

3rd ECATS Conference

Making Aviation Environmentally Sustainable

co-hosted with SARC



Book of Abstracts, Volume 1
Gothenburg June 2020

MAKING AVIATION ENVIRONMENTALLY SUSTAINABLE

3rd ECATS Conference
Co-hosted with Swedish Aeronautical Research Council (SARC)
Book of Abstracts, Volume 1

Title:

Making Aviation Environmentally Sustainable
3rd ECATS Conference, Book of Abstracts, Volume 1, June 2020

ISBN 978-1-910029-58-9

Edited by: Sigrun Matthes, Anja Blum

MAKING AVIATION ENVIRONMENTALLY SUSTAINABLE

3rd ECATS Conference
Co-hosted with Swedish Aeronautical Research Council (SARC)
Book of Abstracts, Volume 1

The original date for the conference was 21-23 April 2020 however due to the COVID-19 pandemic it had to be postponed. The date of the rearranged conference is the 13-15 October 2020. As it is unlikely that we will be able to meet in person due to travel and social distancing restrictions the conference will take place virtually

CONFERENCE LOCATION – THE HOUSE OF WILLIAM CHALMERS

Had travel restrictions allowed the hosting of a face-to-face conference, the venue would have taken place in the former house of William Chalmers.

Once the residence of the founder of Chalmers University of technology, William Chalmers, the house continues to be a meeting place hosting conferences, seminars and workshops. Built from the fortune that William Chalmers amassed from Swedish-Chinese trade, the house has been the residence of many industrialists and merchants.

Banking business has, for a long time, been a key activity in the house and a museum was opened in 1992. In 2006, the house was donated by the Nordic financial group SEB to Chalmers University. The house offers a unique meeting place located in the middle of Gothenburg - and is an obvious choice for making aviation environmentally sustainable. We hope to be able to use these fabulous facilities for a future ECATS conference.



The house of William Chalmers - venue

Title:

Making Aviation Environmentally Sustainable
3rd ECATS Conference, Book of Abstracts, Volume 1, June 2020

ISBN 978-1-910029-58-9

Edited by: Sigrun Matthes, Anja Blum

EDITORIAL FOREWORD

The 3rd ECATS conference brings together researchers from different disciplines working on issues which will help the aviation sector respond to many of the significant environmental challenges it faces. These include alternative fuels for aviation, airport air quality, climate impacts, optimal flight trajectory, future materials for aircraft, propulsion technology.

For over 15 years ECATS has focused on these increasingly important areas of work. The ECATS Network of Excellence was established in 2005 with funding from the EU. In 2010 ECATS formed an International Association with the key objectives to continue to bring together the scientific and technical communities to investigate the impact of aviation on the environment. To this day ECATS continues to work closely with stakeholders from the aero industry, regulatory and scientific communities to support communication, dissemination and exploitation activities. A successful outcome of these endeavours is the establishment of a series of ECATS conferences; the first was held in Berlin in 2013, the second in Athens in 2016 and the third was scheduled for April 2020 in Gothenburg. However, the world has rapidly been engulfed by the COVID-19 pandemic and this conference has been rescheduled for 13-15 October 2020 and will take place virtually.

The call for abstracts for the conference scheduled in April 2020 attracted a large number of excellent, interesting and forward looking submissions. To maintain high momentum the Scientific Committee has decided to compile a book of abstracts. This publication is a combination of short and long format abstracts arranged by session. The abstract collection sets out novel concepts, achievements and present results from a series of recent research projects. Together these provide an outline of the work which will be presented in October.

The **airport air quality** session provides an overview of the impact of aircraft engine emissions on the environment and human health. The session sets the context for many airport studies with an opening contribution describing the investigation of the potential health impacts of emissions of ultra-fine particle matter from aircraft engines. A number of contributions look to expand understanding of modelling emissions from aircraft using CFD and Lagrangian particle models. Advances to our modelling capability will help in providing a better understanding of the impact of aircraft engine emissions on regional and local air quality. Contributions to this session illustrate a potential increase in number concentration of ultra-fine particles in and around airports which can be attributed to aircraft activity. In addition, on-going work to better understand emissions of particle matter from aircraft engines within a major European study are reported. This session brings together the most innovative studies investigating airport air quality to provide a synthesis of developments and outcomes. These outcomes will assist the industry to develop a more robust approach to understanding and mitigating impacts.

The **climate impact and mitigation concepts** session explores atmospheric mechanisms and principles how aviation contributed to a changing climate in particular focussing on non-CO₂ impacts and available promising mitigation options. Comprehensive assessments of quantitative estimates of global aviation impacts and detailed studies on climate impact of contrail and contrail cirrus, nitrogen oxides emissions and aerosol-ice-cloud interactions are shown. Mitigation potentials of alternative technologies and operational concepts comprising studies on contrail mitigation strategies, electric and hybrid-electric aircraft, steam injection and recovering aero engines are presented. Concepts on implementation of such alternative concepts with the help of strategic plans and market based measures are explored.

Additionally, four new research initiatives established within the Horizon2020 Aeronautics work programme on sustainable aviation are presented in this session, which contribute to the overall objective to develop towards sustainable mobility by collaborative research.

As turbofan **propulsion systems** evolve with improved efficiency, their sizes become increasingly large. This brings about a nacelle drag increase and significant aerodynamic interference between the propulsion systems and the airframe. The integration of the propulsion systems therefore needs to be optimized properly. On the other hand, the disruptive aircraft concept, boundary layer ingestion (BLI), has attracted extensive interest due to the efficient aerodynamic performance. The concept demands that a propulsion system and an airframe are designed as integrity. As a consequence, these increasing needs impose growing requirements on the propulsion integration, mostly concerning two subjects -- ultrahigh bypass ratio (UHBPR) engine nacelles and BLI fans – which are presented in this session.

The **green flight** session gives an overview on currently discussed operational climate mitigation options and how to assess these options. The basis of these investigations is the understanding of the relation between weather situations and the impact of non-CO₂ effects from aviation. An overview is given on how to simulate and assess operational options either in an Earth-System model or on the basis of meteorological data. Several contributions explore the idea of formation flight with aspects on fuel planning, climate impact and an overall assessment. Fuel efficient re-routings and tankering options are investigated as well as highflying and hypersonic transport and its impact on atmosphere. Effects from climate change on aviation are discussed and two new projects dealing with climate-optimised trajectories are presented (OP-FLYKLIM, FlyATM4E).

The session on **future materials for aircraft** focuses on novel multifunctional materials. These materials inherently provide multiple functions simultaneously. One example is the structural battery composite, which can carry mechanical loads, while storing electrical energy as a battery. In this way, electrical energy can be stored in a structural load path. As a consequence, mono-functional devices and materials can be reduced and the weight of the aircraft system can be significantly reduced.

The session on **cryogenic fuels and electrofuels** is focused on recent developments of the implementation of cryogenic and electrofuels in the aviation sector. An energy system model of the Nordic countries have suggested that electrofuels is a cost-effective option when carbon capture and storage is not deployed in large-scale. Moreover, hydrogen is presented as an attractive alternative if significant effort is put in the development of critical technologies. Other challenges for hydrogen and electrofuels are the need for fuel production capacity and the large quantities of CO₂ free electricity needed during production. The northern parts of Sweden are particularly interesting for such production, due to abundance of renewable electricity resources and a strong and reliable electric grid.

The **Swedish National Aeronautics Research Programme** (NFFP, started 1994) is an aeronautical research program developing research resources within industry, institutes, and universities. Funded by VINNOVA the NFFP program facilitates activities in a broad field of applied lower TRL aerospace research for both civil and military purposes. This session will showcase the nature of this research program by presenting recent research from a number of active projects, as well as to provide a collaborative event with young researchers within the ECATS network.

Enjoy reading this collection of state-of-the-art research, reviewing recent achievements and providing at the same time a strategic perspective on future directions in environmentally sustainable aviation. Most of the extended abstracts will be submitted as full papers to the special issue "Selected Papers from 3rd ECATS Conference on Making Aviation Environmentally Sustainable" of the MDPI Aerospace journal.



Dr. Sigrun Matthes
ECATS Chair



Prof. Dr. Tomas Grönstedt
ECATS & SARC Conference Chair

on behalf of the ECATS & SARC Conference Committees

CONFERENCE EXECUTIVE COMMITTEE

Dr. Simon Blakey

Lead ECATS Working Group "Alternative Fuels"
University of Birmingham, UK
S.G.Blakey@bham.ac.uk

Prof. Dr. Volker Grewe

Lead ECATS Working Group "Green Flight"
DLR, DE & Delft University of Technology, NL
Volker.Grewe@dlr.de

Dr. Sigrun Matthes (ECATS Chair)

Lead ECATS Working Group "Climate impact"
DLR, Institute Atmospheric Physics, DE
Sigrun.Matthes@dlr.de

Dr. Carlos Xisto

Chalmers University, SE
Carlos.Xisto@chalmers.se

Dr. Simon Christie

Coordinator ECATS Student Schools
The Manchester Metropolitan University, UK
S.Christie@mmu.ac.uk

Prof. Dr. Tomas Grönstedt

ECATS & SARC Conference Chair
Chalmers University, SE
Tomas.Gronstedt@chalmers.se

Prof. Dr. Dave Raper

Vice-Chair ECATS
The Manchester Metropolitan University, UK
D.W.Raper@mmu.ac.uk

SCIENTIFIC PROGRAMME COMMITTEE

- Prof. Dr. David Raper, MMU, UK
- Dr. Didier Hauglustaine, LSCE/CNRS, FR
- Assistant Professor Huadong Yao, Chalmers, SE
- Dr. Jan Middel, NLR, NL
- Prof. Dr. Leif Asp, Chalmers, SE
- Peter Linde, Airbus/Chalmers, DE
- Dr. Sigrun Matthes, DLR, DE
- Dr. Simon Blakey, Sheffield/Birmingham, UK
- Dr. Simon Christie, MMU, UK
- Prof. Dr. Tomas Grönstedt, Chalmers, SE
- Dr. Tomas Mårtensson, FOI, SE
- Prof. Dr. Volker Grewe, DLR, DE and TU Delft, NL

TABLE OF CONTENTS

Conference Programme	12
Introduction Statements	13
AIRPORT AIR QUALITY	
AIRPORT EMISSION PARTICLES: EXPOSURE CHARACTERIZATION AND TOXICITY FOLLOWING INTRATRACHEAL INSTILLATION IN MICE	16
<i>K.M. Bendtsen, A. Brostrøm, A.J. Koivisto, I. Koponen, T. Berthing, N. Bertram, K.I. Kling, M. Dal Maso, O. Kangasniemi, M. Poikkimäki, K. Loeschner, P.A. Clausen, H. Wolff, K.A. Jensen, A.T. Saber & U. Vogel</i>	
REGIONAL SENSITIVITIES OF AIR QUALITY TO AVIATION EMISSIONS	17
<i>F. Quadros & I. Dedoussi</i>	
VARIABILITY IN PARTICLE NUMBER CONCENTRATIONS FROM COMMERCIAL AIRCRAFT EMISSIONS IN THE UNITED STATES	18
<i>S. Arunachalam, J. Huang, L.P. Vennam, B.N. Murphy & F.S. Binkowski</i>	
IMPROVEMENT OF AIRPORT LOCAL AIR QUALITY ASSESSMENT	19
<i>K. Synylo, A. Krupko & O. Zaporozhets</i>	
TIME-RESOLVED AIRCRAFT DISPERSION MODELLING	20
<i>U. Janicke, E. Montreuil, W. Ghedhaïfi & E. Terrenoire</i>	
SIMULATION OF AIRCRAFT EMISSIONS DISPERSION BY TRACKING AIRCRAFT USING CFD	27
<i>W. Ghedhaïfi, E. Montreuil & E. Terrenoire</i>	
AVIATOR PROJECT: AIRCRAFT ENGINE EXHAUST STACK PM CHARACTERISATION AT INTA TEST FACILITY	28
<i>V. Archilla-Prat, D. Hormigo, J. Sánchez-Valdepeñas, M. Sánchez-García, P. Moreno, A. Crayford, M. Pujadas, J. Rodríguez-Maroto, I. Ibarra, E. Rojas, D. Raper & M. Johnson</i>	
AIR QUALITY AT FRANKFURT AIRPORT – WHAT CAN WE LEARN FROM COLLOCATED IAGOS AIRBORNE AND FRAPORT SURFACE MEASUREMENTS	33
<i>J. Glaves, D. Raper, F. Berkes, P. Nedelec & A. Petzold</i>	
CFD AND AEROSOL DYNAMICS BOX-MODEL TO IMPROVE DISPERSION MODELS	34
<i>E. Montreuil, S. Matthes, F. Garnier, V. Archilla-Prat, W. Ghedhaïfi, M. Righi & E. Terrenoire</i>	
AIRPORT AIR QUALITY – EVOLUTION AND STATE-OF-THE-ART OF METHODOLOGIES AND POSSIBLE IMPROVEMENTS.	35
<i>V. Huck, T. Elliff, A. Celikel & F. Murzyn</i>	
CHEMICAL CHARACTERIZATION OF ULTRAFINE PARTICLES NEAR FRANKFURT AIRPORT BY LIQUID CHROMATOGRAPHY	41
<i>F. Ungeheuer, D. Rose, D. van Pinxteren, F. Ditas, S. Jacobi, H. Herrmann & A. L. Vogel</i>	
AIR QUALITY STUDIES AT UKRAINIAN AIRPORTS	45
<i>K. Synylo, K. Ulianova & O. Zaporozhets</i>	
MEASUREMENT OF ULTRAFINE PARTICLES AT PARIS AIRPORT	46
<i>St. Verlhac</i>	
LOW-COST SENSOR DEVELOPMENT AS PART OF THE AVIATOR PROJECT	47
<i>D. Kilic, P.I. Williams, V. Archilla-Prat, D. Raper & S. Lopez</i>	

CLIMATE IMPACT AND MITIGATION CONCEPT

IMPACT OF PRESENT AND FUTURE AIRCRAFT EMISSIONS ON ATMOSPHERIC COMPOSITION AND RADIATIVE FORCING OF CLIMATE <i>E. Terrenoire & D. Hauglustaine</i>	48
TOWARDS DETERMINING THE EFFICACY OF CONTRAIL CIRRUS <i>M. Ponater, M. Bickel, L. Bock & U. Burkhardt</i>	52
THE CONTRIBUTION OF AVIATION NO _x EMISSIONS TO CLIMATE CHANGE <i>V. Grewe, S. Matthes & K. Dahlmann</i>	56
EVALUATION OF THE CLIMATE IMPACT OF THE STEAM INJECTING AND RECOVERING AERO ENGINE <i>R. Pouzolz, O. Schmitz & H. Klingels</i>	57
PARAMETRIC STUDY OF CONTRAILS FORMATION <i>E. Montreuil, W. Ghedhaïfi & E. Terrenoire</i>	61
THE CONTRAIL MITIGATION POTENTIAL OF AIRCRAFT FORMATION FLIGHT DERIVED FROM HIGH-RESOLUTION SIMULATIONS <i>S. Unterstrasser</i>	62
A MODEL STUDY ON CONVECTIVELY GENERATED GRAVITY WAVE AND TURBULENCE <i>W.J. Sang</i>	67
MITIGATING CLIMATE IMPACT OF AVIATION BY MINIMIZING AIRCRAFT CONTRAILS <i>U. Schumann, R. Teoh, and M.E.J. Stettler</i>	68
IMPACT ON CONTRAILS COVERAGE WHEN FLYING WITH HYBRID ELECTRIC AIRCRAFT <i>F. Yin, V. Grewe & K. Gierens</i>	71
THE ROLE OF ELECTRIC-POWERED FLIGHT IN REAL-WORLD COMMERCIAL OPERATIONS <i>A. Sobron, I. Staack & P. Krus</i>	76
AENA PHOTOVOLTAIC PLAN <i>P. Lopez, A. Brea & A. Salazar</i>	80
HOW TO EFFICIENTLY DESIGN AIRCRAFT WITH MINIMUM CLIMATE IMPACT? <i>F. Linke, K. Radhakrishnan, V. Grewe, R. Vos, M. Niklass, B. Lührs, F. Yin, I. Dedoussi, P. Proesmans & K. Deck</i>	81
NEAR-FIELD MODELLING OF CONTRAILS MICROPHYSICS <i>E. Terrenoire, X. Vancassel, W. Ghedhaïfi & E. Montreuil</i>	82
MITIGATION OF NON-CO ₂ AVIATION'S CLIMATE IMPACT BY CHANGING CRUISE ALTITUDES <i>S. Matthes, L. Lim, U. Burkhardt, K. Dahlmann, S. Dietmüller, V. Grewe, A. Haselrut, J. Hendricks, D.S. Lee, B. Owen, G. Pitari, M. Righi & A. Skowron</i>	83
NON-CO ₂ IMPACTS OF AVIATION THROUGH AVIATION-AEROSOL - ICE-CLOUD INTERACTIONS <i>C. Tully, D. Neubauer & U. Lohmann</i>	90
CONCEPT OF CLIMATE-CHARGED AIRSPACE AREAS <i>M. Niklass, V. Grewe & V. Gollnick</i>	93
THE EU PROJECT ACACIA (ADVANCING THE SCIENCE FOR AVIATION AND CLIMATE) <i>R. Sausen, S. Matthes, K. Gierens & the ACACIA team</i>	98

CLIMOP: CLIMATE ASSESSMENT OF INNOVATIVE MITIGATION STRATEGIES TOWARDS OPERATIONAL IMPROVEMENTS IN AVIATION	99
<i>A. Tedeschi & the ClimOP Project Team</i>	

OPTIMIZED FLIGHT TRAJECTORIES TO LIMIT THE CLIMATE CHANGE	103
<i>M. Finke, P. Favier, M. Temme, J. Rataj, M. Kleinert, A. Pasztor, F. Kling & H. Haoliang</i>	

ALTERNATIVE FUELS FOR AVIATION

UNDERSTANDING THERMAL STABILITY OF FUTURE JET FUELS USING COMPUTATIONAL CHEMISTRY	104
<i>C. Adams, S. Blakey, A. Meijer, E. Alborzi & C. Parks</i>	

EFFECT OF FUEL COMPOSITION ON NVPM EMISSIONS PRODUCED BY AN RQL COMBUSTION RIG USING CONVENTIONAL AND ALTERNATIVE FUELS	110
<i>J. Harper, E. Durand, M. Johnson & A. Crayford</i>	

IMPACT OF FUEL COMPOSITION ON AERONAUTIC EMISSIONS	115
<i>A. Berthier, D. Delhaye, I. K. Ortega & C. Focsa</i>	

AIRCRAFT ENGINE PARTICULATE MATTER EMISSIONS USING SUSTAINABLE AVIATION FUELS	116
<i>P. Lobo, T. Schripp, J. Corbin, P. Osswald, M. Shook, E. Crosbie, C. Robinson, Z. Yu, R. Miake-Lye, A. Freedman, G. Smallwood, P. Whitefield, M. Köhler & B. Anderson.</i>	

REVIEWING THE DEVELOPMENT OF ALTERNATIVE AVIATION FUELS AND AIRCRAFT PROPULSION SYSTEMS	117
<i>K. Dahal, S. Brynolf, M. Grahn, J. Hansson & M. Lehtveer</i>	

CONCEPTUAL DESIGN OF A COMPRESSOR-VANE-HEX FOR LH ₂ AIRCRAFT ENGINE APPLICATIONS	125
<i>C. Xisto, I. Jonsson & T. Grönstedt</i>	

NOVEL SMALL SCALE ISOTHERMAL STABILITY TEST METHOD FOR AVIATION FUEL	126
<i>S.Y. Sadat, S. Blakey & E. Alborzi</i>	

IMPACT OF ALTERNATIVE JET FUELS ON AIRCRAFT EMISSIONS IN CRUISE	127
<i>D. Sauer, H. Schlager, B.E. Anderson, P. LeClercq, C. Voigt, T. Bräuer, C. Heckl, S. Kaufmann, R. Moore, M. Scheibe, T. Schripp, M. Shook, K. L. Thornhill, E. Winstead & L. Ziemba</i>	

IMPACT OF ALTERNATIVE FUELS ON CONTRAIL CIRRUS PROPERTIES AND CLIMATE-IMPACT	128
<i>A. Bier & U. Burkhardt</i>	

FUTURE MATERIALS FOR AIRCRAFT

TEACHING ACTIVITIES FOR FUTURE MULTIFUNCTIONAL COMPOSITE MATERIAL	129
<i>J. Xu, D. Carlstedt, S. Duan, L.E. Asp</i>	

MULTI FUNCTIONAL MATERIALS TOWARDS ENVIRONMENTALLY FRIENDLY AVIATION	133
<i>P. Linde & L. Asp</i>	

STRUCTURAL POSITIVE ELECTRODE PRODUCED USING TAPE CASTINGS	134
<i>S. Duan, J. Xu, D. Carlstedt & L.E. Asp</i>	

STRUCTURAL BATTERY COMPOSITE DEMONSTRATOR	135
<i>D. Carlstedt, J. Xu, D. Shanghong, P. Linde, & L.E. Asp</i>	

PROPULSION INTEGRATION

PROPULSION INSTALLATION MODELLING FOR GEARED ULTRA-HIGH BYPASS RATIO ENGINE CYCLE DESIGN	136
<i>J. Andersson, T. Grönstedt & H.D. Yao</i>	
AERODYNAMIC DESIGN OF NACELLES FOR NEXT GENERATION HIGH-BYPASS TURBOFAN ENGINES	140
<i>V.T. Silva, A. Lundbladh & O. Petit</i>	
HARMONIC FORCING IN A BOUNDARY LAYER INGESTING FAN	145
<i>H. Mårtensson</i>	
INSTALLATION EFFECTS ON ENGINE DESIGN	151
<i>X.J. Li & H.D. Yao</i>	
TECHNOLOGY DEVELOPMENT OF UHBPR TURBOFAN ENGINES AND RELATED INSTALLATION	159
<i>J. Andersson, H.D. Yao & T. Grönstedt</i>	

GREEN FLIGHTS

CLIMATE IMPACT MITIGATION POTENTIAL OF FORMATION FLIGHT	162
<i>T. Marks, K. Dahlmann, V. Grewe, V. Gollnick, F. Linke, S. Matthes, E. Stumpf, M. Swaid, S. Unterstrasser, H. Yamashita & C. Zumegen</i>	
ASSESSING THE CLIMATE IMPACT OF FORMATION FLIGHTS	169
<i>K. Dahlmann, S. Matthes, H. Yamashita, S. Unterstrasser, V. Grewe & T. Marks</i>	
HOW WELL CAN PERSISTENT CONTRAILS BE PREDICTED?	174
<i>K. Gierens, S. Matthes & S. Rohs</i>	
WEATHER AND LOCATION DEPENDENCY OF AVIATION CLIMATE EFFECTS: 4-D-CLIMATE- CHANGE-FUNCTIONS	179
<i>C. Frömming, V. Grewe, S. Brinkop, A. S. Haslerud, S. Rosanka, J. van Manen & S. Matthes</i>	
COMPARISON OF VARIOUS AIRCRAFT ROUTING STRATEGIES USING THE AIR TRAFFIC SIMULATION MODEL AIRTRAF 2.0	180
<i>H. Yamashita, F. Yin, V. Grewe, P. Jöckel, S. Matthes, B. Kern, K. Dahlmann & C. Frömming</i>	
REDUCING AVIATION EMISSIONS AND FUEL BURN BY RE-ROUTING TRANSATLANTIC FLIGHTS	184
<i>C. Wells, P. D. Williams, N. K. Nichols, D. Kalise & I. Poll</i>	
HOW WILL CLIMATE CHANGE AFFECT FLIGHT ROUTES AND TURBULENCE?	185
<i>P. D. Williams</i>	
FUEL TANKERING: ECONOMIC BENEFITS AND ENVIRONMENTAL IMPACT	186
<i>L. Tabernier, E. C. Fernández, A. Tautz & R. Deransy</i>	
THE CLIMATE IMPACT OF HYPERSONIC TRANSPORT	187
<i>J. Emmerig, P. Jöckel & V. Grewe</i>	
CLIMATE IMPACT MITIGATION POTENTIAL OF EUROPEAN AIR TRAFFIC	188
<i>B. Lührs, F. Linke, S. Matthes, V. Grewe, F. Yin & K.P. Shine</i>	

ROBUSTNESS OF CLIMATE-OPTIMIZED TRAJECTORIES AND MITIGATION POTENTIAL: FLYING ATM4E	195
<i>S. Matthes, B. Lührs, K. Dahlmann, F. Linke, V. Grewe, F. Yin & K.P. Shine</i>	
ADAPTING THE FUEL PLANNING TO OPERATIONAL UNCERTAINTIES OF AIR-CRAFT WAKE- SURFING FOR EFFICIENCY	205
<i>M. Swaid, T. Marks & V. Gollnick</i>	
OPTIMIZATION OF FLIGHT ROUTES FOR REDUCED CLIMATE IMPACT (OP-FLYKLIM) PROJECT	210
<i>J. Moldanová, J. Langner, M. Lindskog, R. Bergström, T. Mårtensson, M. Wall, H. Ekstrand, M. Rydal & A. Näs</i>	

CRYOGENIC FUELS / ELECTROFUELS

LARGE SCALE BIO-ELECTRO-JET FUEL PRODUCTION INTEGRATION AT CHP-PLANT IN ÖSTERSUND, SWEDEN – PROCESS DESIGN FOR AN ELECTRO FUEL FACTORY.	211
<i>A. Fagerström, D. Grahn, S. Lundberg, O. Wallberg, L. Olsson, D. Creaser, M. Poorsgaard, M. Lindgren, J. Hansson, T. Rydberg & S. Anderson</i>	
DECARBONIZING NORDIC TRANSPORTS – THE ROLE OF ALTERNATIVE AVIATION FUELS	215
<i>J. Hansson, M. Hagberg, S. Brynolf, M. Grahn, K. Karlsson & R. Salvucci</i>	
FUEL TANK SIZING METHODOLOGY FOR CRYOGENIC HYDROGEN FUELLED AIR TRANSPORT	220
<i>D. Nalianda, P. Rompoko, A. Rolt & V. Sethi</i>	
ENERGY TRANSITION IN AVIATION: THE ROLE OF CRYOGENIC FUELS	221
<i>A. Gangoli Rao & F. Yin</i>	

GENERAL SESSION FOR NATIONAL AERONAUTICS PROGRAMME (NFFP)

QUANTIFYING THE ENVIRONMENTAL DESIGN TRADES FOR A STATE-OF-THE-ART TURBOFAN ENGINE	227
<i>E.M. Thoma, T. Grönstedt & X. Zhao</i>	
EXPERIMENTAL STUDY OF TRANSITION IN A TURBINE REAR STRUCTURE	232
<i>I Jonsson. & V.Chernoray</i>	
AERODYNAMIC INVESTIGATION OF THE FLOW IN A TURBINE REAR STRUCTURE AT REALISTIC FLOW CONDITIONS	237
<i>V. Vikhorev & V. Chernoray</i>	
INTEGRATION OF AIRBORNE EARLY WARNING RADAR PLATFORMS ON AIRCRAFT	241
<i>P. Khanal, J. Yang, M. Ivashina, A.Höök, R. Luo, & P. Hallander</i>	
A SYSTEM OF SYSTEMS VIEW IN AEROSPACE PRODUCT DEVELOPMENT	245
<i>L. Knöös Franzén, I. Staack, C. Jouannet & P. Krus</i>	
AUTONOMOUS NAVIGATION SUPPORT FROM REAL-TIME VISUAL MAPPING	250
<i>D. Sabel & D. Åsvärn</i>	
INVESTIGATING FIGHTER PILOT TEAMWORK USING A LOW-COST FLIGHT SIMULATOR	251
<i>U. Ohlander, J. Alfredson & R. Granlund</i>	
CAVITY ACOUSTICS AND ROSSITER MODES - CARE	252
<i>S. Hammer, J. Fridh & M. Billson</i>	

MICROSTRUCTURAL EVOLUTION DURING THERMAL POST-TREATMENT OF ALLOY 718 PRODUCED BY ELECTRON BEAM MELTING <i>S. Goel, U. Klement & S. Joshi</i>	256
Index of Authors	257

CONFERENCE PROGRAMME

Session I Airport Air Quality

Chair: Prof. Dr. Dave Raper

Rapporteur: Dr. Simon Christie

Session II Climate impact and mitigation concepts

Chair: Dr. Sigrun Matthes

Rapporteur: Dr. Didier Hauglustaine

Session III Alternative fuels for aviation

Chair: Dr. Simon Blakey

Rapporteur: Dr. Tomas Martensson

Session IV Future materials for aircraft

Chair: Prof. Dr. Leif Asp

Rapporteur: NN

Session V Propulsion integration

Chair: Dr. Hua-Dong Yao

Rapporteur: Dr. Carlos Xisto

Session VI Green Flights

Chair: Prof. Dr. Volker Grewe

Rapporteur: Dr. Jan Middel

Session VII Cryogenic fuels and electrofuels

Chair: Dr. Carlos Xisto

Rapporteur: Dr. Selma Brynolf

Session VIII National Aeronautics Programme (NFFP)

Chair: Prof. Dr. Tomas Grönstedt

Rapporteur: Prof. Dr. Niklas Andersson

A new dawn of aviation

Henri Werij / Dean Aerospace Engineering at TU Delft

We all know that aviation has a significant effect on World climate, which will further grow if we do not act. The current pandemic demonstrates all too clearly just how much we fly and how much this impacts air quality and climate change. Governments start demanding steps in sustainability from airlines they are currently supporting with public funding. This is the time to start a revolution in aviation.



Despite the fact that modern aircraft at first sight very much resemble their predecessors the fuel consumption per passenger kilometre has decreased impressively, due to vast improvements in propulsion, aerodynamics and materials. However, these improvements are completely nullified by the exponential growth of global air travel. In order to tackle the climate challenges we face a truly holistic approach is needed. We might have to radically change aircraft designs to improve aerodynamic efficiency and allow storage of other fuels, invent new materials to lower weight, and develop new engines running on an energy source different from fossil kerosene. We have to find answers to questions like when to use electrical propulsion and when to rely upon sustainable aviation fuels? And how can we produce the vast amounts of these SAFs? It will also be extremely important to consider the total aircraft emission, including NO_x and water vapour, since CO₂ is only

half the greenhouse story. In this respect we have to make trade-offs in routing, flight altitude and airspeed, which in turn all are likely to affect the aircraft design.

The challenges are enormous, but solutions must and will be found. We must start a revolution, which might exceed the development at the dawn of aviation over a century ago, and will certainly require a concerted international collaboration, long-lasting commitment and a drastic change in mindset to propel aviation into a sustainable future.

US FAA Emissions Research: Characterization, Impacts and Mitigation

S. Daniel Jacob / Emissions Division, Office of Environment and Energy, FAA, USA

The Federal Aviation Administration (FAA) Office of Environment and Energy has a comprehensive end to end research portfolio to characterize aircraft emissions, quantify their impacts on air quality and climate and mitigate such impacts. FAA has facilitated the characterization of gaseous and particle emissions from aircraft engines to enable development of technology-based emissions standards that would reduce emissions at the source. FAA has funded research teams that have informed the development of the first non-



volatile Particulate Matter (nvPM) mass concentration standard and the Landing-Take Off (LTO) nvPM mass and number standards. The FAA is currently funding research to measure ambient concentration of pollutants to quantify aircraft contribution to ambient pollutant concentrations in and around the airports. In addition, research to quantify air quality health impacts are continuing and efforts to improve the performance of regulatory compliance models are underway. There are gaps in our understanding of the impact of current and forecast emissions in the troposphere and stratosphere of subsonic, supersonic and rocket emissions and the FAA is funding research to address these issues. FAA has also funded research to more accurately model aircraft cruise nvPM mass and number emissions as characterization of such cruise emissions remains critical for

quantifying climate impacts of aviation induced cloudiness. In collaboration with other domestic and international agencies, FAA has funded aircraft measurement studies to understand the impact of sustainable aviation fuels on the formation of contrails. Through the Continuous Lower Energy, Emissions and Noise (CLEEN) Program, in close coordination with industry, FAA facilitates the development of technologies that will reduce noise, emissions and fuel burn and expedite the integration of these technologies in to current and future aircraft for a sustainable aviation growth.

Political challenges and a policy perspective

Rickard Nordin, member of Swedish Parliament, Energy/Climate Spokesperson, Center party

To effectively address the Paris agreement, innovation needs to be combined with regulation in a clever way. It is evident that emitting CO₂ into the atmosphere must be associated with a cost and that this cost likely will have to increase with time. More interestingly, technology to achieve net negative CO₂ emissions is now available and should be incentivised to increase innovation and impact. Innovation grows more rapidly under subsidy than regulation.



On medium term Sweden, as does Europe, needs to push greening on several fronts. This includes investing in infrastructure for electrification and stepping up biofuel production. Biofuels will become increasingly more important for transport, in particular in the area of aviation where electrification is technologically more challenging. Synergies between future electrical grid management and fuel supply could provide new opportunity.

Rickard Nordin, climate spokesperson for the Center party will address climate challenge and technological change taking a political and policy making perspective. How can new technological and scientific knowledge be transformed into policies and societal advances? How does the policymaking eco system work and how does it interact with science? How does Sweden and the Center party work with climate change and transport policy?

AIRPORT EMISSION PARTICLES: EXPOSURE CHARACTERIZATION AND TOXICITY FOLLOWING INTRATRACHEAL INSTILLATION IN MICE

K.M. Bendtsen¹, A. Brostrøm^{1,2}, A.J. Koivisto¹, I. Koponen^{1,3}, T. Berthing¹, N. Bertram¹, K.I. Kling², M. Dal Maso⁴, O. Kangasniemi⁴, M. Poikkimäki⁴, K. Loeschner⁵, P.A. Clausen¹, H. Wolff⁶, K.A. Jensen¹, A.T. Saber,¹ & U. Vogel¹

¹ National Research Centre for the Working Environment, Lersø Parkallé 105, DK-2100, Copenhagen, Denmark.

² National Centre for Nano Fabrication and Characterization, Technical University of Denmark, Fysikvej, Building 307, DK-2800 Kgs, Lyngby, Denmark.

³ FORCE Technology, Park Allé 345, 2605, Brøndby, Denmark.

⁴ Aerosol Physics, Laboratory of Physics, Faculty of Natural Sciences, Tampere University of Technology, PO Box 527, FI-33101, Tampere, Finland.

⁵ National Food Institute, Research Group for Nano-Bio Science, Technical University of Denmark, Kemitorvet 201, DK-2800 Kgs, Lyngby, Denmark.

⁶ Finnish Institute of Occupational Health, P.O. Box 40, FI-00032, Työterveyslaitos, Helsinki, Finland.

INTRODUCTION:

There is limited knowledge on exposure levels and adverse health effects following occupational exposure to airport emissions. Diesel exhaust particles are classified as carcinogenic to humans, gasoline engine exhaust is classified as possibly carcinogenic to humans by IARC, and jet engines produce soot particles with similar physico-chemical properties. The potential occupational exposure risk was assessed by analyzing particles from a non-commercial airfield and from a commercial airport. Toxicity of the collected particles was assessed by lung exposure in mice.

RESULTS:

Particle exposure levels were up to 1 mg/m³ at the non-commercial airfield. Particulate matter from the non-commercial airfield air consisted of primary and aggregated nanosized soot particles, whereas commercial airport sampling resulted in a more heterogeneous mixture including soot, salt, and organic compounds. The content of polycyclic aromatic hydrocarbons and metals of the airport particles were similar to the content in standard NIST diesel exhaust particles (NIST2975). Mice were exposed at three dose levels alongside carbon nanoparticles and NIST2975, and followed for 1, 28, or 90 days. Dose-dependent inflammation was observed for all particles. Dose-dependent acute phase response, a biomarker of risk of cardiovascular disease, were observed. Increased levels of DNA strand breaks, a biomarker of cancer risk, were observed at single dose levels in bronchoalveolar lavage cells and liver tissue.

CONCLUSIONS:

Pulmonary exposure of mice to airport emission particles induced acute phase response, inflammation, and genotoxicity similar to standard diesel exhaust particles and carbon black nanoparticles, suggesting similar physicochemical properties and toxicity of jet engine particles and diesel exhaust particles.

Keywords: health effects, risk assessment, occupational exposure

REFERENCE

Bendtsen KM, Brostrøm A, Koivisto AJ, Koponen I, Berthing T, Bertram N, Kling KI, Dal Maso M, Kangasniemi O, Poikkimäki M, Loeschner K, Clausen PA, Wolff H, Jensen KA, Saber AT, Vogel U, 2019. *Airport emission particles: Exposure characterization and toxicity following intratracheal instillation in mice*. Particle and Fibre Toxicology, Vol. 16 (1), 23.

REGIONAL SENSITIVITIES OF AIR QUALITY TO AVIATION EMISSIONS

F. Quadros¹ & I. Dedoussi

¹ Delft University of Technology, Aerospace Engineering, The Netherlands, f.quadros@tudelft.nl

Abstract. Emissions from civil aviation traffic degrade air quality, causing human health problems that have been estimated to result in ~16 000 premature deaths per year globally, potentially making the cost to society of the air quality impacts even greater than the cost of the climate impact of these emissions. Previous studies have indicated that aviation emissions in specific areas can have impacts of significantly different intensities due to variations in population density and background atmospheric composition. We use the GEOS-Chem global atmospheric chemistry-transport model to investigate the air quality sensitivity to aviation emissions in different regions of the world by performing simulations with increased emissions on different locations at a time and comparing the resulting changes in human exposure to air pollutants (fine particulate matter and ozone). We evaluate the impacts of both landing and take-off (LTO) and cruise level emissions. The simulations are used to investigate the drivers of the differences in air quality sensitivity to emission location, shedding light to the previously observed indications that European air traffic leads to more premature deaths per mass of emissions than North American air traffic. These regionally varying air quality effects imply that regionally non-uniform regulations, if feasible, might provide efficient strategies of mitigating costs associated with air quality impacts.

Keywords: aviation, air quality, intercontinental pollution, public health

VARIABILITY IN PARTICLE NUMBER CONCENTRATIONS FROM COMMERCIAL AIRCRAFT EMISSIONS IN THE UNITED STATES

S. Arunachalam¹, J. Huang¹, L.P. Vennam¹, B.N. Murphy² & F.S. Binkowski¹

¹ Institute for the Environment, The University of North Carolina at Chapel Hill, USA, sarav@email.unc.edu

² National Exposure Research Laboratory, U.S. Environmental Protection Agency, USA

Abstract. We present an enhanced approach to characterize fine particulate matter (mass and number concentrations) due to commercial aircraft activity in North America. Currently, the Community Multiscale Air Quality (CMAQ) model treats particles size distributions (PSD) from various emission sectors uniformly. However, field measurements indicate different emission sectors have different PSD. To capture different PSD, we developed a new CMAQ module that treats particle emissions from a specific sector and assigns unique PSD parameters to those emissions. We used this new module to investigate impacts of emissions from aircraft during landing and takeoff operations (LTO) in North America on ambient PM. Our results indicate ultrafine particle number concentrations (UFP) (particles of size < 0.1 μm) dramatically increase in airport grid-cells due to changes in PSD. UFP at the Los Angeles International (LAX) airport are 5.2 times higher than from non-aircraft emissions scenario, matching field measurements at LAX. Although mass concentrations of accumulation mode (size between 0.1 μm and 2.5 μm) particles in airports were lower (up to -34 ng m^{-3} for top 10 airports, and -0.67 ng m^{-3} for domain average), UFP mass concentrations were higher in sensitivity than base scenarios (up to 30 ng m^{-3} for top 10 airports, and 0.83 ng m^{-3} for domain average). Changing aircraft emitted PSD to smaller size increases available surface areas that can impact deposition, aerosol chemistry and gas-particle mass transfer. Our study increases the understanding of UFP spatial variations near airports and provides a blueprint for better UFP estimation from other emission sectors.

Keywords: Aircraft, Emissions, Ultrafine particles, Size distribution, LTO

IMPROVEMENT OF AIRPORT LOCAL AIR QUALITY ASSESSMENT

K. Synylo¹, A. Krupko¹ & O. Zaporozhets¹

¹ Faculty of Environmental Safety, Engineering and Technologies, National Aviation University, Ukraine, synyka@gmail.com, kranig@gmail.com, zap@nau.edu.ua

Abstract. Despite significant economic and social benefits, the aviation brings, its activities also contribute to local air quality impact and affect the health and quality life of people, living near the airports. Number of flights is forecast to grow by a further 42% between 2017 and 2040. The emissions of CO and NO_x are predicted to increase by at least 21% and 16% at 2040.

Inventory emission results at major European and Ukrainian airports highlighted that aircraft (during approach, landing, taxi, take-off and initial climb of the aircraft, engine run-ups, etc.) are the dominant source of air pollution in most cases under consideration. ICAO Doc 9889 recommends few tools for air quality analysis - to model emission inventory from every character groups of the spatially distributed sources as well as atmospheric concentrations resulting from emission dispersion.

As with any dispersion model, the initial properties of a plume are important to model its rise and location. Such plume or jet parameters, as rise height Δh_A due to buoyancy effect, horizontal σ_{2y} and vertical σ_{2z} dispersion parameters are needed as input to dispersion modeling of aircraft sources. The setting of initial plume parameters by default for various types of aircraft fleet in modeling systems is not quite reasonable, since mentioned parameters depend on aircraft and engine type, engine operation mode and meteorological conditions. Air pollution from aircraft engine emissions and engine jet behavior depend both on: number of engines, engine nozzle parameters and height of its installation, distance between engine nozzle centerlines, and where engines are mounted - on fuselage or on wing of the aircraft. Therefore, to assess of aircraft engine emissions contribution to airport air pollution it is important to take into account some features, which define emission and dispersion parameters of the aircraft, as special source of air pollution. Application of CFD-codes allow to improve the models of local air quality and assessment of aircraft engine emissions contribution to total airport air pollution.

Keywords: aircraft engine, emission index, airport air pollution, aircraft engine emissions

REFERENCES (OPTIONAL)

ICAO Environmental Report 2013. Aviation and Climate Change. – 2012 p. // <http://cfapp.icao.int/Environmental-Report-2013>.

Pope, S., Turbulent Flows, Cambridge University Press, 2000.

Zaporozhets O., Fröhlich J., Stiller J., Synylo K. Improvement of Airport Local Air Quality Modeling // Journal of Aircraft, AIAA. -2017. - Vol. 54. – № 5. – P. 1750 –1759.

TIME-RESOLVED AIRCRAFT DISPERSION MODELLING

U. Janicke¹, E. Montreuil², W. Ghedhaïfi² & E. Terrenoire²

¹ Janicke Consulting, Germany, uj@janicke.de

² ONERA, France, emmanuel.montreuil@onera.fr

Abstract. Lagrangian particle models and CFD models allow to model the dispersion of engine exhaust from moving aircraft with a time resolution down to some seconds. This is particularly useful for the investigation of dynamical effects of the engine exhaust and transformation processes within the plume. In addition, it enables direct comparisons with ground-based measurements of the pollutant signal from individual aircraft. The particle model LASAT/LASPORT and the CFD model CEDRE are applied in the EU Horizon2020 research project AVIATOR (2019–2022) to model the ambient transformation and concentration of ultrafine particles at and around airports.

Keywords: dispersion, Lagrangian, CFD, aircraft, airport, ultrafine particles, AVIATOR

INTRODUCTION

Emissions from aircraft have adverse effects on the air quality in and around airports, contributing to public health concerns within neighbouring communities. Therefore, the evaluation of aircraft emissions and dispersion is an important part towards ensuring that local air quality standards in and around airports are not exceeded.

Modelling the dispersion of aircraft engine exhaust plumes and airport emissions provides the basis for a local air quality assessment with spatially and temporally resolved concentration distributions over longer periods of time. This is an essential complement to measurements which are restricted to relatively few locations and which do not allow to assess future trends.

Airports generally have a good understanding of NO_x emissions from a wide range of resident sources including aircraft (Carslaw, 2006), but the emission and dispersion of ultrafine particles (UFP, mass and number) is less understood (ACI, 2019; Agarwal et al., 2019) and may impact health (Cassee et al., 2019). Major uncertainties exist in view of specifying the mass and number emissions and the evolution of volatile UFP during atmospheric transport at and around airports (Timko et al., 2013; Wong et al., 2015). Time-resolved measurements for single aircraft movements and suitable long-time observations can be carried out to gather a better understanding of UFP emission and transformation processes and the UFP contribution from airport-related sources (Fleuti et al., 2017; Vorage et al., 2019).

Time resolved modelling of the emission and dispersion from individual aircraft can help to support these investigations. Models of this type are for example Lagrangian particle models and Computational Fluid Dynamics (CFD) models. In contrast to stationary dispersion models like Gaussian plume models, the models allow to resolve the dispersion process of individual, moving aircraft in a time-resolved manner. This is particularly useful to compare and validate model assumption at hand of measurements that are likewise taken in a time-resolved manner for individual aircraft movements. For example, the time delay between an overflight of an aircraft at approach and the onset of a UFP signal at a measurement device below the approach corridor can be observed (Fleuti et al., 2019) and compared to the model result, providing valuable insight into the dominant transport, dispersion, and transformation processes.

The results of such time-resolved model/measurement comparisons can be used to develop enhanced model parameterizations for the aircraft exhaust dynamics and transformation processes inside the exhaust plume. In addition, the parameterizations can be generalized

such that they can be applied also by stationary dispersion models or for a simplified modelling of long-time averages.

The following provides a short introduction to the particle model LASAT/LASPORT, the CFD model CEDRE and their application in the EU Horizon 2020 project AVIATOR. References given in this document are only a small and non-representative subset of the existing literature.

2. LASAT AND LASPORT

The Lagrangian particle model LASAT (Lagrangian Simulation of Aerosol Transport) is in use for scientific and regulatory purposes since almost 40 years (Janicke, 1983; Janicke & Janicke, 2007). It simulates the dispersion and transport of a representative sample of tracer particles utilizing a random walk process (Markov process in momentum and real space).

The model type intrinsically captures the different diffusion regimes (turbulent diffusion in the near field, classical diffusion in the far field) and allows to account for 3-dimensional wind and turbulence fields in which the particles move. Concentrations are calculated from the time-integrated mass that the particles transport within a given counting volume. Typical resolutions for the concentration are some seconds up to annual averages and about 1 metre up to some hundred metres. Dry and wet deposition, sedimentation of aerosols, and conversions of first order can be modelled directly. For conversions of higher order, a framework has been developed (LASREA) that switches between short time intervals of passive transport and intermediate steps with conversion and redistribution of masses among the particles. The model type has been standardized by the regulation VDI 3945 Part 3 (VDI-3945-3, 2000). A simplified OpenSource version of LASAT, AUSTAL, is applied in Germany since 2002 as regulatory model for the Technical Instruction on Air Quality Control (TA-Luft, 2002). LASAT is part of the modelling tools JRODOS (European off-site emergency management after nuclear accidents), LASAIR (German decision support system for nuclear hazards), ESOFIN (simulation of odour emissions from field inspections), and LASPORT (emission and dispersion calculation for airports).

LASPORT (LASAT for Airports) is a modelling system developed on behalf of the German Airports Association (ADV) as a standard tool for emission and dispersion calculations for airport related sources, in particular aircraft, ground support equipment, motor traffic and other sources at and around an airport. It has been approved for use by ICAO/CAEP (ICAO, 2010), conforms to ICAO document 9889 (ICAO, 2011), and has been applied to model ultrafine particle concentrations (Lorentz et al., 2019).

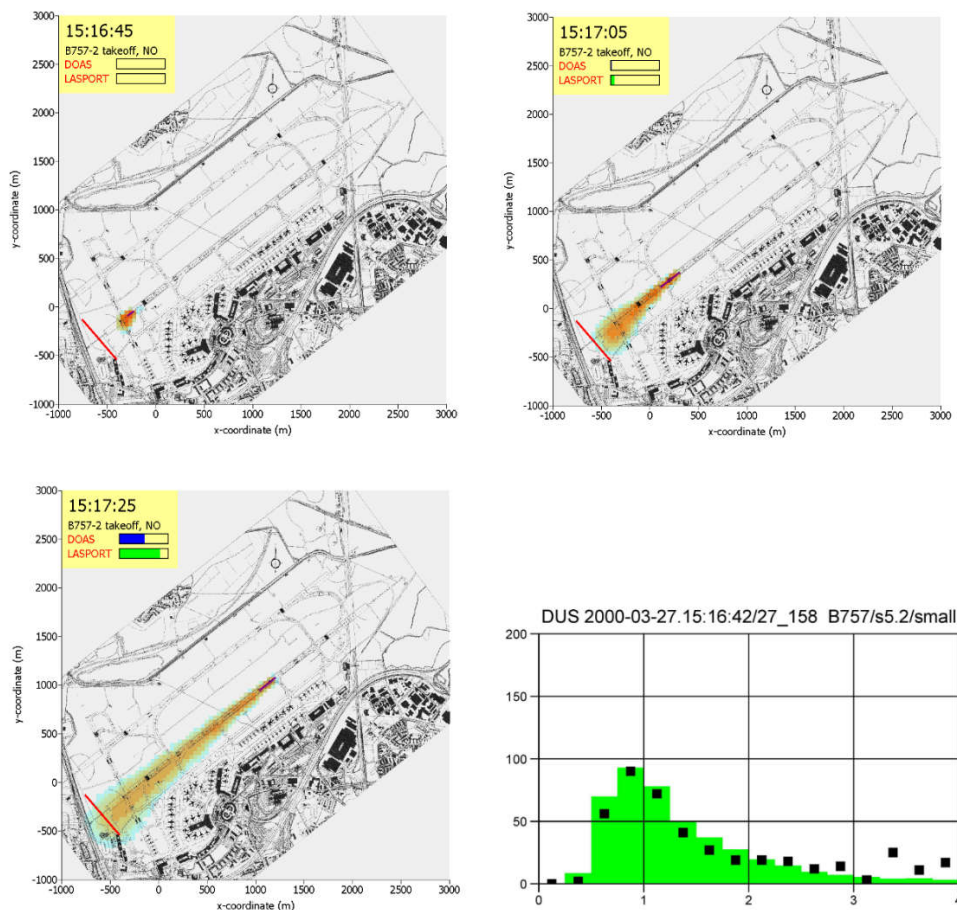


Figure 1. Comparison of measured and modelled near-ground NO concentration behind an aircraft at ground take-off (Janicke, 2008). The three graphs depict Düsseldorf airport with the location of a DOAS device (red line) behind the runway threshold and a subset of 5-second averaged NO concentration plumes behind a moving aircraft at take-off (indicated by the magenta line) modelled by LASPORT. The lower right graph shows the comparison of modelled (green) and measured (squares) concentration averaged over the DOAS line (15-second averages in $\mu\text{g}/\text{m}^3$).

Aircraft traffic can be modelled in LASPORT in two distinct ways. In scenario mode, emissions from aircraft are distributed over systems of stationary line sources with mode-specific dynamical properties and hourly-averaged emissions according to the actual amount of movements. In monitor mode, aircraft traffic is specified in form of a movement journal with individual aircraft movements and every movement is modelled as a moving source with a time resolution of down to about 5 seconds. The scenario mode is useful for quick calculations, long-time averages, and situations for which no detailed information on aircraft traffic is available. It applies a setup similar to the one used with stationary dispersion models. The monitor mode is more demanding with respect to computation time and input detail, but allows to model the three-dimensional, non-stationary concentration distribution from individual moving aircraft with a high temporal resolution. For larger averaging intervals, scenario and monitor mode provide similar results.

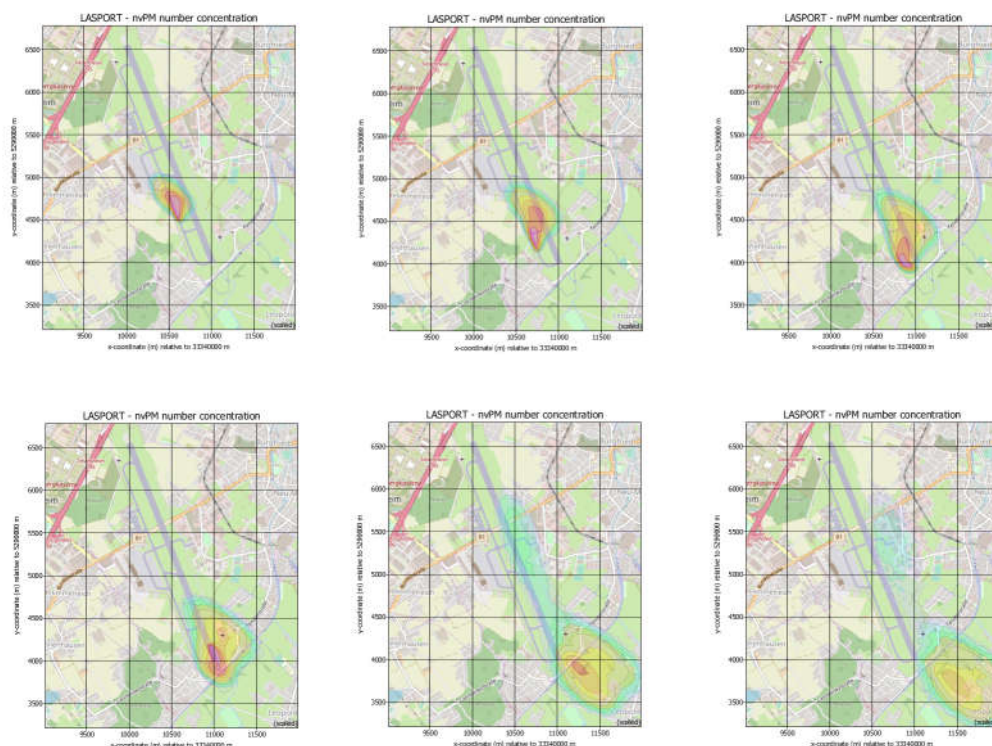


Figure 2. Sub-sequence of 5-second averages of the near-ground number concentration of non-volatile ultrafine particles from an aircraft at taxiing and take-off modelled with LASPORT (setup following Vorage et al., 2019).

CEDRE

Modelling airport air quality is a complex task because it involves multi-scale phenomena such as micro-scale dispersion, microphysics, chemistry. Numerical simulations have often been used to investigate these physical processes and thus providing detailed information in terms of temporal and spatial distribution of species concentrations (Gosseau et al., 2011; Tominaga et al., 2013, 2016). These models were mainly focused on the pollutant dispersion in the urban environment and three-dimensional CFD of aircraft emission dispersion have been little considered over the past few years. A new approach to investigate three-dimensional pollutant dispersion at an airport has been implemented (Ghedhaïfi et al., 2010, 2019) using the CFD code CEDRE (Refloch et al., 2011) which is a MPI parallel, three-dimensional, multi-species, multi-physics compressible Navier-Stokes solver. The numerical method is based on a cell-centered finite-volume approach for general unstructured grids, especially appropriate when complex geometries such as aircraft or jet engine are used. Gas-phase chemistry can also be implemented in specifying kinetic reaction schemes (for example, including SO_x , NO_x , and HO_x chemistry).

In the original methodology developed here, every aircraft engine and APU is considered as an individual source that moves along its own trajectory. The properties of the emissions depend on the engine type, real-time power settings associated with specific exhaust temperature, jet flow velocity and chemical composition. Atmospheric conditions are taken into account through ambient wind speed, temperature, relative humidity and background chemical species concentrations. The air traffic is described using a database that provides aircraft position and current status in the landing/take-off cycle. Numerical simulations give instantaneous and mean distribution of chemical species within the airport platform. In particular, they allow investigations of pollutant concentrations where buildings can influence their spatial distribution.

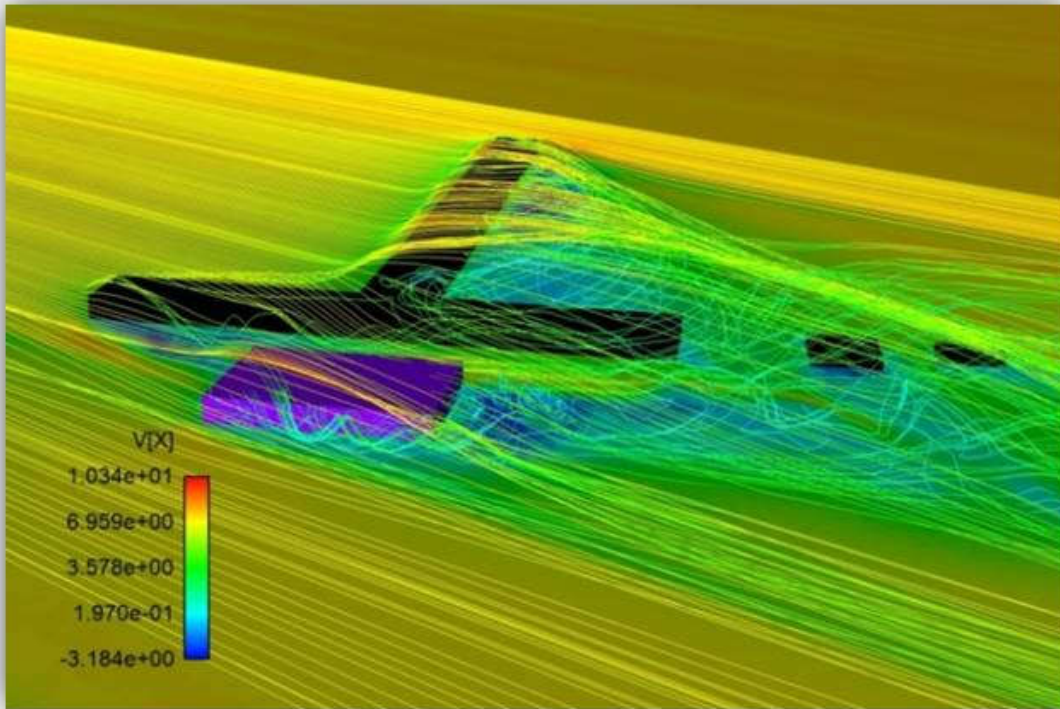


Figure 3. Visualization of the turbulent flow structure around a terminal building as modelled with CEDRE.

4. APPLICATION IN AVIATOR

LASPORT and CEDRE are applied in the EU Horizon2020 project AVIATOR (2019–2022, see aviatorproject.eu). It aims for a better understanding of UFP emission and pollution at and around airports. The models are used to investigate, validate and standardize parameterizations of the engine exhaust properties, the emission of non-volatile UFP and the formation and growth of volatile UFP (mass and number). The work is supported by measurement campaigns at the airports Madrid Barajas and Zurich.

Measurements of UFP and trace gases are carried out at different distances behind an aircraft at rest, with one or more engines operating at different thrust settings. One aim is to enhance the parameterizations of plume dynamics (directed exit velocity and turbulence with according decay times) and to provide more generalized parameterizations that can be applied also by other types of dispersion models (e.g. a smooth and shift of the emission). The measurements are also used to validate parameterizations for the creation and conversion of volatile UFP (e.g. effective emissions or conversion rates).

High fidelity measurements at different locations at the airport are carried out and re-modelled with LASPORT and CEDRE such that the footprint of individual aircraft in the concentration signals can be compared. This will further validate the developed parameterizations of exhaust dynamics and volatile UFP conversion. The high-fidelity measurements are supplemented by a network of local sensors and the results will be compared to modelled ones for longer time averages (hours to weeks).

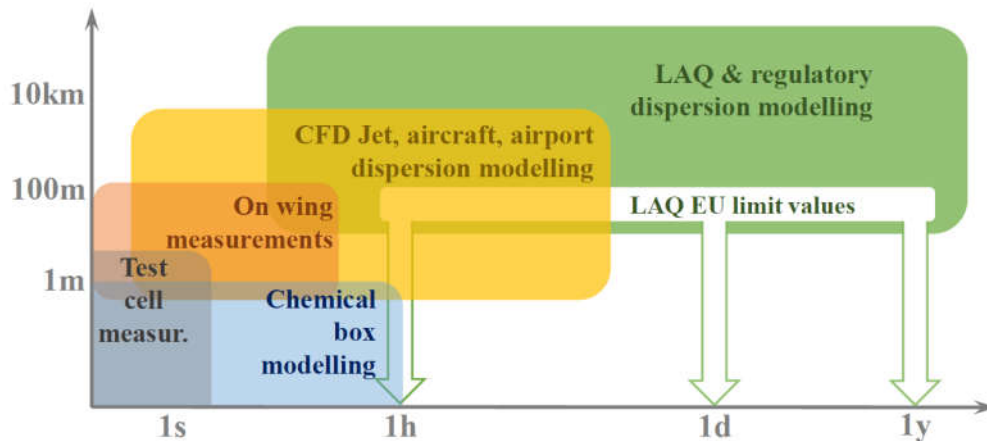


Figure 4. Spatial and temporal scales covered by the AVIATOR model and measurement devices.

CEDRE simulations of an aircraft at departure and arrival will provide further information on the interaction of wing-tip vortices and the engine exhaust. The results are used to enhance according parameterizations in LASPORT and the airport version of CEDRE.

The general aim of this subset of studies within AVIATOR is to provide standardized and validated sets of parameterizations that can be applied both by time-resolving models and simpler dispersion models applied in the context of airport local air quality studies.

ACKNOWLEDGEMENT

This project has received funding from the European Union's Horizon 2020 research and innovation programme under grant agreement No 814801.

REFERENCES

- ACI (2018): *Ultrafine particles at airports*. Airports International Council.
- Agarwal, A., Speth, R.L., Fritz, T.M., Jacob, S.D., Rindlisbacher, Th., Iovinelli, R., Owen, B., Miake-Lye, R.C., Sabnis, J.S., Barrett, S.R.H. (2019): *SCOPE11 method for estimating aircraft black carbon mass and particle number emissions*. Environmental Science & Technology, 53, 1520-5851.
- Carlaw, D.C., Beevers, S.D., Ropkins, K., Bell, M. (2006): *Detecting and quantifying aircraft and other on-airport contributions to ambient nitrogen oxides in the vicinity of a large international airport*. Atmospheric Environment 40, 5424-5434.
- Cassee, F.R., Morawska, L., Peters, A. (2019): *Ambient ultrafine particles: evidence for policy makers*. White paper prepared by the 'thinking outside the box' team.
- Fleuti, E., Maraini, S., Bieri, L., Fierz, M. (2017): *Ultrafine particle measurements at Zurich airport*. Zurich Airport AG.
- Fleuti, E., Ruf, Ch., Maraini, S. (2019): *Ultrafine particle concentrations; Zurich approach runway 14*. Zurich Airport AG.
- Ghedhaïfi, W. (2010): *Chemical impact of aviation in airports*. 27th ICAS Conference, Nice, France.
- Ghedhaïfi, W., Desprez, L., Montreuil, E., Terrenoire, E., Henry-Lheureux, T., Garnier, F. (2019): *3D Simulation of aircraft emissions dispersion in the CAEPport area by tracking aircraft as mobile sources*. 24th ISABE Conference, Canberra, Australia.
- Gousseau, P., Blocken B., Stathopoulos, T. (2011): *Simulation of near-field pollutant dispersion on a high-resolution grid*. Atmospheric Environment, 45, 428-438.
- ICAO (2010): *Environmental Report 2010*. www.icao.int.
- ICAO (2011): ICAO document 9889, *Airport Air Quality Manual*, first edition, www.icao.int.

- Janicke, L. (1983): *Particle simulation of inhomogeneous turbulent diffusion*. In: Weber, B. (Ed.), *Air Pollution Modeling and its Application II*, Plenum Press, New York, 527-535.
- Janicke, U., Janicke, L. (2007): *Lagrangian particle modeling for regulatory purposes; A survey of recent developments in Germany*. Proceedings of the 11th International Conference on Harmonization within Atmospheric Dispersion Modeling for Regulatory Purposes, Cambridge, England.
- Janicke, U. (2008): *Airport air quality: dispersion modelling*. ECATS autumn school, Sinaia.
- Lorentz, H., Janicke, U., Jakobs, H., Schmidt, W., Hellebrandt, P., Ketzler, M., Gerwig, H. (2019): *Ultrafine particle dispersion modelling in the vicinity of the major airport Frankfurt/Main, Germany*. Proceedings of the 19th International Conference on Harmonization within Atmospheric Dispersion Modeling for Regulatory Purposes, Bruges, Belgium.
- Refloch, A., Courbet, A., Murrone, A., Villedieu, P., Laurent, C., Gilbank, P., Troyes, J., Tesse, L., Chaineray, G., Dargaud, J.-B., Quemeraï, E., Vuillot, F. (2011): *Cedre Software*. Aerospace Lab, no. 2.
- TA-Luft (2002): *Technical Regulation on Air Quality Control*. GMBI. 2002, Issue 25-29, 511-605.
- Timko, M.T., Fortner, E., Franklin, J., Yu, Z., Wong, H.-W., Onasch, T. B., Miake-Lye, R.C. and Herndon, S.C. (2013): *Atmospheric measurements of the physical evolution of aircraft exhaust plumes*. *Environmental Science & Technology*, 47, 3513–3520.
- Tominaga, Y., Stathopoulos, T. (2013): *CFD simulation of near-field pollutant dispersion in the urban environment: a review of current modeling techniques*. *Atmospheric Environment*, 79, 716-730.
- Tominaga, Y., Stathopoulos, T. (2016): *Ten questions concerning modeling of near-field pollutant dispersion in the built environment*. *Building and Environment*, 105, 390-402.
- VDI-3945-3 (2000): *Environmental meteorology; atmospheric dispersion models; particle model*. Beuth, Berlin, www.vdi.de.
- Vorage, M., Madl, P., Hubmer, A., Lettner, H. (2019): *Aerosols at Salzburg airport: long-term measurements of ultrafine particles at two locations along the runway*. *Gefahrenstoffe*, 79, 227-234.
- Wong, H.W., Jun, M., Peck, J., Waitz, I.A., Miake-Lye, R.C. (2015): *Roles of organic emissions in the formation of near field aircraft-emitted volatile particular matter: a kinetic microphysical modeling study*. *J. Eng. Gas Turbines and Power*, 137, 072606-1-072606-10.

SIMULATION OF AIRCRAFT EMISSIONS DISPERSION BY TRACKING AIRCRAFT USING CFD

W. Ghedhaïfi¹, E. Montreuil¹ & E. Terrenoire¹

¹ Multi-Physics Department for Energetics, ONERA, France, emmanuel.montreuil@onera.fr

Abstract. Meeting the air quality objectives is becoming a challenging task for the development of the air transport sector since it has to cope with the environmental constraints. At and around airports, aircraft main engines and APU contribute to pollutants emission such as NO_x and Particulate Matter (non-volatile and volatile, Ultra Fine Particles). To evaluate their impact, the present study aims at developing an innovative modelling methodology that better takes into account aircraft emissions evolution at micro-scales, both spatially and temporally in order to increase the accuracy of airport air pollution monitoring and prediction. In this study, the CAEPport airport model has been used as defined in the modelling capabilities and intercomparison ICAO study. This airport is typical of medium size airports infrastructure. In order to achieve CFD simulations, a 3D geometry of the airport is built using CATIA software and the mesh is carried out using ICFM software. In this approach, individual aircraft movements and emissions are tracked with a time resolution down to a second. Meteorological conditions (wind velocity, temperature, relative humidity, etc.) and background species concentrations are also taken into account as they influence dispersion and species chemical evolution respectively. The modelled domain extends up to 8 km around the airport and as the buildings geometry and location influence strongly the dispersion of the pollutants, the spatial resolution can be as fine as 2 m.

Keywords: CAEPport, CFD, emission dispersion

ACKNOWLEDGEMENTS

The authors would like to acknowledge the French Civil Aviation (DGAC) for their funding in the frame of the MOSIQAA project.

REFERENCES

- Ghedhaïfi W., 2010. *Chemical impact of aviation in airports*. In 27th ICAS conference, Nice, France.
- Ghedhaïfi W., L. Desprez, E. Montreuil, E. Terrenoire, T. Henry-Lheureux and F. Garnier, 2019. *3D Simulation of aircraft emissions dispersion in the CAEPport area by tracking aircraft as mobile sources*. In 24th ISABE conference. Canberra, Australia.
- Janicke U. and L. Janicke, 2007. *Lagrangian particle modelling for regulatory purposes - a survey of recent developments in Germany*. In 11th International Conference on Harmonisation within Atmospheric Dispersion Modelling for Regulatory Purposes, Cambridge, UK.
- Tominaga Y. and T. Stathopoulos, 2013. *CFD simulation of near-field pollutant dispersion in the urban environment: a review of current modeling techniques*. Atmospheric Environment, vol. 79, pp. 716-730.

AVIATOR PROJECT: AIRCRAFT ENGINE EXHAUST STACK PM CHARACTERISATION AT INTA TEST FACILITY

V. Archilla-Prat¹, D. Hormigo¹, J. Sánchez-Valdepeñas¹, M. Sánchez-García¹, P. Moreno¹, A. Crayford², M. Pujadas³, J. Rodríguez-Maroto³, I. Ibarra³, E. Rojas³, D. Raper⁴ & M. Johnson⁵

¹. Turbojet Test Centre, INTA, Spain, archillapv@inta.es

². Energy and Environment Department, Cardiff University, UK, CrayfordAP1@cardiff.ac.uk

³. Environmental Department, CIEMAT, Spain, jesus.maroto@ciemat.es

⁴. Centre for Aviation Transport and the Environment, Manchester Metropolitan University, UK, D.W.Raper@mmu.ac.uk

⁵. Measurement Engineering, Rolls-Royce plc, UK, Mark.Johnson3@Rolls-Royce.com

Abstract. Emissions from aircraft engines have adverse effects on air quality in and around airports, contributing to health concerns within neighboring communities. To improve airport local air quality (LAQ) assessment, further understanding and determination of Total Particulate Matter (TPM) within aircraft engine exhaust plumes is required. This study, supported by H2020 funding as part of AVIATOR (Assessing aViation emission Impact on local Air quality at airports: TOwards Regulation), shows initial 'piggyback' experimental data, detailing particle number and mass concentrations and size distributions measured and quantified using both standard and novel techniques in the evolving exhaust measured during Rolls-Royce (RR) large engine development testing campaigns at INTA (Madrid, Spain). The results show that Total PM and Non-Volatile Particulate Matter (nvPM) fractions vary across different engine power conditions. Assessment of low-cost, lower fidelity sensors, provide data which correlates with State-of-the-Art analysers on representative sample potentially highlighting their applicability for local air quality assessment.

Keywords: aviation, airports, emissions, PM, nvPM, VOCs

INTRODUCTION

The historic and future predicted growth of the aviation sector has raised concerns about potential impact of aircraft engines on LAQ in and around airports. Population exposure to Ultra Fine Particles (UFP), especially within neighbouring communities, has received increasing attention because UFP can be readily inhaled, reaching the alveolar regions of the lungs, and penetrating into the circulation system.

The aviation industry has focussed on increasing fuel efficiency and the development of complex design processes aimed at optimising engine performance and combustion processes in compliance with exhaust emission regulations. This has provided a rapid growth in the development of advanced engines focused on reducing regulated gases and smoke. However, this optimisation may affect not only nvPM emission indices, but their size and composition. To improve airport LAQ assessment, further understanding and determination of the concentrations and composition of TPM from aircraft emission plumes is required, building upon the growing knowledge of nvPM emissions. As part of the European project AVIATOR, this study provides additional knowledge of the physical characterisation of UFP (nvPM and TPM) generated by modern large civil aircraft engines (Archilla et al, 2019).

METHODOLOGY

As part of 'piggyback' AVIATOR campaigns, the exhausts of Rolls-Royce large development turbofan engines were sampled using both high fidelity proved and novel measurement techniques. In order to establish a characterisation of the emitted aerosols (vPM and nvPM) as similar as possible to those produced by aircraft engines in and around airports, aircraft engine emissions were sampled and measured at 50m downstream of engine exit in the stack of INTAs test-cell located in Madrid, Spain. This sampling location provides sufficient distance from the engine exhaust to allow physico-chemical processes to occur as the exhaust plume mixes and cools. Consequently, methodology employed during these tests

was required to differ from standard (ICAO Annex 16 Vol II) nvPM emissions measured at engine exit.

Sampling system

Due to the size and height of the stack at INTA's test-cell, a heterogeneous and transient exhaust flow is produced requiring a bespoke multi-orifice probe to obtain representative measurements across the stack (Figure 1).



Figure 1. Multi-orifice probe installation at INTA stack (left and centre), and an individual sampling nozzle (right).

The probe includes six equispaced sampling points (SP) directed into the exhaust flow. Monitoring devices such as thermocouples and Pitot tubes (S-type) are integrated with a modular data acquisition and control system. Samples are transported from each SP by individual transfer lines into an Aerosol Mixing Chamber (AMC). Fixed orifices were calculated and used in each transfer line prior to the AMC in order to equalize the sample pressure drops generated along the lines by the respective differences in length.

The unique AMC, located in a room adjacent to the stack and directly connected to the probe, is made up by three sections: mixing, laminar transport and sub-sampling, to deliver a representative sample to the instrumentation. The mixing section comprises a convergent-divergent nozzle to generate turbulence, resulting in mixing of the six individual samples to produce a homogenous sample. The output sample flow is optimised to be laminar for the transport to the suite of measurement equipment.

Theoretical and experimental validations were performed for each section of the multi-orifice probe, including particle transport efficiency, mixing efficiency in the AMC and the potential effect on the probe of the vibrations of the building. Similarly, theoretical aspiration efficiencies were determined to be nearly 100%, for representative emitted particles $D_p < 600\text{nm}$.

Measurement equipment

In-stack engine emissions characterised particle number concentration (nvPM and TPM), nvPM mass concentrations, and particle size distributions, as well as CO_2 concentration levels necessary to calculate sample dilution. Downstream of the AMC, the sample was carefully split into two sampling lines to provide raw or diluted streams to measurement equipment.

Dilution was achieved using, two ejector dilutors (PALAS) providing a 89:1 dilution stage, required to maintain particle concentrations at sufficiently low levels for single particle counting. Diluted PM number concentrations were measured with a Condensation Particle Counter (CPC TSI 3775) in two different sampling configurations. For TPM characterisation, the CPC and Partector2 (Naneos) were installed in parallel; for nvPM a Catalytic Stripper (Catalytic Instruments), was installed upstream of the CPC to remove volatile compounds.

nvPM mass concentrations and CO_2 measurements were obtained on the raw sampling line. A Laser-Induced Incandescence method (LII-300, Artium), was used for nvPM mass concentrations (as per ICAO standard nvPM measurement), and CO_2 concentration levels

were obtained using two non-dispersive infrared analysers namely; An X-stream (Emerson) analyser that has high accuracy and a lower cost gas analyser LI-850 (LICOR).

Particle size distributions were quantified in both electrical mobility and aerodynamic space using, respectively, an SMPSTM (Scanning Mobility Particle Sizer™) comprised of a NanoDMA 3085A and a CPC 3775 (TSI), and a HR-ELPI+® (Dekati). In this case, the SMPSTM was installed on the diluted sample line; whereas the HR-ELPI+® was installed on the raw sampling line.

Intercomparisons of high fidelity and low cost-equipment was performed for both particle number and CO₂ gas concentration. CPC vs Partector2 (P2) for TPM number concentrations and X-stream vs LI-850 for CO₂ levels, with electrical mobility and aerodynamic diameters also compared.

RESULTS AND CONCLUSIONS

The PM physical characteristics of emissions at different engine power levels are consistent with results from other studies (Lobo et al, 2015; Stacey, 2019), and show good repeatability for the engines tested (Figure 2).

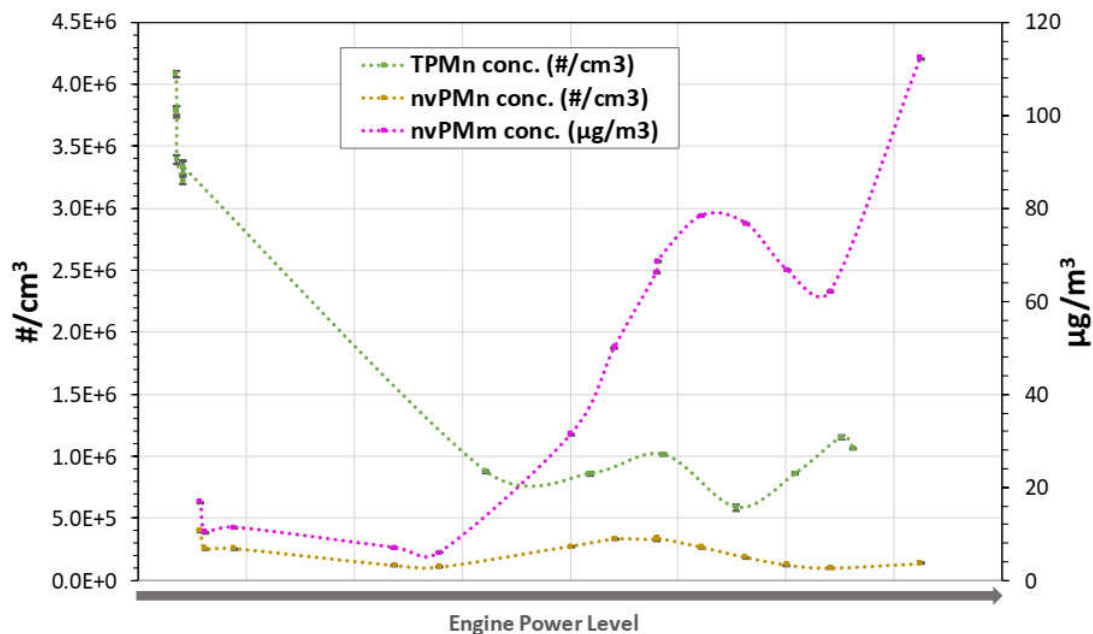


Figure 2. nvPM mass (pink), TPM (green) and nvPM (brown) number concentrations

In agreement with previous work, low engine power (combustor temperature) conditions are dominated by secondary organic aerosols –formed by the oxidation of emitted precursors (Kılıç *et al*, 2018)– result in high TPM number concentrations and low nvPM mass concentrations. This is indicated by a wide single mode particle size distribution with diameters peaking ~10 nm shown in both HR-ELPI+® and SMPS™ distributions (Figure 3). In these cases, this vPM mode dominates such that the nvPM mode distribution cannot be individually distinguished.

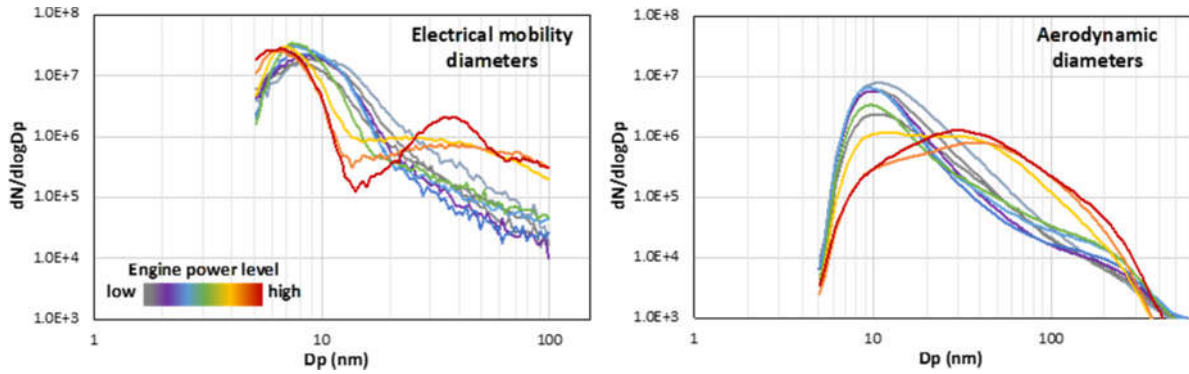


Figure 3. Electrical mobility (NanoDMA) and aerodynamic (HR-ELPI+) TPM size distributions.

As engine power level increases TPM number concentrations vary and particle size distributions become bimodal with a vPM nucleation mode around 6 nm, and an nvPM accumulation mode between 30-40 nm in agreement with nvPM distributions measured at engine exit. In accordance with literature, at higher engine power levels, high combustion efficiency results in low levels of organic compounds and gaseous precursors, exiting the engine, resulting in lower TPM number concentrations downstream in the evolved plume. In addition, formation of SOA is suppressed due to the higher exhaust velocities reducing the exhaust plume residence time before reaching the stack probe.

Results of the intercomparison between high-fidelity and low-cost equipment showed good. TPM number concentration data from CPC and P2, and CO₂ concentration data from X-Stream vs Li-Cor are shown in Figures 4 and 5 respectively.

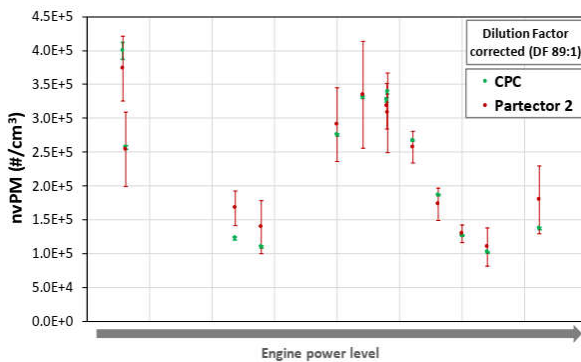


Figure 4. nvPM conc. with CPC & P2

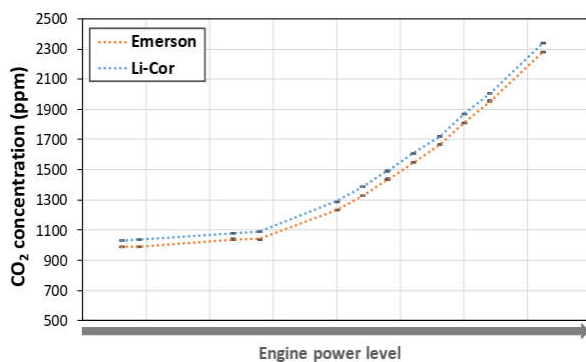


Figure 5. CO₂ conc. with Emerson & Li-Cor

For the TPM number concentration comparison, it was observed that both the CPC and P2 results follow the same trend across engine power levels, with measured concentrations typically within 20%. It is important to highlight that the signal noise variation (shown by the error bars) obtained with P2 is higher than those with the CPC, since the P2 pump is very small and cannot handle pulsations as well as a large pump like in a CPC. Furthermore, this is also due to the P2 is a nanoparticle detector able to measure number concentration in a range up to 1×10^6 #/cm³. However, in these tests the P2 was placed downstream of the dilutor and Catalytic Stripper, where the concentration levels are around $1 - 4 \times 10^3$ #/cm³ (averaged values), even reaching levels of 3×10^2 #/cm³ (instant values). These data are below ambient concentration (10^4 #/cm³). Consequently, the noise of these measurements has been increased, indicating that the P2 should be placed where particle concentration is greater than 1×10^3 #/cm³ (and below 1×10^6 #/cm³, because of its upper limit).

As expected, Figure 5 clearly shows that CO₂ concentration increases with engine power as consequence of a higher fuel flow rate, however the dilution rate in the stack, caused by the bypass and entrainment likely varies with power, hence this trend is not necessarily representative of engine exhaust values. Excellent repeatability is shown between the results

obtained with the high-fidelity sensor (Emerson) and the low-cost sensor (Li-Cor). The uncertainty is shown to be systematic, consistent with an offset rather than a random source. In both cases the low fidelity measurement equipment has been shown to provide reasonable measurements compared to high fidelity equipment. To assess robust performance, longer term datasets are required across different systems and environments.

ACKNOWLEDGEMENTS

This project has received funding from the European Union's Horizon 2020 Research and Innovation Programme under Grant Agreement No 814801.

REFERENCES

- Archilla, V., et al, 2019. AVIATOR - Assessing aViation emission Impact on local Air quality at airports: TOwards Regulation. MATEC Web of Conferences, Vol. 304, 02023.
- Lobo, P., et al 2015. PM emissions measurements of in-service commercial aircraft engines during the Delta-Atlanta Hartsfield Study. Atmospheric Environment. Vol. 104, pp. 237-245.
- Kılıç, et al, 2018. Identification of secondary aerosol precursors emitted by an aircraft turbofan. Atmospheric Chemistry and Physics. Vol. 18, pp. 7379–7391.
- Stacey, B., 2019. Measurement of ultrafine particles at airports: A review. Atmospheric Environment. Vol. 198, pp. 463-477.

AIR QUALITY AT FRANKFURT AIRPORT – WHAT CAN WE LEARN FROM COLLOCATED IAGOS AIRBORNE AND FRAPORT SURFACE MEASUREMENTS

J. Glaves¹, D. Raper¹, F. Berkes², P. Nedelec³ & A. Petzold²

¹ Manchester Metropolitan University, Manchester, UK

² Forschungszentrum Jülich, Institut für Energie- und Klimaforschung – Troposphäre, Jülich, Germany

³ CNRS Laboratoire d'Aérodynamique, and Université Paul Sabatier Toulouse III, Toulouse, France

Abstract. Local air quality near airports and the contribution of air traffic to air quality is gaining increasing attention caused by concerns about adverse health effects of the emissions and the impact of capacity extensions on the air quality close to the airports. Currently, observational data originate from surface-based monitoring stations. Gaussian dispersion models use these observations and gain necessary information on the vertical structure of the atmosphere and respective distributions of trace species from weather data.

In our approach we combine a 6 months record of surface-based NO_x, O₃ and CO observations by FRAPORT AG on the area of Frankfurt airport in 2016 (March – August) with the observations of the same species by IAGOS-CORE aircraft during their ascent from and descent into the airport.

The results show an excellent continuation of IAGOS vertical profiles for NO_x, O₃ and CO by the surface-based observations. Analysing the vertical profiles of the variability of data and the respective variability of data measured near ground, we can identify one regime of the surface measurements which is characterised by the median CO volume mixing ratio from the upper and mixed planetary boundary layer (regional background), and one regime characterised by the polluted lower planetary boundary layer (local pollution).

Starting from this observation we will discuss one potential method of quantifying the aviation contribution to local air quality near airports.

CFD AND AEROSOL DYNAMICS BOX-MODEL TO IMPROVE DISPERSION MODELS

E. Montreuil¹, S. Matthes², F. Garnier³, V. Archilla-Prat⁴, W. Ghedhaifi¹, M. Righi² & E. Terrenoire¹

¹ Multi-Physics Department for Energetics, ONERA, France, emmanuel.montreuil@onera.fr

² Institute of Atmospheric Physic, DLR, Germany, Sigrun.Matthes@dlr.de

³ AEROT-ETS, ETS, Canada, Francois.Garnier@etsmtl.ca

⁴ Turbojet Engine Test Centre, INTA, Spain, archillapv@inta.es

Abstract. To cope with the environmental requirements and the continuous rise of the air traffic, meeting the air quality objectives is becoming a high constraint for the development of the air transport sector. The long-term objective is to answer to the main concern expressed by the ICAO on air pollution issues generated by the air transport sector on the local air quality in the airport area. In the framework of the EU Horizon2020 project AVIATOR (2019 – 2022, see aviatorproject.eu), the program proposed here is aimed at developing an innovative methodology and tools to increase the capability of prediction for the standard dispersion modelling tools in order to better take into account pollutant sources at micro-scales. At this stage, three bricks have been identified:

- The Intra-engine model is a 0-D/1-D gas-turbine model, taking into account combustor, turbine, and nozzles, at different operating conditions, with a kerosene-kinetics scheme, including a soot kinetics model.
- The MADE3 Box-model is applied to investigate the evolution of particle number concentration, size distribution and composition in the aging plume such as condensation on volatile and non-volatile particles, formation of new volatile UFP from gaseous precursors, particle-particle interactions due to coagulation or dilution by mixing with background air.
- The CFD model CEDRE, a compressible Navier-Stokes solver with multi-species, is applied to model the aircraft and its exhaust properties. CFD allows to explicitly model the interaction of the moving aircraft frame and of the emitted exhaust with the ambient flow field but also give plume details such as temperature, pressure, velocity and gas-phase chemistry.

Those models are applied in order to investigate the microphysics and chemistry of pollutant formation and evolution (with emphasis on total PM) from the exit of the main engine and APU and to describe the physical dynamics of the main engine and APU exhaust plume to move towards the development of validated parameterisations suitable for future dispersion modelling and regulatory standard setting. The work is supported by a various measurement campaigns carried out within AVIATOR (test cell, on-wing, and airport). This presentation provides an introduction to MADE3, Intra-engine model and CEDRE and the modelling efforts carried out in AVIATOR.

Keywords: Atmospheric dispersion, dispersion model, aerosol, CFD

ACKNOWLEDGEMENTS

This project has received funding from the European Union's Horizon 2020 research and innovation programme under grant agreement No 814801.

REFERENCES

- Bisson J., P. Seers, M. Huegel and F. Garnier, 2016. *Numerical Prediction of Gaseous Aerosol Precursors and Particles in an Aircraft Engine*. Journal of propulsion, Vol. 32, No. 4, DOI: 10.2514/1.B35943.
- Kaiser J. C., J. Hendricks, M. Righi, P. Jöckel, H. Tost, K. Kandler, B. Weinzierl, D. Sauer, K. Heimerl, J. P. Schwarz, A. E. Perring, and T. Popp, 2019. *Global aerosol modeling with MADE3 (v3.0) in EMAC (based on v2.53): model description and evaluation*. Geosci. Model Dev., Vol. pp. 12, 541–579, <https://doi.org/10.5194/gmd-12-541-2019>
- Montreuil E., W. Ghedaifi, V. Chmielarski, F. Vuillot, F. Gand and A. Loseille, 2018. *Numerical simulation of contrail formation on the common research model wing/body/engine configuration*. In 10th Space and Atmospheric Environment AIAA conference, Atlanta, USA.

AIRPORT AIR QUALITY – EVOLUTION AND STATE-OF-THE-ART OF METHODOLOGIES AND POSSIBLE IMPROVEMENTS.

Violaine Huck¹, Ted Elliff^{1*}, Ayce Celikel¹ & Frédéric Murzyn²

¹ ENVISA, 71 Rue des Desnouettes, Paris, Ile-de-France 75015, France

² ESTACA West Campus, Rue Georges Charpak, Laval 53000, France

* Corresponding author (Email: ted.elliff@env-isa.com)

Abstract. The increase in air traffic over the past years, the growth expectations for the future and the impact of aviation on air quality have become critical environmental issues. Particles and gaseous pollutants emitted by aircraft engines during take-off, cruise and landing phases contribute to climate change and worsening the local air quality (LAQ) around airports. In fact, with the assumed continued growth of air transport, despite the lowering of aircraft emissions associated with the improvements of engine technologies, Particulate Matter (PM), which are one of the most hazardous emissions for health, will continue to create a serious environmental issue. Therefore, PM emissions characterization and dispersion need a special focus, together with predictive numerical models, to direct effective concrete actions and assist airports in managing LAQ. For modelling purposes, an accurate Emissions Index (EI) is required, which can characterise non-volatile PM (nvPM).

Some uncertainties are still to be assessed by measurement campaigns. RAPTOR and AVIATOR projects are addressing these items. The RAPTOR project will also investigate the contribution of measurements to the improvement of existing air quality models. Funded through CleanSky 2 research program, it also aims at improving existing or developing new methods for modelling. Firstly, this paper describes the state-of-the-start of existing methodologies and standards (including regulatory aspects) for assessing aircraft PM emissions. In the second section, existing knowledge of PM characterization for airports will be discussed, with a focus on the latest advances in modelling aircraft PM emissions. A review of critical parameters in numerical models as well as suggestions to improve their accuracy are presented. Finally, some recommendations are given on in situ test measurements that could help improve future EIs, encouraging more robust modelling that will help mitigate the future impact of a growing sector.

Keywords: aviation, airport, air quality, local impact, health effects, methodologies, predictive model, state-of-the-art, Particulate Matter

STATE-OF-THE-ART ON AIRCRAFT PM EMISSIONS

Particulate Matter (PM) is defined as “a solid, a liquid or a solid phase coated with liquid (...) [and] does not necessarily distinguish between solid and liquid phase” (F.Hemond and J.Fechner, 2015). Its chemical composition depends on its source while its phase is often unknown (F.Hemond and J.Fechner, 2015). Though emitted particles can have any shape and asperities, they are often assimilated to a perfectly round particle, characterized by its aerodynamic diameter. PM is a classification based on this physical property rather than a chemical property. PM₁₀ and PM_{2.5} stand for PM with a diameter of respectively 10µm and less, and 2.5µm and less. Some papers also refer to the coarse fraction, which corresponds to PM with an aerodynamic diameter included between 2.5µm and 10µm. PM is divided into two major categories: non-volatile PM (nvPM) and volatile PM (vPM). The former one corresponds to the majority of an engine’s PM direct emission. The size of the corresponding particles ranges from 0.015µm to 0.06µm (Rindlisbacher and Jacob, 2016). nvPM is mostly composed of black carbon and ultrafine soot (Rindlisbacher and Jacob, 2016). Most of the vPMs of a plume engine are the results of transformations of other gaseous pollutants are emitted from the nozzle of the engine into the ambient air. Their composition and phase are more ambiguous as they depend on several parameters, which are not yet fully understood (Rindlisbacher and Jacob, 2016). vPM may also undergo further transformations as it mixes with ambient air. Quite the contrary, as nvPMs are mixed with the ambient air from the engine nozzle, their shape mass and number does not change (Rindlisbacher and Jacob, 2016).

To prevent and mitigate the health impact of PM, aircraft and airport’s air quality are subjected to stringencies and standards from the World Health Organization (WHO), the

International Civil Aviation Organization (ICAO) and in Europe, the European Union (EU). ICAO recommends standards and provides guidelines for nvPM engine emissions while the WHO regularly publishes recommendations for PM concentrations' limit values in the ambient air. EU, as a policymaker, provides directives on Ambient Air Quality, that have to be implemented by all member states.

In 2006, the third edition of Air Quality Guidelines distinguishes for the first time indoor and outdoor air quality (WHO, 2006). This report recommends to increase the stringency for both PM_{2.5} and PM₁₀. For PM₁₀, WHO recommends not to exceed 20µg/m³ on a 1-year averaged concentration and 50µg/m³ on a 24-hour average. For PM_{2.5}, the corresponding values are 10µg/m³ and 25µg/m³, respectively. WHO warns that these concentrations are not a guarantee of safety for health for all the population and adds explicitly "the standard-setting process needs to aim at achieving the lowest concentrations possible in the context of local constraints, capabilities and public health priorities" (WHO, 2006).

Accordingly, ICAO engine emission regulation is based on (measured) ground level emissions, represented by different engine thrust conditions through the Landing-Take-off cycle (LTO). In 1981, ICAO adopts its "first smoke, fuel venting and gaseous emissions standards for turbojet and turbofan" (Rindlisbacher and Jacob, 2016), that is the Smoke Number (SN). SN is dimensionless and measured from "the loss of reflectance of a filter used to trap smoke particle from a prescribed mass of exhaust per unit area of filter" (Rindlisbacher and Jacob, 2016). This is done for the four settings of the LTO cycle (taxiing, take-off, idle, landing). SN does not allow the assessment of PM concentration without assuming certain hypotheses. In 1983, the Committee on Aviation Environmental Protection (CAEP) was established with the objective to develop and maintain the international standards for aircraft noise, aeroplane CO₂ emissions, fuel venting and aircraft engine emissions: nitrogen oxides (NO_x), unburned hydrocarbons (HC), carbon monoxide (CO), smoke and non-volatile particulate matter (nvPM). In 2013, CAEP endorsed the planification of a nvPM certification for turbofan engine emissions of rated thrust larger than 26.7kN. In 2016, it ratifies nvPM certification (ICAO, 2017). Nevertheless, it did not introduce more stringency as it is merely an equivalent of the actual SN certification in terms of nvPM Emissions Indices (EIs). From this point onward (at the latest, 1st January 2020), manufacturers must report for new engines or in-production engines additional information such as fuel flow at each thrust setting of the LTO cycle, nvPM mass and EI numbers for the four LTO points, maximum nvPM EI (in mass and number) and maximum nvPM mass concentration.

In 2019, CAEP announced the end of the SN standard applicability from the 1st January 2023 (except for small engines with rated thrust below 27.6kN) and introduced new stringencies for nvPM emissions. The data available from the previous CAEP standard (2016) allowed the definition of an LTO-based nvPM mass and number metric system. The new standard will apply to new type and in-production engines with rated thrust greater than 26.7kN from 1st January 2023. It introduces a new stringency with respect to the previous standard. There are two different limits for in-production and new engines types (in mass and number) with respect of the rated thrust. In this context, several working groups have been mandated to investigate the possible improvements of PM measurements and assessment. This is the core of AVIATOR and RAPTOR projects. Furthermore, they aim at improving modelling to support and assist the different actors in agreement with CAEP (2019) stringencies on one hand and preparing for the next and new CAEP stringencies on the other hand. New test measurements are led by several actors to better assess relationship between PM emissions and fuel composition (sulphur and aromatics especially), as well as engine technologies, among others.

MODELLING AIRCRAFT PM EMISSIONS

Predicting PM concentration from aircraft engines in the ambient air is particularly complex because it involves the inter-relation between microphysical properties, mixing processes and chemical reactions of the engine's exhaust plume with the ambient air. Various

parameters are involved such as meteorological data, topology and characteristics of the surrounding environment (roughness, obstacles...), unsteadiness (turbulence), buoyancy, deposition, characteristics of sources (localisation, number, strength...). Furthermore, chemical reactions depend also on the background composition (ICAO, 2016). Pollutants emitted by the engine in their final form are called primary pollutants. They encompass Volatile Organic Components (VOC), nitrogen oxides (NO_x), PM, sulphur oxides (SO_x). When released in the atmosphere, some pollutants undergo a transformation (chemical, condensation or coagulation) and form other species. Some secondary pollutants are among other, O₃, PM... (ICAO, 2016). To address the need for a complete air quality modelling solution, different airport air quality models have been developed such as AEDT/EDMS¹ from the Federal Aviation Administration, LASPORT, ADMS and OPENLAQS (Eurocontrol). EDMS, ADMS and AEDT are based on an advanced Gaussian Plume model while LASPORT² (Janicke et al., 2007) and OPEN-ALAQS is based on a Lagrangian dispersion model, though OPEN-ALQS³ allows to switch to Gaussian as well. As dispersion is one of the main aspects of PM emission modelling, existing dispersion models (within these airport air quality models) are further detailed.

Gaussian Plume models in three dimensions the concentration downwind of the source, until the plume reaches the ground (F.Hemond and J.Fechner, 2015). For an expanded 3D plume, the horizontal dispersion is modelled as a function of source-distance and stability class, using eddy diffusivity. This model is based on mass conservation. It is the simplest and most widely used dispersion model (Hoinaski et al., 2016). It assumes a continuous emissions source, steadiness for the source, steady meteorological conditions, 3D dispersion, Gaussian distribution of pollutant, unlimited vertical dispersion upward and ground limited downward (Davis et al., 2008; F.Hemond and J.Fechner, 2015). Concentration fields are modelled using Gaussian Probability Density Functions (PDF) for both lateral and vertical axis (Davis et al., 2008; ICAO, 2016). PDFs reach a maximum value at the centre of the plume and flatten as the distance from the source increases. As pollutants may meet the ground at some point, the PDFs are different for the horizontal (spanwise) and vertical axis. The PDFs on the vertical and spanwise directions are characterized by their standard deviation (σ_y and σ_z , respectively), which are determined empirically from test measurements. Standard deviation also depends on the stability class (stable, neutral or unstable) of the atmosphere (ICAO, 2016), giving indications on how turbulent the flow is. They also characterize the vertical motions as hindered (stable), neutral or enhanced (unstable) (ICAO, 2016). The meteorological conditions play also a key role (wind speed, insolation, or cloudiness) (F.Hemond and J.Fechner, 2015). Standard deviation values are usually taken from empirical tables that consider both the distance to the source and the stability class.

It must be noted that Gaussian Plume model is only reliable for 10-minutes or longer, averaged concentration whereas the influence of averaging time on the concentration level remains unclear (Hoinaski et al., 2016). In addition, this model is usually used to assess single stationary source concentrations. However, its use has also been extended to multi-source areas. Concentrations are then being estimated independently for all single sources, in various meteorological configurations. (Davis et al., 2008; ICAO, 2016). Consequently, in this simple form, flue gases from each source do not interact with one another. This is one of the drawback of this type of model.

The EDMS/AEDT dispersion model AERMOD⁴ uses an advance Gaussian Plume model. It also considers wet and dry depositions and multiple sources, complementary to the Gaussian plume model (Davis et al., 2008). The main advantages of this model are the low level of data required from the user and its low CPU consumption at the expense of the accuracy for complex topologies (Bluett et al., 2004). Only maximum concentrations levels of

¹ Aviation Environmental Design Tool / Emission and Dispersion Modeling System

² LASAT for Airports

³ Airport Local Air Quality Studies

⁴ American Meteorological Society

pollutants or “worst-case scenario”(ICAO, 2016) can be assess (Bluett et al., 2004). More recent dispersion models use a bi-Gaussian distribution for the vertical axis to get a more accurate description of the vertical mixing process (ICAO, 2016). To address the complex topology issue, ADMS uses the FLOWSTAR⁵ model that can simulate flow field and turbulences over complex topologies⁶.

Lagrangian dispersion models suppose a moving referential (“particle” movement). Instead of particles, one considers a “puff” or a small volume of contaminated air. A predetermined number of “particles” or puffs of contaminated air are tracked from the engine nozzle exit plane during a specific timeframe. LASPORT uses LASAT⁷ Lagrangian model. The advantage of the Lagrangian model is that unsteady dispersion configuration is possible (Janicke et al., 2007). Zhang (2007) presented a 1D Lagrangian model based on the 0D Lagrangian model of Kärcher (1998), to study PM formation and evolution in a near-field Aircraft Plume. His model is semi-empirical as initial properties of the engine exhaust plume comes from test measurements. The plume’s mixing profiles have been modelled using a 2D Computational Fluid Dynamics simulation (Eulerian description), Reynolds Averaged Navier Stockes (RANS), from a commercial software. His model can track PM on a centreline trajectory up to 1km from the engine exit plane, and at several planes’ radial location. This model uses 35 chemical species and 181 chemical reaction for NO_x and SO_x. His model considers binary homogeneous nucleation of sulphuric acid and water, coagulation of liquid embryos and droplets and microphysical processes on soot surface.

RECOMMENDATIONS TO IMPROVE FUTURE EIS

As available computational power is increasing and Computational Fluid Dynamics (CFD) tools are developed, new dispersion models using CFD for air quality modelling are being developed. Paoli et al (2008) used 3D Large Eddy Simulation (LES) and 25 000 trajectories from a jet exhaust coupled with a 0D physical model. Khou et al. (2016) simulated an entire 3D exhaust plume using 3D RANS simulation. Ghedhaifi et al. (2019) simulated an entire airport using 3D RANS compressible Navier-Stockes equations in the code CEDRE developed by ONERA⁸. Chemical reactions, meteorological data, background concentrations are also considered as inputs in the model. Additionally, predictions have been extended up to 8km from the airport with a spatial resolution of 1m (at most). CFD dispersion modelling seems to be promising for air quality modelling (Ghedhaifi et al., 2019).

However, estimated concentration can “never be more accurate than the input emissions estimates” (Davis et al., 2008). Developing and improving in-situ data collection of PM emissions will improve assessments of EIs. Literature reports a lack of knowledge or accurate data on two types of in situ test measurements: on one hand, engines emissions characterization depending on engine technology and fuel type and on the other hand transformations of precursors while it mixes in the ambient air.

Uncertainties concerning some aspects of the three major processes (mixing, physical and chemical) involved in air quality modelling have been reported (Davis et al., 2008; ICAO, 2016), such as turbulence (Al Jubori, 2016), plume’s physical properties (Khou et al., 2017), role of organic species in PM evolution (Wong et al., 2015) and freezing properties of fresh exhaust soot (Kärcher et al., 1998).

Regarding engine’s technology, Lobo et al. (2015) showed the influence of the engine type on the exhaust jet aerosol formation, while the influence of the bypass ratio and combustor technology on the exhaust jet aerosol formation have been reported by Yu et al. (2017) and Liu et al. (2017), respectively. Studies have found that nvPM emissions are sensitive to fuel’s sulphur and aromatic concentrations. Test measurements show that using a fuel containing

⁵ <https://www.cerc.co.uk/environmental-software/ADMS-model.html>

⁶ <https://www.cerc.co.uk/environmental-software/FLOWSTAR-Energy-model.html>

⁷ Lagrangian Simulation of Aerosol-Transport

⁸ Office national d’étude et de recherches aérospatiales

less sulphur and aromatics, i.e. species organic species, leads to exhaust plumes with less nvPM (Brem et al., 2015; Moore et al., 2017; Starik et al., 2018)

REFERENCES

- Al Jubori, M. (2016). *ATMOSPHERIC MODELLING*. Gent University.
- Bluett, J., Gimson, N., Fisher, G., Heydenrych, C., Freeman, T., and Godfrey, J. (2004). Good practice guide for atmospheric dispersion modelling. In 522.
- Brem, B. T., Durdina, L., Siegerist, F., Beyerle, P., Bruderer, K., Rindlisbacher, T., Rocci-Denis, S., Andac, M. G., Zelina, J., Penanhoat, O., and Wang, J. (2015). Effects of Fuel Aromatic Content on Nonvolatile Particulate Emissions of an In-Production Aircraft Gas Turbine. *Environmental Science and Technology*, 49(22), 13149–13157. <https://doi.org/https://doi.org/10.1021/acs.est.5b04167>
- Davis, N., He, K., Lents, J., Ossess, M., Tolvett, S., and Walsh, M. (2008). *Foundation Course on Air Quality Management in Asi* (G. Haq and D. Schwela (eds.); Issue March 2008). Stockholm Environment Institute.
- F.Hemond, and J.Fechner, E. (2015). The Atmosphere. In Elsevier (Ed.), *Chemical Fate and Transport in the Environment* (third). <https://doi.org/10.1016/B978-0-12-398256-8.00004-9>
- Ghedhaifi, W., Desprez, L., Montreuil, E., Terrenoire, E., Henry-Iheureux, T., Garnier, F., Ghedhaifi, W., Desprez, L., Montreuil, E., Terrenoire, E., and Henry-, T. (2019). 3D Simulation of aircraft emissions dispersion in the CAEPport area by tracking aircraft as mobile sources To cite this version: HAL Id: hal-02470816 Simulation of aircraft emissions dispersion in the CAEPport area by tracking aircraft as mobile sources. *ISABE*.
- Hoinaski, L., Franco, D., and de Melo Lisboa, H. (2016). Comparison of plume lateral dispersion coefficients schemes: Effect of averaging time. *Atmospheric Pollution Research*, 7(1), 134–141. <https://doi.org/10.1016/j.apr.2015.08.004>
- ICAO. (2016). Airport air quality Manual. In *Air and Space Europe* (Issues 1–2). [https://doi.org/10.1016/s1290-0958\(01\)90012-7](https://doi.org/10.1016/s1290-0958(01)90012-7)
- ICAO. (2017). *Annex 16 : Environmental Protection: Vol. II* (Fourth, Issue January).
- Janicke, U., Fleuti, E., and Fuller, I. (2007). Lasport - A model system for airport-related source systems based on a lagrangian particle model. *Proceedings of the 11th International Conference on Harmonisation within Atmospheric Dispersion Modelling for Regulatory Purposes, HARMO 2007*, 2, 352–356.
- Kärcher, B., Busen, R., Petzold, A., Schröder, F. P., Schumann, U., and Jensen, E. J. (1998). Physicochemistry of aircraft-generated liquid aerosols, soot, and ice particles 2. Comparison with observations and sensitivity studies. *Journal of Geophysical Research Atmospheres*, 103(D14), 17129–17147. <https://doi.org/10.1029/98JD01045>
- Khou, J. C., Ghedhaïfi, W., Vancassel, X., Montreuil, E., and Garnier, F. (2017). CFD simulation of contrail formation in the near field of a commercial aircraft: Effect of fuel sulphur content. *Meteorologische Zeitschrift*, 26(6), 585–596. <https://doi.org/10.1127/metz/2016/0761>
- Liu, Y., Sun, X., Sethi, V., Nalianda, D., Li, Y.-G., and Wang, L. (2017). Review of modern low emissions combustion technologies for aero gas turbine engines. *Progress in Aerospace Sciences*, 94, 12–45.
- Lobo, P., Durdina, L., Smallwood, G. J., Rindlisbacher, T., Siegerist, F., Black, E. A., Yu, Z., Mensah, A. A., Hagen, D. E., Miake-Lye, R. C., Thomson, K. A., Brem, B. T., Corbin, J. C., Abegglen, M., Sierau, B., Whitefield, P. D., and Wang, J. (2015). Measurement of aircraft engine non-volatile PM emissions: Results of the Aviation-Particle Regulatory Instrumentation Demonstration Experiment (A-PRIDE) 4 campaign. *Aerosol Science and Technology*, 49(7), 472–484. <https://doi.org/10.1080/02786826.2015.1047012>
- Moore, R. H., Shook, M. A., Ziemba, L. D., DiGangi, J. P., Winstead, E. L., Rauch, B., Jurkat, T., Thornhill, K. L., Crosbie, E. C., Robinson, C., Shingler, T. J., and Anderson, B. E. (2017). Data Descriptor: Take-off engine particle emission indices for in-service aircraft at Los Angeles International Airport. *Scientific Data*, 4, 1–15. <https://doi.org/10.1038/sdata.2017.198>

- Rindlisbacher, T., and Jacob, S. D. (2016). *New Particulate Matter Standard for Aircraft Gas Turbine Engines*.
- Starik, A. M., Savel'ev, A. M., Favorskii, O. N., and Titova, N. S. (2018). Analysis of emission characteristics of gas turbine engines with some alternative fuels. *International Journal of Green Energy*, 15(3), 161–168. <https://doi.org/10.1080/15435075.2017.1324790>
- WHO. (2006). *WHO Air quality guidelines for particulate matter, ozone, nitrogen dioxide and sulphur dioxide: Global update 2005*. 1–21. [https://doi.org/10.1016/0004-6981\(88\)90109-6](https://doi.org/10.1016/0004-6981(88)90109-6)
- Wong, H. W., Jun, M., Peck, J., Waitz, I. A., and Miake-Lye, R. C. (2015). Roles of Organic Emissions in the Formation of Near Field Aircraft-Emitted Volatile Particulate Matter: A Kinetic Microphysical Modeling Study. *Journal of Engineering for Gas Turbines and Power*, 137(7). <https://doi.org/10.1115/1.4029366>
- Yu, Z., S.Liscinsky, D., C.Fortner, E., Yacovitch, T. I., Croteau, P., C.Herndon, S., and Miake-Lye, R. C. (2017). Evaluation of PM emissions from two in-service gas turbine general aviation aircraft engines. *Atmospheric Environment*, 160, 9–18.
- Zhang, J. (2007). *Study of Particulate Matter Formation and Evolution in Near-field Aircraft Plumes using a One-Dimensional Microphysical Model*. University of Michigan, Ann Arbor.

CHEMICAL CHARACTERIZATION OF ULTRAFINE PARTICLES NEAR FRANKFURT AIRPORT BY LIQUID CHROMATOGRAPHY – HIGH-RESOLUTION MASS SPECTROMETRY (UHPLC/HRMS)

Florian Ungeheuer¹, Diana Rose³, Dominik van Pinxteren², Florian Ditas³, Stefan Jacobi³, Hartmut Herrmann² & Alexander L. Vogel¹

¹*Institute for Atmospheric and Environmental Sciences, Goethe-University, Frankfurt, 60438, Germany*

²*Atmospheric Chemistry Department (ACD), Leibniz Institute for Tropospheric Research (TROPOS), Leipzig, 04318, Germany*

³*Department for Ambient Air Quality, Hessian Agency for Nature Conservation, Environment and Geology, Wiesbaden, 65203, Germany*

Abstract. We present the results from a chemical characterization study of ultrafine particles (UFP). Nano-MOUDI (MSP Model-115) aluminium-filter samples were collected at an air quality monitoring station nearby the Frankfurt airport, where particle size distribution measurements showed number concentrations up to $1 \cdot 10^5$ particles/cm³ for particles with a diameter <30 nm.

The solvent extracts of the UFP samples were measured using liquid-chromatography – Orbitrap high-resolution mass spectrometry (UHPLC/HRMS). More than 500 compounds were detected by nontarget-screening and for each size distribution stage (0.056-0.032 μm ; 0.032-0.018 μm ; 0.018-0.010 μm) molecular fingerprints (m/z vs retention time, Kroll-diagram, Van-Krevelen-diagram, Kendrick mass defect plot) were created to visualize the complex chemical composition.

By the use of fragmentation experiments, various compounds were identified that are considered as molecular markers for jet oil emissions, verified by the analysis of different jet engine oils. Quantification of these compounds was achieved by the use of the standard addition method and the exact standards.

Keywords: ultrafine particles, HPLC-HRMS/MS, non-target analysis, jet engine oil, tricresyl phosphate

INTRODUCTION

Ultrafine particles (UFP) receive increasing attention due to the fact that airports are suspected to be a major source of particles smaller than 100 nm (Yu et al., 2012; Yu et al., 2017; Fushimi et al., 2019). With increasing numbers of flight operations worldwide, aircraft emissions will become more and more relevant regarding the long-term development of local and global air pollution. Ultrafine particles can be transported over long distances towards urban areas (Hudda and Fruin, 2016), and although they are of very low mass, they can cause cell membrane damages, oxidative stress and lead to inflammatory reactions of lung cells (Jonsdottir et al., 2019).

Therefore, it is important to determine the chemical composition of UFPs near airports in order to identify their sources during airport operation, to assess further possible detrimental effects on human health, and finally, to mitigate their emission.

Here, we show the results from a chemical characterization study of UFP. Due to the low mass of nanoparticles the typical sampling and extraction methods need to be refined in order to characterize particles with diameters < 56 nm which requires the detection of low picogram levels of organic molecules.

METHODS

Nano-MOUDI (MSP Model-115) aluminium-filter samples were collected at an air quality monitoring station 4 km north of Frankfurt airport. This 13 stage impactor system is able to collect particles size resolved on the last three stages with a sampling flow rate of 0.6 m³/h. By variation of the sampling time different filter loadings were obtained. The Frankfurt airport is one of the biggest airports in Europe with more than 500,000 flight operations in 2018. Therefore this sampling station is representative for highly-frequented airports over the world which are providing most of the worldwide flight movements.

We used ultrahigh-performance liquid-chromatography (Thermo Scientific: Vanquish Flex) – electrospray ionization hyphenated with an Orbitrap high-resolution mass spectrometer (Thermo Scientific: Q Exactive Focus Hybrid-Quadrupol-Orbitrap) as a sensitive detector. The filter extraction method was developed towards very low amounts of solvent and without any pre-concentration step. We screened extracts of the UFP samples in positive and negative ionization mode.

More than 500 organic compounds were detected by a nontarget-screening approach and for each size distribution stage (0.056-0.032 μm ; 0.032-0.018 μm ; 0.018-0.010 μm) molecular fingerprints (m/z vs retention time, Kroll-diagram, Van-Krevelen-diagram, Kendrick mass defect plot) were created in order to visualize the complex chemical composition. Five different jet engine oils with a high market share of various brands were analyzed identically.

Results

By the use of fragmentation experiments a homologue series of pentaerythritol-esters, N-phenyl-1-naphthylamine, alkylated diphenyl amine and tricresyl phosphate were identified in the ambient UFP samples. The screening of the jet oils showed a matching pattern of the four major compounds which are also mentioned in the safety data sheets of jet lubrication oils (Fig.1). These compounds have been described as molecular markers for jet engine lubrication oil emissions, and are not present in vehicle lubrication oils (Fushimi et al., 2019).

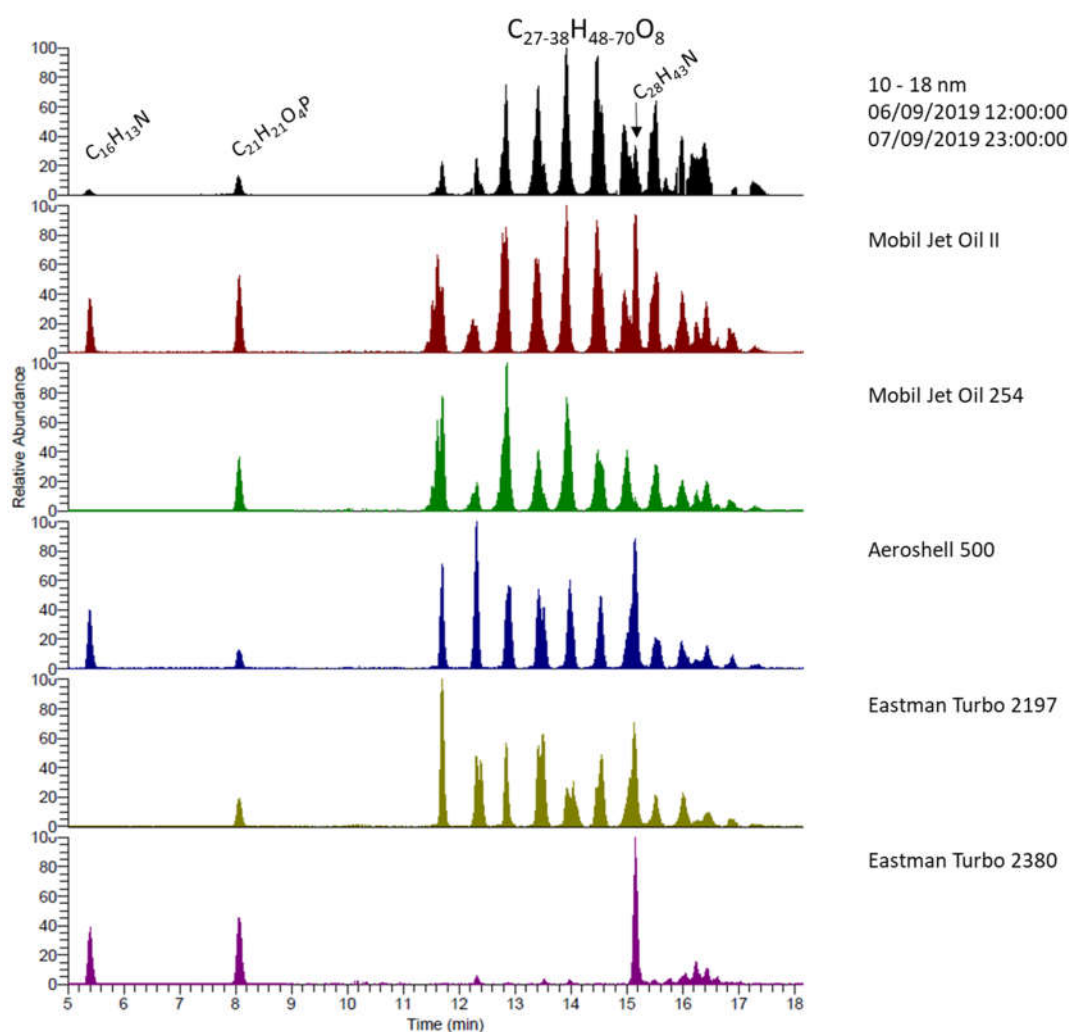


Figure 1. Extracted ion chromatograms (XIC) of an airport-sample (UFP size: 10-18 nm) and five different jet oils, showing a matching pattern of the four major compounds N-phenyl-1-naphthylamine ($\text{C}_{16}\text{H}_{13}\text{N}$), alkylated diphenyl amine ($\text{C}_{28}\text{H}_{43}\text{N}$), tricresyl phosphate ($\text{C}_{21}\text{H}_{21}\text{O}_4\text{P}$) and a homologue series of pentaerythritol-esters ($\text{C}_{27-38}\text{H}_{48-70}\text{O}_8$).

Nontarget-screening of the solvent extracts in the positive ionization mode led to more than 500 compounds whereas the negative ionization mode showed about 16 compounds. The contribution of jet engine oils to the chemical composition of UFP is mainly detectable in the positive ionization mode.

Quantification of these compounds was achieved by the use of a standard addition method with the exact standards N-phenyl-1-naphthylamine, tri-*o*-tolyl phosphate, pentaerythritol tetrahexanoate, Bis(4-(2,4,4-trimethylpentan-2-yl)phenyl)amine. This method was chosen to overcome matrix effects because of the strong tendency of tricresyl phosphate to adsorb on surfaces. By adding tri-*o*-tolyl phosphate to the original samples, a peak is formed besides the original peak signal of the sample (Fig. 2). This indicates that the tri-*ortho*-isomer of tricresyl phosphate cannot be detected in the airport samples. This is in accordance with the reduction of the *ortho*-isomer fraction of tricresyl phosphate used by the oil manufacturers (Winder and Balouet, 2002; Nola et al., 2008) and other research studies which were not able to identify *ortho*-isomers in various sample types (Solbu et al., 2010; Solbu et al., 2011).

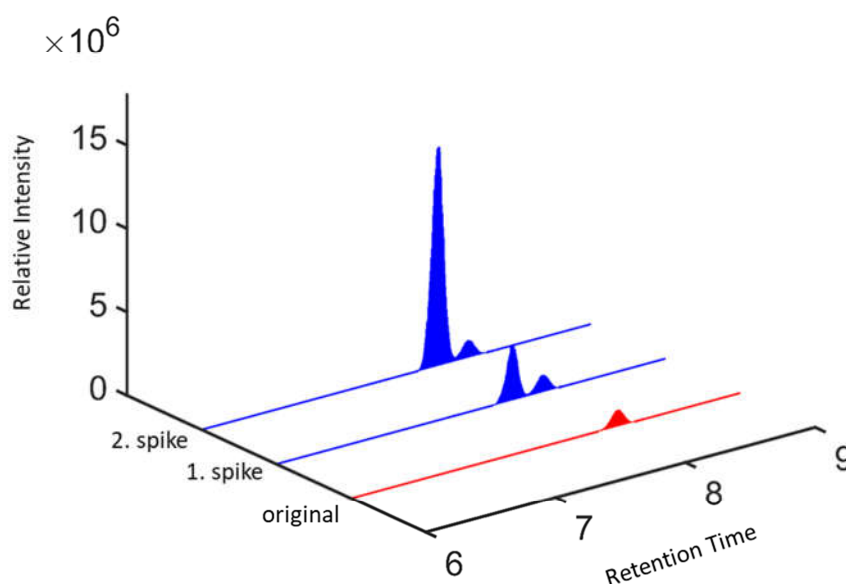


Figure 2. Development of the extracted ion chromatogram (XIC) of tricresyl phosphate ($[M+Na]^+$: 391.1069) during the quantification add-on steps. The added tri-*o*-tolyl phosphate forms a peak signal left of the original sample signal, which indicates no high *ortho*-isomer concentrations in the airport samples.

Further organophosphate compounds like triphenylphosphate can also be detected in UFP samples which can be attributed to hydraulic oils. Different studies already confirmed that these compounds can be found in cabin air because of the air induction throughout the jet engine turbines (Winder and Balouet, 2002; Solbu et al., 2011). Ground maintenance of aircrafts is also a possible source of organophosphates in the environment (Solbu et al., 2010).

Many studies examined possible health effects concerning the exposure of turbine and hydraulic oils to aircraft crews and ground staff. Typical stated symptoms are disorientation, headache, respiratory problems and weakness (van Netten and Leung, 2000; Winder and Balouet, 2001; Winder and Balouet, 2002). Therefore long-term exposure health effects regarding ultrafine particles containing jet engine oil constituents should be assessed.

The overall results show that jet oil emissions contribute to the chemical composition of particles < 30 nm nearby an airport. Further on, different filter materials will be tested in order

to determine the contribution of metals, organic carbon and inorganic salts to the overall mass balance of airport-located UFP.

REFERENCES

- Fushimi, A., Saitoh, K., Fujitani, Y., Takegawa, N. (2019) *Atmos. Chem. Phys.*, Identification of jet lubrication oil as a major component of aircraft exhaust nanoparticles 19, 6389–6399.
- Hudda, N., Fruin, S. A. (2016) *Environ. Sci. Technol.*, International Airport Impacts to Air Quality: Size and Related Properties of Large Increases in Ultrafine Particle Number Concentrations 50, 3362–3370.
- Jonsdottir, H. R., Delaval, M., Leni, Z., Keller, A., Brem, B. T., Siegerist, F., Schönenberger, D., Durdina, L., Elser, M., Burtscher, H., Liati, A., Geiser, M. (2019) *Commun Biol.*, Non-volatile particle emissions from aircraft turbine engines at ground-idle induce oxidative stress in bronchial cells 2, 90.
- Nola, G. D., Kibby, J., Mazurek, W. (2008) *J. Chromatogr. A*, Determination of ortho-cresyl phosphate isomers of tricresyl phosphate used in aircraft turbine engine oils by gas chromatography and mass spectrometry 1200, 211–216.
- Solbu, K., Daae, H. L., Thorud, S., Ellingsen, D. G., Lundanes, E., Molander, P. (2010) *J. Environ. Monit.*, Exposure to airborne organophosphates originating from hydraulic and turbine oils among aviation technicians and loaders 12, 2259–2268.
- Solbu, K., Daae, H. L., Olsen, R., Thorud, S., Ellingsen, D. G., Lindgren, T., Bakke, B., Lundanes, E., Molander, P. (2011) *J. Environ. Monit.*, Organophosphates in aircraft cabin and cockpit air—method development and measurements of contaminants 13, 1393–1403.
- van Netten, C., Leung, V. (2000) *Appl Occup Environ Hyg.*, Comparison of the Constituents of Two Jet Engine Lubricating Oils and Their Volatile Pyrolytic Degradation Products 15(3), 277–283.
- Winder, C., Balouet, J. H. (2001) *J Occup Health Safety*, Aircrew Exposure to Chemicals in Aircraft: Symptoms of Irritation and Toxicity 17, 471–483.
- Winder, C., Balouet, J. H. (2002) *Environ Res A*, The Toxicity of Commercial Jet Oils 89, 146–164.
- Yu, Z., Herndon, S. C., Ziemba, L. D., Timko, M. T., Liscinsky, D. S., Anderson, B. E., Miakel-Lye, R. C. (2012) *Environ. Sci. Technol.*, Identification of Lubrication Oil in the Particulate Matter Emissions from Engine Exhaust of In-Service Commercial Aircraft 46, 9630–9637.
- Yu, Z., Liscinsky, D. S., Fortner, E. C., Yacovitch, T. I., Croteau, P., Herndon, S. C., Miakel-Lye, R. C. (2017) *Atmospheric Environment*, Evaluation of PM emissions from two in-service gas turbine general aviation aircraft engines 160, 9–18.

AIR QUALITY STUDIES AT UKRAINIAN AIRPORTS

K. Synylo¹, K. Ulianova¹ & O. Zaporozhets¹

¹Faculty of Environmental Safety, Engineering and Technologies, National Aviation University, Ukraine, synyka@gmail.com, katia.bolot@gmail.com, zap@nau.edu.ua

Abstract. According to the State Aviation Service of Ukraine, the total passenger traffic of Ukrainian airports in 2018 increased by 25% compared to 2017. The problem of local/regional air pollution of airports is crucial for Ukraine in the context of the increasing approximation of residential areas to airports. The importance of this environmental problem is determined by the adverse impact of aircrafts on the air quality and health of residents of the nearby areas of the airport.

Monitoring of air pollution at airport is necessary for the development, justification and decision-making in the field of regulation of anthropogenic activities and the introduction of measures to reduce the negative effects on environment and public health. Monitoring should be based on the understanding the process of emission, transport and dispersion of air pollutants from an aircraft's engine during the landing-take-off cycle. The chemiluminescence and electrochemical method for the determination of the concentration of nitrogen oxides was considered. The system allows measuring the concentration in the exhaust in real conditions at a distance. The high time resolution (10 s) provides a measurement of the maximum concentrations generated in the jet from each aircraft engine of the aircraft.

The combination of systems for detecting NO_x and CO concentrations in the gas flow from an aircraft engine allows determine the emission indices under real operating conditions at the airport. The results of measurement campaign were used for validation of model.

The emission indices are the fundamental tool applied to make up the inventories and calculate taxes and fares for air pollution from aircraft. Moreover, the real EI is a representative value to get the real pattern of air pollution contributors at the airport as it differs from the indices obtained from the engine bench tests. In addition, the relative contribution is important to develop the strategy for the air pollution decrease.

Keywords: aircraft engine, emission index, airport air pollution, aircraft engine emissions

REFERENCES

ICAO Doc 9889 Airport Air Quality Manual, 2011

Ulianova, K. Synylo, K. Methods of emissions estimation from aircraft engines within the airport. International Scientific and Technical Conference 'Technology and Transport Infrastructure' (May 14-16, 2018) Part 2. Kharkiv. 2018. pp. 124-126.

MEASUREMENT OF ULTRAFINE PARTICLES AT PARIS AIRPORT

St. Verlhac¹

¹ Laboratory, Groupe ADP, France, stephane.verlhac@adp.fr

Abstract. Based on a systematic review of the scientific literature, the French Agency for Food, Environmental and Occupational Health & Safety (ANSES) has confirmed in July 2019 that ultrafine particles (UFP) emitted from road traffic, the burning of coal, petroleum products and biomass have a strong impact on health contributing to numerous diseases. In addition, ANSES stresses the need to pursue research efforts on the health effects of exposure to other sources of particles. Indeed, very few data are available especially those concerning the impact of airport activity. In this context, GROUPE ADP has undertaken exploring measurement of ultrafine particles during a 3-months campaign in 2019 in the axis of the north parallel runway at Paris - Charles de Gaulle Airport (CDG Airport) in France. The objective was to correlate aircraft movements (Landing, take-Off, Taxiing) with total particle number concentrations (PNC) and the size distribution of UFP. To achieve this objective, a scanning mobility particle sizer (SMPS) was deployed to compute the size distribution of aerosol over a size range from 7 to 100 nm and the total PNC was measured by a condensation particle counter (CPC). In addition, meteorological parameters, such as wind speed and direction, and regulated air pollutants and were also measured. This study revealed that the total PNC were higher downwind of the airport activities (10^5 particles/cm³). In addition, the measurements of particle number within the airport perimeter are dominated by the smallest particles (7-30 nm) that represent more than 75% of the total PNC between 6.00 a.m and 11.00 pm and are closely associated with aircraft traffic. Finally, this study has led GROUPE ADP starting 2020 to implement continuous monitoring of UFP on the main platforms (Charles de Gaulle, Orly, Le Bourget) using fixed stations for long term measurements with condensation particle counters.

Keywords: Ultrafine particles, SMPS, CPC, Paris

LOW-COST SENSOR DEVELOPMENT AS PART OF THE AVIATOR PROJECT

D. Kilic¹, P.I. Williams^{2,3}, V. Archilla-Prat⁴, D. Raper⁵ & S. Lopez⁶

¹ The University of Manchester, Manchester, UK, dogushan.kilic@manchester.ac.uk

² The University of Manchester, Manchester, UK, paul.i.williams@manchester.ac.uk

³ National Centre for Atmospheric Science, Manchester, UK paul.i.williams@manchester.ac.uk

⁴ Instituto Nacional de Técnica Aeroespacial, Madrid, Spain, archillapv@inta.es

⁵ Manchester Metropolitan University, UK, D.w.Raper@mmu.ac.uk

⁶ Ramem Research and Development, Madrid, Spain, slopez@ioner.net

Abstract. Emissions from aircraft have adverse effects on the air quality in and around airports, contributing to public health concerns within neighbouring communities. AVIATOR (Assessing aViation emission Impact on local Air quality at airports: TOwards Regulation) will adopt a multi-level measurement, modelling and assessment approach to develop an improved description and quantification of the relevant aircraft engine emissions, and their impact on air quality under different climatic conditions. Engine particulate and gaseous emissions in the INTA test cell and on-wing from an in-service aircraft will be measured to determine pollutant plume evolution from the engine and APU exhaust. This will provide an enhanced understanding of primary emitted pollutants, specifically the nvPM and vPM (down to 10nm), and the scalability between the regulatory test cell and real environments. AVIATOR will develop and deploy across multiple airports, a proof-of-concept low cost sensor (LCS) network for the monitoring of UFP, PM and gaseous species such as NO_x and SO_x, across airport and surrounding communities. This presentation will outline the goals of the project and the pathways to policy, the design for the new proof-of-concept LCS and recent data taken from the INTA test cell in Spain.

Keywords: Low Cost Sensor, aviation, AVIATOR, aircraft engine

ACKNOWLEDGEMENTS

This project has received funding from the European Union's Horizon 2020 research and innovation programme under grant agreement No 814801

IMPACT OF PRESENT AND FUTURE AIRCRAFT EMISSIONS ON ATMOSPHERIC COMPOSITION AND RADIATIVE FORCING OF CLIMATE

E. Terrenoire¹ & D. Hauglustaine²

¹ ONERA – DMPE – Université Paris Saclay, France, etienne.terrenoire@onera.fr

² LSCE – IPSL – Université Paris Saclay, France, didier.hauglustaine@lsce.ipsl.fr

Abstract. Depending on the nature and the location of the emitted chemical agents, aircrafts contribute to warm or cool the climate. The chemical perturbation and the associated radiative forcing of carbon dioxide, ozone, methane, soot carbon (BC), sulphates, nitrates and organic carbon (OC) due to aircraft emissions have been calculated using five different global emission inventories using a carbon cycle compact climate change model and the climate-chemistry global model LMDz-ORCH-INCA. We found that the impact of the aviation CO₂ emissions ranges from $45 \pm 2 \text{ mW/m}^2$ (2.5 % of the total anthropogenic warming) for an ambitious mitigation strategy scenario (Factor 2) to $78 \pm 4 \text{ mW/m}^2$ (2.5 % of the total anthropogenic warming) for the least ambitious mitigation scenario of the study (ICAO based). Apart from CO₂, the total radiative forcing related to aviation and modifications of gases and aerosols calculated in this work is negative and varies from -2.5 mW/m^2 for the present scenario REACT4C (-3.6 mW/m^2 in the case QUANTIFY_2000).

Keywords: present and future aircraft emission, short-term climate impact, global climate model

INTRODUCTION

Depending on the nature and the location of the emitted chemical agents, aircrafts contribute to warm or cool the climate. Three other major effect should be distinguished: the short-term effects (a few weeks at maximum), the long-term effects (from one year to more than 100 years) and the cloud type effects. In this paper, we will present global long-term CO₂ and short-term impacts for present and future aircraft emissions that are predominantly related to the injection of nitrogen dioxides (NO_x=NO+NO₂), water (H₂O) and non-methane hydrocarbon (NMHC) by planes. They perturb the tropospheric and lower stratospheric repartitions of ozone (O₃), methane (CH₄), water (H₂O), sulphur dioxide (SO₂), sulphate (SO₄) and nitrate (NO₃). Other short-term effects are linked with the direct injection of aerosols such as back carbon (BC), organic carbon (OC) and sulphate (SO₄). Other effects that will be evaluated include the long-term effect link to CH₄ concentration decrease due to OH enhancement from the NO_x aircraft emissions. This paper aim to bring an updated estimation of the climate impact of those species based on leading-edge carbon cycle compact climate model and climate-chemistry global model LMDz-ORCH-INCA using multi scenarios analysis.

AIRCRAFT EMISSIONS INVENTORIES

Emission for present comes from the inventory Reducing Emissions from Aviation by Changing Trajectories for the benefit of Climate project (REACT4C) (Sovde et al., 2014). The inventory had to be adapted to our simulations as some species were not available in the original version of the database. First, for NO_x (assimilated as NO₂) and BC the data are taken directly from the original inventory. Second, for H₂O, CO and HC the data comes from the AERO2K project (Eyers et al, 2005). Third, for OC, SO₂ and SO₄, we use the mean emission factors that are reported in Lee et al. (2010). In parallel to the REACT4C inventories, another inventory representative of the 2000 emission was used. The inventory is called QUANTIFY in reference to the project of the same name. For this scenario only the fuel burn, NO₂ and BC are available. For the other species of interest (H₂O, CO, HC, OC, SO₂, SO₄), the emission factors are identical to the ones used for REACT4C. The total emissions of primary species such as NO_x, BC, SO₂ and sulphates from the QUANTIFY_2000 scenario are slightly higher than those of REACT4C (ex: 0.77 kgN/year for REACT4C_2006 against 0.84 kgN/year for QUANTIFY_2000). In QUANTIFY_2000, the species available in the original files are fuel burn, NO₂ and BC. For the other species (CO₂, H₂O, CO, HC, OC, SO₂, SO₄), the emission factors are identical to those used for the

constitution of the basic REACT4C inventory. The spatial distribution is similar for both inventories.

METHODOLOGY

Using the compact Earth System Model (ESM) OSCARv2.2 (Gasser et al., 2017), we quantify the climate impact of present and future (up to 2100) civil aviation carbon dioxide (CO₂) emissions using eight aviation scenarios ranging from 386 Mt CO₂/year (Factor 2 scenario) to 2338 Mt CO₂/year (ICAO/CAEP scenario) in 2050. This approach allows quantifying the uncertainty due to the difficulty to estimate the future mitigation effort. The influence of other emission sectors is evaluated using two background Representative Concentrations Pathways (RCP2.6 and RCP6.0).

For the short-term species, a new version of the LMDz-INCA (LMDz version 5, INCA version 4) have been used. This new version has 39 vertical levels and extends up to 80 km in altitude. The vertical resolution has been improved around the cruise altitude of planes (<1 km). CNRS-LIVE has used the LMDz-INCA global chemistry-aerosol-climate model coupling on-line with the LMDz (Laboratoire de Météorologie Dynamique, version 5) General Circulation Model (Hourdin et al., 2006) and the INCA (INteraction with Chemistry and Aerosols, version 4) model (Hauglustaine et al., 2004). INCA initially included a state-of-the-art CH₄-NO_x-CO-NMHC-O₃ tropospheric photochemistry (Hauglustaine et al., 2004). The tropospheric photochemistry and aerosols scheme used in this model version is described through a total of 123 tracers including 22 tracers to represent aerosols. The model includes 234 homogeneous chemical reactions, 43 photolytic reactions and 30 heterogeneous reactions. Please refer to Hauglustaine et al. (2004) and Folberth et al. (2006) for the list of reactions included in the tropospheric chemistry scheme. The gas-phase version of the model has been extensively compared to observations in the lower-troposphere and in the upper-troposphere. For aerosols, the INCA model simulates the distribution of aerosols with anthropogenic sources such as sulfates, nitrates, black carbon, particulate organic matter, as well as natural aerosols such as sea-salt and dust.

RESULTS

In 2050, on a climate trajectory in line with the Paris Agreement limiting the global warming below 2 °C (RCP2.6), we found that the impact of the aviation CO₂ emissions ranges from 45 ± 2 mW/m² (2.5 % of the total anthropogenic warming) for an ambitious mitigation strategy scenario (Factor 2) to 78 ± 4 mW/m² (2.5 % of the total anthropogenic warming) for the least ambitious mitigation scenario of the study (ICAO based) (Terrenoire et al., 2019). Figure 1 summarizes the radiative forcing calculated for the different scenarios for the short-term species (Terrenoire et al., in preparation). The increase of ozone in the troposphere is responsible for a positive radiative forcing of 15.8 mW/m² for the present reference scenario REACT4C_2006. In the case of methane we calculate a negative forcing of about -15 mW/m² for different simulations by aviation. These two steady-state forcings associated with nitrogen oxides (ozone and methane) largely offset each other. The forcing of methane can in fact be broken down into four distinct forcings: a direct forcing and three indirect forcings. Indirect forcings were recalculated with the LMDZ-OR-INCA model. On the one hand, the increase in OH directly disrupts the methane well in the atmosphere. The increase in this photochemical loss results in a decrease in methane and a direct radiative forcing at equilibrium of -10.7 mW/m² for the present. Concentrations of several types of particles will also be disrupted by aviation-related emissions. Direct emissions of soot carbon (BC) by aviation induce a positive radiative forcing of 0.46 mW/m² in the present case for the REACT4C inventory. In the future, this forcing reaches 1.88 mW/m². Sulfates that are reflective particles will be influenced by SO₂ emissions but also by direct SO₄ emissions. The negative forcing associated with these particles dominates the effect of the other particles (-3.9 mW/m²). The distribution of nitrates is indirectly affected by aviation by the variation of the content in sulphates and the NO_x disturbance. These particles are responsible for a

positive forcing (0.07 mW/m^2). A slight negative forcing is associated with the emission of organic carbon by aviation. In total the particles are responsible for a negative forcing largely dominated by sulphates ranging from -3.4 mW/m^2 in this case REACT4C. Apart from CO_2 and streaks, the total radiative forcing related to aviation and modifications of gases and aerosols calculated in this work is negative and varies from -2.5 mW/m^2 for the present scenario REACT4C (-3.6 mW/m^2 in the case QUANTIFY_2000).

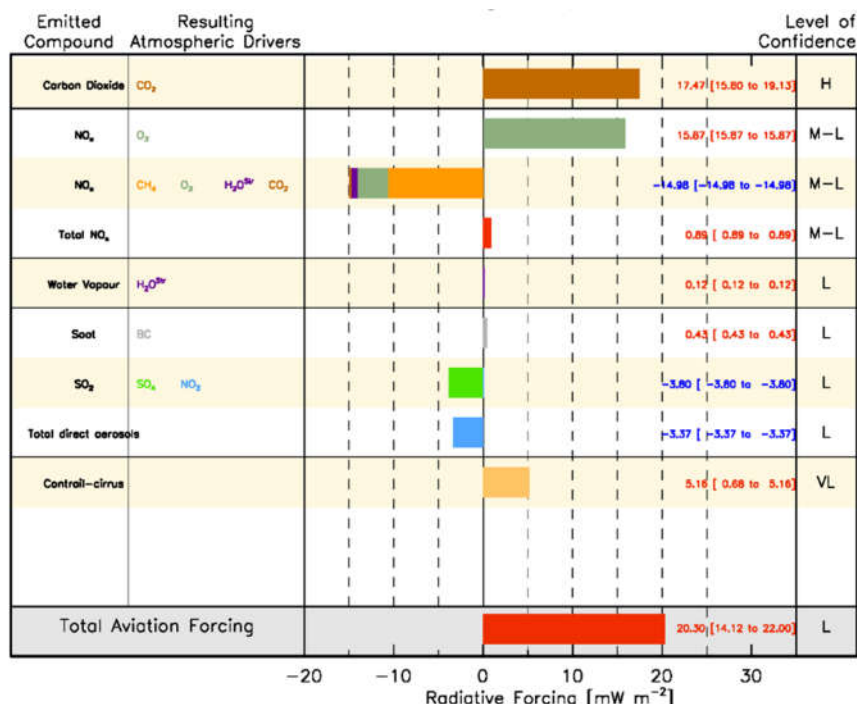


Figure 1: Radiative forcings of climate associated with aircraft emissions REACT4C emission inventory (2006).

CONCLUSION

The chemical perturbation and the associated radiative forcing of carbon dioxide, ozone, methane, soot carbon (BC), sulphates, nitrates and organic carbon (OC) due to aircraft emissions have been calculated using five different global emission inventories using a carbon cycle compact climate change model and the climate-chemistry global model LMDz-ORCH-INCA. We found that the impact of the aviation CO_2 emissions ranges from $45 \pm 2 \text{ mW/m}^2$ (2.5 % of the total anthropogenic warming) for an ambitious mitigation strategy scenario (Factor 2) to $78 \pm 4 \text{ mW/m}^2$ (2.5 % of the total anthropogenic warming) for the least ambitious mitigation scenario of the study (ICAO based). The increase of ozone in the troposphere is responsible for a positive radiative forcing of 15.8 mW/m^2 for the present reference scenario REACT4C_2006. In the case of methane, we calculate a negative forcing of about -15 mW/m^2 . In total, the particles are responsible for a negative forcing largely dominated by sulphates ranging from -3.4 mW/m^2 in this case REACT4C to -10.6 mW/m^2 in 2050. Apart from CO_2 and streaks, the total radiative forcing related to aviation and modifications of gases and aerosols calculated in this work is negative and varies from -2.5 mW/m^2 for the present scenario REACT4C (-3.6 mW/m^2 in the case QUANTIFY_2000).

REFERENCES

- Balkanski, Y., Myhre, G., Gauss, M., Rädcl, G., Highwood, E. J., and Shine, K. P.: Direct radiative effect of aerosols emitted by transport: from road, shipping and aviation, *Atmos. Chem. Phys.*, 10, 4477-4489, doi:10.5194/acp-10-4477-2010, 2010.
- Eyers, C.J., Addleton, D., Atkinson, K., Broomhead, M.J., Christou, R., Elliff, T., Falk, R., Gee, I., Lee, D.S., Marizy, C., Michot, S., Middel, J., Newton, P., Norman, P., Plohr, M.,

- Raper, D., Stanciou, N., 2005. AERO2k Global Aviation Emissions Inventories for 2002 and 2025 QINETIQ/04/01113, Farnborough, Hants, UK.
- Gasser, T., Ciais, P., Boucher, O., Quilcaille, Y., Tortora, M., Bopp, L., and Hauglustaine, D.: The compact Earth system model OSCAR v2.2: description and first results, *Geosci. Model Dev.*, 10, 271-319, <https://doi.org/10.5194/gmd-10-271-2017>, 2017.
- Hauglustaine, D. A., Hourdin, F., Jourdain, L., Filiberti, M. A., Walters, S., Lamarque, J. F., and Holland, E. A.: Interactive chemistry in the Laboratoire de Meteorologie Dynamique general circulation model: Description and background tropospheric chemistry evaluation, *J. Geophys. Res.*, 109, D04314, doi:10.1029/2003JD003957, 2004.
- Hourdin, F., I. Musat, S. Bony, P. Braconnot, F. Codron, J.-L. Dufresne, L. Fairhead, M.-A. Filiberti, P. Friedlingstein, J.-Y. Grandpeix, G. Krinner, P. Levan, Z.-X. Li, and F. Lott, The LMDZ4 general circulation model: climate performance and sensitivity to parametrized physics with emphasis on tropical convection, *Clim. Dyn.*, 27, 787–813, 2006.
- Lee, D. S., Pitari, G., Grewe, V., Gierens, K., Penner, J. E., Petzold, A., Prather, M. J., Schumann, U., Bais, A., Bernsten, T., Iachetti, D., Lim, L. L., and Sausen, R.: Transport impacts on atmosphere and climate: Aviation, *Atmos. Environ.*, 44, 4678–4734, doi:10.1016/j.atmosenv.2009.06.005, 2010.
- Søvde, O.A., S. Matthes, A. Skowron, D. Iachetti, L. Lim, L., Ø. Hodnebrog, G. Di Genova, G. Pitari, D.S. Lee, G. Myhre, I.S.A. Isaksen, Aircraft emission mitigation by changing route altitude: A multi-model estimate of aircraft NO_x emission impact on O₃ photochemistry, *Atmospheric Environment*, 95, 468-479, 2014.
- Terrenoire, E., Hauglustaine, D. A., Gasser, T., and Penanhoat, O.: The contribution of carbon dioxide emissions from the aviation sector to future climate change, *Environ. Res. Lett.*, 14.

TOWARDS DETERMINING THE EFFICACY OF CONTRAIL CIRRUS

M. Ponater¹, M. Bickel¹, L. Bock¹ & U. Burkhardt¹

¹ Deutsches Zentrum für Luft- und Raumfahrt, Institut für Physik der Atmosphäre, marius.bickel@dlr.de

Abstract. Contrail cirrus has been emphasized as the largest individual component of aircraft climate impact, yet respective assessments are based mainly on conventional radiative forcing calculations. Recent climate model simulations have provided the first estimate of contrail cirrus effective radiative forcing (ERF), which turns out to be much smaller, by about 65%, than its conventional radiative forcing. The reason for the reduction is that natural clouds make up for a considerably lower radiative impact in the presence of contrail cirrus. ERF is generally regarded as a superior metric to indicate the efficacy of some forcing agent to induce surface temperature changes. Hence, the new result may suggest a smaller role of contrail cirrus in the context of aviation climate impact (including proposed mitigation measures) than assumed so far. However, any conclusion in this respect should be drawn carefully as long as no simulations of the global mean surface temperature response to contrail cirrus are available. As a next step, these are needed to confirm the power of ERF for assessing the efficacy of contrail cirrus.

Keywords: Contrail Cirrus, Efficacy, Effective Radiative Forcing, Aviation Climate Impact

INTRODUCTION

Based on a number of radiative forcing (RF) estimates yielded over the last 10 years, contrail cirrus is often supposed to form the largest individual contribution to aviation climate impact (Burkhardt and Kärcher, 2011; Schumann and Graf, 2013; Kärcher, 2018, Bock and Burkhardt, 2019). However, in the last (5th) report of the IPCC it has been recommended to use the effective radiative forcing (ERF) as the most appropriate metric for assessing the quantitative importance of various components of a combined climate forcing. The main reason for this is that the fundamental equation linking radiative forcing to the global mean surface temperature response (ΔT_{sfc}) via the so-called climate sensitivity parameter (λ)

$$\Delta T_{sfc} = \lambda RF \quad (1)$$

is better fulfilled with a constant, forcing-independent λ , if the conventional RF is replaced by the ERF. The discovery that certain forcing agents exhibit a climate sensitivity parameter distinctly different from that of CO₂ (λ^{CO_2}) has been accounted for by introducing *efficacy* factors (r), which quantify the specific effectiveness of different forcings to induce surface temperature changes (Hansen *et al.*, 2005).

$$\Delta T_{sfc} = r \lambda^{(CO_2)} RF \quad (2)$$

Since the climate sensitivity parameter is physically related to the various radiative feedback processes caused by a climate forcing (e.g., Rieger *et al.*, 2017), it can be reasoned that forcings associated with an efficacy factor smaller (larger) than unity induce more negative (positive) feedbacks than the reference forcing, i.e., a CO₂ increase. In previous work, line-shaped contrails have been found to exhibit an efficacy considerably less than unity (Ponater *et al.*, 2005; Rap *et al.*, 2010). Hence, respective investigations targeting the more important contrail cirrus forcing are clearly required. A first attempt to do so, as well as consequences arising from the results, is reported here.

EFFECTIVE RADIATIVE FORCING FROM CONTRAIL CIRRUS

Simulation concept and radiative forcing results

The superiority of ERF as a metric is related to the fact that under this conceptual framework 'rapid radiative adjustments', developing on shorter time scales than the slowly responding surface temperature, are included as an integrated part in the radiative forcing value. Hence, a straightforward method to derive ERF is to compare two climate model simulations with fixed sea surface temperature: a sensitivity run including the forcing agent and a reference run omitting it (e.g., Hansen *et al.*, 2005). The ERF is the difference between these two runs

of the global and annual mean radiation balance at the top of the atmosphere. Most recently, Bickel *et al.* (2020) presented results applying this method to CO₂ and contrail cirrus forcings, employing a climate model equipped with a state-of-the-art parameterization for contrail cirrus (Bock and Burkhardt, 2016). It is essential to note that Bickel *et al.* (2020) had to scale the contrail cirrus forcing to yield statistically significant results in their climate model simulations. The scaling is required because ERF (its various indisputable merits notwithstanding) has the disadvantage of being associated with a much weaker signal-to-noise ratio than the classical RF. Therefore, the contrail cirrus simulations used as an input flight distances from a 2050 aircraft inventory (Wilkerson *et al.*, 2010), which were multiplied by a factor 12. This yielded a classical RF value of 701 mWm⁻² and a respective ERF value of 261 mWm⁻² (see Fig. 1), indicating a reduction of ERF of almost 65%. For optimal comparison with the reference (CO₂) case, a CO₂ forcing of nearly the same classical RF was employed, which resulted in a much smaller ERF reduction of only about 10%. Further simulations reported in Bickel *et al.* (2020, their Fig. 1) confirmed the clearly different relative reductions of ERF, with respect to RF, for the contrail cirrus and the CO₂ forcing.

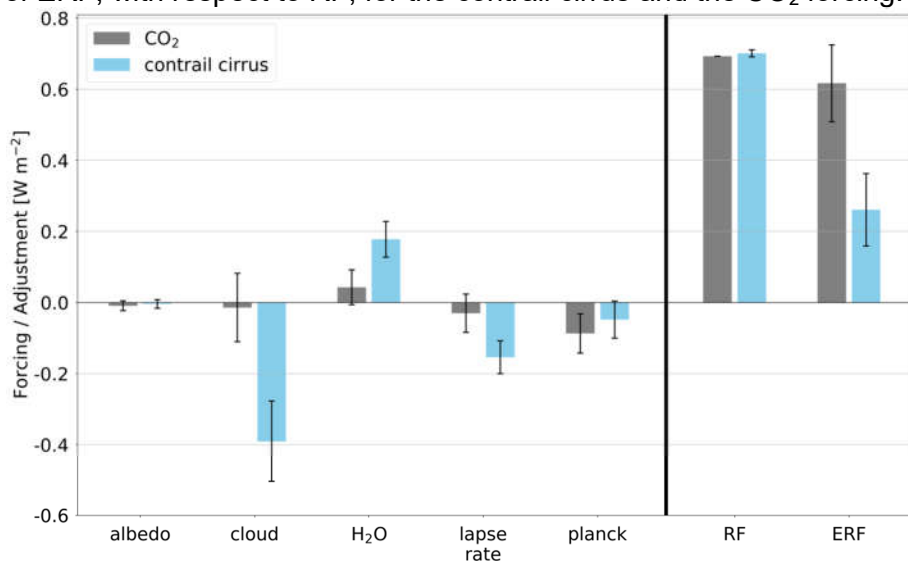


Figure 1. Classical radiative forcing (RF), effective radiative forcing (ERF) and rapid radiative adjustments due to various physical processes (left panel), as yielded by climate model simulations using either contrail cirrus (blue) or CO₂ (grey) as the forcing agent. The forcings in the simulations were scaled (see text) to ensure statistically significant ERF results. Error bars indicate confidence intervals on a 95% significance level.

Analysis of rapid radiative adjustments

As mentioned, the larger reduction of ERF with respect to conventional RF can be traced to its physical origin by means of a complete analysis of feedbacks (Rieger *et al.*, 2017). The result is obvious from the left part of Fig. 1, where the various rapid radiative adjustments contributing to ERF are displayed. The main reason for a stronger reduction auf ERF in the contrail cirrus case is a large negative radiative adjustment from natural clouds. Bickel *et al.* (2020) provide evidence that the (positive, i.e. warming) radiative effect of natural cirrus clouds gets weaker in the contrail cirrus simulation. This can be explained by the physical mechanism that natural and aviation induced cirrus clouds compete with each other, with respect to removing supersaturated water vapor from the ambient atmosphere through condensation to ice particles. Changes of mid-tropospheric clouds may also contribute, but their effect is less statistical significant (Bickel *et al.*, 2020, their Fig. 5b). Rapid adjustments in the CO₂ case are generally smaller (mostly statistically insignificant in Fig. 1). Water vapor and lapse-rate adjustment largely compensate each other, as is usual in feedback analysis.

DISCUSSION: CONTRAIL CIRRUS EFFICACY AND CLIMATE IMPACT RELEVANCE

Is the result of the scaled simulations representative for real contrail cirrus?

The conventional RF of contrail cirrus for year 2006 has been determined as 49 mWm⁻² with reasonable statistical accuracy (Bock and Burkhardt, 2016), but a meaningful value for the respective ERF cannot be simulated directly due to the large statistical uncertainty (Fig. 1). Bickel *et al.* (2020) discuss if the ERF reduction caused by a natural cloud feedback, as derived from scaled inventories, may nevertheless hold for the unscaled case as well. From a series of simulations with gradually increasing scaling factor they conclude that assuming an ERF reduction of similar magnitude for realistic aviation density is tenable. It appears that the underlying physical processes do not depend crucially on the scaling procedure.

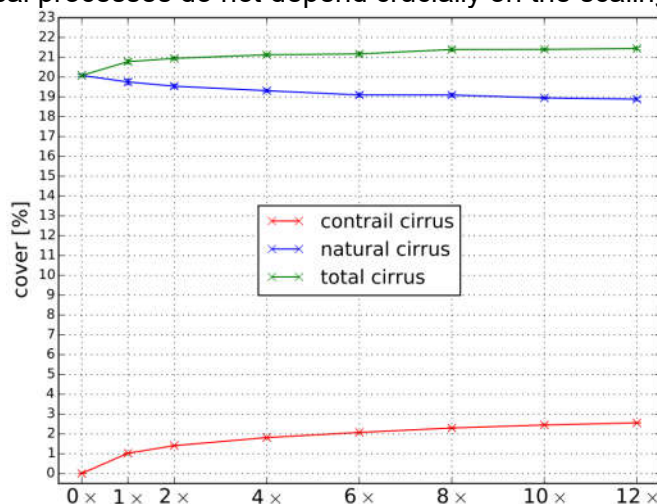


Figure 2. Global mean cover (in %) at 250 hPa for all (green), natural (blue), and aircraft induced (red) cirrus clouds, derived from contrail cirrus simulations using the 2050 aviation inventory with different scaling factors.

For example, cirrus coverage at 250 hPa (Fig. 2) is much less affected by background variability than the radiative impact parameters displayed in Fig. 1. For any scaling factor a substantial decrease of natural clouds in the presence of contrail cirrus is evident, and the effect is also quantitatively similar throughout the simulation series. Hence, the findings for the “scaling factor 12” simulation seem to reflect a consistent process-related interaction.

Is the ERF/RF ratio a reliable substitute for contrail cirrus efficacy?

The conclusion that contrail cirrus ERF is only 35% of the respective classical RF does not automatically imply that the contrail cirrus efficacy will be 0.35. Rather, by formulating Eq. (2) for contrail cirrus (indicated by “cc”) and CO₂ in both the classical and the ERF framework

$$\Delta T_{sfc}^{(CO_2)} = \lambda^{(CO_2)} RF^{(CO_2)} = \lambda'{}^{(CO_2)} ERF^{(CO_2)} \quad (3a)$$

$$\Delta T_{sfc}^{(cc)} = r^{(cc)} \lambda^{(CO_2)} RF^{(cc)} = r'{}^{(cc)} \lambda'{}^{(CO_2)} ERF^{(cc)} \quad (3b)$$

it is easily realized that

$$ERF^{(cc)}/RF^{(cc)} = r^{(cc)} (ERF^{(CO_2)}/RF^{(CO_2)}) / r'{}^{(cc)} \quad (4)$$

Hence, the classical contrail cirrus efficacy, $r^{(cc)}$, only equals $ERF^{(cc)}/RF^{(cc)}$, if $ERF^{(CO_2)}$ and $RF^{(CO_2)}$ are identical *and* if the contrail cirrus efficacy in the ERF framework is unity. The first condition is usually fulfilled within a 10% range (see Fig. 1, or Richardson *et al.*, 2019). The second condition, as mentioned above, is the basic expectation and motivation when using the ERF framework, but examples to the contrary have also been demonstrated (e.g., Marvel *et al.*, 2016). Therefore we state that contrail cirrus efficacy is insufficiently known at the present stage. Direct simulations of the surface temperature response and climate sensitivity, using a coupled atmosphere/ocean model, are necessary for this purpose.

Can contrail cirrus still be regarded as a most relevant part of aviation climate impact?

If the ERF/RF factors reported here are used to convert published estimates of realistic aviation RF to ERF (and if model, parameter, and statistical uncertainties are left aside), it might be argued that contrail cirrus can no longer be regarded as the most important aviation climate impact component (Fig. 3). We think, however, that this would be a superficial and premature conclusion. First, Bickel et al. (2020) point out that contrail cirrus ERF results from only one climate model need independent backing from other models, particularly because cirrus cloud feedbacks (of crucial importance here) have shown large inter-model spread even for the CO₂ case. Second, as mentioned above, the actual efficacy of contrail cirrus is still to be determined by direct simulations. This will be the next step using our climate model.

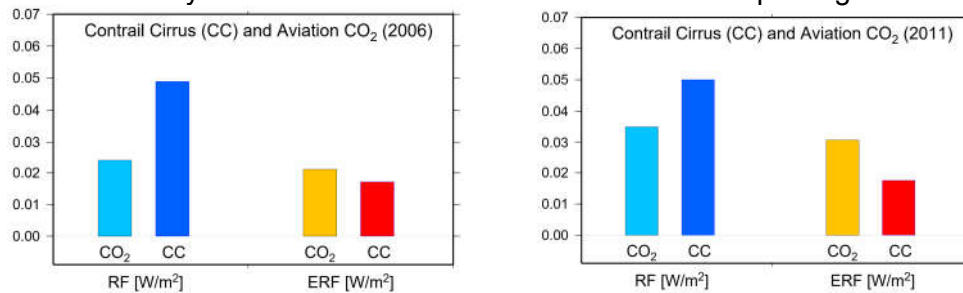


Figure 3. Classical RF from contrail cirrus and CO₂ (dark and light blue, respectively) for realistic aviation scenarios: Values adopted from Kärcher (2018, right) and from Bock and Burkhardt (2019, left). The ERF (red) counterparts have been yielded by using the ERF/RF reduction factors as derived by Bickel *et al.* (2020). Uncertainty bars are deliberately omitted.

REFERENCES

- Bickel M, Ponater M, Bock L, Burkhardt U and Reineke S, 2020. *Estimating the effective radiative forcing of contrail cirrus*. J. Clim., Vol. 33, pp. 1991-2005.
- Bock L and Burkhardt U, 2016. *Reassessing properties and radiative forcing of contrail cirrus using a climate model*. J. Geophys. Res. Atmos., Vol. 121, pp. 9717-9736.
- Bock L and Burkhardt U, 2019. *Contrail radiative forcing for future air traffic*. Atmos. Chem. Phys., Vol. 19, pp. 8163-8174.
- Burkhardt U and Kärcher B, 2011. *Global radiative forcing from contrail cirrus*. Nat. Climate Change, Vol. 1, pp. 54-58.
- Hansen J and co-authors, 2005. *Efficacy of climate forcings*, J. Geophys. Res., Vol. 110, D18104.
- Kärcher B, 2018. *Formation and radiative forcing of contrail cirrus*. Nat. Comm., Vol. 9, 1824.
- Marvel K, Schmidt GA, Miller RL and Nazarenko ES, 2016. *Implications for climate sensitivity from the response of individual forcings*. Nat. Climate Change, Vol. 6, pp. 386-389.
- Ponater M, Marquart S, Sausen R and Schumann U, 2005. *On contrail climate sensitivity*. Geophys. Res. Lett., Vol. 32, L10706.
- Rap A, Forster P, Haywood J, Jones A and Boucher O, 2010. *Estimating the climate effect of contrails using the UK met office climate model*. Geophys. Res. Lett., Vol. 37, L20703.
- Richardson TB and co-authors, 2019. *Efficacy of climate forcings in PDRMIP models*. J. Geophys. Res. Atmos., Vol. 124, pp. 12824-12844.
- Rieger V, Dietmüller S and Ponater M, 2017. *Can feedback analysis be used to uncover the physical origin of climate sensitivity and efficacy differences?* Clim. Dyn., Vol. 49, pp. 2831-2844.
- Schumann U and Graf K, 2013. *Aviation-induced cirrus and radiation changes at diurnal timescales*. J. Geophys. Res., Vol. 118, pp. 2404-2421.
- Wilkerson J and co-authors, 2010. *Analysis of emission data from global commercial aviation: 2004 and 2006*. Atmos. Chem. Phys., Vol. 10, pp. 6391-6408.

THE CONTRIBUTION OF AVIATION NO_x EMISSIONS TO CLIMATE CHANGE

V. Grewe^{1,2}, S. Matthes¹ & K. Dahlmann¹

¹ *Deutsches Zentrum für Luft- und Raumfahrt, Institut für Physik der Atmosphäre, Oberpfaffenhofen, Germany*

² *Delft University of Technology, Aerospace Engineering, The Netherlands*

Abstract. The contribution of aviation to anthropogenic climate change results from CO₂ and non-CO₂ emissions. Latter comprises emissions of nitrogen oxides, water vapour, and aerosols as well as contrail and contrail-cirrus effects. A series of updates can be noted in recent studies related to the effects of NO_x-emissions; the inclusion of two physical processes and an updated radiation calculation (see below). However, in our opinion, two further published methodological shortcomings have not been fully considered which leads to a considerable underestimation of the contribution of aviation's NO_x emissions to climate change. First, methane response calculations implicitly assume steady-state instead of an adequate transient development. Second, most studies determine ozone changes caused by switching off or reducing aviation NO_x emissions, instead of calculating aviation contributions to ozone. Such methodological simplifications largely underestimate the contribution of the aviation NO_x emissions to climate change by a factor of 6 to 7 and can thereby be considered as flaws. Note that the contribution of an emission to climate change ("status report") and the contribution of a change in emissions to climate change ("mitigation option") require different calculation methods. While for calculating the contribution of emissions to atmospheric compositions (and hence climate change), to which we are referring here, a clear recommendation was made, the methodological approach for evaluating mitigation measures might still be ambiguous, but should certainly not ignore the results of contribution calculations.

REFERENCES

Grewe, V. & Matthes S. & Dahlmann K., 2008. The contribution of aviation NO_x emissions to climate change, *Environ. Res. Lett.* 14 (2019) 121003.

EVALUATION OF THE CLIMATE IMPACT OF THE STEAM INJECTING AND RECOVERING AERO ENGINE

R. Pouzolz¹, O. Schmitz² & H. Klingels²

¹ Business Development, MTU Aero Engines, Germany, regina.pouzolz@mtu.de

² Advanced Design, MTU Aero Engines, Germany, oliver.schmitz@mtu.de, hermann.klingels@mtu.de

Abstract. A concept for the enhancement of an aircraft engine by steam injection from recovered water was developed. The concept promises a significant reduction of CO₂ emissions, NO_x emissions, and contrail formation. A standard 800 NM mission of an Airbus A320 using the proposed new engine was calculated. Applying a simplified one-dimensional climate assessment method prospects reduction of more than half of the Global Warming Potential over one hundred years compared to an evolutionarily improved aero-engine. If sustainable aviation fuels were used, climate impact could be reduced by 95 % compared to today's aircraft. The evaluation is a first estimate of effects as a starting point for discussion of such concept in the scientific community, with focus on the radiation properties of potential contrails from the comparatively cold exhaust gases.

Keywords: Climate Impact, Steam Injection, Water Condensation, Aircraft Engine

MOTIVATION: CLIMATE CHANGE TARGETS OF THE AVIATION INDUSTRY

The aviation industry has set itself challenging targets with regard to its contribution to carbon dioxide (CO₂) emissions. ICAO/ATAG states that “by 2050, net aviation carbon emissions will be half of what they were in 2005” (ATAG, 2020). This includes offsetting parts of the CO₂ emissions. Referring to the qualitative illustration published in this context (IATA, 2020, p. 10), offsetting should play a significant role in a transition period between 2020 and say 2035, enabled by the ICAO offsetting scheme CORSIA. Realisation of the potential of “known technology, operations and infrastructure measures” would also cut roughly one quarter of CO₂ emissions, relative to a no-action path. Most of the reduction, however, results from supposedly CO₂-neutrally produced Sustainable Aviation Fuels (SAF) as well as “new-generation” technologies.

Apart from CO₂, aviation contributes to global warming mainly by the emission of nitrogen oxides (NO_x) and the formation of contrails and contrail cirrus. These climate effects have not yet been taken into account in any industrial or regulative initiatives, since there is no common understanding, to which exact extent these effects are relevant, of which operational aspects they depend on, neither which metric should be used for evaluation. All of this is subject to ongoing research. In contrast, NO_x have been regulated for a long time via the ICAO LTO (Landing and Take-Off cycle) certification rules, with a clear objective to reduce effects on local air quality. Due to the lack of certified emission levels at altitude, current climate emission calculation methods use these values certified for low altitudes.

More and more stakeholders acknowledge, that NO_x and contrails have an effect on climate change of the same order of magnitude as that of CO₂. As an example, compensation portals apply a multiplier between two and three on the CO₂ value to factor in the additional effects for the compensation amount. Reducing aviation's climate impact requires considering all effects.

The Steam Injecting and Recovering Aero engine (SIRA) concept discussed in this paper tackles all of the above-mentioned effects. MTU presents the novel concept at an early stage of development (Schmitz et al., 2020a and 2020b) to give an insight on MTU's initiatives towards climate-neutral flight and to foster the discussion in atmospheric sciences on the influence of condensing water vapour in exhaust gases on the formation of contrails.

ENGINE CONCEPT AND EMISSION REDUCTION POTENTIAL

The SIRA concept is introduced in detail by Schmitz et al. (2020a). Figure 1 shows a schematic half-side cut flowchart of the presented concept. Exhaust-heat generated steam is injected into the combustion chamber. The humidified mass flow contains significantly more

extractable energy than air. The pumping of the utilised liquid water up to the necessary pressure requires two magnitudes less power than the compression of air, which reduces the internal power demand. Both lead to a noticeable increase in specific power compared to a conventional gas turbine and, foremost, to a significant increase in thermodynamic efficiency. Through a condenser downstream of the steam generator, the water is brought back to its liquid phase and then recovered from the exhaust gas-steam mixture. The condenser is air-cooled, e.g. from the propulsion system's bypass or from a separate blower.

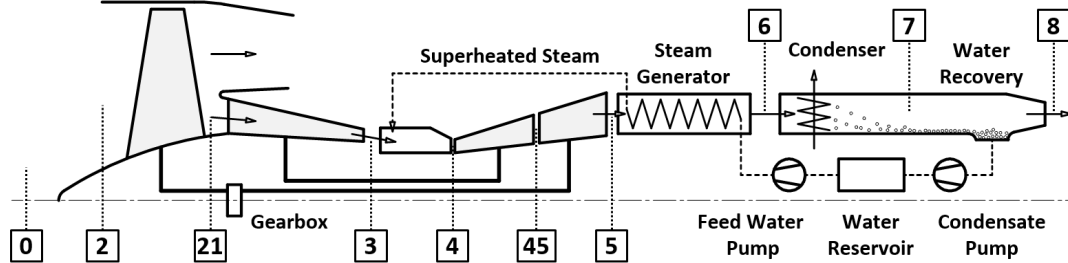


Figure 1: Scheme of a half-side arrangement of the proposed steam injecting and recovering aero engine concept with station nomenclature (taken from Schmitz et al., 2020a)

According to preliminary potential studies outlined by Schmitz et al. (2020a), the proposed water-enhanced gas turbine concept is expected to decrease Thrust-Specific Fuel Consumption (TSFC) in cruise conditions by about 20 % compared to a conventional aero engine of the same technology level. Considering the increase of system mass and drag due to the necessary components (e.g. heat exchanger), the fuel burn saving and, thus, the CO₂ reduction potential is about 15 %. In addition, the injected steam causes a more homogenous temperature distribution during the combustion, leading to a significant lowering of NO_x formation, in the following studies assumed at 90 %. Furthermore, the recovery of water through cooling of the exhaust gas stream below its dew point offers the potential to reduce contrails by at least 90 % or even avoid them completely.

Benefits of this herein presented revolutionary concept shall be evaluated against conventional aero engine technology from 2015 and its evolutionary further development until 2030, both represented by MTU's Clean Air Engine (CLAIRE) technology roadmap. Table 1 summarizes the assumptions taken for the climate evaluation of the SIRA concept.

Table 1: Assumptions for climate impact reduction relative to the 2015 reference

Engine	TSFC	Fuel Burn	NO _x	Contrails
CLAIRE 1 (2015, Reference)	100 %	100 %	100 %	100 %
CLAIRE 2 (2030)	-10 %	-10 %	0 %	0 %
SIRA	-28 %	-24 %	-90 %	-90 %

CLIMATE ASSESSMENT

Choice of climate metric

Climate impact from aviation is generally evaluated in terms of Radiative Forcing (RF) of the entire aviation until a certain reference year (e.g. Grewe et al., 2017). Such RF values cannot be directly used for the evaluation of new engine or aircraft technologies. The quantity of emissions of an aircraft depends on the respective stage length and the payload. The climate impact of these emissions changes significantly with flight altitude, but also with geodetic latitude and longitude. In principal, there are two ways of matching these two different system levels - global aviation vs. one aircraft or engine type. The first one works by embedding a new aircraft or engine technology in a fleet and calculating emission scenarios. These are fed into a 3-D or 4-D atmospheric model, and the scenarios with and without the new technology are compared against each other. The second way of matching derives a

response surface from an atmospheric model, that gives climate feedbacks of all constituents by altitude, latitude and longitude of the emissions, as well as time (daytime, seasonal influence).

The latter approach was pursued in the LEEA (Low Emissions Effect Aircraft) project (Rädel et al. and Köhler et al. in 2008), however, simplified by averaging latitude, longitude and time. The resulting method for the climate impact calculation is applicable for preliminary aircraft design and has been used in this study. In agreement with the Kyoto Protocol, the Pulse Global Warming Potential over a time horizon of 100 years (PGWP) was chosen as metric. With regard to the SIRA concept, the PGWP turns out to be conservative, since short-lived effects (NO_x, contrails) are less valued. For comparison, the Sustained Global Warming Potential (SGWP) as defined in Shine et al. (2005) would yield higher benefits, since short-lived effects are weighted higher. The same is true if applying shorter time horizons, e.g. 50 years. More recent studies (e.g. Dahlmann, 2012, Schwartz Dallara, 2011) use more sophisticated metrics with the objective to be more representative for real air traffic emissions scenarios and less dependent on the time horizon.

Calculation methodology

All aircraft design, mission and emission calculations were performed with the aircraft design and performance program “PIANO”. An Airbus A320 was chosen as reference aircraft. No technological evolutions of the aircraft (e.g. aerodynamics and structure) were modelled, therefore, the results shown in this study purely reflect engine effects. However, a design loop was performed, such that the weight and drag penalties of the novel concept were accounted for in the aircraft weights and design range. Missions of 800 NM and for comparison 2,000 NM were calculated.

PIANO issues one value of NO_x emissions for each cruise segment, spanning over several flight levels. This value is then redistributed on the altitude layers defined in LEEA. The PGWP is calculated based on the formulas defined in Shine et al. (2005), using the same parameters as published in Egelhofer (2009). Since absolute values for the climate impact of a single flight are of no practical use and the LEEA metric was created to compare technologies, all results are shown as relative values to the CLAIRE 1 engine’s total.

Results of the climate impact assessment

According to the results presented in Figure 2, the SIRA engine has in total 60 % less impact (PGWP) on climate than CLAIRE 1. Using the SGWP yields 69 % (not shown). Reducing the time horizon to 50 years results in a 68 % climate impact reduction (not shown).

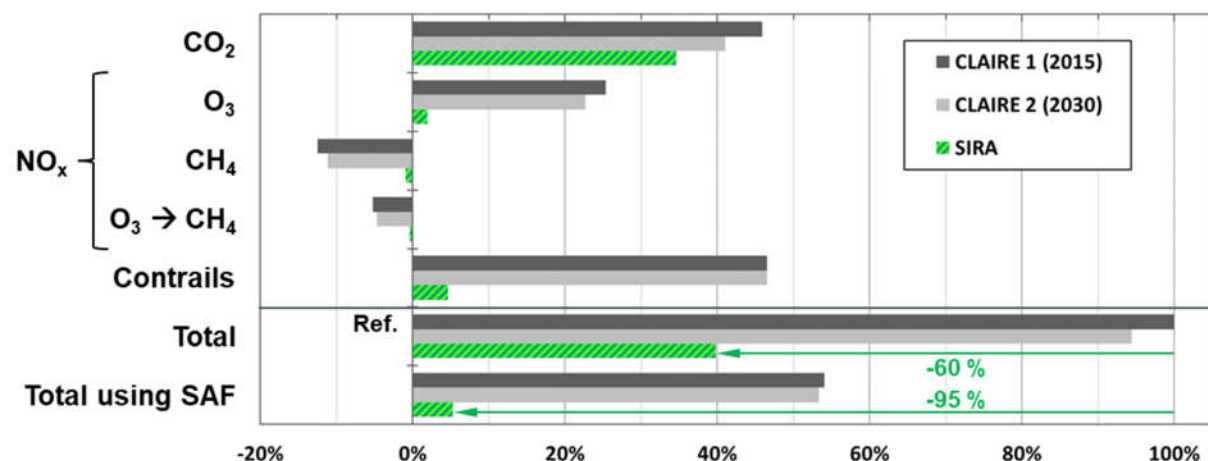


Figure 2: Absolute Global Warming Potentials over one hundred years relative to the total of the CLAIRE 1 reference engine. Stage length: 800 NM. “Contrails” includes contrail cirrus.

The biggest share of these benefits relates to the assumption, that the SIRA’s contrail impact is reduced by 90 % (see Table 1). The NO_x effects are less relevant, since a large portion is emitted at low altitudes during climb, where they have a cooling effect. They would play a

significantly bigger role on long-range flights. On a stage length of 2000 NM, for example, the SIRA's PGWP would be reduced by 65 % instead of 60 %. Operating the SIRA with CO₂-neutrally produced sustainable aviation fuels (SAF) would result in a reduction of 95 % of its climate impact compared to today's aircraft.

CONCLUSION AND OUTLOOK

This simplified approach to evaluate the Steam Injecting and Recovering Aero engine's climate impact reveals large potentials for the reduction of aviation's overall climate impact. If SAFs were used, its impact would almost go down to zero. However, further research is needed to confirm the assumptions for NO_x reduction and contrail impact. On top of the technical uncertainties, the analysis is strongly influenced by parameters, that need further substantiation from atmospheric sciences, e.g. contrail effects, political/societal choices, e.g. applicable time horizon, and the upcoming next cycles of aircraft development, where airframe manufacturers will play a major role in accommodating such systems in future aircraft. By presenting the subject to the ECATS community, the authors hope to foster discussions on both the presented engine concept as well as methods and metrics for evaluation.

REFERENCES

- ATAG, 2020. *Facts & Figures*. www.atag.org/facts-figures.html, retrieved on 28.03.2020.
- Dahlmann K, 2012. *Eine Methode zur effizienten Bewertung von Maßnahmen zur Klimaoptimierung des Luftverkehrs*. Ph.D. thesis, Ludwig-Maximilians-Universität München, Germany.
- Egelhofer R, 2009. *Aircraft Design Driven by Climate Change*. Ph.D. thesis, Technical University of Munich, Germany.
- Grewe V, Dahlmann K, Flink J, Frömming C, Ghosh R, Gierens K, Heller R, Hendricks J, Jöckel P, Kaufmann S, Kölker K, Linke F, Luchkova T, Lührs B, van Manen J, Matthes S, Minikin A, Niklaß M, Plohr M, Righi M, Rosanka S, Schmitt A, Schumann U, Terekhov I, Unterstrasser S, Vázquez-Navarro M, Voigt C, Wicke K, Yamashita H, Zahn A and Ziereis H, 2017. *Mitigating the Climate Impact from Aviation: Achievements and Results of the DLR WeCare Project*. *Aerospace*, 4, 34, doi:10.3390/aerospace4030034
- IATA, 2020. *Aircraft Technology Roadmap*. Company publication. www.iata.org/en/publications/technology-roadmap, retrieved on 30.03.2020.
- Köhler MO, Rädcl G, Dessens O, Shine KP, Rogers HL, Wild O and Pyle JA, 2008. *Impact of perturbations to nitrogen oxide emissions from global aviation*. *J. Geophys. Res.*, 113, D11305, doi:10.1029/2007JD009140.
- Rädcl G and Shine KP, 2008. *Radiative Forcing by Persistent Contrails and its Dependence on Cruise Altitudes*. *J. Geophys. Res.*, 113, D07105, doi:10.1029/2007JD009117.
- Schmitz O, Klingels H and Kufner P, 2020a. *Aero Engine Concepts Beyond 2030: Part 1 – The Steam Injecting and Recovering Aero Engine*. ASME Turbo Expo 2020: Turbomachinery Technical Conference and Exposition, London, England, GT2020-15391. In press.
- Schmitz O, Kaiser S, Klingels H, Kufner P, Obermüller M, Henke M, Zanger J, Grimm F, Schuldt S, Marcellan A, Cirigliano D, Kutne P, Heron-Himmel A, Schneider S, Richter J, Weigand B, Göhler-Stroh A, Seitz A and Hornung M, 2020b. *Aero Engine Concepts Beyond 2030: Part 3 – Experimental Demonstration of Technological Feasibility*. ASME Turbo Expo 2020: Turbomachinery Technical Conference and Exposition, London, England, GT2020-15397. In press.
- Schwartz Dallara E, 2011. *Aircraft Design for Reduced Climate Impact*. Ph.D. thesis, Stanford University, USA.
- Shine, KP, Fuglestedt JS, Hailemariam K and Stuber N, 2005. *Alternatives to the Global Warming Potential for comparing climate impacts of emissions of greenhouse gases*. *Climatic Change*, Vol. 68, pp. 281-302.

PARAMETRIC STUDY OF CONTRAILS FORMATION

E. Montreuil¹, W. Ghedhaïfi¹ & E. Terrenoire¹

¹ Multi-Physics Department for Energetics, ONERA, France, emmanuel.montreuil@onera.fr

Abstract. Condensation trails, usually called contrails, represent an increasing issue for aeronautics. Contrail formation and properties depends on several factors such as ambient atmospheric conditions (temperature and relative humidity), mainly, but also possibly on engine characteristics (e.g. bypass ratio, exhaust temperature), fuel type (e.g. kerosene or alternative fuels), and aircraft geometry (e.g. driving mixing in the aircraft wake). Therefore, parametric studies allow a better understanding of contrails onset mechanisms and assessment of their properties sensitivity in the aircraft near field. This can help to find out smart mitigation solutions to reduce the environmental impact of contrail/induced cirrus by better controlling their formation. In this context, reliable prediction tools as well as technologies input are urgently needed for decision makers. Using the computational fluid dynamics code CEDRE, developed at ONERA and adapted for contrail issues, 3D simulations are carried out to address this need. They take into account the dynamical evolution of the jet plume, the chemical transformations of the exhaust after ejection and the microphysical processes driving contrails formation. The simulations are performed on a realistic aircraft configuration based on the Common Research Model (CRM) with a realistic engine. The objective here is to confront 3D simulation approach with the Schmidt-Appleman criterion, widely used to determine contrails formation areas. In this work, we compare 3D simulations that give local properties within the plume in the aircraft near field and the Schmidt-Appleman predictions, especially for threshold conditions. Several simulations are carried out and analyzed for different atmospheric conditions (particularly temperature and relative humidity) in order to evaluate the sensitivity of contrail formation to meteorological conditions.

Keywords: Contrails; CFD; Schmidt-Appleman

ACKNOWLEDGEMENTS

The authors would like to acknowledge the French Civil Aviation (DGAC) for their funding in the frame of the PHYWAKE program.

REFERENCES

- Ghedhaïfi W., A. Bienner, R. Megherbi, E. Montreuil, E. Terrenoire, X. Vancassel and A. Loseille, 2019. *Influence of atmospheric conditions on contrail formation: 3D simulation versus Schmidt-Appleman criterion*. In 24th ISABE conference. Canberra, Australia.
- Khou J.-C., W. Ghedhaïfi, X. Vancassel, E. Montreuil and F. Garnier, 2017. *CFD simulation of contrail formation in the near field of a commercial aircraft: Effect of fuel sulfur content*. Meteorologische Zeitschrift, Vol. 26, pp. 585 – 596.
- Loseille A., F. Alauzet, A. Dervieux and P. Frey, 2007. *Achievement of second order mesh convergence for discontinuous flows with adapted unstructured mesh adaptation*. In 18th Computational Fluid Dynamics AIAA conference, Miami, USA.
- Montreuil E., W. Ghedaïfi, V. Chmielarski, F. Vuillot, F. Gand and A. Loseille, 2018. *Numerical simulation of contrail formation on the common research model wing/body/engine configuration*. In 10th Space and Atmospheric Environment AIAA conference, Atlanta, USA.
- Schumann U., 1996. *On conditions for contrail formation from aircraft exhaust*. Meteorologische Zeitschrift, vol. 5, no. 1, pp. 4-23.

THE CONTRAIL MITIGATION POTENTIAL OF AIRCRAFT FORMATION FLIGHT DERIVED FROM HIGH-RESOLUTION SIMULATIONS

S. Unterstrasser¹

¹ *Institute of Atmospheric Physics, DLR Oberpfaffenhofen, Germany, simon.unterstrasser@dlr.de*

Abstract. Extended formation flight (with separations of 10 to 40 wing spans) is a viable option to increase the performance of the commercial aviation sector. Fuel savings of around 10% can be expected during such formations (on average over all participating aircraft), which must substantially outweigh re-routing induced fuel penalty. Net fuel savings directly translate into lower CO₂ emissions. Moreover, saturation effects can be expected when contrails of two or more aircraft are produced in close proximity, compete for the available atmospheric water vapour and mutually inhibit their growth. High-resolution simulations of contrails with a well-established model are presented and quantify those saturation effects by comparing long-living contrails behind a two aircraft formation with those evolving behind a single aircraft. The simulations suggest that radiatively-important contrail properties are reduced by 20%-60%. The simulations were performed within the FORMIC project, which also quantified the saturation effects on a regional scale due to non-linear chemistry and the change in the overall global climate impact by the introduction of formation flight (see extended abstract by Dahlmann) and according changes in the flight route cadastre (see also extended abstract by Marks et al).

Keywords: green aviation, formation flight, contrail climate impact, large-eddy simulation, Lagrangian ice microphysics

INTRODUCTION

Formation flight (FF) is a well-known strategy of migratory birds in order to improve their aerodynamic efficiency, save energy and increase their range (Lissaman and Shollenberger, 1970; Hummel, 1983). Similarly, FF can increase the performance in the civil and military aviation sector. In addition to close FF (with separations of a few wing spans in flight direction) in the military sector, extended FF (with separations of 10 to 40 wing spans) is a viable option for the commercial sector. Follower aircraft (AC) encounter uplift from flying in the upwash region created outboard of a leading AC. Numerous numerical, wind tunnel and real flight studies (e.g. Beukenberg and Hummel, 1990; Blake and Multhopp, 1998; Nangia and Palmer, 2007; Kless et al., 2013; Okolo et al., 2014) found that fuel savings of around 10% can be expected during such formations (on average over all participating AC, not only for the follower AC). In order to establish formations in the airspace, re-routing is required. Clearly, re-routing induced fuel penalties should be substantially smaller than the fuel savings during the actual formation. Xu et al. (2014) find net fuel burn reductions of nearly 8% and 6% for different network sizes of cooperating airlines. Fuel savings directly translate into lower CO₂ emissions and would reduce the climate impact of aviation. Besides the emission of carbon dioxide, the formation of contrails and the emission of nitrogen oxides cause a substantial aviation radiative forcing (Sausen et al., 2005; Lee et al., 2010) which would be both affected by the introduction of FF. The contrail radiative forcing (RF) is probably larger than the RF of the total accumulated CO₂ emissions from aviation (Burkhardt and Kärcher, 2011; Bock and Burkhardt, 2016) and the present study focuses on the contrail mitigation potential by FF. Saturation effects can be expected when contrails of two or more aircraft are produced in close proximity, compete for the available atmospheric water vapour and mutually inhibit their growth. In a recent study by Unterstrasser and Stephan (2020), the early evolution of contrails produced by two AC in formation was analysed and compared to classical contrails behind a single aircraft. Classical single aircraft (SA) contrails grow mainly in vertical direction due to the wake vortex descent in the first few minutes (e.g. Lewellen and Lewellen, 2001; Unterstrasser, 2016). In FF scenarios the individual contrails merge quickly after their formation into a single contrail (from now on abbreviated as FF contrail). Unterstrasser and Stephan (2020) found the wake vortex dynamics to be more complex and diverse as vortex pairs happen to also move upwards and sideways. After vortex break-up,

FF contrails are thus not as deep, yet they are broader than SA contrails. Earlier studies already demonstrated that differences in the early contrail properties triggered by differences in wake vortex characteristics can have a long lasting mark. Unterstrasser and Görsch (2014), e.g., simulated contrails produced by various aircraft types and initial differences in ice crystal number and contrail depth lead to quantitative differences between the contrail-cirrus properties that remain over the total simulation period of 6h.

We employ the Large-Eddy Simulation (LES) model EULAG-LCM, which is an established code for performing high resolution simulations of contrails. In this study, we will juxtapose the long-term evolution of contrails generated by a single aircraft, on the one hand, and by a two aircraft formation, on the other hand. First, the model (setup) is described, which is followed by the presentation of the results.

METHOD

Model EULAG-LCM

For the numerical simulations, the model EULAG-LCM has been used. EULAG (Smolarkiewicz and Margolin, 1997) is a widely used, non-hydrostatic anelastic LES (Large-Eddy Simulation) model, which employs the positive definite advection scheme MPDATA (Smolarkiewicz and Margolin, 1998). The ice microphysical module LCM, based on Lagrangian tracking of ice crystals (Sölch and Kärcher, 2010), is fully coupled to EULAG. The model version EULAG-LCM has been used extensively for the simulation of natural cirrus and contrails in the past. The setup of the contrail-cirrus simulations presented here is in many aspects similar to the one in Unterstrasser et al. (2017a, b). A two dimensional model, whose domain is perpendicular to the direction of flight and represents some portion of the UT/LS (upper tropospheric/lower stratospheric) region, is used. In the vertical (z -)direction, the domain dimension is 2.5km. In the horizontal (x -)direction, the domain dimension is 40km or 80km depending on vertical wind shear. Uniform grid boxes with sizes $dx = dz = 10\text{m}$ are used.

Atmospheric scenarios

An ice-supersaturated (ISS) layer of $d_{ISS} \approx 1.2\text{km}$ thickness and an initial relative humidity (with respect to ice) of RHi is prescribed between $z = 1000\text{m}$ and 2000m . Above and below this layer, RHi drops to 20% inside 500m thick transition zones. The flight altitude of the contrail producing aircraft (formation) is at $z = 1500\text{m}$ in the middle of the ISS layer.

In order to quantify the saturation effects for different atmospheric scenarios, several parameters of the idealised atmospheric setup are varied.

The initial relative humidity RHi is either 110% or 120%. Three different synoptic scale updraught scenarios with w_{syn} either $= 1\text{ cm s}^{-1}$, 2 cm s^{-1} or 5 cm s^{-1} are prescribed. By adjusting the updraught period, the prescribed final adiabatic cooling is 2K. The vertical wind shear s is either 0.002s^{-1} or 0.006s^{-1} .

Contrail initialisation

As in previous studies, the contrail initialisation is based on 3D data of contrail vortex phase simulations. The 3D data is averaged along flight direction and inserted into the enlarged domain of the contrail-cirrus simulation. The contrail-cirrus simulations of a classical SA contrail are based on input data of Unterstrasser (2014), whereas the corresponding simulations of a FF contrail-cirrus produced by a two aircraft formation are based on input data of Unterstrasser and Stephan (2020). The latter study compares young contrails after vortex breakup produced behind a formation of two aircraft to those of the classical SA case. Qualitative differences were found: Behind a formation, the wake vortices of both aircraft interact. Often this leads to a strong lateral transport of one vortex pair and moderate sinking of the second pair. Hence, contrails behind a formation are broader, yet their vertical extent is smaller than in the classical case. Moreover, the ice crystal loss is not as pronounced as in the classical case.

All vortex phase simulations used as input in the present study use an ice crystal ‘emission’ index of $2.8 \cdot 10^{14}(\text{kg fuel})^{-1}$ and the aircraft characteristics of an A350/B777 aircraft.

RESULTS

Figure 1 shows the cross-sections of an exemplary contrail after 3 and 6 hours. The highest extinction coefficient values occur close to the contrail top where ice crystals numbers are highest (the so-called contrail core region). The contrail gets deeper as the largest ice crystals start to fall out of the contrail core and make up a fallstreak (lower part of the contrail). Moreover, the contrail becomes tilted due to vertical wind shear. Moreover, many fine-scale structures are apparent due to the high resolution of the simulation.

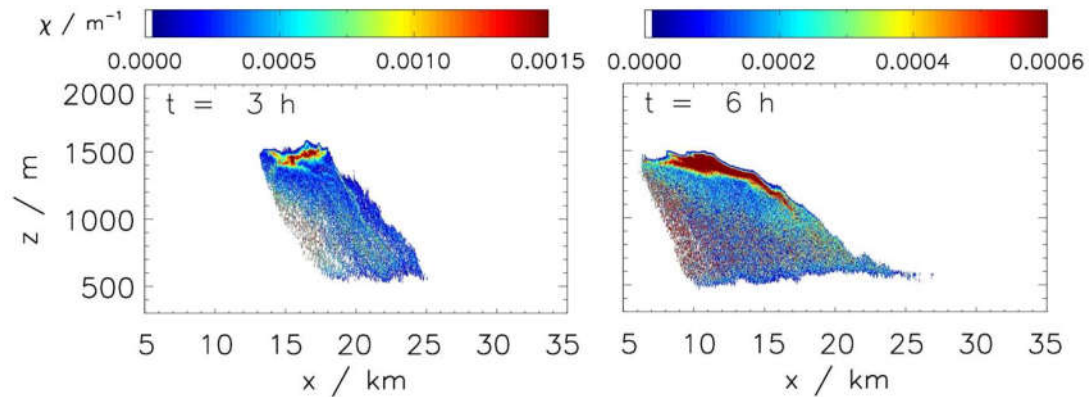


Figure 2: Cross-section of an exemplary contrail after 3 and 6 hours. Displayed is the extinction coefficient. The flight altitude of the contrail producing aircraft is at the model altitude $z=1500\text{m}$.

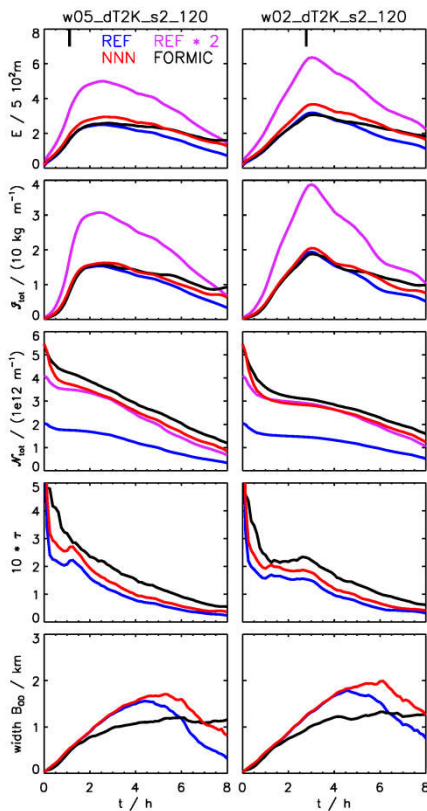


Figure 2 shows integrated contrail properties like the total extinction E (which is the integral of the extinction coefficient over the whole contrail cross-section) and the total ice mass I_{tot} (again integral of ice mass concentration over the 2D area. Note the units “kg per (flight) meter”). Moreover, the total ice crystal number N_{tot} , the mean optical depth τ and the contrail width B_{OD} are displayed. For both atmospheric scenarios (left/right column), four different curves are shown over the simulated period of 8 hours. REF shows properties of the SA contrail and FORMIC properties of the FF contrail. As the formation consists of two aircraft, it is reasonable to compare the FORMIC values to $2 \cdot \text{REF}$ (i.e. two independent contrails spreading unperturbed of each other). The NNN-curves will be explained in the full paper only. The atmospheric scenarios differ only in the prescribed updraught speed w_{syn} (5 cm s^{-1} or 2 cm s^{-1}) and both use $s = 0.002\text{s}^{-1}$ and $RHi = 120\%$.

Due to the initialization, N_{tot} of FORMIC is and remains higher than that of REF and also $2 \cdot \text{REF}$ (as FF contrails are less affected by ice crystal loss during the vortex phase). Contrails mainly get broader due to shear-induced tilting. As SA contrails are initially deeper, their width increases faster than that of FF contrails. Towards the end, those contrails become optically thin and the width (all contrail columns with $\tau > 0.03$ are counted) decreases after 4-5 hours. The width of the FF contrails, on the other hand, grows

continuously; they do not thin out that fast and their optical depth remains higher probably because of higher ice crystal numbers.

With the LES approach it is not possible to derive radiative forcing values; hence we resort to proxy quantities. The total extinction E is a measure of the contrail radiative impact in the shortwave (SW) spectrum and the total ice mass I_{tot} in the longwave (LW) spectrum. For both quantities, the REF and FORMIC values are basically identical over the first 3-4 hours. After that, FORMIC values decrease at a slower rate and are thus higher. Clearly, the FORMIC values are much smaller than the 2*REF values. In terms of the integrated effect, a contrail produced by two aircraft in formation resembles much more a contrail of a single aircraft than that of two independent aircraft.

Contrails warm in the LW and cool in the SW. Both contributions (based on our proxies) are reduced for FF relative to 2*REF, yet the net effect on the overall RF cannot be estimated with the present approach.

In the final paper, also time-integrated proxy quantities are analysed for a much larger set of atmospheric scenarios. We find reductions by 20%-50% in LW and by 30-60% in SW. Hence, this first study of the contrail mitigation potential by formation flight shows promising results.

ACKNOWLEDGEMENTS

The first author is partly funded by the BMWi LuFo project FORMIC (Formation Flight Impact on Climate). Computational resources for EULAG-LCM simulations were made available by the German Climate Computing Center (DKRZ) through support from the German Federal Ministry of Education and Research (BMBF)

REFERENCES

- Beukenberg, M. and Hummel, D., 1990: *Aerodynamics, Performance and Control of Airplanes in Formation Flight*, in: Paper 90-5.9.3, ICAS.
- Blake, W. and Multhopp, D., 1998: *Design, performance and modeling considerations for close formation flight*, in: Guidance, Navigation, and Control and Co-located Conferences, AIAA, doi:10.2514/6.1998-4343.
- Bock, L. and Burkhardt, U., 2016: *Reassessing properties and radiative forcing of contrail cirrus using a climate model*, J. Geophys. Res., 121, 9717–9736.
- Burkhardt, U. and Kärcher, B., 2011: *Global radiative forcing from contrail cirrus*, Nature Clim. Ch., 1, 54–58.
- Dahlmann, K., Matthes, S., Yamashita, H., Unterstrasser, S., Grewe, V., and Marks, T., 2020. *Assessing the climate impact of formation flights*. In Extended Abstracts of ECATS conference 2020.
- Hummel, D., 1983: *Aerodynamic aspects of formation flight in birds*, J. Theor. Biol., 104, 321–347, doi:10.1016/0022-5193(83)90110-8.
- Kless, J. E., Aftosmis, M. J., Ning, S. A., and Nemec, M., 2013: *Inviscid Analysis of Extended-Formation Flight*, AIAA Journal, 51, 1703–1715, doi:10.2514/1.J052224.
- Lee, D., Pitari, G., Grewe, V., Gierens, K., Penner, J., Petzold, A., Prather, M., Schumann, U., Bais, A., Bernsten, T., Iachetti, D., Lim, L., and Sausen, R., 2010: *Transport impacts on atmosphere and climate: Aviation*, Atmos. Environ., 44, 4678 – 4734.
- Lewellen, D. and Lewellen, W., 2001: *The effects of aircraft wake dynamics on contrail development*, J. Atmos. Sci., 58, 390–406.
- Lissaman, P. and Shollenberger, C., 1970: *Formation flight of birds*, Science, 168, 1003–1005.
- Marks, T., K. Dahlmann, V. Grewe, V. Gollnick, F. Linke, S. Matthes, E. Stumpf, S. Unterstrasser, C. Zumegen, 2020. *Climate impact mitigation potential of formation flight*. In Extended Abstracts of ECATS conference 2020.
- Nangia, R. and Palmer, M., 2007: *Formation Flying of Commercial Aircraft, Variations in Relative Size/Spacing - Induced Effects & Control*, in: Fluid Dynamics and Co-located Conferences, AIAA, doi:10.2514/6.2007-4163.

- Okolo, W., Dogan, A., and Blake, W. B., 2014: *A Modified Analysis of Alternate Lateral Trimming Methods for Flying Wing Aircraft at Sweet Spot in Formation Flight*, in: AIAA SciTech Forum, AIAA, doi:10.2514/6.2014-0543.
- Sausen, R., Isaksen, I., Grewe, V., Hauglustaine, D., Lee, D., Myhre, G., Köhler, M., Pitari, G., Schumann, U., Stordal, F., et al., 2005: *Aviation radiative forcing in 2000: An update on IPCC (1999)*, Meteorol. Z., 14, 555–561.
- Smolarkiewicz, P. and Margolin, L.: *On Forward-in-Time Differencing for Fluids: an Eulerian/Semi-Lagrangian Non-Hydrostatic Model for Stratified Flows*, in: Numerical Methods in Atmospheric and Oceanic Modelling: The André J. Robert Memorial Volume, edited by Lin, C., Laprise, R., and Ritchie, H., vol. 35, pp. 127–152, Canadian Meteorological and Oceanographical Society, Ottawa, Canada, 1997.
- Smolarkiewicz, P. and Margolin, L., 1998: *MPDATA: A Finite-Difference Solver for Geophysical Flows*, J. Comput. Phys., 140, 459–480.
- Sölch, I. and Kärcher, B., 2010: *A large-eddy model for cirrus clouds with explicit aerosol and ice microphysics and Lagrangian ice particle tracking*, Q. J. R. Meteorol. Soc., 136, 2074–2093.
- Unterstrasser, S., 2014: *Large eddy simulation study of contrail microphysics and geometry during the vortex phase and consequences on contrail-to-cirrus transition*, J. Geophys. Res., 119, 7537–7555.
- Unterstrasser, S., 2016: *Properties of young contrails - a parametrisation based on large-eddy simulations*, Atmos. Chem. Phys., 16, 2059–2082.
- Unterstrasser, S. and Görsch, N., 2014: *Aircraft-type dependency of contrail evolution*, J. Geophys. Res., 119, 14,015–14,027.
- Unterstrasser, S. and Stephan, A., 2020: *Far field wake vortex evolution of two aircraft formation flight and implications on young contrails*, The Aeronautical Journal, doi:10.1017/aer.2020.3.
- Unterstrasser, S., Gierens, K., Sölch, I., and Lainer, M., 2017a: *Numerical simulations of homogeneously nucleated natural cirrus and contrail-cirrus. Part 1: How different are they?*, Meteorol. Z., 26, 621–642.
- Unterstrasser, S., Gierens, K., Sölch, I., and Wirth, M., 2017b: *Numerical simulations of homogeneously nucleated natural cirrus and contrail-cirrus. Part 2: Interaction on local scale*, Meteorol. Z., 26, 643–661.
- Xu, J., Ning, S., Bower, G., and Kroo, I., 2014: *Aircraft Route Optimization for Formation Flight*, J. Aircraft, 51, 490–501, doi:10.2514/1.C032154.

A MODEL STUDY ON CONVECTIVELY GENERATED GRAVITY WAVE AND TURBULENCE

W.J. Sang¹

¹ Department, Civil Aviation Flight University of China, China, sangwj@cafuc.edu.cn

Abstract. Atmospheric turbulence is one of hazards that can affect aircraft in flight. Using a cloud-resolving large eddy model (LEM), we investigate how gravity wave and turbulence motivated by overshooting convection near the tropopause. We design and conduct a series of sensitivity experiments to diagnose the physical and dynamical generation mechanisms of turbulence caused by convection. The three-dimensional LEM simulations capture the bulk properties of the target case and track microphysical processes using a three-phase microphysical parameterization. The model results indicate that the net effect of overshooting convection on lower stratospheric water content is moistening, primarily due to gravity wave breaking and ice sublimation. Gravity wave activity caused by convection near the tropopause features prominently in these cases. Also, it is found that increased turbulence exchange coefficient near the tropopause correspond to gravity wave breaking well. We have also discussed the feature of convectively generated gravity waves that lead to aviation turbulence.

Keywords: turbulence, gravity wave, deep convection, model, tropopause

REFERENCES

Sang Wenjun; Huang Qian; Tian Wenshou; Wright Jonathon S; Zhang Jiankai; Tian Hongying; Luo Jiali; Hu Dingzhu; Han Yuanyuan; A large eddy model study on the effect of overshooting convection on lower stratospheric water vapor, 2018, J. Geophys. Res., 2018, 123(18): 10023-10036.

MITIGATING CLIMATE IMPACT OF AVIATION BY MINIMIZING AIRCRAFT CONTRAILS

Ulrich Schumann¹, Roger Teoh², and Marc E. J. Stettler²

¹ *Deutsches Zentrum für Luft- und Raumfahrt (DLR), Institut für Physik der Atmosphäre, Oberpfaffenhofen Germany*

² *Centre for Transport Studies, Department of Civil and Environmental Engineering, Imperial College London, London, United Kingdom*

Abstract. For growing air traffic the climate impact of aviation will increase mainly because of slow but long-lasting CO₂ concentration increases in the atmosphere from aircraft burning fossil fuel. The CO₂ enhances the greenhouse effect of the atmosphere globally with positive radiative forcing (RF). The RF from aviation-CO₂ emissions in the past until today very likely caused a slow global warming which keeps increasing for many years even for constant emissions. Besides by fossil CO₂ emissions, aviation impacts climate also by non-CO₂ effects. Among the non-CO₂ effects, contrails and contrail-induced changes of clouds and related atmosphere properties impact the radiative budget of the Earth-atmosphere system at rather short time scales (hours to days) nearly in proportion to the instantaneous traffic, regardless of history. The contrail RF impacts climate not only globally over centuries but also regionally at weather time scales (days). The regional RF and the global RF from contrails and the related surface climate changes have different dynamics, possibly with different signs. For example global changes are mitigated by the thermal inertia of the oceans. Regional effects occur like regional weather. Contrail RF can be predicted for given and for alternative traffic with an available model and with available weather prediction data, quasi operationally. Contrail RF is positive (warming) during night but may, under certain circumstances, be negative (cooling) during day time. Both, a reduction of positive radiative forcing from non-CO₂ effects and an increase of negative RF when occurring may help to reduce or at least retard the climate impact of aviation. Ignoring the latter option by far underestimates the related mitigation potential. This idea is not new, but only a few studies have been performed to assess the contrail climate impact quantitatively and to assess its uncertainties. In this paper we first summarize the results of a recent study of contrail formation and its radiative forcing for regional traffic. In addition we discuss the relative importance of contrail formation and CO₂ emissions on long term global mean surface temperature climate change. Finally we sketch an approach to reduce the uncertainties in assessing the surface climate impact from contrails and related cirrus clouds

Keywords: Climate impact, contrails, CO₂, mitigation potential, efficacy

Recently, the climate forcing impact of aviation by contrails has been studied using the Contrail Cirrus Prediction Model CoCiP (Schumann 2012), together with a new Fractal Aggregates (FA) model of soot number emissions (Teoh et al. 2019), high resolution ECMWF reanalysis data, an aircraft performance model (BADA3 from EUROCONTROL), and a new Monte Carlo method to estimate uncertainties from input data, for six weeks of traffic data available for Japan airspace (CARATS) (Teoh et al. 2020). The mean contrail-induced energy forcing (EF, integral of local contrail Radiative Forcing (RF) over lifetime and contrail cover) per flight distance, about 53 MJ m⁻¹, was found to be 1.6 times higher than the CO₂ EF for a 100-yr time horizon. The EF can be related to the often used Absolute Global Warming Potential (AGWP). Only a small fraction of traffic causes most of the contrail EF. Part of the climate forcing by contrails can be reduced even without extra fuel consumption. Hence, this is an attractive approach.

The method is suited to be extended globally and applied operationally for climate-optimized air traffic. As a new finding, we note that the same approach has been applied also for traffic in the North Atlantic. Here we find that the fraction of flights causing contrails also depends on whether most of the traffic follows the same set of limited oceanic routes or is distributed randomly.

The ratio of climate impact by contrails relative to that by CO₂ can be quantified using various metrics, see Fig. 1. The diagram is computed following older ideas (Sausen and Schumann 2000) and recently published relationships (Fuglestad et al. 2010; Joos et al. 2013) and input data consistent with the cited study for contrails and Japanese traffic (mean contrail EF

= 5.4×10^8 J/m, mean aviation fuel consumption per flight distance = 4.5 g/m). Details will be described and discussed in the extended paper. Taking this figure qualitatively, the figure shows that aviation causes higher absolute global warming potential (AGWP) by forming contrails than by the related fuel consumption/CO₂ emissions, for several decades. The contrail induced AGWP may dominate aviation-CO₂ induced AGWP for more than two centuries. However, the contrail RF induces a heat pulse while CO₂-RF causes warming distributed over a longer time period, and because of finite thermal Earth-Ocean inertia, the surface temperature increase from contrails cools to space more quickly than the CO₂ induced heat so that the ratio of Absolute Global Temperature Change Potentials (AGTP) from contrails and CO₂ is lower. In terms of AGTP, contrails, with the given parameters, may exceed the related CO₂ effects for about 40 years. The temperature change-ratio from contrail RF relative to that from CO₂ RF defines the efficacy. The efficacy depends among others on how quickly heat induced by contrails in the upper troposphere gets transported downward to the surface (Schumann and Mayer 2017). Because of short lifetime of atmospheric temperature changes (hours to weeks), much of the contrail warming disappears to space before reaching the oceans representing most of Earth's thermal inertia. For the global climate system and long time periods various feedback mechanisms, like changes in upper tropospheric cloudiness are also important (Bickel et al. 2020). For low efficacy the time during which contrails may cause more warming than the related CO₂ emissions is much smaller. All this gets complicated by the fact that traffic and weather-dependent regional response patterns may differ from the global mean climate response pattern. The true value of the efficacy is essentially unknown and may be outside the range 0.4 to 1. Hence, in order to assess the climate impact of contrails we need to know far more than RF or EF or AGWP of contrails and aviation fossil fuel consumption.

In particular we need to know more about how contrails or thin cirrus in general heat or cool the Earth surface and cause other climate changes on Earth. The paper will lay out a strategy, using long time series of observed and modelled weather elements, including thin high-level clouds as a surrogate for contrail cirrus, to reduce present uncertainty in an otherwise attractive mitigation procedure

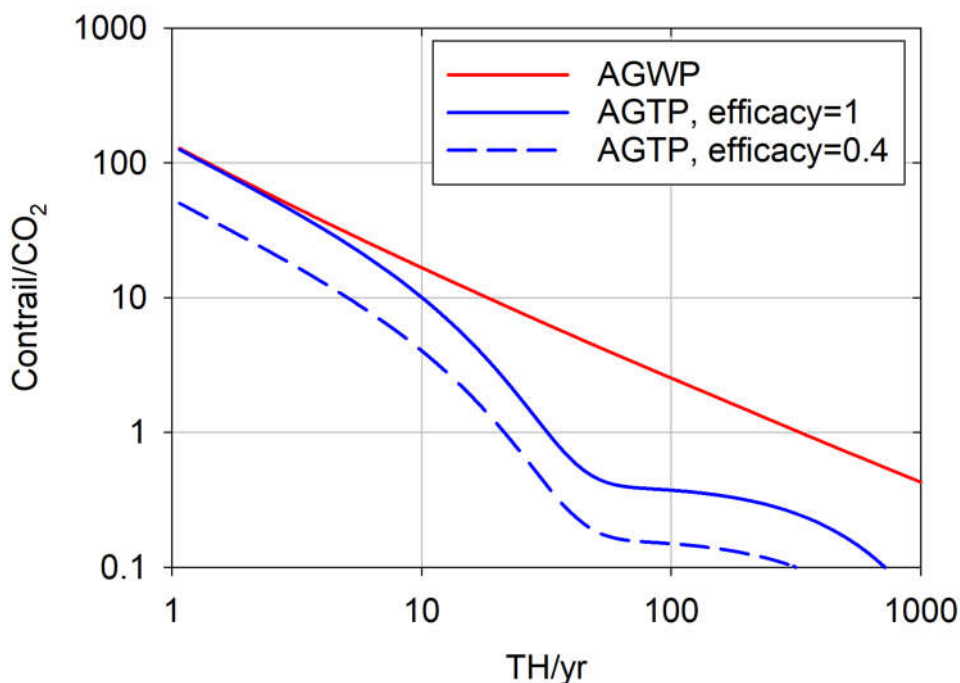


Figure 1. Ratio between climate effects in terms of global mean surface temperature changes from contrails and from CO₂ versus time horizon TH in years in two metrics: Absolute Global Warming Potential (APWG, red) and Absolute Global Temperature Potential (AGTP, blue), for two values of the efficacy (1. and 0.4, full and dashed lines).

REFERENCES

- Bickel, M., M. Ponater, L. Bock, U. Burkhardt, and S. Reineke, 2020: Estimating the effective radiative forcing of contrail cirrus. *J. Clim.*, **33**, 1991-2005, doi: 10.1175/JCLI-D-19-0467.1.
- Fuglestedt, J. S., K. P. Shine, T. Berntsen, J. Cook, D. S. Lee, A. Stenke, R. B. Skeie, G. J. M. Velders, and I. A. Waitz, 2010: Transport impacts on atmosphere and climate: Metrics. *Atmos. Env.*, **44**, 4648-4677, doi: 10.1016/j.atmosenv.2009.04.044.
- Joos, F., R. Roth, J. S. Fuglestedt, and Coauthors, 2013: Carbon dioxide and climate impulse response functions for the computation of greenhouse gas metrics: a multi-model analysis. *Atmos. Chem. Phys.*, **13**, 2793–2825 doi: 10.5194/acp-13-2793-2013.
- Sausen, R., and U. Schumann, 2000: Estimates of the climate response to aircraft CO₂ and NO_x- emission scenarios. *Climatic Change*, **44**, 27 – 58
- Schumann, U., 2012: A contrail cirrus prediction model. *Geosci. Model Dev.*, **5**, 543–580, doi: 10.5194/gmd-5-543-2012.
- Schumann, U., and B. Mayer, 2017: Sensitivity of surface temperature to radiative forcing by contrail cirrus in a radiative-mixing model. *Atmos. Chem. Phys.*, **17**, 13833–13848, doi: 10.5194/acp-17-13833-2017.
- Teoh, R., M. E. J. Stettler, A. Majumdar, U. Schumann, B. Graves, and A. Boies, 2019: A methodology to relate black carbon particle number and mass emissions. *J. Aeros. Sci.*, **132**, 44-59, doi: 10.1016/j.jaerosci.2019.03.006.
- Teoh, R., U. Schumann, A. Majumdar, and M. E. J. Stettler, 2020: Mitigating the climate forcing of aircraft contrails by small-scale diversions and technology adoption. *Env. Sci. Techn.*, doi: 10.1021/acs.est.9b0560.

IMPACT ON CONTRAILS COVERAGE WHEN FLYING WITH HYBRID ELECTRIC AIRCRAFT

F. Yin¹, V. Grewe² & K. Gierens²

¹ Faculty of Aerospace Engineering, Delft University of Technology, the Netherlands, F.yin@tudelft.nl

² Deutsches Zentrum für Luft- und Raumfahrt, Institut für Physik der Atmosphäre, Oberpfaffenhofen, Germany

Abstract Aviation is responsible for approximately 5% of global warming and is expected to increase substantially in the future. In the face of the continuing expansion of air traffic, mitigation of the aviation's climate impact becomes challenging, but imperative. Among various mitigation options, hybrid electric aircraft (HEA) has drawn intensive attention due to its large potential in reducing the greenhouse gas emissions. The non-CO₂ effects (especially the contrails) of the HEA on the climate change, however, remains ambiguous. As the first step to understand the climate impact of HEA, this research aims to investigate the impact on the formation of persistent contrails when flying with HEA. The simulation is performed using the Earth System model (EMAC) coupled with a CONTRAIL submodel, where the Schmidt Appleman Criterion (SAC) is adapted to estimate changes in the potential contrail coverage (PCC) globally. The analysis shows that the HEA forms contrails at relatively lower temperature than conventional aircraft. At the same altitude, the reduction in contrails formation is mainly observed in the tropical regions where the temperature is warmer. With a smaller fraction of electric power in use, the contrail coverage remains nearly unchanged. As the degree of hybridization increases further to 90%, an exponential reduction in the contrail formation is expected with a maximum value of about 40%.

Keywords: Contrail formation; hybrid electric aircraft; degrees of hybridization; seasonal effects; regional effects

INTRODUCTION

Aviation is responsible for approximately 5% of the anthropogenic causes to global warming and is expected to increase substantially in the future. In the face of the continuing expansion of air traffic, mitigation of the aviation's climate impact becomes challenging, but imperative. Among various mitigation options, hybrid electric aircraft (HEA) is drawing intensive attention due to its large potential in reducing the greenhouse gas emissions. Regional/narrow body aircraft are the most promising candidates for this technology (Gladin et al, 2017). On longer-range flights, the additional weight of the electric propulsion system makes it difficult to achieve any substantial fuel saving. Multiple studies have shown that the hybrid electric configuration can reduce the fuel burn in regional flights by around 7-10% with the envisaged 2030-2035 technology in comparison to conventional propulsion system (Gladin et al, 2017; Ang et al, 2019).

The climate impact of HEA, however, remains ambiguous, as the climate impact of aviation includes both CO₂ and non-CO₂ effects from NO_x, H₂O and contrails. The non-CO₂ effects depend not only on the emission quantity but also the geographical location, altitude, time and the local weather condition. Furthermore, among those non-CO₂ effects, the contrails climate impact is more than 50% (Lee et al, 2009, Grewe et al, 2017). As the first step towards understanding of the climate impact of HEA, this research aims to investigate the impact on the formation of persistent contrails when flying with HEA. A parallel hybrid configuration is considered.

The paper is organized as follows: section 2 describes the modelling approach to estimate the potential contrails coverage (PCC) of HEA; section 3 presents the results; finally the conclusions are drawn in section 4.

METHODOLOGY

To predict the PCC by the hybrid electric aircraft, an earth system model (EMAC) coupled with a CONTRAIL submodel is used.

Model framework

The ECHAM/MESSy Atmospheric Chemistry (EMAC) model is a numerical chemistry and climate simulation system that includes submodels describing tropospheric and middle atmosphere processes and their interaction with oceans, land and human influences (Jöckel et al, 2010). For the present study, we applied EMAC (ECHAM5 version 5.3.02, MESSy version 2.52.0) in the T42L31ECMWF-resolution, corresponding to the horizontal grid of about 310km and the vertical resolution of roughly 1 km up to an altitude of roughly 30 km. The simulation time step is 12 minutes. Such a model resolution will provide us with reasonable weather data to calculate the contrail coverage.

The CONTRAIL is one of the submodels in EMAC, which has been developed by Frömming et al. (supplement of Grewe et al, 2014) to calculate the PCC as the difference between the maximum possible coverage of both contrails and cirrus and the coverage of natural cirrus alone. Here we use the CONTRAIL V1.0. The PCC is calculated instantaneously with the EMAC resolution. The threshold for contrail formation is determined using the well-known Schmidt Appleman Criterion (SAC), which will be presented in the next section.

Parameterization of SAC

The contrails form when the mixture of engine exhaust and ambient air reaches water saturation at the sufficient low temperature, and they persist when the ambient air is ice-supersaturated. The mixing process is assumed to be isobaric, therefore, the mixing trajectory is a straight line showing on the T-e diagram (see fig (1) of Gierens et al. (2008); e is the partial pressure of water vapor in the mixture; T is the static temperature of the mixture). The slope of this straight line (G), indicating the threshold of contrail formation, is given by the SAC and calculated using Eqn. (1).

$$G = \frac{p \cdot c_p \cdot EI_{H_2O}}{\varepsilon \cdot Q \cdot (1 - \eta_{orig})} \quad (1)$$

where p is the ambient pressure; ε is the ratio of molar mass of water vapor and dry air (0.622 constantly); c_p is the isobaric heat capacity of air (1004 J/kg/K); Q is the lower heating value of fuel; EI_{H_2O} is the water vapor emission index; η_{orig} is the overall efficiency of the original system.

As for the HEA, the original SAC is adapted following the energy conservation process as described in Eqn.(2)-(3) to consider the effects of various degrees of hybridization.

$$G_{HEA} = \frac{p \cdot c_p \cdot EI_{H_2O}}{\varepsilon \cdot Q \cdot (1 - \eta_{HEA})} \quad (2)$$

where η_{HEA} is a pseudo overall efficiency of the HEA system and is recalculated as in Eqn.(3) and the rest of the parameters remain identical as in Eqn. (1).

$$\eta_{HEA} = \eta_{orig} \cdot \left(1 - \frac{1 - \eta_{elec}}{1 - frac} \cdot \frac{frac}{\eta_{elec}}\right) \quad (3)$$

where η_{elec} is the efficiency of the electric part and is assumed as 0.8 in the current study; *frac* is the fraction of electric power over the overall energy consumption, varying from 0 to 0.99, and the value of 1 indicates a fully electric system with no formation of contrails, whereas the value of 0 indicates no electric power is used. The original SAC in Eqn. (1) is valid; η_{orig} is the efficiency of the original system. We call η_{HEA} pseudo efficiency, since it only reflects that part of the overall efficiency of the aircraft, which relates the power output to the chemical energy from the used kerosene and corrects for the part of the electricity used.

RESULTS

The threshold of contrail formation calculated by SAC

Based on the Eqn. (1)-(3), the parameters for SAC on different aircraft are calculated and given in Table 1. The numbers are calculated at the altitude of 11 km. In Fig. 1, we present three tangential mixing trajectories: one for conventional aircraft with the overall efficiency of

0.4, one for HEA with 45% hybridization, and one for HEA with 80% hybridization. The HEA forms contrails at lower temperatures than conventional aircraft, mainly because the efficiency is smaller due to the extra energy loss through the powertrain.

Table 1: Calculated parameters for the Schmidt Appleman criterion on hybrid electric aircraft

Parameters	Descriptions	HEA (elec.%)			Conv. aircraft	Units
		10%	45%	80%		
EI _{H₂O}	Water emission index		1.25		1.25	kg/kg(fuel)
η	Overall (pseudo for HEA) efficiency	0.39	0.32	0.	0.4	[-]
Q	Lower heating value of the fuel		43.2		43.2	MJ/kg
G	Slope at 11km	1.7	1.6	1.1	1.8	Pa/K

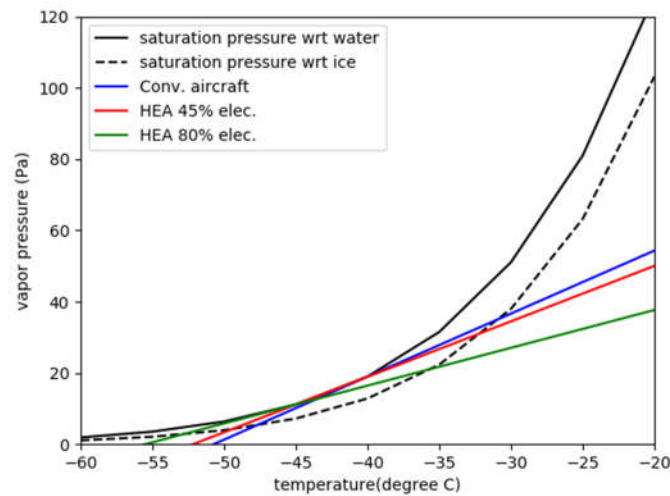


Figure 1: Water vapour pressure vs. temperature phase diagram representing thermodynamics of contrail formation for a conventional aircraft with overall propulsion efficiency of 0.31 (blue line) and for HEA with two different degrees of hybridization: 45% electric power (red line) and 80% electric power (green line). The two black curves are the saturation vapour pressure curves for water (solid) and with respect to ice (dashed).

Changes in the formation of contrails

The PCC for conventional aircraft at 250hPa on a specific day is presented in Fig.2(a), whereas, the changes in PCC caused by 50% hybridization of HEA at the same altitude is given in Fig.2(b). What can be seen is when flying HEA with 50% electric power, the PCC at tropical region can be reduced substantially, since the HEA forms contrails at relative lower temperature.

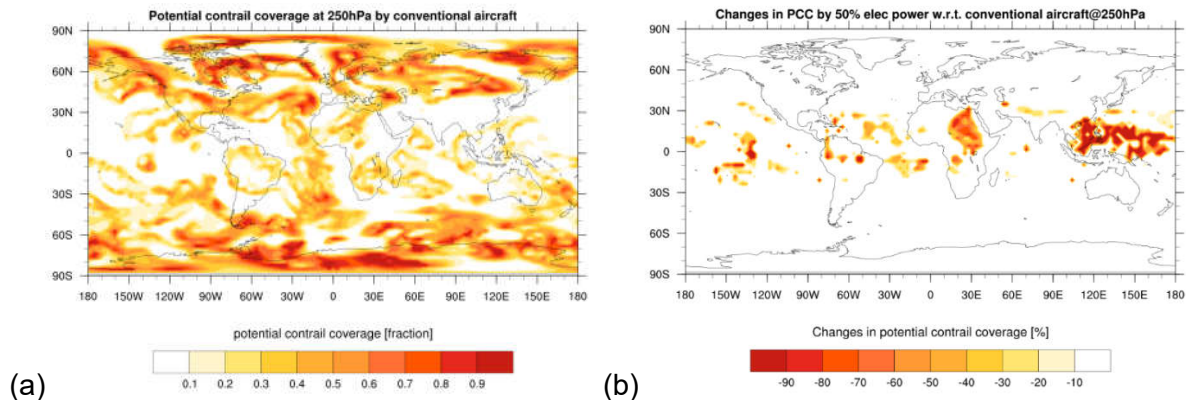


Figure 2: The PCC at 250 hPa on a specific day: (a) conventional aircraft; (b) changes caused by HEA with 50% electric power.

The hybridization effects on the formation of contrails

In Fig.3, we present a statistical analysis on the reduction of contrail coverage when different degrees of hybridization are considered. What we observe is that with a smaller fraction of electric power in use, the contrail coverage remains nearly unchanged. As the hybridization rate increases from 30%-90%, an exponential reduction trend can be expected with a maximum value of about 40%.

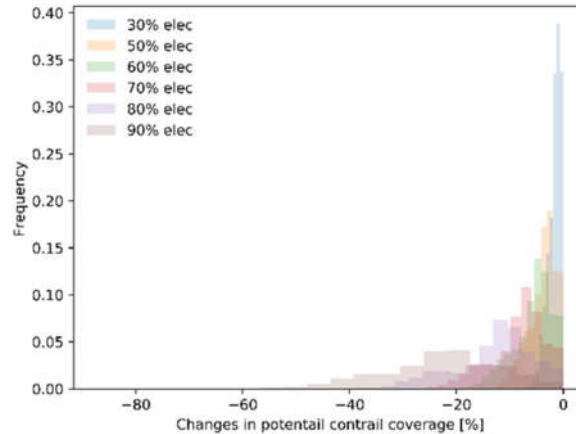


Figure 3: Variation of the reduction in PCC with respect to different degrees of hybridization.

CONCLUSIONS

This paper presents the changes in potential contrail coverage when flying with the hybrid electric aircraft. Based on the analysis, the following conclusions are drawn:

- The hybrid electric aircraft forms contrails at the lower temperature than conventional aircraft.
- The reduction in contrail formation by hybrid electric aircraft mostly happens at tropical region where the temperature is higher.
- With a smaller degrees of hybridization (below 30% in the current study), the contrail coverage remains nearly unchanged. A maximum reduction of about 40% in contrail coverage can be achieved with 90% electric power in use.

A further analysis will be conducted to analyse the seasonal and regional effects on the changes of potential contrail coverage when flying with the hybrid electric aircraft.

REFERENCES

- Ang, A., Gangoli Rao, A., Kanakis, T. and Lammen, W., 2019. *Performance analysis of an electrically assisted propulsion system for a short-range civil aircraft*, Proceedings of the Institution of Mechanical Engineers, Part G: Journal of Aerospace Engineering, vol. 233, nr. 4, pp. 1490-1502.
- Gierens, K., Lim, L. and Eleftheratos, K., 2008. *A Review of Various Strategies for Contrail Avoidance*, The Open Atmospheric Science Journal, 2, pp. 1-7.
- Gladin, J., Perullo, C., Tai, J. and Mavris, D., 2017. *A Parametric Study of Hybrid Electric Gas Turbine Propulsion as a Function of Aircraft Size Class and Technology Level*, in 55th AIAA Aerospace Sciences Meeting. Grapevine, Texas.
- Grewe, V., Dahmann, K., Flink, J., Frömming, C., Ghosh, R., Gierens, K., Heller, R., Hendricks, J., Jöckel, P., Kaufmann, S., Kölker, K., Linke, F., Luchkova, T., Lührs, B., Van Manen, J., Matthes, S., Minikin, A., Niklaß, M., Plohr, M., Righi, M., Rosanka, S., Schmitt, A., Schumann, U., Terekhov, I., Unterstrasser, S., Vázquez-Navarro, M., Voigt, C., Wicke, K., Yamashita, H., Zahn, A. and Ziereis, H., 2017. *Mitigating the Climate Impact from*

- Aviation: Achievements and Results of the DLR WeCare Project*. Aerospace. 4(3), pp. 1-34.
- Grewe, V., Frömming, C., Matthes, S., Brinkop, S., Ponater, M., Dietmüller, S., Jöckel, P., Garny, H., Tsati, E. and Dahlmann, K., 2014. *Aircraft routing with minimal climate impact: the REACT4C climate cost function modelling approach (V1.0)*, Geosci. Model Dev., 7, pp. 175-201.
- Lee, D.S., Fahey, D.W., Forster, P.M., Newton, P.J., Wit, R.C.N., Lim, L.L., Owen, B. and Sausen, R., 2009. *Aviation and global climate change in the 21st century*. Atmospheric Environment. 43(22–23), pp. 3520-3537.
- Jöckel, P., Kerkweg, A., Pozzer, A., Sander, R., Tost, H., Riede, H., Baumgaertner, A., Gromov, S. and Kern, B., 2010. *Development cycle 2 of the Modular Earth Submodel System (MESSy2)*, Geosci. Model Dev., 3(2), pp. 717-752.
- Jöckel, P., Tost, H., Pozzer, A., Kunze, M., Kirner, O., Brenninkmeijer, C. A. M., Brinkop, S., Cai, D. S., Dyroff, C., Eckstein, J., Frank, F., Garny, H., Gottschaldt, K. D., Graf, P., Grewe, V., Kerkweg, A., Kern, B., Matthes, S., Mertens, M., Meul, S., Neumaier, M., Nützel, M., Oberländer-Hayn, S., Ruhnke, R., Runde, T., Sander, R., Scharffe, D., and Zahn, A., 2016. *Earth System Chemistry integrated Modelling (ESCiMo) with the Modular Earth Submodel System (MESSy) version 2.51*, Geosci. Model Dev., 9(3).

THE ROLE OF ELECTRIC-POWERED FLIGHT IN REAL-WORLD COMMERCIAL OPERATIONS

A. Sobron¹, I. Staack¹ & P. Krus¹

¹ Department of Management and Engineering, Linköping University, Sweden, alejandro.sobron@liu.se

Abstract. Following the electrification of the automotive sector, the idea of electric-powered flight for commercial air transportation is becoming, in the eye of the public, the main hope for greener air transportation. To what extent can electric aircraft reduce the energy and environmental footprint of aviation? How should they look like and how does their operation compare to conventional jet aircraft? What technologies are needed, and which of them are already in place? This paper analyses critically some of the unresolved challenges that lay ahead. Current commercial operations are examined and short-term effects of electrification are identified. Fundamental components, basic design and operating concepts are analysed to highlight unavoidable constraints that seem often overlooked. It becomes clear that electric propulsion alone will not fully meet society's expectations even if key enabling technologies develop as forecasted. Nevertheless, this paper suggests that electrification may instead become one piece of a propulsion-technology mix that would address more effectively our short- and long-term goals.

Keywords: Electric aircraft, electric propulsion, low-emissions, air transportation, future concepts.

INTRODUCTION

In the middle of a market pull for sustainable transportation and influenced by the current transition of the automotive sector, electric propulsion is often presented to the public as a key enabler for urban mobility and a potential solution to the growing demand for greener air-transportation. Indeed, civil aviation faces the enormous challenge of absorbing the ever-increasing demand while simultaneously reducing its environmental footprint. Both industry and policymakers have set ambitious goals that go beyond what the current technologies can provide with simple evolutionary improvements (Darecki *et al.*, 2011)(U.N., 2020). I search of more radical solutions to meet these goals; electrification has emerged as a popular candidate. Besides the longstanding efforts to electrify on-board systems (*More-Electric Aircraft*), there is a recent boom in the number of projects that present electric (or hybrid-electric) powertrains as the next paradigm in aircraft propulsion. But, in the near term, are electric-powered aircraft our best strategy to overcome civil aviation's global challenges? The prevalent claims made in civil electric-powered aircraft projects are summarised and briefly discussed in Figure 1. Considering the respective counterarguments found both in literature and in preliminary studies, the primary reason to implement electric propulsion would just be the potential reduction in environmental impact. Assuming green electricity supply and leaving noise, raw materials, and lifecycle concerns aside; the environmental impact can be associated with the amount of energy used and the corresponding emissions produced. This paper aims to shed some light on this matter.

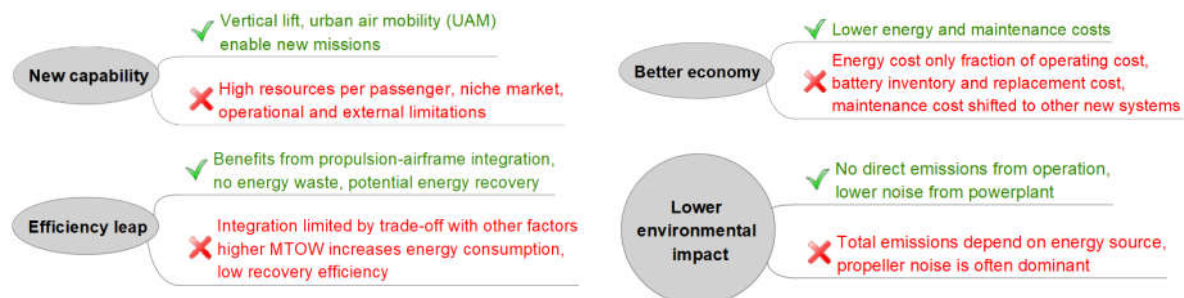


Figure 1. Commonly claimed electric-propulsion benefits for civil air transport along with some corresponding objections or limitations.

ELECTRIC FLIGHT CHALLENGES

There are numerous underlying challenges for the introduction of electric-powered aircraft in commercial service. Fig. 2 presents a collection of identified issues of different nature. Due to space limitations, only few engineering aspects with a significant effect on aircraft design and operation are briefly commented here.



Figure 2. Some of the identified challenges for electric-powered commercial flight.

Energy storage and operating flexibility

An intrinsic disadvantage of electric propulsion derives from its energy storage system: a typical battery carries all its elements on-board during any mission. This increases the gross weight of the aircraft (increasing also manufacturing and operating costs) and degrades its performance. Furthermore, it eliminates all flexibility from the payload-range trade-off, as shown in Fig.3-left. Performance is strongly correlated to the weight of the integrated battery system and the actual available energy for a typical mission, which differs significantly from nominal values of single cells. Fig. 3-right presents an example of these differences.

Mission and turnaround time

For the time being, most applications are based on electric motors driving propellers. This lowers the efficient cruise speeds under those of turboprops and extends the flight duration. Furthermore, a slow turnaround caused by battery recharging could impact regional operators.

Power transmission and management

Managing the high voltage and current as well as thermal losses in multi-megawatt systems is not a trivial problem. For instance, current integrations of power electronics in smaller electro-mechanic flight actuation systems already show a large impact on weight, volume, and cost.

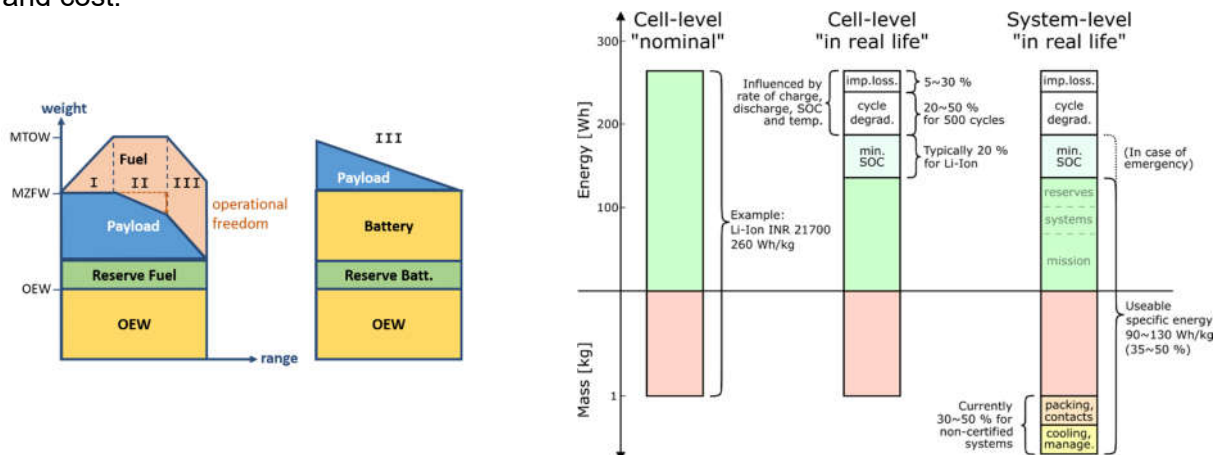


Figure 3. Two often-overlooked factors with important consequences for flight operations: Loss of mission flexibility in payload-range (left), and degradation of nominal specific energy after battery integration and regular use (right).

POTENTIAL IMPACT ON CURRENT CIVIL AIR TRANSPORTATION

Assuming all these challenges can be overcome and time is not an issue, how much impact could electrification have in a market that is not significantly disrupted? An estimation was done by studying all commercial operations to, from, and inside the U.S. during the year 2017 (U.S. Department of Transportation, 2019). From the logistic point of view, the volume of payload is more representative for productivity and energy consumption than the number of flights. Fig.4 shows the distribution per stage length and aircraft class, along with the accumulated total.

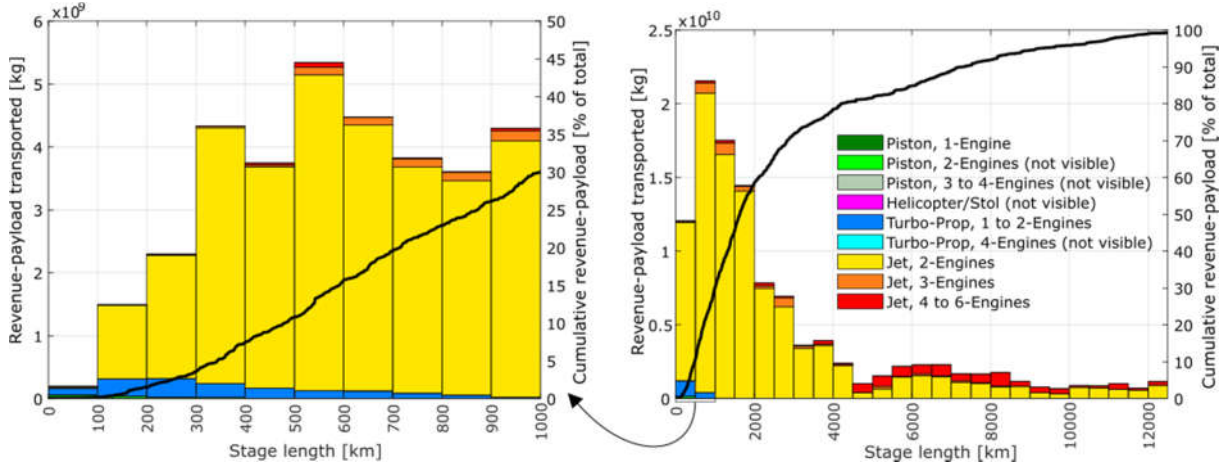


Figure 4. Revenue-payload by stage length for passenger and cargo flights to, inside, and from the U.S. during 2017. Black solid line represents the cumulative fraction of the total. Raw data from U.S. Department of Transportation (2019).

A model of energy consumption per stage length and aircraft class was derived from reported refuelling data from the same source. This model was applied back to the observed distribution of aircraft types and operations to estimate the total energy consumption. According to these results, shown in Fig.5, performing all commercial flights under 500 km (about 25% of the departures and 10% of the payload) with full-electric aircraft would shift about 5% of the total energy consumption. The magnitude of operation-related emissions saved could be similar, assuming a proportional relation between energy consumption and emissions derived from fuel production and combustion (Hileman *et al.*, 2008). Nevertheless, there are additional factors that could motivate both a lower relative impact (high-altitude effects, condensation clouds), or a higher relative impact (local noise and pollution in communities close to airfields).

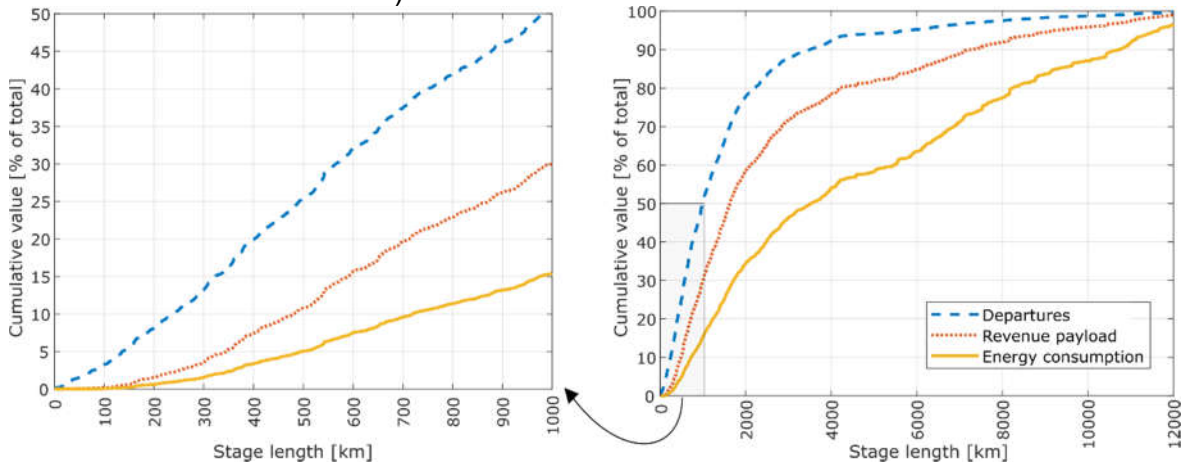


Figure 5. Distribution of number of departures, revenue-payload, and estimated energy consumption according to stage length for passenger and cargo flights to, inside, and from the U.S. during 2017. Elaborated with data from U.S. Department of Transportation (2019).

KEY ENABLERS AND ALTERNATIVE CONCEPTS

While high-power electric motors are readily available and have desirable physical characteristics (efficiency envelope, reversibility, scalability), the bottlenecks of an aircraft electric powertrain are currently the power transmission (conduction, conversion losses and physical limitations for multi-megawatt systems) and especially the energy storage. Indeed, performance and weight of batteries are the main limiting factor for mission range (Hepperle, 2012), especially considering the current regulations on mandatory energy reserves for commercial operations (ICAO, 2016). Both superconducting materials and battery technology are thus key enablers for the electrification of flight, at least beyond the general aviation sector.

Alternatively, allowing for other types of energy transformations in the propulsion system (such as thermal engines and fuel cells), there are fuel types with a good potential for large-scale use in aircraft: alternative, synthetic or bio liquid fuels; gaseous fuels like LNG, LPG; and pressurized or cryogenic hydrogen. It is likely that, for any given aircraft size and range requirement, one of these primary energy sources in combination with a dedicated (possibly hybrid) system architecture could offer the best compromise in terms of overall consumed energy (well-to-wing), environmental footprint, time to market, and costs. Despite an increase in technical complexity, interesting synergies could also be obtained from the combination of these technologies. A good example is the possibility of using liquid hydrogen both as main fuel and as coolant for a high-power electric system based on superconductors, where the electrical losses would also help boiling off the fuel (Smith, 2014).

CONCLUSION

Reducing the operating environmental impact of commercial operations seems the only practical reason to electrify aircraft propulsion. Despite remaining regulatory and engineering challenges, the current technology could soon allow the development of full-electric, fixed-wing commuters in the 10-19 passenger-class for very short missions. However, some of the intrinsic characteristics of such an electric aircraft (heavier T-O weight, intensive battery cycling and inventory, lower availability) may challenge the economical and operational feasibility of such operations. According to estimations based on the current market, full electrification of all missions below 500 km could shift about 5% of the energy consumed by civil air operations; an impact perhaps attainable with simpler initiatives. Besides enabling improvements in battery technology, superconductors, and regulatory standards; a stronger impact could perhaps be achieved in coexistence with other technologies. Alternative fuels such as biofuels in the short term, and hydrogen in the medium/long-term are suggested here as potentially interesting technologies to reach aviation's environmental goals in time.

REFERENCES

- Darecki M *et al.*, 2011. *Flightpath 2050. Technical Report 28*. European Commission.
- Hepperle M, 2012. *Electric flight – Potential and limitations*. In *Energy Efficient Technologies and Concepts of Operation*, NATO RTO, Lisbon, Portugal.
- Hileman *et al.*, 2008. *Payload fuel energy efficiency as a metric for aviation environmental performance*. In *Proceedings of 26th Congress of International Council of the Aeronautical Sciences*, pp. 3314-3324. Anchorage, USA.
- ICAO, 2016. *Operation of aircraft – Annex 6 to the convention on international civil aviation*, 10th edition. International Civil Aviation Organization, Quebec, Canada.
- Smith H, 2014. *Airframe integration for an LH2 hybrid-electric propulsion system*. *Aircraft Engineering and Aerospace Technology*, Vol. 86 No. 6, pp. 562-567.
- United Nations (U.N.), 2020. *The U.N. sustainable development goals*. Online, accessed 07-01-2020.
- United States (U.S.) Department of Transportation – Bureau of Transportation Statistics, 2019. *Air Carrier Summary Data year 2017 (Form 41 and 298C Summary Data)*. Online, accessed 04-12-2019.

AENA PHOTOVOLTAIC PLAN

P. Lopez¹, A. Brea & A. Salazar

¹ AENA S.M.E. SA (AENA), Calle Arturo Soria 109, Madrid 28043, Spain, pjlloeches@aena.es

Abstract. The climate change emergency is one of the most worrying long-term global environmental problem, and its mitigation and adaptation of its effects, one of the significant challenges for States and organizations around the planet.

In this regard, and in line with global energy saving and efficiency policies and the internationally agreed greenhouse gas (GHG) emission reduction commitments, AENA has developed its Climate Change Strategy with the main objective of achieving a progressive decrease in CO₂ emissions derived from our activity through the following lines of work:

- Energy efficiency
- Energy supply from renewable energies
- Reduction of fuel emissions
- Reduction of third-party emissions

Among all these actions, we recently launched an ambitious initiative the AENA Photovoltaic Plan. This will allow Aena to reach 70% of the energy supply in self consumption from solar energy due to the installation of photovoltaic panels in the airports of the AENA network, avoiding the emission of 167,000 tons of CO₂ into the atmosphere each year.

This Plan, with a capital investment of 250 million euros until 2026, which will place AENA as a leading company among European airports for the production of renewable energy in self-consumption (650 GWh/year), and will allow AENA to achieve the following objectives:

- 2025: Reduction of 40% of CO₂ / Traffic Unit
- 2030: Reach carbon neutrality according with level 3+ of Airport Carbon Accreditation in the main airports (Adolfo Suárez Madrid-Barajas and Barcelona-El Prat)
- 2050: Net Zero Emissions at AENA airports according with the ACI Europe initiative.

These goals, part of AENA's commitment to face the climatic emergency, must be addressed, not only carrying out actions at airports, but also working collaboratively with airlines, handling agents, commercial stores, employees and passengers themselves to implement innovative solutions that allow us to achieve a more sustainable and carbon-free aviation.

HOW TO EFFICIENTLY DESIGN AIRCRAFT WITH MINIMUM CLIMATE IMPACT?

F. Linke^{1,2}, K. Radhakrishnan², V. Grewe^{3,4}, R. Vos⁵, M. Niklass^{1,2}, B. Lührs², F. Yin⁴, I. Dedoussi⁴, P. Proesmans⁵ & K. Deck⁴

¹ DLR German Aerospace Center, Air Transportation Systems, Germany

² Hamburg University of Technology, Institute of Air Transportation Systems, Germany

³ DLR German Aerospace Center, Institute of Atmospheric Physics, Germany

⁴ Delft University of Technology, Aircraft Noise and Climate Effects, The Netherlands

⁵ Delft University of Technology, Flight Performance and Propulsion, The Netherlands

Abstract. Given the comparably high impact of aircraft emissions, especially their non-CO₂ effects, on climate in the order of 5%, aviation stakeholders are required to act to reduce the warming effects of air traffic. Besides new operational procedures, like e.g. climate-optimized routing, this demands the development of completely new global-warming optimized aircraft by aircraft manufacturers. The European Clean Sky 2 project "Global-Warming Optimized Aircraft Design" (GLOWOPT) aims at providing aircraft designers an innovative tool to perform aircraft design studies for minimum climate impact, which we call Climate Functions for Aircraft Design (CFAD). The CFAD will substantially change the way aircraft are designed, while maintaining compatibility to existing Multidisciplinary Design Optimization (MDO) methods. The functions need to integrate a lot of information on the typical aircraft usage, including the routes the aircraft will be operated on. This is because, besides the amount of emissions, the impact of aviation non-CO₂ effects, such as NO_x, H₂O as well as contrails, on climate is highly dependent on location (i.e. latitude, longitude) and altitude. So, the representative operating profile of the aircraft needs to be considered in a characteristic route and fleet model. This work will present the interdisciplinary GLOWOPT approach, which comprises expertise on aircraft design, operations, atmospheric physics and climate. Conceptual thoughts on how the complexity of the operating profile in combination with the geographically variable climate impact of aircraft emissions will be reduced such that it can be used in an aircraft design process are given.

Keywords: Aircraft design, Climate impact, CFAD, Climate function, Non-CO₂ effects

ACKNOWLEDGEMENTS

This work has received funding from the Clean Sky 2 Joint Undertaking under the European Union's Horizon 2020 research and innovation programme under grant agreement No. 865300

NEAR-FIELD MODELLING OF CONTRAILS MICROPHYSICS

E. Terrenoire¹, X. Vancassel², W. Ghedhaïfi¹ & E. Montreuil¹

¹ DMPE – ONERA – Université Paris Saclay

² ONERA – Université Paris Saclay

Abstract. Uncertainty about the magnitude of contrails radiative forcing remains high due to the complexity of the mechanisms involved into their formation and therefore the difficulties to accurately represent them within climate models. In order to improve the contrails parametrization in these models, a detailed and comprehensive understanding of the physical and chemical microscale mechanisms during the jet phase is necessary. CFD codes give robust information of the wake dynamics but usually use a simplified description of microphysics and chemistry within the plume whereas microphysical box models generally use simple parametrized dilution along with a detailed description of the plume microphysics. Hence, an efficient hybrid approach based on the use of fluid dynamics trajectories extracted from the CFD CEDRE code coupled to the microphysical trajectory box model MoMiE is proposed. The methodology uses mean/multi fluid trajectories extracted from CFD RANS simulations that solve the full aircraft wake aerodynamics, up to 100 wingspans downstream the wingtip (5000 m behind the engine exit). Note that CEDRE simulations are carried out on the realistic Common Research Model aircraft configuration (CRM, representative of a Boeing 777) which allows a realistic modelling of the aircraft aerodynamics and its wake altogether. Using the modelling coupled approach (CEDRE/MoMiE), the influence of different sustainable alternative fuel (e.g. HEFA, H₂) on contrail characteristics with respect to conventional fuel (e.g. Jet A-1) will be tested. Key contrails properties such as ice crystals density and size distribution will be presented along the plume up to 100 wingspans behind wing tip as a function of fuel properties (e.g. fuel sulfur content and soot number emission index).

MITIGATION OF NON-CO₂ AVIATION'S CLIMATE IMPACT BY CHANGING CRUISE ALTITUDES

S. Matthes¹, L. Lim², U. Burkhardt¹, K. Dahlmann¹, S. Dietmüller¹, V. Grewe¹, A. Haselrut³, J. Hendricks¹, D.S. Lee², B. Owen², G. Pitari⁴, M. Righi¹ & A. Skowron²

¹ DLR Institute of Atmospheric Physics, Department Earth System Modelling, Oberpfaffenhofen, 82334 Wessling, Germany, sigrun.matthes@dlr.de

² MMU, Manchester Metropolitan University, Manchester, UK.

³ Geophysics Department, University of Oslo, Oslo, Norway

⁴ Department of Physical and Chemical Sciences, Università dell'Aquila, L'Aquila, Italy

Abstract. Aviation is seeking for ways to reduce its climate impact caused by CO₂ emissions and non-CO₂ effects. Operational measures which change overall flight altitude have the potential to reduce climate impact of individual effects, comprising CO₂ but in particular non-CO₂ effects. We study impact of changes of flight altitude, specifically aircraft flying 2000 feet higher and lower, with a set of chemistry-climate models integrating alternative emission scenarios. Flying lower leads to a reduction of non-CO₂ effects together with slightly increased CO₂ emissions and impacts, in case cruise speed is not modified. Flying higher increases non-CO₂ effects by about 7%, while flying lower decreases total climate impact by 19%, due to decreasing non-CO₂ impacts (by 29%). In order to improve understanding of mechanisms of aviation climate impact we study geographical distributions of aviation-induced perturbations, together with change in global climate impact.

Keywords: aviation climate impact mitigation, non-CO₂ effects, nitrogen oxides, alternative aircraft trajectories, alternative flight altitudes

INTRODUCTION

Aviation contributes to climate change by its emissions of CO₂, as well as by effects of non-CO₂ species. Hence, aviation contributes to anthropogenic climate change. As future growth of aviation is projected strategic goal has been set to develop aviation efficiently in order to mitigate aviation climate impact. One promising mitigation option is alternative aircraft routing by optimizing aircraft trajectories by operational adopting flight altitudes.

Climate impact of aviation emissions depend on altitude of emission as shown in several papers (e.g., Köhler et al., 1998, Fichter et al., 2005, 2012; Skowron et al. 2013). Hence changing flight altitude changes climate impact of aviation due to a change of both emissions and atmospheric sensitivity at location of emission. Hence, flying higher causes climate impact of one effect to increase, while at the same time another effect decreases. These counteracting effects need to be taken into account to quantify total climate impact and when developing mitigation options. However, an overall assessment which presents such trade-offs between different effects for flying higher or flying lower in a consistent way is missing. An earlier study showed that when aircraft are flying lower radiative forcing from nitrogen oxides decreases by about 30% and increases when they are flying higher (Søvde et al., 2014). An overview how individual effects change calculated by a set of state-of-the-art atmospheric chemistry models was provided by Ling et al. (2015) comprising impacts of nitrogen oxides, contrail-cirrus, water vapour, sulphate, direct soot emissions and soot-cirrus interactions. However a combined assessment has not been made how individual effects change in individual regions of the globe. Additionally, indirect aerosol effect on warm clouds was not yet assessed, as well as further analysis on nitrogen oxide impacts. Hence objective of this paper is (1) to present modelling concept and scenarios for assessing how climate impact changes when aircraft fly higher or lower, (2) to present behaviour of non-CO₂ effects for flight altitude changes, comprising NO_x impacts in different regions, as well as a quantitative estimate of indirect aerosol effect on warm clouds. Finally, this paper intends (3) to provide an overview on set of non-CO₂ effects induced by aviation emissions.

METHOD

Quantitative estimates of aviation climate impact are based on numerical simulations with a set of climate-chemistry models which represent atmospheric, physical and chemical processes influenced by aviation emissions. This concept was used by Lee et al. (2010) to provide radiative impact of aviation emissions comprising CO₂ and non-CO₂ impacts. We present results from a set of separate chemistry climate model simulations, which each represent chemical and physical atmospheric processes for an individual aviation impact. From these simulations we assess the influence of aviation emissions on atmospheric composition of key species and radiative balance, hence climate. The influence of a mitigation scenario is calculated by comparing an individual scenario simulation (having integrated flying higher/lower emission scenario) to the reference (base) case (having integrated the respective reference (base) inventory). From this comparison between alternative routing scenarios with reference case simulation, we can identify impact of flying higher of flying lower. In the presented climate impact assessment of aviation, we consider in detail climate impact of the following emissions: CO₂, NO_x (via formation ozone and influence on methane), soot, H₂O, contrails and contrail-cirrus.

EMISSION INVENTORIES FOR FLYING LOWER AND HIGHER

We have generated a set of three global emission inventories as part of the REACT4C project which describes our reference situation, a so-called base case (R4C), and two scenarios with shifted flight levels, based on information from flight planning data and assumptions on aircraft trajectories. In the reference case it is assumed that aircraft fly at their optimal altitude, while in the flying higher (lower) scenario all aircraft are flying 2000 feet higher (lower), but only if they are able to fly higher. We present geographical distribution of aviation emissions in these global emission inventories in Fig. 1, also comparing flying higher and flying lower scenarios with reference case. We find that fuel consumption and hence CO₂ emissions change, they increase by 1.3% if aircraft fly lower, but decrease by 0.8% if aircraft fly lower.

Vertical distribution of nitrogen oxides exhibits a shift of a part of aviation emissions to higher or lower flight altitudes (Fig. 2). Emission in the flying higher scenario (plus case) are partially shifted to higher altitudes, while in the flying lower scenario (minus case) aircraft trajectories and hence aviation emissions are shifted to lower altitudes. In the vertical distribution the maximum is narrower in the plus case, compared to reference and minus case, which show a broader maximum. All three scenarios show clear maximum in Northern Latitudes at about 30-60°N.

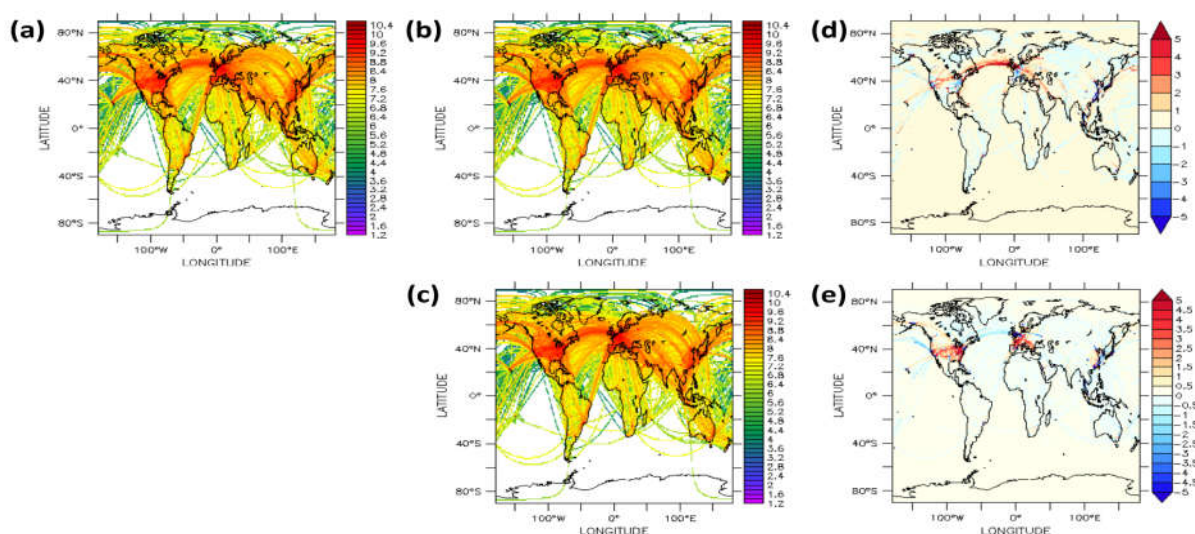


Figure 1. Global distribution of aviation NO_x emission (vertical integrated): reference case (a, R4C), flying higher (b, Plus), flying lower (c, Minus); difference Plus-Ref (d) and Minus-Ref (e).

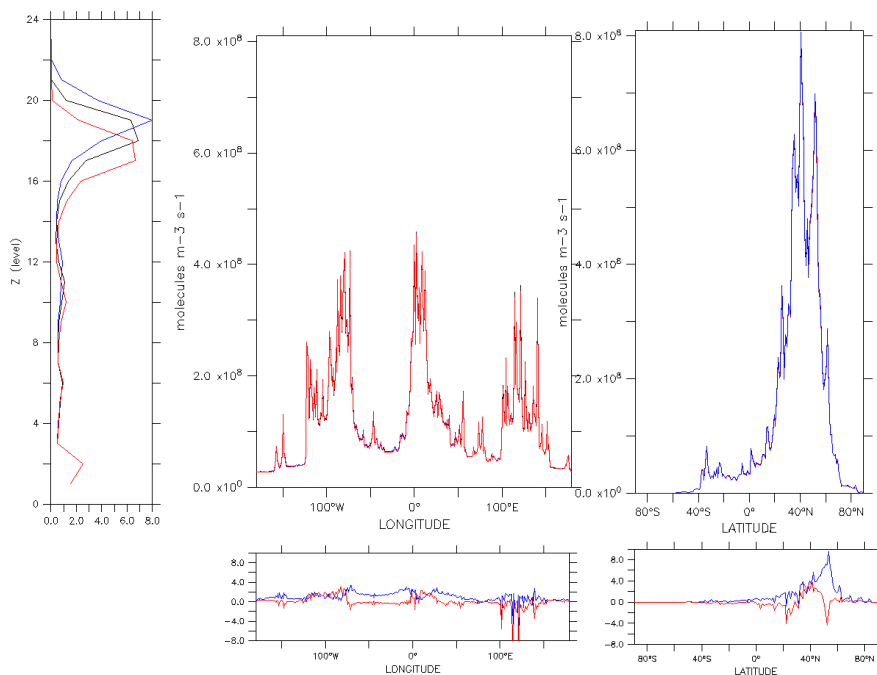


Figure 2. Global distribution of aviation emission; vertical distribution (*left*), meridional distribution (*middle*), zonal distribution (*right*): reference case (REACT4C, *black*), flying higher (plus case, *blue*), flying lower (minus case, *red*).

IMPACTS ON ATMOSPHERIC CONCENTRATION AND CLIMATE IMPACT

Within a set of atmospheric models we use above describe emission inventories and calculate aviation-induced changes of radiative active species. Specifically we apply the following models to investigate NO_x impacts: Oslo CTM, MOZART, EMAC, ECHAM4-CCMod, ULAQ, and AirClim. We calculate aviation induced changes in concentration of radiative active species which are relevant for climate impact, with state of the art atmospheric models. By comparing two distinct simulations, we calculate aviation-induced perturbation signals, comparing impact of the reference (base) case and emission scenarios. In Figure 3 we present changes in net ozone production when flying lower or higher. In the plus (minus) case net O₃ production increases (decreases) considerably at 200 hPa, while it decreases (increases) at 300 hPa.

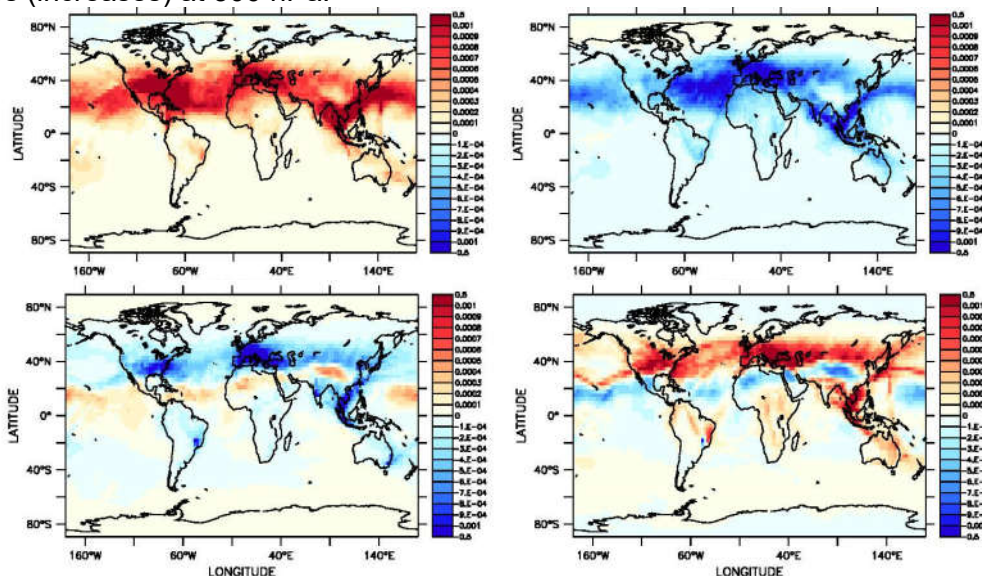


Figure 3. Change in ozone net production [10^{-12} mol/s] flying higher (*left*) and flying lower (*right*) compared to reference case in autumn at 200 hPa (*upper*) and 300 hPa (*lower*).

Impacts of aviation-induced aerosol on warm clouds are given in Tab. 1 and will also be included in the final paper. We are showing climate impact for reference case and both scenarios on non-CO₂ effects of aviation, which are calculated with comprehensive climate chemistry and aerosol models. From the aviation-induced perturbations in atmospheric concentrations caused by aviation emissions we derive radiative forcing from individual components by radiative transfer calculations. In this study we recalculate climate impact of NO_x emissions, comprising effects on O₃ and CH₄, as well as primary mode ozone (PMO), and stratospheric water vapour impacts, according to recent updates (Grewe et al., 2019) based on a multi-model mean with five different comprehensive chemistry climate models (Søvde et al., 2014).

Additionally, this paper presents estimates from aerosol modelling which investigates the impact of aerosol on warm clouds, using the global model EMAC/MADE (Righi et al., 2016). Beside a standard case simulation, a sensitivity study on nucleation properties is performed. Assuming efficient nucleation properties of aviation aerosols, impact of changing flight altitude is smaller than in the standard case simulation. For completing the list of non-CO₂ effects from aviation we included as well estimates from coarse resolution global model ULAQ studying direct sulphate and soot impacts (Ling et al., 2015), which are in the order of 3.5 and 0.8 mW/m², respectively. Beside these complex calculations we have calculated radiative forcing due to CO₂ emissions and linear contrails using a linear response model AirClim (Grewe and Stenke, 2008). Radiative forcing caused by CO₂ emissions is equal to 21.5 mW/m², which increases to 21.8 mW/m² when aircraft fly lower, and decreases to 21.3 mW/m² when aircraft fly higher. Linear contrails alone are associated with 5.7 mW/m² in the reference case, 6.0 mW/m² when flying higher and 5.1 mW/m² when flying lower.

Table 1. Climate impact of individual effects, radiative forcings [mW/m²], non-CO₂ presenting sum of all non-CO₂ effects for reference case and flying higher and lower scenarios.

Impact	Reference	Lower	Higher	Reference
Net NO_x	20.0	17.6	22.6	Update ¹
NO _x -Ozone	30.6	28.5	33.1	Update ¹
NO _x -Methane	-7.0	-7.1	-6.9	Update ¹
NO _x -PMO	-2.8	-2.9	-2.8	Update ¹
NO _x -H ₂ O	-0.8	-0.8	-0.8	Update ¹
Direct H₂O	1.5	1.1	2.0	Multi-model mean ²
Aerosol-Cloud	-15.1	-21.7	-14.5	EMAC/MADE
(sensitivity)	(-65.2)	(-65.8)	(-66.2)	EMAC/MADE
Contrail Cirrus	45	40	48	ECHAM4-CCMod ²
Total³	70.2	55.6	77.1	<i>this work</i>
Total ³ non-CO ₂	48.7	33.9	55.8	<i>this work</i>

¹Søvde et al., 2014, ²Lim et al., 2015, ³comprising CO₂, soot, sulphate mentioned in text

In order to compare non-CO₂ effects to direct warming from CO₂ emissions we calculate the multiplication factor for total impacts (comprising non-CO₂) and CO₂ forcing: For the base case we find a factor of 3.7, when aircraft are flying 2000 feet lower we find 2.9, and when aircraft are flying higher this factor is equal to 4.0, showing that non-CO₂ become more important with higher flight altitudes.

Comparing how climate impact of individual effects change due to the changing flight altitude (Fig. 4) reveals that when aircraft fly higher in general non-CO₂ effects increase (by 13%), and when aircraft fly lower non-CO₂ climate impacts decrease (by 29%). Comparing behaviour of non-CO₂ effects with CO₂ impacts, we find an opposite sign: when aircraft are flying higher (lower) CO₂ emission and hence associated climate impact decreases

(increase) slightly by about 1%. Overall, total climate impact increases by about 8% when aircraft are flying higher, and when flying lower total climate impact decreases by 19%.



Figure 4. Global radiative forcing [mW/m^2] of aviation emissions for REACT4C scenarios: reference case (*solid*), flying higher (*broken blue*) and flying lower (*broken red*) as absolute forcing (*left*) and changes for alternative flight altitudes compared to reference case (*right*).

In the final paper we will present spatial distribution of changes in atmospheric concentrations due to emissions of nitrogen oxide, water vapour, and aerosols. Analysis will focus on both cooling species and warming species. Beside geographic dependence of radiative forcing [W/m^2] we will show global distributions of perturbations induced, zonal distribution, as well as total sum from different species.

DISCUSSION AND CONCLUSION

In our study we calculate for a global fleet changing climate impact when aircraft are flying at an alternative flight altitude: higher CO_2 impacts decrease by 1%, while non- CO_2 effects increase by 13%, causing an increase in overall climate impact of 8%. When aircraft are flying 2000 feet lower CO_2 impacts increase by 1% and non- CO_2 impacts decrease by 29% causing a reduction in total climate impact of 19%. Comparing to the climate impact on individual effects with estimates in Ling et al. (2015) we find that climate impacts of nitrogen oxide emissions in our study are estimated to be higher, as updates on ozone and methane forcing have been published. This comparable higher radiative impact of nitrogen oxides is in agreement with recent estimates provided by Grewe et al. (2019). In terms of climate impacts of water vapour emissions in the stratosphere, values presented here are identical to values in Ling et al. (2015).

In terms of an aerosol indirect effect this study provides additional estimates on aerosol influence on warm clouds. Comparing aerosol forcing in base case, our estimates are close to values provided in Righi et al. (2016). Sensitivity studies introduced here are required as detailed microphysics of aviation aerosols are not yet known; hence assumptions must help to study a range of possible assumption in terms of nucleating properties. The NUC scenario implies a very strong nucleation capacity of aerosols, leading to comparably high numbers of nucleating particles. Comparing influence of changes to aircraft flight altitude shows that flying higher or flying lower in this nucleation sensitivity study causes smaller changes on associated aerosol-cloud interaction, instead of 4% increase when flying lower ($1 \text{ mW}/\text{m}^2$) in the nucleation case an increase of only 2% is calculated ($1 \text{ mW}/\text{m}^2$). When aircraft fly lower radiative forcing changes in the nucleation case as well by only $1 \text{ mW}/\text{m}^2$, which equals 1%, but in the reference case a strong decrease of 44% was calculated ($7 \text{ mW}/\text{m}^2$).

Summarizing behaviour of non- CO_2 effects with a changing flight altitude, we find a uniform behaviour: when aircraft are flying higher non- CO_2 effects generally increase, when aircraft fly lower, non- CO_2 effects decrease. Comparing non- CO_2 effects to CO_2 effects only, our analysis shows that their relative importance increases with increasing flight altitude.

ACKNOWLEDGEMENTS

This work was supported by the European Commission Seventh Framework Project, 'REACT4C' (contract no. ACP8-GA-2009-233772). Special thanks goes to Ivar Isaksen from University of Oslo for his inspiration and enthusiasm to initiate and to work collaboratively in this European collaborative research Project.

REFERENCES

- Burkhardt, U., Kärcher, B., 2011. Global radiative forcing from contrail cirrus. *Nat.Clim. Change* 1, 54-58. <http://dx.doi.org/10.1038/nclimate1068>.
- Dahlmann, K., Grewe, V., Frömming, C., Burkhardt, U., 2016. Can we reliably assess climate mitigation options for air traffic scenarios despite large uncertainties in atmospheric processes? *Transp. Res. Part D Transp. Environ.*, 46, 40 – 55.
- Dahlmann, K., Grewe, V., Ponater, M., Matthes, S., 2011. Quantifying the contributions of individual NO_x sources to the trend in ozone radiative forcing. *Atmos. Environ.*, 45, 2860 – 2868.
- Dameris, M., Grewe, V., Köhler, I., Sausen, R., Brühl, C., Groöß, J.-U., Steil, B., 1998. Impact of aircraft NO_x emissions on tropospheric and stratospheric ozone. Part II: 3-D model results. *Atmos. Environ.* 32 (18), 3185-3199. [http://dx.doi.org/10.1016/S1352-2310\(97\)00505-0](http://dx.doi.org/10.1016/S1352-2310(97)00505-0).
- Fichter, C., Marquart, S., Sausen, R., Lee, D.S., 2005. The impact of cruise altitude on contrails and related radiative forcing. *Meteorol. Z.* 14 (4), 563-572. <http://dx.doi.org/10.1127/0941-2948/2005/0048>.
- Frömming, C., M. Ponater, K. Dahlmann, V. Grewe, D. S. Lee, and R. Sausen (2012), Aviation-induced radiative forcing and surface temperature change in dependency of the emission altitude, *J. Geophys. Res.*, 117, D19104, doi:10.1029/2012JD018204.
- Grewe, V., Dameris, M., Fichter, C., Lee, D.S., 2002. Impact of aircraft NO_x emissions. Part 2: effects of lowering the flight altitude. *Meteorol. Z.* 11 (3), 197e205. <http://dx.doi.org/10.1127/0941-2948/2002/0011-0197>.
- Grewe, V.; Dahlmann, K., 2012. Evaluating Climate-Chemistry Response and Mitigation Options with AirClim, In *Atmospheric Physics: Background-Methods-Trends*; Schumann, U., Ed.; Springer: Berlin/Heidelberg, Germany, 591–606.
- Grewe, V.; Stenke, A., 2008. AirClim: an efficient climate impact assessment tool. *Atmos. Chem. Phys.*, 134 8, 4621–4639.
- Grewe, V., T. Champougny, S. Matthes, C. Frömming, S. Brinkop, O. A. Søvde, E.A. Irvine, L. Halscheidt, 2014: Reduction of the air traffic's contribution to climate change: A REACT4C case study. *Atmospheric Environment* 94, 616–625.
- Grewe, V., Matthes, S., Dahlmann, K., 2019. The contribution of aviation NO_x emissions to climate change: are we ignoring methodological flaws?, *Environ. Res. Lett.* 14, 121003.
- Holmes, C.D., Tang, Q., Prather, M.J., 2011. Uncertainties in climate assessment for the case of aviation NO. *Proc. Natl. Acad. Sci.* 108 (27), 10997e11002. <http://dx.doi.org/10.1073/pnas.1101458108>.
- Lee, D.; Pitari, G.; Grewe, V.; Gierens, K.; Penner, J.; Petzold, A.; Prather, M.; Schumann, U.; Bais, A.; Bernsten, T.; et al., 2010. Transport impacts on atmosphere and climate: Aviation. *Atmos. Environ.*, 137 44, 4678–4734.
- Lim, L.L., Lee, D.S., Owen, B., Skowron, A., Matthes, S., Burkhardt, U., Dietmüller, S., Pitari, G., Di Genova, G., Iachetti, D., Isaksen, I., Søvde, O., 2015. REACT4C: Simplified mitigation studies, TAC-4 Proceedings, 22-25 June 2015, Bad Kohlgrub.
- Matthes, S., 2012. Climate-optimised flight planning – REACT4C in Innovation for a Sustainable Aviation in a Global Environment, Proceedings of the Sixth European Aeronautics Days 2011, IOS Press & European Union, ISBN 978-92-79-22968-8.
- Matthes, S., U. Schumann, V. Grewe, C. Frömming, K. Dahlmann, A. Koch, and H. Mannstein, 2012. Climate optimized air transport, in *Atmospheric Physics, Research Topics in Aerospace*, U. Schumann (ed), DOI: 10.1007/978-3-642-30183-4_44, Springer-Verlag, Berlin, Heidelberg, 727-746.

- Righi, M., Hendricks, J., Sausen, R., 2016. The global impact of the transport sectors on atmospheric aerosol in 2030 – Part 2: Aviation, *Atmospheric Chemistry and Physics* 16(7), 4481-4495, DOI:10.5194/acp-16-4481-2016
- Søvde, O., Matthes, S.; Skowron, A.; Iachetti, D.; Lim, L.; Owen, B., Hodnebrog, T., Di Genova, G., Pitari, G.; Lee, D. et al., 2014. Aircraft emission mitigation by changing route altitude: A multi-model estimate of aircraft NO_x emission impact on O₃ photochemistry. *Atmos. Environ.*, 95, 468–479.

NON-CO₂ IMPACTS OF AVIATION THROUGH AVIATION-AEROSOL - ICE-CLOUD INTERACTIONS

C. Tully¹, D. Neubauer¹ & U. Lohmann¹

¹ *Institute for Atmospheric and Climate Science, ETH Zürich Switzerland, colin.tully@env.ethz.ch*

Abstract.

Clouds currently produce the largest uncertainty in present-day climate estimates and projections¹. A large component of this uncertainty is due to aerosol-cloud interactions, and how these processes may change under further climate change. Aerosols that can act as cloud condensation nuclei and/or ice nucleating particles (INPs) influence the population of cloud droplets and ice particles in clouds, respectively, which in turn affects the radiative properties of clouds. A higher hydrometeor population within a cloud may enhance its radiative effect. For mixed-phase clouds this leads to a stronger cloud albedo effect. For ice clouds, the interactions with aerosols is complicated by the fact that ice may form either homogeneously, without the presence of a nucleation surface at high supersaturation with respect to ice, or heterogeneously with an INP. Both nucleation modes may lead to different ice cloud properties. In general, homogeneous nucleation produces numerous small ice crystals that reflect little incoming solar radiation (shortwave, SW), and “trap” a large portion of outgoing terrestrial radiation (longwave, LW) through absorption and re-emission at much lower temperatures than the underlying surface. On the other hand, heterogeneous ice nucleation with an INP occurs at lower ice supersaturations and higher temperatures. Therefore, the resulting ice particles may have more time to grow larger and sediment earlier. If introduced into homogenous conditions, the INPs may alter ice formation, leading to fewer larger ice particles that preferentially consume available water vapor and reduce the ice-cloud LW trapping effect. However, if the background aerosol environment is already highly populated then the impact of additional aerosols may be dampened or lead to an increase in ice cloud cover, thus increasing radiative effects^{2,3,4}. This ice nucleation competition in naturally occurring ice clouds (cirrus) makes estimating their radiative forcing difficult. Anthropogenic activities like aviation that can have a direct impact on cirrus clouds further complicate this understanding through additional soot emissions.

Due to its daily visibility, the aviation sector is receiving increased attention as an anthropogenic impact on climate. Aircraft emissions not only contribute to rising atmospheric CO₂ concentrations, with the associated greenhouse warming effect, but also have the potential to produce aircraft-induced clouds (AIC)⁵ that have their own radiative forcing. These AICs, known as contrails, are thermodynamically complex, and form in the hot and humid wakes of aircraft jet engines in the upper troposphere. Under the Schmidt-Appleman criterion (SAC), contrails form if the exhaust plume remains above liquid water saturation when mixing with the ambient air that is below a critical temperature (roughly -40°C)^{5,6,7}. The emitted water vapor and other constituents quickly mix and form cloud droplets. After further mixing, rapid homogeneous nucleation of numerous small ice crystals occurs as liquid water is unstable at such low temperatures. The persistence of a contrail after formation is determined by whether the environment remains supersaturated with respect to ice. Upper tropospheric ice supersaturated region occurrence is common^{8,9,10}; however, only a small percentage of aircraft fly through such regions⁵. Simulating ice formation pathways in such environments and the subsequent evolution of the contrails from a climate forcing perspective remains difficult.

Aircraft also emit soot particles from their engine exhaust. Several microphysical parcel-model studies investigated the impact of emitted soot particles on contrail ice formation. The introduction of numerous INPs in the aircraft wake readily consumes available water vapor, preventing supersaturation with respect to liquid water, which defies the SAC for contrail

formation⁵. This may be the case for soot-rich exhaust plumes that show a higher number of nucleated ice particles than soot-poor plumes^{11,12,13}. Ice particle concentrations are lower in these latter plumes, with homogeneous nucleation of cloud droplets dominating at lower threshold temperatures^{5,12}. On the contrary, a laboratory-based study showed that emitted soot particles only act as more efficient INPs after cloud processing due to pore condensation and freezing¹⁴. Testing the ice nucleation ability of soot particles in relation to contrail formation and its climate impact was not previously investigated using a global climate model.

Understanding of the instantaneous forcing of contrails is also uncertain due to their large spatial heterogeneity. After formation, contrails may maintain their linear shape, forming persistent contrails, or spread out due to prevailing environmental conditions to become contrail cirrus⁵. In aircraft-congested regions if contrail cirrus form, they may form ice cloud layers that satellite-based measurements cannot distinguish from naturally occurring cirrus^{5,12}. Recent modelling studies concluded that out of the total AIC radiative forcing of 50 mWm⁻², contrail cirrus overall account for around 80%, making them the most significant contributor to the non-CO₂ impact of aviation emissions⁵. It is unclear whether contrail formation pathways influence their evolution, and what effect this would have on their radiative forcing. A preliminary climate model study on the radiative impact of aircraft soot emissions in high and low background aerosol environments found that the addition of aircraft soot cools in areas dominated by homogeneous nucleation through active nucleation competition, but warms in regions with more heterogeneous nucleation on dust particles⁴.

We use the Max Plank Institute's ECHAM general circulation model (GCM)¹⁵ coupled to the Hamburg Aerosol Module (HAM)^{16,17} to investigate the impact of aircraft soot on naturally occurring cirrus, and to identify regions where these emissions show a significant effect. Aircraft soot was not previously included as an INP species in the GCM. Here, we test the implementation of soot in the model and its impact on ice cloud properties. To investigate contrail ice evolution, we utilize a new single-ice-category microphysics scheme^{18,19} that prognostically predicts bulk ice properties based on mass-to-size relationships. It also includes a new ice-cloud-cover scheme that allows for sub-grid-scale coverage above ice supersaturation, with full gridbox coverage only when homogeneous nucleation conditions are met.

Results of the study will aid in our understanding of AIC, and how their evolution impacts their radiative properties. Furthermore, with the projected rise of aviation traffic during the 21st Century^{20,21,22}, AIC radiative effects may become even more significant. Therefore, this project aims to identify regions suitable for AIC effects in order to mitigate their warming effect, e.g. climate-optimized air traffic routing²². A potential added benefit of this work is to highlight regions where the proposed cirrus cloud thinning climate engineering method^{2,3,23,24,25} may be effective.

REFERENCES

1. Boucher, O., Randall, D., Artaxo, P., Bretherton, C., Feingold, G., Forster, P., Kerminen, V.-M., Kondo, Y., Liao, H., Lohmann, U., Rasch, P., Satheesh, S., Sherwood, S., Stevens, B., and Zhang, X.: Clouds and Aerosols, book section 7, 571–658, Cambridge University Press, Cambridge, UK and New York, NY, USA, doi:10.1017/CBO9781107415324.016, 2013.
2. Gasparini, B. and Lohmann, U.: Why cirrus cloud seeding cannot substantially cool the planet, *J. Geophys. Res. Atmos.*, **121**, 4877–4893, doi:10.1002/2015JD024666, 2016.
3. Penner, J. E., Zhou, C. and Liu, X.: Can cirrus cloud seeding be used for geoengineering?, *Geophys. Res. Lett.*, **42**, 8775–8782, doi:10.1002/2015GL065992, 2015.
4. Zhou, C. and Penner, J. E.: Aircraft soot indirect effect on large-scale cirrus clouds: Is the indirect forcing by aircraft soot positive or negative?, *J. Geophys. Res. Atmos.*, **119**, doi:10.1002/2014JD021914, 2014.

5. Kärcher, B.: Formation and radiative forcing of contrail cirrus, *Nature Commun.*, **9**, 1824, doi:10.1038/s41467-018-04068-0, 2018.
6. Schumann, U.: On conditions for contrail formation from exhaust plumes, *Meteorol. Z., N.F.*, **5**, doi:10.1127/metz/5/1996/4, 1996.
7. Whelan, G.M., Cawkwell, F., Mannstein, H., and Minnis, P.: The use of meteorological data to improve contrail detection in thermal imagery over Ireland, *Conference: Remote Sensing and Photogrammetry*, 2009.
8. Gierens, K., and Spichtinger, P.: On the size distribution of ice-supersaturated regions in the upper troposphere and lowermost stratosphere, *Ann. Geophysicae*, **18**, 499-504, doi:10.1007/s00585-000-0499-7, 2000.
9. Jensen, E.J., Toon, O.B., Vay, S.A., Ovarlez, J., May, R., Bui, T.P., Twohy, C.H., Gandrud, B.W., Pueschel, R.F., and Schumann, U.: Prevalence of ice-supersaturated regions in the upper troposphere: Implications for optically thin ice cloud formation, *J. Geophys. Res.*, **106**, 253-266, doi:10.1029/2000JD900526, 2001.
10. Spichtinger, P. and Leschner, M.: Horizontal scales of ice-supersaturated regions, *Tellus B: Chemical and Physical Meteorology*, **68**, doi:10.3402/tellusb.v68.29020, 2016.
11. Kärcher, B. and Yu, F.: Role of aircraft emissions in contrail formation, *Geophys. Res. Lett.*, **36**, doi:10.1029/2008GL036649, 2009.
12. Heymsfield, A., Baumgardner, D., DeMott, P., Forster, P., Gierens, K., and Kärcher, B.: Contrail microphysics, *Bull. Amer. Meteor. Soc.*, **91**, 465-472, doi:10.1175/2009BAMS2839.1, 2010.
13. Wong, H.W., and Miake-Lye, R.C.: Parametric studies of contrail ice particle formation in jet regime using microphysical parcel modeling, *Atmos. Chem. Phys.*, **10**, 3261-3272, doi:10.5194/acp-10-3261-2010, 2010.
14. Mahrt, F., Kilchhofer, K., Marcolli, C., Grönquist, P., David, R.O., Rösch, M., Lohmann, U., and Kanji, Z.A.: The impact of cloud processing on the ice nucleation abilities of soot particles at cirrus temperatures, *J. Geophys. Res. Atmos.*, **125**, doi:10.1029/2019JD030922, 2020.
15. Stevens et al 2013 Stevens, B., Girogetta, M., Esch, M., Mauritsen, T., Cruegar, T., Rast, S., Salzmann, M., Schmidt, H., Bader, J., Block, K., Brokopf, R., Fast, I., Kinne, S., Kornbluh, L., Lohmann, U., Pincus, R., Reichler, T. and Roeckner, E.: Atmospheric component of the MPI-M Earth System Model: ECHAM6, *J. Adv. Model. Earth Sys.*, **5**, 146-172, doi:10.1002/jame.20015, 2013.
16. Stier, P., Feichter, J., Kinne, S., Kloster, S., Vignati, E., Wilson, J., Ganzeveld, L., Tegen, I., Werner, M., Balkanski, Y., Schulz, M., Boucher, O., Minikin, A. and Petzold, A.: The aerosol-climate model ECHAM5-HAM, *Atmos. Chem. Phys.*, **5**, 1125-1156, doi: 10.5194/acp-5-1125-2005, 2005.
17. Zhang et al Zhang, K., O'Donnell, D., Kazil, J., Stier, P., Kinne, S., Lohmann, U., Ferrachat, S., Croft, B., Quaas, J., Wan, H., Rast, S. and Feichter, J.: The global aerosol-climate model ECHAM-HAM, version 2: sensitivity to improvements in process representations, *Atmos. Chem. Phys.*, **12**, 8911-8949, doi:10.5194/acp-12-8911-2012, 2012.
18. Dietlicher, R., Neubauer, D., and Lohmann, U.: Prognostic parameterization of cloud ice with a single category in the aerosol-climate model ECHAM(v6.3.0)-HAM(v2.3), *Geosci. Model Dev.*, **11**, 1557-1576, doi:10.5194/gmd-11-1557-2018, 2018.
19. Dietlicher, R., Neubauer, D. and Lohmann, U.: Elucidating ice formation pathways in the aerosol-climate model ECHAM6-HAM2, *Atmos. Chem. Phys.*, **19**, 9061-9080, doi:10.5194/acp-19-9061-2019, 2019.
20. Lee, D.S., Fahey, D.W., Forster, P.M., Newton, P.J., Wit, R.C.N., Lim, L.L., Owen, B., and Sausen, R.: Aviation and global climate change in the 21st century, *Atmos. Environ.*, **43**, 3220-3537, doi:10.1016/j.atmosenv.2009.04.024, 2009.
21. Owen, B., Lee, D.S., and Lim, L.: Flying in the future: Aviation emissions scenarios to 2050, *Environ. Sci. Technol.*, **44**, 2255-2260, doi: 10.1021/es902530z, 2010.
22. Grewe, V., Matthes, S., Frömming, C., Brinkop, S., Jöckel, P., Gierens, K., Champougny, T., Fuglestad, J., Haslerud, A., Irvine, E. and Shine, K.: Feasibility of climate-optimized air traffic routing for trans-Atlantic flights, *Environ. Res. Lett.*, **12**, doi:10.1088/1748-9326/aa5ba0, 2017.
23. Mitchell, D. L. and Finnegan, W.: Modification of cirrus clouds to reduce global warming, *Environ. Res. Lett.*, **4**, doi:10.1088/1748-9326/4/4/045102, 2009.
24. Storelvmo, T. and Herger, N.: Cirrus cloud susceptibility to the injection of ice nuclei in the upper troposphere, *J. Geophys. Res. Atmos.*, **119**, 2375-2389, doi:10.1002/2013JD020816, 2014.
25. Gruber, S., Blahak, U., Haenel, F., Kottmeier, C., Leisner, T., Muskatel, H., Storelvmo, T., and Vogel, B.: A process study on thinning of Arctic winter cirrus clouds with high-resolution ICON-ART simulation, *J. Geophys. Res. Atmos.*, **124**, doi:10.1029/2018JD029815, 2019.

CONCEPT OF CLIMATE-CHARGED AIRSPACE AREAS

M. Niklass^{1,*}, V. Grewe^{2,3} & V. Gollnick^{1,4}

¹ *Lufttransportsysteme, Deutsches Zentrum für Luft- und Raumfahrt (DLR), Germany,*

² *Institut für Physik der Atmosphäre, Deutsches Zentrum für Luft- und Raumfahrt (DLR), Germany*

³ *Delft University of Technology (TU Delft), Section Aircraft Noise & Climate Effects, Netherlands*

⁴ *Institut für Lufttransportsysteme, Technische Universität Hamburg (TUHH), Germany*

* Correspondence: malte.niklass@dlr.de; Tel.: +49 (0)40 2489641 214

Abstract. Approximately two third of aviation's climate impact is caused by non-CO₂ effects, like the production of ozone and the formation of contrail-cirrus clouds, which can be effectively prevented by re-routing flights around highly climate-sensitive areas. Although climate-optimized re-routing results in slightly longer flight times, increased fuel consumption and higher operating costs, it is up to 60% more climate-friendly. However, if mitigation efforts are associated with a direct increase in costs, this immediately raises the question of the willingness of primarily profit-oriented airlines to act in a more climate-friendly manner and the passengers' willingness to pay for environmental protection. In order to create an incentive for climate-optimized flying, a climate charge is imposed on airlines when operating in these areas. If climate-charged airspaces (CCAs) are (partly) bypassed, both climate impact and operating costs of a flight can be reduced: a more climate-friendly routing becomes economically attractive ([explanation video](#)). By implementing the precautionary and polluter-pays principles of environmental economics, the concept introduces key requirements of a sustainable development into the field of aviation. The proposed extension of the accounting system clearly reduces the discrepancy between the marginal costs estimated by the airlines and the consequential costs for society. Accordingly, this resolves the trade-off between economic viability and environmental compatibility and creates a financial incentive for climate mitigation. The feasibility of this concept is demonstrated on a small route network in the North Atlantic flight corridor (NAFC). If flights are completely re-routed around altered CCAs, on average more than 90 % of the mitigation potential of climate-optimized flying is achieved.

Keywords: Aviation, Non-CO₂ Effects, Climate Mitigation, Environmental Policy, Cost-Benefit-Analysis

INTRODUCTION

Global air traffic is projected to grow at rates (4-5%) well above the annual increase in fuel efficiency (1-2%). Consequently, aviation's contribution to anthropogenic emissions and the associated global warming is expected to increase. Almost two third of aviation's climate impact is caused by non-CO₂ effects, such as the NO_x-induced production of ozone or the formation of contrail induced cloudiness (CiC). These effects show highly non-linear dependencies on fuel consumption (Lee et al., 2009; Grewe et al., 2017). Therefore, the reduction of emission quantity alone is not a sufficient measure in order to mitigate non-CO₂ climate effects. Due to the high sensitivity of the climate impact on the location and the timing

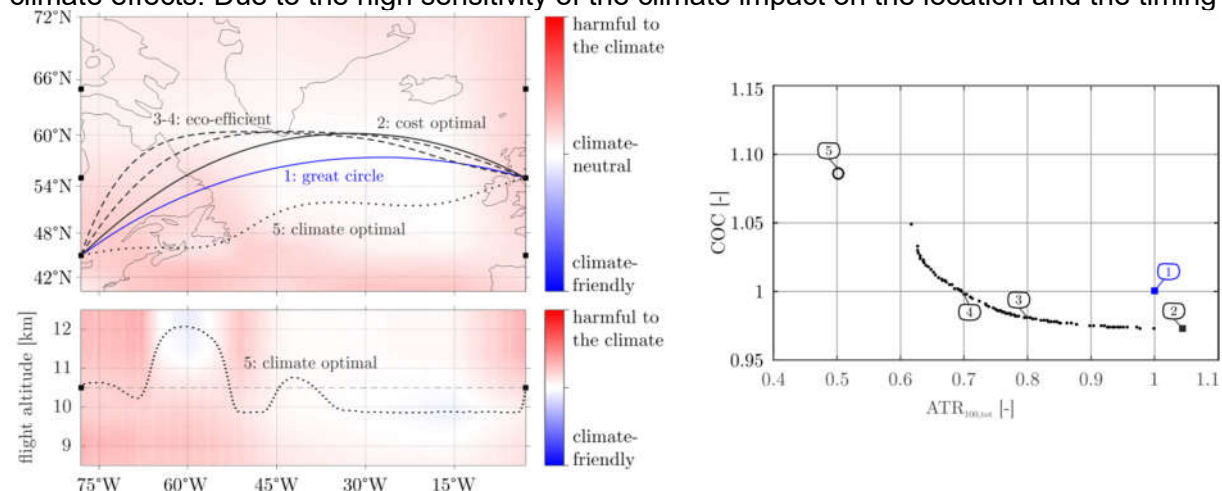


Figure 1: Climate and weather optimized flight trajectories over the North Atlantic (left); colors represent the magnitudes of climate sensitivity. A trajectory is optimal with regard to COC if $c_\psi = 0$, and optimal with regard to climate (ATR_{20}), if $c_\psi = 1$. Pareto elements of climate reduction potential

(ATR) and cash operating costs (COC) (right) are plotted relatively to the great circle trajectory (trajectory 1, blue line, shortest connection; adapted from Lührs et al., 2016, p.6-8) of the emission, the impact can be reduced by changing the flight pattern, represented by an adjustment in routing (see Fig. 1; Lührs et al., 2016; Grewe et al., 2017; Matthes et al., 2017) or a reduction of the general cruising altitude (Dahlmann et al., 2016). Although all of these changes result in slightly increased values of flight time, fuel burn and operating costs, they are significantly more climate compatible (up to -60%). If, however, mitigation efforts are associated with an increase in costs, questions immediately arise whether passengers are willing to pay for environmental protection and whether airlines are willing to act in a more climate-friendly manner. Within this study, the lack of incentivizing airlines to internalize their climate costs is tried to be closed by the introduction of climate-charged airspaces. The CCA concept addresses the question of how to include aviation's climate impact of non-CO₂ effects adequately into an environmental policy measure.

CONCEPT OF CLIMATE-CHARGED AIRSPACES

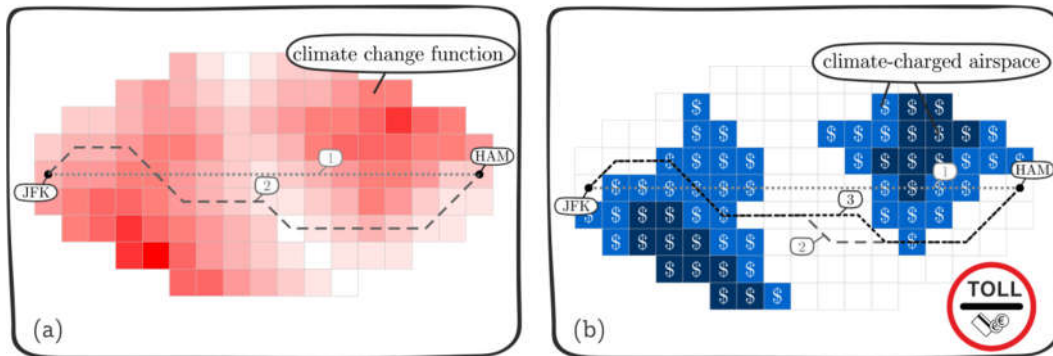


Figure 2: Concept of climate-charged airspaces (CCA): creating a financial incentive for airlines to minimize flight time and emissions in highly climate-sensitive regions: (1) time-optimized, (2) climate-optimized trajectory and (3) cost-optimized trajectory within the CCA concept (Niklaß et al., 2018)

In order to create an incentive for airlines to minimize flight time and emissions in highly climate sensitive regions, Niklaß et al. (2018) and Niklaß (2019) suggested to impose a climate charge for airlines that operate in these areas (see Fig. 2). An airspace area will be levied with an environmental unit charge, U_{cj} , per kilometer flown, d_j , if its climate sensitivity with respect to aircraft emissions⁹ exceeds a specific threshold value (c_{thr}). Resulting climate charges, C_{cj} , are calculated analogously to en-route and terminal charges according to

$$C_{cj} = U_{cj} \cdot \left(\frac{m_{TOW}}{k_1}\right)^{k_2} \cdot I_{ac} \cdot d_j. \quad (1)$$

Parameters under consideration are the maximum take-off weight m_{TOW} of an aircraft, an incentive factor I_{ac} for green technologies¹⁰ as well as specific parameters k_1 , k_2 depending on national territory. For each flight, the operator can individually decide whether to minimize flight time and to pay compensation for higher climate damage (trajectory 1 in Fig. 2b) or to minimize costs and, concurrently, mitigating the climate impact by total or partial avoidance of CCA (trajectory 3). In this manner, climate impact mitigation coincides with the cutting of costs. As CCAs could be defined and monitored by air traffic control, airlines do not have to integrate non-linear relationships of non-CO₂ effects into their flight planning procedures for climate impact mitigation. However, existing uncertainties in modeling the climate impact of a flight could lead to optimized flight trajectories that might either over- or underestimate the impact of different climate agents. For this reason, a resilient management of uncertainties is necessary. In a first step, the implementation of the CCA concept might be limited to selected non-CO₂ effects, e.g. CiC, and those areas that are most likely highly sensitive in this regard (■ in Fig 2b). But its implementation can be adapted any time to the current level of scientific understanding by introducing varying unit charges for areas with different levels of climate sensitivities (■,■) and/or by taking further trace substances, e.g. aerosols, into consideration.

⁹The climate sensitivity of an area is expressed here by climate change functions characterizing the environmental impact caused by non-CO₂ effects of aircraft's emissions at a certain location and time.

¹⁰ $I_{ac} = 1$ for current technology level; $I_{ac} = 0$ for zero-emission aircraft.

In the final expansion phase, the entire airspace and all relevant climate agents should be included into the concept.

COST-BENEFIT AND FEASIBILITY ASSESSMENT

The functionality and effectiveness of the concept is demonstrated below with trajectory simulations on nine North Atlantic routes. The expected impact of CCAs on flight operations is exemplarily illustrated in Fig. 3 for a constant threshold value and varying climate unit charges. Since the “Business as Usual”¹¹ (BAU) trajectory runs straight through the climate-charged area (■), BAU operation is only possible with significantly higher operating costs, partially internalizing the climate-related damage of the flight. The additional costs of internalization, however, can largely be avoided if the aircraft operator changes its flight behavior and (partly) re-routes the flight around CCAs. If CCAs are avoided completely, a maximum cost reduction of 81 % is possible for $U_{c,j} = 5$ \$/km. This results in a 9.4 % climate impact mitigation of the flight. By creating a financial incentive for mitigation, the trade-off between economic viability and environmental compatibility can therefore be solved: climate-friendly flying becomes economically attractive. The higher $U_{c,j}$, the greater the financial incentive for re-routing; the mitigation potential varies with the threshold.¹²

The key parameters of the CCA concept are the independent variables of the threshold (c_{thr}) and the climate unit charge ($U_{c,j}$). An optimal set of these variables can be found for each route to create a monetary incentive for a targeted mitigation potential. On average, more than 90 % of the mitigation potential due to climate-optimized flying (theoretical maximum) is achieved on the simulated route-network. Consequently, the approach of only avoiding the most climate-sensitive regions seems to be extremely effective for a single route.

¹¹ Cost-optimized operation without CCAs

¹² As the threshold value decreases, the size of climate-charged areas increases, which in turn raises the mitigation potential of the CCA concept.

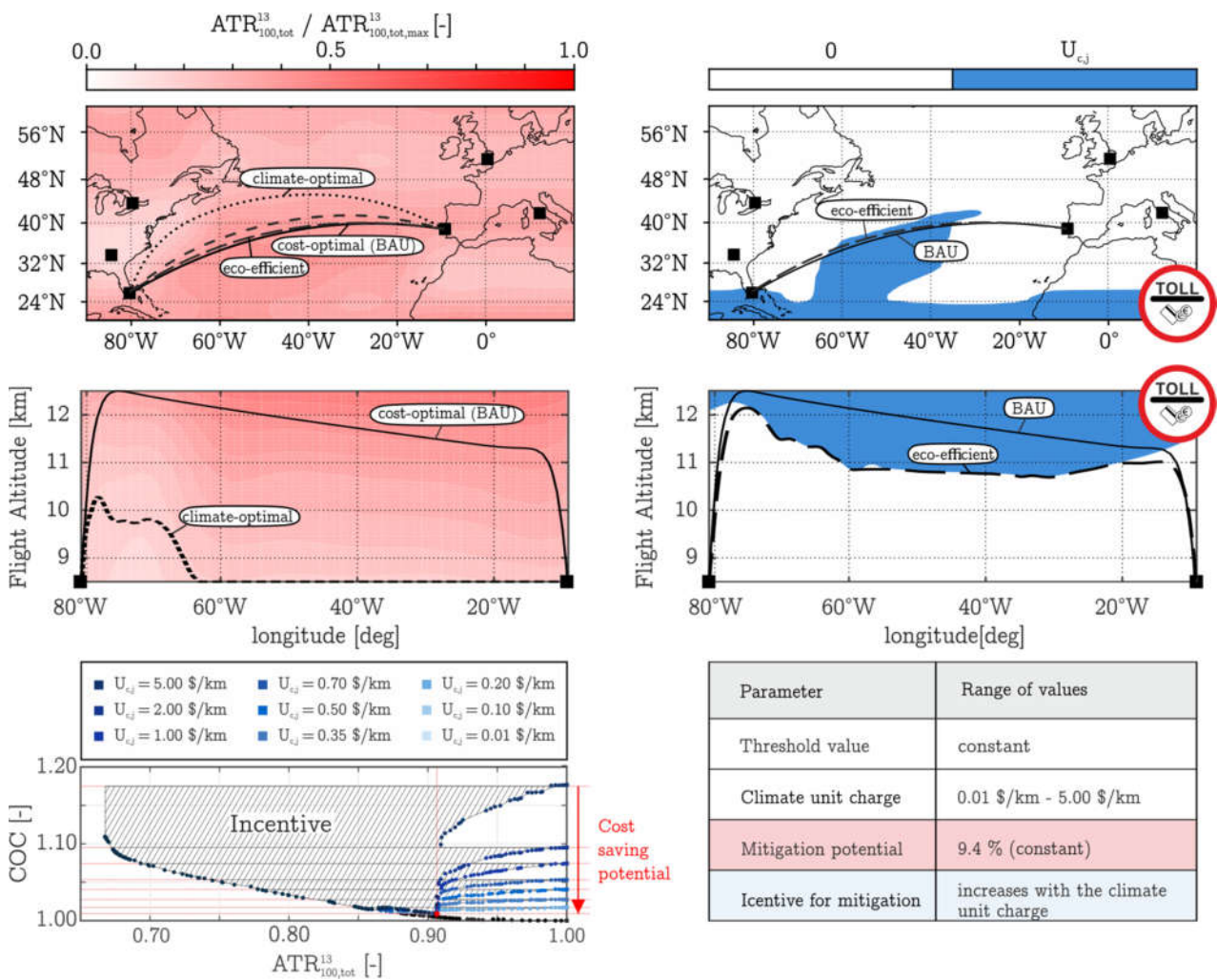


Figure 3: Climate-optimized (left) and cost-optimized flight trajectories after implementing climate-charged airspaces over the North Atlantic. With increasing climate unit charge, the mitigation incentive increases; the mitigation potential remains constant (adapted from Niklaß et al., 2018, p.6-9)

More relevant, however, is the question whether the CCA concept can ensure region- or country-specific environmental targets. Is it possible, for instance, to achieve a climate impact mitigation of 5 % on all North Atlantic flights? For this purpose, the minimum (blue), average (grey) and maximum (red) mitigation potential of all simulated routes are plotted in Fig. 4a over the threshold. Accordingly, a threshold value of 0,564 must be applied. On average, the climate impact is then mitigated by -11.4 % and by a maximum of -17.2 % for the most-efficient re-routing. In order to provide a financial incentive for this mitigation effort, a minimum charge of at least 0.345 \$/km must be levied for the entire route network.

The practicability of our cost-driven re-routing approach can already be demonstrated today with the operating behavior of airlines on trans-European journeys: With the aim of cutting costs, a number of airlines took particularly large detours between 2012 and 2015 – in times when fuel costs were comparatively low – and re-routed their flights as long as possible over countries with lower air traffic control charges, such as Eastern and South-Eastern Europe (see exemplary Fig. 4b; Delgado, 2015; Eurocontrol, 2016). A price-driven re-routing approach is therefore already well-established in the airline industry.

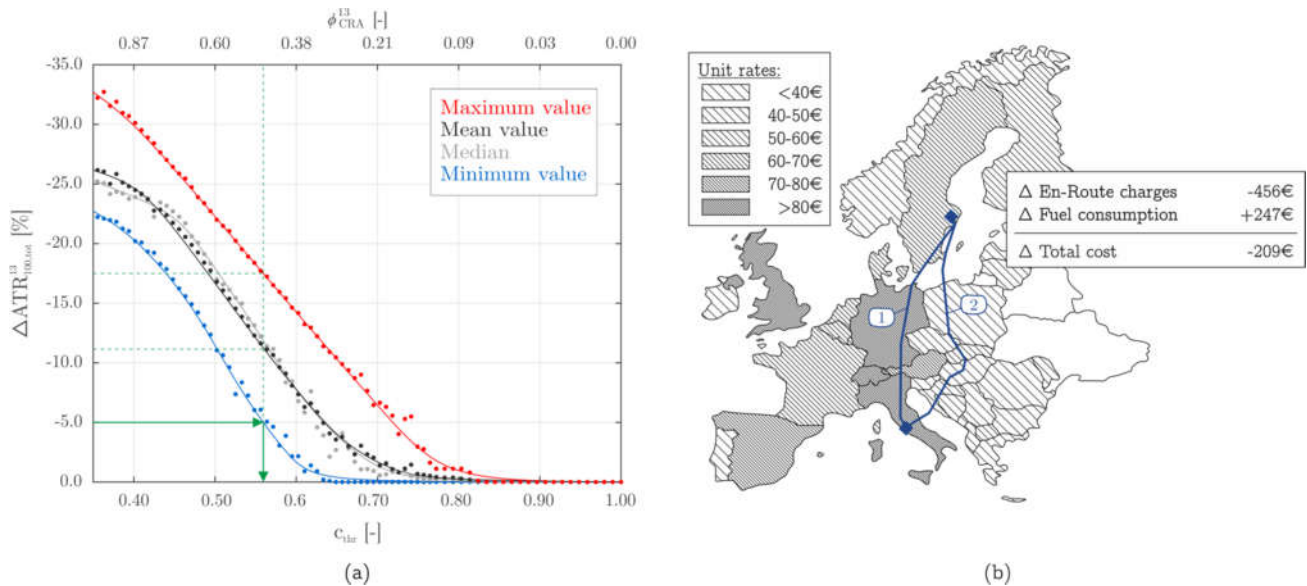


Figure 4: (a) Mitigation potential of the route network depending on the threshold value (c_{thr}) and (b) influence of current ATC unit rates on operating costs and flight route for a full service carrier flight from Stockholm, Sweden to Rome, Italy (adapted from Delgado, 2016); navigation unit rates accord with Eurocontrol (2016)

REFERENCES

- Dahlmann, et al., 2016: Climate-Compatible Air Transport System - Climate Impact Mitigation Potential for Actual and Future Aircraft. *Aerospace*, 3 (38) 38, 10.3390/aerospace3040038
- Delgado, L.: *European route choice determinants: Examining fuel and route charge tradeoffs*. 11th USA/Europe Air Traffic Management Research and Development Seminar, 2015
- Eurocontrol, 2016: *Why variations in navigation charges can influence traffic pattern*. *Skyway Magazine*, 65, p. 31-36.
- Grewe, et al., 2017: *Mitigating the Climate Impact from Aviation: Achievements and Results of the DLR WeCare Project*. *Aerospace*, 44 (3), [10.3390/aerospace4030034](https://doi.org/10.3390/aerospace4030034)
- Lee, et al., 2009: *Aviation and global climate change in the 21st century*, *Atmos. Environ.*, 43, 2009. [10.1016/j.atmosenv.2009.04.024](https://doi.org/10.1016/j.atmosenv.2009.04.024)
- Lührs, et al., 2016: *Cost-Benefit Assessment of 2D- and 3D Climate and Weather Optimized Trajectories*. *AIAA Aviation*, 16, [10.2514/6.2016-3758](https://doi.org/10.2514/6.2016-3758)
- Matthes, et al., 2017: *A Concept for Multi-Criteria Environmental Assessment of Aircraft Trajectories*. *Aerospace*, 4 (42), [10.3390/aerospace4030042](https://doi.org/10.3390/aerospace4030042)
- Niklaß, et al., 2018: *Implementation of eco-efficient procedures to mitigate the climate impact of non-CO₂ effects*. 31st congress of ICAS, Belo Horizonte, Brazil.
- Niklaß, 2019: *A systems analytical approach for internalizing the climate impact of aviation* (German), PhD thesis, Hamburg University of Technology, [DLR-FB-2019-06](https://doi.org/10.2590/dlrfb-2019-06)

THE EU PROJECT ACACIA (ADVANCING THE SCIENCE FOR AVIATION AND CLIMATE)

R. Sausen^{1,*}, S. Matthes^{1,2}, K. Gierens^{1,3} & the ACACIA team

¹ *Deutsches Zentrum für Luft- und Raumfahrt, Institut für Physik der Atmosphäre, Germany*

<https://www.acacia-project.eu>

* robert.sausen@dlr.de

² sigrun.matthes@dlr.de

³ klaus.gierens@dlr.de

Abstract. A short overview of the EU H-2020 Research and Innovation Action ACACIA is given.

Keywords: Climate impact of aviation, indirect aerosol effect, climate assessment, guidance for mitigation strategies

OVERVIEW OF THE ACACIA PROJECT

Non-CO₂ emissions of aviation may impact climate as much as aviation's carbon dioxide (CO₂) emissions do. However, the impact the non-CO₂ effects (e.g., ozone and methane from NO_x emissions, contrails, indirect aerosol effects) is associated with much larger uncertainties; some of these effects might result in a relatively large cooling.

In January 2020, the EU project ACACIA started. It has four aims for scientifically based and internationally harmonised policies and regulations for a more climate-friendly aviation system. (1) We will improve scientific understanding of those impacts that have the largest uncertainty, in particular, the indirect effect of aviation soot and aerosol on clouds. (2) We will identify needs for international measurement campaigns to constrain our numerical models and theories with data and we will formulate several design options for such campaigns. (3) Putting all aviation effects on a common scale will allow providing an updated climate impact assessment. Uncertainties will be treated in a transparent way, such that trade-offs between different mitigation strategies can be evaluated explicitly. This helps our final aim (4) to provide the knowledge basis and strategic guidance for future implementation of mitigation options, giving robust recommendations for no-regret strategies for achieving reduced climate impact of aviation.

To this end, ACACIA brings together research across scales (from plume to global scale), from laboratory experiments to global models, and it proceeds from fundamental physics and chemistry to the provision of recommendations for policy, regulatory bodies, and other stakeholders in the aviation business. ACACIA will cooperate with international partners, both research institutions and organisations. Additionally, ACACIA seeks for synergies with EU partner projects: ALTERNATE (Assessment on aLTERNative AviaTion fuEls development), ClimOp (Climate assessment of innovative mitigation strategies towards operational improvements in aviation), and GREAT (GREener Air Traffic operations)..

ACKNOWLEDGEMENTS

This project receives funding from the European Union's Horizon 2020 research and innovation programme under grant agreement No 875036

CLIMOP: CLIMATE ASSESSMENT OF INNOVATIVE MITIGATION STRATEGIES TOWARDS OPERATIONAL IMPROVEMENTS IN AVIATION

A. Tedeschi¹ & the ClimOP Project Team*,

* Koninklijk Nederlands Lucht- en Ruimtevaartcentrum (NLR),

* Technische Universiteit Delft (TUD),

* Deutsches Zentrum für Luft- und Raumfahrt (DLR),

* Amigo Srl, İstanbul Teknik Üniversitesi (ITU),

* International Air Transport Association (IATA),

* Società Esercizi Aeroportuali (SEA)

¹ Deep Blue Srl, Piazza Buenos Aires 20, 00198, Rome, Italy, E-mail: alessandra.tedeschi@dblue.it

Abstract. Since the end of the 20th century, the urgency of climate change has attracted worldwide attention. The aviation sector is often seen as a major contributor to climate impact and environmental issues, even though its contribution to the anthropogenic greenhouse effect is only about 5%. The aviation industry, considering the expected sector growth, has been working on improvements at different levels. However, more incisive operational improvements remain undervalued. ClimOp aims to contribute to the reduction of the climate impact of aviation by identifying a set of harmonized mitigation strategies. These will be developed from a preliminary list of most-promising operational improvements assessed through different modelling tools. After a validation process with all aviation stakeholders, the mitigation strategies will be proposed as recommendations to policymakers, fostering their implementation.

Keywords: operational improvements, mitigation, climate, impact.

1. INTRODUCTION

Aviation emissions alter the concentration of atmospheric greenhouse gases and trigger the formation of contrails and cirrus clouds. Consequently, the overall impact on climate from aviation emissions has been estimated to roughly 5% of the total anthropogenic radiative forcing (Lee *et al.* 2010). During the last years, the aviation sector has put considerable efforts to stabilise the CO₂ emissions at 2020 levels through a combination of technological innovations and regulation. Unfortunately, a lot needs to be done to reduce the overall impact of aviation on climate. As a matter of fact, ATAG (2018, 2020b) estimated that in 2017 the burning of 341 billion litres of jet fuel produced 859 million tonnes of CO₂, equal to the 2% of man-made CO₂ emissions. In 2019 the global production of CO₂ was over 43 billion tonnes, while flights produced 915 million tonnes (ATAG 2018, 2020a).

In 2008, industry leaders took action to reduce the climate impact of aviation by committing to a high-level strategy based on three major goals (ATAG 2010):

1. Improve the fuel efficiency of a 1.5% average annual from 2009 to 2020.
2. Maintain CO₂ emissions at 2020 levels (carbon-neutral growth).
3. Decrease CO₂ aviation net emissions of 50% by 2050, relative to 2005 levels emissions.

This strategy translated into significant improvements of the fuel efficiency, which brought the aviation industry to surpass its first goal reaching an annual efficiency increase of 2.1% on average between 2009 and 2016 (ATAG, 2018). The implementation of the wingtip technology alone in the aircraft design allowed to save up to 80 million tonnes of CO₂ since 2000 (ATAG 2015, 2018). While these results are encouraging, a comprehensive assessment of all operational improvements with the potential to reduce the climate impact of aviation is still lacking. To address this need, a very diverse Consortium of organisations active in the aviation domain and representative of the research community (ITU, TUD, NLR, and DLR), small-medium enterprises (AMIGO and Deep Blue), airlines (IATA), and airports (SEA Milan), have joined to run the ClimOp project.

ClimOp aims to contribute to the reduction of the climate impact of aviation and provide a harmonized set of the most-effective mitigation strategies. To achieve this result, ClimOp will compile a preliminary list of operational improvements (for example electric taxiing, flexible

runway usage, intermediate stops and formation flights) and subsequently assess them through different modelling tools. After validating the results with all aviation stakeholders, a set of mitigation strategies and recommendations will be proposed to policymakers to foster the implementation of the proposed operational improvements.

2. METHODOLOGY

ClimOp employs a sound six-step methodology that puts the focus on stakeholders' needs by utilizing an iterative validation process. The overall goal of the methodology is to allow ClimOp generating a link between its outcomes and the sectors of interest. A scheme of this methodology is shown in Fig. 1.

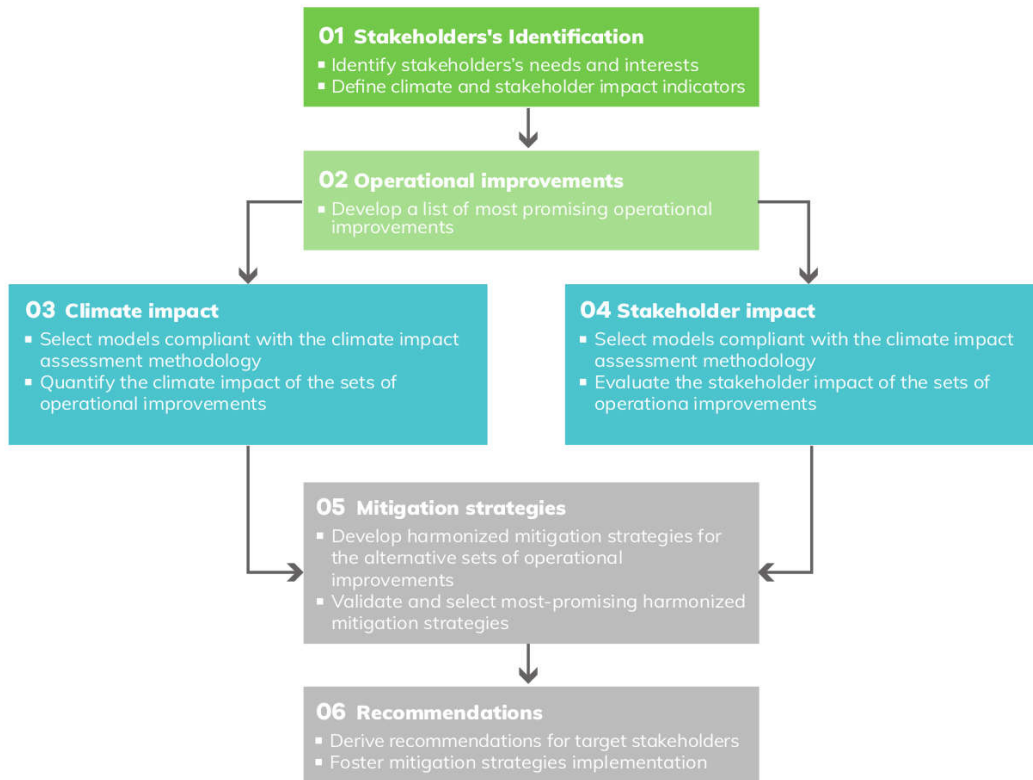


Figure 1. The six-step methodology employed in ClimOp.

As a first task, a set of Key Performance Indicators (KPIs) will be identified to evaluate how future changes of the operations in aviation will impact the climate and the different stakeholders involved in these operations. KPIs that will be taken into consideration include, for example, tonnes of fuel burnt per year, taxiing time, flight time, tonnes of CO₂/NO_x/etc emitted per year, and the Average Temperature Response (ATR) over 20, 50 or 100 years.

Subsequently, the project partners will make a list of the most-promising operational improvements (OIs hereinafter) exploiting their expert judgment. The feasibility and efficacy of these OIs will be assessed with a variety of modelling tools that enable the ClimOp partners to quantify their net impact on the climate and on the involved stakeholders. The results of this analysis will drive the development of harmonized mitigation strategies combining several OIs whose consequences reinforce each other's positive impact on the climate. Alternative mitigation strategies will be proposed to the stakeholders for an iterative process of validations. This validation process will help select the most effective and feasible mitigation strategies, which will then be translated into recommendations for policymakers which will foster the implementation of the proposed operational improvements in the aviation domain.

3. PRELIMINARY RESULTS

3.1. Operational Improvements

In the last years, many OIs have been proven effective in reducing aviation emissions of greenhouse gasses. The members of ClimOp Consortium (2020b) have identified a comprehensive list of potential OIs grouped in four main thematic areas, namely:

1. **Airline network.** This first group of OI includes climate-optimised intermediate stop-over, optimal hub-and-spoke & point-to-point networks, the splitting of long-haul into multiple short-haul flights, and transition from low-capacity, high-frequency to high-capacity, low-frequency flights.
2. **Climate-optimised trajectory.** This category is constituted by avoiding horizontal and vertical climate-sensitive areas, the concept of flying lower and slower, and satellite-based navigation for climate-optimised flight planning.
3. **Terminal movement area (TMA)** mostly regards optimised take-off and approach procedures, to reduce unnecessary waiting time and the related fuel consumption.
4. **Airport ground** operations concern the electrification of ground equipment and operations, more efficient taxiing procedures, renewable energy production at airports and increased runway and airport throughput.

3.2. Key Performance Indicators

The ClimOp consortium (2020a) is selecting a set of KPIs which will be used to quantify the impact of each individual OIs on the climate and on different stakeholders (ANSPs, governments, airlines, airports, manufacturers, passengers, etc.). The purpose is to investigate not only whether an OI, or a combination of OIs, has a net positive effect on climate, but also what are the operational and economical implications for the stakeholders. ClimOp considers quantitative and qualitative KPIs. The consortium employs quantitative metrics to assess the impact of project results at different levels (environmental, economical, safety, etc.). Instead, qualitative KPIs will evaluate the impact that results have on operating staff and processes and analyse stakeholders' acceptance from a passenger to a society level. Examples of the KPIs that ClimOp will apply to assess the impact of the OIs are the fuel consumption, the flight time, the ATR20 and the ATR100, the number of accidents per flight hour, the emissions tons per year and the taxing time. Some KPIs are transversal and will be used to assess the OIs of all the four thematic areas, for instance the ATR20/100 calculations. Other KPIs are instead specific to some OIs, for example total taxiing time will be used to evaluate improvements in ground operations. The qualitative KPIs will evaluate project aspects that rely on the assessment of human performances, e.g. the possible increase in workload for personnel because of new specific tasks that need to be performed, and stakeholder acceptance, such as the passengers' willingness to pay for more climate-friendly operation.

4. SUMMARY AND CONCLUSIONS

The ClimOp consortium has established a preliminary list of OIs and pre-selected promising KPIs to measure their impact on climate and on the aviation stakeholders. While ClimOp is at an early stage, it has a very clear plan and a sound methodology to define, over the 3.5 years of the project, a harmonised strategy to mitigate the impact on climate of the aviation industry as a whole, and to propose robust recommendations to policymakers to help them foster the implementation of the proposed OIs in the aviation domain.

ACKNOWLEDGMENTS

The ClimOp consortium has received funding from the European Union's Horizon 2020 Research and Innovation programme under Grant Agreement No 875503.

REFERENCES

- Air Transport Action Group (ATAG), 2010, *Beginner's Guide to Aviation Efficiency*, available at <https://www.atag.org/component/attachments/attachments.html?id=615>
- ATAG, 2015, *Aviation Climate Solutions*, available at <https://www.atag.org/our-publications/latest-publications.html>
- ATAG, 2018, *Aviation Benefits Beyond Borders*, available at <https://www.atag.org/our-publications/latest-publications.html>
- ATAG, 2020a, *Fact sheet 2: Aviation and climate change*, available at <https://aviationbenefits.org/downloads/fact-sheet-2-aviation-and-climate-change/>
- ATAG, 2020b, *Fact sheet 3: Tracking aviation efficiency*, available at <https://aviationbenefits.org/downloads/fact-sheet-3-tracking-aviation-efficiency/>
- ClimOp Consortium, 2020a, *D1.1 – Definition of climate and performance metrics*.
- ClimOp Consortium, 2020b, *D1.2 – Inventory of operational improvement options*.
- D. Lee, G. Pitari, V. Grewe, et al., 2010, *Transport impacts on atmosphere and climate: Aviation*, *Atm. Env.* Vol. 44, No. 37, pp. 4678–4734

OPTIMIZED FLIGHT TRAJECTORIES TO LIMIT THE CLIMATE CHANGE

Michael Finke¹, Peggy Favier², Marco Temme¹, Jürgen Rataj¹, Matthias Kleinert¹, Attila Pasztor³, Fanni Kling³ & Hu Haoliang⁴

1 Institute of Flight Guidance, DLR Braunschweig, Germany, Michael.Finke@dlr.de

2 L-Up, Paris, France

3 HungaroControl, Budapest, Ungarn

4 CARERI, China Aeronautical Radio Electronics Research Institute, Shanghai

Abstract. The perception of environmental problems especially global warming is more than ever an issue, especially in this day and age when reaching agreements on today's climate targets is a challenge and a topic of concern among European citizens of all ages. Associated effects of global warming, like extreme weather events, are driven primarily by the emission of exhaust gases (especially CO₂, nitrogen oxides and methane) and water vapour creating contrails. Hence, reducing emissions to preserve the environment, while keeping the mobility is a central society need now and in the future.

To reduce the emissions in short and medium term, changes in flight trajectory design and ATC operations are an appropriate means. Thereby, the flight trajectories are influenced on one hand by environmental and aircraft parameters, and on the other by ATC driven parameters, like route length or usable altitudes. During flight execution, re-planning on board of an aircraft using the flight management system enables the consideration of dynamic effects on the tactical level, like changes in the weather situation. For the efficiency of such a greener trajectory, it is necessary that the trajectory can be flown in the planned way, even under the actual traffic situation controlled by ATC, which today is often not the case. Hence, trajectory up-dates and negotiation processes with ATC during the flight execution are crucial to reduce emissions. In order to reduce the environmental impact, it is important to use a holistic approach considering most influencing parts of the ATM system.

The overall objective of the cooperation of Chinese and European partners in the new project Greener Air Traffic Operations (GreAT) is to reduce the fuel consumption and gas emissions during "gate-to-gate" flight phases through developing and assessing environment-friendly air traffic operational concepts, adaptive airspace structures and green trajectory optimization technologies, and supporting avionic systems. Evaluation campaigns between the European partners and in combination with the Chinese partners through cross evaluations are planned to validate the proposed concept and show a potential significant reduction of the aviation's impact on climate change.

Keywords: Green flights, Climate optimal trajectories, GreAT, Greener ATM, Emissions, Fuel Consumption

UNDERSTANDING THERMAL STABILITY OF FUTURE JET FUELS USING COMPUTATIONAL CHEMISTRY

C. Adams¹, S. Blakey², A. Meijer³, E. Alborzi¹ & C. Parks¹

¹ University of Sheffield, Department of Mechanical Engineering

² University of Birmingham, Department of Mechanical Engineering

³ University of Sheffield, Department of Chemistry

Abstract. Chemical composition of jet fuels is expected to increasingly diversify over the coming years as new crude oil sources are identified and sustainable alternative fuels are developed. The increasing diversity of fuel composition will likely impact fit-for-purpose properties like thermal oxidative stability (TOS). Deposits on critical engine components via poor TOS can lead to inefficient and unsafe operation. The Soluble Macromolecular Oxidatively Reactive Species (SMORS) mechanism is the dominant theory for predicting deposit formation in jet fuel, but the mechanistic viability of reactions has had little scrutiny. The aim of the work here was to investigate the chemical pathways in the SMORS mechanism and obtain thermochemistry data using newly available quantum chemical methods. Our calculations suggest that, for the first step of SMORS, the formation of quinones is thermodynamically favorable with modest kinetic barriers. Density functional theory (DFT) calculations were performed using the Gaussian09 program. The functional employed was B3LYP with a cc-pVDZ basis set. The bulk fuel was modelled through a polarizable continuum model (PCM) using the parameters for hexane as implemented in Gaussian. The second step of SMORS is the electrophilic aromatic substitution (EAS) reaction of quinones with indigenous antioxidants in the fuel, represented by a carbazole species. The calculations revealed that the EAS step, as it is proposed, is kinetically prohibited, with a barrier of $\Delta_r G +177.11 \text{ kcal mol}^{-1}$ to the reaction of quinone and carbazole. Furthermore, no mechanistic pathway to the next step of the SMORS mechanism could be elucidated. Thermal stressing of fuels leads to the formation of sulfonic and carboxylic acids. An acid catalyzed route reduced this EAS barrier to $\Delta_r G +6.65 \text{ kcal mol}^{-1}$ and allowed for the subsequent steps of the SMORS mechanism to proceed.

Keywords: Thermal Stability, Future Fuels, Quantum Chemistry, SMORS, Modelling

INTRODUCTION

Climate change and dwindling fossil fuel reserves are driving increased diversification of fuel sources (United Nations 2015). On the one hand, new crude oil fields are producing jet fuel higher in heteroatom and aromatic content (Dwyer et. al 2017). By contrast, fuels produced from Fischer-Tropsch and hydro-processing techniques contain fewer heteroatomics. However, as a result, they have low natural levels of antioxidants (Hazlet 1991). As a consequence, these different sources will have a different fuel chemistry and therefore, have a different thermal stability. Poor thermal stability can lead to deposits on blocked pipes, fouled fuel-oil heat exchangers, and distorted injection nozzle passages. These, all compromising efficiency and increase maintenance requirements (Zabarnick 1993). Thus, a better understanding of the chemical pathways that lead to fouling is needed.

Jet fuel deposition arises from autoxidation chain reactions in the fuel caused by small amounts of dissolved oxygen and temperatures between 100-350°C (Andrésen et. al 2001). The dominant mechanism of deposit formation in the literature is the Soluble Macromolecular Oxidatively Reactive Species (SMORS) mechanism (see Figure 1, Beaver et. al 2005; Sobkowiak et. al 2009; Kabana et. al 2011). The SMORS process involves quinones, formed from the oxidation of phenols. These quinones undergo successive electrophilic aromatic substitution reactions with fuel heteroatoms, such as carbazoles or indoles (see figure 1). A generalized scheme is given below. This scheme starts with phenols (species a), which ultimately form much larger species (k) via a reaction with carbazoles (i), which represent the nitrogen heterocycles found in fuel (Kamin and Ortman 2019). However, despite the extensive experimental investigation into the SMORS process, there has been little mechanistic scrutiny of the reaction scheme. Quantum chemistry is an excellent tool for such mechanistic investigation of reaction schemes. It has been used in previous studies for

investigation jet fuel thermal stability (Zabarnick and Phelps 2006; Dwyer et. al 2017). Moreover, quantum chemical methods can provide thermochemical parameters for eventual use in pseudo-detailed mechanisms.

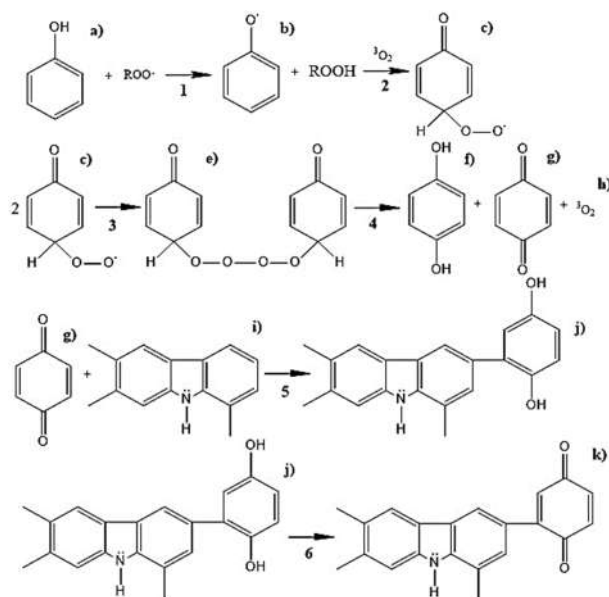


Figure 1 The generalized Soluble Macromolecular Oxidatively Reactive Species (SMORS) mechanism

In a quantum chemical calculation, the structure of the reactants, products and transition states are guessed initially. From these guesses an optimization procedure is initiated. Reactants and products are found in local energy minima, whereas transition states are found at local first-order saddle points. Various ‘methods’ are employed to relate the nuclear coordinates to an electronic energy. Density functional theory (DFT) methods are hugely popular, because of their computational cost and associated accuracy. DFT methods rely on relating the ground state electron density to the energy of the system. This is expressed in the first Hohenberg-Kohn theorem (Hohenberg and Kohn 1964):

$$\rho(x, y, z) \equiv \rho_0(\mathbf{r}) \rightarrow E_0 \quad (1)$$

The total energy of the system can then be expressed as:

$$E_0[\rho_0] = T_{ni}[\rho_0] + V_{ne}[\rho_0] + V_{ee}[\rho_0] + \Delta T[\rho_0] + \Delta V_{ee}[\rho_0] \quad (2)$$

T_{ni} represents the kinetic energy for non-interacting electrons, V_{ne} the nuclear-electron repulsion, and V_{ee} the electron-electron repulsion. ΔT is a correction term for non-interacting electrons and ΔV_{ee} is a correction term for the deviation between real electron-electron repulsion compared to charge Coulomb repulsion. The key issue with DFT is that the last two terms, known collectively as the exchange correlation (E_{xc}), are unknown. Instead a series of approximate terms (functionals) have been proposed (Lewars 2003). The B3LYP functional is one such functional and has been used in the investigations here. Previous work exploring the thermal stability of jet fuel have used DFT methods with a B3LYP functional as well (Zabarnick and Phelps 2006; Dwyer et. al 2017).

METHODS

B3LYP was chosen as a compromise between accuracy and cost. A series of benchmarking reactions revealed B3LYP has a root mean square deviation (RMSD) of 6 kcal mol⁻¹ for barrier heights (Mardirossian and Head-Gordon 2017). A polarizable continuum solvent model (PCM) was used to represent the bulk fuel solvent. Hexane was chosen as the solvent to represent the bulk fuel. The cc-pVDZ basis set, the mathematical representation of

electronic wave function, was chosen. All the calculations were performed on Gaussian 09 (Frisch et. al 2009).

RESULTS AND DISCUSSION

The first step of the SMORS mechanism involves the abstraction of a phenolic hydrogen by a radical species in the fuel (step 1 in figure 1). Several radical species arise from the initial autoxidation of the fuel: peroxy ($\text{ROO}\cdot$), hydroxy ($\text{RO}\cdot$) and alkyl ($\text{R}\cdot$) radicals. When a dodecane moiety is chosen as the R group, the reaction Gibbs energies for the abstraction step are $\Delta_rG(\text{ROO}\cdot) = +4.05 \text{ kcal mol}^{-1}$, $\Delta_rG(\text{RO}\cdot) = -16.95 \text{ kcal mol}^{-1}$, and $\Delta_rG(\text{R}\cdot) = -16.55 \text{ kcal mol}^{-1}$. The exergonicity of the reactions with hydroxy and alkyl radicals demonstrate the antioxidant properties of phenols. In these cases, phenols act as a thermodynamic sink for radical species, slowing down the radical chain reaction. Interestingly, abstraction by peroxy radicals is thermodynamically uphill- implying that the peroxy radical has greater stability than the phenoxy radical (species (b) figure 1). The Gibbs activation energy for abstraction by a dodecane peroxy radical was $+14.42 \text{ kcal mol}^{-1}$.

Steps 2-4, leading to the formation of a quinone species (species (g), figure 1) were thermodynamically downhill by $-7.15 \text{ kcal mol}^{-1}$. These steps yielded a quinone (species (f), figure 1) as well as a half-hydroquinone with a ground-state oxygen molecule (species (h), figure 1). The hydroquinone (species (g), figure 1) did not form, because the distance between the hydrogen atoms in the intermediate species (e) was too large.

Step 5, the reaction between a quinone (species (g), figure 1) and a carbazole (species (i), figure 1), proceeds via an electrophilic aromatic substitution (EAS) reaction. Quinones are highly electrophilic compound. Thus, they are proposed to react with electron-rich heteroatoms in the fuel. Carbazoles, known to be present in the fuel (Balster et. al 2006), is used to represent these heteroatoms here. EAS reactions proceed with two transition states. The first transition state leads to the formation of a non-aromatic intermediate. The second

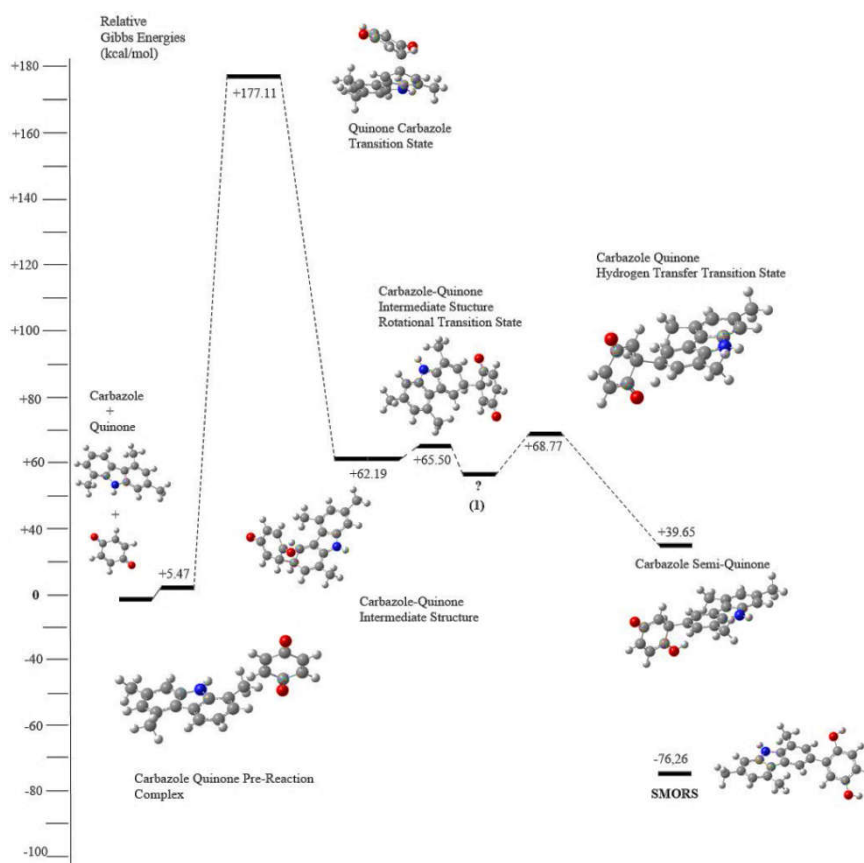


Figure 2 Electrophilic aromatic substitution step between a quinone and carbazole

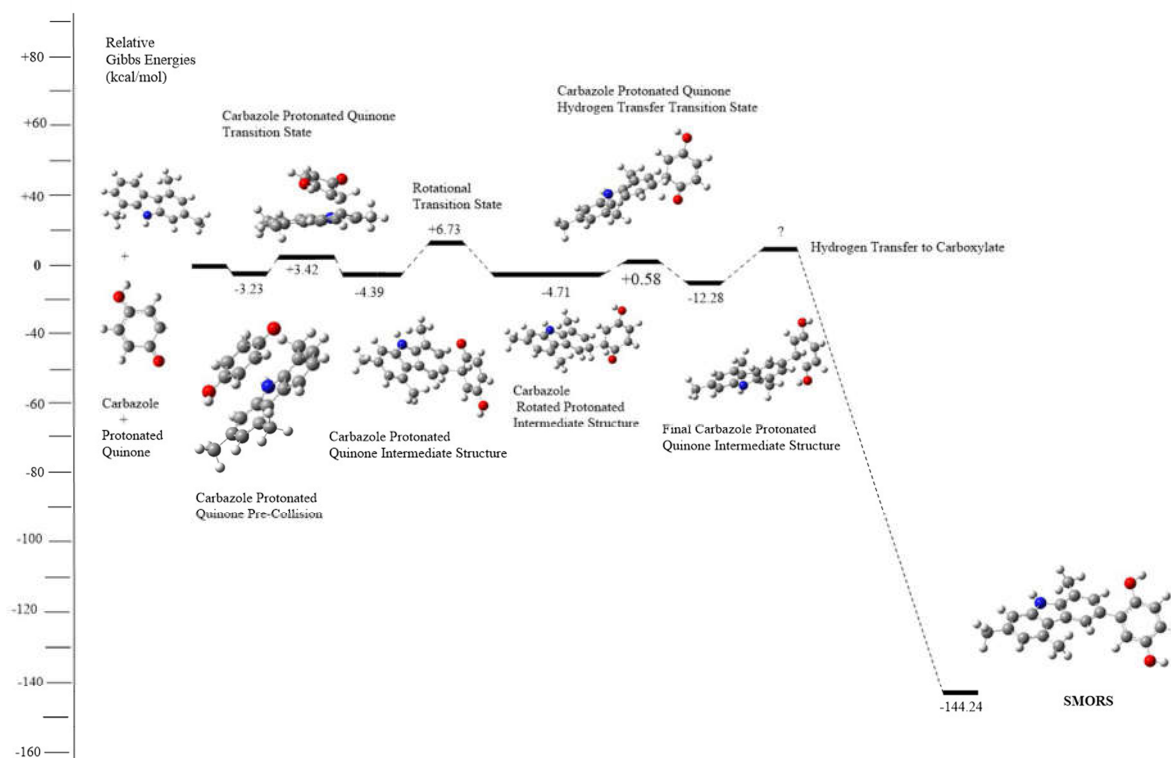


Figure 3 Acid catalysed electrophilic aromatic substitution between a protonated quinone and carbazole

transition state involves a hydrogen transfer. This leads to re-aromatisation and formation of the product. The first transition state, as it is proposed for the SMORS scheme, is kinetically prohibited (Gibbs energy barrier height: +177.11 kcal mol⁻¹). Thus, the final product (species (j), figure 1) cannot be reached (see figure 2).

An analogous reaction in the literature between a quinone and pyrrole, another nucleophilic nitrogen heterocycle, employed an acid acetic acid catalyst. This allowed the reaction between the species to proceed (Lion D. C. et al. 2002). Acids are known to form during the autoxidation of bulk fuel, leading to carboxylic acids (DeWitt et. al 2014). Moreover, oxidation of end-of-chain sulfur species and disulfides leads to sulfonic acids (Naegeli 1999). Therefore, the reaction between a protonated quinone and carbazole was investigated as an alternative to the proposed SMORS scheme. This led to significantly reduced activation energies (maximum barrier height: 6.73 kcal mol⁻¹). As a consequence, the final SMORS product (species (j), figure 1) could be expected to form easily. This scheme is presented in figure 3.

This leaves the question, what the proton source in this case is. Further calculations show that the free energy barriers in hexane solvent are +133.98 kcal mol⁻¹ for carboxylic acid and +88.02 kcal mol⁻¹ for sulfonic acid, respectively. At these levels the barriers are prohibitively high, but small amounts of free water could offer a site for this protonation step to occur.

CONCLUSION

DFT with a B3LYP functional and cc-pVDZ basis set was used to investigate the SMORS jet fuel deposition mechanism. The SMORS mechanism involves the formation of electrophilic quinones which react with electron rich heteroatoms in the fuel. Formation of quinones from phenols was shown to be thermodynamically favourable. However, the subsequent reaction between a carbazole (chosen as a model heteroatomic in the generalised SMORS scheme) was shown to be kinetically prohibited. An acid catalysed scheme reduced the barrier, allowing for the coupling of the quinone and carbazole.

Our work shows the crucial role acids play a role in the formation of deposits. Since sulfonic acids are stronger acids than carboxylic acids, fuels containing end-chain sulfur species would be expected to yield greater amounts of deposits. This has also been demonstrated in several experiments (Taylor and Wallace 1968; Naegeli 1999; Rawson et. al 2018). Here, thiols and disulfides yield sulfonic acids upon reactions with hydroperoxides and radical species formed from autoxidation reactions. However, it is noted that bulk fuel is an unsuitable solvent for protonation of the quinone to occur. Free water, on the other hand, known to be present in fuel, could offer a sight for protonation steps to occur. Particularly, as polar species and acids are known to congregate around free water droplets (Baena-Zambrana et. al 2013).

Our work has implications for building future models for fuels. Our work indicates that fuels rich in acid forming sulfur components and heterocycles will exhibit poor thermal stability. On the other hand, fuels produced from renewable sources with low or zero heteroatom content should exhibit greater thermal stability.

ACKNOWLEDGEMENTS

I'd like to thank my supervisors Anthony, Simon and Ehsan for their help. Anthony for his guidance in the quantum chemistry calculations. Chris Parks for his invaluable guidance on Gaussian. Simon and Ehsan for their rich knowledge of the jet fuels area.

REFERENCES

- Baena-Zambrana, S., Repetto, S. L., Lawson, C. P., & Lam, J. K. W. (2013). Behaviour of water in jet fuel - A literature review. *Progress in Aerospace Sciences*, 60, 35–44.
- Dwyer, M., Blakey, S., Alborzi, E., & Meijer, A. (2017). The role of hydrocarbon composition on the thermal stability of aviation fuels. 15th International Symposium On Stability, Handling And Use Of Liquid Fuels.
- Lewars, E., (2003). Computational chemistry. Introduction to the theory and applications of molecular and quantum mechanics.
- Hazlett, R. N. (1991). Thermal Oxidation Stability of Aviation Turbine Fuels. In *Thermal Oxidation Stability of Aviation Turbine Fuels*. <https://doi.org/10.1520/mono1-eb>
- Andrésen, J. M., Strohm, J. J., Sun, L., & Song, C. (2001). Relationship between the formation of aromatic compounds and solid deposition during thermal degradation of jet fuels in the pyrolytic regime. *Energy and Fuels*, 15(3), 714–723.
- Kabana, C. G., Botha, S., Schmucker, C., Woolard, C., & Beaver, B. (2011). Oxidative stability of middle distillate fuels. Part 1: Exploring the soluble macromolecular oxidatively reactive species (SMORS) mechanism with jet fuels. *Energy and Fuels*, 25(11), 5145–5157.
- Katta, V. R., Jones, E. G., & Roquemore, W. M. (1998). Modeling of deposition process in liquid fuels. *Combustion Science and Technology*, 139(1), 75–111.
- Lion, D. C., Baudry, R., Hedayatullah, M., Da Conceição, L., Genard, S., & Maignan, J. (2002). Reaction of 2, 5-dimethylpyrroles with quinones. Synthesis of new pyrrolylquinones dyes. *Journal of Heterocyclic Chemistry*, 39(1), 125–130.
- Balster, L. M., Zabarnick, S., Striebich, R. C., Shafer, L. M., & West, Z. J. (2006). Analysis of polar species in jet fuel and determination of their role in autoxidative deposit formation. *Energy and Fuels*, 20(6), 2564–2571.
- J. Frisch, G. W. Trucks, H. B. Schlegel, G. E. Scuseria, M. A. Robb, J. R. Cheeseman, G. Scalmani, V. Barone, B. Mennucci, G. A. Petersson, H. Nakat-suji, M. Caricato, X. Li, H. P. Hratchian, A. F. Izmaylov, J. Bloino, G. Zheng, J. L. Sonnenberg, M. Hada, M. Ehara, K. Toyota, R. Fukuda, J. Hasegawa, M. Ishida, T. Nakajima, Y. Honda, O. Kitao, H. Nakai, T. Vreven, J. A. Montgomery, Jr., J. E. Peralta, F. Ogliaro, M. Bearpark, J. J. Heyd, E. Brothers, K. N. Kudin, V. N. Staroverov, R. Kobayashi, J. Normand, K. Raghavachari, A. Rendell, J. C. Burant, S. S. Iyengar, J. Tomasi, M. Cossi, N. Rega, J. M. Millam, M. Klene, J. E. Knox, J. B. Cross, V. Bakken, C. Adamo, J. Jaramillo, R. Gomperts, R. E. Stratmann, O. Yazyev, A. J. Austin, R. Cammi, C. Pomelli, J. W. Ochterski, R. L. Martin, K. Morokuma,

- V. G. Zakrzewski, G. A. Voth, P. Salvador, J. J. Dannenberg, S. Dapprich, A. D. Daniels, Farkas, J. B. Foresman, J. V. Ortiz, J. Cioslowski, and D. J. Fox, (2009). "Gaussian09 Revision D.01." Gaussian Inc. Wallingford CT
- Mardirossian, N., & Head-Gordon, M. (2017). Thirty Years of Density Functional Theory In Computational Chemistry: An Overview And Extensive Assessment of 200 Density Functionals. *Molecular Physics*, Vol. 115, pp. 2315–2372.
- Naegeli, D. W. (1999). The Role Of Sulfur In The Thermal Stability of Jet Fuel. *Proceedings of the ASME Turbo Expo*, 2.
- P. Hohenberg and W. Kohn (1964), "Inhomogeneous Electron Gas", *Physical Review*, Vol. 136, pp. 864–871.
- Rawson, P. M., Webster, R. L., Evans, D., & Abanteriba, S. (2018). Contribution of Sulfur Compounds To Deposit Formation In Jet Fuels At 140 °C Using A Quartz Crystal Microbalance Technique. *Fuel*, 231, 1–7.
- S. Zabarnick, (1993). "Pseudo-Detailed Chemical Kinetic Modeling Of Antioxidant Chemistry For Jet Fuel Applications," *Energy and Fuels*, vol. 12, no. 3, pp. 547–553.
- Sobkowiak, M., Griffith, J. M., Wang, B., & Beaver, B. (2009). Insight Into The Mechanisms of Middle Distillate Fuel Oxidative Degradation. Part 3: Hydrocarbon Stabilizers to Improve Jet Fuel Thermal Oxidative Stability. *Energy and Fuels*, 23(4), 2041–2046.
- Taylor, W. F., & Wallace, T. J. (1968). Kinetics of deposit formation from hydrocarbons: Effect of Trace Sulfur Compounds. *Industrial and Engineering Chemistry Product Research and Development*, 7(3), 198–202.
- United Nations. (2015). Summary of the Paris Agreement. *United Nations Framework Convention on Climate Change*, pages 27–52,
- Zabarnick, S., & Phelps, D. K. (2006). Density Functional Theory Calculations Of The Energetics And Kinetics Of Jet Fuel Autoxidation Reactions. *Energy and Fuels*, 20(2), 488–497.

EFFECT OF FUEL COMPOSITION ON NVPM EMISSIONS PRODUCED BY AN RQL COMBUSTION RIG USING CONVENTIONAL AND ALTERNATIVE FUELS

J. Harper¹, E. Durand¹, M. Johnson² & A. Crayford¹

¹ School of Engineering, Cardiff University, UK, HarperJ4@cardiff.ac.uk

² Measurement Engineering, Rolls-Royce, Derby, UK

Abstract: Emissions produced by aircraft gas turbine engines, such as Particulate Matter (PM), NO_x, and CO₂, have long been a source of concern for their detrimental effects on local air quality and the environment. An ongoing topic of research has been the study of alternative fuels, which have been shown to reduce harmful emissions. As part of the H2020 JETSCREEN program, the impact of fuel composition on gaseous and non-volatile PM (nvPM) emissions was investigated using a scaled tubular Rich-burn quick-Quench Lean-burn (RQL) combustion test rig, which utilised a pre-filming airblast atomiser and was operated at various combustion conditions. Nine fuels consisting of conventional and alternative fuels, and fuel blends were tested, assessing how variations in hydrogen, total aromatics and sulphur mass contents, along with the physical properties of viscosity and surface tension impacted measured emissions. In agreement with previous studies, it was observed that an increase in fuel hydrogen mass content (linked to a reduction in aromatic content) decreased the nvPM Emission Indices (EI) for particle number, mass, and size. Fuels generally followed a well-established hydrogen content trend, with some fuels containing high diaromatics exhibiting higher nvPM emissions compared to fuels with an aromatics content composed mostly of monoaromatics. Deviation from average fuel hydrogen-based correlation also suggests that increased viscosity and surface tension may negatively impact nvPM emissions through reductions in atomisation efficiency.

Keywords: non-volatile Particulate Matter, Aviation emissions, Alternative fuels, Fuel hydrogen content, Fuel aromatic content

INTRODUCTION

Aircraft gas turbine engines produce ultrafine PM and gases which are a growing source of concern for local air quality and the environment (Brasseur et al., 2015; Yim et al., 2015). In order to mitigate harmful aircraft emissions, cleaner alternative fuels have been investigated showing potential reductions in emissions compared with conventional jet fuels (Lobo et al., 2012; Timko et al., 2010). A long-established inverse correlation between hydrogen mass content and nvPM emissions has been demonstrated in both diffusion flames (Calcote and Manos, 1983) and practical gas turbine applications (Lobo et al., 2015). Strong interdependencies are observed between hydrogen and aromatic content; however, hydrogen content alone may be insufficient in accurately predicting the sooting tendencies of alternative fuels. Other fuel parameters which are thought to exacerbate emissions therefore need to be studied experimentally to aid modelling efforts. Previous studies, have noted the significance of di-aromatic compounds (e.g. naphthalenes) on nvPM emissions (Brem et al., 2015), and suggested combined parameters of fuel properties provide improved correlations for soot formation rates and sooting tendencies (Calcote and Manos, 1983; Yang et al., 2007). Meanwhile, fuels of high fuel viscosities and surface tensions are known to reduce fuel atomisation which can impact both the gaseous and nvPM emissions profiles produced by gas turbines (Chin and Lefebvre, 1989).

EXPERIMENTAL METHODS

Experimental Setup and Measurement

Testing was undertaken using an experimental small-scale RQL combustor developed by Cardiff University. The RQL combustor was designed to operate, within the Gas Turbine Research Centres High-Pressure Optical Chamber (HPOC) at power conditions representative of small aircraft engines (250 kW <8 bar, <573 K). The fuel nozzle was a modified version of a prefilming airblast atomiser developed using Additive Manufacturing processes (Crayford et al., 2019). The nvPM number and mass emissions were measured

using an compliant (ICAO, 2017) sampling and measurement reference system (Crayford and Johnson, 2013). Gaseous emissions (NO_x, CO, UHC's & CO₂) were also measured using standard techniques but not presented in this work. Additional particle size distributions were measured using a fast particle analyser (DMS-500), using a monomodal aggregate inversion matrix.

Fuel Properties and Test Matrix

A total of nine fuels were investigated, including conventional jet fuels and alternative fuels (biojet fuels and synthetic fuels), as well as blends of conventional and alternative fuels. Fuel composition uncertainty was shown to present a challenge in this study with quoted compositions varying depending on the fuel test method employed. Several physical and chemical factors are thought to influence the emissions generated, and so accurate and repeatable analysis of fuel composition and physical properties is essential. For the data presented, fuel composition data (mass contents of hydrogen, carbon, mono-aromatics and di-aromatics) were acquired using GCGC analysis, while physical properties of kinematic viscosity and surface tension were measured using a viscometer and tensiometer.

For each fuel, experiments were undertaken at a range of combustor inlet pressures (1-2.5 bar), primary zone AFRs (2.6-3.4) and global AFRs (40-46). The mass flowrates of primary (atomisation) air and secondary (combustion) air were independently controlled and preheated to approximately 75°C and 125°C, respectively. Fuel temperature was maintained at 30°C.

Data Processing

In this study, measured nvPM emissions were converted to their respective EIs as prescribed by ICAO standards (ICAO, 2017) and were subsequently corrected for size-dependent particle loss in the sampling and measurement system using the DMS-500 measured particle size distributions and UTRC particle transport model (SAE international, 2013). This permitted a direct comparison of emissions at combustor exit plane.

Results and Discussion

The effect of specific fuel properties on nvPM emissions was assessed by comparing the combustor exit nvPM EI number, EI mass and Geometric Mean Diameter (GMD) for the nine investigated fuels. **Figure 2** shows nvPM EI number, EI mass and GMD values of each fuel at different test conditions. The effect of fuel hydrogen content, mono-aromatic content and di-aromatic content on nvPM EI mass for a fixed test condition at two different combustor inlet pressures is shown in **Figure 3**. In both figures, each fuel is differentiated by hydrogen content and marked by an associated colour.

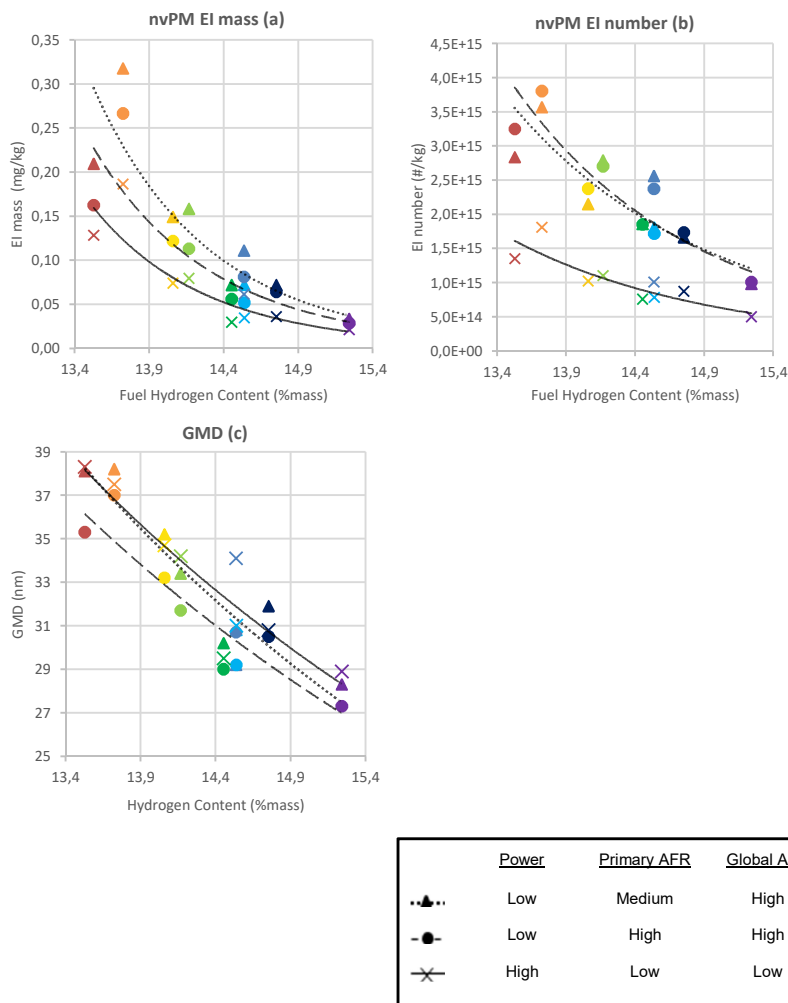


Figure 2: Combustor exit nvPM EI number (a), mass (b) and GMD (c) at a combustor inlet pressure of 2 bar

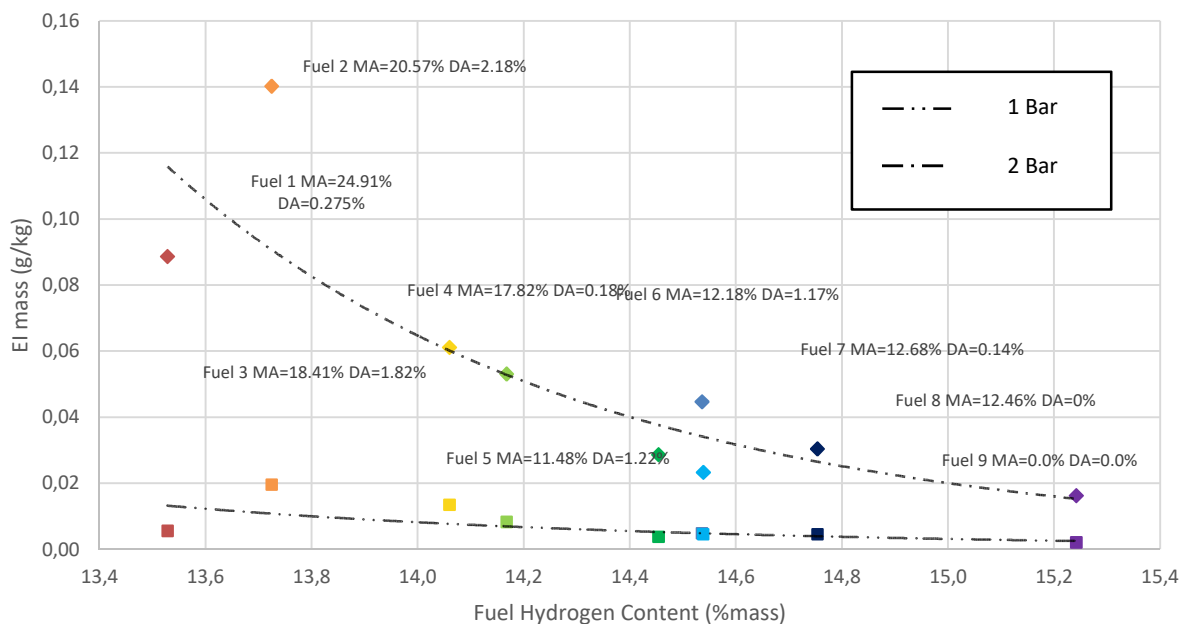


Figure 3: Combustor exit nvPM EI mass emissions against fuel hydrogen content at high power condition for different combustor inlet pressures

It was observed from this data that increasing the combustor inlet pressure generally increased the nvPM EI number, nvPM EI mass and GMD. Increasing the global AFR was shown to decrease both nvPM EI number and mass. Meanwhile, increased atomisation air (i.e. primary AFR) served to decrease nvPM EI mass but had less impact on nvPM EI number. The nvPM emissions are generally seen to decrease with increased fuel hydrogen content, as expected. However, some fuels were observed to deviate from the average trend plotted for visual aid. For example, fuel 6 produced higher nvPM EI number and mass than other fuels with similar hydrogen contents, which may be attributed to a combination of high di-aromatics content and higher kinematic viscosity. Fuel 2 is also observed to produce more nvPM than Fuel 1 across all conditions tested, which can be attributed to its relatively higher di-aromatic content.

CONCLUSION

The nvPM emissions of nine investigated fuels demonstrated that increased fuel hydrogen content generally led to a reduction in nvPM number, mass and size for all the different conditions tested. Increased di-aromatics are shown to exhibit higher nvPM emissions compared to fuels of similar hydrogen content but whose aromatic content is composed of mostly mono-aromatics. The results of this study also suggest that physical fluid properties may impact the witnessed nvPM emissions by reducing injector atomisation efficiency.

ACKNOWLEDGEMENTS

The authors would like to thank GTRC staff members for the operation of the combustor rig and acquisition of gaseous emissions. This project was performed as part of the JETSCREEN Jet Fuel Screening and Optimization research programme and has received funding from the European Union's Horizon 2020 research and innovation programme under grant agreement No 723525.

REFERENCES

- Brasseur, G.P., Gupta, M., Anderson, et al. (2015). Impact of Aviation on Climate: FAA's Aviation Climate Change Research Initiative (ACCRI) Phase II. *Bull. Am. Meteorol. Soc.* 97, 561–583.
- Brem, B.T., Durdina, L., Siegerist, et al. (2015). Effects of Fuel Aromatic Content on Nonvolatile Particulate Emissions of an In-Production Aircraft Gas Turbine. *Environ. Sci. Technol.* 49, 13149–13157.
- Calcote, H.F., and Manos, D.M. (1983). Effect of molecular structure on incipient soot formation. *Combust. Flame* 49, 289–304.
- Chin, J.S. & Lefebvre A.H. (1990) Influence of Fuel Chemical Properties on Soot Emissions from Gas Turbine Combustors, *Combustion Science and Technology*, 73:1-3, 479-486
- Crayford, A., and Johnson, M. (2013). SAMPLE III SC.03- Studying, sAmpling and Measuring of aircraft ParticuLate Emission (EASA).
- Crayford, A.P., Lacan, F., Runyon, et al. (2019). Manufacture, Characterization and Stability Limits of an AM Prefilming Air-Blast Atomizer. (American Society of Mechanical Engineers Digital Collection).
- ICAO (2017). Annex 16 - Environmental Protection Volume 2 - Aircraft Engine Emissions.
- Lobo, P., Rye, L., Williams, P.I., et al. (2012). Impact of Alternative Fuels on Emissions Characteristics of a Gas Turbine Engine – Part 1: Gaseous and Particulate Matter Emissions. *Environ. Sci. Technol.* 46, 10805–10811.
- Lobo, P., Christie, S., Khandelwal, B., et al. (2015). Evaluation of Non-Volatile PM Emissions Characteristics of an Aircraft Auxiliary Power Unit with Varying Alternative Jet Fuel Blend Ratios. *Energy Fuels* 29, 151016011415009.
- SAE international (2013). AIR 6241-Procedure for the Continuous Sampling and Measurement of Non-Volatile Particle Emissions from Aircraft Turbine Engines.

- Timko, M.T., Yu, Z., Onasch, T.B., Wong, H.-W., et al. (2010). Particulate Emissions of Gas Turbine Engine Combustion of a Fischer–Tropsch Synthetic Fuel. *Energy Fuels* **24**, 5883–5896.
- Yang, Y., Boehman, A.L., and Santoro, R.J. (2007). A study of jet fuel sooting tendency using the threshold sooting index (TSI) model. *Combust. Flame* **149**, 191–205.
- Yim, S.H.L., Lee, G.L., Lee, I.H., et al. (2015). Global, regional and local health impacts of civil aviation emissions. *Environ. Res. Lett.* **10**, 034001.

IMPACT OF FUEL COMPOSITION ON AERONAUTIC EMISSIONS

A. Berthier¹, D. Delhaye², I. K. Ortega³ & C. Focsa⁴

¹ *Physique des Lasers, Atomes et Molécules, CERLA – Centre d'Etudes et de Recherches Lasers et Applications, Lille University, CNRS, UMR 8523, F-59000 Lille, France, antoine.berthier@onera.fr*

² *Multi-physics for Energetics Department, ONERA Université Paris Saclay, F-91123, Palaiseau, France, david.delhaye@onera.fr*

³ *Multi-physics for Energetics Department, ONERA Université Paris Saclay, F-91123, Palaiseau, France, ismael.ortega@onera.fr*

⁴ *Physique des Lasers, Atomes et Molécules, CERLA – Centre d'Etudes et de Recherches Lasers et Applications, Lille University, CNRS, UMR 8523, F-59000 Lille, France, cristian.focsa@univ-lille1.fr*

Abstract. Air transport is a steadily growing sector, and this trend is expected to continue in the coming years (ICAO, 2018). As a result, the impact of aviation emissions on climate and air quality is of great concern. Among the various solutions available, the aviation industry has identified the development of new alternative fuels as one of the main tools to reduce its emissions (Vorster S, 2013). Currently, six alternative fuel production streams are technically certified and many more are under review (ASTM D7566). In this context, this study aims to study the emissions of these different alternative fuels to establish a link between their emissions and their chemical composition.

In this work, different fuels have been studied including different Jet A-1 from different productions, biosourced kerosene produced from alcohol or esters, and mixtures at different rates between Jet A-1 and these alternative fuels. Fuels with different levels of sulfur and aromatic compounds will also be studied. The measurement line used allows to study the physical characteristics of the nonvolatile particles, isolated with a catalytic stripper heated to 350 ° C. To complete the physical characterization of the particles, filter samples were taken upstream of the line to perform an off-line chemical characterization of the emissions.

The use of alternative fuels that does not include aromatic compounds resulted in a decrease in concentration both in number and mass of non-volatile particles emitted compared to the combustion of Jet A-1.

Keywords: Alternative fuels, volatile and non-volatile particulate matter, physico-chemical characterization

REFERENCES

ICAO, *Airbus Global Market Forecast*, 2018 (<https://www.airbus.com/content/dam/corporate-topics/pu-blications/media-day/GMF-2018-2037.pdf>).

Vorster S. et al, 2013, *2050 Scenarios for Long-Haul Tourism in the Evolving Global Climate Change Regime*, Sustainability, 5, 1-51.

ASTM D7566-19, 2019, *Standard Specification for Aviation Turbine Fuel Containing Synthesized Hydrocarbons*, ASTM International, West Conshohocken, PA, www.astm.org.

AIRCRAFT ENGINE PARTICULATE MATTER EMISSIONS USING SUSTAINABLE AVIATION FUELS

P. Lobo¹, T. Schripp², J. Corbin¹, P. Osswald², M. Shook³, E. Crosbie³, C. Robinson³, Z. Yu⁴, R. Miake-Lye⁴, A. Freedman⁴, G. Smallwood¹, P. Whitefield⁵, M. Köhler² & B. Anderson³.

¹ Metrology Research Center, National Research Council Canada, Canada

² Institute of Combustion Technology, German Aerospace Center, Germany

³ NASA Langley Research Center, NASA, USA

⁴ Aerodyne Research Inc, USA

⁵ Center of Excellence for Aerospace Particulate Emissions Reduction Research, Missouri University of Science and Technology, USA

Abstract. Aircraft engines are a unique source of emissions both at ground level in the urban environment and at cruise level altitudes. The characteristics of aircraft engine emissions are distinct from other sources, and have been shown to vary with engine type, fuel composition, and engine operating condition. There are increasing concerns about the impact of aircraft emissions on local air quality, health, and climate change.

The ND-MAX / ECLIF II (NASA/DLR-Multidisciplinary Airborne Experiment / Emission and Climate Impact of Alternative Fuel II) measurement campaign was conducted at the Ramstein Air Base in Germany in January 2018 to better understand the impacts of using sustainable aviation fuels to mitigate these environmental impacts. The campaign involved ground-based testing as well as in-flight measurements at cruise conditions of the emissions from a DLR A320 aircraft with V2527 engines. As part of the experimental campaign, 5 different fuels were evaluated in terms of particulate matter (PM) emissions – 2 conventional fossil fuels and 3 blends of conventional and sustainable aviation fuels. The PM emissions (total and non-volatile) were measured at various engine power settings, ranging from idle to maximum continuous thrust using diagnostic instruments for particle number, mass, size, and composition. The resulting data provide an improved understanding of PM physical, optical, and chemical properties as a function of fuel composition and engine operating conditions. The PM emissions were found to be well correlated with fuel hydrogen content, with lower emissions recorded for fuels with higher hydrogen content. The non-volatile PM (nvPM) emissions data was also used to validate the model developed by International Civil Aviation Organization (ICAO) as part of the new nvPM regulatory standard to account for changes in emissions as a function of engine operating condition and fuel hydrogen content.

This work was funded by NASA, DLR, US FAA, NRC, and Transport Canada.

Keywords: Alternative fuels for aviation

REVIEWING THE DEVELOPMENT OF ALTERNATIVE AVIATION FUELS AND AIRCRAFT PROPULSION SYSTEMS

Karna Dahal^{1,*}, Selma Brynolf¹, Maria Grahn¹, Julia Hansson^{1,2} & Mariliis Lehtveer³

¹ Department of Mechanics and Maritime Sciences, Maritime Environmental Sciences, Chalmers University of Technology, SE-412 96, Gothenburg, Sweden

² Sustainable Society, Energy, IVL Swedish Environmental Research Institute, Box 530 21, SE-400 14, Gothenburg, Sweden

³ Department of Space, Earth and Environment, Energy Technology, Chalmers University of Technology, SE-412 96, Gothenburg, Sweden

* corresponding author (karna.dahal@chalmers.se)

Abstract. Alternative aviation fuels such as bio-jetfuels, liquid natural gas (LCH₄), hydrogen (H₂), electro-jetfuels and direct electricity use play an important role in decarbonizing the aviation sector. New aircraft propulsion systems are being developed but low-blending of fuels is possible for some options. It is imperative to understand the technical, environmental and economic performance of the different alternative aviation fuels and the new engine and propulsion technologies for the utilization of these fuels. We have reviewed various literature to map the current status of development on alternative aviation fuels and related aircraft propulsion systems in relation to different perspective such as their cost and technical maturity. There are several challenges related to the design and implementation of the fuels and new propulsion systems. For instance, the volumetric energy content of alternative fuels is lower than the conventional aviation fuels which requires larger fuel storage tanks. Despite the advantageous environmental performance, both the bio-jet and electro-jetfuels are currently not economically competitive. Yet, studies forecast that increased use of alternative aviation fuels is possible after modifications of engines, fuel storage tanks and improvements of the aerodynamics of aircraft and by introducing subsidies and/or carbon taxes on conventional jetfuels.

Keywords: Alternative aviation fuels, aircraft propulsion systems, cost, bio-jetfuels, hydrogen, performance

INTRODUCTION

Alternative aviation fuels are low to zero carbon fuels which can reduce greenhouse gas (GHG) emissions and climate impacts significantly. These include bio-jetfuels, liquid natural gas/liquid methane (LCH₄), hydrogen/liquid hydrogen (H₂/LH₂), electro-fuels [produced from electricity, water (H₂O) and carbon-dioxide (CO₂)], and direct electricity use. The compositions of these alternative aviation fuels differ based on their feedstocks and production processes (Zhang et al., 2016). All aviation fuels must pass laboratory, storage and flight tests to get certified before they can be operated in the aircraft (Yilmaz & Atmanli, 2017). The development and commercialization of different bio-jetfuels and synthetic jetfuels is on-going and other possible alternative aviation fuel options such as LH₂ and LCH₄ are being explored. Several airlines have tested bio-jetfuels in some of their aircraft and minor amounts of bio-jetfuels are being used in low blending with fossil jet kerosene at present (Wang & Tao, 2016; IRENA, 2017). In parallel, there is a growing interest for production and testing of electro-fuels (Zhu, 2019). Electro-fuels are primarily produced via electrolysis of H₂O followed by different synthesis processes combining H₂ and captured carbon. These include electro-methane (e-CH₄), electro-methanol (e-CH₃OH) and electro-n-octane (electro-nC₈H₁₈) (Goldmann et al., 2018).

Some alternative aviation fuels cannot be adapted into the existing aircraft engines which run on fossil jet kerosene (Zhang et al., 2016). Thus, new aircraft propulsion systems are being studied and developed to operate on alternative aviation fuels. This is also the case for all electric and hybrid electric propulsion systems which can significantly reduce both the CO₂ and non-CO₂ emissions from aviation sector (Bogaert, 2015; Voskuil et al., 2018; Schäfer et al., 2019). It is imperative to understand the technical, environmental and economic performance of the alternative aviation fuels and the new engine and propulsion technologies for the utilization of these fuels. Thus, we review various literature to map the current status

of development on all the above-mentioned alternative aviation fuels and related aircraft propulsion systems in relation to their cost and technical maturity.

METHODOLOGY AND REVIEWED LITERATURE

We reviewed 89 different publications published between 2005-2019 for a systematic assessment of alternative aviation fuels and related propulsion systems including electric and hybrid propulsions for future aircraft. The number of scientific publications focusing on alternative aviation fuels and propulsion systems has increased by a factor of five since 2005. To conduct the cost analysis, we reviewed minimum jetfuel selling price (MJFSP) of 12 different alternative aviation pathways including production cost of electro-jetfuel and H₂ from 26 different literatures (Figure 1). MJFSP is the minimum price a customer has to pay for purchasing the jetfuel so that a zero-equity net present value (NPV) is achieved with certain % of return rate (Seber et al., 2014; de Jong et al., 2015). The electro-jetfuel production cost was estimated 'well-to-tank' cost from renewable resources (Schmidt et al., 2018) and H₂ production cost was estimated from different pathways such as electrolysis, hydrolysis of biomass and steam methane reforming (SMR) of natural gas (Gupta et al., 2010; Starik et al., 2018). We compared them with the MJFSPs of other alternative aviation fuel pathways. All obtained cost values were first converted to the same units (USD/GJ) and then made equivalent to 2019 cost with the consumer price index (CPI-U) data to make them comparable to each other. The cost for LH₂ and LCH₄ were purchasing price in the market and we assumed them as the MJFSPs.

TECHNICAL MATURITY OF THE ALTERNATIVE FUELS AND PROPULSION SYSTEMS

At the moment, only some biofuels with certain percentage (10-50%) of blending options with fossil jet kerosene have been certified by the American Society of Testing and Materials (ASTM) for the use in aircraft operation. Considering Technology Readiness Level (TRL) and Fuel Readiness Level (FRL), only Hydroprocessed Esters and Fatty Acids (HEFA) fuel and pathway is commercially ready (Table 1). In addition to the listed fuels in Table 1, both the H₂ and LH₂ as well as LCH₄ have not been certified for the use in aviation.

Table 1: Current status of reviewed alternative aviation fuels (Staples et al., 2014; Atsonios et al., 2015; Mupondwa et al., 2016; Schmidt et al., 2016, 2018; Neuling & Kaltschmitt, 2018; Santos et al., 2018; Wei et al., 2019; Ruzmien, 2020)

Process	Energy efficiency*	Certified level of blending (%)	Technology Readiness Level (TRL)	Fuel Readiness Level (FRL)
Fischer-Tropsch – Synthetic Paraffinic Kerosene/Aromatic (FT-SPK/FT-SPK/A)	0.36	50	6-7	7
Hydroprocessed Esters and Fatty Acids – Synthetic Paraffinic Kerosene (HEFA-SPK)	0.71-0.77	50	9	9
Direct sugar to hydrocarbons (DSCH) or Hydroprocessing of fermented sugars-Synthetic Iso-Paraffinic kerosene (HFS-SIP)	0.50	10	7-9	8
Alcohol-to-Jet Synthetic Paraffinic Kerosene (ATJ-SPK)	0.91	50	6-7	8
Co-processing	N/A	5	7-8	6-7
Catalytic Hydrothermolysis Jetfuel (CHJ)/Hydrothermal Liquefaction (CHJ/HTL)	0.58-0.89	50	4-6	6
Hydroprocessed Depolymerized Cellulosic Jet (HDCJ)	0.36	Under certification	-	6
Aqueous phase processing/reforming (APP/APR)	0.32	Under certification	-	6
Advanced Fermentation/Fermentation	0.31-0.34	No certification	Under demonstration	-
Mixed alcohol synthesis (MAS)	0.40-0.44	No certification	Proposed technology	-
Pyrolysis	0.6-0.8	No certification	Under development	-
Electro-jet [Power to liquids (PtL)]	0.38-0.63	No certification	5-8	-
Electro-jet [Biomass to liquids (BtL)]	0.38-0.63	No certification	5-9	-

*Energy efficiency: The ratio of energy output (upgraded jetfuel) and the total energy input (process energy input and feedstock energy input) (Tzanetis et al., 2017) or thermal efficiency of a refinery.

Likewise, propulsion systems for different alternative aviation fuels and hybrid as well as all electric aircraft are being studied (Felder et al., 2017; Schäfer et al., 2018). Current state of the art of battery pack specific energy is just 200-250 Wh/kg which needs to reach around 800-1200 Wh/Kg for a regional electric aircraft (Schäfer et al., 2018). Fuel cells are also not in operation in commercial aircraft system yet (Taghavi et al., 2014). It is suggested that H₂ fuel cells can save up to 70% weight compared to battery-electric propulsion (Satyapal, 2017).

ECONOMIC PERFORMANCE

Diverse MJFSPs of alternative jet fuels have been estimated in various literature (Figure 1). Overall, Catalytic Hydrothermolysis/Hydrothermal liquefaction (CH/HTL), Pyrolysis, Alcohol-to-Jet (ATJ) and Fischer-Tropsch (FT) Synthetic processes offer the lowest possible MJFSPs while Hydroprocessed Esters and Fatty Acids (HEFA), Hydroprocessed Depolymerized Cellulosic Jet (HDCJ), Advanced Fermentation (AF) and Direct sugar to hydrocarbons (DSCH) pathways offer highest MJFSPs (Figure 1). HEFA fuels are generally less expensive but if produced from microalgae, they become expensive (Tao et al., 2017; Klein-Marcuschamer et al., 2013). The bio-jetfuel MJFSPs from wheat grain, willow, wheat straws, forestry residues and manure have shown lower cost than other feedstocks included in the reviewed literature.

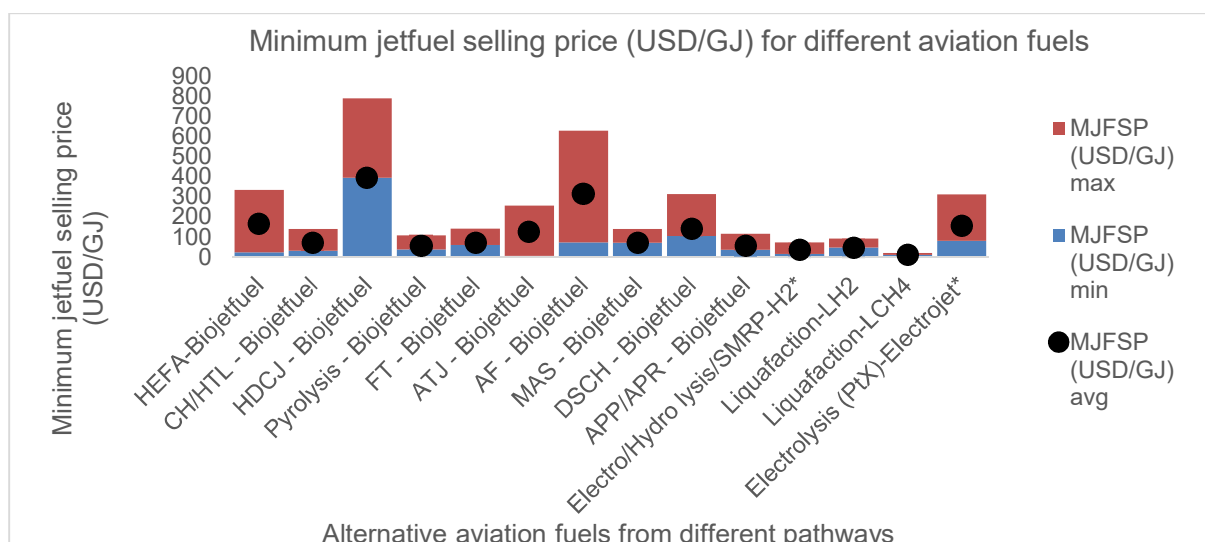


Figure 1: Minimum jetfuel selling price of different aviation fuel pathways (*production cost)

Both the LH₂ and LCH₄ are less expensive than the most bio-jetfuels but LH₂ is more expensive than LCH₄. H₂ production cost is the second smallest among all pathways but their production cost values are contradictory in different literatures as H₂ is produced/utilized in various chemical/fuel production processes. On the other hand, production cost for electro-jetfuel pathway is higher than the MJFSPs of most bio-jetfuel pathways. The average energy based MJFSPs (USD/GJ) of most pathways are 3-22 times higher than the fossil Jet fuel (Jet A-1) purchasing price (17.7 USD/GJ) at the moment (Platts, 2019).

CHALLENGES AND OPPORTUNITIES

Deployment of alternative fuels in aircraft engines is challenging at the moment. For instance, the volumetric energy content of alternative aviation fuels (specially LH₂ and LCH₄) are much lower than the fossil jetfuels which requires larger fuel storage tanks (Khandelwal et al., 2013; Rory et al., 2015). Similarly, some alternative aviation fuels have low flame stability and low combustion efficiencies which obstruct easy work in the existing engines (Zhang et al., 2016; Malins, 2017). Supply of some alternative aviation fuels at airports via existing pipelines is not appropriate due to low production volume of such fuels and leftover impurities in the pipes (Herzig et al., 2017). Lack of suitable fuel storage tanks at airports is also problematic. Similarly, the main challenge of battery-electric aviation is the limited onboard energy storage capacity in batteries (Gnadt et al., 2018). To improve the high specific energy of the battery is material-intensive which increases the weight of batteries and propulsion energy requirement (Hoelzen et al., 2018). The sole use of fuel cells cannot provide enough power required for take-off and hence combustion turbines may be required. Modification of engines and aerodynamic are challenging for new fuel types. The design and construction of tanks for cryogenic liquid storage and controlling the effects of strong thermal stresses in the structural parts are also challenging (Sziroczak et al., 2016).

However, some of the challenges can be resolved by implementing spherical tanks with increased thermal insulation, accommodating reduced surface to volume ratio, and fixing fuel tanks on the top of the fuselage to reduce wing areas (Blakey et al., 2011; Khandelwal et al., 2013; Zhang et al., 2016). Similarly, H₂ and NH₃ can be burnt with oxygen and fuel-air ratio can be altered to mix fuel enough and reduce NO_x emissions (Khandelwal et al., 2013; Goldman et al., 2018). The research and development of suitable new engine types or modification of the combustion chambers are ongoing and will improve the concepts.

DISCUSSION AND CONCLUSION

The results of the literature review show diverse MJFSPs from various pathways primarily due to several factors such as different feedstock, feedstock cost, refinery capital cost, co-product revenues, plant capacity, reactor construction, catalyst used and electricity cost. Bio-jetfuels produced via HEFA, CH/HTL, Pyrolysis, ATJ and FT pathways seem more feasible than other pathways but only HEFA pathway is commercially ready until now. LCH₄ is much cheaper than any other alternative aviation fuels as the market price of the natural gas is relatively low. Similarly, production cost for electro-jetfuel pathway is higher than some bio-jetfuel pathways and 3-6 times higher than fossil jetfuel production (Environment, 2018). However, the average energy based MJFSPs (USD/GJ) of the most pathways are significantly higher than the purchasing price of fossil jet kerosene at the moment. Economic incentives, carbon penalties and other governmental policies are required to further expand the utilization of alternative aviation fuels.

The results also highlight several challenges for the production and implementation of alternative aviation fuels as they possess slightly differing characteristics than fossil jetfuel which limit the performance in the existing engines (Zhang et al., 2016; Malins, 2017). The storage problem is a challenge for all alternative fuels but specifically problematic for H₂ and CH₄ due to their low volumetric energy content. The aircraft using LH₂ or LCH₄ will never be able to fly with the current fuel tanks as the volume limitations prevent the aircraft having enough fuel for take-off, landing and holding (Blakey et al., 2011). Yet, all alternative aviation fuel options have potential to reduce GHG emissions but modifications to engines, fuel storage tanks and aerodynamic systems are required. The research results also show hybrid propulsion systems are more feasible than all electric aircraft in near term.

ACKNOWLEDGEMENT

We gratefully acknowledge financial support from the Swedish Energy Agency and the Swedish Knowledge Centre for Renewable Transportation Fuels (f3) [project carried out within the collaborative research program Renewable transportation fuels and systems program (Samverkansprogrammet Förnybara drivmedel och system) "Project no. P48357-1"]].

REFERENCES

- Atsonios, K., Kougioumtzis, M. A., Panopoulos, K. D., & Kakaras, E. (2015). - Alternative thermochemical routes for aviation biofuels via alcohols synthesis: Process modeling, techno-economic assessment and comparison. - 138, - 366.
- Bogaert, J. V. (2015). Assessment of Potential Fuel Saving Benefits of Hybrid Electric Regional Aircraft. (Master's thesis), Delft University of Technology.
- Blakey, S., Rye, L., & Wilson, C. W. (2011). Aviation gas turbine alternative fuels: A review. *Proceedings of the Combustion Institute*, 33(2), 2863-2885.
- Burston, M., Conroy, T., Spiteri, L., Spiteri, M., Bil, C., & Dorrington, G. E. (2013). Conceptual design of sustainable liquid methane fuelled passenger aircraft. Paper presented at the 20th ISPE International Conference on Concurrent Engineering, CE 2013 - Proceedings.
- de Jong, S., Hoefnagels, R., Faaij, A., Slade, R., Mawhood, R., & Junginger, M. (2015). The feasibility of short-term production strategies for renewable jetfuels - a comprehensive techno-economic comparison. *Biofuels, Bioproducts and Biorefining*, 9(6), 778-800.
- Dincer, I., & Acar, C. (2016). A review on potential use of hydrogen in aviation applications. *International Journal of Sustainable Aviation*, 2, 74.
- Environment, T. (2018). *Roadmap to decarbonizing European aviation*. Retrieved from Brussels:
- Felder, J. L., Marien, T. V., & Bowman, C. L. (2018). Turbo- and Hybrid-Electrified Aircraft Propulsion Concepts for Commercial Transport. In. United States: NASA Center for Aerospace Information (CASI).

- Fleckner, K. M., Neylon, M. K., Roe, G., & Chien, A. (2008). - Multi-fuel reforming and fuel cell systems for aviation applications: The role of bio-diesel and its synergy with global interests.
- Gawron, B., Białecki, T., Janicka, A., Zawisłak, M., & Górniak, A. (2019). Exhaust toxicity evaluation in a gas turbine engine fueled by aviation fuel containing synthesized hydrocarbons. *Aircraft Engineering and Aerospace Technology*.
- Gaspar, R. M. P., & Sousa, J. M. M. (2016). - Impact of alternative fuels on the operational and environmental performance of a small turbofan engine. 130, 90.
- Gnadt, A. R., Speth, R. L., Sabnis, J. S., & Barrett, S. R. H. (2018). Technical and environmental assessment of all-electric 180-passenger commercial aircraft. *Progress in Aerospace Sciences*.
- Gong, A., & Verstraete, D. (2017). Fuel cell propulsion in small fixed-wing unmanned aerial vehicles: Current status and research needs. *International Journal of Hydrogen Energy*, 42(33), 21311-21333.
- Goldmann, A., Dinkelacker, F., Sauter, W., Schröder, U., Oettinger, M., Kluge, T., . . . Friedrichs, J. (2018). A study on electro-fuels in aviation. *Energies*, 11(2).
- Gupta, K. K., Rehman, A., & Sarviya, R. M. (2010). Bio-fuels for the gas turbine: A review. *Renewable and Sustainable Energy Reviews*, 14(9), 2946-2955.
- Herzig, P. L. K. F. S. A. G. C. S. R. M. S., Bob. (2017). Refinery to Wing: Transportation Challenges Associated with Alternative Jet Fuel Distribution.
- Hoelzen, J., Bensmann, B., Winnefeld, C., Hanke-Rauschenbach, R., Liu, Y., Elham, A., & Friedrichs, J. (2018). Conceptual design of operation strategies for hybrid electric aircraft. *Energies*, 11(1).
- IATA. (2019). Now for something completely different. Retrieved from <https://www.airlines.iata.org/analysis/now-for-something-completely-different>
- IRENA. (2017). Biofuels for aviation.
- Jeffrey, C. (2014). Jet-fuel-powered fuel cell developed that produces electricity at room temperature. Retrieved from <https://newatlas.com/jet-fuel-electricity-room-temperature-fuel-cell/34594/>
- Kadyk, T., Schenkendorf, R., Hawner, S., Yildiz, B., & Römer, U. (2019). Design of Fuel Cell Systems for Aviation: Representative Mission Profiles and Sensitivity Analyses. *Frontiers in Energy Research*.
- Kahraman, N., Tangöz, S., & Akansu, S. O. (2018). - Numerical analysis of a gas turbine combustor fueled by hydrogen in comparison with jet-A fuel. - 217, - 77.
- Khandelwal, B., Karakurt, A., Sekaran, P. R., Sethi, V., & Singh, R. (2013). Hydrogen powered aircraft : The future of air transport. *Progress in Aerospace Sciences*, 60, 45-59.
- Klein-Marcuschamer, D., Turner, C., Allen, M., Gray, P., Dietzgen, R., Gresshoff, P., . . . Stephens, E. (2013). Technoeconomic analysis of renewable aviation fuel from microalgae, *Pongamia pinnata*, and sugarcane. *Biofuels Bioproducts and Biorefining*, 7.
- Malins, C. (2017). What role is there for electro-fuel technologies in European transport's low carbon future?
- Moore, R. H., Thornhill, K. L., Weinzierl, B., Sauer, D., Dascoli, E., Kim, J., . . . Anderson, B. E. (2017). Biofuel blending reduces particle emissions from aircraft engines at cruise conditions. *Nature*(7645), 411
- Mupondwa, E., Li, X., Tabil, L., Falk, K., & Gugel, R. (2016). Technoeconomic analysis of camelina oil extraction as feedstock for biojet fuel in the Canadian Prairies. *Biomass and Bioenergy*, 95, 221-234.
- National Academies of Sciences, E., Medicine, Sciences, D. o. E., Physical, Board, A., Space, E., . . . Energy Systems to Reduce Commercial Aviation, C. (2016). *Commercial Aircraft Propulsion and Energy Systems Research : Reducing Global Carbon Emissions*: National Academies Press.
- Neuling, U., & Kaltschmitt, M. (2018). Techno-economic and environmental analysis of aviation biofuels. *Fuel Processing Technology*, 171, 54-69.

- Nojourni, H., Dincer, I., & Naterer, G. F. (2009). Greenhouse gas emissions assessment of hydrogen and kerosene-fueled aircraft propulsion. *International Journal of Hydrogen Energy*, 34(3), 1363-1369.
- Platts, D. (2019). IATA. Retrieved from: <https://www.iata.org/publications/economics/fuel-monitor/Pages/index.aspx>.
- Pereira, S. R., Fontes, T., & Coelho, M. C. (2014). - Can hydrogen or natural gas be alternatives for aviation? - A life cycle assessment. - 39(25), 13275.
- Rory, R., Sean, N., & Mitch, W. (2015). Liquefied Natural Gas as the Next Aviation Fuel.
- Ruzmien M. (2020). Sustainable Aviation Fuel Approval Process. In: Fiskerud M, moderator. Webinar. Fossil-free aviation 2045. Sweden.
- Santos, C. I., Silva, C. C., Mussatto, S. I., Osseweijer, P., van der Wielen, L. A. M., & Posada, J. A. (2018). - Integrated 1st and 2nd generation sugarcane bio-refinery for jet fuel production in Brazil: Techno-economic and greenhouse gas emissions assessment. - 129, - 747.
- Satyapal, S. (2017). *Hydrogen and Fuel Cells Overview*. Paper presented at the DLA Worldwide Energy Conference, National Harbor, MD.
- Schäfer, A. W., Barrett, S. R. H., Doyme, K., Dray, L. M., Gnad, A. R., Self, R., . . . Torija, A. J. (2019). Technological, economic and environmental prospects of all-electric aircraft. *Nature Energy*, 4(2), 160-166.
- Schmidt, P. W., Werner; Roth, Arne; Batteiger, Valentin; Riegel, Florian (2016). Power-to-Liquids Potentials and Perspectives for the Future Supply of Renewable Aviation Fuel.
- Schmidt, P., Batteiger, V., Roth, A., Weindorf, W., & Raksha, T. (2018). Power-to-Liquids as Renewable Fuel Option for Aviation: A Review. *Chemie Ingenieur Technik (CIT)*, 90(1/2), 127.
- Schripp, T., Herrmann, F., Oßwald, P., Köhler, M., Zschocke, A., Weigelt, D., . . . Werner-Spatz, C. (2019). Particle emissions of two unblended alternative jet fuels in a full scale jet engine. *Fuel*, 256.
- Seber, G., Malina, R., Pearlson, M. N., Olcay, H., Hileman, J. I., & Barrett, S. R. H. (2014). Environmental and economic assessment of producing hydroprocessed jet and diesel fuel from waste oils and tallow. *Biomass and Bioenergy*, 67, 108-118.
- Staples, M. D., Malina, R., Olcay, H., Pearlson, M. N., Hileman, J. I., Boies, A., & Barrett, S. R. H. (2014). Lifecycle greenhouse gas footprint and minimum selling price of renewable diesel and jet fuel from fermentation and advanced fermentation production technologies. *Energy & Environmental Science*, 7(5), 1545.
- Starik, A. M., Savel'ev, A. M., Favorskii, O. N., & Titova, N. S. (2018). Analysis of emission characteristics of gas turbine engines with some alternative fuels. *International Journal of Green Energy*, 15(3), 161-168.
- Somarathne, K. D. K. A., Hatakeyama, S., Hayakawa, A., & Kobayashi, H. (2017). Numerical study of a low emission gas turbine like combustor for turbulent ammonia/air premixed swirl flames with a secondary air injection at high pressure. *International Journal of Hydrogen Energy*, 42(44), 27388-27399.
- Sziroczak, D., & Smith, H. (2016). A review of design issues specific to hypersonic flight vehicles. *Progress in Aerospace Sciences*, 84, 1-28.
- Taghavi, R. (2014). General Aviation and Uninhabited Aerial Vehicle Propulsion System In S. Farokhi (Ed.), *Aircraft Propulsion (2nd Edition)* (2nd ed., pp. 283-325): John Wiley & Sons, Ltd.
- Tao, L., Milbrandt, A., Zhang, Y., & Wang, W.-C. (2017). Techno-economic and resource analysis of hydroprocessed renewable jet fuel. *Biotechnology for Biofuels*(1), 1.
- Tzanetis, K. F., Ramirez, A., & Posada, J. A. (2017). Analysis of biomass hydrothermal liquefaction and biocrude-oil upgrading for renewable jet fuel production: The impact of reaction conditions on production costs and GHG emissions performance. *Renewable Energy*, 113, 1388-1398.
- Voskuijl, M., van Bogaert, J., & Rao, A. G. (2018). Analysis and design of hybrid electric regional turboprop aircraft. *CEAS Aeronautical Journal*, 9(1), 15.

- Wang, W.-C., & Tao, L. (2016). Bio-jet fuel conversion technologies. *Renewable and Sustainable Energy Reviews*, 53, 801-822.
- Wei, H., Liu, W., Chen, X., Yang, Q., Li, J., & Chen, H. (2019). - Renewable bio-jet fuel production for aviation: A review. - 254.
- Withers, M. R., Malina, R., Gilmore, C. K., Gibbs, J. M., Trigg, C., Wolfe, P. J., . . . Barrett, S. R. H. (2014). Economic and environmental assessment of liquefied natural gas as a supplemental aircraft fuel. *Progress in Aerospace Sciences*, 66, 17-36.
- Yilmaz, N., & Atmanli, A. (2017). Sustainable alternative fuels in aviation. *Energy*, 140 (Part 2), 1378-1386.
- Zhang, C., Hui, X., Lin, Y., & Sung, C.-J. (2016). Recent development in studies of alternative jet fuel combustion: Progress, challenges, and opportunities. *Renewable and Sustainable Energy Reviews*, 54, 120-138.
- Zhu, Q. (2019). Developments on CO₂-utilization technologies. *Clean Energy*, 3(2), 85-100. *this particular field*. Location, Country.

CONCEPTUAL DESIGN OF A COMPRESSOR-VANE-HEX FOR LH₂ AIRCRAFT ENGINE APPLICATIONS

C. Xisto, I. Jonsson & T. Grönstedt

Department of Mechanics and Maritime Sciences, Chalmers University of Technology, Sweden, carlos.xisto@chalmers.se

Abstract. The density of liquid hydrogen (LH₂), at the normal boiling point, is two times higher than that of highly compressed gaseous hydrogen. This makes LH₂ the prime candidate for hydrogen storage in aviation. However, LH₂ is stored at cryogenic temperatures that require adequate insulation, as well as the integration of heat-exchangers to warm up the hydrogen on its way to the combustion chamber. Ideally, the required heat exchangers are strategically placed in the engine core to produce optimum heat management, thus improving the engine efficiency, increase its durability as well as to reduce emissions. Moreover, the combination of hydrogen high specific heat with cryogenic temperatures results in formidable cooling capacity, that can be explored by more compact heat-exchanger solutions. In the present work a compact vane integrated heat exchanger is introduced. The heat exchanger can be integrated into one or various vanes that comprise the compression system and uses the existing vane surface to reject core heat to the hydrogen fuel. Additional profiled plates can be added spanwise to increase the available surface area. The additional spanwise distributed plates (splitter-vanes) will lead to additional pressure losses in the engine core but can also be designed to enhance the radial turning capability of the vane. The enhanced radial turning capability is expected to allow for a reduction of engine length and weight by reducing the axial length of the transition S-duct between the low- and high-pressure compressors.

Keywords: Compressor, Gas Turbine, Hydrogen, Compact Heat-Exchanger

ACKNOWLEDGEMENTS

The E.U. financially supports this work under the “ENABLEH2 – Enabling cryogenic hydrogen-based CO₂ free air transport” Project co-funded by the European Commission within the Horizon 2020 Programme (2014-2020) under Grant Agreement no. 769241.

NOVEL SMALL SCALE ISOTHERMAL STABILITY TEST METHOD FOR AVIATION FUEL

S.Y. Sadat¹, S. Blakey¹ & E. Alborzi²

¹ *University of Sheffield, Department of Mechanical Engineering*

² *University of Birmingham, Department of Mechanical Engineering*

Abstract

INTRODUCTION

The current Isothermal Temperature Thermal Reactor (ITTR) device at the University of Sheffield has the capability to provide chemical kinetic data to strengthen the understanding of fundamentals of liquid-phase oxidation of hydrocarbons, Jet fuel in particular. Although the products of the autoxidation process are understood to some extent, further fundamental research is required to investigate the underlying reactions ultimately leading to the formation of carbonaceous deposits. The current ITTR rig consists of a fuel supply system, HPLC pump, tubular heater, water jacket followed by an on-line oxygen sensor with a tube length of around 3 meters long.

METHOD

This current formation has a number of limitations; it is a large device which requires a high volume of fuel (around 20L) and a greater power output, resulting in significant operational and maintenance costs. Also, there is a considerable region of non-isothermal flow at the entry and sampling small volumes of fuel for post-test analytical analysis is challenging. The rig has been re-designed with a much smaller formation in order to resolve these shortcomings. The sample is run through pipes immersed into a fluidised sand-bath which offers an evenly distributed temperature profile. Testing the fuel using a static system with no headspace enables us to have the desired residence time, varying the time directly. Having saturated the fuel with air at the start of each test, the oxygen levels are measured to see at the end to examine how much oxygen has been depleted during the thermal stress.

RESULTS

The early results show that the non-isothermal entry region is avoided, operational costs are minimised and oxygen depletion levels are measured for a range of residence times from near zero to 20 minutes. Autoxidation curves have been obtained for surrogate fuel (Banner Solvent), which is very promising. Data obtained from this rig is compared with similar devices such as the NIFTR rig. As the new Isothermal Tube Reactor does not have a fuel headspace, the results can be compared with the PetroOxy to see how the headspace affects the autoxidation results.

CONCLUSION

The new Isothermal Tube Reactor, which is an improved version of previous test methods for thermal stability of aviation fuel, is a promising test rig with an ability to produce highly trustable experimental data to provide a better understanding of autoxidation in jet fuel.

ACKNOWLEDGEMENTS (OPTIONAL)

Grant Support: This work is supported by the FINCAP project - H2020-CS2-CFP04-2016-2

IMPACT OF ALTERNATIVE JET FUELS ON AIRCRAFT EMISSIONS IN CRUISE

Daniel Sauer¹, Hans Schlager¹, Bruce E. Anderson², Patrick LeClercq³, Christiane Voigt¹, Tiziana Bräuer¹, Christopher Heckl¹, Stefan Kaufmann¹, Richard Moore², Monika Scheibe¹, Tobias Schripp³, Michael Shook², Kenneth L. Thornhill⁴, Edward Winstead⁴ & Luke Ziembra²

¹ DLR German Aerospace Center, Institute of Atmospheric Physics, Germany

² NASA Langley Research Center, NASA, USA

³ DLR German Aerospace Center, Institute of Combustion Technology, Germany

⁴ Science Systems and Applications, Inc., USA

Abstract. The project ECLIF (Emissions and CLimate Impact of Alternative Fuels) focused on investigating the effects of alternative jet fuels on aircraft emissions using a wide range of methods from lab experiments and chemical modelling to in-flight emission measurements. In this framework the ECLIF/NDMAX airborne measurement campaigns funded by the German Aerospace center (DLR) and NASA were carried out in 2015 and 2018 to characterize the emissions from a medium-range passenger aircraft in typical cruise conditions operated on a selection of alternative fuels and conventional Jet-A1 fuels as reference. The Advanced Technology Research Aircraft (ATRA), an A320 operated by DLR was used as source aircraft in both experiments; the measurements were performed using the DLR research aircraft Falcon 20 in 2015 and the NASA DC8 airborne laboratory in 2018. Using the ATRA as dedicated source aircraft also permitted to obtain a wide range of engine and operational parameters at high time resolution during flight. Trace gas and particle emissions as well as contrail ice particle properties were probed behind the lead aircraft at distances ranging from ~100m up to 40km. The dataset encompasses a variety of parameters measured during hundreds of individual exhaust plume encounters during defined testpoints at a variety of typical cruise condition. In addition, the airborne measurements were complemented by detailed ground-based measurements using the aircraft and fuels in between the flight missions. The results for particle and trace gas emissions reported here outline the possibilities to mitigate the climate impact of aviation by switching to optimized alternative jet fuels.

Keywords: aircraft emission measurements, contrails

IMPACT OF ALTERNATIVE FUELS ON CONTRAIL CIRRUS PROPERTIES AND CLIMATE-IMPACT

A. Bier¹ & U. Burkhardt¹

¹ *Deutsches Zentrum für Luft- und Raumfahrt, Institut für Physik der Atmosphäre, Germany, andreas.bier@dlr.de, ulrike.burkhardt@dlr.de*

Abstract. Contrail cirrus is the largest known contributor to the aviation climate impact. One possible option to reduce this climate impact is a reduction of aviation soot number emissions by the use of alternative fuels.

We simulate contrail cirrus as an independent cloud class, using a double moment microphysics scheme, within the global climate model ECHAM. Our objective is to analyze the influence of reduced soot particle emissions on contrail formation by including parameterizations of contrail ice nucleation and the subsequent loss in the vortex phase in our climate model instead of prescribing constant initial ice crystal numbers. We also analyze the impact of this improved contrail formation representation on contrail cirrus properties and radiative impact.

In the extratropical cruise altitudes, the number of nucleated ice crystals decreases approximately at the same rate as soot number emissions. In the tropics, contrails form quite frequently close to their formation threshold and the number of formed contrail ice crystals is limited by atmospheric temperature so that the use of alternative fuels is less effective in the tropics than in the extratropics. The ice crystal loss within the vortex phase in general counteracts soot emission reductions since fewer ice crystals sublime within the descending vortices at lower soot emissions influencing changes in contrail cirrus properties. The net radiative forcing by contrail cirrus is non-linearly dependent on the number of emitted soot particles. Due to the compensation effect of the vortex phase, the decrease in the contrail cirrus radiative forcing is lower than proposed by a previous study. Reducing soot number emissions by 50%, 80% and 90% causes the radiative forcing to decrease by around 20%, 42% and 58%, respectively.

Our results emphasize the fact that large soot emission reductions are necessary in order to achieve a significant mitigation of the contrail cirrus climate impact. The abstract of your paper should be located here. It should be a single paragraph and complete in itself (no references or equations). Your abstract should explain the background to the work, a brief summary of the work completed, the results, followed by conclusions and the relevance to other researchers. (Style: ECATS-Abstract, maximum 300 words)

Keywords: alternative fuels, aviation, contrail formation, contrail cirrus radiative impact

TEACHING ACTIVITIES FOR FUTURE MULTIFUNCTIONAL COMPOSITE MATERIAL

Johanna Xu¹, David Carlstedt¹, Shanghong Duan¹, Leif E. Asp¹

¹*Department of Industrial and Materials Science, Chalmers University of Technology, SE-41296 Gothenburg, Sweden*

Abstract. Higher education and skills development are key to develop future materials for aircraft. To meet current and future social needs Chalmers University of Technology launched a new educational model called TRACKS in the academic year 2019/2020. By TRACKS the students have an increased opportunity to choose interdisciplinary courses, thus creating their own educational track. This paper describes the procedure of planning and implementing a research project course as a mean to educate students in the development of future multifunctional composite materials.

Keywords: Carbon fibre reinforced plastics, Multifunctional composites, Energy storage, Mechanical performance, Electrical performance

INTRODUCTION

One of the main goals of higher education is to equip students with adequate competencies (skills and knowledge) in order to prepare them for life and work in the 21st century. TRACKS is Chalmers new educational initiative that offers students multidisciplinary and individualized learning. The initiative has been launched to better prepare students to address the societal challenges of the future, such as energy supply, transport and more efficient use of resources. Most of the studies will take place interdisciplinary. Students are given great opportunities to broaden their knowledge beyond their chosen main area. This educational initiative creates an arena to train students to address major global challenges. It is a way to prepare the students to become more self-sufficient and independent.

Reducing structural weight and electrification are two of the major challenges facing the aviation industry at present. Carbon fibre composites have been at the forefront of lightweight design, providing significant reductions in mass and hence emissions. Likewise, the ambition towards achieving zero-emission flight over the next 20 years via all-electric aircraft has generated a demand for lithium-ion batteries. Researcher at Chalmers, KTH, Imperial College London and IMDEA have, under technical guidance from Airbus, worked on a new type of solution over the past decade. A completely new solution to both weight reduction and energy storage has emerged: structural power composites.

Structural power composites are structural composites with the additional functionality of storing electrical energy. In structural power composites, the constituents (fibres and matrices) synergistically and simultaneously undertake both structural and electrochemical roles. The merge of functions is a step change and potential paradigm shift in how we use polymeric composites, going beyond the conventional monofunctional roles. This emerging field is a prominent research topic as it is presenting considerable technical challenges but promises exciting opportunities in aviation.

By employing commercial carbon fibres as combined electrode and reinforcing elements, and a solid polymer electrolyte as the matrix for simultaneous Li-ion transport and transfer of mechanical loads, a novel Li-ion battery material can be realized. Due to its multifunctional characteristics, this type of material allows for significant weight saving potentials on system level for electric vehicles and devices [1,2]. Two architectures were established for making structural battery materials: the laminated battery and the 3D micro-battery, as shown in Figure 1.

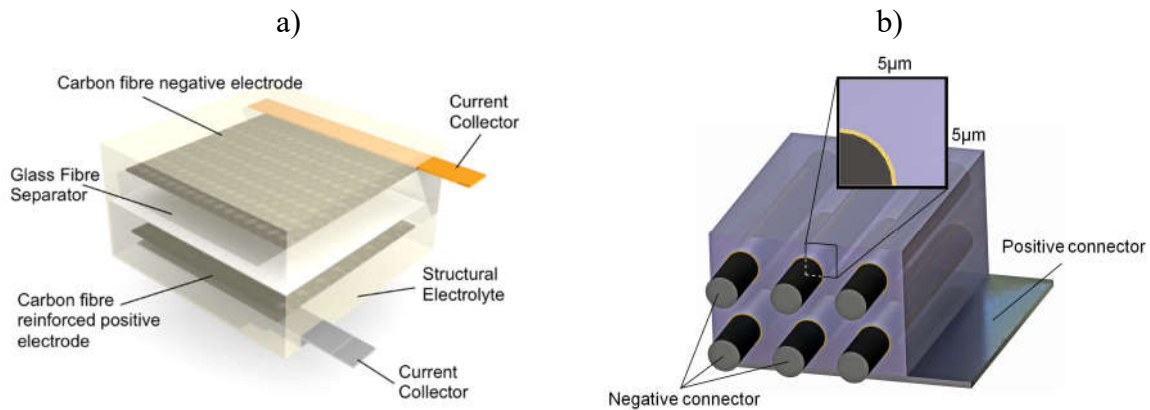


Figure 1. a) Concept of a laminated structural carbon fibre battery. b) concept of a 3D structural carbon fibre micro-battery architecture [3].

The laminated structural battery is a concept that resembles a conventional fibre composite laminate (Figure 1a), where carbon fibres are used as a high-performance structural reinforcement and stacked in an arbitrary angle in the following sequence: Negative electrode/separator/positive electrode. The entire stack is then embedded in the structural battery electrolyte (SBE), to achieve mechanical load transfer and ionic conductivity [4]. The construction of laminated structural battery composites is dependent on access to a highly ion conductive and fairly stiff structural battery electrolyte.

The 3D structural battery composite architecture (Figure 1b) was conceived to elude the low conductivity associated with most solid electrolytes. Each individual carbon fibre is coated with a thin solid polymer electrolyte (SPE) in an electro-polymerisation process. The resulting coating thickness can be less than 500 nanometres, and electrically insulates the carbon fibre (negative electrode) from the positive electrode, which is distributed in the matrix surrounding the coated fibres.

In parallel to realizing these concepts, new phenomena and ideas have emerged, which require further research, experiments, modelling and validation. Many of these activities have been identified as suitable for being part of Chalmers TRACK's initiative.

COURSE ORGANIZATION

Constructive alignment (CA) is a method that is increasingly used in today's higher education. One key feature of the method is to assure that the learning activities are aligned with both assessment and learning objectives. It suggests that course design should start by defining the learning outcomes. Thereafter, the teaching and assessment activities are designed to enable students to achieve these [5].

One of the main intended learning outcome (ILO) for this present course is for the students to gain knowledge, confidence and hands-on experience on state-of-the-art combined mechanical and electrochemical characterisation procedures, their applicability and limitations in multifunctional tests, on constituent-level as well as devices. To achieve this ILO, several research questions comprising experimental and theoretical components were outlined.

Numerous learning activities were designed for the team of students to learn the subject, including lectures, tutorials and lab work. Lectures were given by the teacher and teaching assistants, invited lecturers as well as by the students them self via peer-training. During the peer-training event each student prepared up to a half-day course within their own area of expertise and relevant area for the project and presented that to the team members.

The main theory is presented in these lectures and exemplified during the execution of the project. The students get to study the multifunctional performance of carbon fibers, make and characterize polymer electrolytes, design and manufacture structural battery composites and predict and verify the multifunctional performance of structural battery composite devices. At the end of the course, together with Airbus, a flying glider aircraft is built and demonstrated.

It was identified that a team of 8-12 students is suitable to take on the challenge of design, manufacture and characterise a structural battery composite device. The goal was for the team of students to origin from different programmes across Chalmers. Minimum one student from Mechanical Engineering, Physics, Chemistry and Chemical Engineering as well as Electrical engineering was considered necessary for the team. The admission of students to the course took place in two steps. First, students were asked to write a cover letter, explaining why they were applying for this course. After which interviews took place, much like a job application process. In total, 10 students were accepted, apart from different backgrounds, these students are also different far advanced in their respective education programs. 20% of the students were first-year master's students, 50% were second-year master's students who wanted to write their thesis closely linked to the TRACKS course, finally 30% are first- and second-year PhD-students,

Figure 3. This distribution means that the students in practice have different number of man-hours available, but common to all of them is that they are given the chance to practice taking something from idea to prototype.

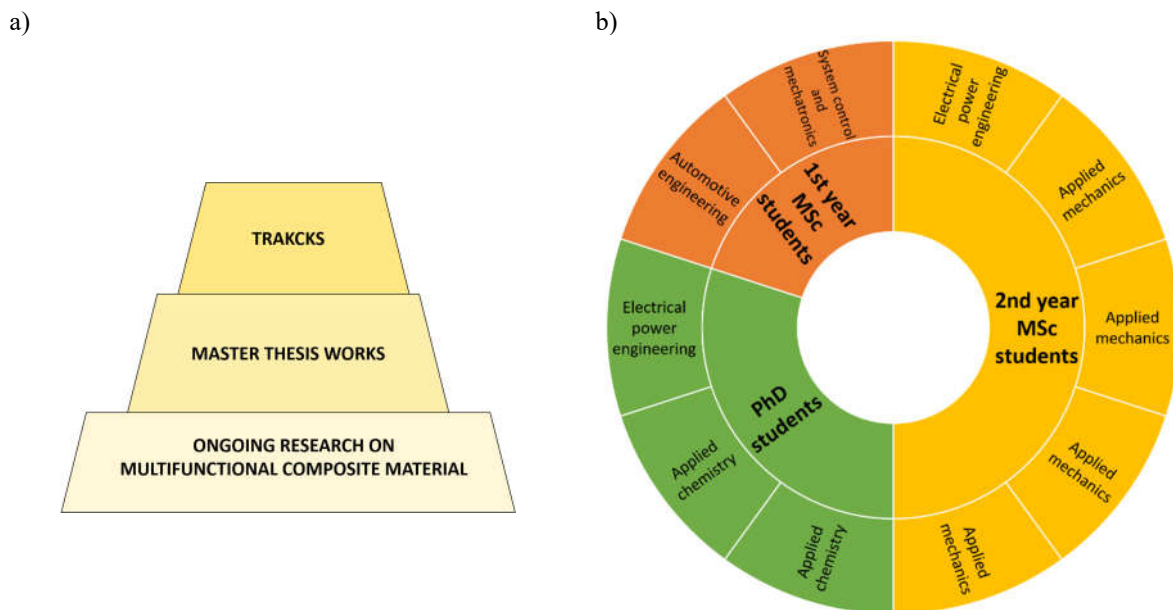


Figure 2. a) Resources needed to solve the interdisciplinary problem. b) Competences in the interdisciplinary TRACKS team.

As examination, a written report lies as a foundation, but it is supplemented with a specially designed dissemination event, where both research cooperation partners (both national and international) as well as industrial actors are invited.

At the time of presentation, the course will have been given in full. However, the course is ongoing at the time of writing, why no evaluation or assessment can be provided.

REFERENCES

- D. Carlstedt, L.E. Asp, Performance analysis framework for structural battery composites in electric vehicles, *Compos. Part B Eng.* 186 (2020).
doi:10.1016/j.compositesb.2020.107822.
- L.E. Asp, E.S. Greenhalgh, Structural power composites, *Compos. Sci. Technol.* (2014).
doi:10.1016/j.compscitech.2014.06.020.
- L.E. Asp, M. Johansson, G. Lindbergh, J. Xu, D. Zenkert, Structural battery composites: a review, *Funct. Compos. Struct.* 1 (2019) 42001. doi:10.1088/2631-6331/ab5571.
- N. Ihrner, W. Johannisson, F. Sieland, D. Zenkert, M. Johansson, Structural lithium ion battery electrolytes: Via reaction induced phase-separation, *J. Mater. Chem. A* 5 (2017) 25652–25659. doi:10.1039/c7ta04684g.
- J. Biggs, Enhancing teaching through constructive alignment, *High. Educ.* (1996).
doi:10.1007/BF00138871.

MULTI FUNCTIONAL MATERIALS TOWARDS ENVIRONMENTALLY FRIENDLY AVIATION

Peter Linde¹ & Leif Asp⁴

¹ *Department of Industrial and Materials Science, Chalmers University of Technology, Sweden, leif.asp@chalmers.se*

Abstract. For efficiency and environmental reasons low weight is of utmost importance in aeronautical applications. Lightweight materials have been well researched and gradually introduced in aeronautical structures, such as carbon fibre reinforced plastics. Recent examples are Airbus A350 and Boeing 787. At the same time systems become more complex and their overall weight tends to increase which counteracts the desire for lightweight. Traditionally structure and systems have been developed and implemented in parallel. The insight that it may be beneficial to integrate structure and systems plus progress in manufacturing processes have led to first concepts of multi functional materials [1]. Some of these will be introduced such as structural function combined with thermal and electrical functions, sensing functions as well as energy storage function [2]. Practical applications will be introduced.

Keywords: lightweight structures, integration of functions, multi functional materials

ACKNOWLEDGEMENTS

Work described in the paper has been partially derived from the SORCERER project – Structural pOwerR CompositEs foR futurE civil aiRcraft, funded by the European Union Clean Sky Program under Grant H2020-CS2-CFP03-2016-01, which is hereby acknowledged.

REFERENCES

- [1] M.O.H. Schutzeichel, T. Kletschkowski, P. Linde, L.E. Asp, Experimental characterization of multifunctional polymer electrolyte coated carbon fibres, *Functional Composites and Structures*, Vol. 1, No. 2, 2019
- [2] L.E. Asp, M. Johansson, G. Lindbergh, J. Xu, D. Zenkert Structural battery composites: a review, *Functional Composites and Structures*, 1, No. 4, 2019

STRUCTURAL POSITIVE ELECTRODE PRODUCED USING TAPE CASTINGS

S. Duan¹, J. Xu¹, D. Carlstedt¹ & L.E. Asp¹

¹ Department of industrial and materials science, Chalmers university of technology, Sweden, duan.shanghong@chalmers.se

Abstract.

INTRODUCTION

Structural battery is a multifunctional carbon fibre reinforced composite material. It can be employed both as mechanical carrier and for electrical energy storage. The multifunctionality of such material can potentially reduce the weight of a structure, where electric energy is used. A laminate structural battery has been designed. Such a battery utilizes carbon fibres as negative electrode, reinforcement material and current collector. It has been studied by several works that carbon fibres can function well as negative electrode and reinforcement material [1-4]. However, the ability of carbon fibre functioning as current collector in positive electrode has only been studied by limited works [5]. To employ carbon fibres as current collector in positive side, the carbon fibres must be electrically connected with the active material (such as LiFePO₄ micro-particles).

In the present work, LiFePO₄ micro-particles are coated on to carbon fibre using conventional tape casting method. The electro-chemical performance of the structural positive electrode is characterised via galvanostatic cycling. In addition, scanning electron microscopy is employed to study the morphology of the positive electrode material.

Keywords: Structural battery, Cathode, Carbon fibre

REFERENCES

- [1] Kjell MH., Jacques E., Zenkert D., Behm M., Lindbergh G., PAN-Based Carbon Fiber Negative Electrodes for Structural Lithium-Ion Batteries. *J. Electrochem. Soc.*, 158 (12), 2011, A1455-60.
- [2] Jacques E., Kjell MH., Zenkert D., Lindbergh G., Behm M., Willgert M., Impact of electrochemical cycling on the tensile properties of carbon fibres for structural lithium-ion composite batteries. *Composites Science and Technology*, 72 (7), 2012, 792-8.
- [3] Jacques E., Kjell MH., Zenkert D., Lindbergh G., The effect of lithium-intercalation on the mechanical properties of carbon fibres. *Carbon*, 68, 2014, 725-33.
- [4] Fredi G., Jeschke S., Boulaoued A., Wallenstein J., Rashidi M., et al., Graphitic microstructure and performance of carbon fibre Li-ion battery electrodes. *Multifunctional Materials*, 1, 2018, 015003.
- [5] Hagberg J., Maples HA., Alvim K., Xu J., Johannisson W., et al. Lithium iron phosphate coated carbon fiber electrodes for structural lithium ion batteries. *Composites Science and Technology*, 162, 2018, 235-43.
- [6] Carlstedt D., Johannisson W., Zenkert D., Linde P., Asp LE., Conceptual design framework for laminated structural battery composites. *Proc. 18th Eur. Conf. Compos. Mater.*, Athens, Greece.

STRUCTURAL BATTERY COMPOSITE DEMONSTRATOR

D. Carlstedt¹, J. Xu¹, D. Shanghong¹, P. Linde^{1,2} & L.E. Asp^{1*}

¹ *Department of Industrial and Materials Science, Chalmers University of Technology, Sweden,*

** leif.asp@chalmers.se*

² *Airbus Operations GmbH, Airbus, Germany*

Abstract. In order to fulfil the aspiration of making all electric commercial aircraft, new energy storage solutions are needed. This is due to the low energy to weight ratio of existing monofunctional battery technologies which results in unrealistically high energy storage per passenger needed to power a commercial aircraft [1]. A potential solution to this problem is "massless" energy storage such as the structural battery composite, where functionalities of existing monofunctional components are combined.

The structural battery composite is a class of composite materials with the ability to carry mechanical loads while simultaneously store electrical energy (i.e. work as a battery) [2]. Due to its multifunctional characteristics, this type of material allows for significant weight saving potentials on system level for electric vehicle and devices [3-4].

As part of the Clean Sky 2 project SORCERER [1], an A4 sized structural battery composite demonstrator is being developed. This demonstrator is intended to replicate the PSU (Personal Supply Unit) in a commercial aircraft. In this work, the multifunctional performance (i.e. capability of providing multiple functions) of this demonstrator and the applicability of structural battery composites in future electric/hybrid aircraft is discussed. Moreover, strategies for predicting the multiphysics behaviour of this material are outlined.

Keywords: Carbon fibre reinforced plastics (CFRP), Functional composites, Energy storage, Finite Element Analysis (FEA), Multiphysics modelling

REFERENCES

- [1] SORCERER - Structural power composites for future civil aircraft, project no. 738085, Clean Sky II, H2020 2017-2020
- [2] L.E. Asp, M. Johansson, G. Lindbergh, J. Xu and D. Zenkert. Structural Battery Composites: A Review, Functional Composites and Structures 1 (2019) 042001.
- [3] W. Johannisson, D. Zenkert, and G. Lindbergh. Model of a structural battery and its potential for system level mass savings. Multifunctional Materials 2 (2019) 035002.
- [4] D. Carlstedt and L.E. Asp. Performance analysis fram

PROPULSION INSTALLATION MODELLING FOR GEARED ULTRA-HIGH BYPASS RATIO ENGINE CYCLE DESIGN

Josefin Andersson^{1*}, Tomas Grönstedt¹ & Hua-Dong Yao¹

¹ Division of Fluid Dynamics, Department of Mechanics and Maritime Sciences, Chalmers University of Technology, Sweden

* E-mail of corresponding author: josefin.andersson@chalmers.se

Abstract. About 3% of the greenhouse gas emissions in the EU are derived from aviation. By 2020, the global international aviation emissions are assumed to be approximately 70% higher than those in 2005 and a strong continued growth in travel demand is expected at least up until 2035. A radical reduction of emissions have to occur on multiple fronts ranging from incremental improvements of advanced propulsion systems to new fuels and electrification. The desire to get higher efficiencies has contributed to the movement from turbojet engines to today's high bypass ratio turbofan engines. The fuel consumption and propulsive efficiency of turbofan engines are highly dependent on the fan pressure ratio (FPR). Decreasing FPR gives an improved fuel and propulsive efficiency as long as installation losses do not exceed potential benefits. As part of the Clean Sky project IVANHOE, new types of nacelles will be developed to enable installation of propulsion systems with radically increased bypass ratio and reduced FPR. In this work the process of describing and selecting a suitable propulsion system is described. The cycle is defined by a multidisciplinary analysis considering nacelle drag, propulsion system weight and engine performance. Effects of variation in turbine cooling with cycle change and small size turbomachinery efficiency is considered defining the core size and pressure ratio. Variations in installed SFC with fan diameter choice is quantified along a suboptimal line of fan pressure ratio and bypass ratio for a specific optimal overall pressure ratio. The final cycle choice is presented.

Keywords: Turbofan engine, Ultra-High Bypass Engine (UHBPR), Installation effects, Engine cycle design

INTRODUCTION

The European union (EU) has been at the forefront of fighting climate change. At the Paris climate conference in 2015, a global framework was set to avoid dangerous climate change (European Commission, 2016). The target is to reduce greenhouse gas emissions at least 40% by 2030 compared to 1990. About 3% of the greenhouse gas emissions in the EU is from aviation. By 2020, the global international aviation emissions are assumed to be approximately 70% higher than those in 2005 (European Commission, 2017).

The desire of the airlines to operate efficient, low cost aircraft, has been contributing to the movement from turbojet engines to today's high bypass ratio turbofan engines (Basher M F, 2013). The fuel consumption and propulsive efficiency of turbofan engines are highly dependent on the fan pressure ratio (FPR). Decreasing FPR gives an improved fuel and propulsive efficiency. As the FPR is reduced it is necessary to address installations to keep losses down. Low weight and nacelle drag as well as fan aerodynamic stability in all operating points are key challenges. In a turbofan engine, efficient lower FPR designs can be achieved by placing a gearbox between the fan and the low-pressure compressor. The components can be run at closer to optimal speeds (Kestner B K et al. 2011).

UHBPR engines experience new challenges for the optimal nacelle design, both in geometry and location. The Clean Sky project IVANHOE will address this challenge, resulting in a new multi-fidelity optimisation method, validated by advanced wind tunnel experiments. A consortium of an SME (HIT09 SRL), an industry (Deharde GmbH), an R&D institute (Stichting Duits-Nederlandse Windtunnels (DNW)) and 3 universities (Chalmers University of Technology, Technical University of Braunschweig, University of Padova) with complementary skills will produce this result in close coordination during 36 months with a budget larger than 3.5 MEuro. As part of this effort a nominal propulsion system is needed, for which the analysis is presented in this work.

In this work the engine cycle selection, as performed in the IVANHOE project, is described. The cycle definition is based on the engine performance computed in the cruise point

including installation effects from the nacelle drag and engine weight. The engine conceptual design and weight analysis is performed by using predicted engine performance data from top-of-climb and take-off. The final cycle is selected by trading installed SFC against complexity of installing a larger engine onto the aircraft.

MODELLING METHODOLOGY

A thermodynamic cycle model for an UHBPR engine was derived using the in-house code GESTPAN (Grönstedt, 2000). Cooling flow is predicted using the methods by (Wilcock, 2005) and small size turbomachinery efficiency effects are taken into account by incorporating the models implemented in (Rolt, 2017). GESTPAN feeds data to the weight and dimensions model WEICO (Grönstedt 2009), to predict component sizes and compute the number of stages. The model also predicts engine weight as well as provide necessary inputs for the nacelle drag estimation, which is based on an ESDU method (ESDU, 1981). The multi-point performance optimization resulted in a one stage fan, three stage IPC, 10 stage HPC, two stage HPT and four stage LPT as depicted in Figure 1 below.

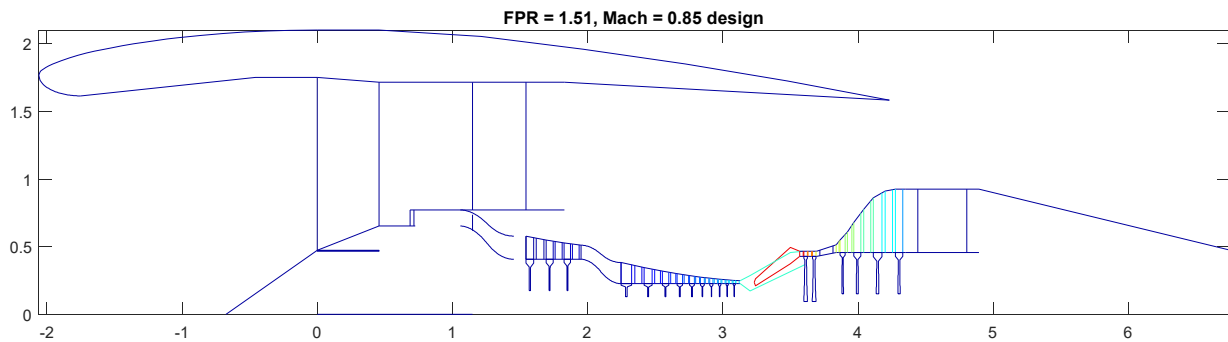


Figure 3. Conceptual design for Mach = 0.85, FPR = 1.51 configuration

Weight and nacelle drag effects are included into an “installed” SFC metric given in Eq.(1) below.

$$SFC_{installed} = \frac{b}{F_{Net} - D_{engine\ mass} - D_{nacelle}} \quad (1)$$

where 70% of the ESDU predicted nacelle drag and 85% of the engine mass related drag is used in Eq.(1) as part of the optimization. In addition to the installation effects captured by Eq. 1 above, models for computing engine bleed and power extraction from the engine are included as well. Key design parameters used for the cycle optimization are found in **Fehler! Verweisquelle konnte nicht gefunden werden.** below. The cycle optimum is established for two different Mach numbers.

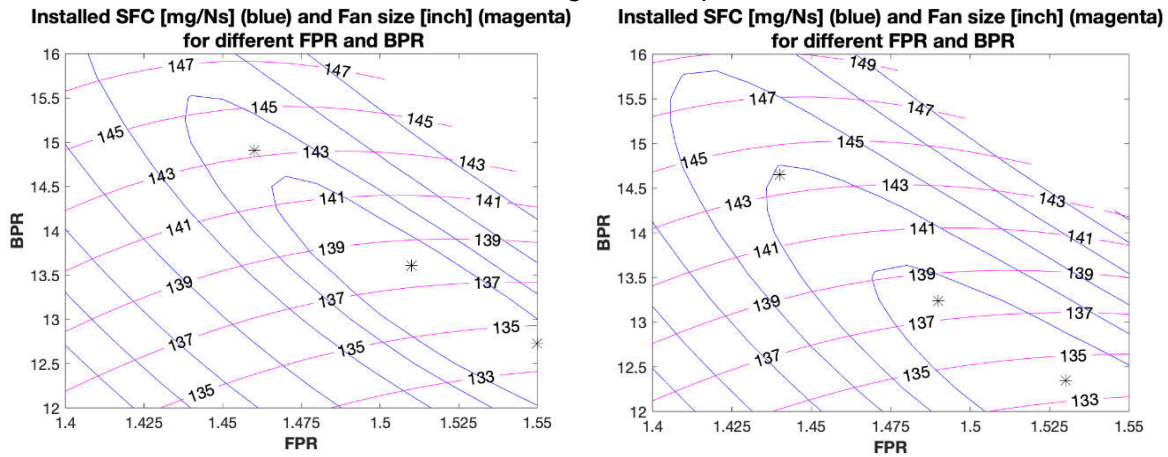
The component efficiencies are estimated to be relevant for an engine to be introduced within the 2027-2030 year range for the thrust class stated in Table 1. Predictions are based on methods presented in Grieb 2003, Samuelsson 2015).

Table 1. Key parameters at the design point.

Altitude	35000 ft	$\eta_{poly,FAN}$	0.925
Mach	0.80 an 0.85	$\eta_{poly,IPC}$	0.920
ISA	+10 K	$\eta_{poly,HPC}$	0.925
Net thrust	17535.97 lbf	$\eta_{poly,HPT}$	0.905
Mass flow	513 kg/s	$\eta_{poly,LPT}$	0.940

RESULTS AND ANALYSIS

After the establishing of a cycle with a minimum installed SFC the design space was analysed keeping the OPR constant but varying FPR and BPR. The results are shown in Figure 2a (Mach 0.8) and Figure 2b (Mach 0.85). Three cycles are extracted for closer analysis for both data sets, as given in Table 2 and Table 3. These are indicated as three asterisks in Figure 2a and Figure 2b. The mid point, with respect to FPR, represents the global optimum. It should be noted however that the minimum installed SFC for Mach 0.85 gives the same installed SFC value for the higher FPR points.



Fehler! Verweisquelle konnte nicht gefunden werden.a. Mach number 0.80

Fehler! Verweisquelle konnte nicht gefunden werden.b. Mach number 0.85

Figure 4. Installed SFC and fan size for two different Mach numbers

A set of suboptimal solutions are obtained if, for each FPR, the BPR with minimum installed SFC is determined. Along this suboptimal line the installed SFC varies quite slowly. Only a variation of 0.13% is observed for a fan diameter variation of 6.2%. This gives the designer a relatively wide choice of parameters without compromising fuel efficiency more than marginally.

Table 2. Key top-of-climb (TOC) and cruise performance parameters for a flight Mach number of 0.80

TOC	FPR	1.46	1.51	1.55
	BPR	15.56	13.92	13.46
	OPR	71.70	66.12	61.40
CRUISE	FPR	1.36	1.40	1.43
	BPR	16.65	15.91	15.36
	SFC_{installed}	15.30	15.25	15.28
	Overall mass flow rate [kg/s]	690.29	638.33	602.35
	FPR_{inner}	1.17	1.20	1.23
Fan size [inch]		143.17	137.97	134.25
Sea-level static thrust [lbf (kN)]		89181.91 (397)	88900.94 (395)	88287.72 (393)

Table 3. Key top-of-climb (TOC) and cruise performance parameters for a flight Mach number of 0.85

TOC	FPR	1.44	1.49	1.53
------------	------------	------	------	------

	BPR	14.61	13.91	13.44
	OPR	69.22	63.15	58.85
CRUISE	FPR	1.35	1.39	1.42
	BPR	16.67	15.85	15.31
	SFC_{installed}	16.29	16.19	16.19
	Overall mass flow rate [kg/s]	730.11	669.84	631.68
	FPR	1.16	1.19	1.22
Fan size [inch]	143.78	137.96	134.19	
Sea-level static thrust [lbf (kN)]	90377.02 (402)	90258.16 (401)	89814.15 (399)	

DISCUSSION AND CONCLUSIONS

The slow variation in installed SFC with FPR along the sub-optimal line gives the designer some freedom to choose the cycle. It was decided that the higher cruise Mach number would be more relevant for the future application and that the fan diameter of 138 would likely be possible to install on the future application. The slight increased installed SFC should be acceptable for the 143.8 inch fan, and could provide a noise benefit through its reduced specific thrust. The additional challenge of installing the larger fan was however not considered worthwhile.

REFERENCES

- European Commission, 2016 (Accessed: 2019-12-10). Paris agreement, https://ec.europa.eu/clima/policies/international/negotiations/paris_en.
- European Commission, 2017 (Accessed 2019-12-10). Reducing emissions from aviation, https://ec.europa.eu/clima/policies/transport/aviation_en.
- Basher M F, 2013. *Optimum turbofan engine performance through variation of bypass ratio*. Journal of Engineering and Sustainable Development.
- Kestner B K, Schutte J S, Gladin J C and Mavris D N, 2011. *Gladin and Dimitri N. Mavris. Ultra-high bypass ratio engine sizing and cycle selection study for a subsonic commercial aircraft in the N+2 timeframe*. Proceeding of ASME Turbo Expo.
- Grönstedt T, *Development of methods for analysis and optimization of complex jet engine systems*, Ph.D. thesis, Chalmers University of Technology, 2000
- Wilcock R C, Young, J. B. and Horlock J. H., *The Effect of Turbine Blade Cooling on the Cycle Efficiency of Gas Turbine Power Cycles*, Journal of Engineering for Gas Turbines and Power, vol. 127, p.109-120, 2005
- Rolt A, Sethi V, Jacob F, Sebastiampillai J., Grönstedt T., Xisto C and Raffaelli L, *Scale Effects on Conventional and Intercooled Turbofan Engine Performance*, Aeronautical journal, vol. 121, Issue 1242, p.1162-1185, 2017
- Grönstedt T, Au D, Kyprianidis K G, Ogaji, S., *Study of Prediction Methods for NOx Emissions and Its Influence on Future Turbofan Engine Emissions*, ASME Turbo Expo, GT2009-60201
- ESDU, 1981. *Drag of Axisymmetry Cowls at Zero Incidence for Subsonic Mach Numbers*. ESDU International, London, UK, Technocal Report ESDU 81024.
- Grieb H, *Projektierung von Turboflugtriebwerken*, Springer 2004
- Samuelsson S, Kyprianidis K and Grönstedt T, *Consistent Conceptual Design and Performance Modelling of Aero Engines*, ASME Turbo Expo, GT2015-43331

AERODYNAMIC DESIGN OF NACELLES FOR NEXT GENERATION HIGH-BYPASS TURBOFAN ENGINES

Vinicius Tavares Silva¹, Anders Lundbladh² & Olivier Petit³

¹ *Mechanics and Maritime Sciences, Chalmers Institute of Technology, Sweden, vincius@chalmers.se*

² *Engine Systems, GKN Aerospace, Sweden, anders.lundbladh@gknaerospace.com*

³ *LFV Operations, LFV, Sweden, olivier.petit@lfv.se*

Abstract. An integrated aerodynamic framework for designing current and future high-bypass turbofan nacelles is developed for this work. It consists of a parametric description of the nacelle shape using the class shape transformation (CST) method, automatic structured mesh generation and computation of the 3D flow-field using computational fluid dynamics (CFD). Two high bypass turbofan nacelles are designed using the described methodology. The first is aimed for a modern current high-bypass turbofan with an inlet length over fan diameter ratio (L/D) of 0.5 and the second targets a future ultra-high bypass turbofan, with an ultra-short inlet with an L/D of 0.3. The aerodynamic performance of the designed nacelles is evaluated for four different operating conditions: cruise at nominal angle of attack, take-off at medium angle of attack and near stall, and finally, at static conditions with maximum crosswind. The nacelle drag and net propulsive force are computed and evaluated for the chosen flight condition, using a well-established thrust and drag bookkeeping method. Two novel contributions are brought by this paper. The first is a CST based methodology for designing asymmetric nacelles considering cruise, low-speed and high incidence conditions, whilst the second is an extension of the CST method for designing nacelles with ultra-short inlets.

Keywords: Nacelle, turbofan, ultra-high-bypass, ultra-short inlet, computational fluid dynamics

INTRODUCTION

In the pursuit of reduced fuel burn and emissions, the next generation of turbofan engines for civil aircrafts will be designed for a higher bypass ratio (BPR) and lower fan pressure ratio (FPR). Future aero-engines are expected to operate with BPR greater than 15, referred to as Ultra High Bypass Ratio (UHBR), in order to achieve reduced specific thrust and higher propulsive efficiency. These configurations, however, require large fan diameters and are likely to be accompanied by increased weight and nacelle drag. Therefore, advanced nacelle designs, with shorter inlets and exhaust nozzles, are required so that the achieved performance benefits are not outweighed by the increased installation drag and weight.

Current engines for long range twin-engine aircraft feature inlets with lengths over fan diameter ratios (L/D) between 0.5 and 0.65. Nevertheless, 2030+ airplanes are expected to have inlets with L/D considerably below 0.5. The design of such short inlets can be highly challenging specifically for low speed and high incidence conditions, since they have reduced internal diffusion capability and boundary layer separation is likely to occur, leading to poor performance and engine instability.

Considerable achievements in modern nacelle design were reached over the last decade. Peters *et al.* (2015) have presented a spline-based framework for designing nacelles with ultra-short inlet and assessed the performance of different short inlet candidates compared to a standard length baseline.

The class shape transformation method (CST) was first presented by Kufan (2008) and further developed by Zhu and Qin (2014). It consists of a versatile parametric airfoil geometry representation method which has recently been applied to the design of nacelles (Christie *et al.*, 2017) and (Stankowski *et al.*, 2017). Class shape transformation curves were also widely used for exhaust nozzles design and optimization (Goulos *et al.*, 2016), (Goulos *et al.*, 2018) and (Otter *et al.*, 2019).

Tejero *et al.* (2019) and Tejero *et al.* (2020) have developed CST based methods for 3D nacelles shape multi-objective optimization. However, they only consider flight conditions under the cruise segment, neglecting other critical conditions within the flight envelope. Therefore, the CST method capability was not yet explored for designing 3D asymmetric

geometries capable of performing well under the most critical flight conditions. Furthermore, the CST method was not extended to the design of ultra-short nacelles, with L/D below 0.4. This paper primarily aims at establishing an integrated aerodynamic framework suitable for designing state-of-the-art and future aero-engine nacelles. Two novel contributions are hereby presented to the field of propulsion integration. The first consists of a CST based methodology for designing asymmetric nacelles considering cruise, low-speed and high incidence conditions, whilst the second is an extension of the CST method for designing nacelles with ultra-short inlets.

METHODOLOGY

The shape of a nacelle is a compromise to satisfy conflicting requirements for different operating conditions. At cruise, the aim is to minimize drag. Therefore, shock waves outside of the fan cowl should be avoided, since they are accompanied by a significant increase in profile drag. At low speed and high incidence conditions, such as end of take-off, initial climb and crosswind, the main design focus is to prevent boundary layer separation inside the inlet. Therefore, the design efforts presented in this article are towards minimizing the super-velocities at the external nacelle surface during cruise while maintaining the inlet boundary layer fully attached for the low speed/ high incidence critical conditions. The following sections present a brief overview of the methodology utilized to conduct the nacelle design and evaluate the aerodynamic performance.

Nacelle Geometry Generation

The Class Shape Transformation (CST) method (Kufan, 2008) was used in this work for the geometrical representation of the nacelles. A total of six CST curves are necessary to define a 2D nacelle shape. Figure 1 shows the main geometric parameters for the inlet, fan cowl and bypass nozzle representation, where A_{hi} , A_{th} , A_{∞} , r_{if} , β_{nac} , β_{core} are respectively defined as highlight area, throat area, streamtube capture area, initial forebody radius, nacelle boat-tail angle and core cowl boat-tail angle. MFR is the mass flow ratio, defined as A_{∞}/A_{hi} . The control points for each curve are shown in blue.

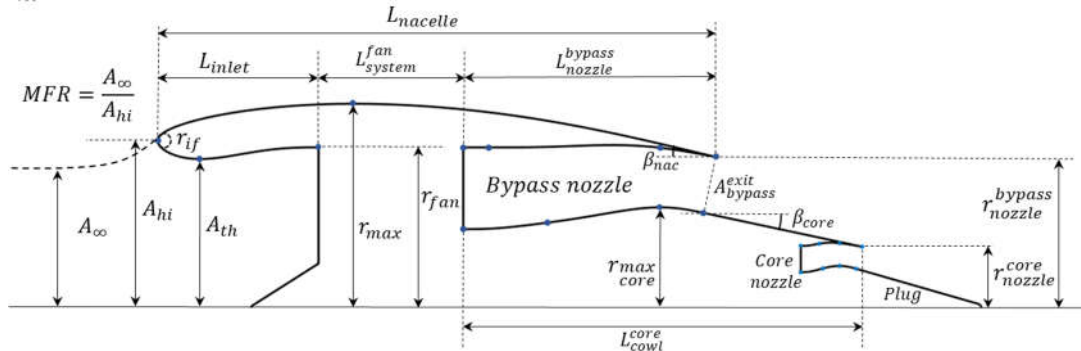


Figure 5. Nacelle main geometric parameters.

Figure 2 shows a 3D nacelle geometric definition. Two dimensional parametrizations are performed for the locations of $\varphi = 0^\circ$, $\varphi = 90^\circ$ and $\varphi = 180^\circ$, referred to as crown, maximum half-breadth (MHB) and keel, where φ is the azimuthal angle in a cylindrical coordinate system. In order to obtain a 3D nacelle shape, sinusoidal interpolations in r (radial coordinate) and x (axial coordinate) are performed circumferentially between the crown and the MHB and, successively between the MHB and the keel. The second nacelle half ($180^\circ \leq \varphi \leq 0^\circ$) is geometrically symmetric to the first one.

The previously mentioned parametrization positions were selected specifically to allow geometric control where local flow effects are critical. At the crown, the strongest shock waves are formed, whilst the keel geometry plays a fundamental role in preventing separation at high incidence and low speed operational conditions. Furthermore, the MHB parametrization is important to avoid crosswind inlet flow separation distortion.

An important characteristic existent in modern turbofan engines is an inlet droop to align the inlet with the wing upwash at cruise (Berry, 1994). A modification was applied to the CST parametrization in order to droop the nacelle inlet over a specified angle (θ_{droop}). The crown and keel highlight positions are rotated around a pivoting point located at the intersection between the fan face plane and the engine centerline. A shape deformation function is then applied to the original CST curves so that the inlet internal and external shapes are stretched from the fan face to the new drooped highlight position, proportional to a cubic function of the axial distance from the pivoting point. The drooping procedure is illustrated in figure 3.

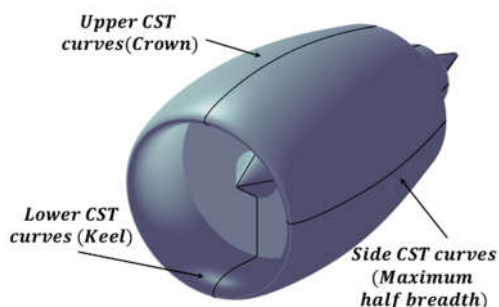


Figure 6. 3D geometric definition.

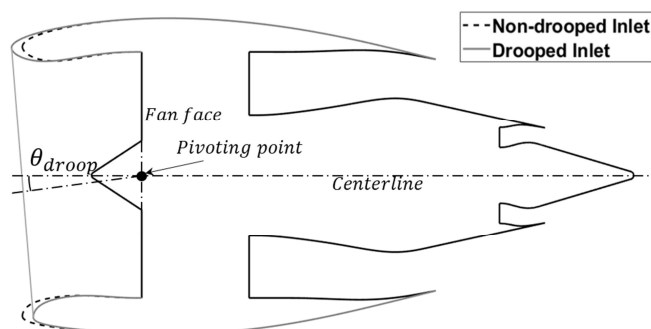


Figure 7. Drooped inlet representation.

Computational approach

Multiblock structured meshes are automatically generated within a computational domain defined between the nacelle and a cylindrical far field, with dimensions equal to 50 times the fan diameter. In order to resolve the viscous sublayer, the first cell height is set so that $y^+ \approx 1$. The flow field around the designed nacelles was computed by the means of computational fluid dynamics (CFD). The commercial software ANSYS FLUENT was used as the CFD solver. The simulations were performed using the Reynolds-Averaged Navier-Stokes (RANS) equations, pressure-based solver, coupled with the $k-\omega$ shear stress transport (SST) turbulence model. The pressure-velocity coupled scheme was selected jointly with second order spatial discretization for all terms.

Aerodynamic performance assessment

Consecutively to the CFD simulations the aerodynamic performance of both the nacelles and nozzles is computed and evaluated. The AGARD nearfield method (MIDAP Study Group, 1979) was used to bookkeep the net propulsive force and nacelle drag from the CFD simulations. The bypass and core nozzles thrust and discharge coefficients, c_v and c_d respectively, were calculated based on the methodology proposed by Mikkelsen *et al.* (2015).

RESULTS

The flight conditions used to assess the designed nacelles performance were based on the critical operating conditions proposed by Peters *et al.* (2015). The selected conditions were cruise, take-off rotation, wing maximum lift coefficient $C_{L_{max}}$, and maximum crosswind.

At cruise, the flight Mach number (M_∞) is 0.8, at an altitude of 10668 m and an angle of attack (AOA) of 5° . At the wing $C_{L_{max}}$ condition, M_∞ is 0.25, AOA is 29° at an altitude of 4267 m. At take-off rotation, M_0 is 0.25, AOA is 17° , at sea level. For the maximum crosswind condition, the forward speed is zero and a crosswind speed is 30 knots.

Figure 4 shows the contours of Mach number for the modern nacelle configuration, with an $L/D=0.5$, for a turbofan with a BPR equal to 12, a FPR of 1.4. Figure 5 shows cruise condition for the future nacelle configuration, with an $L/D=0.3$, for a turbofan with a BPR equal to 16 and a FPR of 1.3.

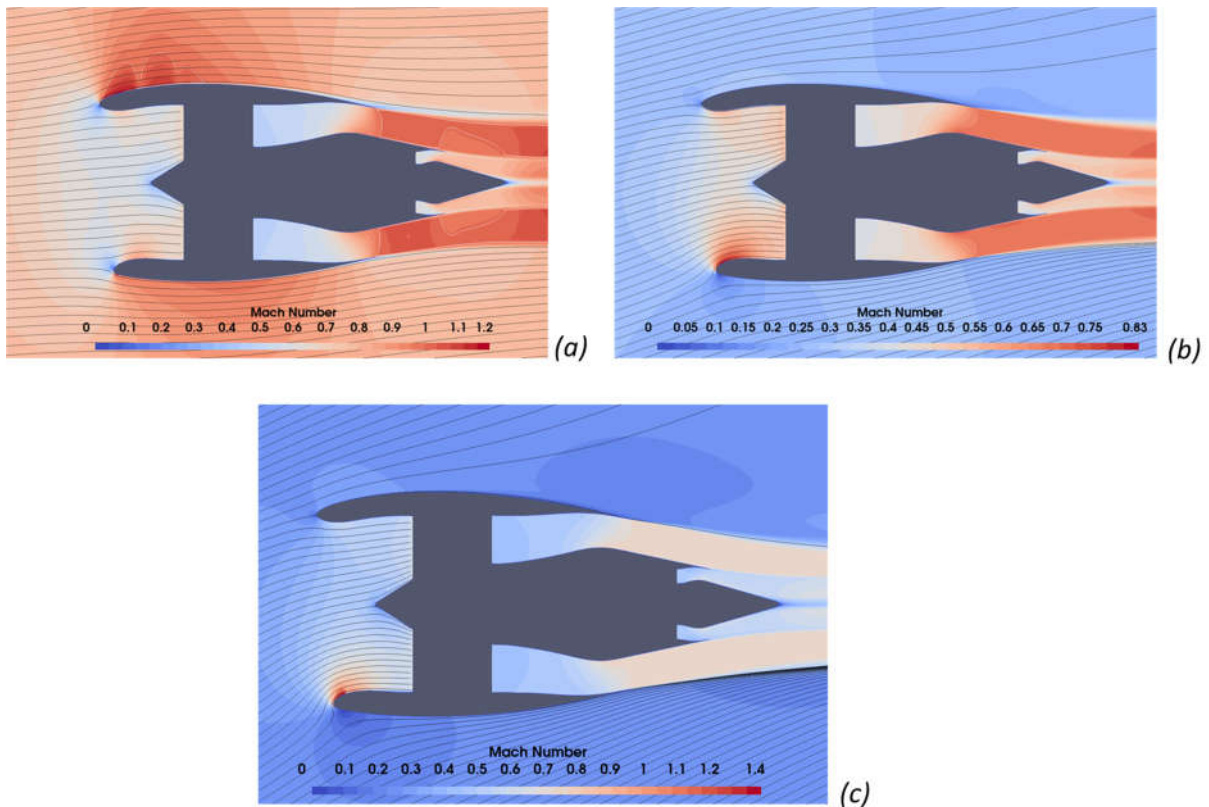


Figure 8. Modern nacelle configuration at (a) cruise, (b) take-off rotation and (c) wing C_{Lmax} .

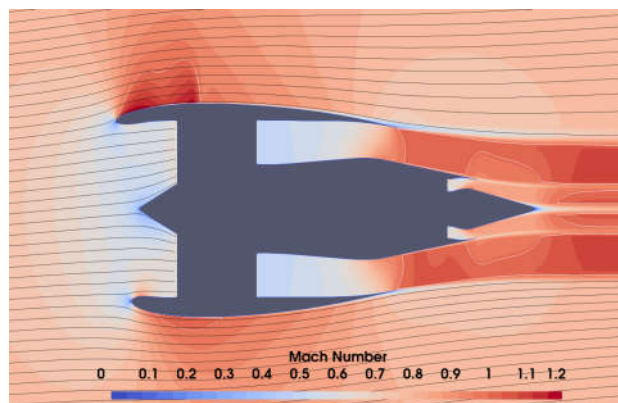


Figure 9. Future short inlet nacelle configuration at cruise.

CONCLUSION

An integrated aerodynamic framework for designing high-bypass turbofan nacelles was presented in this work. The methodology was used for designing two different nacelle geometries. The first for a modern high-bypass turbofan engine, with an inlet $L/D=0.5$ and the second for a proposed future UHBR turbofan, with $L/D=0.3$.

The performance of the nacelles was evaluated, and the presented methodology was shown to be suitable for designing both conventional and future nacelles for high-bypass engines with separated jet exhausts.

Two new contributions have been brought by this article. The first is a CST based methodology for designing asymmetric nacelles considering cruise, low-speed and high incidence conditions, whilst the second is the application of the CST method for designing nacelles with ultra-short inlets.

REFERENCES

- Berry, D. L. (1994). The Boeing 777 Engine/Airframe Integration Aerodynamic Design Process. In ICAS PROCEEDINGS (Vol. 19, pp. 1305-1305). AMERICAN INST OF AERONAUTICS AND ASTRONAUTICS.
- Christie, R., Heidebrecht, A., & MacManus, D. (2017). An automated approach to nacelle parameterization using intuitive class shape transformation curves. *Journal of Engineering for Gas Turbines and Power*, 139(6).
- Goulos, I., Otter, J., Stankowski, T., MacManus, D., Grech, N., & Sheaf, C. (2016). Aerodynamic design of separate-jet exhausts for future civil aero-engines—Part II: design space exploration, surrogate modeling, and optimization. *Journal of Engineering for Gas Turbines and Power*, 138(8).
- Goulos, I., Stankowski, T., MacManus, D., Woodrow, P., & Sheaf, C. (2018). Civil turbofan engine exhaust aerodynamics: Impact of bypass nozzle after-body design. *Aerospace Science and Technology*, 73, 85-95.
- Goulos, I., Stankowski, T., Otter, J., MacManus, D., Grech, N., & Sheaf, C. (2016). Aerodynamic design of separate-jet exhausts for future civil aero-engines—Part I: Parametric geometry definition and computational fluid dynamics approach. *Journal of Engineering for Gas Turbines and Power*, 138(8).
- Kulfan, B. M. (2008). Universal parametric geometry representation method. *Journal of aircraft*, 45(1), 142-158.
- MIDAP Study Group. (1979). Guide to in-flight thrust measurement of turbojets and fan engines. United Kingdom AGARD graph, (237).
- Mikkelsen, K. L., Myren, D. J., Dahl, D. G., & Christiansen, M. (2015). Initial subscale performance measurements of the AIAA dual separate flow reference (DSFR) nozzle. In 51st AIAA/SAE/ASEE Joint Propulsion Conference (p. 3883).
- Otter, J. J., Christie, R., Goulos, I., MacManus, D. G., & Grech, N. (2019). Parametric design of non-axisymmetric separate-jet aero-engine exhaust systems. *Aerospace Science and Technology*, 93, 105186.
- Peters, A., Spakovszky, Z. S., Lord, W. K., & Rose, B. (2015). Ultrashort nacelles for low fan pressure ratio propulsors. *Journal of Turbomachinery*, 137(2).
- Stankowski, T. P., MacManus, D. G., Robinson, M., & Sheaf, C. T. (2017). Aerodynamic effects of propulsion integration for high bypass ratio engines. *Journal of Aircraft*, 54(6), 2270-2284.
- Tejero F, MacManus DG & Sheaf C (2020) Impact of droop and scarf on the aerodynamic performance of compact aero-engine nacelles. In: Proceedings of the 2020 AIAA Scitech Forum, 6-10 January, Orlando, Florida, USA
- Tejero, F., Robinson, M., MacManus, D. G., & Sheaf, C. (2019). Multi-objective optimisation of short nacelles for high bypass ratio engines. *Aerospace Science and Technology*, 91, 410-421.
- Zhu, F., & Qin, N. (2014). Intuitive class/shape function parameterization for airfoils. *AIAA journal*, 52(1), 17-25.

HARMONIC FORCING IN A BOUNDARY LAYER INGESTING FAN

Hans Mårtensson¹

¹ KTH and GKN Aerospace Engine Systems, Sweden; hansmar@kth.se

Abstract. Integrating a fan with the aircraft fuselage in a BLI (Boundary Layer Ingestion) configuration can give improvements in propulsion efficiency. This concept utilizes the lower momentum airflow in the boundary layer developed due to the surface drag of the fuselage. As a consequence, the flow field entering the fan will be distorted with velocity and total pressure variations in the circumferential as well as in the radial direction. A fan design seeking to realize the benefits of BLI will need a design that allows for distortion without large penalties. Full annulus unsteady CFD with all blades and vanes is used to evaluate the effects on aerodynamic loading and forcing on a fan designed to be mounted on an adapted tail cone. The distortion pattern used as a boundary condition on the fan is taken from CFD results on a full aircraft. Results from the fan computation suggest that the harmonic forcing spectrum is correlated to the circumferential variation of inlet total pressure. The change in harmonic forcing resulting from raising the working line, thus increasing the incidence on the fan rotor, increases the forcing moderately.

Keywords: Fan; Distortion; Unsteady aerodynamics; Aeromechanics

1. INTRODUCTION

With an increasing interest in reducing fuel burn, BLI (Boundary Layer Ingestion) among other concepts for future aircraft configurations are being proposed. The main objective of integrating the fan with the fuselage in a BLI configuration is the potential for improvements in propulsion efficiency. The first discussions of benefits of BLI for aircraft date back a long time as in Smith and Roberts (1947), and an early but more modern account is given in Smith (1993). In marine applications similar performance effects have also been established for a long time as described in Betz (1966). Modern concepts for aircraft mainly fall into principal categories with respect to the flow pattern ingested to the fan. Configurations like in Drela (2011), and Uranga et. al (2014), using fans mounted embedded or on top of a surface ingest mainly asymmetric boundary layers. The TCT (Tail Cone Thruster) studied here belongs to configurations as described in Welstead and Felder (2016) will tend to have a large radial variation of the flow, and ideally very small circumferential flow variations.

By the nature of the ingested boundary layer flow the fan will be presented with variations in total pressure and a vortical flow over the fan face. The flow field entering the fan will generally be distorted with variations in the circumferential as well as in the radial direction. The radial variation leads to a change in the velocity triangles, and a redistribution of flow that must be designed for in order to recover efficiency. An example of this for a TCT fan design is reported in Pardo and Hall (2019).

The F100 TCT studied here is depicted in Figure 1 along with a rendering of the pressure distribution over the aircraft. In the analysis of the whole aircraft the TCT fan is represented by an impulse disk which serves to mimic the overall performance of the fan. The ingested flow field from the analysis will provide a representative boundary condition for the analysis of the fan.



Figure 1. Artists view of the F100 TCT configuration and CFD result pressure distribution

Generally, fans for propulsion of aircraft will be subject to distortion some extent. This can be a in the form of streaks of hot air, vortical flow or effects of side wind, separating inlets etc. Mostly these conditions are encountered on some particular operating conditions. The BLI fan will be subject to the distorted flow at design point which merits attention as it persists for a long time. The aerodynamic design condition and details of the fan design used in this study is given in Mårtensson et al (2019). Fidalgo et al. (2012) analyzed the effects of a distorted sector on a transonic fan blade by a full annulus transient CFD model finding good agreement with experimental data on how the distortion evolves through the fan. Bakhle et al. (2018) reported results of aeromechanical analyses and Provenza et al (2018) used a wind tunnel test to map blade vibrations on a BLI fan with asymmetric intake. Whilst the test was successful, the authors also point out the need for further investigations.

2. MATERIALS AND METHODS

Based on CFD results from a complete Fokker 100 aircraft with a TCT mounted, the flow field entering the fan is used to analyze fan aerodynamics. The whole aircraft model uses an actuator disk approach to represent the fan in a simplified manner. At a plane inside the intake lip, the fan flow field is extracted and used as a boundary condition for the fan analysis discussed here. The boundary conditions are imposed on the inlet boundary as distributions of total pressure and flow velocity direction vector. Figure 2 shows the fields applied as boundary conditions over the boundary. Looking at the arrangement of the fan on the tail cone relative to the vertical tail plane wakes at 6 and 12 o'clock. The regions of lowest total pressure deficit are due to the vertical tail plane, and the other visible regions of low total pressure at the 5 and 7 o'clock positions are the wakes downstream of the engine pods. In addition to discrete the non-axisymmetric wakes also an in-plane flow pattern forms due to the flow around the aft fuselage. On the downstream boundary the nozzle back pressure is given as a static pressure satisfying radial equilibrium.

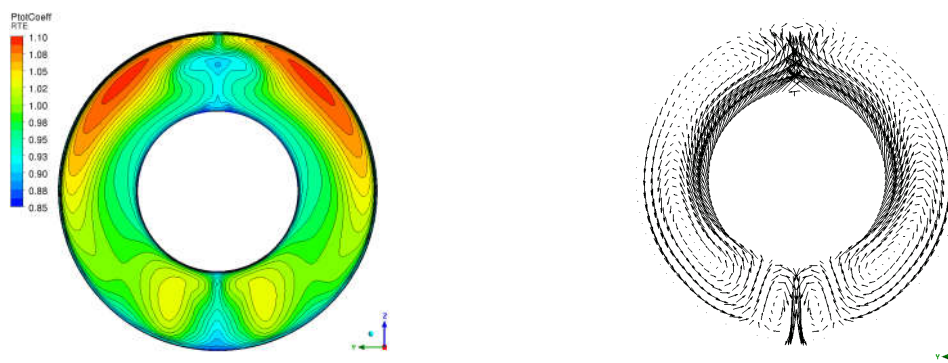


Figure 2. Total pressure and in-plane velocity vectors at inlet boundary

The CFD model of the fan consists of all 18 blades and 46 OGV:s, starting with the inlet boundary just inside the intake lip, and extends to the nozzle. The boundary conditions are applied as profiles in the CFX code, laid out as a variation using a dense mesh distributed over the radius and circumferential coordinates. The simulation is unsteady and is run for several rotations of the fan in order to allow a periodic flow to be established in every case.

A fan designed to fit on the Fokker 100 rear fuselage, Figure 3, is used for this study of the effects of BLI on the aerodynamic forcing of the fan. The fan rotor has 18 blades, and the OGV count is 46. In Figure 3a, the instantaneous field of total pressure at in and outlet, and on blades and vanes the static pressures. Apart from a variation in pressure on the individual blades, it is also worth noting that some variation in total pressure remains at the exit boundary.

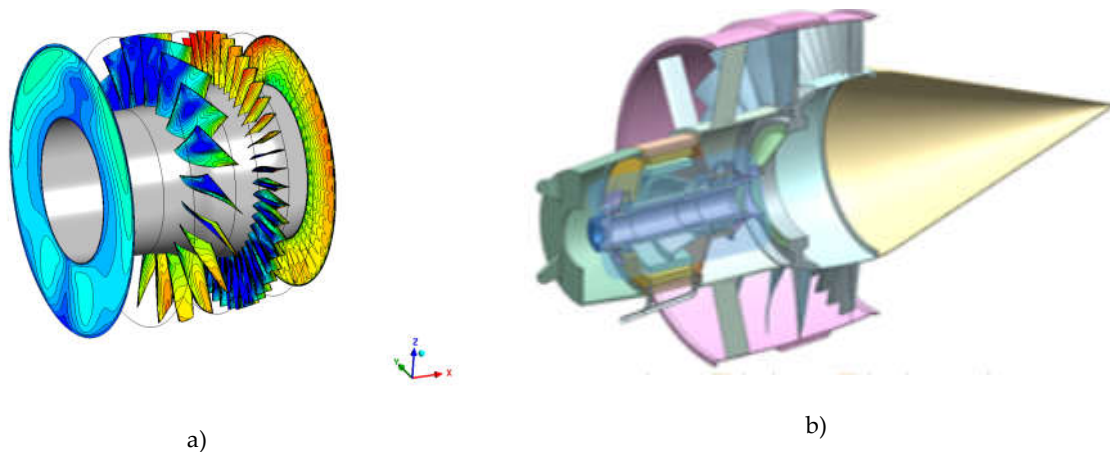


Figure 3 Computational domain a) inlet plane to nozzle, and b) overview of the fan design

In the overview in Figure 3b, struts are visible that are not used in the simulation. These are part of the original fan concept and have no intentional aerodynamic function but may be needed for structural reasons. For the aerodynamics the struts will present a loss of efficiency, but are not used for turning the axisymmetric flow, and would be removed if possible.

3. RESULTS

Pertinent to the aerodynamics of the rotor is the variation of the angle of the incoming flow relative to the leading edge. The inlet flow profile consists of an axisymmetric part and a non-axisymmetric part that will lead to a harmonic forcing and could change the aerodynamic behaviour of the fan. As the blade passes through the different angles a variation in incidence will occur that we can define as the variation around the mean incidence at each span. In Figure 4 the flow angle variation is shown based on a plane 1 axial chord upstream of the rotor leading edge. Figure 4a gives the flow angles in the stationary frame, whereas b) gives the relative flow angle variation.

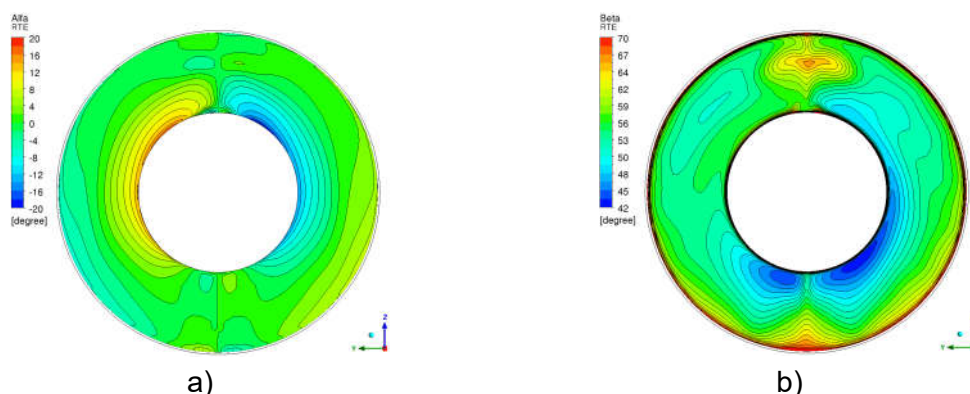


Figure 4 Incidence angle variation 1 axial chord upstream of the rotor leading edge

3.1. Effects on aerodynamics of the fan

The design addresses a radial variation of the total pressure that affects the flow angles and loading distribution by adapting the blade shape. One way of understanding what the

circumferential distortion does to the aerodynamics is to visualize the pressure distribution resulting from the full annulus, or “360” time dependent CFD result. In Figure 5a individual blade pressure distributions shown as dots and the average as a full line. For the rotor this is equivalent to the variation each blade undergoes during one rotation. The variation in the pressure distribution due to the distortion is significantly different from the average, over the entire chord. Figure 5a also shows that the time average pressure distribution on the rotor blade is very similar to the mixing plane (axisymmetric) result.

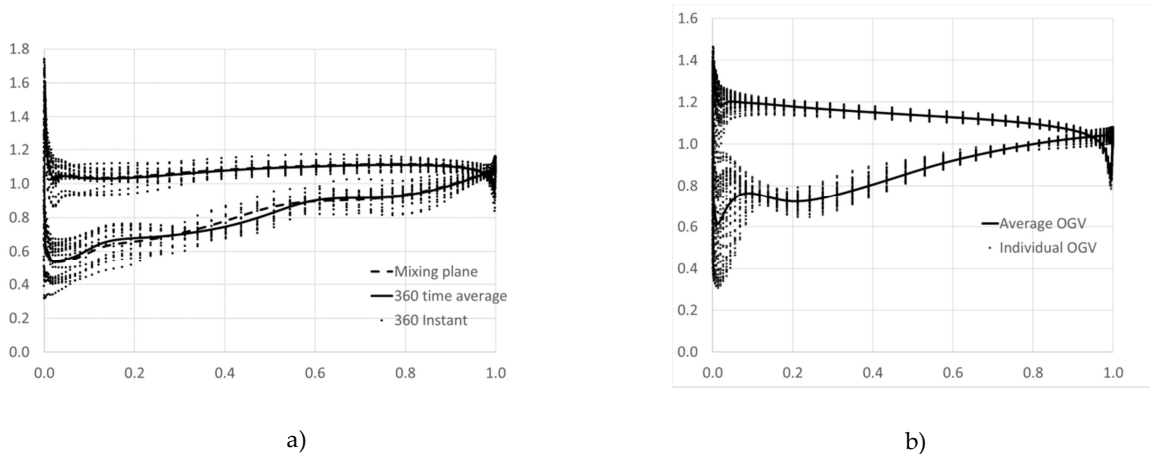


Figure 5 Pressure distributions at ADP 90% span a) Fan blade b) OGV

For the OGV shown in Figure 5b the incidence variation from vane to vane leads to a large variations at the leading edge. As this is a fixed pattern individually re-staggering or modifying the vanes could be considered to mitigate the local incidence effects. The view on the OGV is slightly different from the fan blade as this is the time average over each individual vane.

3.2. Unsteady forcing of the rotor blades

The distortion patterns shown earlier indicates that we should expect unsteady forcing at the lower engine orders. Blade forces from a full 360 rotation of the fan are evaluated and plotted together with a total pressure variation around the circumference as reference. The forces used in the evaluation are the forces on the blade in the circumferential direction normalized with average aerodynamic force in the circumferential direction. By this, the correlation of the blade force with the distortion can be examined.

An interesting issue is whether the effect of the total pressure variation over the inlet plane is dominant, or if the swirling flow swirl at the inlet has large effects. In this case this will be analyzed by simply make a back to back comparison of two cases with the same total pressure distribution but different in the velocity fields at the inflow boundary. The reference model denoted “ADP” in Figure 6 uses the total pressure variation and the flow direction taken from the velocity field as computed in the whole aircraft model. The other model denoted “Axial” uses a boundary condition where the same total pressure variation is used, but the flow at the inlet boundary is axial.

In Figure 6a, the x-axis is the angular position of the rotor could be viewed as the time passed or the angular position of the rotor. The Dloc parameter is the variation of the total pressure for as an average for every 1 degree sector normalized by the dynamic pressure. The variation clearly looks correlated to the blade forces, although not exactly at same angle. It also appears that the force increases where the Dloc is low. In order to understand the harmonic forcing the forces are Fourier transformed. Figure 6b shows the first 14 corresponding Fourier transform amplitudes of the Dloc parameter together with the

normalized forces. The Fourier coefficients can also be interpreted as the amplitudes of circumferential wave numbers or the force amplitude on a single blade at the frequencies also referred to as Engine Orders (EO). Especially from the Fourier coefficients it is quite clear that the normalized forces is correlated to the distortion pattern, even as described by the relatively crude approximation of radial averages.

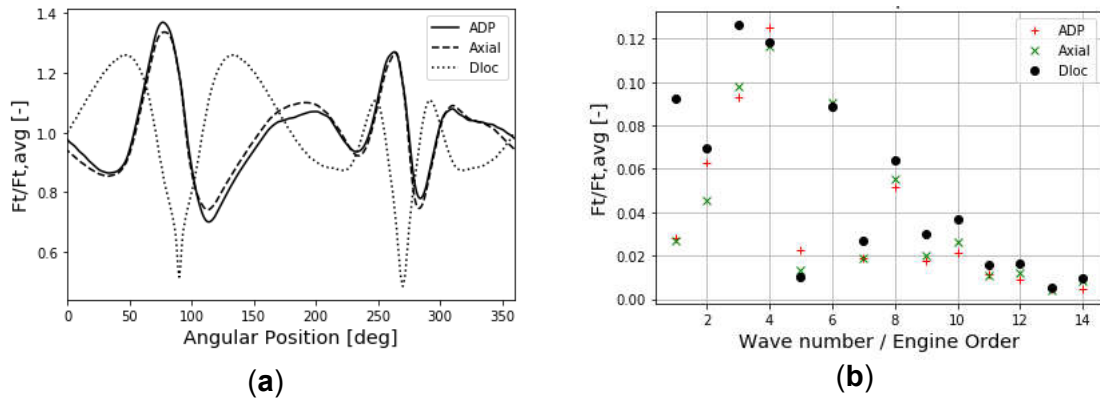


Figure 6 Blade forces and Pt variation a) at a clocking position b) Fourier components per wavenumber

There is a reasonable correlation of the total pressure coefficient with the forcing variation at the angular positions passed by a rotor blade. Where the total pressure is low the force on the blade is high, which is essentially due to the axial velocity being low with a resulting increased incidence on the blade. The similarity largely carries over to the Fourier coefficients where all but the first engine order is well correlated to the distortion coefficient for each wavenumber. Importantly, the pattern is consistent in showing that where the total pressure is generally low the forcing is high.

In Figure 7 results from an increased back pressure is added to the graph showing the sensitivity of the forcing to a raised operating line, the “Hi2” operating point is taken at a mass flow that is 91% of the mass flow at ADP. The ADP data are the same as earlier used in order to provide a reference. The general pattern correlation persists also at the lower mass flow, but the forcing levels show a modest increase over the ADP level.

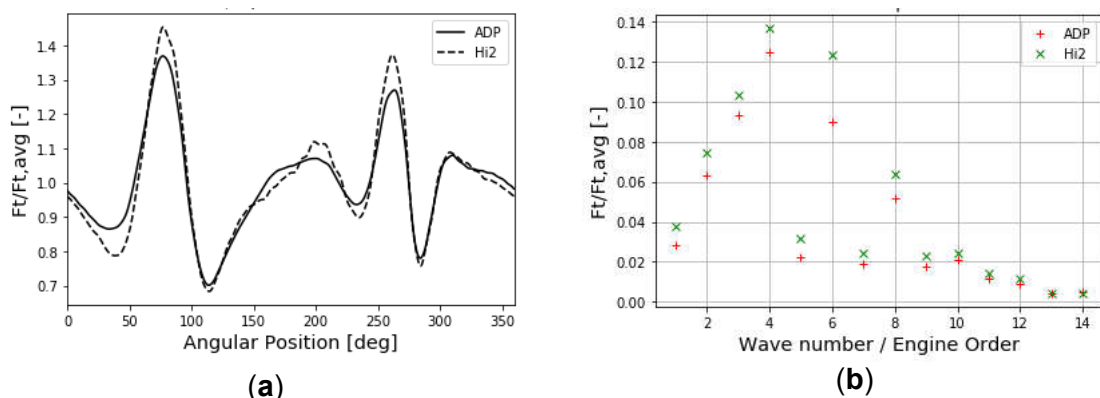


Figure 7 Forcing change with increasing back pressure

DISCUSSION

Transient calculations of a complete fan subject to inlet distortion including all blades and vanes has been performed. This is a computationally demanding way to analyze the fan aerodynamics, but one that relies on relatively few modelling assumptions. The aerodynamic forces vary in general quite a lot around the mean aerodynamic force, with the harmonic

amplitudes above 10% of the average force. It is found that the circumferential variation of total pressure over the inlet has a good correlation with the harmonic forces up to approximately 12EO, with some exception. At this point also the harmonic forces are diminishing. Removing the non-axial flow components at the inlet had only a moderate effect on the forcing, so the main effect in this case is the variation in total pressure. Continued studies will aim to generalize the findings and if possible, formulate more light weight models for the forcing.

ACKNOWLEDGEMENTS

This research was funded by the Swedish National Aeronautics Research Programme NFFP, grant number 2019-02759 and GKN Aerospace Engine Systems. The CFD analysis for the whole aircraft F100 TCT analysis used in this study were made by Martin Laban at NLR as part of a BLI study in collaboration with GKN Aerospace.

REFERENCES

- Bakhle, M.A., Reddy, T.S., Coroneos, R.M., Min, J.B., Provenza, A.J., Duffy, K.P., Stefko, G.L., Heinlein, G., 2018, Aeromechanics Analysis of a Distortion-Tolerant Fan with Boundary Layer Ingestion", AIAA SciTech Forum, AIAA 2018-1891
- Betz, A., 1966, Introduction to the Theory of Flow Machines, ISBN 978-0-08-011433-0, <https://doi.org/10.1016/C2013-0-05426-6>
- Celestina, M., 2019, Long-Davis, M., Large-scale Boundary Layer Ingesting Propulsor Research, ISABE-2019-24264, Proceedings of the 24th ISABE conference, Canberra, Australia
- Drela, M., 2011, Development of the D8 Transport Configuration, Paper 2011-3970, 29th AIAA Applied Aerodynamics Conference, 27–30 June 2011, Honolulu, HI
- Fidalgo et al, 2012, A Study of Fan Distortion Interaction within the NASA Rotor 67 Transonic Stage, J. Turbomachinery, Vol. 134, Sep. 2012
- Mårtensson, H. et al, 2019, Design Conditions For an Aft Mounted Fan With Boundary Layer Ingestion, ISABE-2019-24258, Proceedings of the 24th ISABE conference, Canberra, Australia
- Pardo, A., Hall, C., 2019, Aerodynamics of Boundary Layer Ingesting Fuselage Fans , ISABE-2019-24162, , Proceedings of the 24th ISABE conference, Canberra, Australia
- Provenza, A., et al, 2018, Aeromechanical Response of a Distortion Tolerant Boundary Layer Ingesting Fan, GT2018-77094, Proceedings of ASME Turbo Expo
- Smith, A., Roberts, H., 1947, The Jet Airplane Using Boundary Layer Air for Propulsion, *The journal of Aeronautical Sciences*
- Smith, L. H., 1993, Wake Ingestion Propulsion Benefit, *J. Propulsion and Power* 1993, Vol. 9, 74-82.
- Uranga A., et al, 2014, Preliminary Experimental Assessment of the Boundary Layer Ingestion Benefit for the D8 Aircraft, Proceedings of the 52nd Aerospace Sciences Meeting, AIAA SciTech Forum AIAA 2014-0906, National Harbor, MD, USA, 13–17 January 2014, doi:10.2514/6.2014-0906
- Welstead, J., Felder, J., 2016, Conceptual Design of a Single-Aisle Turboelectric Commercial Transport with Fuselage Boundary Layer Ingestion, 54th AIAA Aerospace Sciences Meeting, doi:10.2514/6.2016-1027
- Yoshihara, H.C.D, 1983. *AGARD Rep. No 712 Special course on subsonic/transonic aerodynamic interference for aircraft*. Technical report, AGARD, Neuilly-sur-Seine.

INSTALLATION EFFECTS ON ENGINE DESIGN

X.J. Li^{1,2} & H.D. Yao^{1,3}

¹ *Chalmers University of Technology/Department of Mechanics and Maritime Sciences/Division of Fluid Dynamics, Sweden*

² *xiaojian@chalmers.se*

³ *huadong.yao@chalmers.se*

Abstract. Increasing the engine bypass ratio is one way to improve propulsive efficiency. However, an increase in the bypass ratio (BPR) has usually been associated with an increase in the fan diameter. Consequently, there can be a notable increase in the impact of the engine installation on the overall aircraft performance. In order to achieve a better balance between those factors, it requires novel nacelle and engine design concepts. This report mainly reviews installation effects on engine design. Firstly, the installation effects assessment methods are introduced. Then, the installation effects on engine cycle design, intake design and exhaust design are sequentially reviewed.

Keywords: Engine design, Installation effects

INTRODUCTION

Concerns over fuel costs, along with the increasing requirement to reduce the impact of emissions, mean that the world's airlines continue to introduce low-noise and more fuel-efficient aircraft into their fleet. Increasing the engine bypass ratio is one way to improve propulsive efficiency. However, historically an increase in the bypass ratio (BPR) has usually been associated with an increase in the fan diameter. Consequently, there can be a notable increase in the impact of the engine installation on the overall aircraft performance (Tejero, et al. 2019). The installation effect in aeronautic engines is usually defined as the difference between the individual component performance in isolated condition and the performance after integration into the wing body (Yoshihara, et al. 1983). This integration has a mutual effect on the flow field of wing and engine nacelle, causing a redistribution of flow and pressure that modify aircraft drag and lift. As a result, although the typical increase in fan diameter is generally beneficial to the uninstalled engine specific fuel consumption, the increase in the nacelle drag and weight are detrimental to the aircraft performance. There is also likely to be a stronger aerodynamic coupling between the engine and the airframe. Overall there is a risk that the gains in uninstalled engine performance are wholly or partly lost due to adverse engine-airframe installation and interference effects as well as additional nacelle weight (Lu, et al. 2019). In order to compensate for the newly introduced weight and drag penalties, it requires novel nacelle and engine design concepts. This report mainly reviews installation effects on engine design.

INSTALLATION EFFECTS ASSESSMENT

The phenomenology of installation effect on engine design is due to alteration of pressure and velocity fields due to the presence of nacelle, pylon and jet efflux from nozzles (Rudnik, et al. 2002). The gulley between nacelle and wing, for instance, creates a velocity jet causing suction peaks, vortex drag penalty and, in some cases, even shock induced separation. Downstream of engine nozzle, the jet/free-flow interaction interferes as well with wing pressure side, inducing viscous and profile drag. To meet the expected future improvements in overall aircraft efficiency, it is necessary to ensure that the installation and integration of the engine with the airframe is properly assessed. Assessment of installation effect can be carried out by comparing the force obtained by superimposition of individually operating components with the force acting on the overall assembly. Traditional workflow for engine integration is based on isolated analysis and successive assembling of aircraft components to evaluate interference effects (Oliveira, et al. 2003).

The development of numerical tools and an increase in computational power lead to a series of Drag Prediction Workshops, where the second series is dedicated to nacelle installation effects (Brodersen, et al. 2005). The success of the initial workshop triggers the design of the more modern aircraft geometry of the NASA Common Research Model (Vassberg, et al. 2008). The publication of substantial experimental datasets with and without through-flow nacelles (Rivers, et al. 2011; Rivers et al. 2014) makes the Common Research Model a benchmark validation activity for the assessment of installation effect. It is anticipated that engine installation will become an increasingly important concern as engine diameters are expected to increase in pursuit of improved propulsive efficiency. It is also expected that knowledge of these aspects at the preliminary design stage will become more important to facilitate timely and informed decisions on engine cycle, size and airframe integration. A key element of the development of future civil aircraft is a robust assessment of the mutual interactions, and therefore of the thrust and drag characteristics, of the combined engine and aircraft configuration. It is necessary to build on experience from the Drag Prediction Workshops, to develop computational tools to evaluate nacelle drag, and to assess the nacelle installation interference drag for a typical civil transport configuration.

Recently, much effort has been made to develop the assessment methods for installation effects. Stankowski et al. (2016) presented the drag assessments for nacelle installation, where the work was carried out with the use of the NASA Common Research Model with through-flow nacelles. A key focus of their work is the use of computational fluid dynamics (CFD) to assess the aerodynamic characteristics for intake and nacelle drag, as well as for the evaluation of installation aerodynamic effects for a through-flow nacelle. Stankowski et al. (2017) described the assessment of the effect of engine installation parameters such as engine position, size and power setting on the performance of a typical 300-seater aircraft at cruise condition. Two engines with very-high by-pass ratio and with different fan diameters and specific thrusts are initially simulated in isolation to determine the thrust and drag forces for an isolated configuration. The two engines are then assessed in an engine-airframe configuration to determine the sensitivity of the overall installation penalty to the vertical and axial engine location. The breakdown of the interference force is investigated to determine the aerodynamic origins of beneficial or penalizing forces.

The quantification of the elements of installation drag is a key aspect in the assessment of the likely developments in engine design as well as on the installation requirements for future airframe architectures (Christie 2016). The overall aim is to determine the effect of nacelle size, weight, geometry and installation on flight efficiency, and to assess the relative importance of various engine installation aspects on the overall flight fuel burn for a range of short-haul and long-haul configurations. The long-term vision is to create a framework that will evaluate the combined engine and aircraft configuration for a specified flight mission and that could be applied at a preliminary design stage.

Stankowski et al. (2016) evaluated the aerodynamics of installation with use of three key computational building blocks such as computation of isolated nacelles, isolated airframe and the aircraft, as airframe with through-flow nacelles. It is the comparison between those three building blocks that allows for the assessment of aerodynamic interference and the decomposition of installation drag. Some elements that are required to evaluate the impact of engine installation on the overall aircraft performance across the flight envelope are also developed. The isolated nacelle modelling criteria have been identified and the assessment of intake performance descriptors such as critical mass flow capture ratio and drag rise Mach number has been established. The effect of the installation of a throughflow nacelle on a transonic civil transport has been considered and the performance of a CFD method to determine the interference aerodynamics has been assessed. Generally good agreement

has been observed between experimental and numerical results for the quantification of installation effects. The numerical results were used for a breakdown of the drag and for the quantification of aerodynamic interference for the aircraft components.

Bijewitz et al. (2015) focused on the comparative assessment of two evolutionary improved Ultra-High Bypass Ratio (UHBPR) turbofan engines for an entry-into-service of year 2035+, a three-spool Direct Drive Turbofan (DDTF) and a Geared Turbofan (GTF). For an initial study, they considered the evaluation of isolated propulsion system performance in terms of specific fuel consumption (SFC) for a broad range of design Bypass Ratios (BPR). In order to additionally capture the effects of propulsion system weight and drag, a trade factor based study was conducted aiming on the identification of fuel burn optimum design values of BPR. It is found that the location of the optimum BPR and the relative improvement potential depends on the assumptions imposed, in particular regarding the technology level and associated component efficiencies as well as the block fuel exchange rates for SFC, drag and weight that were employed. Moreover, apart from the fuel burn improvement potential, fan size and specific thrust levels might also be dictated by noise targets leading to designs that not necessarily coincide with the fuel burn optimum ones. Similarly, the design might also be driven by cost and complexity implications not considered within this paper, which could possibly shift the selected BPR to lower values. A future refined study should take into account more detailed implications of UHBPR engines on the integrated aircraft sizing process. As large engine diameters yield increased wind milling drag, this especially includes appropriate sizing of the vertical tail in order to maintain yaw control under minimum controllable conditions during one-engine-inoperative scenarios. Therefore, integrated aircraft and propulsion system assessment should be conducted to allow for more detailed modeling of further vehicular cascade effects, and to investigate e.g. the sensitivity of optimum cruise speeds for aircraft using UHBPR. In addition, the potentials associated with the exploitation of variable engine geometries in the context of UHBPR such as an adaptable bypass nozzle should be analyzed.

ENGINE CYCLE DESIGN

Based on the quantitative assessment methods of installation effects, different types of engines are conceptually designed. Christie (2016) proposed a Propulsion System Integration Model (PSIMOD) for engine cycle design under installation effects. This model tries to assess propulsion system integration and to enable the overall flight characteristics and mission fuel burn to be evaluated. It also determines the engine requirements and the main aircraft characteristics at each point in a trajectory for a given mission in terms of range, cruise altitudes, payload and engine limitations. At each point in the flight the engine operating point is adjusted to ensure that the thrust requirements are met and the fuel burn is then integrated over the mission.

Larsson et al. (2011) conceptually designed a geared turbofan engine and a geared open rotor engine with year 2020 technology level. The design constraints in the form of customer requirements (such as time between overhaul, runway length, time to height etc.) as well as technology limitations (such as component efficiencies, maximum stage loading, minimum blade height etc.) were taken into consideration. Although the open rotor engine is somewhat heavier, the reduced SFC and nacelle drag makes up for this and the resulting mission fuel burn is improved by approximately 15% compared to the geared turbofan engine. It can also be observed that for the open rotor configuration the location of the mid cruise operating point is not at the bottom of the SFC loop. Sizing the engine and choosing an appropriate design point for the propeller involves complex trade-offs, since for short haul aircraft large parts of the business case mission is spent climbing to cruise altitude, rather than cruising. There is not only a great potential to reduce fuel consumption for the open rotor engine, and consequently decrease the CO₂ emissions, however, the open rotor engine also

demonstrates similar cruise EINO_x figures compared to turbofan concepts, as well as similar margins from ICAO NO_x certification limits. With current fuel prices, 6% lower DOC can be expected from the geared open rotor concept than from the GTF.

Felder J et al. (2009) presented a propulsion system which transmits power from the turbine to the fan electrically rather than mechanically. Recent and anticipated advances in high temperature superconducting generators, motors, and power lines offer the possibility that such devices can be used to transmit turbine power in aircraft without an excessive weight penalty. Moving to such a power transmission system does more than providing better matching between fan and turbine shaft speeds for ultra-high bypass ratio engines. The relative ease with which electrical power can be distributed throughout the aircraft opens up numerous other possibilities for new aircraft and propulsion configurations and modes of operation. They discussed a number of these new possibilities. The Boeing N2 hybrid-wing-body (HWB) is used as a baseline aircraft for this study. The two pylon mounted conventional turbofans are replaced by two wing-tip mounted turboshaft engines, each driving a superconducting generator. Both generators feed a common electrical bus which distributes power to an array of superconducting motor-driven fans in a continuous nacelle centered along the trailing edge of the upper surface of the wing-body. A key finding was that traditional inlet performance methodology has to be modified when most of the air entering the inlet is boundary layer air. A very thorough and detailed propulsion/airframe integration (PAI) analysis is required at the very beginning of the design process since embedded engine inlet performance must be based on conditions at the inlet lip rather than freestream conditions. Examination of a range of fan pressure ratios yielded a minimum Thrust-specific-fuel-consumption (TSFC) at the aerodynamic design point of the vehicle (31,000 ft /Mach 0.8) between 1.3 and 1.35 FPR. This is due to the higher pressure losses prior to the fan inlet as well as higher losses in the 2-D inlets and nozzles. This FPR is likely to be higher than the FPR that yields a minimum TSFC in a pylon mounted engine.

Hall et al. (2007) developed a propulsion system which has a thermodynamic cycle based on an ultrahigh bypass ratio turbofan combined with a variable area exhaust nozzle and an embedded installation. This cycle has been matched to the flight mission and thrust requirements of an all-lifting body airframe, and through precise scheduling of the variable exhaust nozzle, the engine operating conditions have been optimized for maximum thrust at top-of-climb, minimum fuel consumption during cruise, and minimum jet noise at low altitude. Before the parameters of the engine cycle can be specified some characteristics of how the propulsion system is packaged with the airframe need to be considered. For the Silent Aircraft design, the engines are positioned on the upper surface of the airframe, towards the trailing edge. This location was adopted to take advantage of the performance benefits of boundary layer ingestion and to maximize the shielding of forward arc engine noise. It also offers airframe control and safety advantages, because the engines are positioned well behind the passenger bays. The nozzle required has a maximum area variation of 35%. This enables the jet noise target to be reached and also improves the fan efficiency and stability margin during take-off.

Giesecke et al. (2018) thermodynamically designed and mechanically investigated four different engine configurations based on a UHBR turbofan in an embedded installation. For the cycle design, a technology readiness level of 2025 was chosen with an FPR of 1.45, a BPR of 15.5 and a turbine entry temperature (TET) of 1,880 K at top of climb (TOC) condition. Being driven by the vision of the Advisory Council for Aeronautics Research in Europe for 2020 the target SFC was set to less than 15 g/kNs at cruise. An embedded engine configuration was chosen for maximum noise shielding effects of the BWB. The optimization of the variable bypass nozzle leads to a maximum area variation of 35% with a decrease in jet noise of around 10% during approach. Thereby, fan rotor peak efficiency rose

to almost 95%. The concept of increased bypass nozzle area has been tested by NASA for a model turbofan in one of their wind tunnels. Increasing the nozzle area by 5.4% at cutback condition, a fan noise EPNL reduction of 2 dB and 3% higher stage thrust was observed. For higher rotor speeds (take-off condition), a reduction in EPNL of only 1 dB and 2% stage thrust increase were measured. For a further increase in nozzle flow up to 7.5%, an EPNL noise reduction of about 3 dB during approach condition was achieved. No changes were observed for high rotor speeds in the case of a 7.5% increased bypass nozzle area.

Apart from the conceptually overall designed of aeroengines, some important components like intake and exhaust are designed and simulated under installation effects.

INTAKE DESIGN

Florea et al. (2015) demonstrated the aerodynamic feasibility of boundary-layer ingesting embedded-engine inlet designs with low total pressure losses and distortion harmonic content. The study used a fixed, ultra high bypass ratio advanced engine cycle and Boeing N+2 BWB aircraft; engine weight & propulsion / airframe integration effects were not considered. The system study has identified a low-loss inlet and high-performance, distortion-tolerant turbomachinery as key technologies consistent with achieving net system level benefits. Optimization-based parametric design has yielded a significantly improved inlet that meets the requirements identified in the system study. The inlet was designed using a hierarchical multi-objective computational fluid dynamics optimization that combined global and local shaping. Global parameters including duct offset and length, wall curvature and shape, inlet aspect ratio, lip contour and thickness, and upstream airframe contour were used to identify optimal design space regions. Local inlet shaping optimization further reduced total pressure losses and harmonic distortion upstream of the fan. Coupled inlet/fan design iterations were carried out for selected inlet designs to assess the fan/engine stability and operability benefits. The resulting inlet design has the potential of achieving a 3–5% boundary-layer ingesting fuel burn benefit for NASA's Generation-After-Next aircraft relative to a baseline high-performance pylon-mounted propulsion system. It shows significantly improved performance when compared with NASA's "inlet A" reference geometry with a length-to-diameter ratio of 3. The new inlet was shortened to a length-to-diameter ratio of 0.6, total pressure losses were reduced by three times, dominant distortion harmonic amplitudes were reduced by 30–50%, and fan efficiency losses were reduced from 6 to 0.5–1.5%. No flow control was required.

Arend et al. (2012) conducted a high-level vehicle system study based on a large commercial transport class hybrid wing body aircraft, which determined that a 3 to 5 percent reduction in fuel burn could be achieved over a 7,500 nm mission. Both pylon-mounted baseline and BLI propulsion systems were based on a low-pressure-ratio fan (1.35) in an ultra-high-bypass ratio engine (16), consistent with the next generation of advanced commercial turbofans. An optimized, coupled BLI inlet and fan system was subsequently designed to achieve performance targets identified in the system study. The resulting system possesses an inlet with total pressure losses less than 0.5%, and a fan stage with an efficiency debit of less than 1.5% relative to the pylon-mounted, clean-inflow baseline. The subject research project has identified tools and methodologies necessary for the design of next-generation, highly-airframe-integrated propulsion systems. These tools will be validated in future large-scale testing of the BLI inlet / fan system in NASA's 8 ft x 6 ft transonic wind tunnel. In addition, fan unsteady response to screen-generated total pressure distortion is being characterized experimentally in a JT15D engine test rig. These data will document engine sensitivities to distortion magnitude and spatial distribution, providing early insight into key physical processes that will control BLI propulsor design.

Schnell et al. (2014; 2017) provided a general overview of the most recent activities at DLR's Institute of Propulsion Technology dedicated to the appraisal of fan performance under the influence of installation and intake induced flow distortions. A ground induced inlet distortion study was carried out with the V2500 transonic fan stage. One of the objectives was to provide reference results for a realistic and engine representative fan stage with a relatively high fan total pressure ratio. Full scale measurements were taken at DLR's research aircraft ATRA, allowing for a visualization of the flow structures ingested by the fan and a direct comparison with computational data from full annulus, fully coupled and unsteady CFD simulations of the entire ground, nacelle, intake, and fan system. The comparison of the sensitivity of the operational behavior of two fans with different total pressure ratios towards a generic yet realistic inlet distortion was implemented. Results from unsteady CFD computations of the V2500 fan were compared with those of a research fan with a substantially lower fan pressure ratio (Fan135). A design methodology for closely coupled intake and fan systems was introduced, aiming at short and ultra-short inlets in combination with a fan pressure ratio $FPR=1.35$ fan being representative for future UHBR engines.

EXHAUST DESIGN

The European research (FP6) project called VITAL (Vuillemin, et al. 2007; Dezitter et al. 2009) was intended to present the characterisation of installation effects for a typical high bypass ratio engine using advanced numerical and measurement techniques. The third part of this project aims to obtain a better understanding of the link between the jet flow and the noise generated, to validate the methods for computing the flowfield and the noise sources for industrial configurations, and also to assess the benefits of a serrated nozzle when installed under a wing. Dezitter et al. (2009) assessed the capability of the CFD solvers to predict the aerodynamic flow for different nozzles installed under wing, to finally compute the noise sources (Dezitter, et al. 2009). Density gradient and compressibility corrections had been introduced into the SST k- ω turbulence model to better capture the physics related to high speed and hot jet flows, and high order discretization scheme and error estimation techniques were evaluated with the objective of increasing the accuracy of the computations. Particle Image Velocimetry (PIV) measurements were performed in the CEPRA19 anechoic facility to better understand the link between the aerodynamic flow and the noise, and to build experimental database for validation purpose. CFD solvers are able to properly capture the effects related to freestream velocity and installation under wing, at least in terms of the noise deltas. The serrated nozzle produces very surprising and unexpected results: it shows a larger potential core length, thinner mixing layers and a turbulent kinetic energy (TKE) peak that occurs further downstream. However, the acoustic signature remains classical with a low-frequency noise reduction and a high-frequency noise increase.

Goulos et al. (2016) developed an integrated approach which targets the aerodynamic design of separate-jet exhaust systems for future gas-turbine aero-engines. The overall method was based on a set of fundamental modeling theories applicable to engine performance simulation, parametric geometry definition, and viscous/ compressible flow solution. An analytical approach had been developed for the parametric geometry definition of separate-jet exhausts based on CST functions. A suitable aerodynamic modeling approach had been established and validated against publicly available experimental data. The developed design approach had been coupled with a comprehensive formulation for DSE. The overall framework had been deployed to investigate the overall design space for to two civil aero-engines representative of current and future architectures, respectively. The sensitivity of the exhaust systems' performance metrics to parametric design adjustments had been assessed. The inter-relationship between exhaust systems' performance metrics of interest had been quantified and presented. It showed that the developed analytical approach was a powerful mathematical tool for the parametric representation and geometric manipulation of separate-jet exhaust systems. It demonstrated that the use of correlation matrices in the form of Hinton diagrams could be effective in representing the behavior of the

aerodynamic design space for the case of separate-jet exhausts. The proposed approach was successful in identifying effective guidelines for the improved design of separate-jet exhaust systems. Furthermore, it enabled to quantify and correlate the aerodynamic behavior of any separate-jet exhaust system for any specified engine architecture. Therefore, it constituted an enabling technology toward identifying the fundamental aerodynamic mechanisms that govern the aerodynamic performance of current and future civil turbofan engines.

REFERENCES

- Arend D, Tillman G, O'Brien W, 2012. *Generation after next propulsor research: Robust design for embedded engine systems*. 48th AIAA/ASME/SAE/ASEE Joint Propulsion Conference & Exhibit, Atlanta, Georgia, USA.
- Bijewitz, J., Seitz, A., & Hornung, M, 2015. Architectural comparison of advanced ultra-high bypass ratio turbofans for medium to long range application. Deutsche Gesellschaft für Luft-und Raumfahrt-Lilienthal-Oberth eV.
- Brodersen O P, Rakowitz M, Amant S, et al., 2005. *Airbus, ONERA, and DLR results from the second AIAA drag prediction workshop*. Journal of aircraft, Vol. 42(4) pp. 932-940.
- Christie R, 2016. *Propulsion system integration and modelling synthesis*. Cranfield University, UK.
- Dezitter F , Bezard H , Victor X D S , et al., 2009. *Installation Effects Characterization of VHBPR engine PART II: Experimental study using PIV*. AIAA/CEAS Aeroacoustics Conference, Miami Florida, USA.
- Dezitter F , Bezard H , Victor X D S , et al., 2009. *Installation Effects Characterization of VHBR Engines Part III: CFD Assessment for Jet Mixing*. AIAA/CEAS Aeroacoustics Conference, Miami Florida, USA.
- Dezitter F , Bezard H , Victor X D S , et al., 2009. *Characterization of Installation Effects for HBPR Engine, Part IV: Assessment of Jet Acoustics*. AIAA/CEAS Aeroacoustics Conference, Miami Florida, USA.
- Felder J, Kim H, Brown G, 2009. *Turboelectric distributed propulsion engine cycle analysis for hybrid-wing-body aircraft*. 47th AIAA aerospace sciences meeting including the new horizons forum and aerospace exposition, Orlando Florida, USA.
- Florea R V, Matalanis C, Hardin L W, et al., 2015. *Parametric analysis and design for embedded engine inlets*. Journal of Propulsion and Power, Vol. 31(3), pp. 843-850.
- Giesecke D, Lehmler M, Friedrichs J, et al., 2018. *Evaluation of ultra-high bypass ratio engines for an over-wing aircraft configuration*. Journal of the Global Power and Propulsion Society, Vol. 2(10), pp. 493-515.
- Goulos I, Stankowski T, Otter J, et al., 2016. *Aerodynamic design of separate-jet exhausts for future civil aero-engines—Part I: Parametric geometry definition and computational fluid dynamics approach*. Journal of Engineering for Gas Turbines and Power, Vol. 138(8), pp. 081201.
- Goulos I, Otter J, Stankowski T, et al., 2016. *Aerodynamic Design of Separate-Jet Exhausts for Future Civil Aero-engines—Part II: Design Space Exploration, Surrogate Modeling, and Optimization*. Journal of Engineering for Gas Turbines and Power, Vol. 138(8), pp. 081202.
- Hall C A, Crichton D, 2007. *Engine Design Studies for a Silent Aircraft*. Journal of Turbomachinery, Vol. 129(3), pp. 479-487.
- Larsson L, Grönstedt T, Kyprianidis K G, 2011. *Conceptual design and mission analysis for a geared turbofan and an open rotor configuration*. ASME 2011 Turbo Expo: Turbine Technical Conference and Exposition. American Society of Mechanical Engineers, Vancouver, British Columbia, Canada.
- Lu W, Huang G, Xiang X, et al., 2019. *Thermodynamic and Aerodynamic Analysis of an Air-Driven Fan System in Low-Cost High-Bypass-Ratio Turbofan Engine*. Energies, Vol. 12(10), pp. 1917.

- Oliveira G, Trapp L G, Puppim-Macedo A, 2003. *Engine-airframe integration methodology for regional jet aircrafts with underwing engines*. 41st Aerospace Sciences Meeting and Exhibit, Reno Nevada, USA.
- Rivers M, Dittberner A, 2011. *Experimental investigations of the NASA common research model in the nasa langley national transonic facility and NASA ames 11-ft transonic wind tunnel*. 49th AIAA aerospace sciences meeting including the new horizons forum and aerospace exposition, Orlando Florida, USA.
- Rivers M B, Dittberner A, 2014. *Experimental investigations of the NASA common research model*. Journal of Aircraft, Vol. 51(4), pp. 1183-1193.
- Rudnik R, Rossow C C, Geyr H F, 2002. *Numerical simulation of engine/airframe integration for high-bypass engines*. Aerospace Science and Technology, Vol. 6(1), pp. 31-42.
- Schnell R, Schönweitz D, Theune M, et al., 2014. *Integration-and Intake-Induced Flow Distortions and their Impact on Aerodynamic Fan Performance*. Advances in Simulation of Wing and Nacelle Stall, Vol. 131, pp. 251-269.
- Schnell R, Corroyer J, 2017. *Coupled fan and intake design optimization for installed UHBR-engines with ultra-short nacelles*. 23rd International Symposium on Air Breathing Engines, Manchester, UK.
- Stankowski T P, MacManus D G, Sheaf C T J, et al., 2016. *Aerodynamics of aero-engine installation*. Proceedings of the Institution of Mechanical Engineers, Part G: Journal of Aerospace Engineering, Vol. 230(14), pp. 1-40.
- Stankowski T P, MacManus D G, Robinson M, et al., 2017. *Aerodynamic effects of propulsion integration for high bypass ratio engines*. Journal of Aircraft, Vol. 54(6), pp. 2270-2284.
- Tejero F, Robinson M, MacManus D G, et al., 2019. *Multi-objective optimisation of short nacelles for high bypass ratio engines*. Aerospace Science and Technology, Vol. 91, pp. 410-421.
- Vassberg J, Dehaan M, Rivers M, et al., 2008. *Development of a common research model for applied CFD validation studies*. 26th AIAA Applied Aerodynamics Conference, Honolulu Hawaii, USA.
- Vuillemin A, Piccin O, Davy R, 2007. *Installation Effects Characterization of VHBR Engines – Part I: Experimental Setup and Wind Tunnel Improvement*. 1st CEAS European Air and Space Conference, Berlin, Germany.

TECHNOLOGY DEVELOPMENT OF UHBPR TURBOFAN ENGINES AND RELATED INSTALLATION

Josefin Andersson^{1*}, Hua-Dong Yao¹ & Tomas Grönstedt¹

¹ *Division of Fluid Dynamics, Department of Mechanics and Maritime Sciences, Chalmers University of Technology, Sweden*

* *E-mail of corresponding author: josefin.andersson@chalmers.se*

Abstract. In the late 1930s two research groups in different countries worked on turbojet engines. This resulted in the first flight of a turbojet-powered aircraft in 1939 and the first commercial jet transport in 1952. The performance of turbojet engines was much more superior as compared to propeller-driven airplanes during that time. An obvious disadvantage of turbojet engines is the low propulsive efficiency. This disadvantage leads to high fuel consumption and emissions. In comparison with turbojet engines, turbofan engines in general possess better efficiencies. To date the technology development of turbofan engines with high bypass ratio have been driven by the desire to improve modern commercial aviation aircraft. The potential improvements will be beneficial to reach Flightpath 2050 targets, which aim at reducing CO₂ by 75%, NO_x by 90% and noise by 65%. Increased bypass ratio (BPR) can improve specific fuel consumption (SFC) due to the improved engine efficiency. However, this only works up to a specific BPR. The reason is that the large fan associated with large BPR leads to increased drag from the large nacelle, which increases SFC. To improve the SFC with respect to the BPR, the installation effects of UHBPR nacelles needs to be carefully considered. The nacelle geometry, as well as its installation onto an aircraft, should be designed and optimized for the purpose of introducing light weight and less drag. In addition, the installation effects can be optimized by developing new aircraft concepts. This paper is presented to review state-of-the-art of the installation effects on UHBPR engine cycle design.

Keywords: Turbofan engine, Ultra-High Bypass Ratio (UHBPR), Installation effects, Engine cycle design

INTRODUCTION

In the late 1930s two research groups in different countries worked on turbojet engines. This resulted in the first flight of a turbojet-powered aircraft in 1939 (Farokhi, 2014) and the first commercial jet transport in 1952 (Milne et al., 2003). The performance of turbojet engines was much more superior as compared to propeller-driven airplanes during that time. An obvious disadvantage of turbojet engines is the low propulsive efficiency. This disadvantage leads to high fuel consumption and emissions. In comparison with turbojet engines, turbofan engines in general possess better efficiencies (Basher, 2013). To date the technology development of turbofan engines with high bypass ratio have been driven by the desire to improve modern commercial aviation aircraft. The potential improvements will be beneficial to reach Flightpath 2050 targets, which aim at reducing CO₂ by 75%, NO_x by 90% and noise by 65%.

The fuel consumption and propulsive efficiency of turbofan engines are highly dependent on the fan pressure ratio (FPR). Low FPR gives reduced fuel consumption and improved propulsive efficiency. However, as a very low FPR is adopted, it is necessary to address all challenges relevant to the installation of the fan. By placing a gear box between the fan and the low-pressure compressor, the FPR can be decreased (Kestner et al., 2011). Moreover, the components can be run at optimal speeds. An undesired effect is that the thrust decreases with respect to the decreased FPR. To get the same thrust with the lower FPR, the mass flow has to be increased. This results in a larger fan. The ratio of the mass flow going through the bypass duct and the core is called bypass ratio (BPR). Increasing BPR is another way of improving the efficiency. Ultra-high bypass ratio (UHBPR) is the term for engines with a BPR between 12 and 20. The fan of an UHBPR engine has a very large diameter. Therefore, an UHBPR engine needs a larger nacelle to house it, as compared with conventional engines. Potential issues in the usage of larger nacelles are large weight load, drag generation and integration issues (Gomez-Prada, 2009). The benefits of UHBPR (better propulsive and fuel-efficient engine) are traded off by the increased engine diameter and the

nacelle size. To reduce the negative effect, the nacelle geometry and installation location should be optimized. Increased BPR can also improve the specific fuel consumption (SFC) due to the improved engine efficiency. However, this only works up to a specific BPR. The reason is that the large fan associated with large BPR leads to increased drag from the large nacelle, which increases SFC.

The performance of an engine is estimated under an uninstalled or installed condition. The uninstalled situation is that an engine operates isolatedly. The installed situation includes the interference effects of the nacelle, pylon and wing. These installation effects have not been fully addressed for UHBPR engines regarding the adjustment of the SFC with respect to the BPR (Gomez-Prada, 2009). The nacelle geometry, as well as its installation onto an aircraft, should be designed and optimized for the purpose of introducing light weight and less drag (National Academies of Sciences, Engineering and Medicine, 2016). In addition, the installation effects can be optimized by developing new aircraft concepts.

To reach the flightpath 2050 target of reducing the CO₂ by 75%, it is necessary to consider the engine SFC. As the SFC is reduced, the aircraft fuel burn and related CO₂ emission are decreased. The SFC changes with respect to the engine thrust. An engine of small size and light weight could produce a small thrust with a low SFC. Another important concern for the emission reduction is the nacelle installation in terms of the nacelle drag and weight.

The engine exhaust flow is directed to reduce its interaction with the wing and flaps. By doing this, the take-off lift coefficient is increased due to the reduced interference effect from the airframe. The take-off distances are shortened. The noise is also reduced. Nonetheless, it is unclear whether these advantages could be traded off against the aircraft flight efficiency and cruise range (Basher, 2013).

The aerodynamic performance of the wing is affected by the nacelle. For a wing installed with a nacelle under it, the wing bottom surface experiences flow velocity increase and pressure decrease since the flow is interfered by the nacelle. Gomez-Prada (2009) analyzed this effect in relation to the nacelle size and, furthermore, concluded that the effect results in the loss of the wing lift force. Hoheisel (1997) reported that a turbofan engine with higher BPR introduces additional lift loss above 60%, as compared with a conventional engine. However, the loss could be diminished by optimizing the nacelle geometry and position.

The engine propulsive efficiency is defined as the portion of the engine propulsive power that is converted to the kinetic energy added into the ambient air. The thermal efficiency is the same kinetic energy divided by the rate of fuel energy supplied. The propulsive and thermal efficiency are always requested to be maximized, since they directly affect the SFC, which is desired to minimize. There is always a compromise between the high efficiency and the low SFC (Walsh and Fletcher, 2004).

According to the report by National Academies of Sciences, Engineering and Medicine (2016), the propulsive efficiency affects the engine offtake and cruise requirements. As the propulsive efficiency is improved by decreasing FPR and increasing BPR, less power is required to supply the offtake. However, small discrete improvements in individual components are not sufficient. The engine design needs to be optimized in consideration of the overall fuel burn. In addition, it is of interest to estimate the integrated performance of the airframe and engines.

TECHNOLOGY CHALLENGES

To improve the propulsive efficiency, an effective way is to turn down the exhaust velocity and FPR. This is realized by increasing the area of the fan. The large nacelle size due to the increase fan area brings about technology challenges in the installation of the nacelle onto the aircraft.

ACKNOWLEDGEMENTS

This study is financed by the Clean Sky 2 project IVANHOE (Installed adVAnced Nacelle uHbr Optimisation and Evaluation). The project has received funding from the European

Union's Horizon 2020 research and innovation programme under grant agreement number 863415.

REFERENCES

- Basher M F, 2013. *Optimum turbofan engine performance through variation of bypass ratio*. Journal of Engineering and Sustainable Development.
- Farokhi S, 2014. *Aircraft propulsion*. John Wiley & Sons Ltd.
- Gomez-Prada J, 2009. *Parametric Analysis of the Drag Produced by a VHBR Engine using CFD*. PhD thesis, Cranfield University, Great Britain
- Hoheisel, H, 1997. *Aerodynamic Aspects of Engine-Aircraft Integration of Transport Aircraft*. Aerospace Science and Technology.
- Kestner B K, Schutte J S, Gladin J C and Mavris D N, 2011. *Gladin and Dimitri N. Mavris. Ultra-high bypass ratio engine sizing and cycle selection study for a subsonic commercial aircraft in the N+2 timeframe*. Proceeding of ASME Turbo Expo.
- Milne I, Ritchie R O, and Karihaloo B, 2003. *Comprehensive Structural Integrity*. Elsevier Ltd
- National Academies of Sciences, Engineering, and Medicine. 2016. *Commercial Aircraft Propulsion and Energy Systems Research: Reducing Global Carbon Emissions*. Washington, DC: The National Academies Press. <https://doi.org/10.17226/23490>.
- Walsh P P and Fletcher P, 2004. *Gas Turbine Performance*. John Wiley & Sons Ltd.

CLIMATE IMPACT MITIGATION POTENTIAL OF FORMATION FLIGHT

T. Marks¹, K. Dahlmann², V. Grewe², V. Gollnick¹, F. Linke¹, S. Matthes², E. Stumpf³, M. Swaid¹, S. Unterstrasser², H. Yamashita² & C. Zumege³

¹ German Aerospace Center (DLR), Air Transportation Systems, Hamburg, Germany

² German Aerospace Center (DLR), Institute of Atmospheric Physics, Weßling, Germany

³ RWTH Aachen University, Institute of Aerospace Systems (ILR), Aachen, Germany

Abstract. The aerodynamic formation flight that is also known as aircraft wake-surfing for efficiency (AWSE) enables aircraft to harvest the energy inherent in another aircraft's wake vortex. As the thrust of the trailing aircraft can be reduced during cruise flight, the resulting benefit can be traded for longer flight time, larger range, less fuel consumption or cost savings accordingly. Furthermore, as amount and location of the emissions caused by the formation are subject to change and saturation effects in the cumulated wake of the formation can occur, AWSE can result in a change in the climate effect of the affected flights. In order to quantify these effects, this paper presents an interdisciplinary approach combining the fields of aerodynamics, aircraft operations and atmospheric physics. The approach comprises an integrated model chain to assess the climate impact for a given air traffic scenario based on flight plan data, aerodynamic interactions between the formation members, detailed trajectory calculations as well as on an adapted climate model accounting for the saturation effects in the cumulated wake of the formation. Based on this approach, representative AWSE scenarios for the world's major airports were derived by analyzing and assessing flight plans. The resulting formations were recalculated by a trajectory calculation tool and emission inventories for the scenarios were created. Based on these inventories, the climate impact was quantitatively estimated using the average temperature response (ATR) as climate metric, calculated as an average global near surface temperature change over a time horizon of 50 years. It is shown, that AWSE as a new operational procedure has a significant mitigation potential on climate impact.

Keywords: aircraft wake-surfing, formation flight, air traffic management, fuel savings, climate impact

INTRODUCTION

The principle of aerodynamic formation flight as it can be observed at migratory birds is known for over a century and is nowadays also called aircraft wake-surfing for efficiency (AWSE). It enables aircraft to tap an external source of energy as it is given by another aircraft's wake vortex. As the thrust of an aircraft flying in the upwash of another aircraft's wake can be reduced during cruise flight, the harvested energy can be traded for longer flight time, larger range, less fuel consumption or cost savings accordingly (see e.g. Erbschloe et al. (2020)). Especially in the context of climate change the reduced fuel consumption yields a reduction of the emission of greenhouse gases. Additionally, as location and amount of the emissions caused by the formation can change due to the adapted routing and saturation effects in the cumulated wake of the formation can occur (see Unterstrasser et al. (2020)), AWSE holds the potential to change the climate effect of the affected flights.

SCOPE

In order to quantify climate impact mitigation potential for formation flights, this paper presents an interdisciplinary approach combining the fields of aerodynamics, aircraft operations and atmospheric physics in an integrated model chain. The approach followed in the study is depicted in figure 1. It shows the two main studies that were conducted in order to assess the climate impact of AWSE as two branches with the global study in contrast to a geographically confined study focusing on the North Atlantic Flight Corridor. For the latter for the optimization of the formation routing wind effects were taken into account. Generally for both studies two-aircraft formations were evaluated assuming both aircraft maintaining a stable AWSE formation during the cruise flight constituting one single formation segment and, therefore, no positional changes, breakups and rejoins. Furthermore, it is assumed, that the formation maintains a fixed altitude (formation cruise altitude; FCA) as well as a fixed speed (formation cruise Mach number; FCM) during the AWSE formation.

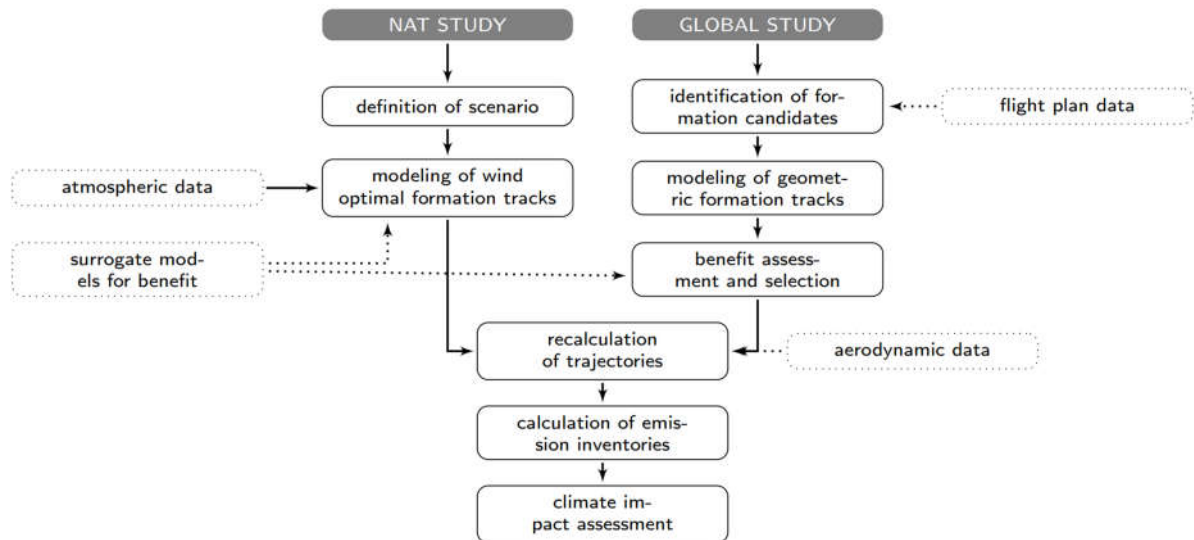


Figure 1. General approach as followed in this paper

The emissions of both formation members will be compared to the emissions of both reference flights which are given by the direct flights each aircraft would take in solo mission. In order to establish comparability and to properly assess the effects of the AWSE benefits the reference missions can be set to use the same altitude and cruise speed as the formation in contrast to the standard cruise speed (SCS) and optimal step climb profiles that the solo flight would otherwise choose. Hence, several settings are distinguished as presented in table 1. Here *XX* denotes the setting with optimal vertical profile and SCS for the reference missions whereas *AM* in contrast describes the assumption, that the reference missions are conducted at the same altitude and speed as the formation missions. *AX* and *XM* are the corresponding settings with only formation altitude or formation speed for the reference missions.

Table 1. Settings used in the study and the corresponding altitude and speed assumptions for reference missions

setting	altitude	speed
XX	Optimal	SCS
AX	FCA	SCS
XM	Optimal	FCM
AM	FCA	FCM

Global Study

In the global study, representative AWSE scenarios for the world's major airports are derived by assessing global flight plans. The huge amount of possible formations is filtered and all valid formation candidates are subsequently evaluated using surrogate models that can predict the formation efficiency based on the formation route geometry and the general mission data. Based on this assessment, the formations with the largest relative benefit are selected to constitute a formation flight plan. The selected formations are subsequently recalculated by the trajectory calculation tool using databases to assess the aerodynamic interactions between the formation members and emission inventories for the evaluated scenario are created. Based on these inventories, the climate impact is quantitatively estimated using the average temperature response (ATR) as climate metric, calculated as an

average global near surface temperature change over a time horizon of 50 years using an adapted climate model accounting for the saturation effects in the cumulated wake of the formation.

North Atlantic Study

For the North Atlantic (NAT) study, a special focus is set on the influence of wind, as it was shown by the authors, that it has a strong effect on the optimal routing and the achievable benefits (see Marks *et al.* (2018)) as well as on the timing (see Marks *et al.* (2020)) of an AWSE formation. In order to give a more complete picture of the potential AWSE benefits while focusing on the climate effects, the scope of the study as used by the authors in the study of Marks *et al.* (2020) is likewise used for the NAT study within this paper. Here, for a set of major European (AMS, CDG, AMS) and North American (ATL, JFK, ORD) airports all possible combinations of two-aircraft formations were calculated for eight representative weather patterns characterizing the weather on the North Atlantic according to Irvine *et al.* (2013). For each scenario wind optimal formation and reference routes were estimated showing a strong geographic deviation of the routes. These routes are used in the NAT study to assess the climate impact by detailed recalculation, creation of emission inventories and climate assessment as in the global study described above.

METHODS

The methods used in this study comprise the identification of formation candidates, route modelling and optimization, surrogate modelling of benefits, trajectory calculation, aerodynamic modelling, climate impact modeling and more as shown in figure 1. All these methods are shortly presented in the following.

Identification of formation candidates

For the global study an identification of possible formation candidates is performed using flight plan data. In order to reduce the enormous amount of possible formations several filters reduce the viable formation candidates based on flight time, location of origin and destination airports, range and the direction of the particular flight tracks. Further filters can be set for aircraft types, carrier, airports and more.

Geometric modeling of formation routes

The formations identified during the previously described process are modeled by a geometric approach as presented by Kent and Richards (2012). However, if the departure time offsets are taken into account, the geometric optimal rendezvous point cannot be reached by the formation members simultaneously. Therefore, the geographically closest applicable location that fulfills this timing constraint is selected for the rendezvous point as presented by Drews *et al.* (2017).

Benefit assessment by surrogate modeling

The benefit estimation is based on surrogate models for the relative AWSE efficiency metric for the whole formation λ_f that represents the difference of the blockfuel mass for the reference mission m_{Bref} to the AWSE mission m_{Bawse} relative to the blockfuel mass of the reference mission m_{Bref} aggregated for both formation members according to eq. 1. The benefits of any formation route geometry (FRG) can then be estimated using a set of parameters that can be directly derived from the FRG and the according mission settings. The models are created using the kriging method on a set of sample data constituting various FRGs and missions settings. The benefits for the sample data are estimated using the trajectory calculation and aerodynamic modelling as described in the next section. A detailed description of this process can be found in Marks *et al.* (2019a).

$$\lambda_f = \frac{\Delta m_{Bf}}{m_{Bfref}} = \frac{\sum m_{Bref} - \sum m_{Bawse}}{\sum m_{Bref}} \quad (1)$$

Trajectory calculation and aerodynamic modelling

For the recalculation of the trajectories, the Trajectory Calculation Module (TCM) is applied, which calculates 4D aircraft trajectories using the total-energy model for solving the flight mechanical equations of motion in combination with aircraft performance data, Base of Aircraft Data (BADA 4.2) from EUROCONTROL (see Linke *et al.* (2009) and Lührs *et al.* (2014)). As the strength of the wake vortex of the leader depends on its flight state and weight, the leader's trajectory is handed over to the follower during the calculation process and the vortex strength is accounted for in the calculation of the aerodynamic benefit of the follower. Here, a database of previously calculated drag values for AWSE condition (drag reduction database, DRD) and solo flight (base drag database; BDD) depending on the leader's and follower's masses as well as on altitude, speed and the follower's position in the vortex is used to interpolate the follower's benefits for the current flight states of both aircraft. The process to set up the corresponding databases is described by Zumegen and Stumpf (2018). A comparison of a simple analytical model and the approach used in this paper can be found in Marks *et al.* (2019b). Wind effects are accounted for during the trajectory calculation using European Centre for Medium-Range Weather Forecasts (ECMWF) wind data.

Wind optimal route optimization

Not only the AWSE benefits of a formation are influenced by wind, also the optimal FRG is affected. For the estimation of wind optimal formation and reference tracks an optimal control approach is used as presented by Marks *et al.* (2018). Each FRG is built up by seven segments (approach, continuation and reference for leader and follower as well as the formation segment for both) and for each segment a wind optimal track is calculated. All segments are then connected in order to build up a full FRG. The resulting FRGs are subsequently assessed using the surrogate models as described in section *benefit assessment*. To find the wind optimal geographic locations of the rendezvous and separation points a higher level pattern search algorithm is used varying both locations simultaneously pinpointing the combination with maximum benefit.

Derivation of emission inventories

As input for the climate impact assessment, the changes in the geographical distributions of engine emissions are determined. So called emission inventories, i.e. 3-dimensional grids (horizontal and vertical) that contain the amount of emissions per species in each grid cell, are created. For this purpose, the engine state is evaluated along each trajectory and from the fuel flow in each trajectory segment the amount of emissions are calculated. For CO₂ and H₂O emissions this is done by multiplying the fuel flow with a constant emission index (EI) of 3.15 (CO₂) and 1.24 (H₂O), respectively, and integrating it over time. The EI of NO_x is not constant, but strongly dependent on the engine thrust and thermal conditions in the combustor, which is why here the Boeing Fuel Flow Method 2 (see Dubois and Paynter (2006)) is used in conjunction with engine certification data provided in the ICAO Engine Emission Databank. Since this database contains ground test measurement data valid for the landing and take-off cycle (LTO), the in-flight conditions have to be translated ("reduced") to equivalent sea-level conditions to correlate the fuel flow with the measured fuel flow data and obtain the corresponding NO_x EI, which is finally re-transformed to in-flight conditions. Based on the resulting segmented emission data, a gridding algorithm calculates the emission portions and assigns it to the relevant grid cells.

Climate impact assessment

The climate response model AirClim (see Grewe et al. (2008) and Dahlmann et al. (2016)) is used to calculate the differences in climate impact between the different scenarios (with and without the effects of AWSE), based on the emission inventories (see section). The tool is a non-linear climate-response model which comprises the atmospheric response to local emissions and thereby establishes a direct link between emission location and their associated radiative forcing, resulting in an estimated near surface temperature change, which is presumed to be a reasonable indicator for climate change. AirClim has been designed to be applicable to (changes in) aircraft technology, including the climate agents CO₂, H₂O, CH₄ and O₃ (latter two resulting from NO_x emissions) and contrail cirrus. The climate response model combines a number of previously calculated atmospheric data with aircraft emission data to obtain the temporal evolution of atmospheric concentration changes, radiative forcing and temperature changes. Dedicated simulation of contrail processes with LES (Large Eddy Simulations) and atmospheric chemical responses with climate chemistry models show, that the ozone and contrail-cirrus impact in formation flight is reduced by 5% and 50%, respectively; see Dahlmann *et al.* (2020), for the NO_x effects and Unterstrasser *et al.* (2020), for the contrail mitigation potential. Thereby the mitigation impact is split evenly between leader and follower. The climate impact is calculated as an average global near surface temperature (average temperature response, ATR) over a time horizon of 50 years. For quantitative estimates of climate impacts presented in this paper the relative difference of the temperature responses δATR is used as climate metric. δATR is defined as the difference of the temperature responses from the AWSE (ATR_{awse}) and the reference scenario (ATR_{ref}) related to the reference scenario (see eq. 2).

$$\delta ATR = \frac{ATR_{awse} - ATR_{ref}}{ATR_{ref}} \quad (2)$$

RESULTS

This section presents results on overall climate impact mitigation gain from the global study. The final paper will contain all major results for both the global and the NAT study, including analyses of the overall benefits and formation statistics, formation route geometry analysis, distributions of emissions and overall climate impact. The flight plan data used for the studies contained all commercial flights from October 2014. As not all aerodynamic databases (DRD) were available for each combination of aircraft types at the time of writing, this preliminary evaluation focuses on the Boeing 777 aircraft being both leader and follower. Concerning the overall scope of the global analysis, three main scenarios were evaluated, constituting different sets of origin and destination airports: *top30* (30 most popular world airports), *top50* (50 most popular world airports) and *all* (all airports). Figure 2 (a) shows the achievable benefits in terms of relative (λ_f) and absolute (Δm_{Bf}) efficiency metrics for the different scenarios and the AM setting (see table 1). It can be seen in this figure, that for the different scenarios similar distributions of the relative benefits are obtained for all identified formations with average values between 5 % and 6 % resulting in average absolute savings of 6500 kg to 7200 kg of fuel per formation. For the different scenarios and the AM setting the resulting ATR50 relative temperature responses δATR in total are representatively shown in figure 2 (b) both for the leader (ld), follower (fw) and the whole formation (form). The figure shows, that in all scenarios a positive effect of AWSE regarding the climate impact is given for the whole formation with the follower contributing more to the effect as its fuel burn is reduced. As the effects of the combined contrail are equally distributed between leader and follower, the leader also shows a reduced climate impact even without reduced fuel burn. The climate impact mitigation gain for the identified formations averages out at 22% to 24% for the different scenarios. A more detailed analysis of the climate effects of AWSE is presented in by Dahlmann et al. (2020), presenting changes for individual direct and indirect effects.

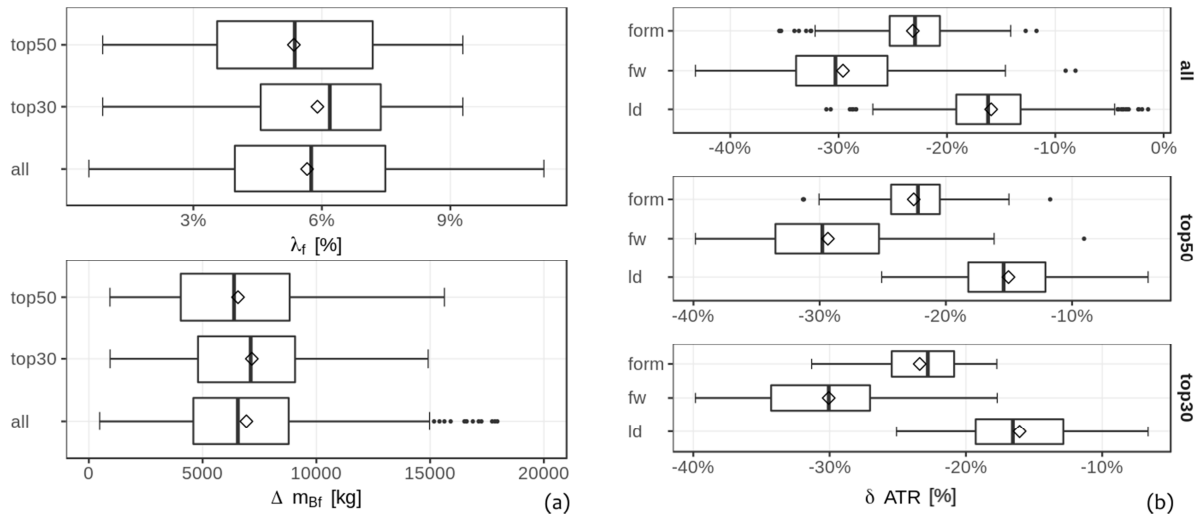


Figure 2. Relative (λ_f) and absolute (Δm_{Bf}) efficiency metrics for the different scenarios and the AM setting (a); relative temperature responses δATR for the AM setting separated by leader (ld), follower (fw) and formation (form) (b)

CONCLUSIONS

The results show, that AWSE as a new operational procedure has a significant mitigation potential on climate impact. The final paper will include detailed descriptions of the methods used as well as the main results both for the global and the NAT study in the different settings and scenarios.

GRANT SUPPORT

This work has received funding from the German Ministry of Economic Affairs and Energy (BMWi) under the National Aeronautical Research Programme (LuFo) V-2 under the grant agreement no. 20E1508.

REFERENCES

- Dahlmann, K., Grewe, V., Frömming, C., and Burkhardt, U., 2016. *Can we reliably assess climate mitigation options for air traffic scenarios despite large uncertainties in atmospheric processes?*, Transportation Research Part D: Transport and Environment, 46, 40 – 55.
- Dahlmann, K., Matthes, S., Yamashita, H., Unterstrasser, S., Grewe, V., and Marks, T., 2020. *Assessing the climate impact of formation flights* (abstract submitted). ECATS 3rd Conference.
- Draws, K., Marks, T., Konieczny, G., Linke, F., and Gollnick, V., 2017. *Identification and modeling of civil formation flight routes based on global flight schedule data*. 66. Deutscher Luft- und Raumfahrtkongress (DLRK), Munich, Germany
- Dubois, D. and Paynter, G. C., 2006. *“Fuel Flow Method2” for Estimating Aircraft Emissions*. SAE International.
- Erbschloe, D., Carter, D. L., Dale, G. A., Doll, C., Niestroy, M. A., and Marks, T., 2020. *Operationalizing Flight Formations for Aerodynamic Benefits*. In proceedings of AIAA Scitech 2020 Forum, Orlando, USA.
- Grewe, V. & Stenke, A., 2008. *Airclim: An efficient tool for climate evaluation of aircraft technology*. Atmospheric Chemistry and Physics, 8, 4621–4639.
- Irvine, E. A., Hoskins, B. J., Shine, K. P., Lunnon, R. W., and Froemming, C., 2013. *Characterizing north atlantic weather patterns for climate-optimal aircraft routing*. METEOROLOGICAL APPLICATIONS, 20, 80–93.

- Kent, T. and Richards, A., 2012. *A Geometric Approach to Optimal Routing for Commercial Formation Flight*. In Proceedings of AIAA Guidance, Navigation, and Control Conference.
- Linke, F. (2014). *Trajectory Calculation Module (TCM) - Tool Description and Validation*. Internal Report, German Aerospace Center.
- Lührs, B., Linke, F., and Gollnick, V., 2014. *Erweiterung eines Trajektorienrechners zur Nutzung meteorologischer Daten für die Optimierung von Flugzeugtrajektorien*. 63. Deutscher Luft- und Raumfahrtkongress (DLRK), Augsburg, Germany
- Marks, T., 2019a. *Modellansätze zur Bewertung von Formationsflügen im Lufttransportsystem*, Ph.D. thesis, Hamburg Technical University, Germany
- Marks, T. and Swaid, M., 2020. *Optimal Timing and Arrangement for Two-Aircraft Formations on North Atlantic under Consideration of Wind*. In proceedings of AIAA Scitech 2020 Forum, Orlando, USA.
- Marks, T., Swaid, M., Lührs, B., & Gollnick, V., 2018. *Identification of optimal rendezvous and separation areas for formation flight under consideration of wind*. In proceedings of 31st Congress of the International Council of the Aeronautical Sciences, Belo Horizonte, Brasil
- Marks, T., Zumegen, C., Gollnick, V., & Stumpf, E., 2019b. *Assessing formation flight benefits on trajectory level including turbulence and gust*. Italian Association of Aeronautics and Astronautics XXV International Congress, Rome, Italy
- Unterstrasser, S. & Stephan, A., 2020. *Far field wake vortex evolution of two aircraft formation flight and implications on young contrails*, (pp. 1–36). Cambridge University Press.
- Zumegen, C. & Stumpf, E., 2019. *Flight behaviour of long-haul commercial aircraft in formation flight*. Air Transport Research Society, ATRS World Conference, Amsterdam, the Netherlands

ASSESSING THE CLIMATE IMPACT OF FORMATION FLIGHTS

K. Dahlmann¹, S. Matthes¹, H. Yamashita¹, S. Unterstrasser¹, V. Grewe^{1,2} & T. Marks³

¹ *Deutsches Zentrum für Luft- und Raumfahrt, Institut für Physik der Atmosphäre, Oberpfaffenhofen, Germany*

² *Delft University of Technology, Aerospace Engineering, The Netherlands*

³ *German Aerospace Center (DLR), Air Transportation Systems, 21079 Hamburg, Germany*

Abstract. An operational measure to aim for mitigation of aviation climate impact that is inspired by migrant birds is to fly in aerodynamic formation. This operational measure adapted to human aircraft would eventually save fuel and is, therefore, expected to reduce the climate impact of aviation. As this method changes beside the total emission also the location of emission it is necessary to assess its climate impact with a climate response model to assure a benefit for climate. Therefore, the climate response model AirClim was adopted to account for saturation effects occurring for formation flight. The results for case studies comprising typical air traffic scenario show that on average the fuel consumption can be decreased by 5%, the climate impact, however, can be reduced by up to 24%.

Keywords: climate impact, formation flight, mitigation potential, aircraft wake-surfing for efficiency

INTRODUCTION

Aviation aims to reduce its climate impact. Hence, quantitative estimates of potential reduction in climate change from individual mitigation strategies are required, in order to identify promising mitigation options. Operational measures offer mitigation potentials that are accessible without adapting the aircraft structure, aerodynamics or engine technology, and might be available within shorter time scales. Such an operational mitigation strategy is inspired by migrant birds that fly in formation to save energy. This method can be adopted by aircraft and lead to substantial fuel savings as the thrust of the trailing aircraft, which is literally surfing on the vortex of the leading aircraft, can be reduced during cruise flight. This procedure can likewise be called aircraft wake-surfing for efficiency (AWSE). This in turn changes the climate effect of aviation as the amount and the location of the emissions change due to the formation flight and the AWSE benefits. This effect is even enlarged, as saturation effects occurring behind the formation can lead to an additional benefit in terms of climate impact.

METHOD

The nonlinear climate response model AirClim (Grewe and Stenke, 2008; Dahlmann *et al.*, 2016) is used to calculate the change in climate impact due to formation flight. AirClim comprises a linearization of atmospheric processes to establish a direct link between emission and near surface temperature change, which is presumed to be a reasonable indicator for climate change. AirClim has been designed to be applicable to climate assessment of different aircraft technologies and operations. It includes the climate impacts of the climate agents CO₂, H₂O, CH₄ and O₃ (latter two resulting from NO_x-emissions) and contrail cirrus (CiC). The climate response model combines a number of previously calculated atmospheric data with aircraft emission data to obtain the temporal evolution of atmospheric concentration changes, radiative forcing and temperature changes.

For formation flights of two aircraft the trailing aircraft (follower) maintains a position in the vortex of the leading aircraft (leader). The close proximity of the aircraft leads to the creation of only one contrail, which incorporates different geometrical, microphysical and optical properties compared to a contrail created by a single aircraft (Unterstrasser and Stephan, 2020). Dedicated Large Eddy Simulations (LES) of the contrail-cirrus evolution showed that in formation flight scenarios the total ice mass, which is used as a proxy for changes in the longwave radiation, is reduced by 20-50%, while the total extinction (proxy for shortwave radiation changes) is reduced by 30-60% (Unterstrasser, 2020). The reduction in longwave forcing reduces the warming effect of contrails, while the reduction of shortwave forcing

reduces the cooling effect from contrails. The net effect depends on the ratio between longwave and shortwave forcing. As the contrail cirrus parametrization in AirClim is based on simulations from Burkhardt and Kärcher (2011), we used the longwave-shortwave ratio from these simulations. In total this leads to a mean net reduction of radiative forcing of 48% in our simulations.

In addition to the saturation effects from contrail, saturation effects for NO_x can occur during formation of aviation-induced ozone. The ozone chemistry is highly nonlinear, which can lead to saturation effects if instead of two aircraft flying separately the two aircraft fly in formation and emit in the identical air mass. Therefore, climate model simulations with EMAC were performed in order to study non-linearities within the North Atlantic Flight corridor (NAFC), studying an emission between 50% and 100% of NO_x emissions. The results on aviation-induced ozone formation show that if NO_x is emitted in the identical air mass, ozone production efficiency decreases by 5%, which causes a lower overall efficiency of emitted NO_x emissions, hence leading to a weaker associated climate effect.

The climate response model AirClim was adapted to account for these saturation effects occurring while flying in formation. Therefore AirClim decreases the CiC and ozone impact by 48 and 5%, respectively when the aircraft fly in formation. Thereby the mitigation benefit is split evenly between leader and follower. The climate impact is calculated as an average global near surface temperature (Average temperature response, ATR) over a time horizon of 50 and 100 years:

$$ATR_{100} = \int_0^{100} \Delta T(t) dt \quad (1)$$

Calculation of the climate impact with the climate response tool AirClim requires emission data as input for individual model simulations. AirClim analyses the mitigation potential by comparing the climate impact of two distinct emission inventories for a given set of city pairs, a reference case which represents aircraft routing in a conventional way (fuel optimal) and a formation case which assumes aircraft to fly in formation with AWSE benefits whenever it is favorable under fuel optimal conditions. Individual traffic samples used in this study as input for AirClim are described in more detail in the next section.

EMISSION INVENTORIES: CASE STUDIES OF AIRCRAFT ROUTES

In this paper we use four set of city-pairs that were identified to have a potential for formation flight between most active airports in the world. A detailed description on the construction of the emission inventories is provided in Marks *et al.*, (2020). They analyzed a global study involving all airports leading to a set of 555 flights (All). In a similar way the 50 most popular airports (TOP50) and the 30 most popular airports (TOP30) were analyzed in order to identify city pair connections with a potential for formation flight. Additionally we used emission inventories of a North Atlantic study (NAT) with a special focus on the influence of wind on the formation.

RESULTS

In order to provide a quantitative estimate of the formation flight mitigation potential, this paper presents differences in the climate impact between the formation flight case and a reference case for four distinct scenarios. Relative changes in climate impact, indicated as average temperature response (ATR100) for the leading and following aircraft as well as for the total formation for the TOP50 scenario are presented in Figure 10 (left). The total climate impact mitigation potential for the formation is about 23%, while the climate impact of the leading aircraft (leader) is reduced by 15% and the climate impact of the following aircraft (follower) is reduced by 31%. Specifically, AWSE increases the fuel consumption and NO_x emissions of the leader, but leads to reduced fuel consumption and NO_x emissions of the follower (Figure 10 right). For the total formation (both aircraft together) fuel consumption as well as NO_x emissions decreases by 5% and 10%, respectively. The total flown distance increases as both aircraft have to fly detours to the rendezvous points (geographic location

where aircraft are scheduled to meet the other aircraft in order to start formation flight with AWSE).

Changes in total climate impact originate from individual effects of aircraft emissions, comprising CO₂ and non-CO₂ effect. Detailed analysis of individual effects can provide information which effects dominate the mitigation potential. The main contributor to the reduced climate impact is the reduced impact of contrail cirrus (CiC) due to the saturation effects described above. This shows a mitigation potential associated with a reduced contrail cirrus effect of about 15%. Additionally 7% reduction can be attributed due to reduced NO_x emissions, while the impact of CO₂ due to reduced fuel consumption amount to only about 1%. Summing up these relative contributions results in an overall mitigation potential of 23% of the total formation (Total).

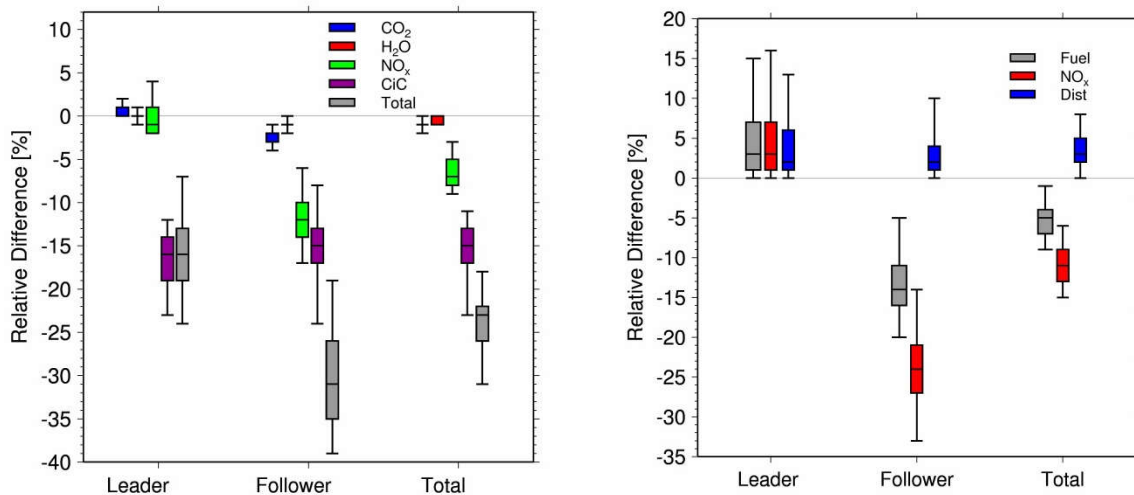


Figure 10 Relative change in climate impact of the different species (left) and fuel consumption, NO_x emissions and flown distances (right) for leader, follower and the Total formation and the Top50 scenario.

Comparing individual impacts between leader and follower shows that while contrail effects are estimated to be reduced by about the same amount for both aircraft, this is not the case for CO₂ and NO_x. Here stronger differences of attributable reductions between leader and follower become apparent. Change of climate impact of CO₂ amounts to +1% versus -2%, comparing leader to follower. This difference can be directly attributed to the changed emissions, as the impact is directly proportional to emitted amounts. For the NO_x impact we find reductions of -1% and -12% comparing leader to follower. This difference is partly attributed to changed emissions, which then have a different impact, as non-linear photochemical processes drive ozone formation in the atmosphere.

Beside the TOP50 scenario, three additional cases were analyzed: All, Top30 and NAT. Comparing the total mitigation potential of these case studies shows only a small variation of the median of the estimated mitigation potential between 23 and 24% (Figure 11 left). Nevertheless the total impact of the individual formations in the traffic sample provides a spread between 13 and 33%. Only the NAT study shows reduced spread from 13 to 27% reduction. The fuel consumption and NO_x emissions for the formation flights of the global study are reduced by about 6% and 12%, respectively (Figure 2 right). In contrast the flown distances are increased by about 3%. For the NAT study the fuel consumption and NO_x emissions are reduced by 7% and 13%, respectively, while the flown distance is increased by only 1%.

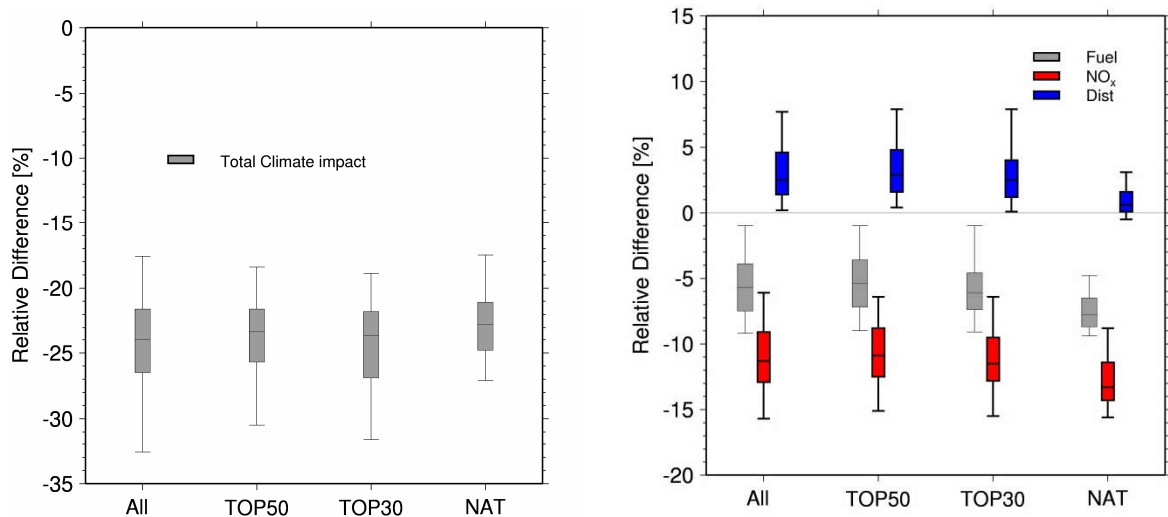


Figure 11: Overview of the total climate impact mitigation potential (left) and the change in fuel consumption, NO_x emission and flown distances (right) for the analyzed studies.

CONCLUSION

Several case studies indicate that the climate impact of aviation could be reduced by one quarter by introducing formation flight procedure with AWSE benefits. While one part of this reduction potential can be attributed to reduced emissions, 5% in CO₂ and 10% in NO_x, a second part can be attributed to changes in the atmospheric processes involved, during contrail processes and formation of aviation-induced ozone in the atmosphere. Due to formation flight the flown distance increases by 1-3%. This is more than only the effect due to the reduced emissions would suggest.

This mitigation potential is achievable for those formations that have a potential for formation flight and which currently (using available flight plans) represent only a small fraction of global flights according to Marks *et al.* (2020). An optimization of the flight plans in favor of the creation of AWSE formations would eventually raise the full climate mitigation potential.

ACKNOWLEDGEMENTS

This work has received funding from the German Ministry of Economic Affairs and Energy (BMWi) under the National Aeronautical Research Programme (LuFo) V-2 under the grant agreement no. 20E1508C.

REFERENCES

- Burkhardt, U., Kärcher, B., 2011. Global radiative forcing from contrail cirrus. *Nat. Clim. Change* 1, 54–58.
- Dahlmann, K., Grewe, V., Frömming, C., & Burkhardt, U. (2016). Can we reliably assess climate mitigation options for air traffic scenarios despite large uncertainties in atmospheric processes? *Transp Res Part D: Transport and Environment*, 46, 40 – 55.
- Grewe, V. & Stenke, A., 2008. Airclim: An efficient tool for climate evaluation of aircraft technology. *Atmospheric Chemistry and Physics*, 8, 4621–4639.
- Marks, T., Dahlmann, K., Grewe, V., Gollnick, V., Linke, F., Matthes, S., Stumpf, E., Unterstrasser, S., Yamashita, H., Zumegen, C., 2020. Climate Impact Mitigation Potential of Formation Flight, in "Making Aviation environmentally sustainable", ECATS 3rd Conference.
- Unterstrasser, S. & Stephan, A. (2020). Far field wake vortex evolution of two aircraft formation flight and implications on young contrails, (pp. 1–36). Cambridge Univ. Press.

Unterstrasser, S (2020). The contrail mitigation potential of aircraft formation flight derived from high-resolution simulations, in "Making Aviation environmentally sustainable", ECATS 3rd Conference, April 2020.

HOW WELL CAN PERSISTENT CONTRAILS BE PREDICTED?

K. Gierens¹, S. Matthes¹ & S. Rohs²

¹ *Deutsches Zentrum für Luft- und Raumfahrt, Institut für Physik der Atmosphäre, Germany, klaus.gierens@dlr.de, sigrun.matthes@dlr.de*

² *Forschungszentrum Jülich, IEK-8, Germany, s.rohs@fz-juelich.de*

Abstract. Persistent contrails and contrail cirrus are responsible for a large part of aviation induced radiative forcing. A considerable fraction of their warming effect could be eliminated by diverting only a quite small fraction of flight paths, namely those that produce the highest individual radiative forcing (iRF). In order to make this a viable mitigation strategy it is necessary that aviation weather forecast is able to predict (i) when and where contrails are formed, (ii) which of these are persistent, and (iii) how large the iRF of those contrails would be. Here we study data from scheduled aircraft measurements and satellites together with weather data from reanalysis in order to see whether such a forecast would currently be possible.

Keywords: Contrails, climate impact, mitigation, Big Hits, weather forecast

INTRODUCTION

Persistent contrails contribute substantially to the climate effect of aviation (for recent estimates see, e.g., Lee et al. 2009, Grewe et al. 2017). The annual and global mean radiative forcing (RF) of all contrails is of the order 50 mW/m, which represents a third to one half of the total estimated RF of aviation. The instantaneous RF (iRF) of a single contrail can, however, be two orders of magnitude larger with both negative (cooling) and positive (warming) sign, such that the value reported by the Intergovernmental Panel on Climate Change (IPCC) and in the estimates mentioned above are just the small net effect that remains when large negative and positive contributions almost balance. The balance is not perfect, such that a small positive RF remains.

To mitigate contrail induced warming of the climate, it is not efficient to avoid all persistent contrails. Avoiding only those ones that produce individually the largest warming, so called Big Hits, suffices to largely eliminate the overall climate effect of persistent contrails and represents an efficient mitigation strategy. For instance, Teoh et al. (2020) demonstrated in a study using data from six weeks of air traffic in Eastern Asia that only about 2% of all flight distances contribute 80% to the total energy forcing (EF, a time and space integral of iRF, see Schumann and Heymsfield 2017) of all flights together. Selectively diverting 1.7% of the considered flights could lead to almost 60% reduction of contrail EF, while the corresponding increase in fuel consumption and CO₂ emission would be 0.0014% for the considered fleet. The authors considered a low-risk strategy as well, where flights are only diverted if there is no need for additional fuel; in this case the total contrail EF could still be reduced by 20%.

This indicates that a large fraction of contrail induced aviation climate warming could be avoided at relatively low cost for additional fuel and at relatively little additional emissions of other greenhouse gases, if we knew in advance, where and when an aircraft will produce not only a contrail, but a persistent one with large individual instantaneous radiative forcing, and perhaps with long life-time and large horizontal spreading (inducing large EF). Thus we need the capability to predict Big Hits, which is a challenge because, as mentioned, we are looking for those few percent of flight distances that are prone to produce Big Hit contrails. Such a capability entails the possibility to predict (i) when and where contrails are formed, (ii) which of these are persistent, and (iii) how large the iRF of those contrails would be. Point (i) is termed the Schmidt-Appleman criterion (Schumann 1996), (ii) implies the prediction of ice-supersaturation, and (iii) implies that the amount of condensable water vapour can be predicted reliably.

In the present paper we compare measurement data from satellites and passenger flights with reanalysis data of the European Centre for Medium-Range Weather Forecast (ECMWF), the so called ERA-5 data, to assess how good a state-of-the-art weather forecast model is able to predict contrail formation, persistence, and iRF.

DATA

The Measurement of Ozone and Water Vapour on Airbus In-service Aircraft (MOZAIC) programme (Marenco *et al.* 1998) is an observing system installed on a small number of commercial passenger aircraft. It runs since 1994; in 2011 it was integrated into the European Research Infrastructure IAGOS (In-service Aircraft for a Global Observing System, Petzold *et al.* 2015). Until today (March 2020) more than 60,000 flights contributed to the data base. Here we use temperature and relative humidity with respect to liquid water (RHL). Flight position (longitude, latitude, pressure altitude) are given for each data record. The data contain also quality labels for each record. We use only data with quality flag "0", which means that the measurement is reliable. Records with $RHL > 100\%$ (i.e. water supersaturation) are rejected. We select four months of data that represent the four seasons: January, April, July and October 2014. From these, approximately 1 percent of cruise level data with pressure altitudes between 310 and 190 hPa are used. For each selected data point we then collect the corresponding data (humidity, temperature, ice cloud water content, radiation quantities) from ERA-5 in $1^\circ \times 1^\circ$ spatial and 1 hr temporal resolution. The MOZAIC vs. ERA-5 comparison is of statistical nature, as we did not perform an online sampling.

The Automatic Contrail Tracking Algorithm (ACTA, Vázquez-Navarro *et al.* 2010) is a tool to spot and track individual contrails during part of their life. It uses the Rapid Scan Service of the Meteosat Second Generation satellite to track contrails in 5 minute intervals over the heavily flown areas of the North-Atlantic and Europe. The ACTA data set spans a full year and comprises over 2300 contrails. It contains observational records of 2305 individual contrails, including their optical thickness, computed using the COCS algorithm (Kox *et al.* 2014), their effects on the radiation field at the top of the atmosphere, computed using the RRUMS algorithm (Vázquez-Navarro *et al.* 2013), as well as their length and width. The data set is described in detail in Vázquez-Navarro *et al.* (2015). From this data set we select two cases where very strong warming contrails have been detected: a) 25 August 2008, between 2235 and 2255 UTC at about $7^\circ W$, $41^\circ N$ in about 12 km altitude, and b) 15 May 2009, between 1740 and 1830 UTC at about $25^\circ W$, $33^\circ N$ in about 12 km altitude, about 750 km west of Madeira. Both cases are night-time cases, such that the shortwave fluxes are zero. The iRF indicated in the data exceeds for both cases 50 W/m^2 . The optical thicknesses of these contrails (or more precisely, contrail segments) are 0.4 to 0.5 and 0.6 to 0.7, respectively. The corresponding ERA-5 data are in $0.25^\circ \times 0.25^\circ$ spatial and 1 hr temporal resolution.

RESULTS

Statistical comparison

Conditions for contrail formation and persistence

The Schmidt-Appleman criterion (Schumann 1996) sets an upper temperature limit for contrail formation, T_{\max} . When the hot exhaust plume gets colder than this threshold by mixing with ambient air, a contrail can form if the mixture is water supersaturated when T_{\max} is reached. That is, one can compute the saturation ratio at T_{\max} , S_{\max} , and if this value exceeds 1.0 a contrail forms. S_{\max} has been computed for the MOZAIC data and compared to the corresponding values at the nearest grid point and time from ERA-5.

The upper half of table 1 casts the comparison between the two data sets into a 2×2 contingency table with entries: Y/Y (hits), Y/N (miss), N/Y (false alarm) N/N (correct negatives). We use the equitable threat score, ETS (Kästner *et al.* 2006), to interpret the contingency table. ETS is unity for a perfect agreement, zero for a totally random relation between the two data sets, and negative when the two datasets tend to contradict each other. The rightmost column in the table lists the ETS. The values range from 0.47 in July to 0.78 in January. These values confirm that the agreement between the two data sets with respect to the possibility of contrail formation is not bad. It is reasonably fair in fall and winter, a bit less good in spring and, say, mediocre in summer.

Table 4: Contingency table for the comparison of MOZAIC with ERA-5 contrail formation and persistence criteria

Month	Y/Y	Y/N	N/Y	N/N	# data	ETS
Contrail formation						
January	3553	100	88	858	4599	0.78
April	1680	22	115	388	2205	0.68
July	617	35	367	1512	2531	0.47
October	788	29	37	224	1078	0.71
Ice supersaturation ($RH_i \geq 100\%$)						
January	249	411	173	3766	4599	0.24
April	47	81	164	1913	2205	0.12
July	14	55	147	2315	2531	0.05
October	9	48	66	955	1078	0.04

Next we compare the measured relative humidity with respect to ice (RH_i) from MOZAIC with the corresponding data from ERA-5. Remember that contrail persistence requires $RH_i > 100\%$. The result is presented in the lower half of table 1. The entries of the contingency table and the corresponding ETS values show that the degree of agreement between the two data sets is quite low. There is a weak coherence in the colder seasons fall and winter with ETS values of 0.12 and 0.24, respectively, but in the warmer seasons the relation is mostly random.

The instantaneous radiative forcing

Now we provide an estimate of radiative impacts of contrails induced at individual positions of aircraft along the trajectory, by using an empirical (parametrical) formula. Figure 1 shows cumulative distribution functions (cdf) of instantaneous radiative forcing (iRF) for all cases where persistent contrails are diagnosed, for the four months considered (colour coded) and separately for MOZAIC and the corresponding ERA-5 grid and time points.

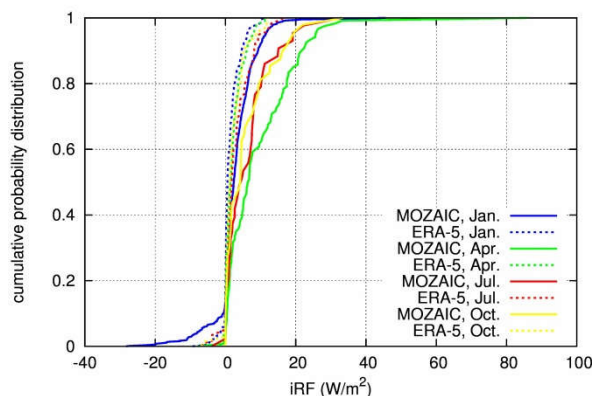


Figure 12: Cumulative distribution functions of iRF in MOZAIC and ERA-5 for 4 months in 2014

The most general observation is that cooling contrails (negative iRF) occur rarely, in less than 20% of the cases. Rather the cdfs rise steeply at zero and small positive values which shows that most persistent contrails in the data sets have a slightly positive warming effect up to 10 W/m^2 . The mean values of iRF for the four months (01, 04, 07, 10) are in the MOZAIC data (2.85, 9.49, 6.25, 5.95) W/m^2 and in the ERA-5 data (1.36, 2.18, 2.94, 2.13)

W/m^2 . That is, the iRF tends generally to higher values in MOZAIC than in ERA-5. The only difference in the calculation is that we use the measured humidity and temperature for the radiation calculation in the MOZAIC case, which then translates into differences in the optical thicknesses. It turns out that these MOZAIC optical thickness values are often larger than their reanalysis counterparts.

Case studies

The case of 25 August 2008 is a short story. We find that at the position and time when ACTA detects very strong contrails, ERA-5 confirms the validity of the Schmidt-Appleman criterion but is far from ice supersaturation with $RH_i \approx 0.6$. This miss is not just a question of an error of a few degrees or a temporal mismatch of an hour or so. In fact, there is no ISSR closer than 10° in both longitude and latitude directions.

The case of 15 May 2009 is more yielding. The Schmidt-Appleman criterion is fulfilled with $S_{max} > 1.8$ and there is an ISSR at the time and position of the contrail. However, ERA-5 indicates low ice-supersaturation; RH_i only slightly exceeds 100%. Thus the contrail as predicted from ERA-5 data would perhaps just be visible under very clear conditions with an optical thickness between 0.01 and 0.03 instead of 0.6-0.7. Consequently, the estimated iRF using ERA-5 data is lower than $1 W/m^2$, much smaller than what the ACTA data suggest.

Although this looks discouraging, let us consider the meteorological situation for 15 May 2009 a bit closer. At the location of the contrail there is a local minimum in the temperature field (215 K), which implies a local minimum in water vapour saturation pressure which hence promotes the formation of ISSRs. The vertical air motion is relatively fast upward, about $-0.2 Pa/s$ (or about 5-6 cm/s). These circumstances promote not only ice supersaturation but also cirrus formation and indeed the contrail is found close to the western edge of a cirrus cloud. The contrail is in tropospheric air, but the dynamic 2-PVU tropopause in the reanalysis data is only $\sim 40 km$ to the west. The upward motion is accompanied with a divergence of higher than $10 \times 10^{-6} s^{-1}$, a value that is typical for ISSRs but untypical for non-ISSRs (Gierens and Brinkop 2012). The relative vorticity is about $-20 \times 10^{-6} s^{-1}$, that is again a value rather typical for ISSRs than for non-ISSRs. The relative vorticity in the nearby stratosphere is strongly positive, that is, the contrail is close to the rims of two counter-rotating vortices; it is itself in the anticyclonic rotation.

Summary and conclusions

In order to see whether a promising strategy to eliminate a considerable share of contrail's warming impact on climate is ready to be realized, namely to avoid the formation of Big Hits, we tested whether a state-of-the-art weather prediction model, represented by the ERA-5 reanalysis, is able to predict reliably (i) the formation of contrails, (ii) their persistence, and (iii) the magnitude of their instantaneous radiative forcing. For a statistical comparison we used four months of MOZAIC data. Additionally we considered two cases from a satellite based data set.

It turns out that the thermodynamic condition for contrail formation can be predicted quite reliably. However, the weather model has only a minor ability to predict ice supersaturation at the right location and right time, and it generally underestimates the degree of supersaturation (see also Dyroff et al. 2015). Thus, it under predicts optical thickness of contrails and in turn iRF as well. It seems this reanalysis data has only limited capabilities for estimating real-world contrail formation along an aircraft trajectory.

ACKNOWLEDGEMENTS

This work contributes to an ambition initiated by John Green and the Greener by Design working group of the Royal Aeronautical Society to take steps towards a real trial of reducing contrail formation by ATM measures. Furthermore this work has received funding from the European Union's Horizon 2020 research and innovation programme under grant agreement

No 875036. We thank Margarita Vázquez-Navarro (EUMETSAT) for provision of the ACTA data.

REFERENCES

- Dyhoff C., Zahn A., Christner E., Forbes R., Tompkins A.M. and van Velthoven, P.F.J., 2015: *Comparison of ECMWF analysis and forecast humidity data with CARIBIC upper troposphere and lower stratosphere observations*. Q. J. Roy. Meteor. Soc., 141, 833–844.
- Gierens K. and Brinkop, S., 2012: *Dynamical characteristics of ice supersaturated regions*. Atmos. Chem. Phys., 12, 11933–11942
- Grewe V. et al., 2017: *Mitigating the climate impact from aviation: Achievements and results of the DLR WeCare project*. Aerospace 2017, 4, 34, 50 pp.
- Kästner M., Torricella F. and Davolio S., 2006: *Intercomparison of satellite-based and model-based rainfall analyses*. Meteorol. Appl., 13, 213–223.
- Kox S., Bugliaro L. and Ostler, A., 2014: *Retrieval of cirrus cloud optical thickness and top altitude from geostationary remote sensing*. Atmosph. Meas. Techn., 7, 3233–3246.
- Lee D., Fahey D., Forster P., Newton P., Wit R., Lim L., Owen B. and Sausen, R., 2009: *Aviation and global climate change in the 21st century*. Atmos. Env., 43, 3520–3537.
- Marenco A., Thouret V., Nedelec P., Smit H., Helten M., Kley D., Karcher F., Simon P., Law K., Pyle J., Poschmann G., von Wrede R., Hume C. and Cook T., 1998: *Measurement of ozone and water vapor by Airbus in-service aircraft: The MOZAIC airborne program, an overview*. J. Geophys. Res., 103, 25631–25642.
- Petzold A., et al., 2015: *Global-scale atmosphere monitoring by in-service aircraft - current achievements and future prospects of the European Research Infrastructure IAGOS*. Tellus B, 67, 28452.
- Schumann U., 1996: *On conditions for contrail formation from aircraft exhausts*. Meteorol. Z., 5, 4–23.
- Schumann U. and Heymsfield A.J., 2017: *On the Life Cycle of Individual Contrails and Contrail Cirrus*. Meteorol. Monogr., 58, 3.1, 24 pp.
- Teoh R., Schumann U., Majumdar A. and Stettler, M., 2020: *Mitigating the climate forcing of aircraft contrails by small-scale diversions and technology adoption*. Environ. Sci. Technol., 54, 2941–2950.
- Vázquez-Navarro M., Mannstein H. and Mayer, B., 2010: *An automatic contrail tracking algorithm*. Atmos. Meas. Tech., 3, 1089–1101.
- Vázquez-Navarro M., Mayer B. and Mannstein H., 2013: *A fast method for the retrieval of integrated longwave and shortwave top-of-atmosphere upwelling irradiances from MSG/SEVIRI (RRUMS)*. Atmos. Meas. Tech., 6, 2627–2640.
- Vázquez-Navarro M., Mannstein H. and Kox S., 2015: *Contrail life cycle and properties from 1 year of MSG/SEVIRI rapid-scan images*. Atmos. Chem. Phys., 15, 8739–8749.

WEATHER AND LOCATION DEPENDENCY OF AVIATION CLIMATE EFFECTS: 4-D-CLIMATE-CHANGE-FUNCTIONS

C. Frömming¹, V. Grewe^{1,2}, S. Brinkop¹, A. S. Haslerud³, S. Rosanka^{1,2,4}, J. van Manen² & S. Matthes¹

¹ *Deutsches Zentrum für Luft- und Raumfahrt, Institut für Physik der Atmosphäre, Oberpfaffenhofen, Germany*

² *Delft University of Technology, Aerospace Engineering, The Netherlands*

³ *Center for International Climate and Environmental Research, Oslo, Norway*

⁴ *Forschungszentrum Jülich GmbH, Institute of Energy and Climate Research, IEK-8: Troposphere, Jülich, Germany*

Abstract. Emissions of aviation include CO₂, H₂O, NO_x and particles. While CO₂ has a long atmospheric residence time and is uniformly distributed in the atmosphere, non-CO₂ gases, particles and their products have short atmospheric residence times and are heterogeneously distributed. Their climate effects depend on chemical and meteorological background conditions during emission, which vary with geographic location, altitude, time, local insolation, actual weather, etc. This spatial and temporal variability can be utilized for aviation climate impact mitigation by identifying aircraft trajectories which avoid climate-sensitive regions. To determine the climate change contribution of individual emissions as function of 3-dimensional position, time and weather situation, contributions of local emissions to changes in O₃, CH₄, H₂O and contrail-cirrus were computed by means of the ECHAM5/MESy Atmospheric Chemistry model and four-dimensional climate change functions (CCFs) were derived thereof. Typical weather situations in the North Atlantic region were considered for winter and summer. For all non-CO₂ species included in the study, we found distinct weather related differences with respect to their climate impact. Depending on the species, we found enhanced significance of the position of emission release in relation to high pressure systems, in relation to the jet stream, in relation to polar night and in relation to the tropopause altitude. The dominating parameters were found to be contrail-cirrus and total NO_x. The results of this study represent a comprehensive basis for weather dependent flight trajectory optimization studies. Furthermore it constitutes the groundwork for the development of more generally applicable algorithmic CCFs.

Keywords: non-CO₂ emissions, weather dependency, climate optimal trajectories

COMPARISON OF VARIOUS AIRCRAFT ROUTING STRATEGIES USING THE AIR TRAFFIC SIMULATION MODEL AIRTRAF 2.0

H. Yamashita¹, F. Yin², V. Grewe^{1,2}, P. Jöckel¹, S. Matthes¹, B. Kern¹, K. Dahlmann¹ & C. Frömming¹

¹ German Aerospace Center, Institute of Atmospheric Physics, Germany, Hiroshi.Yamashita@dlr.de

² Delft University of Technology, Aerospace Engineering, The Netherlands

Abstract. A climate-optimized routing is expected as an operational measure to reduce the climate impact of aviation, whereas this routing causes extra aircraft operating costs. This study performs some air traffic simulations of nine aircraft routing strategies which include the climate-optimized routing, and examines characteristics of those routings. A total of 103 trans-Atlantic flights of an Airbus A330 is simulated for five weather types in winter and for three types in summer over the North Atlantic by using the chemistry-climate model EMAC with the air traffic simulation submodel AirTraf. For every weather type, the climate-optimized routing shows the minimum climate impact, whereas a trade-off exists between the costs and the climate impact. The cost-optimized routing lies between time- and fuel-optimized routings, and minimizes the costs. The aircraft routing for minimum contrail formation shows the second-lowest climate impact, whereas this routing also causes extra costs.

Keywords: Climate impact of aviation, Climate-optimized routing, North Atlantic weather patterns

INTRODUCTION

A climate-optimized routing has been examined to reduce the climate impact of aviation. This routing significantly reduces the climate impact by optimizing flight routes to avoid regions where released emissions and formed contrails have a large climate impact. Previous studies show that the climate-optimized routing greatly decreases the impact, whereas the routing increases aircraft operating costs (Grewe *et al.*, 2014, Ng *et al.*, 2014). Thus, if additional costs for the climate impact of aviation, such as environmental taxes, are included in the current operating costs, a cost increase due to the climate-optimized routing is possibly compensated. This inclusion can change the current routing strategy of minimum costs and incentivize airlines to introduce a climate-optimized flight planning. This study simulates 103 trans-Atlantic flights for not only the climate-optimized routing but also different aircraft routings by using the chemistry-climate model EMAC (Jöckel *et al.*, 2010, 2016) with the air traffic simulation submodel AirTraf (Yamashita *et al.*, 2016, 2019). The simulations are performed for representative weather types over the North Atlantic and common characteristics of those aircraft routings are examined.

METHODOLOGY

To analyze weather patterns over the North Atlantic, a ten years EMAC simulation was carried out for the time period from December 2008 to August 2018 (Table 1). The EMAC model is a numerical chemistry and climate simulation system that includes submodels describing tropospheric and middle atmosphere processes and their interaction with oceans, land, and influences coming from anthropogenic emissions (Jöckel *et al.*, 2010, 2016). EMAC comprises the Modular Earth Submodel System MESSy (version 2.54) to link multi-institutional computer codes and the 5th generation European Centre Hamburg general circulation model ECHAM5 (version 5.3.02; Roeckner *et al.*, 2006). For this study, the model was nudged towards the realistic meteorology (ERA-Interim reanalysis data; Dee *et al.*, 2011).

Next, air traffic was simulated by coupling of AirTraf (version 2.0; Yamashita *et al.*, 2019) with EMAC. AirTraf consists of the total energy model, the DLR fuel flow correlation method and a genetic algorithm. A flight trajectory is optimized including altitude changes according to a selected aircraft routing strategy (called an option): great circle, flight time, fuel use, NO_x emission, H₂O emission, contrail formations, simple operating cost, cash operating cost (COC), and climate impact estimated by the algorithmic Climate Change Functions (aCCFs;

Van Manen, 2017, Yin *et al.*, 2018, Van Manen and Grewe, 2019). These options represent the objects to be minimized (we abbreviate the options to, e.g. the ‘climate option’). AirTraf considers only a cruise flight phase; trajectory conflicts and operating constraints are neglected. Further details are given by Yamashita *et al.* (2016, 2019).

Table 1. Model setup for EMAC and AirTraf models

Parameter	Description
ECHAM5 resolution	T42L90MA (2.8° by 2.8° in latitude and longitude, up to 0.01 hPa)
Simulation period	Dec. 2008-Aug. 2018 (ten years), representative days (Table 2)
Flight plan	103 trans-Atlantic flights (52 eastbound/51 westbound)
Aircraft/engine type	A330-301/CF6-80E1A2, 2GE051 (with 1862M39 combustor)
Mach number	0.82
Flight altitude change	[8.8, 12.5] km (fixed at 10.7 km for the great circle option)

NORTH ATLANTIC WEATHER PATTERN ANALYSIS

Weather patterns were classified into types from the ten years EMAC calculation, which provided ten complete winters (December, January and February) and summers (June, July and August). Diagnostic indices of the North Atlantic Oscillation (NAO) and the East Atlantic (EA) were calculated by considering a similarity of daily-mean geopotential height anomalies at 250 hPa to typical NAO and EA teleconnection patterns over the North Atlantic (80°W-0, 30°N-75°N; Woollings *et al.*, 2010, Irvine *et al.*, 2013). The indices characterize a jet stream position and strength, so that all days of the ten complete winters and summers are classified into five types for winter (W1-W5) and three types for summer (S1-S3). Table 2 lists the types and the representative days for each type; for example, when observing type W3 (Fig. 1), we see that blocking over southwest Europe occurs and diverts the jet stream to the north. As a result, the jet stream becomes weak and tilts southwest-northeast.

Table 2. North Atlantic weather types for winter and summer. This classification refers to Table 1 of Irvine *et al.* (2013). “+” and “-” stand for positive and negative values.

Type	NAO/EA indices	Jet stream position/strength	Representative day in 2008-2018
W1	EA+	Zonal/strong	January 12, 2010
W2	NAO+	Tilted/strong	January 1, 2015
W3	EA-	Tilted/weak	January 9, 2012
W4	NAO-	Confined/strong	December 20, 2009
W5	Mixed	Confined/weak	February 19, 2012
S1	EA+	Zonal/strong	July 11, 2009
S2	Mixed	Weakly tilted/weak	August 1, 2016
S3	EA-	Strongly tilted/weak	July 26, 2011

AIRCRAFT ROUTING CHARACTERISTICS

Some simulations of the nine aircraft routing options were carried out for the trans-Atlantic flights for every representative day (Table 2). Here, we briefly illustrate three characteristics of those routings with the calculation for type W3, focusing on relative changes (in %) to the calculation obtained by the COC option. First, the COC and the climate options are analyzed. COC for the COC and the climate options are 5.35 and 5.85 Mil.USD, whereas the estimated

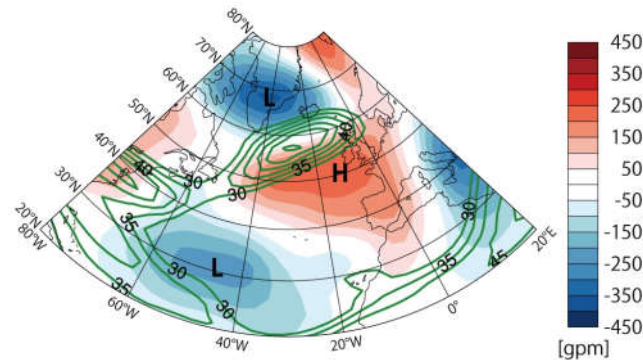


Figure 1. Daily-mean geopotential height anomaly (red-blue contours) and zonal wind above 30 m s^{-1} (green contours) at 250 hPa on January 9, 2012 (type W3)

climate impact $\text{ATR20}_{\text{total}}$ (the average temperature response over 20 years) of the two options are 4.1×10^{-7} and 1.8×10^{-7} K, respectively. The climate option decreases $\text{ATR20}_{\text{total}}$ by 56.5 % (Fig. 2) with an extra COC of 9.2 %. Of the nine routing options, the climate option shows the lowest $\text{ATR20}_{\text{total}}$, whereas a trade-off is observed between the cost and the climate impact. This trade-off agrees with that indicated by the previous studies.

Second, the time, the fuel and the COC options are compared. To minimize COC, a reduction of both flight time and fuel is desirable, because COC depends on the two factors; however, a trade-off generally exists between them. For type W3, the time penalty of flying minimum fuel trajectories is 1.4 percentage points (%pt), whereas the fuel penalty of flying minimum time trajectories is 14.8 %pt. On the other hand, the COC option takes 1.3 % more flight time (with 14.7 % less fuel) than the time option takes, and consumes 0.07 % more fuel (with 0.09 % less flight time) than the fuel option consumes. The COC option lies between the time and the fuel options, and yields the best compromised values of the flight time and the fuel to minimize COC (COC for the time and the fuel options are 5.60 and 5.36 Mil.USD). Last, the contrail option shows the second-lowest $\text{ATR20}_{\text{total}}$ of 2.9×10^{-7} K, which corresponds to a decrease in $\text{ATR20}_{\text{total}}$ by 30.7 % (Fig. 2); however, as with the climate option, this option increases COC by 9.3 % (COC for the contrail option is 5.9 Mil.USD). The point is that these three characteristics are common to every representative day (the quantitative values of the relative changes vary with the days).

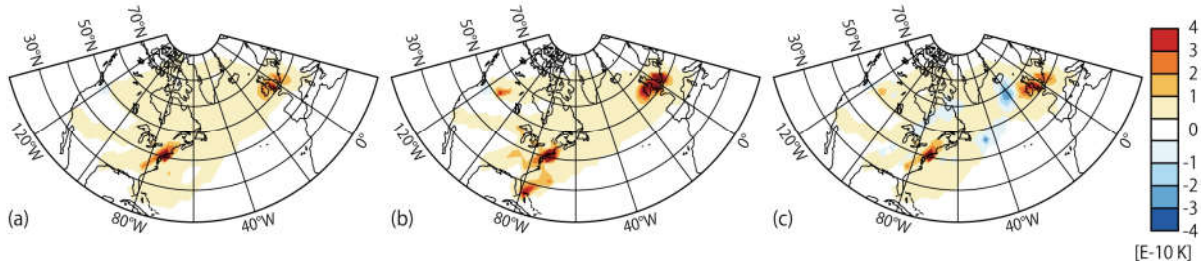


Figure 2. Estimated climate impact ($\text{ATR20}_{\text{total}}$) for contrail (a), COC (b) and climate routing options (c) on January 9, 2012 (type W3)

CONCLUSIONS

Weather patterns over the North Atlantic were classified into five types for winter and three types for summer from the ten years EMAC calculation, and representative days for each type were selected. The EMAC/AirTraf calculations for those days revealed the common characteristics of the aircraft routings. The climate option reduces $\text{ATR20}_{\text{total}}$ most and shows a trade-off between COC and $\text{ATR20}_{\text{total}}$; the COC option lies between the time and the fuel options and achieves the minimum COC successfully; and the contrail option shows the second-lowest $\text{ATR20}_{\text{total}}$, which causes an increase in COC.

ACKNOWLEDGEMENTS

This study was supported by the DLR project Eco2Fly. The flight plan was provided by the European Union FP7 project REACT4C (grant ACP8-GA-2009-233772). The computational resources for the simulations were provided by the German Climate Computing Center.

REFERENCES

- Dee, DP., Uppala, SM., Simmons, AJ., Berrisford, P., Poli, P., Kobayashi, S., Andrae, U., Balmaseda, MA., Balsamo, G., Bauer, P., *et al.*, 2011. *The ERA-Interim reanalysis: configuration and performance of the data assimilation system*. Q. J. R. Meteorol. Soc., 137, pp. 553-597, doi: 10.1002/qj.828.
- Grewe, V., Champougny, T., Matthes, S., Frömming, C., Brinkop, S., Søvde, O. A., Irvine, E. A. and Halscheidt, L., 2014. *Reduction of the air traffic's contribution to climate change: A REACT4C case study*. Atmospheric Environment, 94, pp. 616-625, doi: 10.1016/j.atmosenv.2014.05.059.
- Irvine, E. A., Hoskins, B. J., Shine, K. P., Lunnon, R. W. and Froemming, C., 2013. *Characterizing North Atlantic weather patterns for climate-optimal aircraft routing*. Meteorol. Appl., 20, pp. 80-93, doi: 10.1002/met.1291.
- Jöckel, P., Kerkweg, A., Pozzer, A., Sander, R., Tost, H., Riede, H., Baumgaertner, A., Gromov, S. and Kern, B., 2010. *Development cycle 2 of the modular earth submodel system (MESSy2)*. Geosci. Model Dev., 3, pp. 717-752, doi: 10.5194/gmd-3-717-2010.
- Jöckel, P., Tost, H., Pozzer, A., Kunze, M., Kirner, O., Brenninkmeijer, C. A., Brinkop, S., Cai, D., Dyroff, C., Eckstein, J., Frank, F., Garny, H., Gottschaldt, K.-D., Graf, P., Grewe, V., Kerkweg, A., Kern, B., Matthes, S., Mertens, M., Meul, S., Neumaier, M., Nützel, M., Oberländer-Hayn, S., Ruhnke, R., Runde, T., Sander, R., Scharffe, D. and Zahn, A., 2016. *Earth system chemistry integrated modelling (ESCiMo) with the modular Earth submodel system (MESSy, version 2.51)*. Geosci. Model Dev., 9, pp. 1153-1200, doi: 10.5194/gmd-9-1153-2016.
- Ng, H. K., Sridhar, B., Chen, N. Y. and Li, J., 2014. *Three-dimensional trajectory design for reducing climate impact of trans-atlantic flights*. 14th AIAA Aviation Technology, Integration, and Operations Conference. Atlanta, USA, doi: 10.2514/6.2014-2289.
- Roeckner, E., Brokopf, R., Esch, M., Giorgetta, M., Hagemann, S., Kornblueh, L., Manzini, E., Schlese, U. and Schulzweida, U., 2006. *Sensitivity of simulated climate to horizontal and vertical resolution in the ECHAM5 atmosphere model*. Journal of Climate, 19, pp. 3771-3791, doi: 10.1175/JCLI3824.1.
- Van Manen, J., 2017. *Aviation H₂O and NO_x climate cost functions based on local weather*. Master thesis, Delft University of Technology, The Netherlands.
- Van Manen, J. and Grewe, V., 2019. *Algorithmic climate change functions for the use in eco-efficient flight planning*. Transportation Research Part D: Transport and Environment, 67, pp. 388-405, doi: 10.1016/j.trd.2018.12.016.
- Woollings, T., Hannachi, A. and Hoskins, B., 2010. *Variability of the North Atlantic eddy-driven jet stream*. Q. J. R. Meteorol. Soc., 136, pp. 856-868, doi: 10.1002/qj.625.
- Yamashita, H., Grewe, V., Jöckel, P., Linke, F., Schaefer, M. and Sasaki, D., 2016. *Air traffic simulation in chemistry-climate model EMAC 2.41: AirTraf 1.0*. Geosci. Model Dev., 9, pp. 3363-3392, doi: 10.5194/gmd-9-3363-2016.
- Yamashita, H., Yin, F., Grewe, V., Jöckel, P., Matthes, S., Kern, B., Dahlmann, K. and Frömming, C., 2019. *Various aircraft routing options for air traffic simulation in the chemistry-climate model EMAC 2.53: AirTraf 2.0*. Geosci. Model Dev. Discuss., doi: 10.5194/gmd-2019-331, in review.
- Yin, F., Grewe, V., Frömming, C. and Yamashita, H., 2018. *Impact on flight trajectory characteristics when avoiding the formation of persistent contrails for transatlantic flights*. Transportation Research Part D: Transport and Environment, 65, pp. 466-484, doi: 10.1016/j.trd.2018.09.017.

REDUCING AVIATION EMISSIONS AND FUEL BURN BY RE-ROUTING TRANSATLANTIC FLIGHTS

C. Wells¹, P. D. Williams¹, N. K. Nichols^{1,2}, D. Kalise³ & I. Poll⁴

¹ University of Reading, UK, c.a.wells@student.reading.ac.uk

² National Centre for Earth Observation, UK

³ University of Nottingham, UK

⁴ Poll AeroSciences Ltd., UK

Abstract. After decades of limited situational awareness in the mid-North Atlantic, full satellite coverage will soon be available. Routes could now be altered to exploit the wind field fully and reduce fuel use. When aircraft speed and altitude are constant, the fuel flow rate per unit time is also constant and the optimal route has the minimum journey time. Here we show that changes to current practice could significantly reduce fuel use.

Flights between New York and London, from 1st December, 2019 to 29th February, 2020 are considered. Optimal control theory is used to find the minimum flight time through wind fields from a global atmospheric re-analysis dataset. The aircraft is assumed to fly at Flight Level 340 with airspeeds ranging from 200 to 270 m s⁻¹. Since fuel burn and greenhouse gas emissions are directly proportional to the product of time of flight and airspeed, this quantity, air distance, is used as a measure of route fuel efficiency.

Minimum time air distances are compared with actual Air Traffic Management tracks. To allow clearer comparisons between the fuel efficiency of daily ATM tracks and optimised routes a new quantity, W_{route} , is introduced. This is defined as the ratio of the average headwind along the route to the airspeed. Potential air distance savings range from 0.9 to 7.5% when flying west and from 0.8 to 16.3% when flying east. Thus large reductions in fuel consumption and emissions are possible immediately, without waiting decades for incremental improvements in fuel-efficiency through technological advances.

Keywords: route optimisation, fuel efficiency, ATM tracks, minimum flight time, mid-North Atlantic wind field

HOW WILL CLIMATE CHANGE AFFECT FLIGHT ROUTES AND TURBULENCE?

P. D. Williams¹

¹ *Department of Meteorology, University of Reading, UK, p.d.williams@reading.ac.uk*

Abstract. The atmosphere's meteorological characteristics affect flight routes, journey times, and turbulence. Therefore, climate change has potentially important consequences for aviation.

To investigate the influence of climate change on turbulence, we diagnose an ensemble of 21 clear-air turbulence measures from climate model simulations. We find that turbulence strengthens significantly under climate change, all around the world, in all seasons, and at a wide range of aircraft cruising altitudes. For example, within the transatlantic flight corridor in winter at around 39,000 feet, the occurrence of light turbulence increases by an ensemble-mean value of 59% (with an intra-ensemble range of 43–68%), moderate by 94% (37–118%), and severe by 149% (36–188%). The prospect of more unplanned deviations around turbulence threatens to increase fuel consumption and emissions, at a time when the aviation sector has committed to lowering them.

To investigate the influence of climate change on journey times between London and New York, we feed atmospheric wind fields generated from climate model simulations into a flight routing algorithm. We find that a CO₂-induced strengthening of the prevailing jet-stream winds causes eastbound flights to shorten and westbound flights to lengthen in all seasons. For example, eastbound and westbound crossings in winter become approximately twice as likely to take under 5 hours 20 minutes and over 7 hours, respectively. Even assuming no future growth in aviation, these results suggest that transatlantic aircraft will collectively be airborne for an extra 2,000 hours each year, burning an extra 7.2 million gallons of jet fuel at a cost of \$22 million, and emitting an extra 70 million kilograms of CO₂.

The above examples illustrate how climate change may inadvertently increase the environmental impact of aviation. The two-way interaction between aviation and climate change is an emerging research area that deserves further study.

Keywords: turbulence, jet stream, flight routes, flight times

FUEL TANKERING: ECONOMIC BENEFITS AND ENVIRONMENTAL IMPACT

L. Tabernier¹, E. C. Fernández¹, A. Tautz¹ & R. Deransy¹

¹ *Eurocontrol*

Abstract. The majority of emissions from aviation come from the combustion of the fuel required to operate the aircraft. Therefore, limiting the consumption of fuel required for a safe journey to the absolute minimum is the simplest and most effective way to ensure that emissions from that journey are kept to a minimum.

In practice, however, the fuel load is determined by each aircraft operator on the basis of a number of criteria maximising cost efficiency rather than fuel efficiency.

This is perfectly understandable in a highly competitive market and the non-harmonization of certain operating costs, such as route charges and fuel costs at airports, leads to practices that increase the environmental impact of the aviation sector.

Fuel tankering is one such practice. It consists of transporting more fuel than necessary for the safe execution of the flight in order to avoid or minimise refuelling at the destination airport. It offers an economic benefit when there is a significant difference in fuel prices between departure and arrival airports but greatly increases the amount of emissions produced, because the more kerosene an aircraft carries, the more fuel it consumes and the more it emits.

This paper presents the steps followed by EUROCONTROL in conducting a first study to estimate the number of times this practice would offer an economic benefit and the amount of CO₂ emissions that would result.

This study, limited to short-haul flights, estimates that 21% of ECAC flights would perform fuel tankering beneficially. This would represent a net saving of 265 M€ per year for the airlines, but the burning of 286,000 tonnes of additional fuel (equivalent to 0.54% of ECAC jet fuel used), or 901,000 tonnes of CO₂ per year. At a time when aviation is challenged for its contribution to climate change, the use of fuel tankering is highly questionable.

Keywords: fuel tankering, CO₂ emissions, economic benefit, fuel price.

THE CLIMATE IMPACT OF HYPERSONIC TRANSPORT

J. Emmerig^{1,2}, P. Jöckel¹ & V. Grewe^{1,2}

¹ *Institut für Physik der Atmosphäre, DLR-Oberpfaffenhofen, Germany, johannes.emmerig@dlr.de*

² *Delft University of Technology, Aircraft Noise and Climate Effects, The Netherlands*

Abstract. Supersonic transport was the subject of intense debate in the 1970s and commercial operation was eventually abandoned until recently due to economic and environmental concerns. Flight emissions at stratospheric altitude differ from tropospheric emissions mainly in terms of longevity. Long lifetimes of chemically reactive emissions, especially in the presence of the stratospheric ozone layer, require a detailed investigation of the long-term impact of emissions at this altitude.

Recent studies show a faster degradation of stratospheric water vapor with increasing altitude, driven by photolysis and chemical reaction with O¹D. This is seen as an opportunity for civil hypersonic transport. However, the climate impact of hypersonic flight has not yet been investigated.

This is why our study focuses on the emissions of hydrogen-powered hypersonic aircraft fleets (H₂O, NO_x, H₂) in the middle and upper stratosphere (27 and 36 km). Three different scenarios based on the HIKARI emission data allow an altitude dependent comparison of hypersonic emissions. The scenarios were simulated with ECHAM5/MESSy (v2.54.0), including a newly developed submodel H2OEMIS to integrate external water vapor emissions into the cycle of specific humidity.

Additional simulations using different models for comparison are planned with Didier Hauglustaine (LSCE) in the context of project 'Stratofly' funded by EU-Horizon 2020.

ACKNOWLEDGEMENTS

The authors received funding from the European Union's Horizon 2020 research and innovation programme under grant agreement No 769246 (project STRATOFly).

CLIMATE IMPACT MITIGATION POTENTIAL OF EUROPEAN AIR TRAFFIC

B. Lührs¹, F. Linke², S. Matthes³, V. Grewe^{3,4}, F. Yin⁴ & K.P. Shine⁵

¹ *Institute of Air Transportation Systems, Hamburg University of Technology, 21079 Hamburg, Germany, benjamin.luehrs@tuhh.de*

² *DLR Air Transportation Systems, 21079 Hamburg, Germany*

³ *DLR Institute of Atmospheric Physics, Earth-System-Modelling, Oberpfaffenhofen, 82334 Wessling, Germany*

⁴ *Faculty of Aerospace Engineering, Delft University of Technology, Section Aircraft Noise and Climate Effects, 2628 HS Delft, The Netherlands*

⁵ *Department of Meteorology, University of Reading, RG6 6BB Reading, UK*

Abstract. Air traffic contributes to anthropogenic global warming by about 5% due to CO₂ emissions (about 1/3) and non-CO₂ effects (about 2/3) primarily caused by emissions of NO_x and water vapour as well as the formation of contrails. Since aviation is expected to maintain its trend to grow over the next decades, mitigation measures are required counteracting its negative effects upon the environment. One of the promising operational mitigation measures which has been subject of the EU project ATM4E, is climate-optimized flight planning using algorithmic climate change functions describing the climate sensitivity as a function of emission location and time. The methodology developed for the use of algorithmic climate change functions in trajectory optimization is described and results of its application to the planning of about 13,000 intra-European flights on one specific day are presented. The optimization problem is formulated as bi-objective continuous optimal control problem with climate impact and fuel burn being the two objectives. Results on individual flight basis indicate that there are three major classes of different routes which are characterized by different shapes of the corresponding Pareto-fronts. For the investigated scenario, results show a climate impact mitigation potential of about 73% which is related with a fuel penalty of 14.5%. However, a climate impact reduction of 50% can already be achieved with 0.75% additional fuel burn.

Keywords: climate optimization, eco-efficient trajectories, optimal control

INTRODUCTION

Global air traffic has been growing over the past decades and was able to withstand a number of global crises despite temporary declines in flight movements. In the long-term, air travel demand is expected to grow and since the fuel performance improvement rates due to a continuous development of enhanced aircraft technologies will not exceed growth rates, aviation's impact on global gaseous emissions and hence climate is expected to increase. Besides CO₂-emissions, air traffic causes non-CO₂ effects, due to the emission of NO_x and water vapour as well as the formation of contrails which change the concentration of radiative forcing agents in the atmosphere and influence the climate. Overall, aviation's contribution to the anthropogenic climate change is estimated to be about 5%, of which approximately two thirds can be attributed to the non-CO₂ effects (Lee et al., 2009). Therefore, mitigation actions have to be taken as soon as possible considering both, CO₂ and non-CO₂ effects. Since the latter ones are strongly dependent on the geographic location, altitude, time of the day and the current atmospheric conditions, on the operational side the avoidance of climate sensitive regions is a very promising means. Those regions are characterized by a particularly high impact of the non-CO₂ emissions on climate, e.g. due to a high contrail formation probability. The European project ATM4E carried out in the SESAR Exploratory Research programme was dedicated to the scientific investigation of the potential of optimizing flights with respect to their climate impact already during flight planning (Matthes et al., 2017).

Prior to that, there have been several approaches to climate optimized routing, e.g. by Schumann et al. (2011), Sridhar et al. (2013), Grewe et al. (2014a, b), Hartjes et al. (2016), Zou et al. (2016), Lührs et al. (2016), Rosenow et al. (2017) and Grewe et al. (2017), which vary in the considered emission species, the geographic variability of the effects, the climate metric used and the degrees of freedom in the trajectory optimization.

At the heart of the ATM4E project was the development of algorithmic Climate Change Functions (aCCF), which allow for an efficient computation of the climate impact of different emission species purely based on available weather (forecast) data. Thanks to the aCCFs, it was possible for the first time to do fast-time flight planning for reduced climate impact for any given weather situation.

Within this study, we describe the methodology developed for the use of aCCFs in trajectory optimization for flight planning and present results for a traffic scenario which consists of about 13,000 intra-European flights on a selected day.

MODELING APPROACH

Within this section, the continuous trajectory optimization approach is illustrated. Since the climate impact prediction is mandatory for the optimization with regard to climate, the concept of aCCFs is explained in more detail.

Trajectory Optimization

In order to determine continuous climate optimized trajectories, the Trajectory Optimization Module (TOM) is used (Lühns et al., 2016, 2018). Following an optimal control approach, aircraft's motion is described as temporal evolution of state variables $\mathbf{x}(t)$ (e.g. location, speed, emission flows) and control variables $\mathbf{u}(t)$ (e.g. thrust, heading, acceleration). Optimal trajectories are obtained by identifying the control input $\mathbf{u}(t)$ which minimizes the cost functional J while satisfying dynamic constraints (e.g. equations of motion) as well as control (e.g. maximum thrust), state (e.g. maximum speed), and path limitations (e.g. maximum pressure altitude). The resulting continuous optimal control problem is converted into a discrete non-linear programming problem (NLP) with the MATLAB optimal control toolbox GPOPS-II (Patterson and Rao, 2014) and solved with the NLP-solver IPOPT (Wächter and Biegler, 2006).

Cost functional

In order to determine trajectories which are Pareto-optimal with respect to fuel burn and climate impact, the cost functional is expressed as the weighted sum of climate impact (curly brackets) and fuel burn (squared brackets). Both, climate impact and fuel burn are normalized with respect to the corresponding reference values of the minimum fuel burn trajectory (ATR_{ref} , $m_{fuel,ref}$). The climate impact is obtained as temporal integral of the product of the aCCF and the associated emission flow \dot{m}_i for CO_2 , NO_x and H_2O or the true airspeed v_{TAS} in the case of contrail induced cirrus cloudiness (CIC).

$$J = c_{clim} \cdot \left\{ \sum_i \int_{t_0}^{t_f} aCCF_i(\mathbf{x}, t) \cdot \dot{m}_i(t) dt + \int_{t_0}^{t_f} aCCF_{CIC}(\mathbf{x}, t) \cdot v_{TAS}(t) dt \right\} \cdot ATR_{ref}^{-1} \\ + c_{fuel} \cdot [m_0 - m_f] \cdot m_{fuel,ref}^{-1}; \quad i \in \{CO_2, NO_x, H_2O\} \quad (1)$$

$$c_{clim} + c_{fuel} = 1 \quad \text{with} \quad c_{clim}, c_{fuel} \in [0,1] \quad (2)$$

Varying the weights of climate impact and fuel burn (c_{clim} and c_{fuel}) yields Pareto-optimal trajectories. Minimum climate impact trajectories are determined with $c_{clim} = 1$ and minimum fuel burn trajectories with $c_{fuel} = 1$.

Dynamic constraints

The dynamic constraints are formulated based on the equations of motion given by Eurocontrol's Base of Aircraft Data (BADA) 4.0 performance models which assume a point-mass model with three degrees of freedom and variable aircraft mass (Nuic and Mouillet, 2012). In order to estimate aircraft's emissions, the Eurocontrol modified Boeing Fuel method 2 is used (Jelinek et al., 2004; DuBois and Paynter, 2006).

Control, state and path limitations

In order to avoid violations of the aircraft's flight envelope, control, state and path limitations are introduced. The limitations are extracted from the BADA 4.0 dataset and cover aircraft mass, fuel capacity, pressure altitude, calibrated airspeed, Mach number and maximum lift coefficient. Additional geographic boundaries are set up to reduce the solution space, and hence the computational effort.

Algorithmic Climate Change Functions

Climate Change Functions (CCFs) allow for the quantification of the global climate impact of local aircraft emissions as a function of emission location and time (Grewe et al., 2014; Frömming et al. 2020). Since the calculation of CCFs using complex climate-chemistry models is computationally expensive and hence cannot be performed in real-time, algorithmic Climate Change Functions (aCCFs) were developed in the course of the project ATM4E. These aCCFs consider both CO₂ and non-CO₂ effects and measure global climate impact using the average temperature response integrated over a 20-year period (ATR₂₀). The robustness of climate optimized trajectories with regard to different metrics is discussed by Matthes et al. (2020). By design, aCCFs allow for a fast-time calculation of the climate impact of ozone and methane changes resulting from NO_x emissions, water vapour emissions and persistent contrail formation using standard weather forecast data which is available for flight planning (Van Manen and Grewe, 2019; Yin et al., 2018, 2020; Yamashita et al., 2020).

The water vapour and nitrogen oxide aCCFs were created by applying correlation analyses using the CCFs estimated by Grewe et al. (2014) and are based on four meteorological parameters which show a reasonable statistical significance. While for water vapour, the potential vorticity is best suited to correlate the effects, the warming effect of ozone caused by NO_x is modeled as a function of the local temperature and the geopotential. The cooling effects of the methane reductions were captured by a relationship which includes the geopotential and the amount of incoming solar radiation at the top of the atmosphere.

Contrail-aCCFs were derived separately for night-time contrails and day-time contrails since the net contrail climate effect is hugely influenced by the time of the day. It was found that temperature (which strongly determines the amount of contrail ice content) and the outgoing infrared radiation provide reasonable approximations to the climate effect in regions where the Schmidt-Appleman criterion predicts persistent contrails to form (Appleman, 1953).

RESULTS

Below, the chosen reference day for the case study is characterized. Then, Pareto-fronts for exemplary routes are presented. Finally, the individual Pareto-fronts are consolidated in order to formulate more general statements.

One-day Case Study of European Air Traffic

Using the modelling approach described above, en-route climate optimized trajectories within Europe are estimated and evaluated with respect to fuel burn and climate impact of CO₂ and non-CO₂ effects for the 18th December 2015. This day is characterized by a high traffic volume with unaffected traffic flows indicated by a low number of weather-, ATC-, and aerodrome related regulations. Additionally, the weather situation shows persistent contrail formation areas over central Europe.

The corresponding traffic inventory is extracted from Eurocontrol's Demand Data Repository 2 (DDR2) database and contains 28,337 flights. After filtering by restricting to intra-ECAC (European Civil Aviation Conference) flights only and by restricting to flights covered by Eurocontrol's BADA 4.0 models, a traffic sample containing 13,276 flights is generated. Although this seems to be a large reduction of flights, the amount of considered available seat kilometres only decreases by about 9% since especially large Airbus and Boeing aircraft are part of BADA.

Meteorological parameters which are required for both the aircraft performance calculations as well as the aCCF evaluation are determined based on ECMWF ERA-Interim reanalysis data (Dee et al., 2011).

Results for individual routes

Assuming that climate impact is considered along with economical aspects in the trajectory planning process, approximately 100 Pareto-optimal trajectory options for each route within the traffic sample have been calculated by systematically varying the weighting factors c_{clim} and c_{fuel} according to Eq. (2). During the analysis of the results, three characteristic shapes have been identified including smooth curves and discontinuous Pareto-fronts (see figure 1). The first shape is characterized by a smooth overall Pareto-front which has no contrail impact and is dominated by the climate impact reduction of NO_x (see figure 1, left). Caused by detours compared to the minimum fuel solution, the fuel burn and hence the climate impact of CO_2 is increasing. In the second case, various contrail areas along the route are involved. Only minor trajectory changes lead to the avoidance of contrail sensitive areas and hence lead to large climate impact reductions (see figure 1, middle). In the third case, the minimum fuel trajectory passes a contrail sensitive region at its edge. Small trajectory changes causing only low amounts of additional fuel lead to a full avoidance of contrails. Further climate impact reduction is possible by deviating to regions with lower climate sensitivities with respect to NO_x emissions (see figure 1, right).

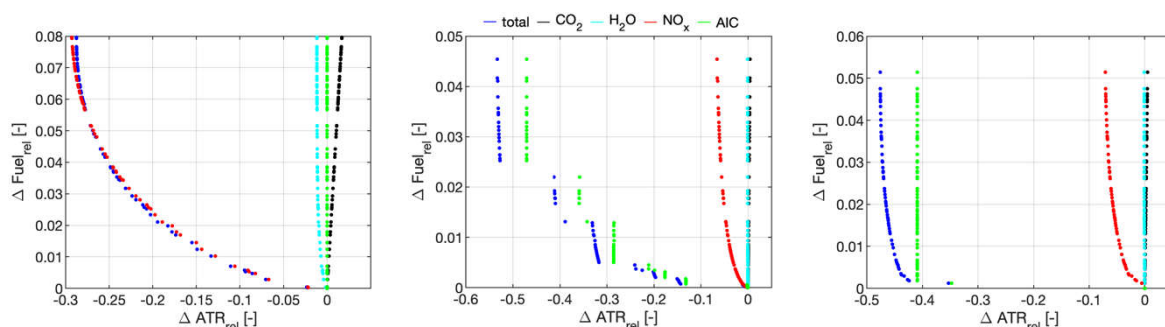


Figure 1. Pareto-fronts for Baku-Luxembourg (left) Lulea-Gran Canaria (middle) Helsinki-Gran Canaria (right). The coloured dots indicate the individual contribution of CO_2 (black), H_2O (cyan) NO_x (red) and contrails (green) to the overall climate impact reduction (blue) for a given fuel increase. Results are expressed relative to the minimum fuel case.

Consolidated Results

The individual Pareto-fronts are estimated for all 13,276 routes of the traffic scenario. Based on these, an average Pareto-front is created, where one point on each individual Pareto-front (index i) is selected such, that a given overall fuel penalty for all routes is not exceeded and the total climate impact of all routes is minimized according to Eq. (3). Finally, the average Pareto-front is obtained by varying the accepted fuel penalty.

$$\begin{aligned} \min \sum_i \text{ATR}_{20,i} \\ \text{subject to } \sum_i m_{\text{fuel},i} < m_{\text{fuel,penalty}} \end{aligned} \quad (3)$$

Figure 2 (left) shows the individual Pareto-fronts of the top 10 routes (coloured) of the traffic scenario in terms of available seat kilometers as well as the resulting average Pareto-front (black curve). The black circle indicates the +5% fuel burn point on the average Pareto-front which corresponds to a total climate impact reduction of about 42% for these routes. The red circles highlight the points which are chosen on each route's Pareto-front in order to achieve an overall +5% fuel burn increase while minimizing the total climate impact. Depending on the shape and slope of each individual Pareto-front, climate impact mitigation and additional fuel burn may vary strongly between the routes.

Moreover, figure 2 (right) shows the Pareto-front for the top 2,000 routes. A maximum climate impact reduction of about 73% can be achieved if a fuel penalty of 14.5% was

accepted. Higher climate impact mitigation efficiencies (climate impact reduction per fuel increase) are obtained at low fuel penalties, e.g. a fuel penalty of 0.75% may already lead to a climate impact reduction of about 50%. The individual contribution of the species indicates that the climate impact reduction is dominated by the reduction of the contrail climate impact shown in green. Because of the importance of the contrail impact, a more comprehensive evaluation of contrail radiative forcing will be included in Matthes et al. (2020). However, for this study, a weather situation with high contrail formation probabilities over central Europe has been chosen. Consequently, mitigation potentials and efficiencies may look very different for other weather situations.

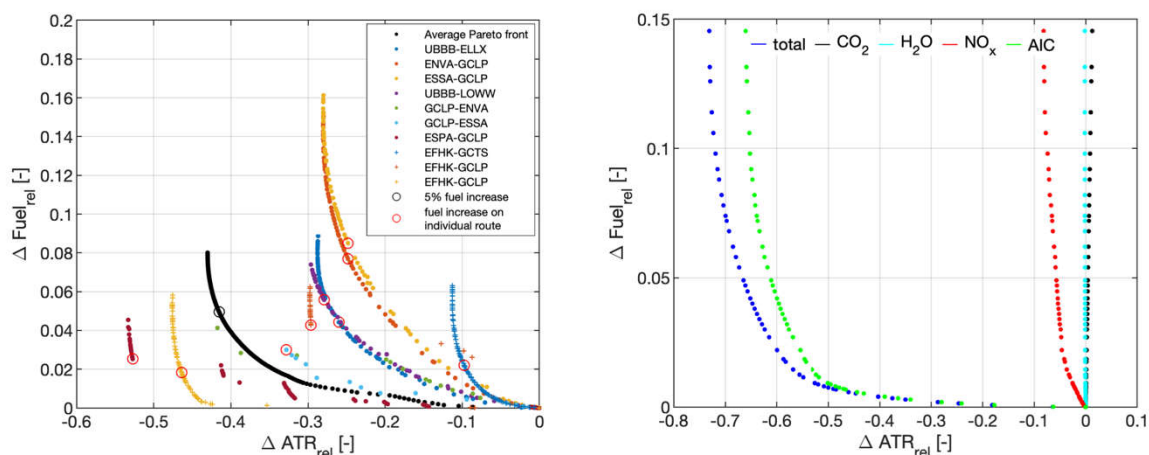


Figure 2. Top 10 single route Pareto-fronts and corresponding average Pareto-front (left) and average Pareto-front (right) for the top 2000 routes with individual contribution of the species CO₂ (black), H₂O (cyan), NO_x (red) and AIC (green) to the overall climate impact reduction (blue) for a given fuel increase. Results are expressed relative to the minimum fuel case.

Figure 3 shows the cumulative climate impact reduction as a function of the number of changed routes for different fuel penalties. The routes have been sorted according to their absolute climate impact reduction. At a fuel penalty of 1% which is related to a climate impact reduction of approximately 53% (see figure 2), the adaption of only 500 of the total 2,000 routes would already yield more than 85% of the potential for all routes (left). This effect slightly decreases for increasing fuel penalties: at 14.5% fuel penalty, 500 routes are related with about 75% of the overall potential (right). Since the slope of the individual contribution of contrails tends towards zero after about 1,000 changed routes in all three cases, it can be concluded that routes which allow the avoidance of contrails areas are characterized by high climate impact mitigation potentials and hence should be changed first.

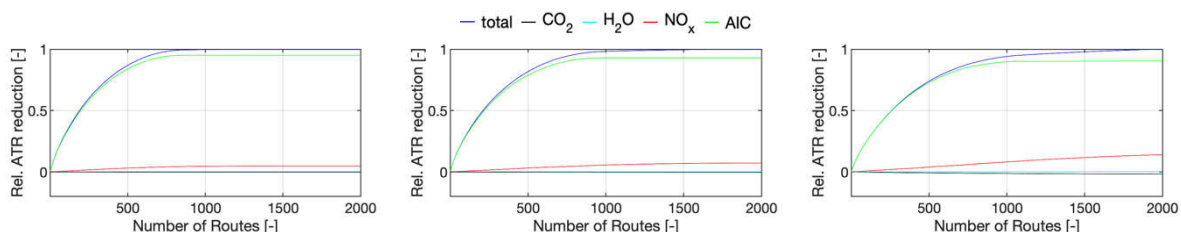


Figure 3. Cumulative ATR reduction as a function of the number of changed routes for 1% (left), 2% (middle) and 14.5% (maximum) increase in fuel burn (right) for the top 2,000 routes. Individual contributions to the total ATR reduction (blue) are shown for CO₂ (black), H₂O (cyan), NO_x (red) and contrails (green).

CONCLUSION AND OUTLOOK

Within this study, the climate impact mitigation potential of intra-European air traffic is estimated for a one-day case study. For this purpose, aircraft trajectories are optimized with regard to climate impact by avoiding regions in which the atmosphere shows a high climate

impact sensitivity with regard to non-CO₂ emissions. Climate impact sensitivities are determined based on algorithmic Climate Change Functions measuring the climate impact per unit emission based on meteorological parameters which can be obtained from weather forecasts.

Results of the top 2000 routes (in terms of available seat kilometres) show a maximum climate impact mitigation potential of up to 73% related with additional fuel burn of about 14.5% compared to the minimum fuel solution. However, a climate impact reduction of 50% can already be achieved with only 0.75% additional fuel burn. Since a case study day with high persistent contrail formation probability was chosen, the climate impact reduction is dominated by a reduction of the contrail impact. Therefore, in following studies different weather situations will be evaluated with regard to potential climate impact savings. Additionally, results indicate, that a large fraction of the overall climate impact mitigation potential can already be achieved with the modification of a comparably low number of routes with particularly high climate impact reduction potential. This finding will be addressed in more detail in upcoming studies.

ACKNOWLEDGEMENTS

The project leading to this study has received funding from the SESAR Joint Undertaking under grant agreement No 699395 (ATM4E) under European Union's Horizon 2020 research and innovation programme. Work in this article was supported by DLR project Eco2Fly (2018-2022). The Base of Aircraft Data (BADA) aircraft performance models and the access to the Demand Data Repository were kindly provided by Eurocontrol. High performance supercomputing resources were used from the German DKRZ Deutsches Klimarechenzentrum Hamburg.

REFERENCES

- Appleman, H., 1953: The Formation of Exhaust Condensation Trails by Jet Aircraft. Bull. Amer. Meteor. Soc., 34, 14–20, <https://doi.org/10.1175/1520-0477-34.1.14>
- Dee, D.P. et al.: The ERA-Interim reanalysis: configuration and performance of the data assimilation system. Quarterly Journal of the Royal Meteorological Society (2011), April, pp. 553–597.
- DuBois, D.; Paynter, G.: 'Fuel Flow Method 2' for Estimating Aircraft Emissions. Society of Automotive Engineers (SAE), SAE Technical Paper 2006-01-1987, 2006.
- Frömming, C., Grewe, V., Matthes, S., Brinkop, S., Haslerud, A.S., Irvine, E.A., Rosanka, S., van Manen, J., 2020. Influence of weather situation on aviation emission effects: The REACT4C climate change functions (in preparation).
- Grewe, V.; Champougny, T.; Matthes, S.; Frömming, C.; Brinkop, S.; Søvde, O.; Irvine, E.; Halscheidt, L. Reduction of the air traffic's contribution to climate change: A REACT4C case study. *Atmos. Environ.* 2014, 94, 616–625, 2014a.
- Grewe, V.; Frömming, C.; Matthes, S.; Brinkop, S.; Ponater, M.; Dietmüller, S.; Jöckel, P.; Garny, H.; Tsati, E.; Dahmann, K.; et al. Aircraft routing with minimal climate impact: The REACT4C climate cost function modelling approach (V1.0). *Geosci. Model Dev.* 2014, 7, 175–201, 2014b.
- Grewe, V., Matthes, S., Frömming, C., Brinkop, S., Jöckel, P., Gierens, K., Champougny, T., Fuglestedt, J., Haslerud, A., Irvine, E., Shine, K.: Feasibility of climate-optimized air traffic routing for trans-atlantic flights. *Environ. Res. Lett.* 12, 034003. <https://doi.org/10.1088/1748-9326/aa5ba0>, 2017.
- Hartjes, S., Hendriks, T., Visser, H.G.: Contrail mitigation through 3D aircraft trajectory optimization. In: 16th AIAA Aviation Technology, Integration, and Operations Conference, American Institute of Aeronautics and Astronautics. doi:<https://doi.org/10.2514/6.2016-3908>, 2016.
- Jelinek et al.: Advanced Emission Model (AEM3) v1.5 - Validation Report. EEC Report EEC/SEE/2004/004, 2004.

- Lee, D. S. et al.: Aviation and global climate change in the 21st century, *Atmospheric Environment journal*, Volume 43, 2009, pp.3520-3537.
- Lührs, B.; Niklaß, M.; Frömming, C.; Grewe, V.; Gollnick, V.: Cost-Benefit Assessment of 2D- and 3D Climate and Weather Optimized Trajectories. 16th ATIO conference, 2016.
- Lührs, B.; Niklaß, M.; Frömming, C.; Grewe, V.; Gollnick, V.: Cost-Benefit Assessment of Climate and Weather Optimized Trajectories for different North Atlantic Weather Patterns. 31st Congress of the International Council of the Aeronautical Sciences (ICAS), 2018.
- Matthes S., Grewe, V., Dahlmann, K., Frömming, C., Irvine E.; Lim L., Linke F., Lührs B., Owen B., Shine K. P., Stromatas S., Yamashita, H., and Yin F., 2017. A Concept for Multi-Criteria Environmental Assessment of Aircraft Trajectories, *Aerospace* 2017, 4, pp. 42; doi:10.3390/aerospace4030042.
- Matthes, S. Lührs, B., Dahlmann, K., Linke, F., Grewe, V. Yin, F., Shine, K., Robustness of climate-optimized trajectories and mitigation potential: Flying ATM4E, in in "Making Aviation environmentally sustainable", Vol 1, ECATS 3rd Conference 2020.
- Nuic, A.; Mouillet, V.: User Manual for the Base of Aircraft Data (BADA) Family 4. ECC Technical/Scientific Report No. 12/11/22-58, 2012.
- Patterson, M.A.; Rao, A.V.: GPOPS-II: A MATLAB Software for Solving Multiple-Phase Optimal Control Problems Using hp-Adaptive Gaussian Quadrature Collocation Methods and Sparse Nonlinear Programming. *ACM Transactions on Mathematical Software*, Vol. 1, No. 1, Article 1, 2014.
- Rosenow, J., Lindner, M., Fricke, H.: Impact of climate costs on airline network and trajectory optimization: a parametric study. *CEAS Aeronaut. J.* 8, 371–384. <https://doi.org/10.1007/s13272-017-0239-2>, 2017.
- Schumann, U., Graf, K., Mannstein, H.: Potential to reduce the climate impact of aviation by ight level changes. 3rd AIAA Atmospheric Space Environments Conference. AIAA paper 2011-3376, 2011.
- Sridhar, B., Chen, N.Y., Ng, H.K.: Energy efficient contrail mitigation strategies for reducing the environmental impact of aviation. 10th USA/Europe Air Traffic Management Research and Development Seminar, 2013.
- Van Manen, J.; Grewe, V.: Algorithmic climate change functions for the use in eco-efficient flight planning. *Transportation Research Part D: Transport and Environment*, Vol. 67, pp. 388-405, <https://doi.org/10.1016/j.trd.2018.12.016>, 2019.
- Wächter, A.; Biegler, L. T.: On the implementation of an interior-point filter line-search algorithm for large-scale nonlinear programming. *Mathematical Programming*. Vol. 106, pp. 25-57, 2006.
- Yamashita, H., Yin, F., Grewe, V., Jöckel, P., Matthes, S., Kern, B., Dahlmann, K., and Frömming, C. Various aircraft routing options for air traffic simulation in the chemistry-climate model EMAC 2.53: AirTraf 2.0, *Geosci. Model Dev. Discuss.*, <https://doi.org/10.5194/gmd-2019-331>, in review, 2019.
- Yin, F., Grewe, V., van Manen, J., Matthes, S., Yamashita, H., Irvine, E., Shine, K.P. Lührs, B., Linke, F., Verification of the ozone algorithmic climate change functions for predicting the short-term NOx effects from aviation en-route, 8th international conference on air transportation (ICRAT), Barcelona, Spain, 2018.
- Yin, F., Grewe, V., Matthes, S., Yamashita, H., Irvine, E., Shine, K.P. Lührs, B., Linke, F., Predicting the climate impact of aviation for en-route emissions: The algorithmic climate change function sub model ACCF 1.0 of EMAC 2.53, GMDD in preparation, 2020.
- Zou, B., Buxi, G.S., Hansen, M.: Optimal 4D aircraft trajectories in a contrail-sensitive environment. *Networks Spat. Econ.* 16, 415–446. <https://doi.org/10.1007/s11067-013-9210-x>, 2016.

ROBUSTNESS OF CLIMATE-OPTIMIZED TRAJECTORIES AND MITIGATION POTENTIAL: FLYING ATM4E

S. Matthes¹, B. Lührs², K. Dahlmann¹, F. Linke³, V. Grewe^{1,4}, F. Yin⁴, & K.P. Shine⁵

¹ DLR Institute Atmospheric Physics, Earth-System-Modelling, Oberpfaffenhofen, 82334 Wessling, Germany, sigrun.matthes@dlr.de

² Institute Air Transportation Systems, Hamburg University of Technology, 21079 Hamburg, Germany

³ DLR Air Transportation Systems, 21079 Hamburg, Germany

⁴ Faculty of Aerospace Engineering, Delft University of Technology, Section Aircraft Noise and Climate Effects, 2628 HS Delft, The Netherlands

⁵ Department of Meteorology, University of Reading, RG6 6BB Reading, UK

Abstract. Aviation can reduce its climate impact by controlling its CO₂-emission and non-CO₂ effects, e.g. aviation-induced contrail-cirrus and ozone caused by nitrogen oxide emissions. One option is the implementation of operational measures which aim to avoid those atmospheric regions that are in particular sensitive to non-CO₂ aviation effects, e.g. where persistent contrails form. Quantitative estimates of mitigation potentials of such climate-optimized aircraft trajectories are required, when working towards sustainable aviation. Results are presented from a comprehensive modelling approach which is working towards identifying such climate-optimized aircraft trajectories. The overall concept relies on a multi-dimensional environmental change function concept, which is capable of providing environmental impact information to air traffic management (ATM) and which in principal could include the noise and air quality impacts. A one-day case study with a weather situation containing regions with high contrail impacts for European air traffic estimated an overall climate impact reduction of about 30% for an increase of costs of 0.5%, relying on best estimate for climate impact information. The climate impact reduction and mitigation potential varies strongly with individual routes. By using a range of different climate metrics, the robustness of proposed mitigation trajectories is assessed. Sustainable ATM needs to integrate comprehensive environmental impacts and associated forecast uncertainties into route optimisation in order to identify robust eco-efficient trajectories.

Keywords: climate optimisation, air traffic management, eco-efficient trajectories

INTRODUCTION

The impact of aviation on the environment can be reduced by adopting climate-optimized aircraft trajectories, which preferentially fly in regions where aviation emissions have lower climate impact, so-called green trajectories, e.g. Green (2005). The climate impact of aviation is caused by CO₂ and non-CO₂ effects; hence for climate-optimisation, individual effects have to be taken into account simultaneously, in order to assess and minimize the total climate impact. Impacts of non-CO₂ effects depend on the location and time of emission, e.g. contrail formation and photochemical ozone production. Hence, planning green trajectories requires spatially and temporally resolved information on climate impact of aviation emissions to be available. A methodology for performing a multi-criteria environmental and climate impact assessment of aircraft trajectories has been established (Matthes et al., 2017) within the SESAR Exploratory Project ATM4E. It relies on a concept of climate change function (CCF) or environmental change function (ECF) (which in principal can also include metrics to measure noise and air quality impacts) as described in Matthes et al. (2012). This was applied to North Atlantic Air Traffic in Grewe et al. (2014a,b), to provide a quantitative measure of climate impact of an emission at a specific location and time of emission. When working towards climate-optimisation of air traffic trajectories in Europe, the identification of mitigation potential is crucial. It is necessary to provide a quantitative estimate of the possible reduction of climate impact of aviation, its mitigation potential, due to climate-optimized trajectories compared to an associate increase in direct operation costs. However, identifying climate-optimized trajectories has to overcome the issue of uncertainties related to quantitative estimates of aviation climate impact. In addition to uncertainties of weather forecast and climate impact estimates, also the choice of climate metric constitutes a source

of uncertainty. However, the overall climate objective largely determines the choice of the climate metric (Grewe and Dahlmann, 2015). Here, we evaluate the climate impact as near-surface temperature change, or indicators thereof, for a strategic change in routing (Grewe et al. 2014a), not only applied once, but generally in future. This largely limits the choice of climate metrics, but still some choices are to be made, such as the time horizon, e.g. 20, 50 or 100 years, on which physical climate impacts are analysed. In order to deal with uncertainties, methodologies are required which have the capability to identify robustness of an alternative trajectory.

Hence, this paper presents a methodology on how to investigate and integrate uncertainty when identifying climate-optimized trajectories, in order to characterise and consider the robustness of an identified mitigation trajectory. As a case study for introducing a robustness measure in climate-optimisation of trajectories we use a one-day traffic sample of air traffic in Europe using realistic weather reanalysis data to characterise the atmosphere from ERA-Interim. Objectives of this paper are (1) to present environmental and economic performance of individual city pairs under different optimization criteria resulting in a set of distinct alternative aircraft trajectories, (2) to compare climate optimized trajectories to fuel optimal trajectories in order to provide an estimate of overall mitigation gain associated with environmentally optimized aircraft trajectories. We evaluate the climate impact using a set of different climate impact metrics in order to identify robustness of proposed solutions. We do not consider here explicitly the important issue of the reliability of weather forecasts, which are required to enable flight planning in practice, nor do we take into account that, in reality, many real world trajectories depart from fuel-optimal trajectories.

METHOD TO IDENTIFY CLIMATE-OPTIMISED AIRCRAFT TRAJECTORIES

The concept applied in this study to optimize aircraft trajectories, while simultaneously taking into account climate impact, relies on a concept explored within the Aeronautics research project REACT4C by expanding an air traffic management system to include climate impact information (Matthes et al., 2012; Grewe et al., 2017). In this study we perform a multi-criteria trajectory optimisation under different target functions (Matthes et al., 2017). Our methodology to assess the climate impact of aircraft operations, and to identify climate optimal aircraft trajectories, requires having environmental impact information available during the flight and trajectory planning process. In order to calculate total climate impact of aircraft operations, both CO₂ and non-CO₂ effects have to be taken into account. While climate impact of CO₂ emission is proportional to the emitted amount of CO₂ (and fuel), and is independent of where that emission occurs, the climate impact of non-CO₂ effects shows a strong dependency on location, geographic position and altitude, as well as background conditions and/or time of emission. We apply an expansion of the CCF concept (Frömming et al., 2020) to an algorithmic CCF (aCCF) as developed in van Manen and Grewe (2019) and Yin et al. (2018), partially verified in Yin et al. (2018) and applied, e.g., in Yamashita et al. (2019). These algorithmic CCFs provide an easy to use estimate of the climate impact of a local emission and hence constitute a tradeoff between applicability (fast calculation time) and accuracy. They provide a quantitative measure of climate impact by using standard climate metrics, such as the global warming potential (GWP) or average temperature response (ATR), derived from standard meteorological parameters though following the overall climate objective (see above). This climate impact information is provided in our methodology to the ATM trajectory planning by integrating 4-dimensional climate change functions, during trajectory optimisation within TOM (trajectory optimisation module) into the overall target function (Matthes et al., 2012). By varying weights of individual components in this overall target function (e.g. by putting more weight on environmental and climate impacts) a set of distinct aircraft trajectory optimisation solutions is calculated for individual city pairs (Lühns et al., 2020). In our analysis of routing options we calculate for each city pair a set of 75 alternative trajectories using different weights. Overall climate impact of alternative trajectory solutions is provided as CO₂ and non-CO₂ effects of emissions comprising NO_x (on ozone and methane), contrail cirrus and water vapour.

PERFORMANCE AND ROBUSTNESS ASSESSMENT OF CLIMATE-OPTIMIZED TRAJECTORIES

Within a collaborative decision making framework it is crucial to quantify potential benefits and associated costs of alternative routing strategies. For this purpose, in our study of climate-optimized trajectories we have expanded performance assessment of key performance areas by a comprehensive climate impact assessment. Standard performance indicators we provide in our performance assessment are estimates on fuel efficiency, time efficiency as well as emissions and associated climate impact. As a novel aspect in our overall performance assessment we provide estimates of robustness parameters of proposed alternative climate-optimized trajectory solutions. We introduce robustness of a climate-optimized trajectory with a parameter characterising if climate impact of a trajectory under variation of relevant external parameters remains lower than impact of reference solution. Specifically, we assess if the alternative solution has a lower climate impact under different physical metrics over different time horizons (e.g. ATR_{20} , GWP_{100} where the number indicates the time horizon in years). A robust solution is characterised by presenting a benefit under every variation. However, if a variation exists, e.g. one metric indicates a higher climate impact while another indicates a lower climate impact, such an alternative trajectory is not a robust solution in terms of climate-optimization. As a parameter of robustness, we present for each alternative trajectory solution its range of mitigation benefits. As part of our robustness analysis, we calculate climate impact for a set of different available climate impact metrics, comprising GWP, ATR and global temperature change potential (GTP). In practice, the particular choice of emission/climate metric depends on the overall aims of a mitigation policy and policymaker preference.

ONE-DAY CASE STUDY OF EUROPEAN AIR TRAFFIC

This methodology of identifying climate optimized trajectories is applied in a case study for Europe, simulating and optimising one full day of air traffic using realistic meteorological data from weather reanalysis data. Performance analysis of aircraft routing comprises, beyond fuel and time efficiency, additional quantification of total emissions and an assessment of total climate impact due to CO_2 and non- CO_2 effects. The meteorology used for this case study corresponds to real world meteorological situation from 18 December 2015 based on ECMWF reanalysis data. This day is characterised by a high traffic volume, a low number of regulations (weather-, ATC-, and aerodrome related) as well as an interesting weather situation. For a one day traffic sample trajectory optimisation was performed within an expanded TOM calculating for each city pair a set of alternative aircraft trajectories (Lührs et al., 2020). In the next step, air traffic has been climate-optimized in four different dimensions focusing on the climate impact of the en-route segment of the flight.

Based on this meteorological data, we calculate algorithmic climate change functions for non- CO_2 impacts on that specific day comprising impacts of nitrogen oxides (on ozone and methane), water vapour and contrail cirrus. The target function in the optimisation combines economic costs with environmental impacts. Within the traffic sample described above we have analysed the importance of individual city pairs for capacity in European airspace and ranked them according to their transport capacities. Individual trajectories analysed in this paper represent the top-10 connections in terms of available seat kilometres, as identified in an analysis of seat kilometres in the reference year according to scheduled flights data.

MITIGATION POTENTIAL OF CLIMATE-OPTIMIZED TRAJECTORIES

We present results on climate-optimized trajectories comparing flight altitude and position of trajectories on top-10 connections in Europe showing overall performance in terms of fuel efficiency and environmental efficiency by comparing the fuel-optimal solution with climate-optimized solutions. We analyse individual components in the total climate impact, identifying role and importance of non- CO_2 contributions. Additionally, we will present an overall climate-optimisation of the top-2000 routes by identifying routing options with lowest mitigation costs.

Alternative trajectories with lower climate impact

As a result of the climate optimisation of aircraft trajectories between each city pair we achieve from our modelling approach a set of alternative trajectories. We present horizontal track and vertical profile of three top-10 connections in Europe (Fig. 1).

Climate impact metrics are used to quantify the climate impact of aviation. Choice of metric corresponds to priority and societal issues, in term of selected time horizon, with typical values ranging from 20 to 100 years. Average temperature response provides mean change of surface temperature over a selected time horizon. Recent studies are proposing novel concepts to overcome challenges for adequate representation of short-term effects (Etmiman et al., 2016; Allen et al., 2016; Grewe et al., 2019) which can be integrated in the concept developed.

We present results for distinct city pairs, which are amongst the top-10 connections in Europe with regard to passenger kilometres. Flight corridors are located in areas where contrails can form (e.g. the dark red patches shown in Fig. 1). Trajectory calculation in TOM results in environmental-optimized trajectories which avoid these regions by flying slightly lower in order to avoid high values of the aCCF associated with contrails. By comparing mitigation potentials [pK/kg fuel] it is possible to identify those alternative city pairs where most efficiently climate-optimisation of trajectories should be implemented.

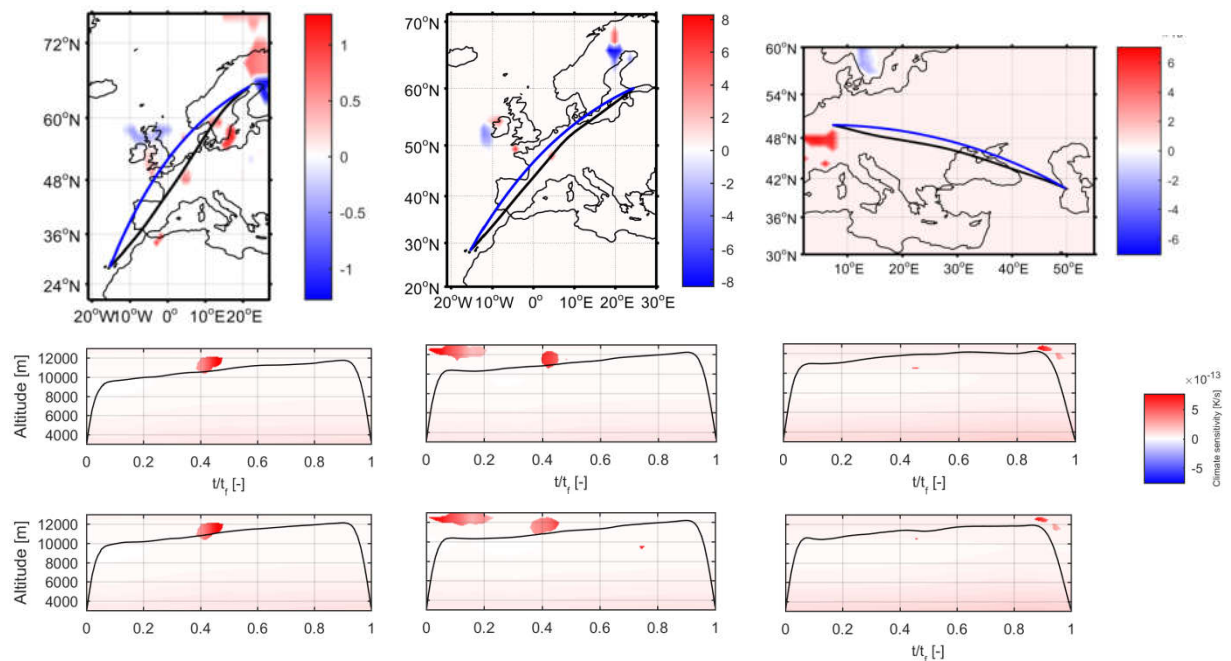


Figure 1. Aircraft trajectories (*top*) Lulea-Gran Canaria (*left*), Helsinki-Gran Canaria (*middle*), Baku-Luxembourg (*right*): great circle (blue), fuel-optimized trajectory (black). Altitude profile: fuel optimal case (*middle row*) and climate optimized case with 0.5% cost (*bottom row*), indicating algorithmic climate change functions warming (red) and cooling impacts (blue).

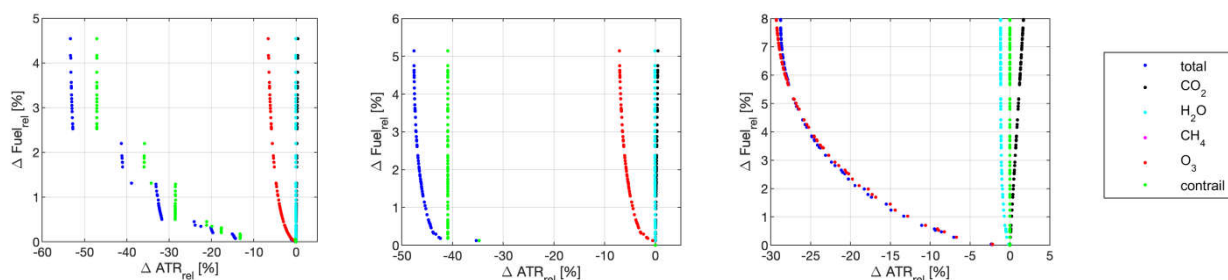


Figure 2. Pareto fronts for aircraft trajectory optimisation showing average temperature response (ATR_{20}) vs. fuel increase Lulea-Gran Canaria (*left*), Helsinki-Gran Canaria (*middle*), Baku-Luxembourg (*right*) and individual effects. For given fuel increase, dark blue dots show the optimal climate change impact from the possible routes available. Other individual dot colours indicate the CO_2 and non- CO_2 climate impacts for that alternative route.

In order to identify the role and importance of individual aviation emission effects as well as their importance in mitigation solutions, we present individual components of total climate impact (CO_2 and non- CO_2 effects) of the climate-optimal trajectories for a given fuel penalty compared to (theoretical) fuel optimum (Fig. 3). Due to climate-optimisation, the relative contributions from non- CO_2 effects to total climate impact decreases as the fuel use increases; depending on the particular route and meteorological conditions along the trajectory, reductions are dominated by either contrail cirrus avoidance or reduction in nitrogen oxides effects. On the route between Baku and Luxembourg (Figure 3, right) on the specific day no contrails can form along the trajectory and hence the climate impact from aviation induced cloudiness is zero. On the fuel optimal trajectory, the climate impact of CO_2 emissions account for 23% of total climate impact, hence non- CO_2 effects contribute 77%. Specifically, impacts of nitrogen oxides contribute 74% and direct water vapour emissions 3%. On the climate-optimised trajectories, these relative contributions change: contributions due to non- CO_2 effects decrease to 74%, 73%, 70%, and 65% for climate-optimised cases considered, respectively for the 0.5%, 1%, 2% and 5% fuel increase that results from climate-optimisation. This additional fuel enables a reduction in total climate impact calculated to be equal to 9%, 15%, 20%, and 30%, respectively. On the route *Helsinki-Gran Canaria* (Figure 3, middle) contrails can form over France (Fig. 1). On the fuel optimal trajectory CO_2 impacts contribute 11% while non- CO_2 effects contribute 89%, with impacts from nitrogen oxides and contrail cirrus contributing about the same order of magnitude, 45% and 43% respectively, and water vapour 1%. Following climate-optimisation, relative CO_2 contributions increase while non- CO_2 contributions decrease. Specifically with a fuel increase of 0.5%, climate impacts due to contrail cirrus can be completely avoided resulting in a reduction of total climate impact by 47% (individual contributions: CO_2 20%, NO_x 78%, water vapour 2%).

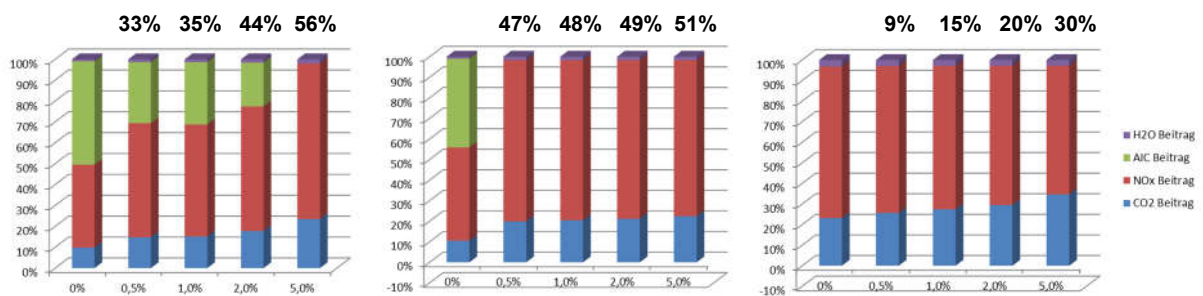


Figure 3. Individual contributions to total climate impact (ATR_{20}) Lulea-Gran Canaria (*left*), Helsinki-Gran Canaria (*middle*), Baku-Luxembourg (*right*); shown for individual mitigation trajectories allowing fuel increase by 0.5%, 1%, 2% and 5% and fuel optimal (0%). Numbers on top indicating decrease of total climate impact for respective alternative trajectory.

During climate optimisation relative contributions from non- CO_2 effects decrease from 89% to 80%, 79%, and 78%, for fuel increases by 0.5%, 2%, and 5%.

Similarly, on the route *Lulea-Gran Canaria* on that day fuel optimal trajectory CO_2 contributes only 10% (Fig 3, left), while non- CO_2 impacts contribute 90%; nitrogen effects 40% and contrail cirrus 50%, respectively. Following climate optimisation these non- CO_2 contributions drop to 85%, 82% and 77%, respectively, associated with reductions of climate impact by 33% of up 56%, for increases in fuel burn between 0.5% and 5%.

On this route it is most efficient to mitigation contrail cirrus effects. On the Helsinki to Gran Canaria route our analysis shows, initially efficient mitigation originates from contrail cirrus

effects. Once contrail cirrus impacts are avoided, further reductions at higher costs, can be achieved due to mitigation of the nitrogen oxide effect. In our feasibility study using aCCFs initial mitigation gains of up to 18 pK/(kg fuel), an alternative trajectory is calculated with small fuel penalties here, avoiding more than 40% climate impact. Later mitigation associated to nitrogen oxide effects show considerably lower gains of only up to 8 pK/(kg fuel), which then decrease down with 1-2 pK/(kg fuel). On the connection Baku-Luxembourg our analysis calculates lower values of mitigation gains starting from values of about 1 pK/(kg fuel), followed by smaller values, by an order of magnitude.

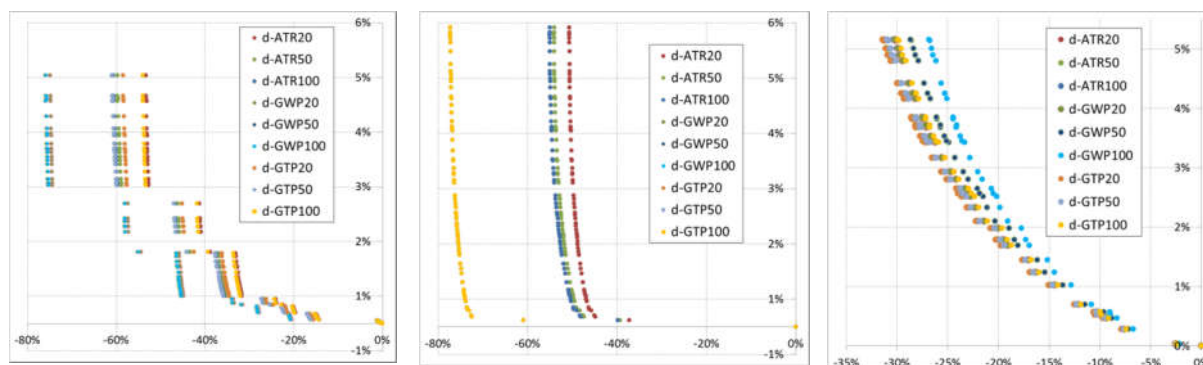


Figure 4. Pareto front on climate impact reduction vs. fuel change [%] for different climate metrics: Lulea-Gran Canaria (*left*), Helsinki-Gran Canaria (*middle*), Baku-Luxembourg (*right*);

In order to investigate robustness of identified alternative trajectories we calculate associated climate impact using a set of different climate impact metrics (Fig. 4). We calculate three different climate impact metrics using ATR, GWP, and GTP, over three distinct time horizon, leading to nine different climate impacts metrics, and evaluate associated change in climate impact. Identified trajectories show positive mitigation gains, hence they are robust under different climate impact metrics. On the Lulea-Gran Canaria range of climate impact reduction for a fuel penalty of 0.5% is equal to 8-10% using different climate metrics, and 13-15% for 1% fuel penalty. We propose to use this range of climate impact reduction as robustness parameter, testing sign of climate impact changes calculated. Overall robustness analysis on our presented alternative trajectories shows that identified alternative trajectories are robust under the selected set of climate impact metrics.

The decrease of non-CO₂ impacts due to climate optimization can also be illustrated in the concept of calculating total impacts, CO₂ and non-CO₂, with a simple multiplication factor based on CO₂ impacts, a weighting factor to obtain equivalent CO₂ (Table 1). We calculate on the Baku-Luxembourg in the fuel optimal case that CO₂ impacts have to be multiplied by a factor of 4.3 in order to quantify total climate impacts, but only with a lower value of 2.9 in the climate-optimised case. On the Helsinki-Gran Canaria route this factor reduces from 9.5 down to 4.5, and on the Lulea-Gran Canaria route drops from 10.2 down to 4.3. Our analysis shows that with climate optimisation, we find a clear reduction in the multiplication factor, from values of up to 10 down to about 3, hence a reduction of non-CO₂ impacts.

Table 1. Multiplier to CO₂ emissions in order to represent the total CO₂ and non-CO₂ climate impact for individual city pairs for relative fuel increases up to 5%.

Route / Fuel increase	0%	0.5%	1%	2%	5%
EFHK-GCLP	9.5	5.0	4.9	4.7	4.5
UBBB-ELLX	4.3	3.9	3.7	3.4	2.9
ESPA-GCLP	10.2	6.8	6.6	5.6	4.3

Our feasibility study provides initial estimates for European air traffic, involving intra-ECAC flights, applying a bottom-up approach. An assessment of the top-2000 routes shows (Lührs et al., 2020) on that specific day climate impact can be mitigated by 46% for an increase of

0.5% fuel. Climate impact in the fuel optimal case is dominated by non-CO₂ effects (90%), getting lower flying on alternative trajectories (down to 83% for 0.5% fuel increase).

DISCUSSION

This study demonstrates the feasibility of an approach to optimize aircraft trajectories by using spatially and temporally resolved aCCFs in order to reduce their environmental impact, while providing parameters on robustness of identified mitigation solutions. We have applied this approach for a full traffic sample for a single day in Europe, showing results in more detail for three European city-pairs. Analysis shows the clear potential to optimize for environment and economic aspects simultaneously, by avoiding non-CO₂ effects in particular from nitrogen oxides, and contrails, while also assessing the robustness of these optimised trajectories to the choice of climate metric. A sensitivity analysis shows clearly a small impact of the choice of the climate metric if they all follow a given political objective (here: climate impact evaluation of a strategic and durable change in routing).

As part of our analysis in this feasibility study we have the ability to identify routes and associated trajectories which offer a large mitigation potential with high mitigation gains. Specifically, we presented alternative routes which showed a strong mitigation gain due to contrail avoidance in our feasibility study in that specific meteorological situation that day over Europe. Our full paper will comprise a more comprehensive evaluation on total impacts for full traffic sample and on strong forcing calculated for contrail cirrus, in order to assess to what extent our estimates can be confirmed from, e.g. considerations of radiative transfer in the atmosphere and satellite images. In our feasibility study they appear as big hits, in terms of offering a large mitigation gain, and hence merit further investigation.

Comparing our estimates of climate impact from European Air Traffic on that specific one-day case study with estimates on global climate impact, we find that our analysis covers about 3% of global fuel consumption. Comparing total climate impacts of our top-2000 routes with impact of a global fleet (e.g. Matthes et al., 2020) we find that our estimates on total climate impact are about 6% higher, and contributions from non-CO₂ differ slightly.

The presented study considers aircraft performance, realistic meteorological conditions from reanalysis, and algorithmic climate change functions (aCCF) originating from complex chemistry-climate model simulations which were derived by van Manen and Grewe (2019) and Yin et al. (2020). However, the analysis presented does not take into account airspace structure, e.g. ATC sectors, route charges. It also does not account for other environmental impacts beyond climate change, or the ability to accurately forecast the weather conditions sufficiently far ahead for flight planning; this would be a necessity for optimisation to be effective.

We suggest that integration of such an advanced MET service should be done via the meteorological information interface to flight-planning processes, due to the fact that aCCF are calculated as a function of specific weather forecast meteorological information (ATM4E final report, 2017) Combination of environmental and climate impact services can be done in conjunction with other services for the purpose of safety relating to weather events, e.g. thunderstorm and convective hazards (Matthes et al., 2018).

Depending on the atmospheric region where aircraft fly, overall climate impact of trajectories is dominated by individual non-CO₂ impacts. This becomes also apparent when identifying from which effect mitigation gains originate. On the city pair between Lulea and Gran Canaria, a considerable reduction in overall climate impact can be achieved by avoiding regions which are sensitive to contrail formation. By contrast, on the connection between Baku and Luxembourg, mitigation gain originates from lowering the flight altitude and avoiding warming effects of nitrogen oxides emissions. We have applied a climate metric which assumes sustained emissions, as we assume that a respective routing strategy would be flown on every day of the year, leading to sustained impacts.

CONCLUSION AND OUTLOOK

The overall approach of climate-optimisation of aircraft trajectories has been successfully applied within this feasibility study for Europe using algorithmic climate change functions and optimizing a one day full traffic sample of European air traffic. This extends previous work on trans-Atlantic flights (Grewe et al. 2017). As a result of this analysis, climate-optimized trajectories have been identified and characterised by their potential mitigation gain and their non-CO₂ associated contributions, as well by demonstrating their robustness to different climate impact metrics, within the prototypic aCCFs adopted.

We conclude that climate optimization of aircraft trajectories can be enabled by expanding an ATM system with an advanced MET service for environmental impacts relying on Environmental change functions (ECFs). An efficient way to generate climate change functions is to use algorithms which calculate impact from standard meteorological parameters that are available in a weather forecast system. For this we introduced the aCCFs which enable providing climate impact information directly from standard meteorological parameters at each location and time of emission. Potential mitigation gains and potentials and robustness of green trajectories can be quantified for each optimized trajectory by using a set of distinct climate impact metrics, in order to identify mitigation options which are robust under different climate impact metrics. Mitigation potential in the order of 10's of percent can be achieved for an increased fuel burn of a few percent. Implementation of state of the art knowledge on aviation non-CO₂ effects is required, comprising in particular contrail cirrus, nitrogen oxides (ozone, methane) as well as, potentially, indirect aerosol effects, once these aerosol effects are better understood.

The implementation of such environmental optimized routing would need quantitative performance indicators to be able to demonstrate benefits for the environment and more specifically to climate impacts relating to the key performance area environment (KP05), in order to gain the confidence of the stakeholder community.

This concept lays the basis for performing route optimizations in the European airspace using advanced MET information in the light of climate impact assessment and optimization of aircraft movements in Europe. To further advance efficient implementation of eco-efficient (green) trajectories, a strategic roadmap has been defined (ATM4E, 2018b). This proposes a route to implement such a multi-criteria and multi-dimensional environmental assessment and optimization framework into current ATM infrastructure by integrating tailored MET components, in order to make future aviation sustainable. ATM4E roadmap identified as future research and development activity to increase the technological readiness level of algorithmic environmental change functions. Using algorithmic ECFs allows efficient implementation of environmental optimization in an overall information infrastructure. Ignoring the representation of relevant non-CO₂ impacts in an overall assessment framework, e.g. because they are considered negligible (or too uncertain), can lead to wrong estimates of total climate impact, and even create misleading incentives, if trade-offs are not adequately taken into account.

With this study an important step towards assessment of robustness information was made, while further research should address the incorporation of information on robustness of the environmental aircraft trajectories, considering uncertainties from weather and climate impact data, as well as representations of aircraft/engine dependence. An adequate implementation of individual sources of uncertainty should help to identify robust climate impact mitigation solutions and trajectories.

However, as estimated by climate impact assessment studies, e.g. Lee et al. (2010), Grewe et al. (2017), there still exists uncertainties in the quantitative estimates of climate impact of aviation using radiative forcing as a metric. Here, our approach introduced could also be applied in order to estimate parameters of robustness of identified alternative, climate-optimized trajectories with regard to its environmental impact. The ultimate goal of such a concept is, to make available an efficient, comprehensive assessment framework for environmental performance of aircraft operations, by providing key performance indicators on environmental impacts comprising climate impact, air quality and noise, which enables identification and environmental optimization of aircraft trajectories. Eventually, such a

framework will allow the quantification of the climate impact mitigation potential, studying and characterizing changes in traffic flows due to environmental optimization, as well as studying trade-offs between distinct strategic measures.

ACKNOWLEDGEMENTS

The project leading to this study has received funding from the SESAR Joint Undertaking under grant agreement No 699395 under European Union's Horizon 2020 research and innovation programme" within the Exploratory Research project ATM4E. Part of the work has Individual authors of this study receive funding from the European Union's Horizon 2020 research and innovation programme under grant agreement No 875503 (ClimOP). Work in this article was supported by DLR project Eco2Fly (2018-2022). High performance supercomputing resources were used from the German DKRZ Deutsches Klimarechenzentrum Hamburg.

REFERENCES

- Allen, M., Fuglestvedt, J., Shine, K., Reisinger, A., Raymond T., Pierrehumbert, R.T., Forster P.M., New use of global warming potentials to compare cumulative and short-lived climate pollutants. *Nature Clim Change* 6, 773–776. <https://doi.org/10.1038/nclimate2998>, 2016.
- ATM4E, Conceptual Roadmap, D4.3, June 2018, deliverable available under www.atm4e.eu/workpackages/pdfs, Exploratory Project, SESAR-04-2015, Grant No. 699395, 2018.
- Frömming, C., Grewe, V., Brinkop, S., Haslerud, A.S., Rosanka, S., van Manen, J., and Matthes, S., The REACT4C Climate Change Functions: Impact of the actual weather situation on aviation climate effects, in preparation, 2020.
- Green, J. Air Travel-Greener by Design. Mitigating the environmental impact of aviation: Opportunities and priorities. *Aeronaut. J.* 2005, 109, 361–418
- Grewe, V., Matthes, S., Dahlmann, K., The contribution of aviation NO_x emissions to climate change: are we ignoring methodological flaws, *Environ. Res. Lett.*, 14, 121003, 2019.
- Grewe, V.; Frömming, C.; Matthes, S.; Brinkop, S.; Ponater, M.; Dietmüller, S.; Jöckel, P.; Garny, H.; Tsati, E.; Dahlmann, K.; et al. Aircraft routing with minimal climate impact: The REACT4C climate cost function modelling approach (V1.0). *Geosci. Model Dev.*, 7, 175–201, 2014a.
- Grewe, V.; Champougny, T.; Matthes, S.; Frömming, C.; Brinkop, S.; Søvde, O.; Irvine, E.; Halscheidt, L. Reduction of the air traffic's contribution to climate change: A REACT4C case study. *Atmos. Environ.*, 94, 616–625, 2014b.
- Lee, D.; Pitari, G.; Grewe, V.; Gierens, K.; Penner, J.; Petzold, A.; Prather, M.; Schumann, U.; Bais, A.; Bernsten, T.; et al. Transport impacts on atmosphere and climate: Aviation. *Atmos. Environ.* 2010, 44, 4678–4734.
- Lührs, B., Linke, F., Matthes, S., Grewe, V., Yin, F. Shine, K.P. Climate optimized trajectories in Europe, in "Making Aviation environmentally sustainable", Vol 1, 3rd ECATS Conference 2020.
- Matthes, S., Ling, L., et al., Mitigation of aviation's non-CO2 climate impact by changing cruise altitudes, in "Making Aviation environmentally sustainable", Vol 1, ECATS 3rd Conference, 2020.
- Matthes S, Grewe, V, Dahlmann, K, Frömming, C, Irvine E; Lim L, Linke F, Lührs B, Owen B, Shine K P, Stromatas S, Yamashita H, and Yin F, 2017. A Concept for Multi-Criteria Environmental Assessment of Aircraft Trajectories, *Aerospace* 2017, 4, pp. 42; doi:10.3390/aerospace4030042.
- Matthes, S.; Schumann, U.; Grewe, V.; Frömming, C.; Dahlmann, K.; Koch, A.; Mannstein, H. Climate optimized air transport. In *Atmospheric Physics: Background-Methods Trends*; Schumann, U., Ed.; Springer: Berlin/Heidelberg, Germany, 2012; pp. 727–746, doi: 10.1007/978-3-642-30183-4_44.

- van Manen, J., and Grewe, V., Algorithmic climate change functions for the use in eco-efficient flight planning, *Transp. Res. Part D* 67, 388-405, doi:10.1016/j.trd.2018.12.016, 2019.
- Yamashita, H., Yin, F., Grewe, V., Jöckel, P., Matthes, S., Kern, B., Dahlmann, K., and Frömming, C. Various aircraft routing options for air traffic simulation in the chemistry-climate model EMAC 2.53: AirTraf 2.0, *Geosci. Model Dev. Discuss.*, <https://doi.org/10.5194/gmd-2019-331>, in review, 2019.
- Yin, F., Grewe, V., van Manen, J., Matthes, S., Yamashita, H., Irvine, E., Shine, K.P. Lührs, B., Linke, F., Verification of the ozone algorithmic climate change functions for predicting the short-term NO_x effects from aviation en-route, 8th international conference on air transportation (ICRAT), Barcelona, Spain, 2018.
- Yin, F., Grewe, V., Matthes, S., Yamashita, H., Irvine, E., Shine, K.P. Lührs, B., Linke, F., Predicting the climate impact of aviation for en-route emissions: The algorithmic climate change function sub model ACCF 1.0 of EMAC 2.53, GMDD in preparation, 2020.

ADAPTING THE FUEL PLANNING TO OPERATIONAL UNCERTAINTIES OF AIRCRAFT WAKE-SURFING FOR EFFICIENCY

M. Swaid^{1,3}, T. Marks¹ & V. Gollnick²

¹ German Aerospace Center (DLR), Air Transportation Systems, Hamburg, Germany

² Hamburg University of Technology (TUHH), Institute of Air Transportation Systems, Hamburg, Germany

³ Correspondence: Majed.Swaid@dlr.de; Tel.: +49 (0)40 248 96 41-282

Abstract. The operational concept of aircraft wake-surfing for efficiency (AWSE) holds a high potential in terms of fuel savings and regarding the climate impact mitigation of aviation. In order to implement this concept, many technological and operational challenges have to be coped with. As the fuel consumption during a mission strongly depends on a successful formation execution, the existing uncertainties regarding flight planning increase. While a conservative fuel planning ensures a follower to complete the mission even in the case of a formation failure, it might result in high amounts of excess fuel and, therefore, additional fuel consumption. This problem is addressed in this study by the adaption of flight planning procedures to the requirements of AWSE with fuel planning in particular, considered from the perspective of a designated follower aircraft of a two-aircraft formation. This trade-off is modeled as an n-action two-event decision making problem. Each of the possible actions is represented by a combination of mission routing and a corresponding amount of trip fuel, taking atmospheric effects (e.g. wind) into account as well as the distances to suitable diversion airports. The two events under consideration are a total formation failure in contrast to a complete success. Based on a scenario with a set of double origin destination pairs characterizing the formation and representative weather patterns for the North Atlantic region, each action is analyzed with regard to the expected fuel consumption and expense.

Keywords: aircraft wake surfing for efficiency, aerodynamic formation flight, fuel planning, route optimization, decision making

INTRODUCTION TO FUEL PLANNING FOR AWSE FOLLOWER AIRCRAFT

The concept of aerodynamic formation flight, also known as aircraft wake-surfing for efficiency, allows the follower aircraft to utilize the energy in the leader aircraft's wake vortex, which can result in high savings with regard to burned fuel. However, the follower aircraft in such a two-aircraft formation faces an increased level of uncertainty in the process of fuel planning. Referring to [Swaid et al. \(2018\)](#) it was investigated to what extent a reduction of the follower aircraft take-off mass due to a consideration of the expected fuel savings in the process of fuel planning can save fuel in addition to the primary savings induced by AWSE. Based on a North Atlantic scenario with 14 different routings under consideration (each track optimized to a specific atmospheric day) it could be shown, that due to fuel planning alone, the amount of burned fuel can be reduced by up to 5% (~2000 kg), which corresponds to a reduction of 1.3% with regard to direct operating costs (DOC).

For the follower aircraft, this savings potential comes in exchange for a reduced flight plan reliability. The fuel planning procedure presented in this study is based on the established Decision Point Procedure (DPP), which allows a reduction of the contingency fuel of a conventional mission depending on the availability of potential diversion airports along the track, so called En-Route-Alternates (ERAs), and considers the possibility of an intermediate stop for refueling. The concept of DPP requires the definition of a Decision Point (DEC) in advance of the mission. When passing the DEC, it is the pilot's responsibility to decide whether the remaining fuel is sufficient in order to safely continue to the commercial destination. Otherwise, the pilot will divert to the predefined ERA for a refueling stop before proceeding to the destination.

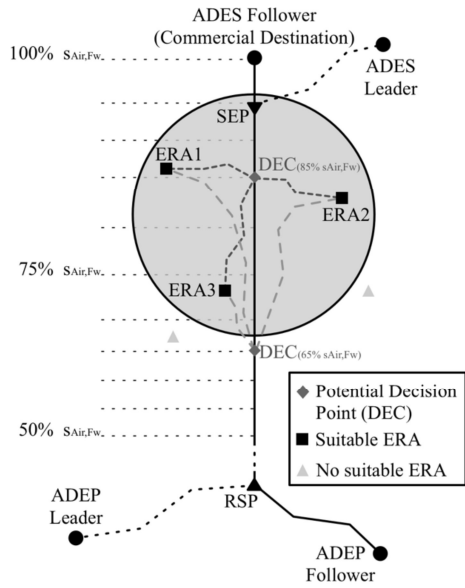


Figure 1. Formation flight route with relevant checkpoints regarding DPP (adapted from Swaid et al., 2018).

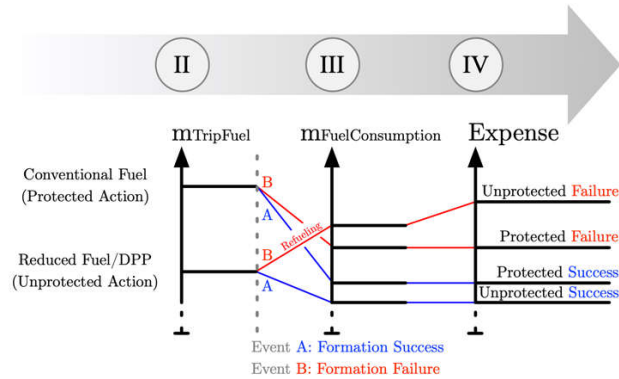


Figure 2. Schematic overview on fuel amount and monetary expense, depending on event and protection level of the action.

The calculation of the required trip fuel according to the adapted DPP as proposed in Swaid et al. (2018) is summarized in Equations (1-3) with regard to denomination from Figure 1. In a first step, the required trip fuel between the origin airport and the respective ERA via the investigated DEC is computed and charged with a contingency share of 3%. Subsequently, the trip fuel between DEC and the destination is computed and a 5% share of this amount is added to the required trip fuel from origin to destination. Only in the latter case, the expected fuel savings due to AWSE, which occur on the segment between the rendezvous point (RSP) and the separation point (SEP), are considered for calculation of trip fuel, reflecting the assumption that the follower will proceed to the commercial destination as scheduled in the event of a formation success, and divert to the ERA in the event of a formation failure. Whichever value of trip fuel is higher, will be selected as the corresponding amount m_{TF} for a combination of DEC, ERA and lateral track. In the course of these investigations, this combined data set represents a fuel plan and will be henceforth designated as possible *action* for the decision maker to pick.

$$m_{TF,Diversion} = 1.03 \cdot m_{TF,NoCont.}(ADEP \rightarrow DEC \rightarrow ERA) \quad (1)$$

$$m_{TF,Schedule} = m_{TF,NoCont.}(ADEP \rightarrow DEC \rightarrow ADES) + 0.05 \cdot m_{TF,NoCont.}(DEC \rightarrow ADES) \quad (2)$$

$$m_{TF} = \max(m_{TF,Schedule}, m_{TF,Diversion}) \quad (3)$$

The atmospheric data used for route optimization and fuel computation are based on the European Reanalysis Interim data set and can be obtained by the European Center for Medium-Range Weather Forecasts (ECMWF). A detailed description of the data is provided by Berrisford et al. (2011). The investigations are carried out for a set of eight weather patterns, which were identified to be representative for the North Atlantic region in Irvine et al. (2013). In order to reflect a varying degree of route geometries, a set of at least 4 double origin destination pairs is investigated, comprising all combinations of common and separate origin and destination airports.

DERIVATION OF EXPECTED FUEL CONSUMPTION AND EXPENSE

It was shown in Swaid et al. (2018) that the ratio between possible savings due to lean fuel planning and the additional costs due to a diversion to the ERA significantly varies with the atmospheric days. This is caused by the variability of the tracks, which are optimized for the

respective weather patterns (according to Marks et al., 2018) and, therefore, suitable ERAs can be missing on some days. It was assumed that for a minor shift of a track, the amount of fuel consumption stays almost constant while simultaneously the time-dependent expense for a diversion from DEC to ERA might be visibly reduced, favorably changing the ratio of potential additional costs to potential rewards.

Based on this assumption, in this study, an expanded search space is generated around the reference track, as summarized in Step I of Figure 3. Each of the points in the expanded search space is used as an offside DEC for testing the optimization potential due to a deviation from the reference track. For each of these potential DEC, an adapted wind optimal routing is derived between the DEC and the closest checkpoints along the track with regard to Figure 1. In accordance with Lührs et al. (2014), a Zermelo's problem is formulated on a spherical earth, applying an optimal control approach to the heading angle of the aircraft in order to derive the minimum time track, especially taking the impact of wind into consideration.

In step II, fuel planning scenarios are calculated according to the adapted DPP on the one hand, and a conventional fuel planning without consideration of AWSE benefits as a reference on the other hand. Each of the combined data sets (DEC, ERA and tracking) are considered as a possible action with an assigned value m_{TF} . Depending on the fuel planning procedure, each action is considered to be protected or unprotected, defining whether the viability of the scheduled mission can be maintained even in case of a formation failure.

In step III, all generated actions are evaluated for the two possible events. In the case of a formation success, all actions can be carried out as scheduled and the follower reaches the commercial destination, taking advantage of the AWSE benefits (compare Figure 2). In the case of a formation failure, the follower will divert to the predefined ERA, refuel and subsequently continue to the commercial destination.

In step IV, each action is evaluated for both regarded events, taking the total fuel consumption, mission time, and further aspects into consideration. Based on these results, the expenses are derived applying the DOC method presented in Thorbeck (2012). A schematic overview on the interdependencies of the investigated parameters trip fuel (result of step II), fuel consumption (result of step III), and expense (result of step IV) is depicted in Figure 2 for all combinations of actions - with and without protection - and the possible events, i.e. formation success and formation failure.

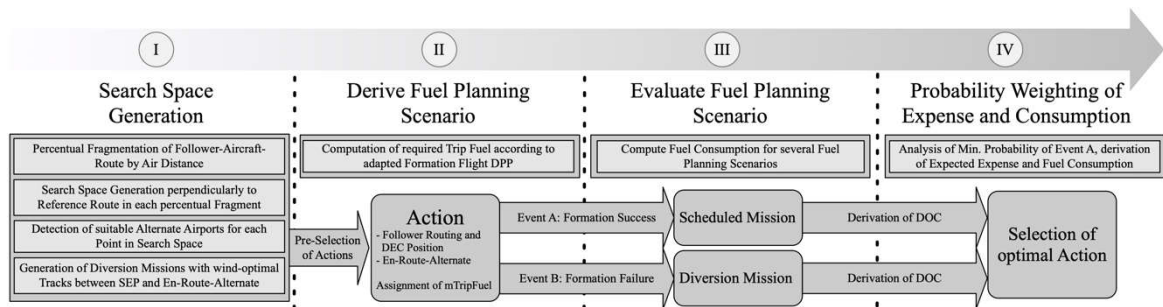


Figure 3. Proposed workflow for optimal action selection with regard to expected expense.

In compliance with Murphy (1984), the values of expense of an action are associated to the corresponding likelihood P of each event j , yielding the Expected Expense

$$EE(\text{Action } i) = \sum_{\text{Event } j}^2 [P(j) \cdot \text{Expense}(i, j)]. \quad (4)$$

Since the likelihood of a formation success is assumed to have many complex dependencies on the air traffic system (congestion, weather, airport specific delay), it is not possible to quantify the exact likelihood of events A and B. Therefore, the minimum value of probability for event A is derived from the required probability of success $P(A)_{Min}$, such that the

additional expenses of both formation partners due to a detour in the case of a formation failure are compensated long-term. The probability $P(A)$ is finally varied in the interval $P_{Min}(A) \leq P(A) < 1$ in order to identify the sensitivity of the expected fuel consumption and expense on the formation success rate.

FIRST RESULTS

In Figure 4, an exemplary search space is depicted for a two-aircraft formation with the common destination airport JFK. The circles represent potential DEC points, that are placed on the reference track (depicted as gray line), while crosses mark potential off-track DEC points. The ERAs under consideration are represented by squares. The color code assigns a DEC to the corresponding ERA, that was taken into consideration for deriving the amount of trip fuel and is consistent with Figure 5.

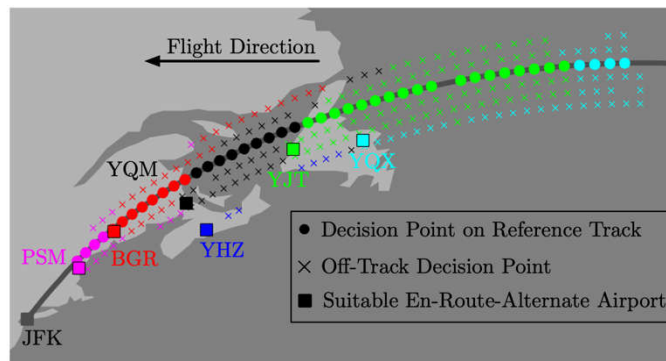


Figure 4. Exemplary search space of DEC points around a reference route with destination JFK.

In Figure 5 the relative change in expected fuel consumption for a follower aircraft with unprotected fuel planning is illustrated in comparison to the reference scenario, in which the follower aircraft conducts a protected fuel planning on the reference track. On the left-hand side, the formation success probability is assumed to be 80%, on the right-hand side it is supposed to be 99%. For actions with a DEC position between 65% and 75% of air distance along the track and the airport YJT (depicted in green) as designated ERA, the highest changes in expected fuel consumption can be identified with -3.2% for $P(A) = 80\%$, respectively -4.4% for $P(A) = 99\%$.

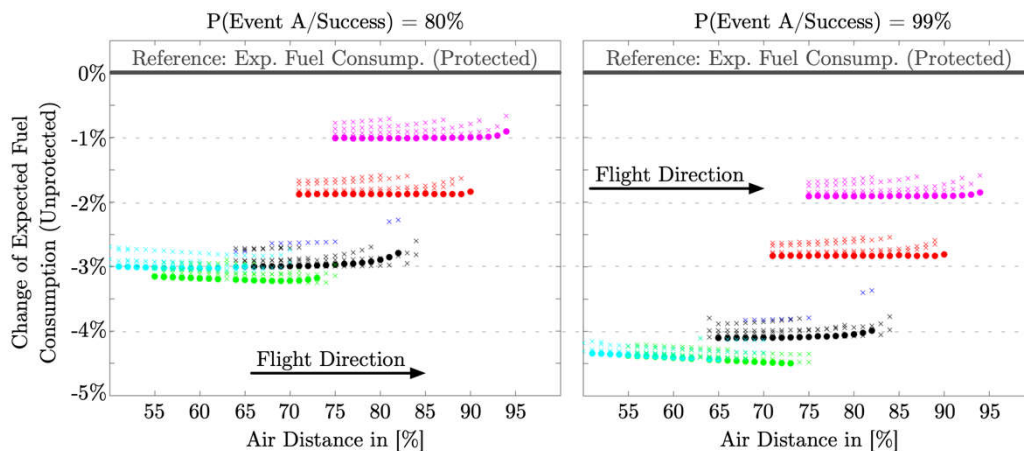


Figure 5. Change of expected fuel consumption due to application of unprotected fuel planning in comparison to protected fuel planning. Left: Assumed formation success probability of 80%. Right: Assumed formation success probability of 99%.

GRANT SUPPORT

This work has received funding from the German Ministry of Economic Affairs and Energy (BMWi) under the National Aeronautical Research Programme (LuFo) V-2 under the grant agreement no. 20E1508.

REFERENCES

- Berrisford P. et al., The ERA-Interim Archive. European Center for Medium-Range Weather Forecasts, 2011.
- Irvine, E. A., Hoskins, B. J., Shine, K. P., Lunnon, R. W., & Froemming, C. (2013). Characterizing north atlantic weather patterns for climate-optimal aircraft routing. *METEOROLOGICAL APPLICATIONS*, 20, 80–93.
- Lührs B., Linke F., Gollnick V., Erweiterung eines Trajektorienrechners zur Nutzung meteorologischer Daten für die Optimierung von Flugzeugtrajektorien., 63. Deutscher Luft- und Raumfahrtkongress (DLRK), Augsburg, Germany, Sep. 16-18, 2014
- Marks, T., Swaid, M., Lührs, B., & Gollnick, V. (2018). Identification of optimal rendezvous and separation areas for formation flight under consideration of wind. International Council of the Aeronautical Sciences, ICAS.
- Murphy, A. (1984). Decision Making and the Value of Forecasts in a Generalized Model of the Cost-Loss Ratio Situation. *Monthly Weather Review*, Volume 113.
- Swaid, M., Marks, T., Lührs, B., & Gollnick, V. (2018). Quantification of formation flight benefits under consideration of uncertainties on fuel planning. International Council of the Aeronautical Sciences, ICAS.
- Thorbeck J., TU Berlin, DOC Method as proposed in lecture notes „Flugzeugentwurf“, 2012.

OPTIMIZATION OF FLIGHT ROUTES FOR REDUCED CLIMATE IMPACT (OP-FLYKLIM) PROJECT

J. Moldanová¹, J. Langner², M. Lindskog², R. Bergström², T. Mårtensson³, M. Wall⁴, H. Ekstrand⁵, M. Rydal² & A. Näs⁶

¹IVL, Swedish Environmental Research Institute, Sweden, jana.moldanova@ivl.se

²Swedish Meteorological and Hydrological Institute, Sweden, joakim.langner@smhi.se

³FOI, Swedish Defence Research Agency, Sweden, tomas.martensson@foi.se

⁴LFV, Sweden, martin.wall@lfv.se

⁵Nova Airlines AB (Novair), Sweden, Henrik.Ekstrand@novair.se

⁶Swedavia, Sweden, Näs, anette.nas@swedavia.se

Abstract. The objective of the project 'Optimization of flight routes for reduced climate impact (OP-FLYKLIM) is to study the potential for mitigation of climate effects of aviation contrails and Short-Lived Climate Pollutants (SLCP) through alternative 3D routes for flights operating in Swedish controlled airspace compared to today's nominal operation where direct routing dominates.

To link the climate impact of contrails and SCLP to flight optimization, avoidance of operating in ice-saturated, cloud-free areas with maintained climate benefit will be studied through combination of atmospheric modelling and simulation of day-to-day flight route planning with and without climate optimization. The latter will be done by Novair, using their flight planning system on the city pair Stockholm – Kiruna through support of SMHI, providing forecasts of ice-supersaturated regions for climate optimized routes which is calculated and used as an alternative to the conventional route optimization typically done by airlines. Impact of the climate optimization on the routes selected will then be analyzed with support of atmospheric models.

The modelling part of the project employs plume model for calculation of the formation of contrails and the short-term effects linked to the aircraft NO_x emissions under the entire flight mission, taking into account conditions in the atmosphere where the emissions take place and climate cost functions from Grewe et al. (2017), as well as the chemistry-transport model MATCH which calculates impact of emissions on selected flight routes during 1 year to scale-up the study to national aviation in Sweden. The flight emissions for modelling are calculated with FOI3 aircraft emission model and validated with fuel consumption data which will be provided by SAS.

Keywords: flight route optimization, climate impact, short-lived climate pollutants, plume modelling, chemistry transport modelling

ACKNOWLEDGEMENTS

The study is financed by Swedish Transport Administration and Swedish Transport Agency.

REFERENCES

Grewe, V., Matthes, S., Frömming, C., Brinkop, S., Jöckel, P., Gierens, K., Champoungny, T., Fuglestedt, J., Haslerud, A., Irvine, E., Shine, K., 2017. *Feasibility of climate-optimized air traffic routing for trans-Atlantic flights*. Environmental Research Letters, Vol. 12, 034003.

LARGE SCALE BIO-ELECTRO-JET FUEL PRODUCTION INTEGRATION AT CHP-PLANT IN ÖSTERSUND, SWEDEN – PROCESS DESIGN FOR AN ELECTRO FUEL FACTORY.

A. Fagerström¹, D. Grahn², S. Lundberg³, O. Wallberg⁴, L. Olsson⁵, D. Creaser⁶, M. Poorsgaard⁷, M. Lindgren⁸, J. Hansson⁹, T. Rydberg¹⁰ & S. Anderson¹¹

¹ IVL Swedish Environmental Research Institute, Sweden, anton.fagerstrom@ivl.se

² IVL Swedish Environmental Research Institute, Sweden, desiree.grahn@ivl.se

³ IVL Swedish Environmental Research Institute, Sweden, susanne.lundberg@ivl.se

⁴ Lund University, Sweden, ola.wallberg@chemeng.lth.se

⁵ Chalmers University of Technology, Sweden, louise.olsson@chalmers.se

⁶ Chalmers University of Technology, Sweden, derek.creaser@chalmers.se

⁷ Nordic Initiative for Sustainable Aviation, Denmark / Fly Green Fund, Sweden, map@cleancluster.dk

⁸ City of Östersund / The Power Region, Sweden, magnus.lindgren@ostersund.se

⁹ IVL Swedish Environmental Research Institute, Sweden, julia.hansson@ivl.se

¹⁰ IVL Swedish Environmental Research Institute, Sweden, tomas.rydberg@ivl.se

¹¹ IVL Swedish Environmental Research Institute, Sweden, sara.anderson@ivl.se

Abstract. The aviation sector will need to transition to renewable fuels. Considering a future scarcity in biofuels, electro fuel from renewable feedstocks is an attractive option. Bio-electro-Jet fuel production integration at CHP plants in northern Sweden, where renewable electricity is plentiful and growing, has a currently untapped potential that can be used for greater synergy in existing heat and power production while at the same time significantly reduce the climate impact for future air-travel. This project is an in-depth feasibility study for the establishment of a production facility for Bio-electro-Jet fuel at the current location of an existing CHP plant. The entire value chain for Bio-electro-Jet fuel is represented within this project. The study at hand promotes bio-based economy through the re-utilization of carbon and production of high-value products. Jämtkraft currently produces a large amount of electricity from renewable sources in this region and control a good point source for green carbon dioxide to be utilized through Carbon Capture and Utilization (CCU) for electro fuel production. The project provides an excellent example of industrial symbiosis between a power company (Jämtkraft), a fuel producer (Fabriken AB), a fuel distributor (AFAB) and representatives from the user-side (FGF and NISA), and has strong involvement of academia (Chalmers University of Technology and Lund University) and research institutes (IVL Swedish Environmental Research Institute). The project runs between fall of 2019 and the end of 2020. The work is divided into work packages that will deliver results on: i) Process identification, ii) Unit operations, iii) Mass transport effects during CO₂-hydrogenation to Jet fuel, iv) Process integration, v) Capital- and operational costs, vi) the Factory, vii) LCA, viii) Distribution, ix) Usage, and x) Sustainable business models. Preliminary results will be available during spring 2020.

Keywords: Bio Jet fuel, Electro Fuel, CCU, CHP, Process integration

INTRODUCTION

There is a great potential to increase the use of biofuels, electricity and hydrogen in many sectors of society, including the transport sector, to meet emission and climate goals. For hydrogen and electricity, there is uncertainty to what extent batteries and fuel cells are suitable solutions in, e.g. aviation, freight and long-haul transport by road; requiring new infrastructure etc. (Ball & Wietschel, 2009). Large-scale use of biofuels produced from biomass is facing sustainability challenges and the future supply of conventional biofuels seems to be limited in relation to the expected global transport needs (Mendes Souza, et al., 2015; Grahn, et al., 2009; Azar, 2011). Based on future scenarios on biomass accessibility, it's probable that the aviation sector will need access to energy-dense hydrocarbon fuels for the foreseeable future. Aviation will need to transition to renewable fuels to contribute to goals set by policy, e.g. (SOU 2013:84, 2013; ER 2017:07, 2017; ER 2017:14). Accounting for future scarcity in biofuels, electro fuel from renewable feedstocks for aviation, e.g. - Bio-electro-Jet fuel – is an attractive option. Large scale electro fuel production requires access to large quantities of electricity. Therefore, the production facility should not be placed where a shortage of power is prevalent, to prevent unnecessary strain on the transmission grid.

Hence, production of electro fuels is suitable in the northern parts of Sweden, where renewable electricity is plentiful and growing, and the grid is both strong and reliable. Additionally, a well-developed district heating system which can mitigate peaks in power demand during the cold winter months and allow utilization of electro fuel production process heat is an asset for this type of production.

GOALS

The process

1. Best available technology for sub-processes and unit operations, i.e. hydrogen production, CO₂-capture and utilization, and Bio-electro Jet A1 production, etc. Evaluation of the best current technology for at least four sub-processes with at least two possible options for each.
2. Integration design and total efficiency of the process for both evaluated production paths (LU resp. CU) to Bio-electro Jet A1. Determination of the total conversion efficiency and the amount of Bio-electro Jet A1 produced per supplied MWh for the two paths.

The plant

3. Estimation of plant size, and the capital- and operational costs for the new plant based on desired amount of produced Bio-electro Jet A1.
4. Identification of at least three possible stakeholders to operate the prospective company Fabriken AB at an organizational level.

The product

5. Comparative Life cycle assessment on: Bio-electro-Jet A1, Bio-Jet A1 (gasification of biomass), and conventional Jet A1 (fossil petroleum-based). Determination of the reduction in CO₂-emission per amount of raw-material.
6. Identification of at least two sustainable business models that can be created in the Bio-electro Jet A1 value chain including distribution paths and taking economic instruments and policies into account.

PROJECT UTILITY

This project has a strong potential to contribute to the development and increased use of biofuels for flights in Sweden. The cost and resource efficiency of the proposed concept is high due to: All raw materials are already in place at the site, good access to large amounts of renewable electricity, there is a dedicated site, economy of scale applies, efficient process integration, there is strong demand for the product, efficient use of by-products, CO₂ is captured and utilized in this process, promotion of circular- and bio-based economy.

The sustainability aspects of the project are high due to: Incoming streams are of completely renewable origin (electricity and CO₂), the product will have a very high degree of renewability (close to 100%, to be verified within the project), unnecessary transport of raw materials is avoided, unnecessary transmission of electricity is avoided, and transmission bandwidth is freed up for other purposes, minimal additional investments in infrastructure is required.

The novelty of this project is high. While previous projects have demonstrated the feasibility, this would be the first study, to the best of our knowledge, which investigates a potential factory at commercial scale for electro-aviation fuel. The utilization and dissemination of this project is high due to: The results from this project will be used to construct the production plant, this is a pioneer project and the results can be utilized also by other external stakeholders for similar purposes domestically or internationally.

The goals and feasibility of the project are reasonable and high, respectively. The goals have been set in a way that they are reachable within the available timeframe and that they reflect

the overall purpose of the project and the call. The feasibility is high due to: The project team is very strong, the project is closely tied to other ongoing projects in the same area, the project partners are dedicated to deliver high-quality, useful results.

RESULTS AND DISCUSSION

Results have been produced on the identification and mapping of preferred sub-processes and unit operations within the Bio-electro Jet fuel (Bio-Jet) production process, including the qualitative identification of mass- and energy flows between the subprocesses. A schematic overview of the Bio-Electro Jet fuel production process is shown in Figure 1.

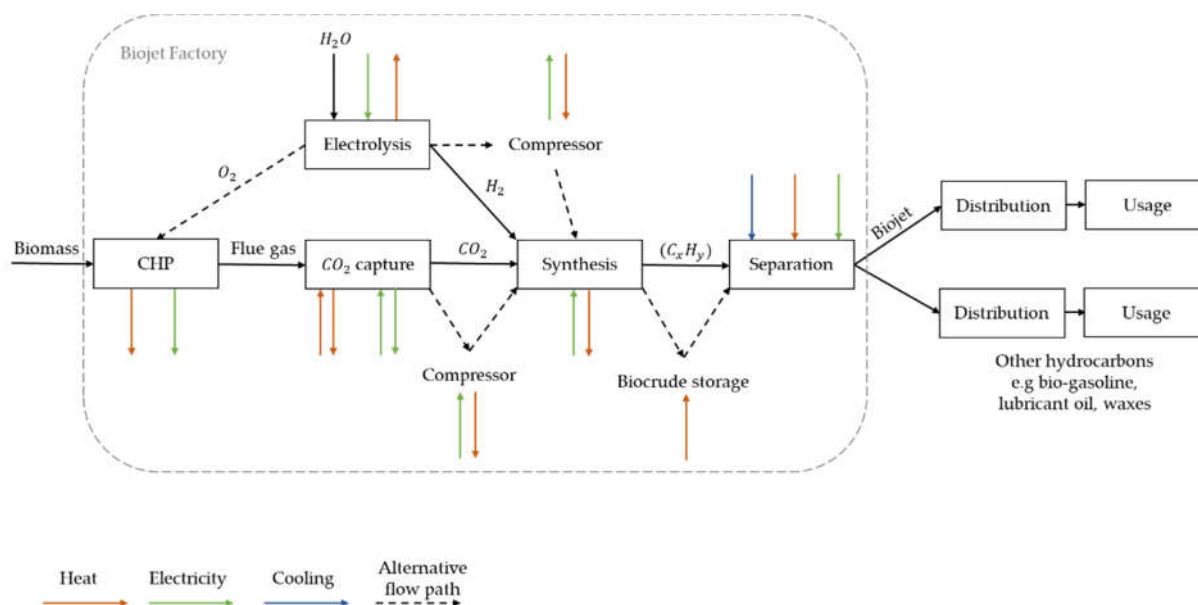


Figure 1. An overview of the process for Bio-electro Jet fuel production.

Five main steps (or subprocesses) have been identified for the overall Bio-Jet production process, see figure 1, and this publication is based around these individual steps:

1. **Combined Heat and Power Production**, where the raw material CO_2 is produced.
2. **Carbon capture**, where CO_2 is isolated from the rest of the flue gasses from the CHP-production.
3. **Electrolysis**, where the raw material H_2 is produced from electricity and water.
4. **Synthesis**, where the Bio-Jet is produced along with other hydrocarbons.
5. **Separation**, where the different hydrocarbons are separated into discrete streams.

These five sub-processes make up the Bio-Jet factory and the boundaries are drawn around this system. Different options for each subprocess are presented and discussed within each separate section of the paper and the results in are based on scientific literature, applied to the specific case in question for this study.

CONCLUSIONS

The process of Bio-electro Jet fuel production has been identified and the unit operations in play have been reviewed. This has resulted in two different options for each process-step as listed below.

Combined Heat and Power

Option 1: The CHP process is suggested to be run at normal operation with minimal change.

Option 2: The oxyfuel technology is included to the process.

Carbon Capture

Option 1: MEA is used as CC technology because of its technological maturity, high CC capacity and suitability for the current CHP process.

Option 2: AMP-NMP is used as CC technology because of its higher efficiency and suitability for energy integration.

Electrolysis

Option 1: AEL is preferred as first-hand option for the production site for the bio-electro jet fuel production plant because of the high production capacity, long lifetime, suitability for continuous production processes and for its technological maturity.

Option 2: SOEC is considered as a second-hand option due to its low electricity demand when heat is available e.g. waste heat from other machines, its ability to produce hydrogen gas with high purity and its suitability for a continuous process. It is not considered as a first-hand option since it is in an early R&D phase and has limited lifetime expectancy compared to AEL.

Synthesis

The synthesis process will focus on two different types:

- The Fischer-Tropsch reaction with Reverse-Water-Gas-Shift reaction
- The modified Alcohol to Jet reaction.

Both will be studied separately as alternative options for the synthesis step of the production process.

Separation

Option 1: A simplified separation process based around distillation to separate hydrocarbons of different chain-lengths.

Option 2: A more intricate separation process that produces fuels containing aromatics.

ACKNOWLEDGEMENTS

The Swedish Energy Agency, Jämtkraft Environmental Fund, and The Research Foundation IVL is recognised for financial support of the project. Ulf Lindqvist, Jonas Vestun, Staffan Swedin and Karl Selander at Jämtkraft and the Lugnvik CHP plant are recognised for valuable contributions to this work.

REFERENCES

- Azar , C., 2011. Biomass for energy: a dream come true... or a nightmare?. Wiley Interdiscip Rev: Clim Change, Volume 2, pp. 09-23.
- Ball , M. & Wietschel , M., 2009. The future of hydrogen – opportunities and challenges.. Int J Hydrog Energy, Volume 34.
- ER 2017:07, 2017. Strategisk plan för omställning av transportsektorn till fossilfrihet, s.l.: Statens Energimyndighet.
- ER 2017:14 , n.d. Luftfartens omställning till fossilfrihet, 2017: Statens Energimyndighet.
- Grahn , M., Azar , C. & Lindgren, K., 2009. The role of biofuels for transportation in CO2 emission reduction scenarios with global versus regional carbon caps.. Biomass Bioenergy, 33(3), p. 60–71.
- Mendes Souza , G., Victoria, R., Joly, C. & Verdade , L., 2015. Bioenergy & sustainability: bridging the gaps., São Paulo: Brazil: Scientific Committee on Problems of the Environment (Scope).
- SOU 2013:84, 2013. Fossilfrihet på väg, s.l.: Statens Offentliga Utredningar.

DECARBONIZING NORDIC TRANSPORTS – THE ROLE OF ALTERNATIVE AVIATION FUELS

J. Hansson^{1,2}, M. Hagberg³, S. Brynolf², M. Grahn², K. Karlsson¹ & R. Salvucci⁴

¹ Sustainable Society, IVL Swedish Environmental Research Institute, Sweden; julia.hansson@ivl.se

² Department of Mechanics and Maritime Sciences, Maritime Environmental Sciences, Chalmers University of Technology, Sweden; selma.brynolf@chalmers.se, maria.grahn@chalmers.se

³ Profu, Sweden; martin.hagberg@profu.se

⁴ Department of Management Engineering, Technical University of Denmark, Denmark; rafs@dtu.dk

Abstract. In order to meet future climate targets, aviation, shipping and road transport need to reduce their climate impact, partly by introducing alternative transportation fuels. There are several possible fuel options. The purpose of this study is to provide an initial assessment of what fuels that are most cost-effective for first and foremost aviation but also other transport modes in the future Scandinavian region in an energy system context given carbon reduction requirements. The cost minimizing energy systems model TIMES Nordic covering national energy systems in Sweden, Norway and Denmark is used for the assessment. We find that a combination of transport mitigation measures is the most cost-effective scenario for decarbonizing the Nordic transport sector. A considerable electrification seems cost-effective for passenger and freight road transport. However, biofuels are needed too, not least in aviation. The findings indicate that bio-jet fuels represent cost-effective mitigation measures in the aviation sector for 2030 and 2050 in all studied scenarios. Electrofuels in the aviation sector is to some extent also a cost-effective option but only when carbon capture and storage is not deployed in large-scale. Thus, the introduction of alternative aviation fuels will play a crucial role in the decarbonization of the Nordic transport sector. Updated transport demand scenarios and improved cost estimates for different fuel production pathways and propulsion systems will further improve the assessment and likely provide new insights for the potential role for different alternative aviation fuel options.

Keywords: Alternative aviation fuels, bio-jet fuels, hydrogen, electrofuels, cost-effectiveness

INTRODUCTION

In order to meet future climate targets, aviation, shipping and road transport need to reduce their climate impact. The amount of alternative and renewable fuels needs to increase in all transport sectors. Biomass-based fuels, electrification, hydrogen and so called electrofuels (produced from carbon dioxide, CO₂, and water using electricity) are being developed for different parts of the transport sector and specifically for the aviation sector.

Transforming transport is a key energy challenge in the Nordic region to achieve the ambitious climate targets set by the Nordic governments (Hansson *et al.*, 2019). This will require changes in all transport sectors, also aviation (Wormslev *et al.*, 2016). The low-carbon transition of the international aviation sector is being encouraged through the Carbon Offsetting and Reducing Scheme for International Aviation (CORSIA), the regulatory framework that aims to stabilize GHG emissions from the aviation sector by 2020 (ICAO, 2019).

The development and in some cases commercialization of different bio-jetfuels, synthetic jetfuels, hydrogen concepts and electric and hybrid electric propulsion systems is on-going (Dahal *et al.*, 2020; IRENA, 2017; Wormslev *et al.*, 2016; Wormslev and Broberg, 2020). Currently, minor amounts of bio-jet fuels are used as low blending with conventional fossil jet kerosene (Wang and Tao, 2016; IRENA, 2017; Wormslev and Broberg, 2020). The potential to develop and use sustainable aviation fuels in the Nordic countries, including Denmark, Finland, Norway, Iceland and Sweden has been examined by Wormslev *et al.* (2016) and updated by Wormslev and Broberg (2020). However, the potential role of different alternative aviation fuels introduced in the future will beside technical and cost development depend on the development in the other transport sectors.

This paper aims for an initial study of what fuels and propulsion technologies that are most cost-effective for first and foremost aviation but also in other transport modes in the future Nordic region in an energy system context given carbon reduction requirements and what factors that influences the prerequisites for different options in these sectors. The focus is on the Scandinavian countries.

METHOD

The TIMES Nordic Model

The study uses a quantitative model-based approach based on the TIMES energy system model. TIMES (The Integrated MARKAL-EFOM System) is an internationally well-established model generator for energy system analysis developed and maintained within the Energy Technology Systems Analysis Program (ETSAP) linked to the International Energy Agency (IEA) (ETSAP, 2018). TIMES is a technology rich, bottom-up model generator, which uses linear-programming to produce a least-cost energy system, optimized according to several user constraints, over medium to long-term time horizons (ETSAP, 2018).

The TIMES application used in this study is a newly developed model named TIMES Nordic presently covering the Scandinavian countries Sweden, Norway and Denmark (Salvucci *et al.*, 2019a,b; Hansson *et al.*, 2019; Salvucci *et al.*, 2018). It is based on the structure of the TIMES-Denmark model (Balyk *et al.*, 2018), which has been extended and developed further.

The TIMES Nordic model is a multi-region model covering all sectors of the national energy systems, including power and heat, industry, service, residential and transport. The comprehensive coverage ensures that relevant connections and interactions over sector boundaries are captured. In its current version the model has a time horizon extending to year 2050 and a yearly time resolution of 32 time slices. Passenger transport is represented by 12 different modes, of which passenger air transport is one. Air transport is also available for freight. Passenger and freight air transport is described by a selection of fuel and vehicle technology options, including conventional jetfuels, bio-jetfuels, hydrogen and electrofuels (Hansson *et al.*, 2019; Salvucci *et al.*, 2018). The technologies differ in terms of fuel use, efficiencies and costs. Both domestic and international aviation is included. The model satisfies the defined modal demands for the entire time horizon by deploying the technology mix with the lowest levelised costs while fulfilling the CO₂ constraint.

Some of the base assumptions for the TIMES Nordic modelling in Shift builds upon the scenario work of the Nordic Energy Technology Perspectives (NETP) 2016, primarily the carbon neutral scenario (CNS) (IEA and NER, 2016). This include the energy service end-use demand projections (such as transport demand) and future price developments for fossil fuels.

Scenarios

The scenarios assessed represent different cost-effective technology pathways to reach the goal of no net CO₂ emissions in the Scandinavian countries by 2050 under different circumstances. All national energy related CO₂ emissions as well as CO₂ emission associated with fuel use for international shipping and aviation (represented by the share filled in the included Nordic countries) are included in the model. Decarbonization is achieved by applying a yearly CO₂ emission bound which is gradually decreased until (close to) net zero emissions are reached by 2050. No other policy measures are included.

The model is run with one main scenario in which five key aspects are varied, resulting in 32 model cases. The main scenario has a technology focus and include a range of transport technology options and future development of them. However, no external shift and avoid measures are assumed possible for meeting the CO₂ target. The introduction of external shift and avoid measures (i.e., shift to more energy-efficient modes and avoided travel demand)

represent a case with reduced transport demand. The key aspects (switches) for the development that can be varied in our scenarios include (i) external shift and avoid measures (yes and no), (ii) biofuel import bound (yes or no), (iii) large-scale introduction of carbon capture and storage (CCS) (yes or no), (iv) high cost for electric vehicles and fuel cell vehicles (yes or no), and (v) large-scale introduction of shared autonomous cars (yes or no).

The introduction of external shift and avoid measures (i.e., shift to more energy-efficient modes and avoided travel demand) represent a case with reduced transport demand. The biofuel import bound represent the limited global bioenergy potential, and with the biofuel import bound, the bioenergy use in the included countries is restricted to the domestic biomass supply potentials. Without the import bound, biofuels can be imported from the rest of the world at an assumed market price. CCS technologies imply that CO₂ can be captured from point sources, transported and stored permanently in storage sites. CCS could potentially be a future key technology for CO₂ mitigation but with limited deployment so far. The cost development of electric and fuel cell vehicles is a central factor for their deployment but relatively uncertain. To test the influence of the development of future vehicle cost reductions, a 20% higher investment costs for all electric vehicle options for road transport compared to the base assumption are assumed in this case. Shared autonomous vehicles can in the future function as driver-less taxis and reduce the need for privately-owned vehicles which may influence the fuel availability also in the other transport sectors. In the case with shared autonomous cars such technologies can supply up to 25% of the delivered car passenger km in 2050.

COST-EFFECTIVE FUEL CHOICES

The total fuel use in the Scandinavian transport sector in 2050 for different scenario conditions are shown in Figure 1. Biofuels and electricity are cost-effective in all cases and hydrogen in quite many cases. Electrofuels on the other hand are only cost-effective as transport fuel in the cases where large-scale introduction of CCS is not assumed to happen.

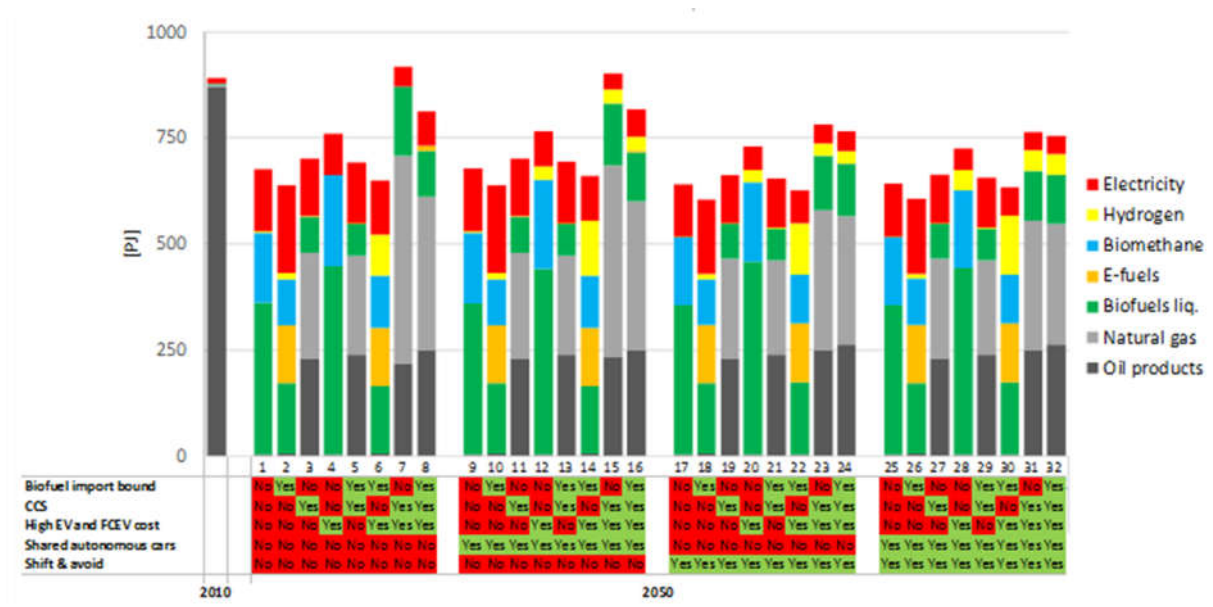


Figure 1. Fuel use in the Scandinavian transport sector in 2050 for the 32 different scenario cases. E-fuels represent electrofuels, CCS – carbon capture and storage, EV – electric vehicles, FCEV – fuel cell vehicles, and Shift & Avoid represents a case with reduced transport demand.

For aviation, bio jetfuels are cost-effective in all scenario cases both in 2030 and 2050 (Figure 2). Electrofuels are cost-effective in some cases, mainly in 2050 and in the cases

with an assumed biomass import bound limiting the total availability of biomass and assuming that there will be no large-scale introduction of CCS. Hydrogen does not seem to be cost-effective in any of the assessed cases, but this needs to be studied further and the cost data updated before any firm conclusions can be drawn on the potential role for hydrogen as an aviation fuel in the Nordics.



Figure 2. Fuel use in the Scandinavian aviation sector in 2030 and 2050 for 16 different scenario cases. The fuel use in 2010 is included for comparison. E-fuels represent electrofuels, BN/Y: biofuel bound Yes/No, CN/Y: Carbon capture and storage (CCS) Yes/No, EN/Y: High electric and fuel cell vehicle cost Yes/NO.

DISCUSSION AND CONCLUSION

The cost-effectiveness of different fuel options in different transport sectors in the Scandinavian countries when striving for low CO₂ emissions has been assessed using energy systems modelling with the TIMES Nordic Model. In general, the assessment shows that it is possible to drastically reduce Nordic transport CO₂ emissions to 2040-2050. However, to achieve this, the deployment rate of low carbon technologies and fuels as well as shift and avoid measures need to be accelerated, not the least in the aviation sector. As expected, a combination of transport mitigation measures is the most cost-effective scenario for decarbonizing the Nordic transport sector. A considerable electrification seems cost-effective for passenger and freight road transport. However, biofuels are needed too, not least in aviation.

For the aviation sector, the assessment indicate that bio-jet fuels represent cost-effective mitigation measures in the Scandinavian aviation sector in 2030 and 2050 in all studied scenarios. Electrofuels in the aviation sector also seem like a cost-effective option to some extent but only under certain circumstances (limited availability of biomass and no large-scale introduction of CCS). The cost-effectiveness of hydrogen in the aviation sector need to be further assessed, by updated estimates for cost and technology performance. The introduction of alternative aviation fuels will play a crucial role in the decarbonization of the Nordic transport sector.

A cost-effective fuel and technology mix in the Nordic transport sector and specifically in the aviation sector depend on several key factors. These include availability of sustainable biofuels, the development and cost reductions of new aircraft propulsion systems (e.g., hydrogen based concepts and all electric and hybrid concepts), the expansion of low-carbon electricity generation, cost development of electrified options in other sectors as well as the development of biomass-based carbon capture and storage (bio-CCS) enabling negative emissions which may facilitate for the aviation and the entire transport sector. Most of these factors have been varied and thereby considered in the different scenarios.

Updated transport demand scenarios and improved cost estimates for different fuel production pathways and propulsion systems will further improve the assessment and clarify the potential role for different alternative aviation fuel options. The implementation and design of policies and targets linked to alternative aviation fuels in the Nordic countries will also influence the development for different options.

ACKNOWLEDGEMENTS

This study is part of the collaborative research program Renewable transportation fuels and systems, with funding from the Swedish Energy Agency and f3 Swedish Knowledge Centre for Renewable Transportation Fuels (project title: Future fuel choices for low-carbon shipping, aviation and road transport). Funding from Nordic Energy Research (via the Shift project) is also acknowledged.

REFERENCES

- Balyk O, Andersen Steen K, Dockweiler S, Gargiulo M, Karlsson K, Næraa R, 2019. *TIMES-DK: technology-rich multi-sectoral optimisation model of the Danish energy system*. Energy Strategy Reviews, Vol. 23, pp. 13-22.
- ETSAP, 2018. *Energy Technology Systems Analysis Program*. Available at <https://iea-etsap.org/>
- Hansson J, Hagberg M, Hennlock M, et al., 2019. *Sustainable Horizons in Future Transport - with a Nordic focus. Project summary 2015-2019*. Available at: <https://www.nordicenergy.org/wp-content/uploads/2019/10/Summary-and-briefs.pdf>
- IEA and NER, 2016. *Nordic Energy Technology Perspectives 2016*. Available at: <https://www.nordicenergy.org/project/nordic-energy-technology-perspectives/>
- International Civil Aviation Organisation (ICAO), 2019. *Carbon Offsetting and Reduction Scheme for International Aviation (CORSIA)*. Available from: <https://www.icao.int/environmental-protection/CORSIA/Pages/default.aspx>.
- Irena, 2017. *Biofuels for aviation: Technology brief*. Available at: <https://www.irena.org/publications/2017/Feb/Biofuels-for-aviation-Technology-brief>
- Salvucci R, Petrovic S, Karlsson K., Wråke M, Priya Uteng T, Balyk O, 2019a. *Energy scenario analysis for the Nordic transport sector: A critical review*. Energies Vol 12 (11), 2232.
- Salvucci R, Gargiulo M, Karlsson K, 2019b. *The role of modal shift in decarbonising the Scandinavian transport sector: Applying substitution elasticities in TIMES-Nordic*. Applied Energy Vol 253, 113593.
- Salvucci R, Tattini J, Gargiulo M, Lehtilä A, Karlsson K, 2018. *Modelling transport modal shift in TIMES models through elasticities of substitution*. Applied Energy 232, pp. 740-751.
- Wang W-C, Tao L, 2016. *Bio-jet fuel conversion technologies*. Renewable and Sustainable Energy Reviews, Vol. 53, pp. 801-822.
- Wormslev E, Broberg M, 2020. *Sustainable Jet Fuel for Aviation Nordic perspectives on the use of advanced sustainable jet fuel for aviation - Update 2019*. Report published by Nordic Energy Research (NER). Available at: <https://www.nordicenergy.org/wp-content/uploads/2020/01/Sustainable-Jet-Fuel-Update-FinalNER.pdf>
- Wormslev E, Pedersen J, Eriksen C, et al., 2016. *Sustainable jet fuel for aviation – Nordic perspectives on the use of advanced sustainable jet fuel for aviation*. TemaNord 2016:538. Available at: <https://norden.diva-portal.org/smash/get/diva2:956135/FULLTEXT01.pdf>
- <https://norden.diva-portal.org/smash/get/diva2:956135/FULLTEXT01.pdf>

FUEL TANK SIZING METHODOLOGY FOR CRYOGENIC HYDROGEN FUELLED AIR TRANSPORT

D. Nalianda¹, P. Rompoko¹, A. Rolt² & V. Sethi¹

¹ Centre for Propulsion Engineering, Cranfield University, Bedfordshire, UK

² School of Aerospace, Transport and Manufacturing, Cranfield University, Bedford, UK

Abstract. Flightpath 2050 ambitiously targets 75% CO₂ and 90% NO_x emissions reductions, relative to year 2000. However, there is increasing evidence from a number of research projects that these targets will not be met using fossil fuels. This is despite extensive research on advanced, and in many cases disruptive, airframe and propulsion technologies, and improvements in aircraft asset management.

Liquid hydrogen (LH₂) has long been seen as a technically feasible fuel for a fully sustainable and decarbonised aviation future, but its use is still subject to widespread scepticism particularly related to the costs associated with its introduction. In order to revitalise interest in the adoption of LH₂ within the aerospace industry, the presentation will describe the strategy, focus and key research activities of ENABLEH2 (**ENAB**ling cryogenic **H**ydrogen-based CO₂- free air transport). This pivotal EU H2020 research and innovation project, is investigating novel technologies to facilitate the utilisation LH₂ in civil aviation and aims to provide a potential roadmap for completely decarbonising civil aviation in the long term.

ENABLEH2 is maturing critical technologies for LH₂ based propulsion to achieve zero mission-level CO₂ and ultra-low NO_x emissions, together with long term safety and sustainability. An overview of experimental and numerical work will be presented for two key enabling technologies: H₂ micromix combustion, and fuel system heat management. The techno-economic and environmental risk evaluation process applied to assess these technologies on long-range and short-medium range LH₂-fuelled, 2050 EIS, aircraft concepts will also be covered. Finally, the presentation will describe an innovative LH₂ cryogenic tank sizing methodology, developed within the project. This allows the optimisation of the LH₂ tank dimensions including its insulation, accounting for the changing loads and temperatures experienced by the pressurised cryogenic tank throughout typical flight missions.

ENERGY TRANSITION IN AVIATION: THE ROLE OF CRYOGENIC FUELS

A. Gangoli Rao* & F. Yin

Faculty of Aerospace Engineering, Delft university of Technology, the Netherlands

[*A.Gangolirao@tudelft.nl](mailto:A.Gangolirao@tudelft.nl)

Abstract. Aviation is the backbone of our modern society. At present, around 4.5 Billion passengers travel through the air every year and aviation is responsible for around 5 % of anthropogenic causes of Global Warming (Lee et al, 2009). With the increase in global GDP, the number of travellers is expected to increase to 7.5 Billion by 2037 and to around 15 Billion by 2050. Even though the crude oil prices are low at the moment, with finite petroleum reserves available on our planet, it is expected that the Jet fuel prices will increase in the future. Moreover using kerosene causes several emissions which are bad for the environment. Liquefied Natural gas (LNG) and Liquid Hydrogen (LH2) can provide an attractive alternative for aviation.

Keywords: aviation, energy transition, cryogenic fuels

INTRODUCTION

The air traffic is expected to grow at a rate of approximately 5% per year for the next couple of decades (Airbus, 2017), implying that numbers of aircraft will double every 15 years. As a result, the environmental impact of aviation will increase significantly. Moreover, whereas surface transportation systems are able to reduce their CO₂ and other emissions significantly, thanks to the increased use of electric/hybrid vehicles, the aviation sector is restricted in the energy source. The European Advisory Council for Aeronautical Research and innovation in Europe (ACARE), has set challenging goals for reducing the environmental impact of aviation. Targets for the year 2050 include a 75% reduction of CO₂ emissions per passenger kilometre and a 90% reduction in NO_x emissions. These targets are relative to the capabilities of typical new aircraft in 2000 (ACARE, 2011).

One of the other main challenges for future aviation is the energy source. Currently, aviation consumes around 1.1 Billion litres of Jet Fuel every day and it is anticipated this would increase by 3% every year despite the improvements in aircraft efficiency. On the other hand, the oil reserves are depleting, thus creating a discrepancy in the supply and demand which will lead to an increase in the fuel cost. This increase in fuel cost has already increased the fuel share in the total operating cost of an airline to around 30% to 40% (IATA, 2010). Further increase in fuel prices would have disastrous consequences for airlines. Therefore other means of releasing energy to drive the aircraft engines will have to be tapped.

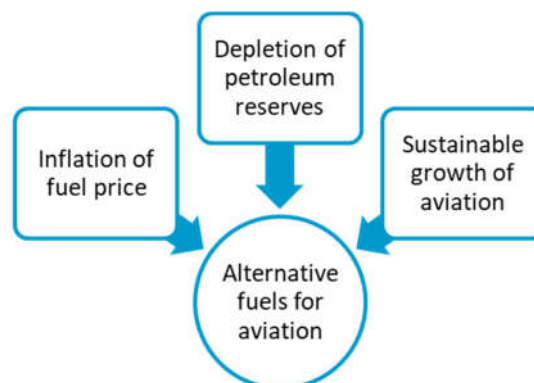


Figure 1. Motivation of alternative fuels for aviation.

LIQUEFIED NATURAL GAS AND LIQUEFIED HYDROGEN AS FUELS

Thus if aviation has to maintain its growth then the problem of energy source for aviation has to be solved first. Some analysts have high hopes on biofuels however there are serious problems with biofuel which include; scaling of production, fuel consistency, availability of

biomass, conflict with the food chain, high price, competition with surface transport, unavailability of subsidies in aviation, etc. Therefore biofuel can be a part of the solution but not the solution itself.

There are several criteria in selecting a fuel for aviation. One of the main criteria is the energy density, as reducing weight and volume is of paramount importance for aviation. Both Specific Energy Density (SED, amount of energy per unit mass of the fuel) and Volumetric Energy Density (VED, amount of energy per unit volume) is important in this regard. Fig. 2 shows several fuels/ energy sources in terms of their SED and VED (Gangoli Rao et al, 2014). It can be seen that Jet-A / kerosene has good SED and VED and therefore is suitable for aviation. It can also be seen that LH2 has high SED but a poor VED, implying that we would require a huge volume to carry any reasonable amount of hydrogen. The main advantage of carrying LH2 is that there is no CO₂ emission from the combustion of fuel. The engine will emit water vapour and some amount of NO_x as exhaust. Researchers have shown that there are several positive effects of using LH2 for aviation on the environment. At present LH2 production is expensive and not environmentally friendly; however as we move towards a hydrogen-based economy by utilizing renewable energy sources, the price of hydrogen is expected to reduce substantially. The recent future energy scenario from Shell (Sky Energy Scenario (Shell Scenarios, 2018)), lays out a roadmap for the usage of hydrogen in various sectors in order to meet the Paris Climate goals (UN, 2015). Hydrogen can be produced from renewable energy and is seen as a long term fuel for aviation (Rondinelli, 2014). But using LH2 in aviation has several challenges including large volume required for fuel storage, safety, logistics, passenger perception, etc, as investigated in the Cryoplane Project (Slingerland, 2005).

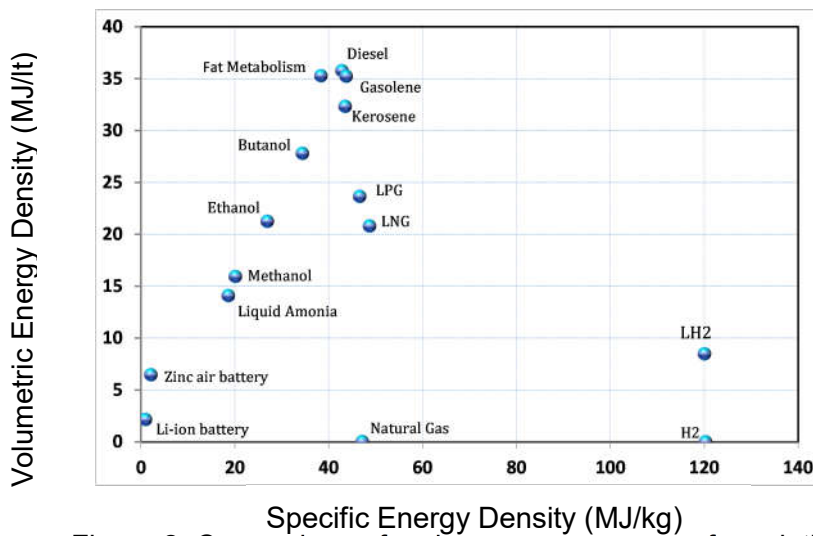


Figure 2. Comparison of various energy sources for aviation

From Fig. 2 it can also be seen that LNG is in between kerosene and LH2, both in terms of SED and VED. Currently, LNG is one of the cheapest fuels available (Nicotra, 2012). The gas reserves in the world are enormous, especially with the discovery of shale gas, thus implying that LNG prices would be stable. LNG is one of the cleanest fuels and recently it has been proved that LNG can be generated by using renewable energy. Due to a higher energy density than kerosene, using LNG can reduce the amount of fuel that needs to be carried on board. Moreover, being a low carbon fuel, burning LNG or LH2 will reduce the CO₂ emission significantly. Some of the advantages and disadvantages of using LNG is summarized below.

There are several criteria for fuel selection in aviation. The table below gives a simplistic comparison of different energy sources. It can be seen that apart from emissions, there are really no other disadvantages of kerosene and that is why it is widely used. It can also be

seen that LNG has several advantages as compared to other fuels/energy sources (apart from kerosene).

Parameter	Kerosene	Biofuel	Syn-Ker	Batteries	LNG	LH2
Energy Density	+	+	+	--	+	++
Vol. Density	++	++	++	--	+/-	-
Emissions	--	+	+	++	+	+
Cost	++	-	--	+	++	-
Availability	++	-	--	--	+	+/-
Infrastructure	++	-	--	+/-	+	-
Safety	+	+	+	-	+/-	--
Compatibility	++	++	++	-	+/-	-
Policy	-	+	+	+	+/-	+

Advantages of LNG

- Lower fuel weight compared to kerosene.
- ~25 % reduction in CO₂ emission.
- > 60% reduction in NOx and particulate emissions.
- Usage of the cryogenic heat sink can increase engine thermal efficiency.
- The LNG is substantially cheaper than conventional jet fuels.

Disadvantages of LNG

- Requires pressurized tanks for storage resulting in increased aircraft Operating Empty Weight (OEW).
- Requires insulation to keep the fuel cool, increasing aircraft OEW further.
- Increased storage space for LNG compared to conventional jet fuels.
- Airport facilities and logistics for tanking LNG are required.

Using natural gas as a fuel is not a problem for the engine as natural gas is a clean fuel and can be burnt in a premixed or partially premixed mode. This substantially reduces the NOx formation within the combustor when compared to kerosene. However, an additional heat exchanger has to be used for evaporating the LNG to natural gas. Since LNG is a cryogenic fuel and therefore a good heat sink, it can be used in a beneficial manner to enhance the thermodynamic efficiency of the engine for intercooling, bleed cooling, air-conditioning, etc (van dijk et al, 2009). Using the cryogenic fuel for cooling the bleed air used for turbine cooling was found to be most beneficial with SFC reductions in the order of 6%.

AIRCRAFT DESIGNS USING CRYOGENIC FUELS

A Multi-Fuel Blended Wing Body (MF-BWB) aircraft was designed in the AHEAD project. The aircraft uses LNG and Biofuel as energy sources (shown in Fig. 3). The fuel is stored in cylindrical insulated tanks within the fuselage of this aircraft and the biofuel is stored in the wings. The energy ratio between the two fuels is around 75-25.

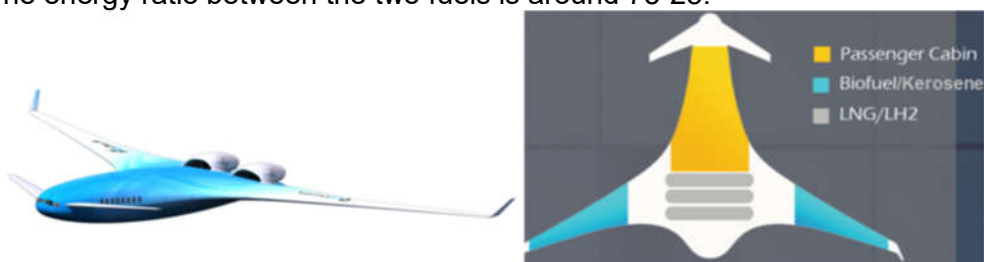


Figure 3. The Multi-Fuel Blended Wing Body investigated in the AHEAD project.

The Multi-Fuel aircraft requires a new type of engine can burn two different types of fuels. The engine that was investigated and designed within the project is shown below. The main features of this engine are:

Multi-fuel Capability:

One of the primary requirements of the multi-fuel BWB aircraft propulsion system is the capability of using multiple fuels. The engine features two combustion chambers, one in between the high pressure compressor and the high pressure turbine which uses the cryogenic fuel, and the other in between the high pressure turbine and the low pressure turbine that uses biofuel (Gangoli Rao, 2015; Yin et al, 2018).

Low Emissions:

The combination of these fuels reduces CO₂ emission. The vitiated products of combustion from the first combustor enables the usage of flameless combustion technology in the second combustion chamber, thereby reducing the NOx emission substantially (Levy et al, 2012).

Bleed Cooling:

The cryogenic fuel is used to cool the turbine bleed cooling air. This is done by a cryogenic heat exchanger in which the compressed air from the last stages of the compressor is extracted to heat up the cryogenic fuel. The colder bleed air is then used to cool the high pressure turbine blade. This process reduces the amount of air required for turbine cooling air substantially and increases the performance of the engine (Yin et al, 2018).

The first combustion chamber (located between the HPC and HPT) burns cryogenic fuel (such as liquid hydrogen/liquid natural gas) in a vaporized state, whereas, the second combustor is an Inter-stage Turbine Burner (ITB) and uses kerosene/biofuels in the flameless combustion mode. Since the flammability limit for Hydrogen / Methane is wider than for kerosene, the combustion in the first combustion chamber can take place at very lean conditions and is beneficial from NOx emission perspective (Reichel et al, 2015). A combustor capable of working on H₂ was designed within the AHEAD project and was demonstrated at atmospheric conditions by the group of Prof. Paschereit (Reichel et al, 2018).

Using Hydrogen / Methane in the first combustion chamber increases the concentration of water vapour and reduces the oxygen concentration within the gases, thereby creating a high temperature vitiated environment at the inlet conditions at the Inter Turbine Burner (ITB). This is beneficial to obtain Flameless Combustion (FC) which takes place at low O₂ concentration and high temperatures (above the auto-ignition temperature of the fuel). This helps to minimize emissions of CO, NOx, UHC, and soot (Perpignan et al, 2018; Perpignan et al, 2018)

The initial results are promising as the CO₂ emission can be reduced by more than 50% when compared to B777-200 ER for a long-range mission (>10,000 km). The climate impact of such an aircraft was evaluated in detail and it was found to be substantially lower than a conventional aircraft (Grewe et al, 2017). The operating cost is also lower by 20-25% due to the lower cost of LNG. The CO₂ emissions can be further reduced by using LH2 instead of LNG.

A group of students worked on the design of a Multi-Fuel A320 class of aircraft for short and medium-range mission (Fig. 4). The results showed that the operating cost and emissions from the aircraft can be reduced substantially when compared to a conventional A320 aircraft. The operating cost was reduced by 10% due to lower emissions and cheaper fuel (Cont et al, 2014).

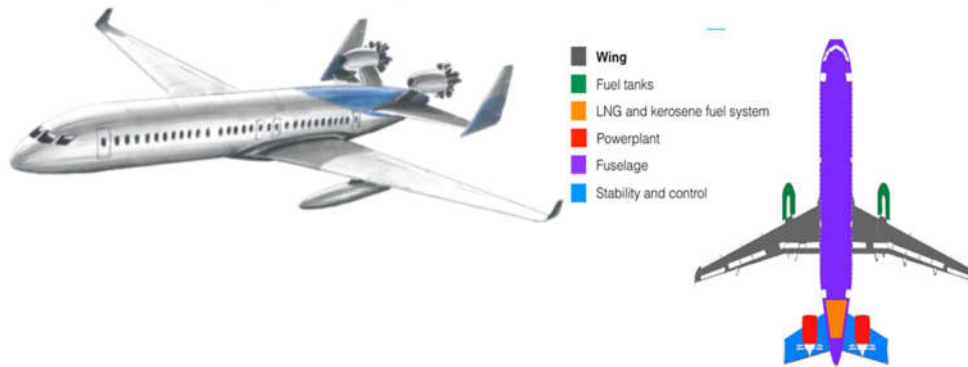


Figure 4. A Multi-Fuel A320 class of aircraft with podded LNG tanks and open rotors designed by students at TU Delft.

The mission of the aircraft is shown in Fig. 5. LNG is used as a fuel in the LTO (landing – takeoff) cycle and in the climb and descent phase. This is done to reduce the local pollution around the airport (soot, CO₂, NO_x, UHC, VoC, etc) while in the cruise phase, kerosene is used in order to limit the emission of water vapour, which can lead to contrail formation. However, the main advantage of using such a multifuel configuration is the flexibility to use the aircraft in places where LNG is not available.

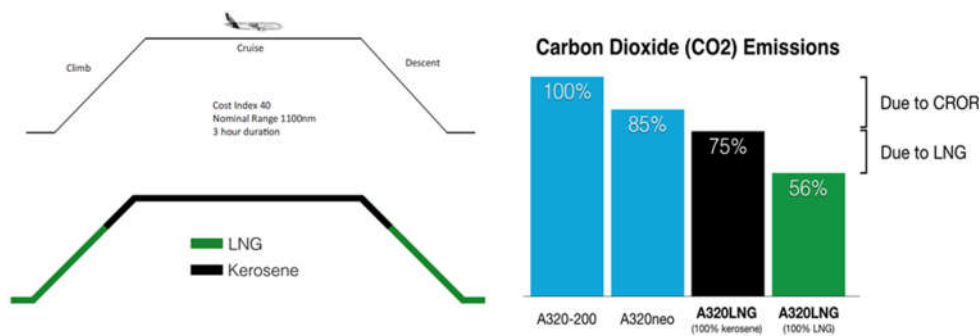


Figure 5. Mission and CO₂ emission reduction from the hybrid A320 class aircraft using LNG and kerosene on a typical mission

Both LNG and LH₂ can offer several advantages as an alternative fuel for aviation, the logistical challenges and the high aircraft development cost are the main hindrances. However as the society will demand lower emissions from aircraft in the future (with the enforcement of the Emission Trading Scheme) and as the fuel will become more expensive in future, the breakeven point for switching over to a new fuel will become viable.

REFERENCES

- Airbus, 2017. *Growing Horizons 2017/2036*, Airbus, Toulouse, France.
- Cont, B., Doole, M.M., Driessen, C.L.V., Hoekstra, M., Jahn, P.B., Kaur, K., Klespe, L., Ng, C.H.J., Rezunencko, E.M., and van Zon, N.C.M., 2014. *A320 Alternative Fuel Design the next generation sustainable A320 operating on Liquefied Natural Gas for the year 2030*, TU Delft.
- Gangoli Rao, A., Yin, F. and van Buijtenen, J. P., 2014. *A Hybrid Engine Concept for Multi-fuel Blended Wing Body*, Aircraft Engineering and Aerospace Technology, Vol. 86 (6).
- Grewe, V., Bock, L., Burkhardt, U., Dahlmann, K., Gierens, K., Hüttenhofer, L., Unterstrasser, S., Gangoli Rao, A., Bhat, A., Yin, F., Reichel, T.G., Paschereit, O., and Levy, Y., 2017. *Assessing the climate impact of the AHEAD multi-fuel blended wing body*, Meteorologische Zeitschrift.

- Gangoli Rao, A., 2015. *No Smoking: Towards a Hybrid Engine*, CleanEra: A Collection of Research Projects for Sustainable Aviation, IOS Press, Amsterdam.
- United Nations, 2015. *Paris Agreement*, Report.
- IATA Economics, 2010. *IATA Economic Briefing*, Report.
- Levy Y, Sherbaum V, Erenburg V, Krapp V, Paschereit CO, Göke S, Reichel T, and Grey J., 2012. *Chemical kinetics of the hybrid combustion system – Deliverable 2.1. Advanced Hybrid Engines for Aircraft Development*, Report.
- Lee, D.S., Fahey, D.W., Forster, P.M., Newton, P.J., Wit, R.C.N., Lim, L.L., Owen, B., and Sausen, R., 2009. *Aviation and global climate change in the 21st century*, Atmos. Environ. Vol. 43, 3520–3537.
- Nicotra, A., 2012. *LNG is the sustainable fuel for aviation*, 25th World Gas Conference—Gas: Sustainable Future Global Growth, Kuala Lumpur, Malaysia.
- Perpignan, A.A.V., Talboom, M.G., Levy, Y. and Rao, A.G., 2018. *Emission Modeling of an Interturbine Burner Based on Flameless Combustion*. Energy & Fuels, 32(1), pp.822-838.
- Perpignan, A.A.V., Gangoli Rao, A., and Roekaerts, D.J.E.M., 2018. *Flameless combustion and its potential towards gas turbines*, Progress in Energy and Combustion Science, Vol. 69, pp. 28-62.
- Reichel, T. G., Terhaar, S., Paschereit, O. C., 2015, *Increasing Flashback Resistance in Lean Premixed Swirl-Stabilized Hydrogen Combustion by Axial Air Injection*, J. Eng. Gas Turbines Power 137(7).
- Reichel, T. G., Terhaar, S., and Paschereit, C.O., 2018. *Flashback Resistance and Fuel–Air Mixing in Lean Premixed Hydrogen Combustion*, Journal of Propulsion and Power, Vol. 34(3):670-701.
- Rondinelli, S., Sabatini, R., and Gardi, A., 2014. *Challenges and benefits offered by liquid hydrogen fuels in commercial aviation*, in: *Practical Responses to Climate Change (PRCC)*, Melbourne, Australia.
- Slingerland, R., 2005. *Innovative Configurations and Advanced Concepts for Future Civil Aircraft*, VKI Lecture Series on Aircraft Design.
- Van Dijk, I.P, Rao, G.A., and Van Buijtenen, J.P., 2009. *Stator Cooling and Hydrogen Based Cycle Improvements*, Int. Soc. of Air Breathing Engines, Montreal Canada, ISABE 2009-1165.
- Yin, F., Gangoli Rao, A., Bhat, A. and Chen, M., 2018. *Performance assessment of a multi-fuel hybrid engine for future aircraft*, Aerospace Science and Technology. 77, p. 217-227.

QUANTIFYING THE ENVIRONMENTAL DESIGN TRADES FOR A STATE-OF-THE-ART TURBOFAN ENGINE

Evangelia Maria Thoma^{1*}, Tomas Grönstedt¹ & Xin Zhao¹

¹ *Division of Fluid Dynamics, Department of Mechanics and Maritime Sciences, Chalmers University of Technology, Sweden*

* *E-mail of corresponding author: marily@chalmers.se*

Abstract. Aircraft and engine technology have continuously evolved since its introduction and significant improvement has been made in fuel efficiency, emissions and noise reduction. One of the major issues that the aviation industry is facing today is pollution around the airports, which has an effect both on human health and on the climate. Although noise emissions do not have a direct impact on climate, variations in departure and arrival procedures influence both CO_2 and non- CO_2 emissions. Thus, multidisciplinary modelling is required for the assessment of these interdependencies for new aircraft and flight procedures. A particular aspect that has received little attention is the quantification of the extent to which early design choices influence the trades of CO_2 , NO_x and noise. In this study, a single aisle thrust class turbofan engine is optimized for minimum installed SFC. Close to optimal cycles are then studied to establish how engine size trades with noise certification and LTO (Landing and Take-Off) emissions.

Keywords: Turbofan engine, Ultra-High Bypass Engine (UHBPR), Installation effects, engine cycle design, LTO cycle, NO_x emissions, Noise emissions, OPR, FPR.

INTRODUCTION

State-of-the-art turbofan engines convert chemical energy to useful propulsive thrust power with an efficiency of around 40%. This represents an immense historical improvement manifesting a reduction in fuel burn with about 75% since the introduction of the Comet 4 aircraft in the early 1960ies (Peeters 2005). While noise and NO_x emissions are subject to regulatory limits the fuel burn reduction achievements have been pushed primarily by the airlines' drive to invest in more fuel and cost efficient aircraft.

Long-term exposure to high levels of aircraft noise is known to have a significant impact on human health, e.g. cardiovascular disease and sleep disturbance. Therefore, reduction of aircraft noise has been a major issue leading to ICAO issuing a series of regulation recommendations. Most recently, this is manifested by the adoption of the ever stringent ICAO Chapter 14 noise standard.

Clearly, the interdependency between fuel efficiency and NO_x emissions has been recognized for a long time. Even with the first CAEP/1 standard adopted in 1981, this interdependency was accounted for by allowing the emission certification levels to be relaxed with increasing overall pressure ratio (OPR).

In this work four different softwares are integrated to simulate interdependencies: 1) engine performance and aircraft flight trajectories, 2) engine conceptual design and sizing, 3) noise modelling and 4) emissions modelling. Propulsion system efficiencies are defined to model a state-of-the-art single aisle thrust class propulsion system. A simplified metric for mission fuel burn, installed SFC, is then used to define an optimal cycle and trades are then studied around this optimum to quantify on the design choices that engine manufactures have to make upon freezing the cycle of a new engine. Three fan diameters 81, 77 (the optimal) and a 74 inch fan engine are then analysed, each engine representing a minimum installed SFC for the given fan diameter. The main intent is to quantify the design range in which a modest fuel burn penalty can be traded for noise and NO_x emissions as well as to predict their values.

MULTIDISCIPLINARY OPTIMIZATION SOFTWARE AND MODELLING

To allow the coupled study of aircraft trajectories, noise, NO_x and CO_2 emissions a number of software components are linked together. At the heart of the simulation the Chalmers in-

house code for aircraft engine simulations, GESTPAN, is used (Grönstedt 2000). GESTPAN is a simulation system for aircraft and propulsion performance that allows the user to perform design, off-design and transient analysis. GESTPAN feeds data to the weight and dimensions model WEICO (Grönstedt 2009), the emissions model CHEESE (Chalmers Engine Emissions Simulation Environment) and the noise model CHOICE (CHalmers nOise CodE, Ellbrant et al 2008).

CHOICE is a tool for the estimation of noise from engine and airframe components using semi-empirical source models (Ellbrant et al 2008). It can either be used as a stand-alone simulation tool or it can be run directly linked with GESTPAN. Trajectories are established by integrating the flight dynamic equations for the aircraft, including its mass (solving for 5 differential equations – 2D trajectories in time):

$$\begin{aligned} F_x &= F_N \cos(\gamma + \alpha) - L \sin(\gamma) - D \cos(\gamma) \\ F_y &= F_N \sin(\gamma + \alpha) + L \cos(\gamma) - D \sin(\gamma) - mg \end{aligned}$$

where F_x and F_y represent net thrust to the cartesian coordinate directions, α is the angle of attack, γ the centre of gravity motion, and L and D are the lift and drag respectively. The trajectories computed are coupled directly to algebraic equations for the propulsion system resulting in a non-linear differential algebraic system of typically around 15 equations. Having take-off and landing trajectories available together with aircraft and engine performance modelling, allows estimating noise emissions from semi-empirical noise source models coupled with noise propagation methods (Ellbrant 2008).

Similar to noise emissions, NO_x is estimated based on semi-empirical modelling (Green 2002, Chandrasekaran 2012, Kyprianidis 2017). The optimal engines are evaluated according to the ICAO NO_x certification procedures (LTO NO_x). For the thrust class and performance most relevant here the Leap-1A was selected as a calibration case. Matching the cycle to public data and using component efficiency predictions (Grieb 2004, Samuelsson 2015), assessed NO_x levels similar to the Leap-1A26 case found in the ICAO NO_x data bank at the take-off, approach and idle points. However NO_x at the climb-out point deviated substantially, despite that the simulated fuel flow for the LTO points differs less than 0.5% compared to the data bank. It is then observed that the Leap-1A26 shows an atypical characteristic for the climb-out point, compared to other engines of similar thrust class. This characteristic is attributed to the novel GE combustor type (Twin Annular Premixing Swirler) TAPS II, which can not be captured by the semi-empirical models found in public literature.

ENGINE CYCLE SELECTION

To analyse the thermodynamic performance of a state-of-the-art turbofan engine a model was set up for an engine with a take-off thrust (Mach 0.2) of 29,000 lbf. Component efficiencies are based on trending performance parameters (Grieb 2003) and trends develop based on research data as presented in (Samuelsson 2015). Top-of-climb key design data together with thrust requirements are presented in Table 1 below:

Table 5. Key parameters at top-of-climb.

Altitude	35000 ft	$\eta_{poly,FAN}$	0.917	OPR	55.0
Mach	0.78	$\eta_{poly,IPC}$	0.902	T4 (TET)	1650 K
ISA	+10 K	$\eta_{poly,HPC}$	0.896	FPR	1.51
Net thrust	5400 lbf	$\eta_{poly,HPT}$	0.900	BPR	10.4
Mass flow	205 kg/s	$\eta_{poly,LPT}$	0.912	Fan dia.	77.4 inch

The installed drag includes not only conventional installation effects such as engine bleed and power extraction but also the detrimental effect of nacelle drag and added drag due to carrying the weight of the engine.

$$SFC_{installed} = \frac{b}{F_{Net} - D_{engine\ mass} - D_{nacelle}} \quad (1)$$

The basic expression used to establish the optimal engine is included in Eq.(1) above as evaluated in the cruise point. Additionally, the cycle is evaluated in the take-off point ($M_n=0.2$ and ISA+15) to check against a turbine entry temperature constraint.

The cycle optimum is located close to an FPR of 1.51 in top-of-climb. The bypass ratio in this point is 10.4. The optimal OPR is computed to 55.0. The search space is reproduced in Figure 1a below. The red triangle point represents the optimal point given in Table 1 above. The lower FPR point results in a 74 inch fan, where as the high FPR design has a 81 inch fan. Despite the relatively large variation in fan diameter the installed SFC remains almost constant.

Mechanically the engine is a direct driven single stage fan with a three stage booster a ten stage high pressure compressor a two stage high pressure turbine and a seven stage low pressure turbine.

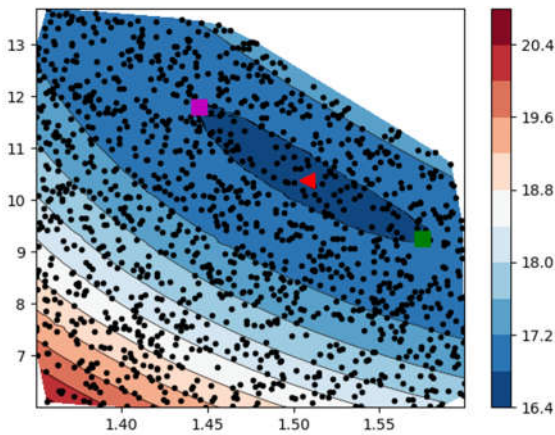


Figure 13: Installed SFC contoured for the FPR/BPR design space (top-of-climb)

Table 2: Key cruise data for the 74, 77 and the 81 inch engine designs.

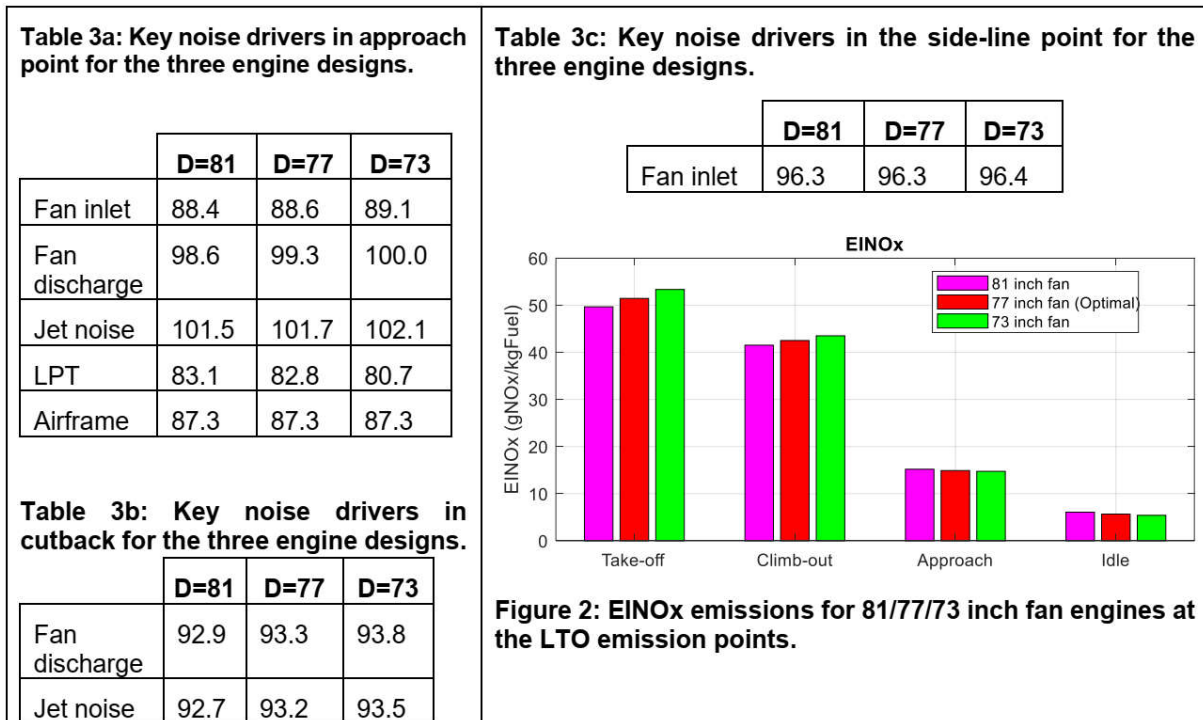
	D=81	D=77	D=74
FPR	1.39	1.44	1.50
Inst. SFC mg/Ns	16.8	16.8	16.8
SFC mg/Ns	14.2	14.3	14.5
OPR	48.2	48.0	47.9
BPR	12.7	11.2	9.95
Mass flow kg/s	218.5	196.1	178.2
Weight	8.9% ¹	8.3%	8.0%
Nacelle drag	6.1% ¹³	5.6%	5.2%

MULTIDISCIPLINARY TRADES

Although the mass flow drops by approximately 20% between the three cruise points and the FPR increases from 1.39 to 1.50 the installed SFC remains virtually constant over this relatively large design range. This indicates that the fuel burn trade is rather weak in this region and that the designer can choose diameter within a relatively large range in the FPR/BPR space with a very modest fuel burn penalty. Thus, this should allow a relatively large design freedom with respect to noise.

¹³ Relative to net thrust.

The main output from the semi-empirical noise and emissions models are collected in Table 3a/Table 3b/Table 3c and Figure 2 below.



Regarding the NO_x emissions it is clear that the variation is notable between the three fan options. It is mainly the Take-off and Climb-out points that are indirectly influenced by the specific thrust of the three designs. The smaller engine has a higher FPR and hence has a smaller thrust lapse. With other words the thrust of the higher FPR engine does not go up as much as the lower FPR engines when running in take-off. Thus it does not throttle down as much and the resulting temperature in take-off remains somewhat higher than for the lower specific thrust configurations. Interestingly enough, since the off-design trend is opposite in the lower thrust points (approach and idle), i.e. low specific thrust engines tend to get hotter in idle, this results in a compensating trend. In total, the LTO cycle NO_x emissions mass for the three engines are 7.89 kg, 8.08 kg and 8.52 kg respectively. The relatively large difference in the total NO_x mass is mainly driven by the fuel flow difference.

Clearly, large variations in NO_x emissions and design trades are mostly relevant for defining the OPR. If the cycle selection is unconstrained by its temperature limits, then a similar flat variation in installed SFC and to a larger extent also in SFC occurs around the optimal OPR. Then, OPR can be traded against emissions. However, if the take-off constraint set for compressor exit temperature is active (set to 1000 K) for the three engines overall pressure ratio can only be reduced down for these cycle selections. For the optimal 77 inch fan engine we observe a 6% total NO_x reduction dropping the OPR from 55 to 52.5 at an increase in installed SFC around 0.2%.

Since the parameter variation in FPR/BPR carried out here, only influence the propulsion system and the airframe noise remains constant, the total EPNdB estimates are computed from the engine noise sources only, as given in Table 3a/Table 3b/Table 3c. It should be noted that, because the airframe noise source is large, frequently the largest in the approach point, we expect that the predicted improvement from the engine will be less important in this point.

Albeit the total engine noise goes down with increasing BPR and decreasing FPR, as can be seen from Table 3a/Table 3b/Table 3c, the relative importance of the fan noise increases as expected at sideline and cutback while jet noise decreases significantly (Daroukh 2017). On the other hand, the LPT noise at approach increases with increasing BPR which mitigates

the noise reduction from the lower FPR fan.

In general, the trade between noise and engine performance is strongly dependent on the technology level assumed. For the state-of-the-art high BPR engines described in this paper, the rate of noise reduction is diminishing since the jet velocities and jet noise is no longer so predominant. Except the fan as still the major source of the total noise, the LPT becomes more important than ever (Nesbitt, 2010).

DISCUSSION AND CONCLUSIONS

It is observed that although SFC varies with 2.1% across the three engine designs studied, installed SFC remains almost constant. Since the installed SFC accounts for the effect of engine weight and nacelle drag, this measure is expected to be a better metric for engine selection than pure SFC. The relevance of the simplified installed SFC metric is supported by that the optimal cycles predicted are quite realistic for a state-of-the-art turbofan engines of the given thrust class. Public data on BPR for the Leap-1A/Leap-1C engines are within the trade range predicted for the three engines. So are publically stated diameters for these engines. If the pure SFC metric is used optimal BPR values larger than 12.5 are observed together with diameters outside the range of existing state-of-the-art engines for this thrust class.

After quantifying the range within which engine size and related BPR/FPR can be traded without a notable installed SFC penalty, a corresponding range in noise can be evaluated. For the engine size and technology level assumed here a cumulative EPNdB decrease by 2.2 dB from the 74 inch to the 81 inch fan is observed. Clearly larger noise reductions can be attained for further increases in fan diameter, but then with notable installed SFC penalties and associated fuel burn penalties. Further increase in fan diameters also increase installation challenges.

When exploring the design space for OPR a limit the compressor exit temperature limit was active meaning that the trade space opens only in the direction of lower OPR. A 6% total NO_x reduction is observed for a lower OPR engine with the same FPR of the optimal 77 inch fan engine at a 0.2% penalty in installed SFC.

REFERENCES

- Chandrasekaran N and Guha A, Study of Prediction Methods for NO_x Emissions form Turbofan Engines, *Journal of Propulsion and Power*, 185 (2012): 1506-1516
- Daroukh, Majd. "Effects of distortion on modern turbofan tonal noise." PhD diss., 2017.
- Ellbrant L, Karlson D, A Noise Prediction Tool for Subsonic Aircraft and Engines including a Numerical Investigation of Noise Radiation, M.Sc., Chalmers, 2008
- Green J, Greener by Design – the technology challenge, *The Aeronautical Journal* 106.1056 (2002): pp 57-113
- Grieb H, Projektierung von Turboflugtriebwerken, Springer 2004
- Grönstedt T Development of methods for analysis and optimization of complex jet engine systems, Ph.D. thesis, Chalmers University of Technology, 2000
- Grönstedt T, Au D, Kyprianidis K G, Ogaji, S., Low-Pressure System Component Advancements and Its Influence on Future Turbofan Engine Emissions, ASME Turbo Expo, GT2009-60201
- Kyprianidis K G, Dahlqvist E, On the trade-off between aviation NO_x and energy efficiency, *Applied energy*, 185 (2017): 1506-1516
- Nesbitt, Eric. "Towards a quieter low pressure turbine: design characteristics and prediction needs." *International Journal of Aeroacoustics* 10.1 (2010): 1-15.
- Peeters P M, Middel J, Hoolhorst A Fuel efficiency of commercial aircraft – an overview of Historical and future trends, NLR-CR-2005-669
- Samuelsson S, Kyprianidis K and Grönstedt T, Consistent Conceptual Design and Performance Modelling of Aero Engines, ASME Turbo Expo, GT2015-43331
- Zhang M, Filippone A, Bojdo N, Multi-objective optimisation of aircraft departure trajectories. *Aerospace Science and Technology* 79 (2018) 37–47.

EXPERIMENTAL STUDY OF TRANSITION IN A TURBINE REAR STRUCTURE

Jonsson I.¹ & Chernoray V.¹

¹ Fluid Dynamics Dept., Chalmers University of Technology, Sweden, isak.jonsson@chalmers.se

Abstract. In modern commercial aviation engines, the low-pressure turbine (LPT) has a high outlet swirl to maximize turbine power to weight ratio. Downstream of the last LPT rotor is the turbine rear structure (TRS) that with relatively few low-aspect-ratio outlet guide vanes (OGV), de-swirls the flow to maximize the thrust. In the wide operational envelope of the TRS, both transition location and mode can change during a normal operating cycle. Hence, accurately predicting transition is critical for the development of future TRS modules.

This work discusses the experimental method and results of laminar-turbulent transition in a TRS module at engine representative conditions at Reynolds Number of 235,000. This was done in Chalmers

1.5 stage LPT-OGV facility. The transition was measured on the entire span using IR-thermography. The technique was specially developed at Chalmers for this particular purpose and validated by boundary layer hot-wire measurements.

The technique provides both steady-state heat transfer with high confidence of 2-8% and time-resolved temperature fluctuations. This paper describes a collection of how this data can be used for transition detection, how it compares to fundamental correlations and as a tool for flow visualization.

The facility was built thanks to the financial support of Energimyndigheten, Nationella flygtekniska forskningsprogrammet, the EU Commission, GKN Aerospace Sweden AB and the department of Mechanics and Maritime Sciences at Chalmers. The aerosurface of the LPT and TRS is designed by GKN Aerospace solely for the experimental rig and is not related to any GKN Aerospace product characteristics.

Keywords: Experimental, Turbomachinery, Transition, Aerothermal

INTRODUCTION

The relatively high Reynolds number and turbulence levels present in turbomachinery lead to that most boundary layers are transitional (Mayle R. E. 1993). There is a large difference between laminar and turbulent boundary layer in terms of skin friction, heat transfer and separation resilience. The transition location is, hence, critical for both aerodynamic performance and thermal loads in core components. More specific for turbomachinery is also the added complexity from the ambient in highly complex flowstructures with strong pressure gradient making predictions on transition location more challenging.

The measurement of boundary layer transition in real engines might be very hard if not impossible for most components. Therefore, detailed studies in representative conditions in specified facilities are required. One test facility of such nature is the Chalmers OGV-LPT facility where detailed studies of the TRS can be investigated with great details.

The established method to measure boundary development is by using hotwire anemometry. This method provides velocity with very high sample frequency, enabling both velocity distribution and turbulence to be deduced. Hotwire anemometry is very reliable and has been extensively used in the last century. However, it is a time-consuming process and can be challenging on most geometries in turbomachinery. One of the main challenges on the static components is to position the very sensitive hotwire within a few hundreds of a millimetre of the surface repeatedly.

Alternative methods to directly measure the boundary layer profile such as miniature Prandtl tube or particle image velocimetry (PIV) are also available. The Prandtl tube is less sensitive to wall collisions but does normally not have the time resolution as a hotwire. PIV can produce time resolve full plane data but requires substantially more preparations and providing enough tracing particles can be challenging in turbomachinery.

As an alternative to these two methods, several indirect methods of transition detections can be utilized with a wide range of confidence. In this work, the validity of using Infrared thermography to deduce the boundary layer development and transition location is discussed.

METHOD

Steady-state convective heat transfer measurement is achieved by using a uniformly heated core with an isolation layer between the core and the freestream flow. From the temperature difference between the core and the surface temperature of the isolation, the heat flux through the wall can be calculated. The total heat flux through the wall is transported away by radiation and convective processes. As interest is on the convective part the radiative part needs isolated or minimized, this is commonly the most arduous part of the problem. Earlier studies in Chalmers fluid dynamics lab by Arroyo .C (2012), Rojo B. (2014) and Chenglong C. (2016). have been using the principle of a heated core but have had challenges with background radiation. Recently Kirillos B. and Povey T. (2017) showed a relatively easy method to estimate the background radiation. A slightly modified version of this is incorporated in results presented by Jonsson I. (2020) together with an extensive uncertainty analysis indicating a confidence interval of 2-8% on heat transfer coefficient on the surface on the OGV. The results from the latter is presented in this work.

The heat transfer distribution can reveal information about the boundary layer development. As the laminar boundary layer develops, the skin friction reduces and according to Reynolds analogy so does the heat transfer as well. At transition, there is a rapid increase in mixing and heat transfer increases. When the boundary layer is fully turbulent and a start to develop the skin friction and heat transfer starts to reduce again. This is valid if the boundary development is typical with limited acceleration or other interferences on the boundary layer development. Steady-state results can be at minimum used as a strong indicator where the transition zone is located.

The surface temperature is sampled using an IR camera. The IR camera provides full-frame time-dependent data. This allows for further details to be extracted than only average values.

As the turbulent streaks are formed there is a rapid increase in skin friction and heat transfer. This causes a surface temperature change which, if large enough, can be detected by the camera. The problem is often that the streaks are formed and traversed downstream in a too short time frame to be fully resolved in time by the camera.

Larger structures such as separations and secondary flow structures cause local changes in heat transfer that is in most cases causes both larger and during a longer time frame compared to individual turbulent streaks

RESULTS

Figure 1 shows the steady-state heat transfer along the OGV at midspan. In the graph three points, A, B and C are marked out. From steady-state heat transfer, the transition is expected to begin at A and end at C, B was selected as an arbitrary point in between. At these three points, boundary layer hotwire anemometry was used to investigate the boundary layer development. At point A the boundary layer was fully laminar. At point C the boundary layer was fully turbulent and B the intermittence was around 0.45 meaning that the flow is 45% turbulent during the sample time.

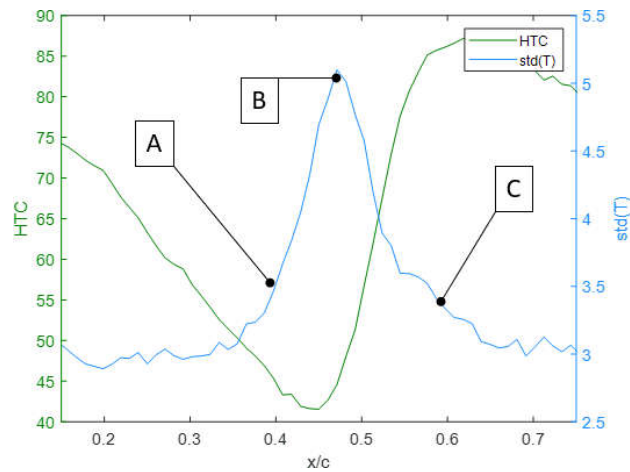


Figure 1. OGV midspan distribution at design conditions of the convective heat transfer coefficient, temperature fluctuation and location of the boundary lay studies.

In Figure 1 there the temperature fluctuation is shown as a blue line and temperature fluctuations. The high temperature fluctuations start to increase at A and ends at C with peak values near point B. Before A there is no fluctuation and after C there are slightly higher values compared to before A.

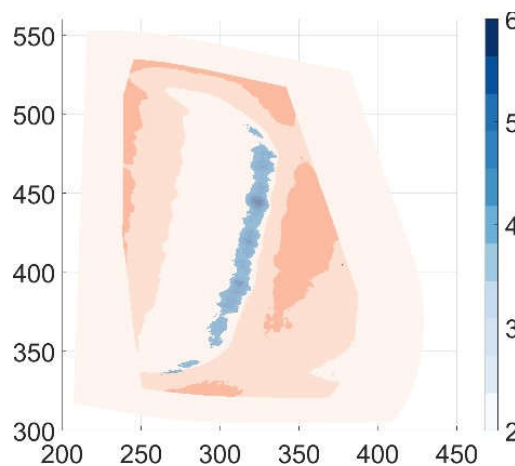


Figure 2. The suction side convective heat transfer coefficient together with the temperature fluctuations along the full span at design conditions.

Figure 2 shows heat transfer coefficient and temperature fluctuation on the suction side of the OGV. Using the same rationale as for midspan the transition distribution for the span can be observed in fig 2. The high temperature fluctuation observed reaching from the leading edge and expanding along the vane indicate a corner vortex that expands along the vane near the hub. This corner vortex disturbs normal boundary layer development and can be argued to be the main reason for the front shift in transition near the end wall. As the OGV is much heavier loaded near the hub the effect is larger near the hub while at the shroud very little of the expanding stream tube can be observed.

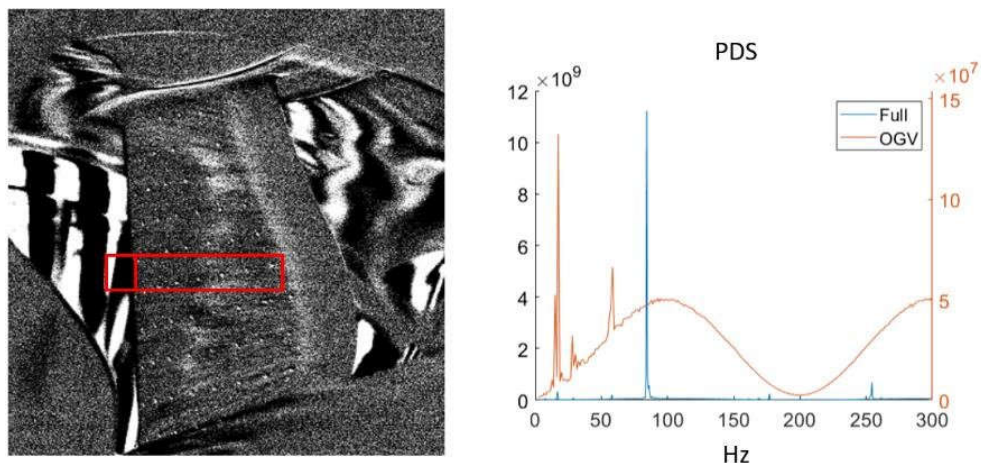


Figure 3. (a) Sliding frame subtraction of OGV suction side ADP, red rectangle show area for POD studies. (b) Dominant frequencies from the POD performed in subframe or the rotor and boundary layer at midspan of the suction side.

Figure 3a show a single sliding subtraction of the OGV suction side at design conditions and shows that individual streaks which can be identified even though very faint. In Figure 3b, a comparison of the dominant frequencies found in the area cover the rotor compared to the area in the transition zone near midspan. This is done using power density spectrum (PDS) analysis on the two areas are marked with two red rectangles in Figure 3.

DISCUSSION AND CONCLUSIONS

At midspan, the steady-state heat transfer, hotwire anemometry and high temperature fluctuation indicate the same transition location. As only three points of the boundary layer studies were performed, with this an upper and lower limit of the transition zone could be decided. Transition onset moment thickness correlates well with fundamental boundary layer correlations as shown in Jonsson I (2020).

The secondary flow structures observed in the full span data correlate well with earlier presented results from flow visualization and wake studies.

Initially, the authors believed that the rotor wakes from the upstream LPT would be enough to cause a transition in the boundary layer on the OGV, but initial data indicate no coupling between the two. The sampling speed or camera sensitivity might not be enough to capture the weaker coupling between the rotor and transition, this require further investigation.

The method presented in this work can be implemented on other geometries with very little geometrical limitation as a free-form additive manufacturing method SLA is used. The wall thickness and water channel height could need adjustment to the fit the case specific conditions. However, for most cases with wind speed below 60m/s, similar accuracy and observation possibilities should be viable.

ACKNOWLEDGEMENTS

The facility was built thanks to the financial support of Energimyndigheten, Nationella flygtekniska forskningsprogrammet, the EU Commission, GKN Aerospace Sweden AB and the department of Mechanics and Maritime Sciences at Chalmers.

REFERENCES

Arroyo C, Johansson G, Wallin F. 2012, *Experimental Heat Transfer Investigation of an Aggressive Intermediate Turbine Duct*. Journal of Turbomachinery. Vol 134, nr 051026.

- Chenglong W. et al. 2016. *Experimental and numerical investigation of outlet guide vane and endwall heat transfer with various inlet flow angles*. International Journal of Heat and Mass Transfer. Vol 95, pp 355-367.
- Geankoplis, C.J. 2003. Transport processes and separation process principles, Fourth Edition, p. 475.
- Kirollos B, and Povey T. 2017. *High-accuracy infra-red thermography method using reflective marker arrays*. Measurement Science and Technology. Vol. 28, 9
- Jonsson I. et al. 2020a. *Infrared Thermography Investigation of Heat Transfer on Outlet Guide Vanes in An Engine Exit Module*. International Journal of Turbomachinery, Propulsion and Power. ijtp-746488 (under review).
- Jonsson I et al. 2020b. *Experimental and Numerical study of laminar-turbulent Transition on a Low-pressure Turbine Outlet Guide Vane*. Proc. ASME Turbo Expo 2020. GT2020-14990
- Mayle R. E. 1993. *The Role of Laminar-Turbulent Transition in Gas Turbine Engines: A Discussion*. Journal of turbomachinery. Vol 115, pp 207-2016.
- Rojo B, Jimenez C. 2014. *Experimental heat transfer study of endwall in a linear cascade with ir thermography*. In Proceedings of EPJ Web of Conferences Vol. 6

AERODYNAMIC INVESTIGATION OF THE FLOW IN A TURBINE REAR STRUCTURE AT REALISTIC FLOW CONDITIONS

V. Vikhorev¹ & V. Chernoray¹

¹ *Mechanics and Maritime Sciences, Chalmers University of Technology, Sweden, valvik@chalmers.se, valery.chernoray@chalmers.se*

Abstract. The development of the current geared engines has increased the demands of its components' investigation. This article is focused on the last stage of the turbofan engine – turbine rear structure (TRS), a good design of which is crucial for higher efficiency and lower emissions. Studies were performed in an annular rig located at Chalmers University of Technology, Sweden which represents an engine realistic TRS stage. The static structure of TRS is equipped with 12 outlet guide vanes (OGV) of three different types: regular, thick and bumped vane. Each type of vane was tested under on- and off- design conditions with swirl angle varying at ± 5 degrees from the aerodynamic design point and fixed Reynolds number of 235000. Measurements were done using multi-hole pressure probes and monitoring inlet and outlet planes. Moreover, to visualize the near-wall streamlines and flow separations the oil-film visualization was used. The study shows that the OGVs with increased thickness and with a vane shroud bump are shown to affect the performance of the TRS by influencing the losses on the OGV suction side near the hub. Besides, the implementation of vane equipped with bump leads to a significant influence on the outlet flow from the low-pressure turbine and noticeable downstream influence on the wakes from the OGVs.

Keywords: turbine rear structure, engine exit structure, outlet guide vane, low-pressure turbine, engine mount recess.

INTRODUCTION

In modern geared turbofan engines, the low-pressure system is composed of low-pressure turbine (LPT), turbine rear structure (TRS) and the core exhaust nozzle, so that LPT provides the initial conditions for the TRS.

The TRS is designed to satisfy two main functions: to support the engine rear bearings and to remove the exit swirl from the LPT to maximize the thrust. This de-swirling provided by Outlet Guide Vanes (OGV) in TRS leads to the development of the diffusive flow with the risk for the flow separation both on end-walls and vanes. Therefore, the implementation of static vanes requires a good design of the TRS with further aerodynamic investigation of the flow which is particularly challenging.

The first evaluation of the flow field around OGVs in a linear cascade was made by Hjärne *et al.* (2005). The authors introduced a two-dimensional approximation of vanes based on modern CFD techniques. Furthermore, Hjärne *et al.* (2006) performed experimental investigations of the secondary flow development and provided a detailed comparison between different numerical models noting the effect of the free-stream turbulence.

A novel approach for investigating the effect of the turbine tip clearance on pressure losses was introduced by Selic *et al.* (2012). Unlike the previous studies, the authors provided experimental results in an annular rig with an unshrouded turbine. Moreover, special attention is given to the impact of leakage flow on the flow structures.

Further investigations were carried out in an engine realistic facility equipped with a shrouded turbine stage located at Chalmers University of Technology. Jonsson *et al.* (2018) studied the effect of surface roughness on secondary flows and transition behaviour in TRS. Later, Jonsson *et al.* (2019) have conducted the heat transfer experiments on the OGV's surface, which allowed to indicate the laminar-turbulent transition for several aerodynamic load cases. However, a typical modern TRS design includes not only regular vanes but also several vanes equipped with an engine mount recess provided on the TRS shroud, where the engine mounts are attached and several vanes with enlarged thickness to provide additional space for oil tubes.

Neither bumped vane nor the thickened vane have previously been studied in an annular rig with an upstream LPT. The current investigation aims at studying aerodynamic performance

of a realistic TRS with implemented thick and bump vanes under on- and off-design conditions.

EXPERIMENTAL SETUP AND METHODS

The experimental study was conducted in a newly built TRS facility in Chalmers Laboratory of Fluids and Thermal Sciences (Fig. 1).

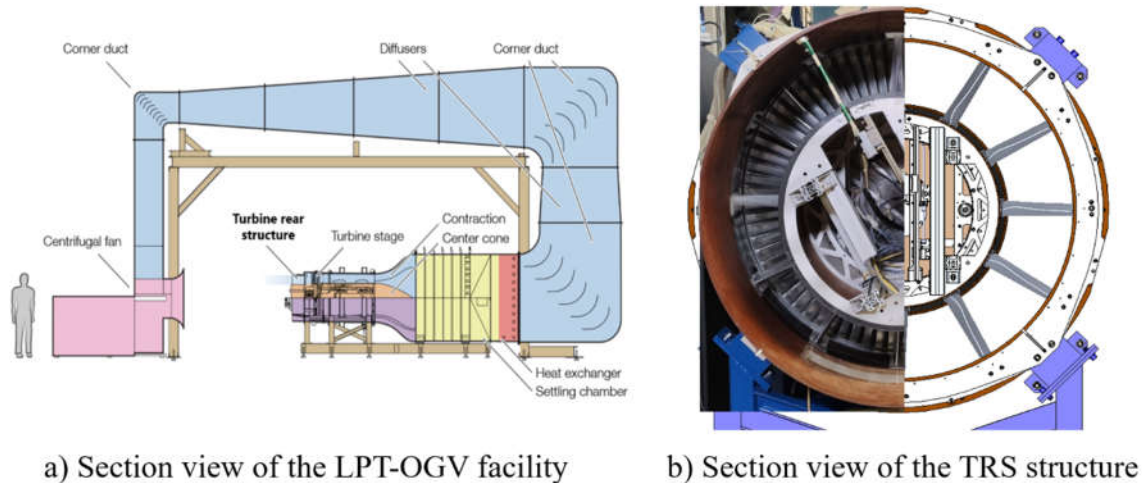


Figure 1. LPT-OGV Facility

The facility is capable of performing EEM studies for a large variety of engine representative flow conditions up to $Re = 450,000$. The facility is of a semi-closed loop type that operates at a steady state at atmospheric pressure with controlled temperature. A single-stage shrouded LPT is controlled by a hydraulic brake and is providing realistic inflow conditions to the tested TRS module. The TRS includes 12 OGV which are positioned with a 30-degree spacing. It shall be noted that the LPT and TRS components have been designed solely for the experimental rig and are not related to any GKN Aerospace product characteristics. The turbine braking torque and the axial velocity in the test section are controlled in order to obtain constant values of the flow Reynolds number and the flow coefficient (FC), defined as the ratio of the axial velocity to the blade speed. The TRS module has baseline instrumentation consisting of two traversing systems with multi-hole pressure probes and reference Prandtl tubes.

Pressure measurements

Total pressure measurements were done for Inlet and Outlet planes which are located upstream and downstream respectively (Fig. 2a).

The Inlet measurements were performed with L-shaped five-hole probe (Fig. 2b) while the Outlet measurements are performed with a straight 7-hole probe. Pre-calibration was carried out in an in-house calibration facility at velocities from 5 to 60 m/s with high accuracy of probe's positioning which is determined by the resolution of the optical encoders. Surface static pressure distributions were measured by embedded surface pressure taps. The OGV with pressure taps was manufactured by a rapid prototyping method – stereolithography (Fig. 2c).

Oil-film interferometry

This technique is used as a qualitative tool to identify topological surface structures on the vane, hub and shroud. In our case, an oil-film visualization on the OGV suction side was carried out to visualize the near-wall streamlines and flow separations. The facility is instrumented with an embedded video camera for photo and video recording of the oil-film

development. An oil-kerosene mixture with pigment particles is adapted for operating velocity and blade loading by changing the proportion of the components to control the evaporation rate and viscosity of the mixture.

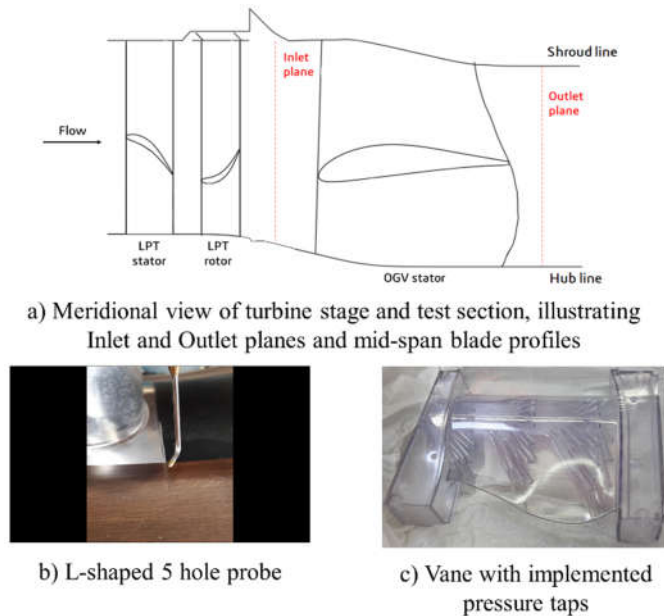


Figure 2. Setup and equipment for total and static pressure measurements

RESULTS AND CONCLUSIONS

Measurements of the flow around OGVs were performed at fixed Reynolds number, $Re = 235,000$ and three different flow coefficients (0.588, 0.662 and 0.657). For the first time, the investigated TRS configuration includes three types of vanes: regular, thick and bumped. To investigate the flow coefficient impact, the thick OGV oil-visualizations were performed (Fig. 3). It shows clear changes in the surface streamlines with the flow coefficient increase. At the lower off-design point the streamlines are smooth without any flow separations (Fig. 3a). Furthermore, under the on-design condition (Fig. 3b) the region with accumulating particles is clearly visible, indicating local laminar separation followed by transition and further reattachment. Finally, as the load increases, the flow pattern illustrates the developed vortices near the OGV trailing edge close to the hub (Fig. 3c).

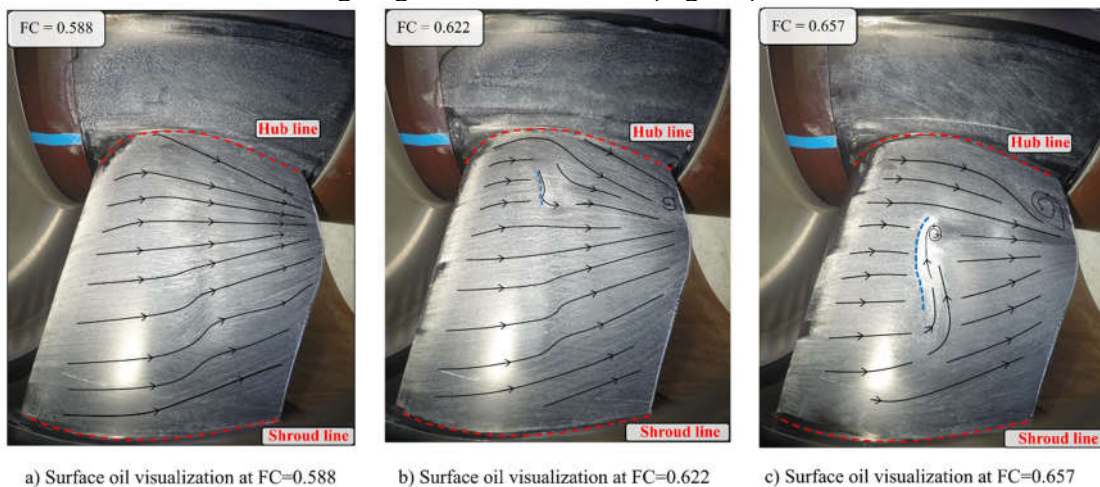


Figure 3. Oil-film visualizations on a thick OGV suction side at on-design flow coefficient (0.622) and two off-design flow coefficients (0.588, 0.657).

Figure 4 shows the wake comparison of the total pressure coefficient for the regular, thick and bump vanes under on-design condition for Outlet plane and for 12% span.

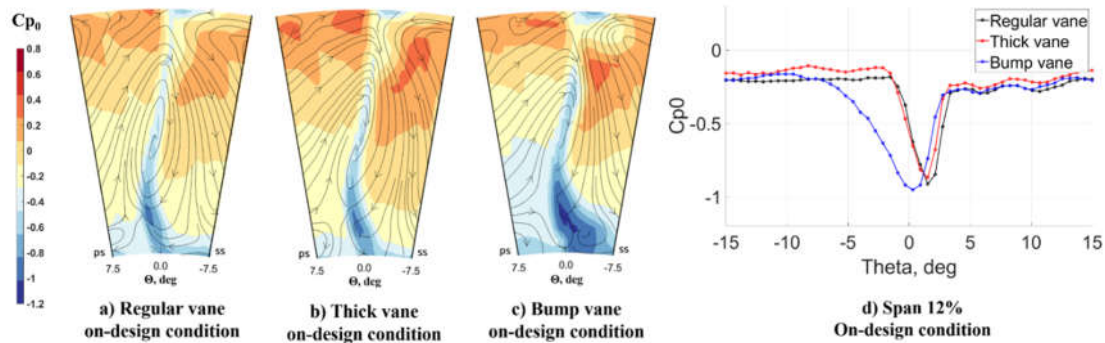


Figure 4. Total pressure coefficient distribution for the regular, thick and bump vanes.

As seen, the shape and intensity of the wake for the thick vane are similar to the regular vane (Fig. 4a–b), while the presence of the bump on the OGV is significantly changing the total pressure distribution due to the bump influence as a blockage to the passing flow (Fig. 4c). Moreover, there is an additional area with low pressure created near the hub, which indicates a hub wall flow separation due to the extra adverse streamwise pressure gradient induced by the bump. Quantitative comparison shown in Fig. 4d supports previous conclusions that the thickening of the vane doesn't influence the aerodynamic performance in terms of pressure losses. For the bump case, the wake increases about twice compared to the regular and thick vanes. More detailed results can be found in the paper written by Vikhorev *et al.* (2020).

ACKNOWLEDGEMENTS

The authors would like to thank Isak Jonsson for the regular vane data presented in this work. The financial support from the Nationella flygtekniska forskningsprogrammet and the EU-commission is highly appreciated. Chalmers Laboratory of Fluids and Thermal Sciences is acknowledged for hosting the facility and for the measurement equipment.

REFERENCES

- Hjärne J., Chernoray V., Larsson J, and Löfdahl, L., 2005. *Experimental Evaluation of the Flow Field in a State-of-the-Art Linear Cascade with Boundary Layer Suction*. In Proceedings of ASME Turbo Expo 2005. Reno, USA.
- Hjärne J., Chernoray V., Larsson J. and Löfdahl L., 2006. *An Experimental Investigation of Secondary Flows and Loss Development Downstream of a Highly Loaded Low Pressure Turbine Outlet Guide Vane Cascade*. In Proceedings of ASME Turbo Expo 2006. Barcelona, Spain.
- Jonsson I, Chernoray V. and Rojo B., 2018. *Surface Roughness Impact on Secondary Flow and Losses in a Turbine Exhaust Casing*. In Proceedings of ASME Turbo Expo 2018. Oslo, Norway
- Jonsson I., Chernoray V. and Dhanasegaran R., 2019. *Infrared Thermography Investigation of Heat Transfer on Outlet Guide Vanes in an Engine Exit Module*. In Proceedings of 13th European Turbomachinery Conference on Turbomachinery Fluid Dynamics and Thermodynamics. Torino, Italy.
- Selic T., Lengani D., Marn A. and Heitmeir F., 2012. *Aerodynamic Effects of an Unshrouded Low Pressure Turbine on a Low Aspect Ratio Exit Guide Vane*. In Proceedings of ASME Turbo Expo 2012. Copenhagen, Denmark.
- Vikhorev V., Chernoray V., Thulin O., Deshpande S., Larsson J., 2020. *Detailed Experimental Study of the Flow in a Turbine Rear Structure at Engine Realistic Flow Conditions*. In Proceedings of ASME Turbo Expo 2020. London, United Kingdom.

INTEGRATION OF AIRBORNE EARLY WARNING RADAR PLATFORMS ON AIRCRAFT

Prabhat Khanal¹, Jian Yang¹, Marianna Ivashina¹, Anders Höök², Ruoshan Luo², & Per Hallander²

¹ *Department of Electrical Engineering, Chalmers University of Technology, Sweden.
prabhat@chalmers.se, jian.yang@chalmers.se, marianna.ivashina@chalmers.se*

² *SAAB AB, Sweden.
anders.hook@saabgroup.com, ruoshan.luo@saabgroup.com, per.hallander@saabgroup.com*

Abstract. The need for a long-range and complete Air Picture has long since motivated the presence of airborne early warning (AEW) radar platforms. Later developments, such as stealth and advancing threats at low altitudes or hypersonic speeds have nothing but reinforce the need for increased-performance AEW. However, the high costs for the platform, integration, and operations restrict the number of platforms to a point where these high-value assets become sensitive to preemptive actions by an adversary. Therefore, SAAB has within the NFFP7 framework launched a series of studies aiming at smaller, adapted, and cost-efficient unmanned AEW platforms with extreme endurance. Thus, the aerodynamic performance of the carrier plus radar must be optimized, which implies that the projected area of the radar must be minimized. In this project, we study the possibility of integrating the antenna layer in the fuselage structure of the aircraft, thus gaining (i) body width and (ii) a more optimal wet geometry.

Keywords: Airborne early warning (AEW), Sensor integration, surveillance radar, wide coverage antenna, phased array antenna.

INTRODUCTION

An Airborne Early Warning (AEW) system is an airborne solution equipped with radar and other sensors. It detects and tracks targets like aircraft, ships, and vehicles at vast distances and allowing defences to be alerted as early as possible before the intruder reaches its destination, giving the air defences the maximum time in which to operate. It is also capable of providing command and control information to other units and act as the air traffic controller at the battlefield. Apart from military applications, AEWs can be used in other surveillance applications like detecting illegal drones, drug smuggling, deforestation and illegal mining, used in search and rescue in emergencies, illegal fishing, pirates and many more.

The AEWs play a vital role in air defence and other operations. The primary role of an AEW aircraft is to provide the detection of low-flying aircraft. Surface radar is good at delivering ample early warning of high-flying aircraft; however, if aircraft is flying low, the radar horizon is reduced to less than 20 kilometres (McCarry, 2001). It minimizes the warning time to the point where defending fighters do not have enough time to intercept the intruders before they reach the target. Modern aircraft often fly at a very low level — as little as 10 metres, use stealth and hypersonic aircraft and fly behind hills and down valleys, using terrain features to mask their approach. It further decreases the radar horizon and warning time. To overcome the horizon limitation, one needs to get the radar higher. An AEW at the altitude of ten kilometres above the surface of the earth can 'see' everything from directly below out to a range of hundreds of kilometres. Additionally, since the platform is highly mobile, the effective coverage area of an AEW is even larger than the range of the radar taken by itself (Berkner, 1946). The AEW System may have secondary roles such as signal interception, act as a communications relay, detect targets at land and sea, locate bearings of jammers, or to provide surveillance over regions for which surface-based radar coverage is not available.

The design requirements for an AEW radar comes from the role and objectives of the AEW System, of which the radar is only one (though important) element. The high costs for the

AEW platform, integration, and operations restrict the number of platforms to a point where these high-value assets become sensitive to preemptive actions by an adversary. Smaller, adapted, and cost-efficient unmanned AEW platforms with extreme endurance might help to deploy adequate numbers of platforms. The aerodynamic performance of the carrier plus radar must be optimized together, which implies that the projected area of the radar must be minimized. In this project, we study the possibility of integrating the antenna layer in the fuselage structure of the aircraft, thus gaining (i) body width and (ii) a more optimal wet geometry.

AEWS MAIN SENSOR

The physical size of the antenna becomes too big for practical aircraft platforms below upper UHF frequencies, and the two ways propagation loss is very high above S-band for the long-range detection, especially in poor weather (Clarke, 1985). Therefore most AEWs use L or S-bands antenna for the long-range detection. Commonly, two different antennas configurations are used in AEW. 1) A fixed beam antenna like the reflector antenna in AVS21 (Watts, 2017) or the fixed beam antenna array in Boeing E-3A (Clarke, 1985), and 2) A beam-scanning antenna like the phased array antenna in SAAB Erieye (Heed, 2000). The fixed beam antenna only radiates at one direction, and it is mechanically steered to the desired radiation direction. In contrast, the beam scanning antenna is mechanically fixed to the aircraft body, and it is electronically steered to the desired radiation direction. In this project, we shall study a body-wide fixed antenna geometry similar to the SAAB Erieye.

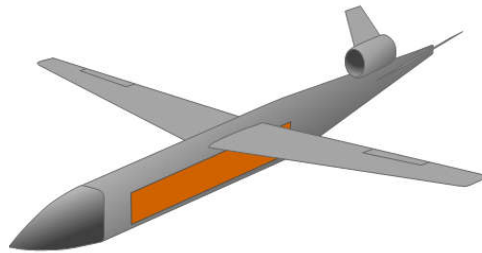


Figure 1. A concept model of the proposed fuselage integrated antenna (in the orange colour) on an aircraft.

One of the approaches of designing the body-wide antenna for an aircraft is to use very thin conformal antennas like those in (Kemkemia et al., 2013) and (Qiang et al., 2017). The main advantage of this approach is that the fuselage can be built using the conventional method, and the antenna can be installed on top of the fuselage later. However, this approach is not suitable for wide scanning antenna arrays. Wide-angle scanning antenna arrays are not very thin (Jonsson et al., 2013); as a result, installing them on top of the conventional fuselage will create protrusion in the fuselage and change the aerodynamic of the aircraft significantly. Therefore, such antennas should be integrated with the fuselage, and the aerodynamic performance of the aircraft plus radar must be optimized together. One of the early published research on the fuselage integrated phased array antennas were (Yee and Furlong, 1981). It gives us the importance of fuselage integrated antennas and the antenna design approach at that time. More recently, a fuselage integrated antenna array was studied under NFFP4 (Swedish National Aeronautics Research Programme 4) project (Eilgardt, 2009). However, the study focused on a wide-band antenna and to reduce the radar cross-section for the antenna's cross-polarization. As a result, the antenna was not low profile.

In this project, we are investigating a low volume, lightweight, high endurance load-carrying fuselage integrated antenna. Figure 1 shows a conceptual model of an aircraft consisting of the desired antenna. It shall be a large, high gain, wide scanning, fixed phased array

antenna consisting of antenna elements in the order of thousands. The size of the antenna shall be comparable to the size of the aircraft. Hence, the reduction of weight and volume of the radar sensor will help us to reduce the weight, volume, and drag of the aircraft and improve the sensor coverage. As a result, we expect to have increased mission time, lower operating costs, and better coverage due to the freedom of sensor integration. Research results of the project could be applied to unmanned ISR platforms, large AEWs, small UAV AEWs and mid-life fighter upgrades.

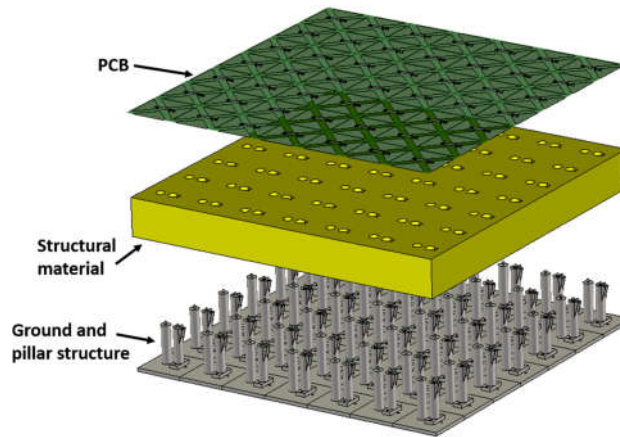


Figure 2. One of the proposed concepts for the structural integration of connected cross bowtie antenna array.

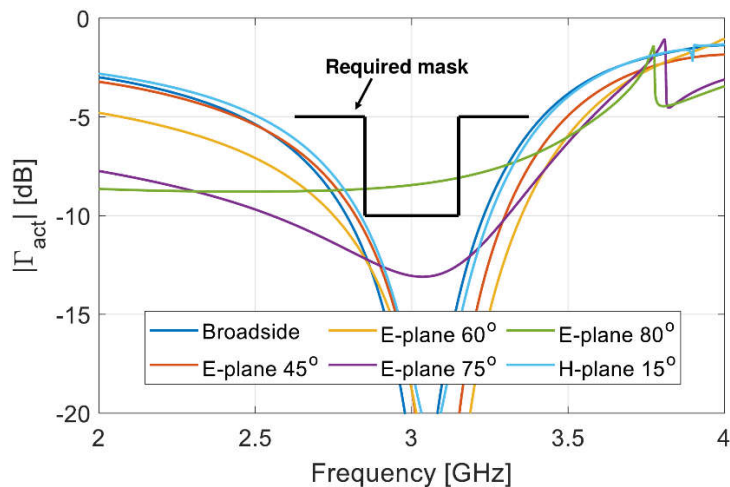


Figure 3. The active reflection coefficients of the uniformly excited infinite phased array of the connected cross bowtie antenna array.

For the project, we selected a cross bowtie antenna element (Khanal et al., 2019) as one of the possible solutions. Figure 2 shows the proposed concept for structural integration of the cross-bowtie antenna element. The antenna has two parts, 1) A PCB consisting of the radiating elements: bowties elements and 2) Ground and pillar structure consisting of a ground plane and the feeding structure: coaxial pillars and solid (metal) pillars. A pair of the coaxial and solid pillars act as a balun transforming single-ended antenna port to the differential port of the bowties. We have proposed to use Rohacell sandwich or similar material as a structural material. The structural material is sandwiched between the PCB and ground and pillar structure to provide the antenna with the rigidity and mechanical strength.

Figure 3 shows the active reflection coefficient of an infinitely large cross bowtie antenna array. Here we can see that the antenna array is capable of providing coverage up to $\pm 75^\circ$ in azimuth (E-plane) and $\pm 15^\circ$ in elevation (H-plane) with the desired performance: active reflection coefficient of -10 dB and -5 dB at 10% and 25% bandwidth respectively. Next phase of the project is to build a prototype antenna and study its electrical and mechanical performance.

REFERENCES

- Berkner L.V. 1946. Naval airborne radar. Proceedings of the IRE, vol. 34, pp. 671-706.
- Clarke J. 1985. Airborne early warning radar. Proceedings of the IEEE, vol. 73, pp. 312-324.
- Ellgardt A. 2009. Ph.D. thesis. Wide-angle scanning wide-band phased array antennas. KTH School of Electrical Engineering, Sweden.
- Heed M. 2000. The erieye phased array antenna – from a system viewpoint. Proceeding 2000 IEEE International Conference on Phased Array Systems and Technology, pp. 391-394.
- Jonsson B. L. G., Kolitsidas C. I. and Hussain N. 2013. Array antenna limitations. IEEE Antennas and Wireless Propagation Letters, vol. 12, pp. 1539-1542.
- Kemkemian S., Roy-Naneix I. Le, Mallegol S., Perpere B. and Renard C. 2013. Wideband and very wideband thin structural tiles for airborne active antennas. 7th European Conference on Antennas and Propagation (EuCAP), pp. 2744-2747.
- Khanal P., Yang J., Ivashina M., Höök A. and Luo R. 2019. A wide coverage s-band array with dual polarized connected bowtie antenna elements. 2019 IEEE International Symposium on Antennas and Propagation and USNC-URSI Radio Science Meeting, pp. 2001-2002.
- McCarty P. 2001. Airborne Early warning and Control: A piece of The Puzzle. Aerospace Centre, RAAF Base, Fairbairn, Australia.
- Qiang Y. F., Guo L, Zhu Q. C. and Yao Y. F. 2017. A conformal low-profile series-fed microstrip array for aircraft applications. 2017 International Applied Computational Electromagnetics Society Symposium (ACES), pp. 1-2.
- Watts S. 2017. The asv 21 maritime surveillance radar. 2017 IEEE Radar Conference (RadarConf), pp. 0027-0032.

A SYSTEM OF SYSTEMS VIEW IN AEROSPACE PRODUCT DEVELOPMENT

L. Knöös Franzén¹, I. Staack¹, C. Jouannet² & P. Krus¹

¹ Department of Management and Engineering (IEI), Fluid and Mechatronic Systems (FLUMES), Sweden, ludvig.knoos.franzen@liu.se

² Overall Design and Systems Integration, Saab Aeronautics, Linköping, Sweden

Abstract. This paper presents ongoing research that aims to produce methods for performing design and trade space explorations on system-of-systems. Aerospace systems are becoming more and more complex due to the increasing connectivity with the operational environment and other systems in general. The focus is shifting from a singular system's perspective to a system-of-system's perspective. This increasing complexity gives rise to new levels of uncertainty that needs to be understood to produce aerospace solutions for an everchanging future. The intention of this research is to provide methods that can aid in aircraft conceptual design from a system-of-systems perspective and allow designs to be holistically explored in the early stages of their development. Proposed methods for using ontology and description logic reasoning are presented together with additional approaches that could address the added complexity of a system-of-systems viewpoint in the design process. Search and Rescue operations based on the Swedish Maritime Administration are used as case-studies to test the developed methods. At the end, a possible future direction for the research is presented together with an outline for an envisioned holistic system-of-systems design approach.

Keywords: System-of-Systems, Ontology, Description Logic Reasoning, Search and Rescue

INTRODUCTION

Systems of systems engineering (SoSE) has become a growing field within aerospace product development. Aerospace systems are becoming more and more connected with the operational environment and other systems in general. This consequently leads to new and higher levels of complexity and uncertainty, which creates a desire for understanding systems and their connections early in the development process. A holistic view of the systems is needed to explore the influence of possible changes in the outside world, such as changing politics and environmental aspects. Systems capable of delivering capabilities throughout time and under changing circumstances can thereby be identified by exploring the available design space early in the development process. Having a holistic view also implies that more aspects than just single system solutions need to be considered during the design phases. The increasing connections with other systems take the development into a system-of-systems (SoS) perspective. While the term system can be referred to as *“a set of elements or parts that is coherently organized and interconnected in a pattern or structure that produces a characteristic set of behaviours”* (Meadows, 2008); the term SoS can be defined as *“an interoperating collection of component systems that produce results unachievable by the individual systems alone”* (INCOSE, 2006). A SoS can be distinguished from a system with five different characteristic properties proposed in (Maier, 1998). Systems engineering (SE) has been widely used in aerospace product development and have well established practices. The SoS view might however require different approaches to achieve satisfactory results.

This paper presents ongoing research that aims to develop design and trade space exploration methods for SoS that can be used in the early stages of aircraft conceptual design. It summarizes methods for approaching aerospace product development with a SoS view and highlights current results and the planned future work for the research project.

APPROACHES

Suggestions on how SoS can be used in aeronautical product development has been presented in (Amadori, et al., 2019). The design process can here be divided into five different levels of interest. These are represented in Fig. 1.

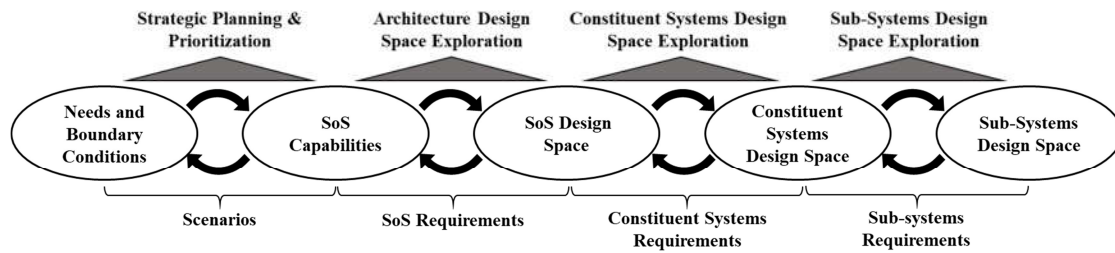


Figure 14. The holistic design process for a SoS. Adapted from (Amadori, et al., 2019).

The five levels presented in Fig. 1 are associated with different design spaces that are intercorrelated with each other. This means that a change in needs or boundary conditions will propagate and consequently influence all design spaces of the different levels. A change in the sub-system design space will therefore influence the other levels in a similar fashion. There are many ways of approaching the complex problems related to SoS and an overall holistic perspective. One of the commonly used approaches is to use modelling and simulation to perform SoS analyses. A common approach to model-based systems engineering (MBSE) is to use modelling languages such as the unified modelling language (UML) or the systems modelling language (SysML). These languages can be used to describe important aspects such as the architecture and information exchange between systems that are connected in a SoS. Architecture frameworks have been developed for the purpose of describing complex systems and SoS. Examples of such frameworks are the department of defence architecture framework (DoDAF) and the unified architecture framework (UAF), where UAF is tightly connected with UML and SysML (UAF, 2020). A complementary approach to MBSE, that has been used in both SE and SoSE, is ontologies. The field of ontology can be used to describe entities and their relationships in a domain, similar to UML and SysML models. An ontology implemented in the web ontology language (OWL) can be processed by a description logic reasoner. A reasoner can check the consistency of an implemented ontology, but also infer new relationships within the domain. Ontology could be a way of understanding the emergent behaviour of a complex system (Mittal, et al., 2018). Other approaches for understanding the emergent behaviours have shown that different kinds of simulations can be used for this purpose. System dynamics can be used to investigate and increase the understanding of systems through simulations (Meadows, 2008). It can be used to indicate how desired emergent behaviours can be achieved in SoS. Emergent behaviours of systems are important to understand in SoSE development. Complex emergent behaviours of SoS can be produced and analysed with agent-based simulation (ABS). This can be used to increase the understanding of the dynamics in SoS during the early stages of system design (Rainey & Tolk, 2015). Many traditional SE approaches for product development are still applicable in SoS contexts. Matrix-based approaches for representing relationships between means and functions can generate available design spaces using morphological matrices. An interactive reconfigurable matrix of alternatives (IRMA) can be used for design space refinement and allow designers to see interrelationships between concept options (Dickerson & Mavris, 2010). A general problem with matrix-based approaches is however that the available combinations of solutions grow at an exponential rate. This is especially true for the large design spaces available for a SoS.

CURRENT RESULTS

Work that has been done to approach the holistic view levels shown in Fig. 1 are presented in (Jouannet, et al., 2019) and (Amadori, et al., 2020). These papers have shown that ontology and description logic reasoning together with ABS can be used to generate, reduce and evaluate a SoS design space and to give performance measures for different solution alternatives. Search and rescue (SAR) operations of the Swedish maritime administration have been used as case-studies to show the usefulness of presented methods in the

papers. A SAR scenario with e.g. available SAR assets, rescue subjects, capabilities and identified SAR needs are represented in an ontology model. Description logic reasoning is subsequently used to automatically generate and narrow down a design space of possible SAR assets that can fulfil the identified needs. The performances of different suitable asset combinations are then investigated using ABS. A summary of this approach is illustrated in Fig. 2.

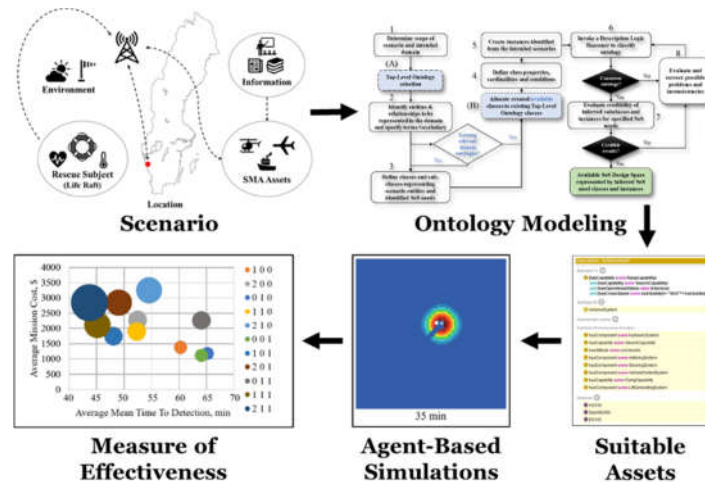


Figure 15. A summary of the approach used to generate, reduce and evaluate a SoS design space. From the work presented in (Amadori, et al., 2019) and (Amadori, et al., 2020).

This is an initial approach that enables an increased understanding for the different designs during the early stages of aerospace product development. There is still much work to be done to generate a process that includes more aspects of the SoS view. The performed investigations have so far only covered existing resources and how to best use them from a SoS perspective. A SoS that consists of currently available systems can be referred to as a near-term SoS. Future expansions of the studies would be to include SoS where some of the involved systems are new and not yet developed. Such a composition of systems could be defined as a mixed SoS. Similarly, a long-term SoS would correspond to a composition where all the involved systems are yet to be developed. Incorporation of traditional product development methods and techniques would have to be done in order to expand the produced methods so that all the different SoS compositions can be investigated.

THE WAY FORWARD

The performed work has so far investigated currently available SAR resources and how to best use them. A future abstraction is to generate and evaluate concepts using the previously mentioned approaches. In order to do this, an understanding of how SoS needs connect to capabilities and subsequently functions and means must be obtained. One possible way of identifying these connections are through architecture frameworks, such as DoDAF or UAF. A breakdown of a SAR enterprise using such a framework can indicate how a typical SoS should be broken down starting from the stakeholder needs level. The area of search and rescue has a basic goal which is to find and rescue subjects in distress. A black box could act as a good starting point in the breakdown from needs to capabilities. A question that arises is consequently how capabilities can be differentiated from functions. A coherent understanding of this must be achieved to allow consistent breakdowns from needs to capabilities to functions. Means that can achieve the functions can then be investigated using function/mean trees or similar approaches. An ontology approach could then be used to represent the relationships between needs, capabilities, functions and means. Any potential incompatibilities could also be included in the ontology so that unreasonable designs can be ruled out early in a design space reduction. The suitable design options

captured in the ontology can subsequently be extracted and used in combination with e.g. an IRMA. Different alternatives can then be generated using the IRMA, and afterwards tested using ABS. An illustration of the envisioned process can be seen in Fig. 3.

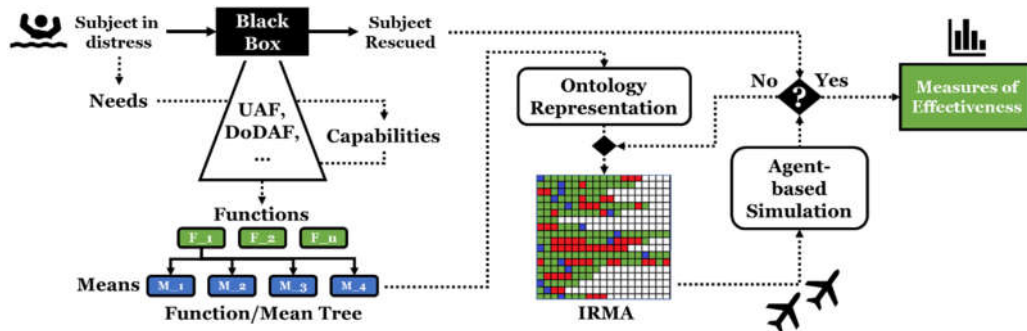


Figure 16. An illustration of an envisioned holistic SoS design approach.

Additional future work includes the incorporation of changing boundary conditions, such as environmental changes. This could be used to show how changes influence all levels of the holistic view in an early stage. The designs that are least sensitive to changes in the initial conditions could then be regarded as the ones most resilient to possible changes in the near-term future. Finally, the intention is to provide methods for performing analyses on any SoS and not just on SAR and in aerospace product development. The produced methods will therefore be generalized to possibly allow the analyses of any domain from a SoS perspective.

CONCLUSIONS

The presented work indicates that there are potential benefits with seeing aerospace product development from a system-of-systems (SoS) perspective. Methods for approaching and analysing SoS have been presented, together with current results from ongoing research. Ontology, description logic reasoning and agent-based simulations (ABS) have so far been used to generate, reduce and evaluate a SoS design space of different search and rescue (SAR) assets. Future work includes the incorporation of architecture frameworks and matrix-based approaches to create new concepts that can be tested and evaluated.

GRANT SUPPORT

The research presented in this paper is financially supported by the Swedish Innovation Agency (VINNOVA) by the grant no. NFFP7/ 2017-04838.

REFERENCES

- Amadori, K. et al., 2020. A System of Systems Approach for Search and Rescue Missions. Orlando, AIAA SciTech Forum.
- Amadori, K., Jouannet, C. & Staack, I., 2019. A holistic engineering approach to aeronautical product development. *The Aeronautical Journal*, 123(1268), pp. 1545-1560.
- Dickerson, C. E. & Mavris, D. N., 2010. *Architecture and Principles of Systems Engineering*. 1st ed. Boca Raton: Auerbach Publications.
- INCOSE, 2006. *Systems Engineering HandBook: A Guide for System Life Cycle Processes and Activities*. Seattle: INCOSE.
- Jouannet, C., Knöös Franzén, L., Krus, P. & Staack, I., 2019. An Ontological Approach to System-of-Systems Engineering in Product. Stockholm, Aerospace Technology Congress.
- Maier, M. W., 1998. Architecting Principles for System-of-Systems. *SYstems Engineering: The Journal of the International Council on Systems Engineering*, 1(4), pp. 267-284.
- Meadows, D. H., 2008. *Thinking in Systems: A Primer*. 1st ed. Chelsea: Chelsea Green Publishing.

- Mittal, S., Diallo, S. & Tolk, A., 2018. Emergent Behavior in Complex Systems Engineering - A Modeling and Simulation Approach. 1st ed. New York: John Wiley & Sons.
- Rainey, L. B. & Tolk, A., 2015. Modeling and Simulation Support for System of Systems Engineering Applications. 1st ed. New Jersey: Wiley.
- UAF, 2020. Object Management Group - Unified Architecture Framework. [Online]
Available at: <https://www.omg.org/uaf/index.htm> [Accessed 17 March 2020].

AUTONOMOUS NAVIGATION SUPPORT FROM REAL-TIME VISUAL MAPPING

D. Sabel¹ & D. Åsvärn²

¹ Division of Robotics, Perception and Learning, KTH Royal Institute of Technology, Stockholm, Sweden, dosabel@kth.se

² Spacemetric AB, Sollentuna, Sweden, dag@spacemetric.com

Abstract. The last few years have seen a rapid technological development in the field of unmanned aerial vehicles, with increasing degrees of autonomy. Autonomous navigation is expected to greatly benefit a range of different applications, such as reconnaissance, search and rescue operations, inspection of forest fires or power lines and delivery of supplies in disaster areas. Autonomous outdoor aerial navigation commonly depends on Global Navigation Satellite Systems (GNSS) which can be unreliable in case of occlusion from terrain or buildings or due to intentional disruption through electronic attacks as well as unintentional radio frequency interference.

One aerial positioning method not using GNSS is "visual mapping", which estimates the aerial vehicle's position and orientation by comparing images from an on-board camera with geolocated reference images of the ground. The research project will investigate how position and orientation can be estimated with visual mapping in order to support autonomous aerial navigation. The research focusses on i) optimal on-board camera characteristics, ii) choice of ground reference data (e.g. aerial or satellite images, terrain models, 3D point clouds) and iii) algorithms for real time visual mapping with high enough accuracy and reliability in order to support autonomous aerial navigation.

The outcomes of the project will provide a foundation for the development of visual mapping-based systems. Such a system will be useful not only as a backup in cases when GNSS positioning fails, but also for improving the accuracy of position and orientation estimates of aerial vehicles. The project will conclude with a proof-of-concept demonstration.

Keywords: autonomous navigation, drone, unmanned aerial vehicle, GPS-denied environment, vision-based positioning

ACKNOWLEDGEMENTS

This project receives funding from the National Aeronautics Research Programme (NFFP) through the Swedish Agency for Innovation Systems (Vinnova).

INVESTIGATING FIGHTER PILOT TEAMWORK USING A LOW-COST FLIGHT SIMULATOR

U. Ohlander¹, J. Alfredson² & R. Granlund³

¹ Saab AB, Sweden, ulrika.ohlander@saabgroup.com

² Saab AB, Sweden, jens.alfredson@saabgroup.com

³ RISE SICS East, Sweden, rego.granlund@ri.se

INTRODUCTION

The field of System-of-Systems Engineering has become a growing area within Aerospace product development. Aerospace systems are becoming more and more interconnected with the operational environment and other systems in general, which consequently leads to new and higher levels of complexity and uncertainty. A desired for understanding systems and their connections early in the development process therefore arises. A holistic view is also needed to explore the influence of possible changes in external factors such as politics, technology and environmental aspects.

METHODS

The work presented in this paper summarizes methods for approaching aerospace product development with a System-of-Systems (SoS) view. It presents developed methods for holistically exploring SoS design spaces using ontology, description logic reasoning and Agent-Based Simulations (ABS). Swedish Search and Rescue (SAR) is used as a case study to evaluate the developed methods. Ontology is used to model a SAR scenario with e.g. available SAR assets, rescue subjects, environmental conditions, capabilities and identified SAR needs. Description logic reasoning is subsequently used to automatically generate and narrow down a design space of possible SAR assets that can fulfil the identified needs. The performance of different constellations of available assets are then investigated using ABS. The influence of possible changes in external factors are envisioned to be propagated and investigated using the methods.

RESULTS AND CONCLUSIONS

The case study has shown that the presented methods can be used to generate and reduce a SoS design space, and that the performance of different solutions can be investigated. Ontology, description logic reasoning and ABS can be used to model and simulate a SoS to increase the overall knowledge and understanding of different designs during the early stages of aerospace product development.

GRANT SUPPORT

The research presented in this paper is financially supported by the Swedish Innovation Agency (VINNOVA) by the grant no. NFFP7/ 2017-04838.

CAVITY ACOUSTICS AND ROSSITER MODES - CARE

S. Hammer¹, J. Fridh¹ & M. Billson²

¹ Heat and Power Technology, KTH, Sweden, steffenh@kth.se, jens.fridh@energy.kth.se

² GKN Aerospace Sweden AB, Sweden, mattias.billson@gknaerospace.com

Abstract. Acoustic resonance in cavities in aero engines is a current and major concern due to the detrimental effect the unsteady loads have on the nearby components in the engine. An example is the bleed system resonance in the intermediate compressor duct that may cause failure to the low-pressure compressor. The basic acoustic phenomena of quarter pipe length or Helmholtz resonances may occur for any given cavity geometry and calculations of those are not straightforward for complex cavity geometries with several exits. So-called Rossiter's resonance may occur due to an interaction between the radiating cavity acoustic resonance frequency and any dominant boundary layer vortex frequency from passing over the cavity that can lead to severe structural forces generating high vibration amplitudes, which in turn may lead to pre-lifetime failure of components. The main overall objective is to experimentally quantify the coupled resonance occurring due to interaction between vortex oscillations from the shear layer flow passing over a cavity and the acoustic cavity. This targeted to provide validation data for analysis methods at industry in order to strengthen design prediction capabilities.

Keywords: Cavity, Resonance, Rossiter, Acoustic

INTRODUCTION

The objective of the project is the numerical and experimental study of acoustic resonance due to flow over a cavity. Experiments will be performed in a wind tunnel test rig at KTH – Royal Institute of Technology.

Especially of interest is the interaction of this shear layer instability with the acoustic resonance of a cavity. Herein a quantifiable database shall be established in regards of geometric shape of the cavity and the flow conditions in the shear layer when interacting with the cavity. The research aim is to characterize the flow physics and the coupling of shear layer instabilities (Rossiter modes) with cavity acoustics in relation to geometric parameters. This shall help refine the prediction of the acoustic resonance phenomena with GKN in-house tools. The database shall help to minimize the error margin of the numerical predictions. Therefore the interaction phenomena of boundary layer and cavity is studied with 3 test objects with increased geometric complexity. The first cavity will be used as generic study to establish a baseline. The second cavity will increase the depth of the cavity to quantify the results of the baseline and further characterize the phenomena. The 3rd cavity shall represent a more industry-like geometry which uses the outcome of the first two test campaigns to reduce the acoustic interaction.

The first cavity with limited instrumentation but several cavity depths will be run to compare with initial 2D numerical studies presented below.

EXPERIMENTAL TEST FACILITY

This section describes the test facility used for the experimental study (Bron, 2003).

The air supply consists of an opened wind tunnel facility in which the air is sucked by a screw compressor, driven by a 1MW electrical motor, from the atmosphere into a dryer, and compressed at a fixed operating point. Three valves allows to control both the mass flow and the pressure level in the test section.

A drawing of the exchangeable wind tunnel VM100 which will be used in the experiments can be seen in **Fehler! Verweisquelle konnte nicht gefunden werden.** It consists of a square settling chamber (250mm²) with screens and honeycombs. The test section of the wind tunnel is modular and can be equipped with different geometries (**Fehler! Verweisquelle**

konnte nicht gefunden werden.). All 4 walls around the rectangular test section have large openings for instrumentation or optical access.
 Due to the small size of the settling chamber it is planned to measure the flow at the outlet of the settling chamber to ensure isotropic conditions.

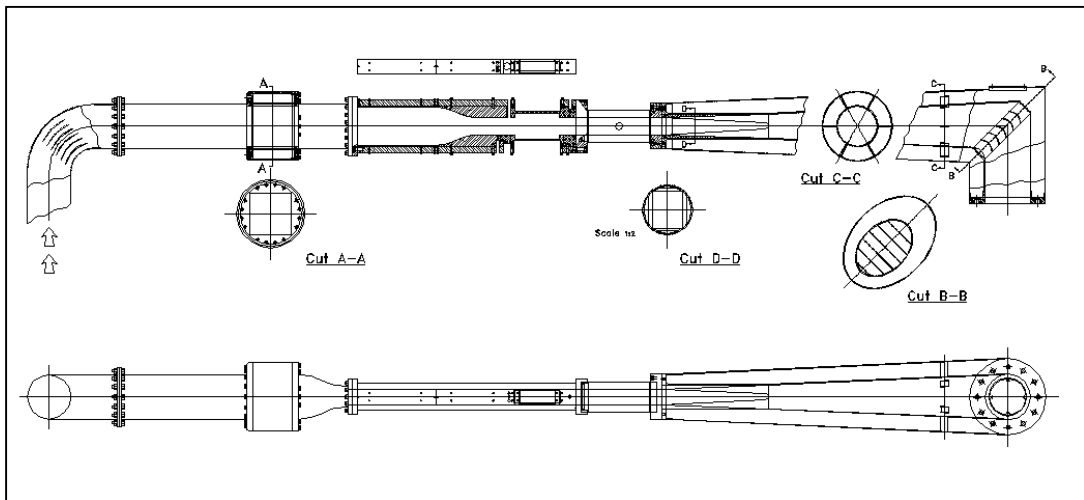


Figure 17. Drawing of the exchangeable wind tunnel VM100 (Bron, 2003)

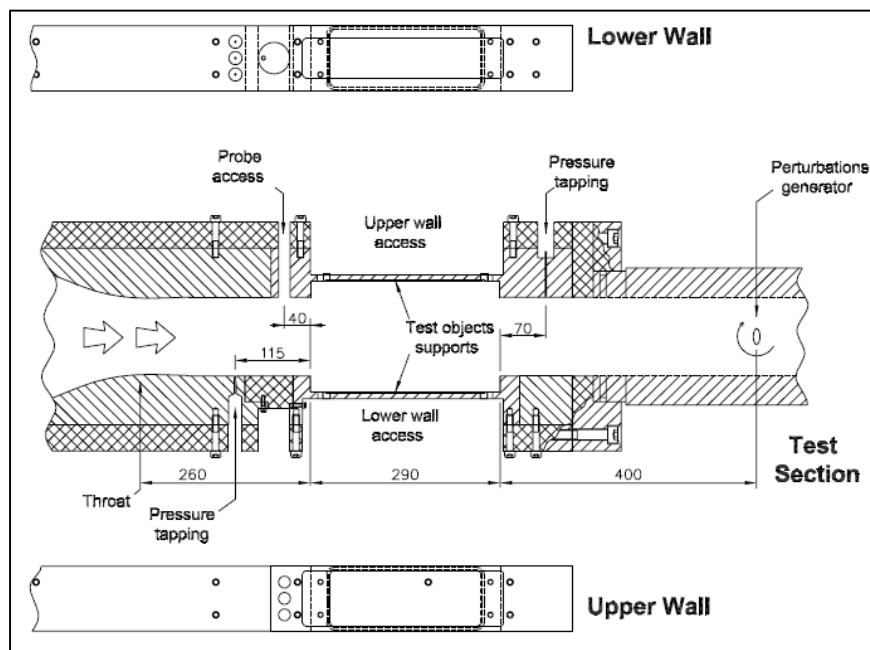


Figure 18. Detailed drawing of the VM100 test section (Bron, 2003)

Cavity design for initial study

A cavity with a length of $L = 40$ mm and a depth $D = 10-80$ mm is designed for the initial test. The full duct height ($H = 120$ mm) available in the test section of the wind tunnel will be used during these runs. Different cavity ratios of length to depth will be achieved with a combination of different plugs showcased in Fehler! Verweisquelle konnte nicht gefunden werden.. In the center of the bottom and the trailing edge upstream facing wall of the cavity Kulite pressure transducers will be placed.

The 3 more complex measurement campaigns will use a reduced duct height later on. The reduction in height is achieved with a vertically converging flow path at hub and shroud in the test section.

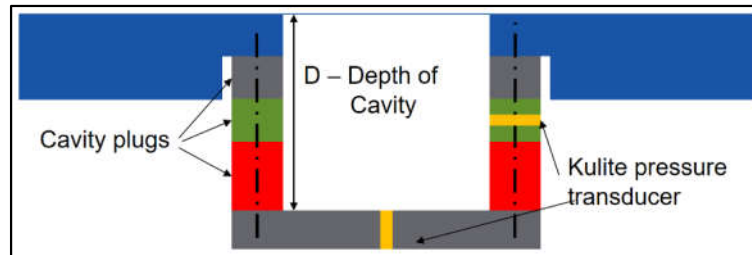


Figure 19. Symbolic drawing of the cavity with multiple plugs

The initial test will include 4 cavity length to depth ratios. **Fehler! Verweisquelle konnte nicht gefunden werden.** shows the expected results. For each cavity depth a range of Mach numbers between 0.2 and 0.8 will be tested to reach resonance.

Table 6. Cavity design and expected results for pre-test

Cavity depth	Expected result
$L/D = 4$	Shallow cavity, expected to result in wake mode
$L/D = 2$	Intermediate cavity depth, may produce wake modes and Rossiter modes
$L/D = 1$	May produce wake modes and Rossiter modes
$L/D = 0.5$	Deep cavity, deep enough that the depth is not a parameter (except for possible acoustic feedback), Rossiter modes expected

The initial test will use 3 steady pressure taps upstream of the cavity. One in the centreline and 2 away from the center to control 2D predictability of the steady flow.

Further Kulite transducers will be placed in equal distances downstream of the cavity along the centreline of the test section. Here 2 additional Kulite transducers are placed left and right of the first location to check the 2D predictability of the unsteady flow as shown in **Fehler! Verweisquelle konnte nicht gefunden werden.**

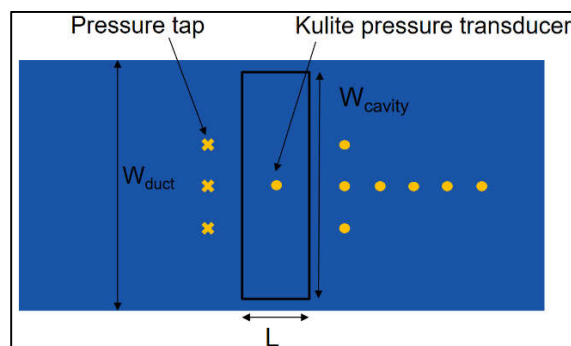


Figure 20. Pressure measurement positions around cavity

NUMERICAL PRE-STUDIES

A simplified CFD approach for predicting oscillations over open cavities has been set up. It is based on a 2D grid of a duct with an open cavity (one cell layer) shown in **Fehler! Verweisquelle konnte nicht gefunden werden.**

The duct flow is varied by setting the inlet speed to 80, 160 and 240 m/s at 288K. The outlet is set to 101325 Pa static pressure. Large eddy simulations (LES) are used as turbulence model.

The cavities are varied in depth such that L/D ranges from 1 to 4. Shown here are only cavities L/D of 1 and 4.

Monitors of pressure and y-component of velocity are used to determine the shear layer and cavity oscillation.

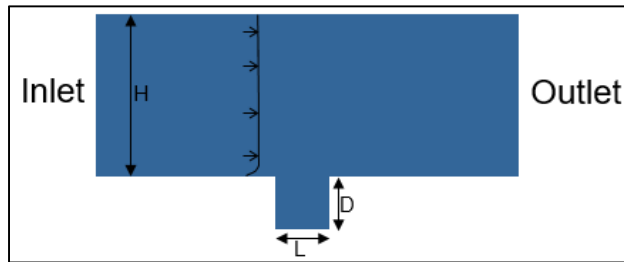


Figure 21. Sketch of the 2D test section with cavity

Fehler! Verweisquelle konnte nicht gefunden werden. shows the results of a cavity of $L/D = 4$ and inlet speed of 160 m/s. Depicted are the pressure and the normalized vorticity. The simulations show a clear wake mode.

In comparison **Fehler! Verweisquelle konnte nicht gefunden werden.** shows a cavity of $L/D = 1$ with the same inlet conditions. Here no clear resonance mode can be seen.

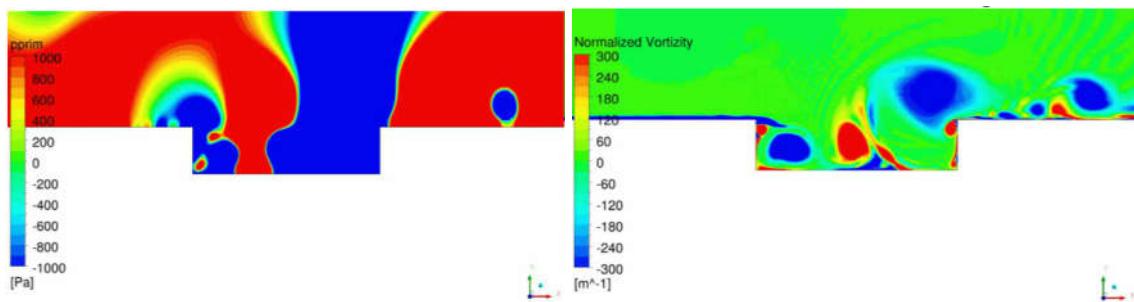


Figure 22. Cavity $L/D = 4$ with $U = 160$ m/s, Pressure on the left and normalized vorticity on the right

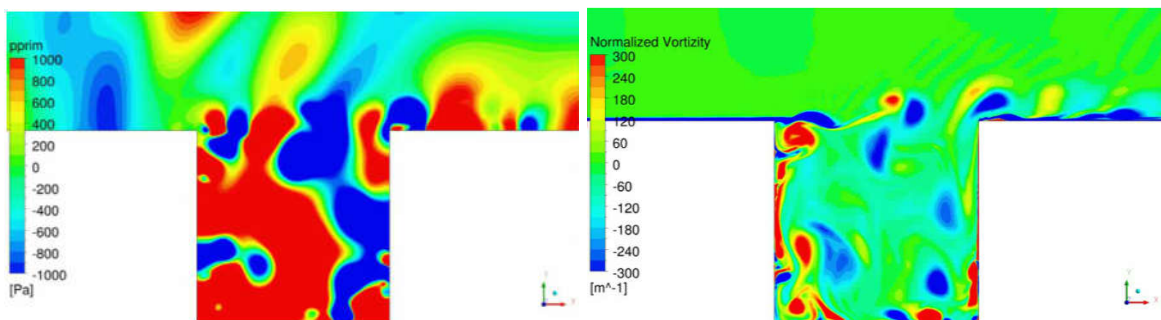


Figure 23. Cavity $L/D = 1$ with $U = 160$ m/s, Pressure on the left and normalized vorticity on the right

REFERENCES

- Tracy M. B. and Plentovich E.B., 1997. *Cavity Unsteady-Pressure Measurements at Subsonic and Transonic Speeds*. NASA Technical Paper 3669
- Jones M. B., Watmuff J. H. and Henbest S. M., 2010, *Aeroacoustic measurements of a deep cavity in a low speed flow*. Proceedings of 17th Australian Fluid Mechanics Conference. Auckland, New Zealand
- Bron O., 2003. *Numerical and Experimental study of shock boundary layer interaction in unsteady transonic flow*. Ph.D. thesis, Royal Institute of Technology, Sweden

MICROSTRUCTURAL EVOLUTION DURING THERMAL POST-TREATMENT OF ALLOY 718 PRODUCED BY ELECTRON BEAM MELTING

Sneha Goel¹, Uta Klement² & Shrikant Joshi¹

¹ Department of Engineering Science, University West, Sweden

² Department of Industrial and Materials Science, Chalmers University of Technology, Sweden

Abstract.

INTRODUCTION

Electron beam melting (EBM) is an additive manufacturing technology which is gaining rapid popularity for production of complex customized parts for diverse sectors such as aerospace, medical etc. High value difficult-to-machine materials like superalloys, e.g. Alloy 718, extensively used in aerospace sector are attractive candidates for being produced using EBM technique. Processing of EBM Alloy 718 builds free from detrimental defects and/or phases is challenging and microstructural inhomogeneity, inappropriate phase constitution, etc. are additional concerns. The above facets of EBM Alloy 718 builds suggest the need for appropriate thermal post-treatments and encourage comprehensive investigation of the outcomes.

Keywords: Additive manufacturing, Electron beam melting, Superalloy, Hot isostatic pressing, Heat treatment

METHODS

EBM built Alloy 718 specimens were subjected to two different HIPing treatments: (a) HIP1 (1120°C/100 MPa/4h), and (b) HIP2 (1185°C/100 MPa/4h) based on recommendations of ASTM (F3055) standard for post-treatment of powder bed fusion built Alloy 718. Select HIPed and as-built samples were also subjected to heat treatments (HTs) comprising solution treatment (954°C) and two-step aging (740°C, 635°C). The duration of HTs was systematically varied to investigate the evolution of microstructure to explore the possibility of shortening the post-treatment protocols. The specimens were extensively characterized using microscopy to investigate the influence of the different post-treatments on porosity, lack-of-fusion defects, NbC segregation, δ -phase and γ'' -phase, etc. The tensile behaviour of selected samples was also evaluated.

RESULTS AND CONCLUSION

It was observed that, through choice of appropriate HIPing parameters, defects in EBM Alloy 718 can be closed without significantly affecting the as-built grain structure. Detailed investigation of microstructural evolution during subsequent heat treatments revealed that a significantly shortened aging treatment (7h) compared to the 'standard' long treatment (18h) traditionally developed for conventionally produced Alloy 718 might be realizable. These results can have significant techno-economic implications in encouraging adoption of additively manufactured material.

ACKNOWLEDGEMENTS

Grant Support

This project was supported by KK-foundation (grant-number 20160281).

INDEX OF AUTHORS

- Adams C. 104
Alborzi E. 104, 126
Alfredson J. 251
Anderson B.E. 116, 127
Anderson S. 211
Andersson J. 136, 159
Archilla-Prat V. 28, 34, 47
Arunachalam S. 18
Asp L.E. 129, 133, 134, 135
Åsvärn D. 250
Bendtsen K.M. 16
Bergström R. 210
Berkes F. 33
Berthier A. 115
Berthing T. 16
Bertram N. 16
Bickel M. 52
Bier A. 128
Billson M. 252
Binkowski F.S. 18
Blakey S. 104, 126
Bock L. 52
Bräuer T. 127
Brea A. 80
Brinkop S. 179
Brostrøm A. 16
Brynolf S. 117, 215
Burkhardt U. 52, 83, 128
Carlstedt D. 129, 134, 135
Celikel A. 35
Chernoray V. 232, 237
Clausen P.A. 16
Corbin J. 116
Crayford A. 28, 110
Creaser D. 211
Crosbie E. 116
Dahal K. 117
Dahlmann K. 56, 83, 162, 169, 180, 195
Dal Maso M. 16
Deck K. 81
Dedoussi I. 17, 81
Delhaye D. 115
Deransy R. 186
Dietmüller S. 83
Ditas F. 41
Duan S. 129, 134, 135
Durand E. 110
Ekstrand H. 210
Elliff T. 35
Emmerig J. 187
Fagerström A. 211
Favier P. 103
Fernández E.C. 186
Finke M. 103
Focsa C. 115
Freedman A. 116
Fridh J. 252
Frömming C. 179, 180
Gangoli Rao A. 221
Garnier F. 34
Ghedhaïfi W. 20, 27, 34, 61, 82
Gierens K. 71, 98, 174
Glaves J. 33
Goel S. 256
Gollnick V. 93, 162, 205
Grahn D. 211
Grahn M. 117, 215
Granlund R. 251
Grewe V. 56, 71, 81, 93, 162, 169, 179, 180, 187, 188, 195
Grönstedt T. 125, 136, 159, 227
Hagberg M. 215
Hallander P. 241
Hammer S. 252
Hansson J. 117, 211, 215
Haoliang Hu 103
Harper J. 110
Haselrut A. 83
Haslerud A.S. 179
Hauglustaine D. 48
Heckl C. 127
Hendricks J. 83
Herrmann H. 41
Höök A. 241
Hormigo D. 28
Huang J. 18
Huck V. 35
Ibarra I. 28
Ivashina M. 241
Jacobi S. 41
Janicke U. 20
Jensen K.A. 16
Jöckel P. 180, 187
Johnson M. 28, 110
Jonsson I. 125, 232
Joshi S. 256
Jouannet C. 245
Kalise D. 184
Kangasniemi O. 16
Karlsson K. 215
Kaufmann S. 127
Kern B. 180

- Khanal P. 241
Kilic D. 47
Kleinert M. 103
Klement U. 256
Kling F. 103
Kling K.I. 16
Klingels H. 57
Knöös Franzén L. 245
Köhler M. 116
Koivisto A.J. 16
Koponen I. 16
Krupko A. 19
Krus P. 76, 245
Langner J. 210
LeClercq P. 127
Lee D.S. 83
Lehtveer M. 117
Li X.J. 151
Lim L. 83
Linde P. 133, 135
Lindgren M. 211
Lindskog M. 210
Linke F. 81, 162, 188, 195
Lobo P. 116
Loeschner K. 16
Lohmann U. 90
Lopez P. 80
Lopez S. 47
Luo R. 241
Lührs B. 81, 188, 195
Lundberg S. 211
Lundblad A. 140
Marks T. 162, 169, 205
Mårtensson H. 145
Mårtensson T. 210
Matthes S. 34, 56, 83, 98, 162, 169, 174,
179, 180, 188, 195
Meijer A. 104
Miake-Lye R. 116
Moldanová J. 210
Montreuil E. 20, 27, 34, 61, 82
Moore R. 127
Moreno P. 28
Murphy B.N. 18
Murzyn F. 35
Nalianda D. 220
Näs A. 210
Nedelec P. 33
Neubauer D. 90
Nichols N.K. 184
Niklass M. 81, 93
Ohlander U. 251
Olsson L. 211
Ortega I.K. 115
Osswald P. 116
Owen B. 83
Parks C. 104
Pasztor A. 103
Petit O. 140
Petzold A. 33
Pitari G. 83
Poikkimäki M. 16
Poll I. 184
Ponater M. 52
Poorsgaard M. 211
Pouzolz R. 57
Proesmans P. 81
Pujadas M. 28
Quadros F. 17
Radhakrishnan K. 81
Raper D. 28, 33, 47
Rataj J. 103
Righi M. 34, 83
Robinson C. 116
Rodríguez-Maroto J. 28
Rohs S. 174
Rojas E. 28
Rolt A. 220
Rompoko P. 220
Rosanka S. 179
Rose D. 41
Rydal M. 210
Rydberg T. 211
Sabel D. 250
Saber A.T. 16
Sadat S.Y. 126
Salazar A. 80
Salvucci R. 215
Sánchez-García M. 28
Sánchez-Valdepeñas J. 28
Sang W.J. 67
Sauer D. 127
Sausen R. 98
Scheibe M. 127
Schlager H. 127
Schmitz O. 57
Schripp T. 116, 127
Schumann U. 68
Sethi V. 220
Shine K. 188, 195
Shook M. 116, 127
Silva V.T. 140
Skowron A. 83
Smallwood G. 116
Sobron A. 76
Staack I. 76, 245
Stettler E.J. 68
Stumpf E. 162

- Swaid M. 162, 205
Synylo K. 19, 45
Tabernier L. 186
Tautz A. 186
Tedeschi A. 99
Temme M. 103
Teoh R. 68
Terrenoire E. 20, 27, 34, 48, 61, 82
Thoma E.M. 227
Thornhill K.L. 127
Tully C. 90
Ulianova K. 45
Ungeheuer F. 41
Unterstrasser S. 62, 162, 169
van Manen J. 179
van Pinxteren D. 41
Vancassel X. 82
Vennam L.P. 18
Verlhac St. 46
Vikhorev V. 237
Vogel A.L. 41
Vogel U. 16
Voigt C. 127
Vos R. 81
Wall M. 210
Wallberg O. 211
Wells C. 184
Whitefield P. 116
Williams P.D. 184
Williams P.I. 47
Winstead E. 127
Wolff H. 16
Xisto C. 125
Xu J. 129, 134, 135
Yamashita H. 162, 169, 180
Yang J. 241
Yao H.D. 136, 151, 159
Yin F. 71, 81, 180, 188, 195, 221
Yu Z. 116
Zaporozhets O. 19, 45
Zhao X. 227
Ziemba L. 127
Zumegen C. 162

Making Aviation Environmentally Sustainable
3rd ECATS Conference, Book of Abstracts, Volume 1, June 2020
ISBN 978-1-910029-58-9

© ECATS 2020